UNIVERSIDAD COMPLUTENSE DE MADRID
FACULTAD DE FARMACIA
Departamento de Edafología

SOIL-WATER SYSTEM RESPONSE IN AN ANTHROPIZED MEDITERRANEAN WETLAND DURING DRYING CYCLES : LAS TABLAS DE DIAMIEL NATIONAL PARK

MEMORIA PARA OPTAR AL GRADO DE DOCTOR
PRESENTADA POR

Héctor Aguilera Alonso

Bajo la dirección de los doctores

Luis Moreno Merino
Miguel Ángel Casermeiro Martínez

Madrid, 2014

UNIVERSIDAD COMPLUTENSE DE MADRID

FACULTAD DE FARMACIA

Departamento de Edafología

Soil-water system response in an anthropized Mediterranean wetland during drying cycles: Las Tablas de Daimiel National Park

This thesis is submitted in fulfilment of the requirement for the degree of Doctor of Philosophy by

Héctor Aguilera Alonso

Supervisors

Promoter: Luis Moreno Merino

Co-promoter: Miguel Ángel Casermeiro Martínez

Madrid, 2013

UNIVERSIDAD COMPLUTENSE DE MADRID

FACULTAD DE FARMACIA

Departamento de Edafología

Respuesta del sistema suelo-agua en periodos de sequía en un humedal mediterráneo antropizado: el Parque Nacional de Las Tablas de Daimiel

Memoria para optar al grado de Doctor presentada por

Héctor Aguilera Alonso

Bajo la dirección de los Doctores

Luis Moreno Merino

Miguel Ángel Casermeiro Martínez

Madrid, 2013

Respuesta del sistema suelo-agua en periodos de sequía en un humedal mediterráneo antropizado: el Parque Nacional de Las Tablas de Daimiel

Directores

Luis Moreno Merino

Miguel Ángel Casermeiro Martínez

V°B° Director de Tesis

V°B° Codirector de Tesis

Luis Moreno Merino
Investigador Titular
Instituto Geológico y Minero de España

Miguel Ángel Casermeiro Martínez
Profesor Titular Edafología
Facultad de Farmacia

Memoria presentada por

Héctor Aguilera Alonso

Para aspirar al grado de Doctor

Madrid, 2013

UNIVERSIDAD COMPLUTENSE DE MADRID

FACULTAD DE FARMACIA

Departamento de Edafología

D. Antonio López Lafuente, Director del Departamento de Edafología de la Facultad de Farmacia de la Universidad Complutense de Madrid,

CERTIFICA,

Que el trabajo que constituye la presente memoria "Respuesta del sistema suelo-agua en periodos de sequía en un humedal mediterráneo antropizado: el Parque Nacional de Las Tablas de Daimiel", que presenta D. Héctor Aguilera Alonso, para optar al grado de Doctor, ha sido realizada bajo la dirección del Dr. Moreno Merino y del Dr. Casermeiro Martínez.

Y para que así conste, firmo la presente certificación en Madrid, de septiembre de 2013.

Antonio López Lafuente

To my parents, for a life of trust and support

Acknowledgements

Such a long work as a PhD thesis involves the direct or indirect participation and support of many different persons, organizations and institutions to which I need to be extremely grateful. They all deserve my acknowledgement and appreciation and will try not to forget anyone in the following lines.

First, I am very grateful to my main supervisor, Dr. Luis Moreno, for allowing me to enrol in the world of soil and water science. Also from his expertise in field work planning and designing I learnt the relevance of "measured" data against "estimated" or "bibliographic" data in site-specific soil science studies. He has always been there to support, encourage, and welcomed to discuss and contribute original ideas. I very much appreciate his patience and clear guidance for overcoming my difficulties. Secondly, my special thanks to my co-supervisor, Dr. Miguel Ángel Casermeiro, facilitating my integration in the Department of Edaphology of the Complutense University in Madrid, the use of laboratory equipment and being always open to discuss and provide contacts for scientific collaboration in specific fields and matters.

I am grateful to the Ministries responsible for the official research project, in particular to the Research State Department for providing me with the financial support through the Predoctoral Research Education (FPI) program referenced as BES-2006-11997, which has allowed me to fully focus on the research tasks of this thesis.

Furthermore, I am very grateful to the Geological Survey of Spain (IGME) for offering a PhD position in unsaturated zone dynamics and surface water-groundwater relations within their research projects in Las Tablas. In particular, my works coincided with projects CGL2005-06458-C02-01/HID and CGL2009-13507 from which funding for sampling campaigns and "in situ" field tests as wells as hydrochemical and isotopic water analyses was obtained. From the previous project (REN2002-04433-C02) I

gathered background and initial information for my research, whereas from the subsequent most recent one (CGL2011-30302-C02-01) I got updated information of the studied environment for contrasting and validation purposes.

During the whole process I've been part of an exceptional team at the IGME without which I would not have accomplished this mission: my supervisor Dr. Luis Moreno mentioned above, Dr. Silvino Castaño, Dr. Mª Emilia Jiménez-Hernández and technical expert Almudena de la Losa. Dr. Castaño, an expert in the hydrology of Las Tablas de Daimiel National Park, always keen on teaching, showing, discussing and challenging me, has contributed significantly to improve the quality of this research. Also, several foreign and Spanish master students have collaborated in our researches as part of their master studies. Special mention for Patricia Jiménez-Pinilla, who shared with me countless hours of field work to carry out an exhaustive study on peat physical and chemical properties. Field and laboratory work as well as writing support for publications have always been there at once when needed. This group has also provided valuable advice and guidance in different situations related to this thesis. I consider myself extremely lucky for having found out how important teamwork in science is through the experience of working with them. Besides them, all the administrative and technical staff from IGME has always been keen on helping and providing resources for either field or desk work. I am also highly acknowledged to all the staff from the Department of Edaphology, particularly laboratory technicians, always kind and helpful with the soil physical and chemical laboratory analyses performed there.

Without access to experimental sites this study would not have been possible. Here the collaborative attitude of Las Tablas de Daimiel National Park Managing Authorities has been fundamental. Special thanks to National Park's Director Carlos Ruíz de la Hermosa for providing data, technical and human support whenever required. How could I forget all those times when Park staff came to rescue our four-wheel drives when they got stuck in the hidden phreatic mud? I hope the findings presented in this thesis will somehow compensate their helpfulness.

Successful completion of this thesis has been based on two research stays with the Soil Physics and Land Use team from Alterra Research Centre of Wageningen University where I substantially improved my knowledge of soil physics. I spent over 7 months in Wageningen divided in two visits, in 2008 and 2010. I am very grateful to my supervisor there Coen Ritsema and the other members of the team I worked with: Louis Dekker, Klaas Oostindie and Jan Wesseling. It was really nice and fun to go in the field with Louis and Klaas to learn about soil water repellency by helping them with their experimental setups in golf courses. Jan has been essential for my understanding and application of the SWAP vadose zone water flow model. My whole professional as well as personal experience in Wageningen and the Netherlands was unforgettable. Shared a lot of nice dinners and evenings with students from different countries, played football and watched the Holland-Spain final of the 2010 World Cup with Dutch friends, discovered beautiful natural and urban sites, and so on.

I would also like to highlight the role of the IGME PhD-students collective for sharing a great working environment, full of unselfish support and concern for each other. Luckily, I have discovered that can exist. Struggling together for collective's rights at the same time as struggling with our own researches, all in a nice cooperative mood both inside and outside the office. Actually, I have to speak of most of them as real friends: Juan Vázquez, Alberto Jiménez, Manuela Chamizo, Marta Diéz Ercilla, Francisco Javier Montalván, Rut Sánchez, Mónica Marina, and many others.

Finally, my special gratitude and affection for my family and friends who have always supported and care about me all through this journey they could only follow from the distance. Their unselfish love and encouragement have kept me standing in the difficult moments. My father, Mariano, my mother, Pilar, my sisters, Cristina and Elvira, my close friends and partners, Marta, Annemiek, Juanes, Dani, Alvaro, Ana, Puel, Francesca, Paloma, Alberto, Driss, and my love, Arantxa. Thanks to you all I am what I am and this thesis has become real. Oh, almost forget Bilbo, my dog, always so happy to see me back after my long field work trips. Many ideas and hypotheses have

popped up during our walks and either confirmed or rejected through deep barking scientific discussions.

Abstract

The semiarid wetland area of Las Tablas de Daimiel National Park (TDNP) is located in central Spain. The peculiar mix of water qualities and geographical location conferred TDNP a special relevance among European wetland areas as an ecological refuge for singular waterfowl and plant species. This ecosystem linked to groundwater dynamics (former discharge area) was recognized as Biosphere Reserve by UNESCO and included in the Ramsar Agreement under the category of Wetlands of International Importance.

Since the 1960s strong human intervention and disturbance has led to system denaturalization (ditching, damming, pollution, artificial drainage and flooding etc). Mainly due to excessive groundwater pumping for irrigation in the Mancha Plain region coupled to inherent climatic variability in semiarid Mediterranean environments, the wetland area was disconnected from the underlying aquifer system and now suffers from alternating flooding and drainage cycles. This process induces severe impacts and modifications in the ecological characteristics of the wetland, both in the biotic as well as the abiotic environment. From a hydrogeological point of view the hydraulic gradient shifted from upward to downward, turning TDNP into a recharge area. The most striking representative of human-induced degradation on TDNP physical-chemical structure is the process of peat cracking, subsidence and fire caused by desiccation.

Artificial management aiming to sustain flooding conditions has also contributed to system disturbance and degradation turning the wetland into a regulated system of connected reservoirs which operates as an aquifer recharge area sustained through water transfers and groundwater pumping. One of the main limitations for suitable TDNP management has been the lack of precise knowledge of the physical and hydrological environments, particularly below the wetland surface.

The understanding of the behaviour of the TDNP soil-water system during drainage periods has been the reason motivating this research. The two major goals have been:

- Hydrological-based physical-chemical characterization of the soil-water system
- Analysis of environmental and management implications and development of support tools for hydro-environmental planning.

An integrated methodological approach has been followed to deal with system complexity and heterogeneity and the lack of detailed geological and hydrogeological knowledge. The subsurface system has been tackled through vadose zone (VZ) physical and chemical determinations and analyses. Soil chemistry was studied through descriptive statistics and multivariate analysis (principal component analysis and redundancy analysis) of 1:5 soil-water extracts and soil matrix samples. Intensive field and laboratory work has allowed for the determination of several soil physical parameters: texture, bulk density, saturated hydraulic conductivity, infiltration curves, water repellency, capillary wetting rate, and water retention and hydraulic conductivity curves. Special attention has been given to peat degradation characteristics following desiccation: hydrophobicity, shrinking and cracking properties, and combustion risk and propagation mechanisms.

VZ physical-chemical characterization has led to the definition and mapping of soil functional types (SFT) regarding their hydraulic properties as water and solute transmitters and storage. Besides this, one-dimensional VZ water flow models in different soil profiles representing typical arrangement of SFT in TDNP have been successfully calibrated and validated using measured and estimated data.

The interrelation between the surface water (SW) and groundwater (GW) environments has been inferred from a simple stepwise approach combining basic hydrochemical, hydrodynamic and isotopic data from a sampling network of monitoring points through clustering techniques and long-term time series analysis. A conceptual model of TDNP hydrological behaviour based on the interrelation between

flooding, groundwater level and hydrochemistry, involving both spatial and temporal considerations in SW-GW interactions, is proposed.

Environmental and management implications of soil and water physical-chemical characterization have been derived focusing on water availability and risk of groundwater contamination. Critical soil water contents for the development of soil hydrophobicity, reed (*Phragmites australis*) invasive expansion and peat combustion risk have been determined. Furthermore, usefulness of VZ water flow models as a management tool to simulate soil moisture progress and critical soil water contents reach during a drying scenario has been assessed.

Eight SFT have been identified based on soil physical and chemical properties which are defined by different degrees of evolution, anthropization and edaphization. They belong to four major soil materials: charophyte layers (unconsolidated carbonated sediments biologically produced), clay, fluvial silt (fluvial deposits in rivers, ditches and drains) and organic (high organic matter content). A map of the average spatial distribution of SFT inside TDNP based on the information provided by more then 120 soil columns bored all around the Park is presented.

The results show and that during drying periods TDNP becomes a highly saline and eutrophicated environment as inferred from both VZ and SW-GW chemical analyses. Median electrical conductivity (EC) in soil-water extracts of soil profiles is 3,280 $\mu S\ cm^{-1}$, and median organic matter (OM) content in the soil matrix is 5.33%. Median EC values in SW range between 2,973 and 11,739 $\mu S\ cm^{-1}$, and in GW between 677 and 15,383 $\mu S\ cm^{-1}$. Median total organic carbon concentrations in some groundwater monitoring points reach over 9 mg l^{-1}. However, large variability is observed in the whole soil-water system conditioned by lithology, evaporation, vegetation, microtopography, soil degradation and anthropization (i.e. dams, pumps, ditches, water transfers and wastewater inflows).

Physical properties of SFT show large variability reflecting high system heterogeneity. Lower bulk densities in organic SFT are associated to higher saturated hydraulic conductivities (K_s), infiltration capacities and OM contents, conditioning a less compact structure which enhances water transmissivity capacities. TDNP peats show extremely high K_s values [$(2.2. \pm 0.9)\cdot10^4$ cm d^{-1}] due to secondary porosity and swelling capacity. Average infiltration capacities in dry SFT range between 159 cm d^{-1} in clay to over 2,000 cm d^{-1} in peat, with all organic materials exceeding 1,000 cm d^{-1}. Only two organic SFT (peat and edapizhed charophytes) show soil water repellency conditioned by amount and type of OM, soil water content and drying conditions. Peats develop extreme soil water repellency after oven-drying at 105 °C, a laboratory condition not far from reality given the high topsoil temperatures observed in the field. A threshold 45% OM content and 9-22 vol% critical soil water content range have been defined for soil water repellency development in TDNP peats.

Desiccation decreases peat total porosity making it shrink and giving rise to cracks and hollows which constitute preferential flow paths for both air and infiltrating waters. High soil temperatures and low water contents promote exponential increase in cracks and hollows number, dimension and extension in short time (i.e. less than one year), reaching up to half meter wide and two meters deep. Soil water content and organic fraction are the main controlling properties for smouldering fires ignition and spread. Fire irreversibly modifies soil physical properties, increasing the risk of solute mobilisation and, thus, groundwater pollution.

During drying periods, the combination of large SW and soil nutrient contents with high water transmissivity capacities in the VZ of the left TDNP margin where higher degree of SW-GW interactions have been observed, conditions groundwater pollution. Anthropic management (soil compacting by heavy machinery, recirculation of low quality groundwater, reed reaping, water transfers or smouldering fire extinction) increases the risk of releasing stored nutrients. As organic soils are widespread in the left TDNP margin area, it is likely that increased SW-GW interactions in this area are enhanced by soil physical degradation. Preferential flow paths through peat cracks and

hollows in S and SE areas constitute freeways for water and solute transport. Fluvial silts in ditches, which store large amounts of nutrients and OM, as well as low permeability Tertiary levels, hold perched poor-quality groundwater levels connected to deeper layers.

The closing effect of the dams and the functioning of the system as an artificial recharge pond causes that the overall effect of management measures during drying periods is solute accumulation in the VZ. Besides this, the extent of SW-GW interactions condition a higher risk that groundwater pollution is spread through the groundwater flow that percolates from TDNP to deeper aquifer layers and meets the regional flow towards pumping irrigation areas.

Increased understanding of the TDNP physical-chemical environment has allowed for the development of tools to support Park management during a system dry out. The classification and mapping of SFT involves an enhancement of current knowledge of the physical environment and will contribute to management actions planning. It has allowed to delimit areas showing homogeneous behaviour and, thus, modelling time as well as monitoring systems expenses can be optimized.

VZ water flow simulations under different climatic and management scenarios can, for example, help to foresee the development of soil moisture conditions suitable for reed overgrowth (36-51 vol% in charophytes and 21-30 vol% in peat) and peat combustion risk (below 23 vol%). This way, management actions could be less dependent on improvisation and their impact to the physical system minimized. Modelling can be complemented with a monitoring network of soil moisture and temperature sensors at different depths. With these sensors underground cracks and hollows development or surface water inflows arrival could be detected and monitored in real time.

The huge amount of compiled data on soil and water physical-chemical properties is in itself a valuable management tool. Qualitative and quantitative characteristics of

drying processes in the Park can be used as input data for different eco-hydrological modelling approaches suitable for managing needs.

To summarize, the two main objectives previously mentioned have been successfully achieved through an integrated methodological approach of VZ and SW-GW study tackling with system complexity, heterogeneity and lack of geological and hydrogeological knowledge.

In order to build more accurate flux and transport hydrological models further research on local geological characteristics (i.e. geophysical studies) and hydrological and hydrochemical dynamics in flooding periods is still required. Besides this recommendation, there is still a need to quantify impacts influence and degree of disturbance on soil and water physical-chemical properties. Also the knowledge of shrinking characteristics and piping development in Mediterranean semiarid peatlands should be improved.

Hopefully, the information provided in this research will contribute to support and enhance management actions in Las Tablas de Daimiel National Park.

Resumen

Introducción

La zona húmeda semiárida del Parque Nacional de Las Tablas de Daimiel (TDNP) se encuentra situada en el centro de la Península Ibérica. La posición geográfica junto con la particular mezcla de aguas de diferente calidad confiere al TDNP una relevancia especial entre las zonas húmedas europeas como refugio para especies singulares de aves y plantas acuáticas. Este ecosistema ligado a su vez a la dinámica de las aguas subterráneas (antigua zona de descarga), fue reconocido como Reserva de la Biosfera por la UNESCO e incluido en el Convenio Ramsar como Humedal de Importancia Internacional.

El enorme grado de intervención y alteración humana desde la década de 1960 ha llevado a la completa desnaturalización del sistema (canalizaciones, represamientos, contaminación, drenajes e inundaciones artificiales, etc.). El bombeo excesivo de agua subterránea para regadío en la Llanura Manchega junto con la variabilidad climática inherente a los ambientes mediterráneos semiáridos, han sido los condicionantes principales de la desconexión del humedal del sistema acuífero y de que en la actualidad en el TDNP se sucedan ciclos alternos de inundación-desecación. Este proceso induce impactos y modificaciones severas sobre las características ecológicas, tanto bióticas como abióticas, del humedal. Desde del punto de vista hidrogeológico, se ha producido una inversión del gradiente hidráulico de vertical ascendente a vertical descendente, con lo que el TDNP se ha convertido en una zona de recarga. El exponente más llamativo de la degradación y desecación sobre la estructura físico-química del TDNP es el proceso de agrietamiento, subsidencia e incendio de las turbas del Parque.

La gestión artificial enfocada al mantenimiento de condiciones encharcadas ha contribuido también a la alteración y degradación del sistema, convirtiendo el humedal en un sistema regulado de embalses conectados en serie que opera como un sistema de recarga artificial mantenido a través de trasvases y bombeo de aguas subterráneas. Una de las principales limitaciones que ha impedido una gestión más adecuada del TDNP ha sido la falta de un conocimiento preciso de los ambientes físico e hidrológico, especialmente bajo la superficie del humedal.

Objetivos

La motivación fundamental de esta investigación ha sido la de intentar entender el comportamiento del sistema suelo-agua del TDNP durante periodos de desecación. Los dos objetivos principales han sido:

- La caracterización físico-química con base hidrológica del sistema suelo-agua.
- El análisis de las implicaciones ambientales y de gestión y el desarrollo de herramientas de apoyo a la gestión hidro-ambiental del TDNP.

Metodología

Para poder enfrentarse a la gran complejidad y heterogeneidad del sistema y a la ausencia de un conocimiento geológico e hidrogeológico detallado, se ha utilizado un enfoque metodológico integrado. El sistema subsuperficial se ha abordado a través de determinaciones y análisis físicos y químicos de la zona no saturada (VZ). La química del suelo se ha estudiado con herramientas de estadística descriptiva y análisis multivariante (análisis de componentes principales y análisis de redundancia) sobre muestras de la matriz sólida y extractos suelo-agua 1:5. Un intensivo trabajo de campo y de laboratorio ha permitido determinar varios parámetros físicos de los diferentes suelos del TDNP: textura, densidad aparente, conductividad hidráulica saturada, curvas de infiltración, repelencia al agua, tasa de humectación capilar, y curvas de retención y conductividad hidráulica. Se prestado especial atención a las características de

degradación de la turba causadas por la desecación: hidrofobicidad, propiedades de contracción y agrietamiento, y riesgo de combustión y mecanismos de propagación.

La caracterización físico-química de la VZ ha permitido la definición y elaboración de un mapa de tipos funcionales de suelo (SFT) en base a sus propiedades hidráulicas como almacenes y transmisores de agua y solutos. Además, usando los datos medidos y estimados, se han calibrado y validado satisfactoriamente modelos unidimensionales de flujo de agua en VZ en distintos perfiles tipo representativos de la disposición en profundidad de SFT en el TDNP.

La interrelación entre aguas superficiales (SW) y aguas subterráneas (GW) se ha inferido a través de un enfoque metodológico sencillo combinando datos hidroquímicos, hidrodinámicos e isotópicos elementales tomados de una red de puntos de muestreo, a través de técnicas de análisis cluster y análisis de series temporales. A partir de este estudio se propone un modelo conceptual de funcionamiento hidrológico del TDNP basado en la interrelación entre superficie inundada, nivel de agua subterránea e hidroquímica, que tiene en cuenta consideraciones tanto espaciales como temporales en las interacciones SW-GW.

Las implicaciones ambientales y de gestión derivadas de la caracterización físico-química del suelo y el agua en el entorno del TDNP se han abordado desde el punto de vista de la disponibilidad hídrica y el riesgo de contaminación de las aguas subterráneas. Se han determinado los contenidos de humedad críticos para el desarrollo de hidrofobicidad en el suelo, la expansión de carrizo (*Phragmites australis*) y el riesgo de combustión de turba. Además, se ha evaluado la utilidad de los modelos de flujo en VZ como herramienta de gestión para simular la evolución de la humedad del suelo y el desarrollo de los contenidos de humedad críticos bajo un escenario de desecación.

Resultados

Se han identificado ocho SFT en base a sus propiedades físicas y químicas atendiendo a los diferentes grados de evolución, antropización y edafización. Los tipos definidos están englobados dentro de cuatro materiales principales: capas de caráceas (sedimentos carbonatados no consolidados de origen biológico), arcilla, limo fluvial (depósitos fluviales en ríos, zanjones y drenes) y orgánico (elevado contenido en materia orgánica). Se ha elaborado a su vez un mapa de la distribución espacial media de estos SFT en el interior del TDNP en base a la información proporcionada por más de 120 perfiles de suelo muestreados en el entorno del Parque.

Los resultados de los análisis químicos tanto de la VZ como de SW-GW indican que durante los periodos de desecación el TDNP se transforma en un ambiente altamente salino y eutrofizado. La mediana de la conductividad eléctrica (EC) en los extractos suelo-agua de muestras de suelo en profundidad es 3,280 $\mu S\ cm^{-1}$ y la mediana del contenido en materia orgánica (OM) de la matriz sólida del 5.33%. Las medianas de EC en SW varían entre 2,973 y 11,739 $\mu S\ cm^{-1}$, y en GW entre 677 y 15,383 $\mu S\ cm^{-1}$. La mediana de carbono orgánico total en algunos puntos de agua subterránea alcanza valores superiores a 9 $mg\ l^{-1}$. Sin embargo, la química del sistema conjunto suelo-agua muestra una elevada variabilidad condicionada por la litología, evaporación, vegetación, microtopografía, degradación del suelo y antropización (ej. presas, bombeos, zanjones, trasvases y entrada de aguas residuales).

Las propiedades físicas de los SFT muestran una gran variabilidad que refleja la heterogeneidad del sistema. Los SFT orgánicos presentan bajas densidades aparentes asociadas a mayores conductividades hidráulicas saturadas (K_s), capacidades de infiltración y contenidos en OM, lo que condiciona una estructura menos compacta que incrementa la capacidad de transmisión de agua. Las turbas del TDNP muestran valores extremos de K_s ($22{,}161.3 \pm 9{,}008.9\ cm\ d^{-1}$) debido a la porosidad secundaria y la capacidad de hinchamiento. Las capacidades de infiltración medias en SFT inicialmente secos varían entre 159 $cm\ d^{-1}$ para arcillas y 2,000 $m\ d^{-1}$ para turbas,

excediendo los 1,000 cm d^{-1} en todos los materiales orgánicos. Únicamente dos SFT (turba y caráceas edafizadas) muestran repelencia al agua condicionada por la cantidad y tipo de OM, contenido de humedad del suelo y condiciones de secado. Las turbas desarrollan una repelencia extrema tras el secado en estufa a 105 °C, condición de laboratorio que, dadas las elevadas temperaturas observadas en campo en las capas superficiales, no se aleja mucho de la realidad. Se han determinado unos umbrales de 45% de contenido en OM y 9-22 vol% de rango crítico de humedad del suelo para la aparición de repelencia al agua en las turbas del TDNP.

La desecación disminuye la porosidad total de la turba provocando su contracción y dando lugar al desarrollo de grietas y cavidades que constituyen vías de flujo preferencial para el aire y las aguas de infiltración. Las altas temperaturas del suelo unidas a bajos contenidos de humedad favorecen el crecimiento exponencial en poco tiempo (ej. menos de un año) del número, dimensión y extensión de grietas y cavidades, llegando a alcanzar medio metro de anchura y dos metros de profundidad. El contenido de humedad del suelo y la fracción orgánica son los factores principales que controlan la ignición y expansión de los incendios latentes. La combustión modifica las propiedades físicas del suelo de forma irreversible, aumentando el riesgo de movilización de solutos y, por tanto, de contaminación del agua subterránea.

Conclusiones

La combinación de altas concentraciones de nutrientes en el SW y en el suelo con elevadas capacidades transmisivas en la VZ de la margen izquierda del TDNP, donde se han observado los mayores grados de relaciones SW-GW, condiciona la contaminación del agua subterránea. La gestión antrópica (compactación del suelo por maquinaria pesada, recirculación de agua subterránea de baja calidad, siega de carrizo, trasvases, labores de extinción de incendios latentes) incrementa el riesgo de liberación de los nutrientes almacenados. Dado que además los suelos orgánicos se encuentran muy extendidos en la margen izquierda del TDNP, es muy posible que el alto grado de relación SW-GW en esta zona se vea favorecido por la degradación física de estos

suelos. Las vías de flujo preferencial a través de las grietas y cavidades de las turbas del área S y SE constituyen autopistas para el transporte de agua y solutos. Tanto los limos fluviales que rellenan los zanjones, los cuales acumulan grandes cantidades de nutrientes y OM, como ciertos niveles Terciarios de baja permeabilidad, provocan la aparición de niveles colgados conectados a capas acuíferas más profundas que almacenan agua subterránea de baja calidad.

El cierre a través de las presas y el funcionamiento del sistema como embalse de recarga artificial origina que el resultado global de las medidas de gestión del TDNP durante periodos de desecación sea la acumulación de solutos en la VZ. Aparte de esto, el nivel de relaciones SW-GW condiciona un mayor riesgo de que la contaminación del agua subterránea se extienda hacia capas acuíferas más profundas a través del flujo que percola desde el TDNP y enlaza con el flujo regional hacia las zonas de bombeo para regadío.

El aumento del conocimiento del sistema físico-químico del TDNP ha permitido el desarrollo de herramientas de apoyo a la gestión del Parque durante un episodio de desecación. Por un lado, la clasificación y mapa de SFT implica una mejora del conocimiento del medio físico y servirá de apoyo a la toma de decisiones. La delimitación de áreas de comportamiento más homogéneo redundará en una optimización del tiempo de modelización y gastos en sistemas de monitorización.

Las simulaciones de flujo de agua en VZ bajo diferentes escenarios climáticos y de gestión pueden contribuir, por ejemplo, a predecir el desarrollo de condiciones de humedad del suelo favorables a la expansión del carrizo (36-51 vol% en caráceas y 21-30 vol% en turba) y al riesgo de combustión de la turba (humedad inferior a 23 vol%). De este modo, se podría minimizar el grado de improvisación y el impacto sobre el sistema físico de las medidas de gestión. La modelización se puede complementar con una red de sensores de humedad y temperatura del suelo a diferentes profundidades. Con la ayuda de estos sensores se podría detectar y monitorizar en tiempo real el desarrollo de grietas y cavidades o la llegada de aportes externos de agua.

La enorme cantidad recopilada de datos de propiedades físico-químicas del suelo y el agua implica en sí misma una valiosa herramienta potencial de gestión. Las características cualitativas y cuantitativas de los procesos de desecación del Parque pueden ser usadas como datos de entrada para diferentes modelos eco-hidrológicos adecuados a las necesidades de gestión.

En resumen, se han cumplido los dos objetivos principales mencionados al principio a través de un enfoque metodológico integrado de estudio de zona no saturada y aguas superficiales-aguas subterráneas capaz de abordar la complejidad, heterogeneidad y falta de conocimiento geológico e hidrogeológico del sistema.

Recomendaciones

Para poder elaborar modelos hidrológicos de flujo y transporte más precisos, es necesario profundizar en el conocimiento de las características geológicas locales (ej. estudios geofísicos) y de la dinámica hidrológica e hidroquímica durante los periodos de inundación. Aparte de esta recomendación, también es preciso cuantificar la influencia y grado de alteración de los impactos sobre las propiedades físico-químicas del suelo y el agua. El conocimiento de las propiedades de contracción y los mecanismos de desarrollo del sistema de grietas en zonas de turberas mediterráneas semiáridas debería, a su vez, mejorarse.

Con todo, se espera que la información aportada por esta investigación sirva de apoyo y mejora para la gestión del Parque Nacional de Las Tablas de Daimiel.

List of contents

List of figures

List of tables

List of pictures

Abbreviations and symbols

(appearing more than once)

Abbreviations

ANOVA: one-way analysis of variance

BD: bulk density

CEDEX: Centre for Study and Experimentation of Public Works

CSIC: Spanish Council for Scientific Research

CV: coefficient of variation

EC: electrical conductivity

ET_p: potential evapotranspiration

ET_{ref}: reference evapotranspiration

FAO: Food and Agriculture Organization

GW: groundwater

HRP: Hydrological Restoration Plan

IGME: Geological Survey of Spain

IW: incoming water

LOI: loss on ignition

LSD: least significance difference

MARM: Ministry of Rural and Marine Environment

OC: organic carbon

OM: organic matter

PCA: principal component analysis

RDA: redundancy analysis

REGATA: Gradual Restoration Plan of Las Tablas

RMSE: root mean squared error

SFT: soil functional types

SW: surface water

SWAP: Soil-Water-Atmosphere-Plant model

SWR: soil water repellency

TDNP: Tablas de Daimiel National Park

TOC: total organic carbon

TSA: trend surface analysis

TU: tritium units

VZ: vadose zone

WDPT: water drop penetration time

Symbols

$\theta(h)$: volumetric soil water content (cm^3 cm^{-3}) as function of of soil water pressure head h (cm)

α: empirical shape factor in the Mualem-van Genuchten soil hydraulic functions (cm^{-1})

ϑ_0: moisture ratio at the transition of the near-normal shrinkage stage to the subnormal shrinkage stage in the peat shrinkage curve (cm^3 cm^{-3})

θ_r: residual soil water content (cm^3 cm^{-3})

ϑ_s: moisture ratio (moisture volume to solid phase volume) at saturation in the peat shrinkage curve (cm^3 cm^{-3})

θ_s: saturated soil water content (cm^3 cm^{-3})

e_0: void ratio (pore volume to solid phase) at moisture ratio equal to 0 in the peat shrinkage curve (cm^3 cm^{-3})

f_c: final infiltration capacities of soil materials (cm d^{-1})

G: groundwater monitoring point

H: soil moisture sensor

h_e: minimum capillary height as a cut-off point for air-entry value in the soil hydraulic functions (cm)

$K(h)$: unsaturated hydraulic conductivity (cm d^{-1}) as function of soil water pressure head h (cm)

K_c: crop factor

K_s: saturated hydraulic conductivity (cm d^{-1})

K_{soil}: soil factor

L: empirical shape coefficient for the hydraulic conductivity function (dimensionless)

n: empirical shape factor in the Mualem-van Genuchten soil hydraulic functions (dimensionless)

P: soil profile

S: surface water monitoring point

T: soil temperature sensor

CHAPTER 1

General introduction and motivation

Springtime in 2013. The wetland area of Las Tablas de Daimiel National Park (TDNP), located in the Mancha Plain in central Iberian Peninsula, remains fully flooded (Pic. 1.1). Around 2,000 ha flooded through water inputs from Azuer and Cigüela rivers as well as several northern creeks.

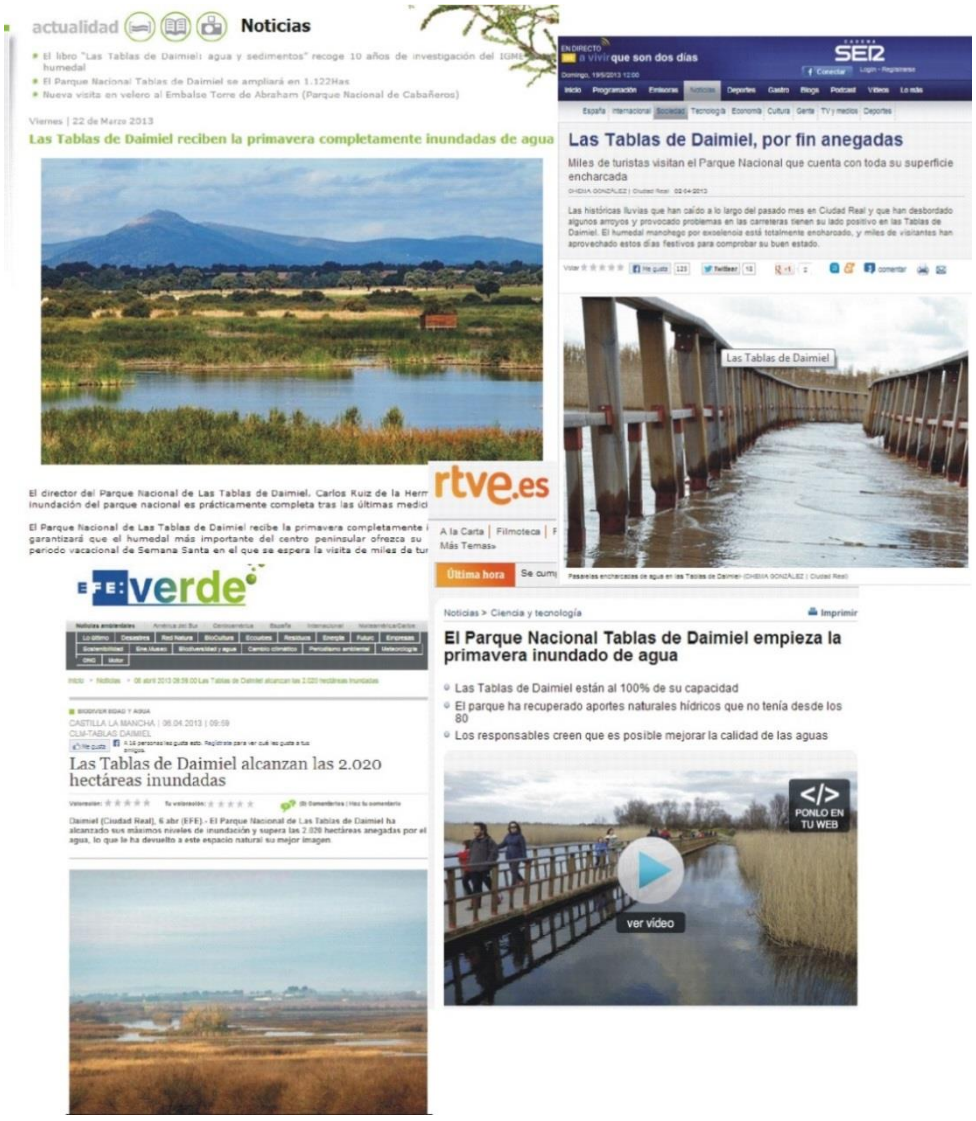

Picture 1.1. Press news emphasizing the extraordinary flooding conditions in Las Tablas de Daimiel National Park (TDNP) at the beginning of spring in 2013.

By the end of 2012, groundwater discharges (real groundwater!) were observed in the Guadiana riverbed just 6 km away from the Park limit. These were flowing like a river

towards TDNP at approximately 200 litres per second. In 2011, non-flowing groundwater reaching the surface in the valley of the former Guadiana River was visible until the summer. Hope. Euphoria. “Let’s get the irrigation pumps ready”, some say. “Caution”, others say; a riverside generation has grown by a wetland in a coma which has briefly revived several times to end up relapsing again.

The present moment constitutes a clear proof of system’s dynamism which, without anthropic impact, tends to go back to its origins in a natural way. But that seems difficult to happen nowadays when mankind’s footprint on Earth has reached such magnitude that it could be depicted as a huge hand playing basketball with the bluish ball…

If the current favourable situation lasts for two or three more years, many could forget about the weak environmental and hydrologic equilibrium of this Mediterranean area, and that it in 2009 the whole National Park was completely dry. Groundwater and pumps are great contributors for this fragility. In 2009 managers were even struggling against smouldering soil combustion inside TDNP. The human being has a poor memory and soon memories start vanishing like “tears in rain”, as the replicant explains Harrison Ford at the end of the futurist film Blade Runner, by director Ridley Scott.

In the same way as it has been forgotten that until just 200 years ago it was common that countrymen would make mass pleadings for rain, either for it to start or cease (“agua por San Juan, quita vino, aceite y pan” popular proverb that can be translated as “water for Saint John, takes away wine, oil and bread”), as registered by ecclesiastic archives. Going further back in time, fortified structures to protect wells locally known as “motillas”, which were also flooded during wet periods, reflect the importance of water in the Mancha Plain in Bronze Age. Here we have to make use of archaeology.

During all these times, and even before, terrain and vegetation have been part of the wetland. The terrain, as the basis supporting water and living beings, has also

developed and evolved together with the wetland. This is registered in a storage "written in rock" that can be read with geology and palaeontology. Through their tools and interpretations several researches carried out by the Geological Survey of Spain (IGME) and other organizations have come to the conclusion that Las Tablas, the most emblematic wetland in La Mancha and its environmental health representative, has suffered, all through its history, extraordinary floodings and freshets and complete dry outs, as well as changes in morphology and location.

The water loss situation differs noticeably of what books and leaflets tell ("Las Tablas de Daimiel is the last representative of an ecosystem known as fluvial tablas that developed due to overflowing of Cigüela and Guadiana Riversin their confluence, supported by the limited slope…The mix of saline (Cigüela) and freshwaters (Guadiana) provides singular conditions allowing for the existence of a unique diversity of plant species…)". At the same time, this situation conditions different modifying processes as those taking place in wetland areas permanently flooded.

The hydrologic drought situation in the last decades in TDNP has been motivated, however, by human action, or, rather, by technology and human economies. Because of them there have been long periods where the wetland has been dry or almost dry since the 1980s. This gave the chance to know, not only theoretically, system's behaviour under these circumstances and how it could affect the wetland and its environment. This motivated IGME, together with other partner institutions in climate and sedimentology researches in Las Tablas, to perform specific studies on the water transit area from the visible surface zone to that other important invisible zone belowground where exploitable groundwater accumulates. And here I come.

Chance or nature made possible that during most of the sampling and fieldwork period for the thesis a strong drought leading to complete emptying of Las Tablas facilitated in situ works and tests. Also chance or nature wanted that the last year of fieldworks was the beginning of a wet period that still remains at present, and that allowed for an analogue of system's behaviour following extreme freshets under dry conditions.

Much is known so far, mainly due to the studies performed by a group of ecologists from the Spanish Council for Scientific Research (CSIC), about the ecosystem and how it functions when flooded. And also about the changes that have taken place in the surface environment after its degradation. However, little is known regarding system's properties when it dries out, a moment when huge disturbances of the physical environment take place conditioned by the development of a unsaturated zone between the surface and the groundwater level. Soil physical-chemical processes derived from desiccation have devastating consequences on the hydrologic resource, both in amount as well as in quality. During those periods, the desperate fight of managers, conservationist institutions and scientific community against water loss, reed invasion, subsidence, cracking and peat combustion, turns grey and, to great extent, lonely.

TDNP management in dry periods is continuously overwhelmed by environmental alterations. Reed stands overgrow and invade former flooded areas, water derived to the Park from water transfers or emergency wells infiltrates and evaporates very fast, the soil starts shrinking, cracking and subsiding in peat areas, underground fires take place, etc. Urgent management measures are constantly applied trying to alleviate continuous setbacks. Nevertheless, as it is usual in these cases, the complex rate of the administrative machinery is overwhelmed by the speed of degradation. Furthermore, the lack of scientific knowledge of the subsurface environment hinders suitable planning and decision making against situations on many occasions. This fact conditions failure of adopted measures and the need to resort to trial-and-error with subsequent loss of time and resources.

The work presented here is intended as a novel contribution for the knowledge of the Park, as little or none was known so far about the hydraulic behaviour of the underlying sediments from the first centimetres from the surface. Physical-chemical characteristics of these materials determine the hydrologic functioning of the system during drying periods. The decrease in groundwater levels due to water demands in dry times conditions hydraulic gradient inversion and the disconnection of a multi-

layer aquifer system in which flux in the upper levels is predominantly vertical downwards through a vadose zone constituted by the Quaternary sediments of fluvial and marshy-lacustrine origin filling the Park. In this environment, edaphic processes of organic matter accumulation and mineralization, solute accumulation and leaching, and redox as well as decarbonation reactions, happen at high speed.

An intensive work of soil and water physical and chemical characterization in TDNP has been carried out. Special attention has been give to peat, one of the most dynamic elements when the system dries out. The surface water-soil-groundwater integration approach used becomes fundamental for such a complex system as TDNP in which previous hydrologic studies have always had a partial character.

Perhaps I drew the short straw in the sense of having to spend hours, days and weeks of sampling in an arid desolated landscape, scorching on many occasions (Pic. 1.2). But this is far from reality. I am pleased of contributing with this work to the knowledge of the least idyllic but most relevant environment from the point of view of management and environmental implications. Along the lengthy journey of this thesis, besides the classic mood bipolarities inherent to a work of such intensity and characteristics, of learning and learning to relearn, of drifting out and then finding the track again or finding a different one, I have found out the great importance of a tough and poorly gratifying environment such as the soil, far from current research panaceas (medicine, neuroscience, new materials or aerospace), but which constitutes, without a doubt, the engine for the biogeochemical and hydrological processes that support life on solid earth and, thus, us.

The only medicine capable of healing the Park completely has been known for a long time and no alternative magic formula or miraculous elixir have been sought in this study. Water is life, even more for TDNP, and the only way to cure the disease is letting the aquifer bottle to be filled up to the brim. This thesis aims to become part of the foundation for building up the knowledge of the hydrologic behaviour of TDNP during

its lowest moments when dry and degraded is left alone and the Park management team tries to relieve the patient's agony.

Picture 1.2. Field work in an extensive dry area of Las Tablas de Daimiel National Park (TDNP) during the warm summer season in 2008.

The question may arise: can the work carried out be of use in a situation like the present one where saturation predominates or in the future? As stated at the beginning of this motivation, humans have a weak memory and tend to forget most features of the past easily. Nevertheless, they can rely on written testimonies or interpretations based on research of natural and artificial remains to understand what has happened before. For now, humans only have a blur picture of the future in their imagination. Although numerical predictions are constantly improved, still they often fail (economical models, for example) due to the human factor. And I am human. I only expect this work will contribute to enhance our general knowledge of the environment and of the particular area of the world where it focuses, and that it can help to improve management in such a needy environment.

CHAPTER 2

Background

2.1. Ecological and environmental significance of semiarid wetlands. Human degradation. Water: the limiting factor

This section illustrates the relevance of wetland ecosystems and their vulnerability, particularly in Mediterranean regions such as central Spain. This outlines the need for the development of suitable management strategies based on rigorous scientific research.

The interest for wetlands conservation worldwide has experienced an important growth due in part to the recognition of their high ecological and environmental value (Mitsch and Gosselink, 2000). Wetlands constitute extraordinary refuges for biodiversity of both plants and animals, and also play an essential role in hydrological and biogeochemical cycles by regulating both river flows and the fate of sediments and nutrients (Phillips, 1989). Actually, they perform a fundamental ecological-economical function as natural water filters and buffers, by storing nutrients and carbon in their sediments (van der Peijl et al., 2002; Pfadenhauer and Klötzli, 1996; Reddy and DeLaune, 2008; Bohn et al., 2001; Phillips, 1989; Mitsch and Gosselink, 2000; Mitsch et al., 2005), and decreasing surface runoff peaks during storm events (Kazezyılmaz-Alhan et al., 2007). The functionality of these ecosystems provides goods and services of environmental, economic and social interest. In fact this type of ecosystem is the most valuable from the environmental services produced point of view (Costanza et al., 1997). However, equilibrium in wetland ecosystems is very fragile, showing high sensibility and vulnerability as they are exposed to impacts that are not always evident or reversible (Johnston, 1994; Pfadenhauer and Klötzli, 1996; Manzano et al., 2002; Niedermeier and Robinson, 2007; Boswell and Olyphant, 2007; Aguilera et al., 2011; Rodríguez-Rodríguez, 2007; Rodríguez-Rodríguez and Benavente, 2008). Their progressive disappearance is a problem of major concern worldwide (Mitsch and Gosselink, 2000; Zedler and Kercher, 2005; Biggs et al., 2005; Kingsford, 2000; Moiwo et al., 2010; Rudolph et al., 2006; Biebighauser, 2007; Gerakis and Kalburtji, 1998; Harvey and McCormick, 2009; Rodríguez-Rodríguez and Benavente, 2008).

Wetlands linked to groundwater dynamics suffer from an added weakness due to their dependency on groundwater levels which, in turn, depend on aquifers' management, especially in regions under Mediterranean semiarid climates (Acreman and Miller, 2006; Jolly et al., 2008; Moiwo et al., 2010; Patten et al., 2008; Rodríguez-Rodríguez et al., 2007; Wolski and Savenije 2006). Some of the most important wetlands of the world such as the Okavango Delta (Botswana), the Kafue Flats (Zambia), the Hadejia-Jamaare (Nigeria), the Prairie Potholes (North America), the lower River Murray wetlands (Australia), and Doñana (Spain), are located in arid-semiarid areas. However, they have received little attention compared to humid continental and tropical regions (Álvarez-Cobelas et al., 2005; Gerakis and Kalburtji, 1998; Jolly et al., 2008; Zhao et al., 2009). Wetland areas in semiarid Mediterranean regions are generally quite accessible and fragile and therefore an easy target for human alteration (Gerakis and Kalburtji, 1998; Manzano et al., 2002; Martínez-Santos et al., 2008a; Rodríguez-Rodríguez, 2007; Rodríguez-Rodríguez and Benavente, 2008).

The combination of water scarcity and irregular climate conditions on highly sensitive hydrological balances increases the risk of modification. In Mediterranean semiarid climates water scarcity, usually induced by droughts and high demands, becomes an essential socio-political and economical issue which is aggravated under climate change scenarios where increased aridity is predicted (MED WS&D WG, 2007; Abouabdillah et al., 2010; Gao and Giorgi, 2008). In this context, often less attention is paid to wetlands and as water becomes a limited resource, unequally distributed in space and time and widely exploited, the risks and impacts on them increase. Eutrophication, development of invasive species, biodiversity loss, accelerated oxidation of soil organic matter and CO_2 release, solute mobilization to groundwater, and smouldering peat fires constitute strong degradation processes that take place as wetlands dry out. Wetlands lose their ecological function and the negative consequences of these processes are extrapolated to other natural and socio-economic systems (Costanza et al., 1997; Zedler and Kercher, 2005). However, unsuitable management of Mediterranean wetlands is more the rule than the exception (Kingsford, 2000; Amezaga and Santamaria, 2000; Melendez-Pastor et al.,

2010). Therefore, the development of appropriate management tools to help sustaining these vital natural systems plays a key role for present and future decision making (Trepel et al., 2000). These management tools need to be based on accurate scientific knowledge of the hydro-ecological processes and interactions that take place in these complex ecosystems.

2.2. Las Tablas de Daimiel National Park case study: background and current situation

In this section background context on the degradation process suffered by the case study TDNP wetland area leading to its actual state is given. The review focuses on the relevant aspects from a hydrological point of view.

TDNP, located in semiarid central Spain (Fig. 2.1), constitutes an example of a human modified and regulated ex-natural wetland (Álvarez-Cobelas et al., 2001). The peculiar mix of water qualities and geographical location conferred TDNP a special relevance among European wetland areas as an ecological refuge for singular waterfowl and plant species. Therefore, various protection forms were established to preserve the wetland: National Park declaration in 1973; Special Bird Protection Area (SPA) in 1979; Biosphere Reserve by UNESCO in 1981; and was included in the Ramsar Agreement under the category of Wetlands of International Importance in 1982.

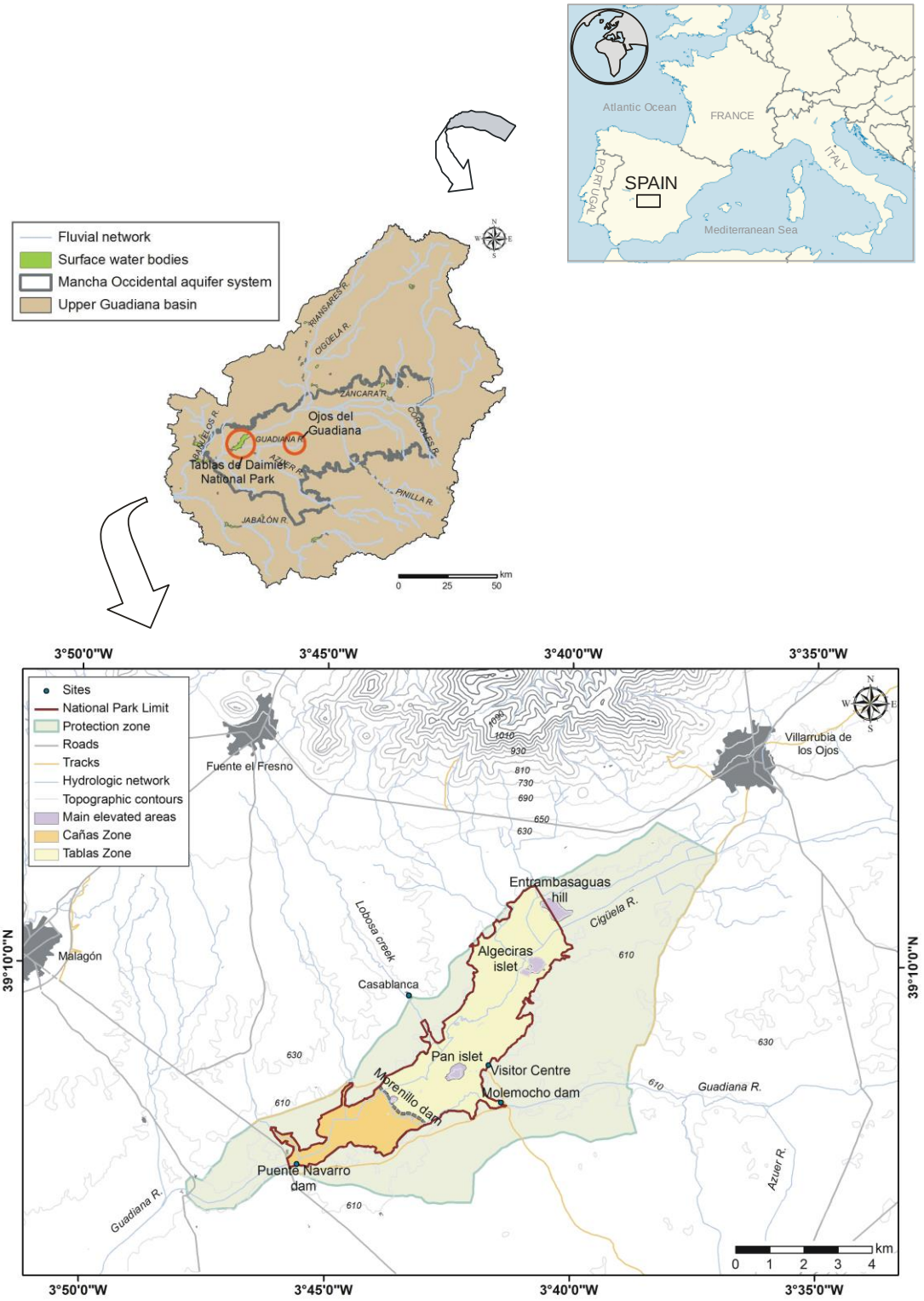

Fig. 2.1. Geographical setting of Las Tablas de Daimiel National Park (TDNP) in Spain in relation to the Upper Guadiana basin and the Mancha Occidental aquifer system. Both National Park limit and protection zone area are depicted. TDNP representative sites, main surrounding urban areas as well as hydrologic and road networks are shown. TDNP is further subdivided into two major areas upstream (Tablas zone) and downstream (Cañas zone) the central Morenillo dam. Topographic elevations are expressed in meters above sea level (masl).

The global TDNP significance has also made this wetland area the focus of scientific research in different fields in recent years: ecology (Álvarez-Cobelas and Cirujano 2007; Álvarez-Cobelas et al., 2008; Angeler et al., 2003; Angeler et al., 2010; Cirujano et al., 1996; Sánchez-Carrillo and Angeler, 2010); biology (Angeler et al., 2001; Ortega-Mayagoitia et al., 2000; Rojo et al., 2010); remote sensing (Riaza et al., 2004, 2006; Schmid et al., 2004, 2005; Koch et al., 2008, 2012); hydrochemistry (Álvarez-Cobelas et al., 2007; Berzas et al., 2000); hydrology (Navarro et al., 2011, 2012; Castaño 2004; Castaño et al., 2008; Sánchez-Carrillo et al., 2001; Sánchez-Carrillo et al., 2004); water pollution (Aranda et al., 1993; Berzas et al., 1999; Sánchez-Carrillo and Álvarez-Cobelas 2001); soil science (Aguilera et al., 2009a,b; Aguilera et al., 2011; Rodríguez-Murillo et al., 2011), microbiological (D'Auria et al., 2010), global change (Álvarez-Cobelas et al., 2001; Domínguez-Castro et al., 2006; Domínguez-Castro et al., 2008; Dorado-Valiño et al., 2002; Gil-García et al., 2007); water management (Aldaya et al., 2010; Amezaga and Santamaría 2000; Martínez-Santos et al., 2008a), although these last ones about water management refer to the whole Mancha Occidental aquifer system. Currently, Las Tablas de Daimiel is becoming one of the most studied Mediterranean wetland ecosystems in Europe (Angeler and Sánchez-Carrillo, 2010).

The former natural wetland of TDNP was originated at the outflow boundary of two hydrological basins, a surface one, the 15,000 km^2 Upper Guadiana basin, and a groundwater one, the 5,500 km^2 Mancha Occidental aquifer system, in the confluence of the Cigüela and Guadiana Rivers (Fig. 2.1). In 1940, thirty three years before National Park declaration, the wetland area was around 150 km^2 (Álvarez-Cobelas et al., 2001), and it constituted the widest flooded area among the set of wetlands that form the La Mancha Húmeda Biosphere Reserve (8,000 km^2) within the Upper Guadiana basin. The seasonal flooding pattern was a mixture of oligohaline inflows through the Cigüela River (Álvarez-Cobelas et al., 2000) and carbonated groundwater discharge through the so-called "Ojos" and "Ojillos" to the Guadiana River. In winter and spring Cigüela inflows were dominant, whereas during summer and the beginning of autumn groundwater discharge through the Guadiana River predominated (Álvarez-Cobelas et al., 2001).

Until the 1970s the wetland area represented an integrated model of human-nature interrelation where over 300 families lived from fish and crab fishing (Álvarez-Cobelas et al., 2000). Furthermore, the wetland's flooded area was also maintained by human buildings, such as small water-mill dams which helped to retain water inside TDNP. Fifteen water-mill dams have been identified along the Cigüela and Guadiana Rivers (Álvarez-Cobelas et al., 1996). Thus, the waterscape of TDNP appeared as the result of both natural flooding and human-induced inundation in an area where rainfall is scarce (Álvarez-Cobelas and Cirujano, 1996). Nowadays, none of these water-mills are functional and only the Molemocho one has been reconstructed for exhibition purposes (Sánchez-Carrillo et al., 2010).

However, conservation measures have not been able to stop the increasing anthropogenic degradation and desiccation since the 1960s (Martínez-Santos et al., 2008a). Since then, human impacts and interventions such as pollution, overexploitation of groundwater resources, artificial drainages, ditching of riverbeds, building of dams for surface water regulation, and artificial flooding through water transfers or low quality groundwater, have disturbed the near-natural behavior of the system. Besides this, the fact that the wetland is located at the outflow edge of the Upper Guadiana basin (both surface water and groundwater) has to be taken into account, as any impact on the hydrological environment of the basin affects the wetland either directly or indirectly (wastewater, spills, etc). As a consequence, major ecological disturbances such as biodiversity loss, expansion of invasive species such as reed (*Phragmites australis*) (Álvarez-Cobelas et al., 2001), eutrophication (Sánchez-Carrillo and Álvarez-Cobelas, 2001) and peat fires (Moreno et al., 2010), have taken place, becoming indicators of this human degradation (Pic. 2.1).

Picture 2.1. Indicators of human degradation of Las Tablas de Daimiel National Park (TDNP): eutrophication, reed (*Phragmites australis*) invasion and smouldering peat fires.

TDNP was one of the last representatives of Mediterranean wetland areas linked to groundwater dynamics (Álvarez-Cobelas et al., 2001; Castaño et al., 2008; García Rodríguez, 1996; González Monterrubio, 1992; Llamas, 1988). TDNP used to be the discharge area for the aquifer, but the depletion of groundwater levels due to intensive pumping for irrigation all through the Mancha Plain caused an inversion of the hydraulic gradient from upward to downward. Hence, TDNP turned into a recharge area as the regional groundwater flow shifted from westerly to easterly (Llamas, 1988). The TDNP disease became chronic in 1983, when the main groundwater discharge area feeding the Guadiana River, the so-called "Ojos del Guadiana" springs, located at approximately 20 km east from the Park limits, dried out. This has led to major changes in the TDNP hydrologic system:

- Disappearance of flooded areas where no additional water inputs exist due to hydraulic gradient inversion (Llamas, 1988; Martínez-Santos et al., 2008a).
- Development of a vadose zone (VZ) during drying periods with different physical-chemical properties where leaching, redox, soil decarbonation, mineralization and solute transport processes are activated.
- Modification of the hydrochemical composition due to the substitution of natural groundwater inputs by artificial inflows of different origins such as water transfers, freshets, sewage water, and groundwater recirculation from a set of emergency pumping wells (Aguilera et al., 2011; Berzas et al., 2000).

Since the 1980s the aim of different institutions, organizations and especially Park managers has been to achieve stable surface flooding levels to be able to recover and preserve ecological, social and economical benefits of this peculiar and unique ecosystem. Within the management framework of the Hydrological Restoration Plan (HRP) developed by the consultancy EPTISA (1986), besides water transfers, three dams were built inside TDNP to retain water (Molemocho, Morenillo and Puente Navarro), and a minimum flooded area in the visitor's zone tried to be maintained by groundwater pumping from a system of wells installed inside and nearby the Park limits (Fig. 2.2). However, this plan was developed without prior assessment of all the relevant features of the hydrological cycle and did not take some essential aspects of wetland restoration into account: water quality, hydrological balance, and, most importantly, a thorough follow-up monitoring to evaluate its success (Cirujano et al., 2010; Sánchez-Carrillo et al., 2004). In fact, measures have often been undertaken as emergency patches more than based on a thorough knowledge of the system and, consequently, have had limited efficiency (Sánchez-Carrillo and Álvarez-Cobelas, 2010). As outlined by Sánchez-Carrillo et al. (2004), from an ecological viewpoint, these measures were unsatisfactory and brought no significant functional or structural improvements to the area. Actually, increased knowledge on the local wetland hydrology is still seen as a main research priority nowadays (Angeler and Sánchez-Carrillo, 2010).

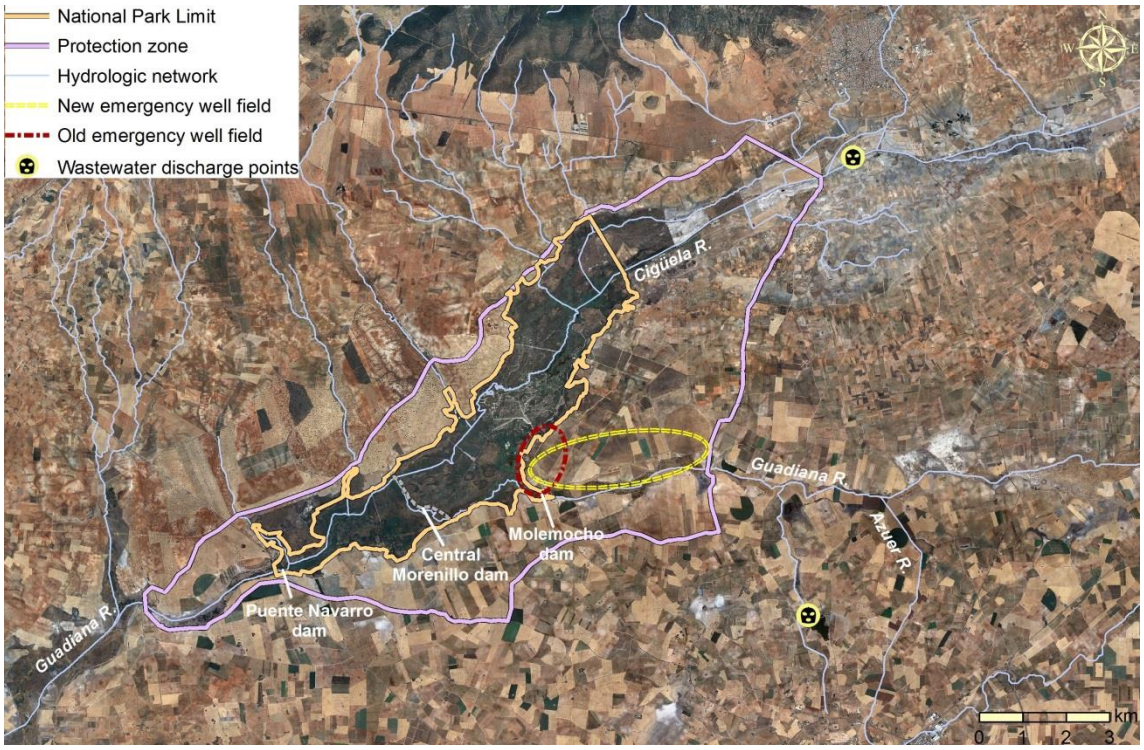

Fig. 2.2. Orthophoto of the TDNP area showing agricultural lands within the Protection zone and surrounding Park limits, particularly in the eastern and southeastern sides. Infrastructures for anthropic management built upon the 1987 Hydrological Restoration Plan (HRP) such as dams and emergency well fields are shown. The effluent discharge points to the Cigüela and Azuer rivers from Villarrubia de los Ojos and Daimiel wastewater treatment plants, respectively, are also shown.

Nowadays, TDNP has become an artificial system of connected reservoirs (Castaño, 2004) that behaves as an "artificial recharge pond" where infiltration plays a major role (Aguilera et al., 2009a,b; Angeler and Sánchez-Carrillo, 2010; Castaño et al., 2008; Martínez-Santos et al., 2008a, Navarro et al., 2011, 2012). Artificial management has turned the TDNP into what Wang et al. (2010) call an "anthropogenic wetland", completely dependent on human intervention. The water budget has substantially changed, flooding periods being shorter and more intermittent (Sánchez-Carrillo and Álvarez-Cobelas, 2010). Maximum flooding area has been reduced to less than 19 km^2 (Castaño, 2004). In all the changes, both in the unsaturated and saturated zones, water acts as the modifying factor, not only of the hydrological system but of the biotic and abiotic systems as well.

In spite of the different socio-economical and political efforts to restore TDNP (European Agro-Environmental Program UE 2078/92) by means of compensatory incomes for voluntarily cutting down on water use; acquisition of surrounding lands with pumping wells by the Public Administration since 2004 to avoid groundwater pumping; launching of the Upper Guadiana Special Plan (PEAG) in 2008, intending to recover groundwater levels by 2027, incorporating a smaller Plan to restore TDNP, the so-called REGATA (acronym for Gradual Restoration of Las Tablas), designed to act at two spatial levels, namely, that of the wetland and that of the Upper Guadiana basin, both impinging on water quantity and the quality, to guarantee enough water of good quality for the wetland), TDNP situation is far from a plausible full restoration scenario (Martínez-Santos et al., 2008a). Currently, TDNP degradation continues, mainly due to water input deficit and water quality impairment (Sánchez-Carrillo et al., 2010). In the last years (2010-2013), extraordinary flooding conditions supported by and an unusual wet period and artificial dams mean a temporary relief for TDNP situation. However, the lack of continuity between the wetland and the saturated zone makes Park recovery to its natural state quite difficult, at least on a human time scale. Furthermore, increased aridity predicted for the Mediterranean region under climate change scenarios (MED WS&D WG, 2007; Abouabdillah et al., 2010; Gao and Giorgi, 2008) will further increase the uncertainty regarding rehabilitation outcomes (Harris et al., 2006). Paying attention to wetland degradation, UNESCO has fixed a deadline in year 2015 to achieve the ecosystem restoration; otherwise it will be withdrawn from Biosphere Reserve status.

2.3. Anthropization and its consequences: main impacts

This section presents anthropization of natural systems as a global phenomenon that has to be considered more the rule rather than the exception. The Upper Guadiana basin and TDNP constitute a prefect example of anthropization. Drastic changes in the TDNP abiotic and biotic systems derived from artificial management have further

impoverished ecosystem's health and quality. Main impacts induced by management practices on TDNP, particularly on the soil hydrological system, are summarised.

At the beginning of the 21st century unsustainable development, population growth and climate change pose a serious risk not only to the survival of major ecosystems worldwide, but especially to their "natural" existence (Jia and Luo, 2009; Wang et al., 2010). Anthropization often reduces their buffering capacity through modifications of physical, chemical and biological properties which might in turn not be reversible (Cirujano et al., 2010; Hattermann et al., 2008; Johnston, 1994; Litaor et al., 2006; Mitsch and Gosselink, 2000; Pfadenhauer and Klötzli, 1996). This is particularly the case of wetland areas, where the paradigm framework of wetland restoration to a previously existing state renders more an idealistic approach than a reachable goal (Harvey and McCormick, 2009; Larsen et al., 2007; Martínez-Santos et al., 2008a; Niedermeier and Robinson, 2007; Pfadenhauer and Klötzli, 1996; Shaffer et al., 1999; Zedler, 2000; Zedler and Kercher, 2005).

Nowadays, despite the different protection attempts to preserve their ecological identity and value, anthropization of earth systems should be seen as an added intrinsic property rather than an external disturbance (Messerli et al., 2000; Moiwo et al., 2010; Sutula et al., 2003; Thiere et al., 2009). Hence, understanding "natural systems" as "disturbed natural systems" becomes a key issue in order to define appropriate management strategies to prevent wetland ecosystems from disappearing (Amezaga and Santamaría, 2000; Harvey and McCormick, 2009; Messerli et al., 2000; Wang et al., 2010). These strategies should be based on realistic conceptual hydrological models which represent current conditions of hydrological behaviour and not past natural or future desirable situations (Krause et al., 2007; Manzano et al., 2002; Pfadenhauer and Klötzli, 1996; Richter et al., 1996; Rudolph et al., 2005; Sikdar and Sahu, 2009; van Duren and Pegtel, 2000; Zedler, 2000).

The Upper Guadiana basin constitutes an excellent natural laboratory to evaluate the effects of human-related activities on wetland degradation patterns (Sánchez-Andrés

et al., 2010a). In the particular case of TDNP described in the previous section, degradation lead to a series of management interventions from the 1980s that, in turn, generated more impact than repair (Cirujano et al., 2010). As argued by these authors, in the beginning, wetlands management schemes had a narrow target focus (i.e. priority habitat for waterfowl). Therefore, the main goal was to maximize flooding area for rare and endangered bird species, without taking other wetland functions into account. Management success was evaluated only on the basis of an increase in bird populations and the occurrence of a protected species in censuses. In TDNP this was exemplified by the HRP, which pursued maintenance of suitable flooding levels for waterfowl through water transfers, groundwater pumping and dam retention.

Water transfers from the Tajo-Segura aqueduct are carried out through the channelized Cigüela River over a distance of 150 km. Derivations started in 1988 and since then they have had an average yield (percentage of volume of water arriving to TDNP) of approximately 50%, with a minimum of 3.8% in the transfer of 2009 (data provided by TDNP Managing Authorities). The underlying reason is that, due to bureaucratic issues, they have often been carried out during spring or summer when evaporation and infiltration rates are highest and when increased demands of water for irrigation promote illegal extractions. Flooding with pumped groundwater is a management tool used constantly during dry periods to keep a minimum flooded area (Pic. 2.2). Both management tools induce quantitative and qualitative impacts to the system as will be argued throughout this study.

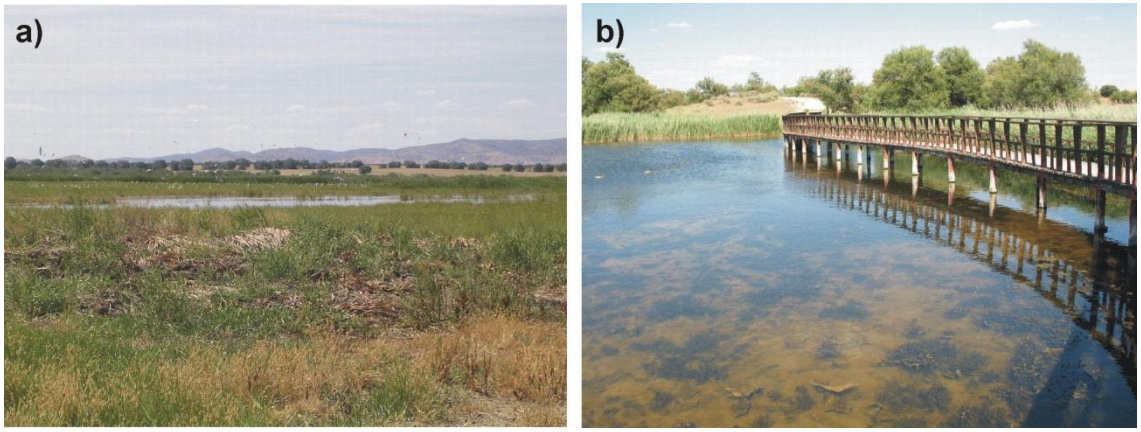

Picture 2.2. a) Limited flooding conditions in the central area of Las Tablas de Daimiel National Park (TDNP) in August 2007 after the inefficient water transfer carried out that season where only 1.5 hm^3 out of 10 hm^3 derived (Fig. 4.2); b) minimum flooding conditions in the visitor's TDNP area mantained through groundwater pumping during dry periods.

Due to unsuitable planning and quality of resources, hydrological and hydrochemical modifications have so far been the main outcome of the HRP. Given the limitation of such a narrow-focused management plan, undesired results of degradation (i.e. biodiversity loss) resulting from other forms of impacts (i.e. eutrophication) also took place. The resulting loss of food resources for birds or the increased frequency of massive bird kills through botulism outbreaks even counteracted management goals in the long term. Rather than protecting and enhancing waterfowl populations, the results were impoverishment of communities and loss of desired species (Cirujano et al., 2010).

Recently, from the mid 2000's, a management focus integrating dynamic ecosystem processes is being implemented, based upon global ecosystem studies. What matters is to restore the wetland physiognomy and to attain the maximal biological diversity, while respecting the environmental characteristics of the wetland (Cirujano et al., 2010). However, under this scope, alterations of the abiotic environment are often overlooked.

In this way, actions such as the disposal of sediment and decaying vegetation, particularly reed beds, construction of ditches and fire breaks began to be

implemented (Sánchez-Carrillo et al., 2010; Aguilera et al., 2011). These measures imply the use of heavy farm machinery inside TDNP which alters soil properties as water and solute transmitters (Pic. 2.3).

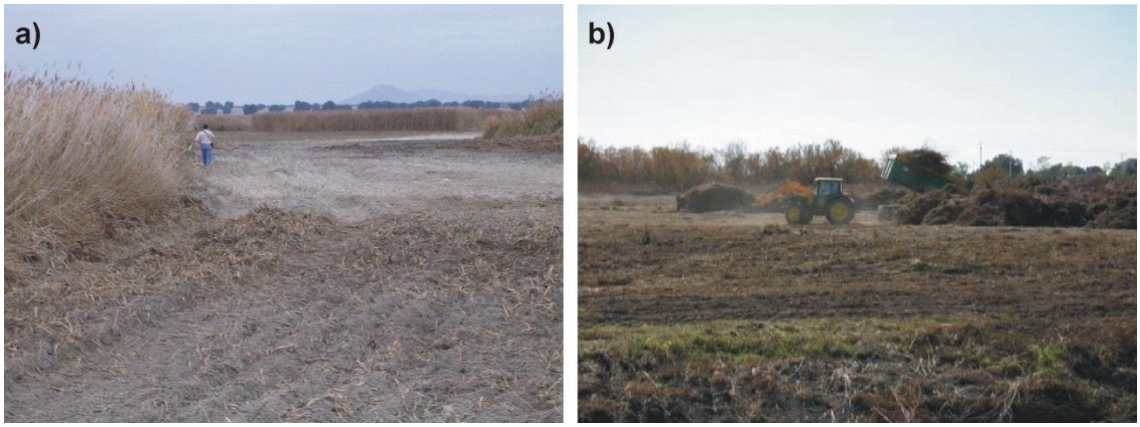

Picture 2.3. Examples of use of heavy machinery inside Las Tablas de Daimiel National Park for a) construction of fire breaks and b) reed reaping.

Anthropic water management can induce a high degree of stochasticity and uncertainty in the hydrological behaviour of the TDNP system where complexity and irregularity are enhanced (Sánchez-Carrillo and Álvarez-Cobelas, 2010; Cirujano et al., 2010; Zorrilla et al., 2010). For example, increasing variability of hydroperiods and vegetation management modify macrophyte cover patterns which, in turn, determine the evapotranspiration term of the hydrological balance (Sánchez-Carrillo et al., 2004). Far from stopping wetland degradation, management practices have increased the degree of disturbance and significantly contributed to system "denaturalization". Therefore they can be considered as indicators of anthropic impact on the weakened TDNP system.

2.4. Specific degradation effects on VZ: Peatlands and smouldering fires

The most striking representative of human-induced degradation on TDNP physical-chemical structure is the process of peat cracking, subsidence and fire. The desiccation process has modified the morphological and hydraulic properties of peats, turning them into an extremely fire vulnerable material posing a continuous threat for system's integrity during dry periods. These facts have motivated the more specific and exhaustive study of peat presented in this thesis. In the following lines, a general description of peatlands formation and smouldering fire occurrence is given.

Organic matter accumulation in percentages exceeding those of typical mineral soils gives rise to the development of humic soils. Peat or organic soils originate when this accumulation is very large and takes place under reducing conditions (Guerrero, 1985). A peatland is a complex open system associated to water depth which exchanges energy and matter with the outside. Plant debris deposited on the soil surface undergo fast mineralization with production of CO_2, NH_3, NH_4^+, NO_3^-, SO_4^{2-}, PO_4^{3-}, etc, and release of cations such as Ca^{2+}, Mg^{2+}, Na^+ and K^+ which either remain in the soil solution or are absorbed to the exchange complex. In some cases these nutrients can be taken by aquatic plants or transported by infiltrating waters.

Peatlands are the most widespread of all wetland types in the World, representing 50 to 70% of global wetlands. They cover over four million km^2 or 3% of the land and freshwater surface of the planet (Joosten and Clark, 2002). These ecosystems are supported by particular hydrological systems and are especially important for organic carbon storage (Parish et al., 2008). They hold one-third of the world's soil carbon and 10% of global freshwater resources. Their total carbon pool exceeds that of the world's forests and is comparable to that of the atmosphere (Joosten and Clark, 2002).

The existence of peatlands under Mediterranean climate is infrequent, being the necessary conditions for their development hard to find in this kind of environment

characterized by water shortage in the soil. Therefore, Mediterranean peatlands such those developed in the TDNP area are more valuable and fragile than those under wetter climates. The genesis of peat deposits in TDNP lies on the successive flooding periods supported by low salinity groundwater discharges from the Mancha Occidental aquifer (ITGE, 1988). The peatland system developed in TDNP and its surroundings during the Holocene transition from a fluvial stage to a marshy-lacustrine stage (García-Hidalgo et al., 1995) and shows an overall intermediate decomposition stage. Peat formation is conditioned by the interrelation of several factors which support the physical, chemical and biological processes required (Guerrero, 1985). These factors are: climate (as determinant factor on soil development and classification), geomorphology, lithology, vegetation, time, flooding area and water's salt content (García Rodríguez, 1996).

Smouldering fires are characterized by a combustion without flame at relatively low temperatures around 500-700 °C (Rein, 2009). The basic difference between smouldering and flaming combustion is that, in the former, the oxidation reaction and the heat release occur on the solid surface of the fuel or porous matrix and, in the latter, these occur in the gas phase surrounding the fuel (Rein, 2009). The characteristic temperature, spread rate and heat released during the smouldering combustion of a solid are low compared to those of a flaming one. Typical propagation speeds are in the range 10-30 mm h^{-1} (Rein, 2009). Furthermore, large amounts of toxic gases such as CO are produced as a consequence of low combustion temperatures. There are many porous substances constituted by the aggregation of fibers, grains or dust of combustible nature (cotton, coal, tobacco, paper, carton, peat, synthetic materials such as polyurethane, etc.).

The occurrence of smouldering fires in natural environments is quite common, particularly in coal areas, organic soil horizons and peatlands. Smouldering fires are a serious problem in coal mining exploitations and are frequently the cause for the reactivation of apparently extinguished wildfires. Peatland fires are very common in tropical, temperate and boreal climates (Rein et al., 2008). They can consume more

than half of the biomass burned during wildfires (Rein et al., 2008). Thus, they contribute significantly to atmospheric emissions from wildfires. On the other hand, smouldering fires of peatlands and other organic-soil systems represent a large perturbation of the global atmospheric chemistry. When active, the burning of ground and subsurface biomass layers can last for long periods of time and emit large quantities of combustion products causing the deterioration of the air quality (Page et al., 2002; Stracher and Taylor, 2004).

Factors governing the ignition, depth, duration and extend of a smouldering fire are primarily diffusion of heat and oxygen through the porous fuel layers from/to the propagation front (Rein et al., 2008). Also, the peat properties affecting these two mechanisms are, in turn, moisture and inert contents, botanical composition, bulk density, matrix permeability, and presence of cracks and deep channels (Rein et al., 2008). Studies of smouldering limits conducted using peat moss showed that sustained smouldering was influenced by both moisture and mineral content (Frandsen, 1987).

Both surface flaming fires and smouldering peat fires have been relatively frequent in the TDNP surroundings (Pic. 2.4) during the last decades (1977, 1987 and 1991) (García Rodríguez, 1996). In fact, most natural peatlands outside the Park limits have disappeared. Smouldering peat fires have even been reported inside the Park in 1986, 1987 and 1994 (Cirujano, 1996), but they occurred under relatively wet soil conditions, with a shallow water table located less than 1 m below the surface, and affected small areas. In 2009 fires, on the contrary, soil moisture was much lower and the water table was located deep below the surface, so they represented a much bigger problem.

Picture 2.4. Warning signs of peat fire risk in the surroundings of Las Tablas de Daimiel National Park.

2.5. Specific degradation effects on VZ: Soil hydrophobicity

Among soil physical properties, a relevant phenomenon developing on dry soils which had so far been overlooked in TDNP is hydrophobicity or water repellency. It involves drastic changes in the properties of soils as water and solute storages and transmitters towards lower layers of the VZ and the aquifer. A general review on the occurrence, causes and consequences of soil water repellency is presented in this section.

Soil water repellency (SWR) is a measure of soil hydrophobicity, this is, the degree of resistance of a soil to be wetted. SWR is a worldwide phenomenon both in arid and humid climates (Jaramillo et al., 2000; Doerr et al., 2000; Dekker et al., 2005). It has become an issue of major concern and scientific research on this topic has been increasing exponentially since the 1960s (DeBano, 2000a; Dekker et al., 2005). SWR has been found to have several hydrological implications summarised in the work by Jaramillo (2006): hinders infiltration and enhances surface runoff and erosion; conditions irregular wetting patterns and the development of preferential flow paths in the soil (i.e. fingered flow) which trigger rapid leaching of solutes to the groundwater; affects stability and structure of soil aggregates. These hydrological alterations can result in losses of plant-available water and nutrients, reduced

agricultural crop production, and deterioration of turf quality on sports fields (Dekker et al., 2009).

As reported by Dekker et al. (2005) in their review paper, although water repellency is most common in sandy soils and in nature reserves, it has also been observed in a wide range of other soil types such as loam, heavy clay, peat or volcanic ash. It is highly variable both spatially and temporally (Doerr et al., 2000; Ritsema and Dekker, 1994; Dekker et al., 2001; Dekker et al., 2009; Buczko et al., 2006).

It is widely acknowledge that SWR is basically due to the coating of soil aggregates by hydrophobic organic compounds released by plants, fungi and soil microorganisms (Doerr et al., 2000). The amount and nature of soil organic matter content has been found as one of the main controlling factors on SWR (Harper et al., 2000; Doerr et al., 2000; Ellies et al., 2005; Taümer at al., 2005; Hurra and Schaumann, 2006; Rodríguez-Alleres et al., 2007a; Blanco-Canqui and Lal, 2009). Moreover, Doerr et al. (2000) referenced in their review Berglund and Persson (1996), who reported that *Phragmites* spp., the main current macrophyte in TDNP (see section 3.6), are associated to SWR.

Another controlling factor on SWR is the soil moisture content. Some studies have found that the occurrence of SWR depends on a critical soil water content, above which the soil is wettable and below which it becomes repellent (Doerr and Thomas, 2000; Dekker et al., 2001; Ziogas et al., 2005; Taümer et al., 2005; Rodríguez-Alleres et al., 2007b; Sonneveld, 2008). This critical soil water content is specific for each particular soil. However, the development of SWR has not always been found to be directly related to the water content (Doerr et al., 2000; Hurra and Schaumann, 2006; Bayer and Schaumann, 2007). On contrary, it is globally acknowledged that SWR is influenced by seasonal conditions, mainly (not only) through variations in the soil moisture status, as reported in many studies (Ritsema and Dekker, 1994; Doerr et al., 2000; Sonneveld, 2008; Buczko et al., 2006; Dekker et al., 2001; Dekker et al., 2009; Ziogas et al., 2005; Keizer et al., 2007). As argued by Dekker et al. (2009), it is likely that SWR is most pronounced during periods with drier weather conditions (generally in

spring and summer) and decreases or disappears during wetter periods (late autumn and winter).

Other environmental factors that have been reported to affect SWR are soil texture (Bisdom et al., 1993; Harper and Gilkes, 1994 in Harper et al., 2000), soil pH (Bayer and Schaumann, 2007; Mataix-Solera et al., 2007), relative air humidity (Doerr at al., 2002; Wallach and Graber, 2007), aggregate size and stability (Hallet et al., 2001; Ellies et al., 2005; Goebel et al., 2004; Graber et al., 2006; Rodríguez-Alleres et al., 2007a; Blanco-Canqui and Lal, 2009), and faunal activity (Garkaklis et al., 2000; Cammeraat et al., 2002; Contreras et al., 2008).

On the other hand, SWR might also be locally induced or enhanced by wildfires (Giovannini and Lucchesi, 1997; DeBano, 2000b; Doerr et al., 2000; Lewis et al., 2007). According to DeBano (2000b), during a forest fire, heat from combustion vaporizes organic substances that migrate downwards into the soil where they condense at cooler temperatures and coat mineral particles. At temperatures below about 175 °C, there is little or no change in SWR; temperatures between about 175 and 280 °C increase SWR; and temperatures above 280 °C tend to destroy it. The effect of fire-induced SWR on other soil properties is increasingly being studied (Gonzalez-Pelayo et al., 2006; Fox et al; 2007; González-Pérez et al., 2004). Due to wildfire abundance, special attention is recently being given to Mediterranean areas, particularly in the Iberian Peninsula, concerning the occurrence of SWR under both typical natural vegetation stands in calcareous soils and following fire (Hubbert et al., 2006; Cerdà and Doerr, 2007; Mataix-Solera et al., 2007; Rodríguez-Alleres et al., 2007b; Verheijen and Cammeraat, 2007; Jordan et al., 2008). However, no literature has been found regarding the effect of smouldering peat fires on the hydrophobic properties of these soils. This is especially relevant for TDNP due to the recurrent occurrence of smouldering peat fires, the last one taking place in 2009. In this sense, the works developed throughout the present thesis constitute a pioneer approach relating the hydrophobic properties of a semiarid peatland with the occurrence of smouldering fires and the implications for fire prevention and control.

Given the above mentioned, the characterization of SWR in TDNP is an essential task due to the organic nature of some wetland soils, the expansion of reed beds and the recurrent drying conditions in the Park. The development of SWR involves drastic changes in the properties of soils as water and solute storages and transmitters towards lower layers of the VZ and the aquifer. Moreover, it can happen, that those materials that have turned into hydrophobic during drying do not easily recover their wettability after subsequent wetting or vice versa (Diehl and Schaumann, 2007; Hurra and Schaumann, 2006; Doerr and Thomas, 2000), thus, prolonging the effects of any preferential flow patterns that might have developed.

2.6. The global outcome of TDNP anthropization: System complexity

TDNP degradation and anthropization have developed an actual system much more complex than a simple floodplain, conditioned by the existence of perched water tables, aquitards, lateral geological changes, varying water qualities and infiltration rates in different zones, etc. System's reality is that of a drained potentially flooded area where inflowing water tend to infiltrate rapidly (Castaño et al., 2008; Aguilera et al., 2009b; Navarro et al., 2012) through a relatively thin (1-10 m) heterogeneous VZ, towards a multi-layer aquifer constituted by variably interconnected Tertiary and Quaternary materials. This complex system is a recipient for water and nutrients which are prone to be transported to deeper carbonate layers and exported through the regional water flux. Peat shrinking and cracking aggravate this problem and increase mentioned complexity.

Soil's VZ plays an essential role as nutrients and pollutants storage. It regulates their flux through different chemical and biological reactions. Successive drying-flooding cycles "activate" VZ processes which modify the original functioning of the system as a wetland area turning it into a "time bomb". VZ saturation by means of extraordinary

hydrologic (i.e. freshets) and/or climatic events (i.e. heavy rainfalls), or through water transfers, support ponding water stay in TDNP flooding areas for some time.

In spite of mentioned complexity, only few hydrological studies incorporating spatial-temporal variability have been conducted so far (Navarro et al., 2011, 2012). Furthermore, the interactions between the surface and groundwater systems have always been considered as a black box where the specific properties of the VZ have never been taken into account. This thesis expects to increase the hydrological knowledge of the degraded and anthropized wetland area through the integration of VZ studies, hydrology and soil science. It is hoped that increased knowledge of the hydrologic functioning as well as the belowground physical-chemical processes that take place in TDNP will contribute to the development of a more solid and structured management model far from current improvisation.

CHAPTER 3

Questions, objectives and hypotheses

3.1. Questions, objectives and hypotheses

In the previous chapter TDNP system anthropization and degradation was described. Management actions to enhance its quantitative and qualitative state have been mostly inefficient. How can management strategies and practices be improved? To be able to answer this question it is essential to polish up the knowledge of the physical-chemical system. For example, the relations between surface water bodies and groundwater in the area remain unknown. A better understanding of these processes seems crucial in a disturbed semiarid system conditioned by water shortage episodes. From a qualitative point of view, what happens with the nutrients stored in the VZ? How is the anthropic action affecting the system? To which extent do VZ physical hydraulic parameters change from flooding to drying conditions? Can peat fires be predicted? Which could be system's hydrological dynamic under different future management scenarios? The results presented in this thesis will contribute to answer these questions.

The specific objectives of this thesis focus on the achievement of two major goals:

1. Hydrological-based physical-chemical characterization of the TDNP soil-water system under dry conditions.

2. Analysis of environmental and management implications and development of support tools for hydro-environmental planning in TDNP.

3.1.1. Objectives for physical-chemical characterization of the soil-water system

3.1.1.1. Vadose zone chemistry

- Characterization of both the amount and distribution of mobile solutes stored in TDNP VZ that are readily available to be washed and transported to the groundwater by infiltrating waters.
- Assessment of the relationship of solutes with certain human-influenced environmental factors (soil type, depth, microtopography and central dam).

3.1.1.2. Vadose zone physics

- Determination of the most relevant physical properties of TDNP soils from a hydraulic point of view: bulk density, hydraulic conductivity, infiltration, water repellency, wetting rate, and water retention curves.
- Application of soil physical data to develop a VZ water flow model.

3.1.1.3. Peat combustion characterization

- Determination of physical-chemical variables controlling peat smouldering combustion and propagation.

3.1.1.4. Hydrology and hydrochemistry

- Characterization of the surface water and groundwater hydrochemical environments.
- Enhancement and refinement of the conceptual model of surface water-groundwater interactions.

3.1.2. Objectives for environmental and management implications analysis and support tools

- Definition and mapping of specific soil units within the TDNP area, referred as "soil functional types", regarding their hydraulic properties as water and solute transmitters and storage, as complementary information for Park managers.
- Environmental and management implications of physical-chemical characterization of the soil-water system: water availability and risk of groundwater contamination
- Determination of critical soil water contents for the development of soil hydrophobicity, reed (*Phragmites australis*) invasive expansion and peat combustion risk.
- Assessment of the performance of a soil moisture-temperature monitoring network as a tool for smouldering peat fire prevention and detection.
- Assessment of the usefulness of the VZ water flow model as a management tool to simulate soil moisture progress and critical soil water contents reach during a drying scenario.

3.2. Initial assumptions and hypotheses

The consistency (applicability) of the methodology used in this thesis is conditioned by the validity of several facts and hypotheses which are considered to apply based on current knowledge and literature review. The starting point is that the TDNP system is strongly anthropized and restoration to its natural state is difficult under the current socio-economical context. Other specific assumptions are:

- Natural flooding in TDNP only takes place during extraordinary wet periods.

- Nowadays, under average regional climatic conditions, TDNP wetland area always ends up drying out.
- Due to hydraulic gradient inversion and wetland disconnection (see section 2.2) the system behaves as a disconnected multi-layer aquifer system.
- The top Quaternary aquifer has preferential flow zones where water percolates faster towards the carbonated regional aquifer.
- Water flow in TDNP VZ is predominately vertical due to hydraulic gradient inversion and can be simulated with a one-dimensional model.
- Critical soil water contents for peat combustibility, reed (*Phragmites australis*) growth dynamics and soil water repellency can be used for modelling and planning.

CHAPTER 4

The physical environment

This chapter is focused on the description of main features of the physical environment of TDNP and its surroundings: geography and geomorphology, climate, hydrology, geology and hydrogeology, soil and vegetation. The chapter has been devised to focus on the relevant aspects for the study of the soil-water system directly linked to the analyses carried out and the results attained throughout this research.

4.1. Geography and geomorphology

As stated in section 2.2, the TDNP wetland area was originated at the outflow boundary of the 15,000 km^2 Upper Guadiana basin and the 5,500 km^2 Mancha Occidental aquifer system (Mancha Occidental I groundwater body according to the European Water Framework Directive nomenclature), in the confluence of the Cigüela and Guadiana Rivers in the Ciudad Real province (39°08'N, 3°43'W; Fig. 2.1). The extension of TDNP is 1,928 ha plus 5,410 ha of protection zone, this is, a total of 7,338 ha, divided among the municipalities of Daimiel (5394 ha), Villarrubia de los Ojos (1,914 ha) and Torralba de Calatrava (30 ha) (González Monterrubio, 1992).

TDNP lies on the alluvial plains of the Palaeozoic reliefs of the Toledo Mounts at the western end of the Mancha Plateau and it has NE-SW orientation (Fig. 2.1). The small altitudinal gradient of the floodplain region, with slopes lower than 1 ‰ (Sáez-Royuela, 1977) and average topographic elevation of 604.7 $\pm$ 1.06 m (Cirujano et al., 1996), leads to a flat landscape where only small islet outcrops, constituted by Upper Pliocene calcareous loamy facies and/or calcareous crusts, emerge (García Rodríguez, 1996). This fact, together with the geological and climatic characteristics, allows for the occurrence of semi-endorheic depressions that in the past constituted large flooding areas. TDNP, with a total surface over 150 km^2, was the most interesting and extensive of these areas (Álvarez-Cobelas et al., 2001).

Nowadays, with an approximate extension of 20 km^2, the TDNP possesses a maximum flooded area of 18.4 km^2 (data from the 1997 freshet reported by TDNP Managing Authorities and compiled in Castaño, 2004). The average depth of the water column is 0.90 m (Álvarez-Cobelas and Cirjuano, 2007), highly variable inter and intra-annually due to fluctuating climatic and hydrologic conditions as well as artificial management (i.e. floodgates at the Puente Navarro and Molemocho dams).

The study of the geomorphology is interesting as it allows to explain processes such as sedimentation, genesis of riverbeds and erosion surfaces, peatland formation and disposition, etc (García Rodríguez, 1996). Alluvial wetlands are depositional features in the geomorphological sense, since all appear as a result of sediment deposition (Richards, 1982 in Álvarez-Cobelas et al., 2010). Following the study by Rodríguez-García and Pérez-González (1999), TDNP can be classified as "wetlands linked to alluvial plains and bottoms".

TDNP belongs to the Mancha Plateau geomorphological unit which has E-W orientation and is located between three other different morphostructural units: the Palaeozoic Toledo Mounts in the north, the volcanic "Campo de Calatrava" in the west, and "Sierra Morena" in the south. The Mancha Plateau is dominated by extensive plains filled with recent Miocene-Pliocene continental sediments. It is also related to erosion surfaces situated at different elevations, close to each other. The fluvial hydrologic network is poorly embedded, showing undefined riverbeds with large flooding areas, little development of terraces and a seasonal pattern. The terrain is essentially flat or gently rolling with an average elevation around the TDNP area between 600-630 m (Pérez-González, 1996). Palaeozoic outcrops constitute regular ancient residual reliefs elevated from the plain, in which eventually can stand some structural relief of quartzite. These Palaeozoic reliefs show soft hillslopes covered with colluvials and west from TDNP they constitute a natural limit to the La Mancha Occidental aquifer, avoiding the deepening of the Guadiana River and, thus, supporting the development of large flooding areas (García Rodríguez, 1996).

As reported by García Rodríguez (1996), the most relevant geomorphological features in the study site are calcareous crusts, karstic processes and endorheism. The outcropping continental Tertiary materials include Pliocene limestone and marls to a depth of 100-110 m. To the north, these lacustrine or marshy-lacustrine carbonated deposits shift to more detrital materials such as sand, mud, clay and highly karstified calcareous crusts. The most recent materials (Upper Pliocene and Pleistocene) are constituted by karstified calcareous crusts of up to 1 m thick, which are the correlative deposits of an erosion surface embedded 10-15 m over the Tertiary deposits. This erosion surface shapes the overlying Quaternary relief in the area (Pérez-González, 1996). The generalized crusting is likely due to the Pliocene limestone-marly lithology and to the capillary rise and evaporation of groundwater with calcium bicarbonate character (García Rodríguez, 1996). This phenomenon would be further enhanced by agricultural tillage.

The landscape morphology is, therefore, directly linked to karstic processes, particularly circular or semi-circular sinkholes, either opened or closed, which can reach a few kilometres in length and tens of meters in depth. They are usually filled with fine materials such as organic silts and clays, and salts. In the past, they used to constitute temporary lagoon systems fed by groundwater discharge. Actually, it is possible that the whole Guadiana riverbed between the "Ojos" and TDNP corresponds to the main sinkhole system in the western Mancha Plain (García Rodríguez, 1996).

Finally, the materials in the valley bottoms, to which TDNP belongs, are besides detrital (silt, clay), organic and saline. Salts accumulate in drier areas giving rise to "solonchack" soils (see section 4.5), whereas peatlands develop in wetter areas (Pérez-González, 1996). The eolian shapes, such as sand dunes in the northern area of TDNP, have a policlinic genesis which began in the Upper Pleistocene.

Currently, due to both anthropic and climatic causes, the poorly developed fluvial network, basically constituted by the Cigüela, Záncara, Guadiana and Azuer Rivers, is only functional during extraordinary wet periods. According to García Rodríguez,

(1996), the morphology of the Guadiana and the Azuer, with few terraces and large floodplain areas, is related to subsidence and karstic processes of carbonate dissolution by the groundwater flux. Nevertheless, the Azuer River could be artificial from Daimiel or have been deviated through minor riverbeds.

4.2. Climate

Climatic conditions constitute a core aspect for hydrological studies, particularly rainfall and temperature. Since climate change has become a central topic in scientific research, it is very important to consider its potential effects on fragile ecosystems such as wetlands. Special attention must be given to Mediterranean climates, characterized by strong inter and intra-annual irregularity and subjected to periodical drought episodes. Nevertheless, recent studies predict increased aridity under climate change scenarios (Abouabdillah et al., 2010; Gao and Giorgi, 2008). In this section, a brief summary of available information on local climatic trends in the TDNP area for the 20th century and the first decade of the 21st is presented.

The climate in TDNP is dry Continental Mediterranean, with annual average values of precipitation and temperature for the 20th century of 412.6 mm and 14.3 °C, respectively, with dry hot summers and cold winters (Domínguez-Castro et al., 2006). The potential evapotranspiration estimated by the Thornthwaite method is about 850 mm yr^{-1}, revealing an annual water deficit over 400 mm (Sánchez-Carrillo et al., 2004). Droughts are usual in this semiarid region with recurrent periods where total rainfall amounts less than 300 mm yr^{-1}.

Three studies have extended the analysis to the first years of the 21st century. Martínez-Santos et al. (2004) analysed the climatic trends in 9 weather stations, one within and the rest close to TDNP, comprising the period 1904-2002. Besides this, they studied the association of these trends to the main events of human-induced

modifications to the hydrological system. They observed large variability in both annual and monthly data. The overall average rainfall of the 9 stations for the considered period, 412.6 mm, is the same as that reported by Domínguez-Castro et al. (2006) for TDNP, whereas the average temperature differs, being noticeable higher (21.1 °C). These authors identified four thermal periods: 1904-1937, cold; 1938-1958, warm; 1959-1990, cold; 1991-2002, warm. Other four periods were identified on basis to rainfall analysis: 1904-1954, dry; 1955-1979, wet; 1980-1995, dry; 1996-2002, wet. However, superposition of these series to the main human impacts on the TDNP environment revealed no relation of these events to climatic trends. Consequently, they argued that there has been a clear human control on the environment overlying the climatic and endogenic controls.

The second climatic study, carried out by Sánchez-Carrillo and Álvarez-Cobelas (2010), expands the previous time series until 2008. They analysed data from the weather station located inside TDNP (4112U), complemented with data from two other stations, one from Ciudad Real and another from Daimiel. They obtained a yearly average air temperature at TDNP of 14.2°C, a very similar value to that reported by Domínguez-Castro et al. (2006), with strong differences between summer and winter (up to 35°C). However, average annual rainfall, seasonally distributed between winter and spring, decreased to 402 mm. Interannual differences in monthly rainfall were quite accentuated and statistically significant (Rank test $p< 0.05$). On the basis of the accumulated deviations of rainfall from the average, they identified three hydrological periods between 1904 and 2008: a dry period until 1950, a humid one from 1951 to 1979, and a dry one from 1980 until today. This subdivision essentially coincides with that of Martínez-Santos et al. (2004), with the difference that Sánchez-Carrillo and Álvarez-Cobelas (2010) did not consider the wetter period 1996-2002. From their analysis they conclude that the climate of TDNP can, thus, be classified as semi-arid.

Finally, Santisteban and Mediavilla (2012a) integrated the information from six meterological stations in the TDNP surrounding area. They found a relative similarity of annual temperature and raifall values in all the stations. Based on the longer series

from the Ciudad Real station they report an average annual temperature of 14.6 °C and an average annual rainfall of 406.8 mm for the extended period 1904-2011. These authors also performed a drought analysis based on the SPEI index (standarized precipitation-evapotranspiration index) at different time scales (12, 24, 36 and 48 months). Their results show a significant increase of dry cycles from the late 1960s until 2009.

The reviewed studies show a somehow coarse scale of climatic analysis. This thesis will add a contribution by narrowing (zooming) the cycles of wet and dry periods to a time scale more suitable for hydrological management and planning. Due to the apparent homogeneity of temperature within TDNP, rainfall will be the main target variable. Nevertheless, rainfall is the most important variable to characterize hydrological conditions, both in the unsaturated and saturated zones. Furthermore, due to its anthropic management, surface water in TDNP, although highly controlled by evaporation and evapotranspiration, also depends on the socio-economic and political context for the authorization of water transfers and on upstream regulation, which are conditioned by the precipitation pattern.

4.3. Hydrology

An outline of the hydrological context of TDNP was presented in the Background section (see sections 2.2 and 2.3). This section will complement and detail the above mentioned, describing the modifications suffered by the surface water network, the water budget and the flooding area from natural to anthropized conditions.

The Cigüela and Guadiana Rivers, which directly arrive and cross the National Park, and two of their tributaries, the Záncara and the Azuer, respectively, can be considered as the main fluvial network of TDNP (Fig. 2.1). Under natural conditions, before de 1970s, the main surface water inputs to the wetland area were provided by the Cigüela and

the Azuer, especially by the former. The discharges from both rivers have always been highly variable, although the Azuer was a bit more regular as it is supported by the neighbouring aquifer of Campo de Montiel (ITGE, 1980; Esnaola, 1991; Martínez Cortina, 2003; de la Losa et al., 2012). The contribution of the Cigüela ranged between 0 and 324 $hm^3\ yr^{-1}$ and the Azuer's between 0 and 67 $hm^3\ yr^{-1}$, although the last one remained virtually dry from 1980 to 1996 (López Camacho et al., 1996). Moreover, groundwater discharge through the Guadiana used to play a crucial role in the support of the hydrologic system until the beginning of the 1980s (García Rodríguez, 1996; Álvarez-Cobelas et al., 2001; Sánchez-Carrillo and Álvarez-Cobelas, 2010). In 1983, its main groundwater supplier before the confluence with the Azuer, the Ojos del Guadiana, discharged for the last time (Cruces and Martínez Cortina, 2000). Different estimations on the average contribution of the Guadiana upstream from the confluence with the Azuer for the period 1915-1932 are 61 $hm^3\ yr^{-1}$ (Álvarez-Cobelas et al., 2001), 72 $hm^3\ yr^{-1}$ (García Rodríguez, 1996) and 73 $hm^3\ yr^{-1}$ (data provided by the Centre for Study and Experimentation of Public Works, CEDEX).

A thorough review and analysis of the historical evolution of flow rates in these rivers along the 20th century can be found in de la Losa et al. (2012). Despite the paucity of data, some general features are observed: i) high seasonal and interannual irregularity, linked to precipitation and surface water-groundwater interactions; ii) global change of river dynamics from 1978-79 associated to anthropization, particularly the expansion of irrigation agriculture and river abstractions during dry periods; iii) decrease of flow rates since 1980 due to infiltration from riverbeds enhanced by aquifer disconnection. From the 1960s, ditching and channelization of rivers as well as construction of reservoirs upstream such as Peñarroya for Záncara and Cigüela (1959) and Vallehermoso for Azuer (1988), has also conditioned the modification of the hydrological patterns (INYPSA, 1990; Sáez-Royuela, 1977, Esnaola, 1991). In the case of the Guadiana River, flow rates used to be quite regular due to groundwater discharge before the drying out of the Ojos del Guadiana in 1983. The analysis points out that the rivers are mainly conditioned by rainfall and infiltration, being the last supported by groundwater abstractions. The decline of groundwater levels caused a shift in the

functioning of the rivers, which turned from areas of natural discharge into areas of preferential infiltration (Esnaola, 1991).

The average water table drawdown in the period 1980-2011 is 8.5 m, which is equivalent to a 1,070 hm^3 decrease in aquifer's storage (Mejías et al., 2012). Greatest extractions took place between 1985 and 1990 when withdrawals were over 500 hm^3 yr^{-1} (with a declared historic record of 570 hm^3 in 1988), while renewable resources under natural conditions were estimated in 340 hm^3 yr^{-1} (SGDGOH, 1989; Martínez Cortina, 2003). Figure 4.1 shows a schematic representation of the TDNP water budget components under natural and anthropized conditions. Different figures for these components depending on estimation methods, both for natural and degraded conditions, can be found in the various water budgets performed since the 1980s compiled in García Rodríguez (1996) and Castaño (2004). These budgets have been highly unreliable on the estimation of the infiltration term, which is acknowledged as the current key variable in TDNP hydrological dynamics (García Rodríguez, 1996; Castaño et al., 2008; Sánchez-Carrillo and Álvarez-Cobelas, 2010; Angeler et al., 2010; Navarro et al., 2011).

Castaño (2004) and Castaño et al. (2008) estimated an average infiltration rate of 1 cm d^{-1} for the whole TDNP through a daily water balance model, where volume stored is calculated as a function of flooding area. This model has been recently improved by Navarro et al. (2011, 2012) who refined the functional relationship between flooding area and infiltration rate. Their model considers infiltration rate as function of flooding area, water level, surface elevation, ground profile thicknesses from the surface to the groundwater level and saturated hydraulic conductivities of soil materials. The model takes into account the spatial variability of the infiltration rate in different TDNP areas, particularly for the Cañas zone, where they simulated the drying processes of 1996, 2000 and 2003 with considerable accuracy (Navarro et al., 2012). However, these authors assumed a very simplified and homogeneous hydrogeological arrangement of materials without considering lateral changes, and used literature based average saturated hydraulic conductivity values for each material while no measurements were

carried out. Estimated infiltration rates ranged between 0.33 cm d^{-1} and and 0.73 cm d^{-1} in the Cañas zone, and from 0.85 cm d^{-1} to 2.1 cm d^{-1} in other TDNP areas. Their estimates agree reasonable well with the overall 1 cm d^{-1} proposed by Castaño (2004) and Castaño et al. (2008). Therefore, in spite of the lack of knowledge of physical characteristics and that the effects of small-scale variability in hydraulic parameters is hardly considered in these models, successful approximations of TDNP infiltration rates seem to have been achieved.

The mentioned infiltration studies have something in common: they consider infiltration from flooded conditions, quasi-hydrostatic inundations as Navarro et al. (2011) define them. The similarity of estimated rates indicates a relative uniform predictable behaviour of the infiltration term when TDNP is flooded. But this implies infiltration from saturated soil conditions, which, obviously, might quite differ from those in unsaturated soils.

The quantitative hydrological disturbance was coupled to a qualitative one enhanced by the decrease in river flow rates. Water quality deterioration in the Upper Guadiana basin caused by wastewater and industrial spills to the rivers, and agriculture runoff pollution, had an obvious negative impact on its TDNP outflow system (INYPSA, 1990; Cirujano et al., 1996; Álvarez-Cobelas et al., 2001; Berzas et al., 2000). All these hydrological changes have severely damaged the ecological properties of the wetland.

The flooding area of TDNP has followed seasonal patterns as long as water inputs from Cigüela, either natural or transferred, have taken place (Fig. 4.2). Under natural conditions, these patterns showed a peak in mid-spring and a drought in late summer and early autumn (Sánchez-Carrillo and Álvarez-Cobelas, 2010). According to Sánchez-Carrillo and Álvarez-Cobelas (2010), a decreasing trend in mean annual levels has been observed for the period 1944-2008. However, monthly flooding areas have only been continuously monitored since 1988, when the first water transfer was carried out, whereas earlier data were mostly estimated (Álvarez-Cobelas et al., 2001).

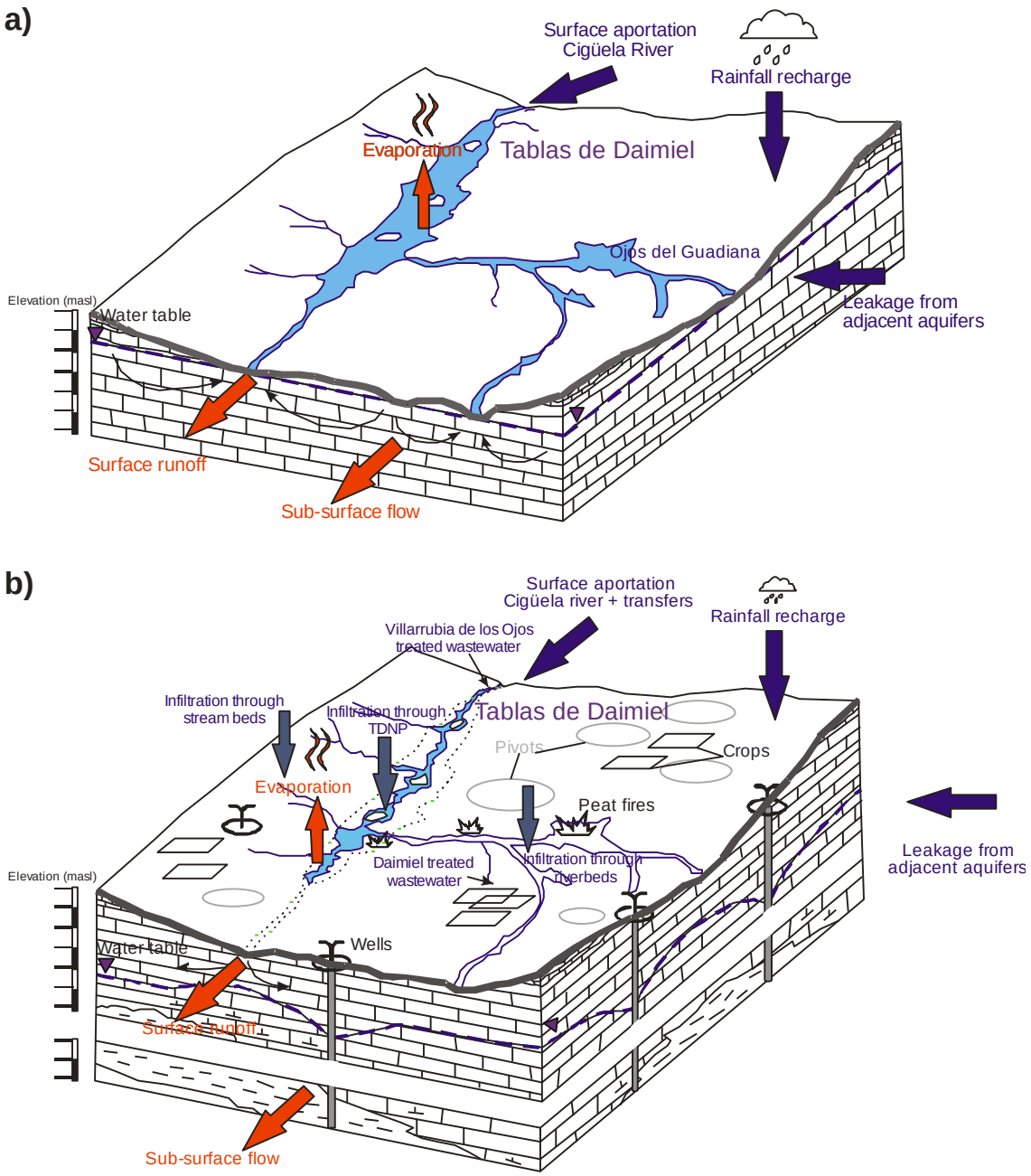

Fig. 4.1. Diagram of main water budget components in Las Tablas de Daimiel National Park area under a) natural and b) anthropized conditions (modified from García Rodríguez and Llamas, 1993). Note that the vertical scale in b) has been extended to represent deeper areas of the multi-layer aquifer system. Main human impacts and pressures are also depicted.

As depicted by the graph, after the disappearance of groundwater discharges in the early 1980s and the decrease in surface water inputs through the Cigüela, frequent hydrologic drought periods (1981–1988, 1991–1995 and 2006–2009) have kept the wetland almost dry during the whole year. In extreme situations, only a minimum

flooded area around 50-100 hm^2 in the visitor's zone maintained by groundwater pumping from the system of wells installed inside and nearby the Park limits remains (Fig. 2.2). Flooding conditions have depended almost exclusively on water transfers or, as in the case of the period 1996-1997 and the recent 2010-2013, on extraordinarily wet events (see section 4.2). During this wet periods stable flooding levels are supported by the re-activation of the hydrologic network as water is released from upstream reservoirs. It can be observed that the undertaken water transfers have yielded varying flooding areas. Although derived volumes have usually been around 15-20 hm^3, low performances were observed in years where transfers were carried out in spring or summer (1992, 1994, 2000, 2007 and 2009) when evaporation and infiltration rates are highest and when increased demands of water for irrigation promote illegal extractions.

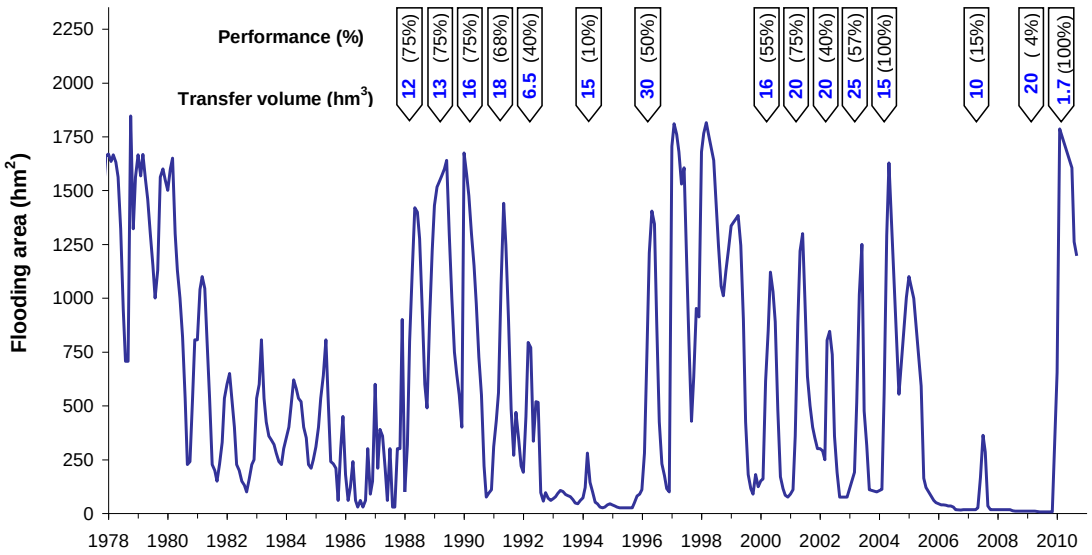

Fig. 4.2. Monthly flooding area pattern in Las Tablas de Daimiel National Park (TDNP) from 1978 to 2010. Data prior to 1988 was estimated either through remote sensing (García Jiménez et al., 1992) or by multiple linear regression (Álvarez-Cobelas et al., 2001). Volume and performance of the water transfers carried out in the period 1988-2010 to sustain flooding conditions are shown.

The implementation of the HRP in 1987 has determined an increase in the variability of the flooding area (López-Camacho et al., 1996). Besides water transfers and

emergency wells, three dams were built inside TDNP to retain water (Molemocho, Morenillo and Puente Navarro) (Fig. 2.1). From this moment, TDNP became an artificial system of connected reservoirs that behaves as an "artificial recharge pond" where infiltration plays a major role (see section 2.2). Evaporation and infiltration are the only outputs, except for when water surpluses in the closed artificial reservoir system need to be evacuated through the outlet Puente Navarro dam, or even upstream the Guadiana River by tearing down the Molemocho weir, as happened in 1997.

Summarizing, human intervention has significantly altered and disrupted the hydrological system of TDNP. Nowadays the Park behaves as an artificial recharge reservoir system which suffers from long periods of drought, with the exception of small areas flooded with groundwater pumped from emergency wells. It only receives sporadic natural water inputs after intense rainfall periods, either through small streams on the northwestern side or through the Cigüela and Azuer Rivers, which also receives treated wastewater discharges from Villarrubia de los Ojos and Daimiel, respectively (Fig. 2.2). These sporadic inputs become more continuous during extraordinary wet years, when water is released from upstream reservoirs and fluvial network is re-activated. Besides this, occasional water transfers of varying efficiency are derived through the Cigüela riverbed into TDNP, which are usually dependent on the socio-political context. Outputs only take place through infiltration and evaporation. Nevertheless, when occasional surpluses need to be evacuated, water is released downstream the Guadiana River at the outlet Puente Navarro dam, and even upstream this river through the Molemocho weir. Therefore, the Guadiana River has turned from being a source of groundwater discharge to TDNP under natural conditions to a two-ways drainage path, both downstream and upstream, under extraordinary circumstances.

4.4. Geological and hydrogeological environment

One of the main limitations for the study of the hydrological behaviour of TDNP is the lack of detailed geological and hydrogeological information. Actually, drilling of boreholes is not allowed inside the National Park, so geophysical studies can not be fully performed. Although the general geological features of the Mancha Plain and in the TDNP surroundings are well documented (Molina et al., 1972 and Molina, 1974, 1975 in García Rodríguez, 1996; ITGE, 1988; Pérez-González, 1996; García Rodríguez, 1996; González Monterrubio, 1992), the extreme local heterogeneity regarding degrees of karstification and contacts between Tertiary and Quaternary deposits underneath the wetland area makes geology a crucial conditioning factor (Castaño et al., 2013). An overview of the finest geological and hydrogeological available information within the TDNP environment is given in this section.

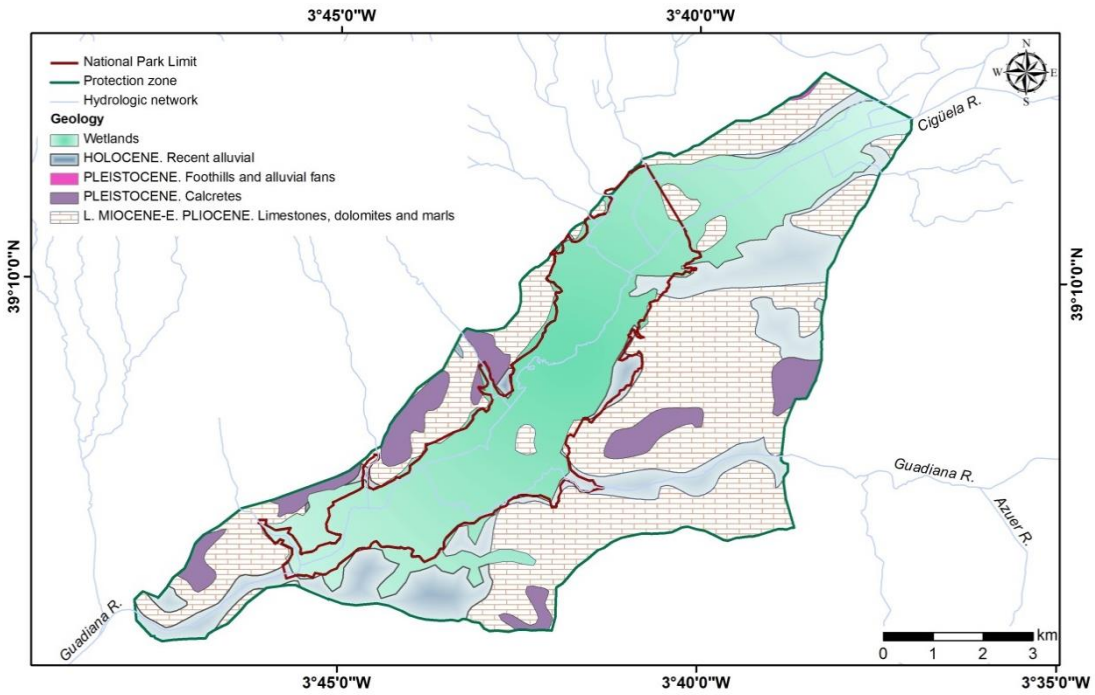

Fig. 4.3. Geological setting of Las Tablas de Daimiel National Park (TDNP).

The geological setting is constituted by a Palaeozoic basement of quartzites and shales, overlaid by discordant Miocene-Pliocene sands, limestone, muds, clays, dolomites, gypsum and marls (Fig. 4.3). Upper Pliocene materials (sands, clays, limestone, marls and calcareous crusts) are the most widely represented in the study area (García Rodríguez, 1996). As already mentioned, the Pliocene-Pleistocene transition in the TDNP area is constituted by calcareous crusts (calcretes), which are the correlative deposits of an erosion surface that shapes the Quaternary relief in the area (Pérez-González, 1996). The most recent deposits are sandy, clayey and silty fluvial materials with varying gypsum content from the Guadiana, Azuer and Cigüela Rivers, overlaid by marshy-lacustrine sediments such as peat and clay in the flooding areas inside TDNP (García-Hidalgo et al., 1995; Aguilera et al., 2011; Domínguez-Castro et al., 2006). Besides that, alluvial fans, colluvials and deposits in the bottom of sinkholes and from eolian origin are also present (see section 4.1).

According to García-Hidalgo et al. (1995) and Mediavilla et al. (2011) the Holocene TDNP sedimentary evolution reflects a transition from a fluvial stage dominated by sandy and silty materials (siliciclastic facies) to a marshy-lacustrine stage mainly represented by organogenic materials (peat and clay) and carbonate facies (charophytes biogenic deposits). This transition reflects an increase of the water level and a shift to permanent flooding conditions which would have been either due to a climatic change to wetter conditions or to downstream damming of the Guadiana River. Charophytes, locally known as “ovas”, are algae that colonize the bottom of ponds (tablas) and induce biogenic precipitation of calcium carbonate. Organogenic facies were generated in a permanently flooded environment with almost null energy. The presence of peat indicates an anaerobic environment whereas the existence of charophytes supports water oxygenation and carbonate deposition.

Outcropping Palaeozoic materials can be found in the northern area of Villarrubia de los Ojos at the foot of the hills (González Monterrubio, 1992). Available lithostratigraphic information from individual piezometers, boreholes and hydrogeological profiles (García Rodríguez, 1996; MARM, 2011) indicates a general W-

E transition underneath TDNP from Miocene-Pliocene clay and marl, which are dominant on the right margin, to thick layers of Miocene-Pliocene limestone and marl, in the left one, with gypsum lenses appearing randomly at various depths in the entire area, particularly in the north. Limestone show varying degrees of intensive karstification, constituting the main aquifer unit in the whole Mancha Plain with thickness ranging between 30 and 100 m (García Rodríguez, 1996). Sporadic outcropping limestones overlaid by calcareous crusts constitute the so-called islets within TDNP. Finally, the diverse Quaternary deposits are widespread over the entire area. Alluvial fans from the Palaeozoic reliefs can be found in the N-NW limits.

Hydrogeologically, the TDNP area comprises the edge part of the Miocene-Pliocene unit of the Mancha Occidental aquifer, constituted by limestone and marl materials, which has an average thickness of 200 m and behaves in an unconfined manner (Martínez-Santos et al., 2008b). The impervious bottom is constituted by Palaeozoic materials of negligible permeability. The hydraulic conductivity values range from below 1 m d^{-1} near the system boundaries to nearly 100 m d^{-1} in its central areas. The same occurs with specific yield values, which roughly vary between 0.01 and 0.06 (Martínez-Santos et al., 2008b). Transmissivity ranges from 50 m^2 d^{-1} in the northwestern border to 20,000 m^2 d^{-1} in the eastern valley area of the Ojos del Guadiana springs, where pumps concentrate (García Rodríguez, 1996). The Quaternary and Plioquaternary fluvial and marshy-lacustrine deposits of varying permeability overlay the Tertiary permeable (i.e. limestone) and semi-permeable materials (marls, gypsum and clays). The heterogeneous vertical and horizontal lithologies (García Rodríguez, 1996), differential karstification and subsidence effects determine varying degrees of interconnection between all these Tertiary and Quaternary materials which condition the complex local hydrogeological behaviour of the system (Castaño et al., 2013). Therefore, it can be initially assumed that the whole system operates as a multi-layer aquifer (see section 4.1), where some low permeability Quaternary and Tertiary materials might behave as semiconfining aquitards that give rise to shallow perched water tables in the TDNP area (García Rodríguez, 1996).

The multi-layer aquifer system represents a complex and heterogeneous sequence of alternant unsaturated and saturated levels constituted by the Quaternary and Tertiary materials described above. The first level, from the surface to a variable depth between 1 and 10 m as inferred from field observations and literature review (García Rodríguez, 1996; García-Hidalgo et al., 1995; Domínguez-Castro et al., 2006; Gil-García et al., 2007; Castaño et al., 2013), is formed by the fluvial and marshy-lacustrine sediments which are the target of the analyses presented in this thesis.

4.5. Soil

Soils in the TDNP basically consist on fluvial and marshy-lacustrine sediments. The Soil Taxonomy on its eleventh edition (USDA, 2010) excludes from the soil definition all those "areas where the surface is permanently covered by water too deep (typically more than about 2.5 m) for the growth of rooted plants. This is not the case of the TDNP wetland area, with an average water depth of less than 1 m and well developed hydrophytic and helophytic vegetation. Furthermore, increasing drying cycles due to anthropization have caused that TDNP soils are no longer permanently submerged and edaphization processes take place.

In the present thesis, the study of soils has been addressed from a pure hydrological context as constituents of the vadose zone. Therefore, it was considered convenient to define specific soil units within the TDNP area regarding their hydraulic properties as water and solute transmitters and storage. These units haven been termed "soil functional types" (SFT) and they have allowed to group materials with similar hydraulic behaviour, independently from other characteristics of their genetic classification (Aguilera et al., 2009a, 2011). However, a genetic classification of soils for the whole area of influence of TDNP will be given based on the Food and Agriculture Organization (FAO) World Reference nomenclature (IUSS Working Group WRB, 2007).

The most important work on the edaphic characteristics of the TDNP area can be found in de la Horra (1996). According to this study, there are two main lithological domains with different chemical and mineralogical compositions which have determined the edaphic evolution of the area: an acid environment represented by the Palaeozoic reliefs of the Toledo Mounts, and a neutral or basic one corresponding to the Tertiary and Quaternary deposits that extend through the Mancha Plain.

Acid lithologies can be found north from TDNP in the area of influence of the Toledo Mounts. They are mainly represented by *Dystric Cambisols* associated to *Dystric Leptosols* and *Lithic Leptosols*. *Dystric Cambisol* is the most widespread, showing an ochric A horizon with low organic matter content, and a percent base saturation below 50%, between 20 and 50 cm from the surface. *Leptosols* are limited by Palaeozoic quartzite bedrock, with a maximum depth of 10 cm in the case of *Lithic Leptosols* and up to 30 cm in the case of *Dystric Leptosols*, where a xeric ochric A horizon a percent base saturation below 50% can also be found.

Closer to TDNP limits in the northwestern area, coarse grained colluvial deposits of shales and quartzites, with a clay matrix and a Ca horizon, appear. It can be considered as a transition lithology due its location between the acid Toledo Mounts and the basic Mancha Plain. The soils that develop from these materials are *Calcic-Chromic Luvisols* and *Chromic Cambisols*, characterized by a bright red colour in all their horizons.

Within the TDNP area, two main lithologies condition the characteristics of soils: i) calcareous crusts with silt, sand and gravels; ii) recent alluvial and alluvial-colluvial deposits, with or without salinity and/or organic matter in endorheic zones (see section 4.1). The most representative soils developed from calcareous crusts are *Petric Calcisols* which are closely associated to *Calacaric-Chromic Cambisols*. Their profiles are completely carbonated, but *Petric Calcisols* have a petric-calcic horizon shaped as a calcareous crust which allows to characterize them as *Calcisols*. This edapohological association shows inclusions of two other soil types, *Calacaric Regosols* and Calcic-*Chromic Luvisols*, which genesis is closely linked to that of crust soils.

On the other hand, recent alluvial and alluvial-colluvial deposits in TDNP correspond to the sediments deposited by the Cigüela, Guadiana and Azuer Rivers. The overflowing of these rivers in the past flooded large areas with water rich in silt, clay and dissolved salts (sulphate, calcium and, in less proportion, magnesium and chloride) washed from the marly lithologies crossed by these rivers. The combination of salt-rich waters and shallow phreatic levels caused the development of large permanently flooded areas where significant amounts of peat accumulated, especially in the alluvial areas of the Azuer and the Guadiana. Moreover, drought episodes in the topographically higher areas during low water seasons conditioned the deposition of evaporites on the soil surface, resulting in what today are saline environments. Nevertheless, salinization can not be considered as a generalized process, being more intense in the alluvial zones of the Cigüela and the Zancara, where saline soils predominate. The most widespread type is the *Mollic Solonchak*, characterized by an organic carbon rich A horizon. In steppe zones with natural vegetation, *Mollic Solonchaks* are associated to isohumic *Calcic Kastanozems*. To a lesser extent, other soil types such as *Calcaric Regosols*, in non-flooded areas, and *Petric Calcisols*, where the characteristic calcareous crust lithology dominates in elevated areas next to riverbeds, are also present. *Petric Calcisols* would be the representatives of the calcareous islets inside TDNP.

Finally, in the northeastern area of TDNP, there is a recent dune system due to the accumulation of eolian sandy deposits with rare gravels with an alluvial origin. The structure is of sand and gravel banks overlaying calcareous crusts. Soils are sufficiently elevated in respect to riverbeds so they are not influenced by flooding episodes. They can be classified as *Calcaric Arenosols* or as *Albic Arenosols*, when a clear albic horizon is present.

4.6. Vegetation

Vegetation constitutes a key element for wetland functioning through its decisive involvement in processes such as water distribution and balance, sedimentation and nutrient cycle, conditioning both the structure and physical-chemical properties of soils (Mitsch and Gosselink, 2000; Aguilera et al., 2011). Some examples of the environmental roles played by wetland plants, mostly helophytes, are: to control evapotranspiration dynamics (Sánchez-Carrillo et al., 2004); to limit surface water motion and, thus, the distribution and flow of particulate and dissolved material in the wetland (Kadlec and Knight, 1996 in Cirujano et al., 2010); to increase nutrient and organic matter contents in soils when decaying; to provide refuge for animals.

Macrophytes in wetlands usually operate as ecosystem engineers and some of them, mostly helophytes, provide the characteristics of the wetland (Keddy, 2000 in Cirujano et al., 2010). Peat soils, for example, are entirely dependent on the characteristics of the plant species from which they develop. Therefore, the knowledge of the physical-chemical growth parameters of vegetation becomes essential to understand the properties of the vadose zone as water and solute transmitter and storage. In the case of TDNP this is particularly relevant due to the anthropic management of macrophyte vegetation (i.e. reaping).

The dynamics of hydrophytic and helophytic vegetation has been extensively studied by a group of ecologists from the Spanish Council for Scientific Research (CSIC) since the 1990s (Cirjuano et al., 1996; Álvarez-Cobelas et al., 2001; Sánchez-Carrillo and Álvarez-Cobelas, 2001; Sánchez-Carrilo et al., 2004; Álvarez-Cobelas and Cirujano 2007; Álvarez-Cobelas et al., 2008; Cirujano et al., 2010). Their main goal has been to analyse the relation between vegetation dynamics and environmental factors conditioned by anthropogenic impacts, particularly those related to hydrological characteristics and water quality (Cirujano et al., 2010). In this section, a summary of the historical

evolution of wetland vegetation and the characteristics of the main species related to soil, water and nutrient dynamics will be presented.

In TDNP, as in other wetlands, vegetation is determined by several factors such as water seasonality, salinity, organic matter, microtopography, edaphic moisture, etc. In wetland ecosystems the presence of plant species mostly depends, among other factors, on the soil moisture pattern, and not on the local microclimate. Communities are subjected to a high number of constantly changing variables, even in short periods of time. According to Cirujano et al. (2010), structural and dynamical changes in TDNP vegetation in the last 40 years are related to the same impacts that affect all wetlands in Mediterranean Europe: diminishing water availability as a result of agricultural practices, drying, changing morphometry of their basin, water pollution, salinization, invasive species and fires. Space (as a surrogate for water quality), water depth and plant cover of the other species (as an index of competition between emergent species) could be considered the main environmental controlling factors of the cover of emergent plants other than the biological traits of a given species.

Under natural conditions, in the shallow areas, and growing on sulphate-carbonate-rich limestone that were transported by the Cigüela River, there were compact submerged meadows comprising several charophyte species (*Chara canescens*, *C. hispida*, *C. aspera*, *C. hispida* var. *major*, etc.). These charophytes were essential for waterfowl feeding and as refuge for fish and other aquatic animals (Pascual, 1976). Submerged meadows of charophytes are the best index of ecological conservation for this wetland, its occurrence and abundance being mostly dependent upon hydroperiod and water quality (Cirujano et al., 2010).

Helophytic vegetation was very homogenous and dominated by large formations of cut-sedge (*Cladium mariscus*) which could be considered the highest population on a single site in Western Europe (Álvarez-Cobelas et al., 2001). Riverine areas were covered by the remaining helophytes, mostly *Phragmites australis*, *Typha domingensis*, *T. latifolia*, *Carex riparia* and *C. hispida* (Fig. 4.4). The landscape structure was based

upon the equilibrium between helophyte patches and helophyte-free areas, the latter being more frequent and extensive in the eastern, shallower area of the wetland, whose bottom areas were mostly covered by charophytes.

The main change was towards a chemically more homogeneous environment, but more fluctuating and somewhat stochastic as well, as a result of strong changes in water availability and ongoing eutrophication (Cirujano et al., 2010). This influenced plant species richness in a variety of ways. While the absence of fresh and permanent waters was the cause for the disappearance of large macrophytes (33.3% of species lost, Álvarez-Cobelas et al., 2001), water pollution, lower hydrolevels and hydroperiods and salt contents increasingly enhanced the occurrence of plant species that were better adapted to these conditions (i.e. *Lemna minor, L. gibba, Chara connivens*, *Ranunculus peltatus*, *R. trichophyllus* and *Ruppia maritima*).

From a spatial perspective, changes in emergent vegetation resulted in strong fragmentation and cover loss of cut-sedge patches (Álvarez-Cobelas et al., 2008), with a decrease of 89% of the original cover, and a variable increase of reed (*Phragmites australis*) and cattail (*Typha domingensis*) cover, up to 24% and 237%, respectively (Fig. 4.4). Apparently, low oscillating water levels and poor water quality support reed growth and spread against cut-sedge (Álvarez-Cobelas et al., 2001; Álvarez-Cobelas et al., 2008). Saltmarsh et al. (2006) report that, as water stress increases, photosynthetic efficiency of reed is higher than that of cut-sedge. Therefore, random flooding following system anthropization has enhanced reed growth. However, the spatial pattern of reed distribution has been unclear, perhaps because of its faster growth which might make species cover more fluctuating and unpredictable (Álvarez-Cobelas et al., 2008).

In recent years, during dry periods invasive nitrophilous plants (*Conya Canadensis, Cochlearia glastifolia, Erygeron bonariensis*, *Aster squamatus*) widely spread in drained soils rich in nutrients and organic matter, occupying 79% and 95% of total helophyte-free areas in 2007 and 2008, respectively (Cirujano et al., 2010). Furthermore, there is

a growing contribution of woody species (*Tamarix canariensis*, *T. gallica*) in clayey soils of TDNP margins which comprise the potential forest vegetation of wet and saline soils, together with other salt tolerant plants such as *Juncus maritimus* (Pic. 4.1).

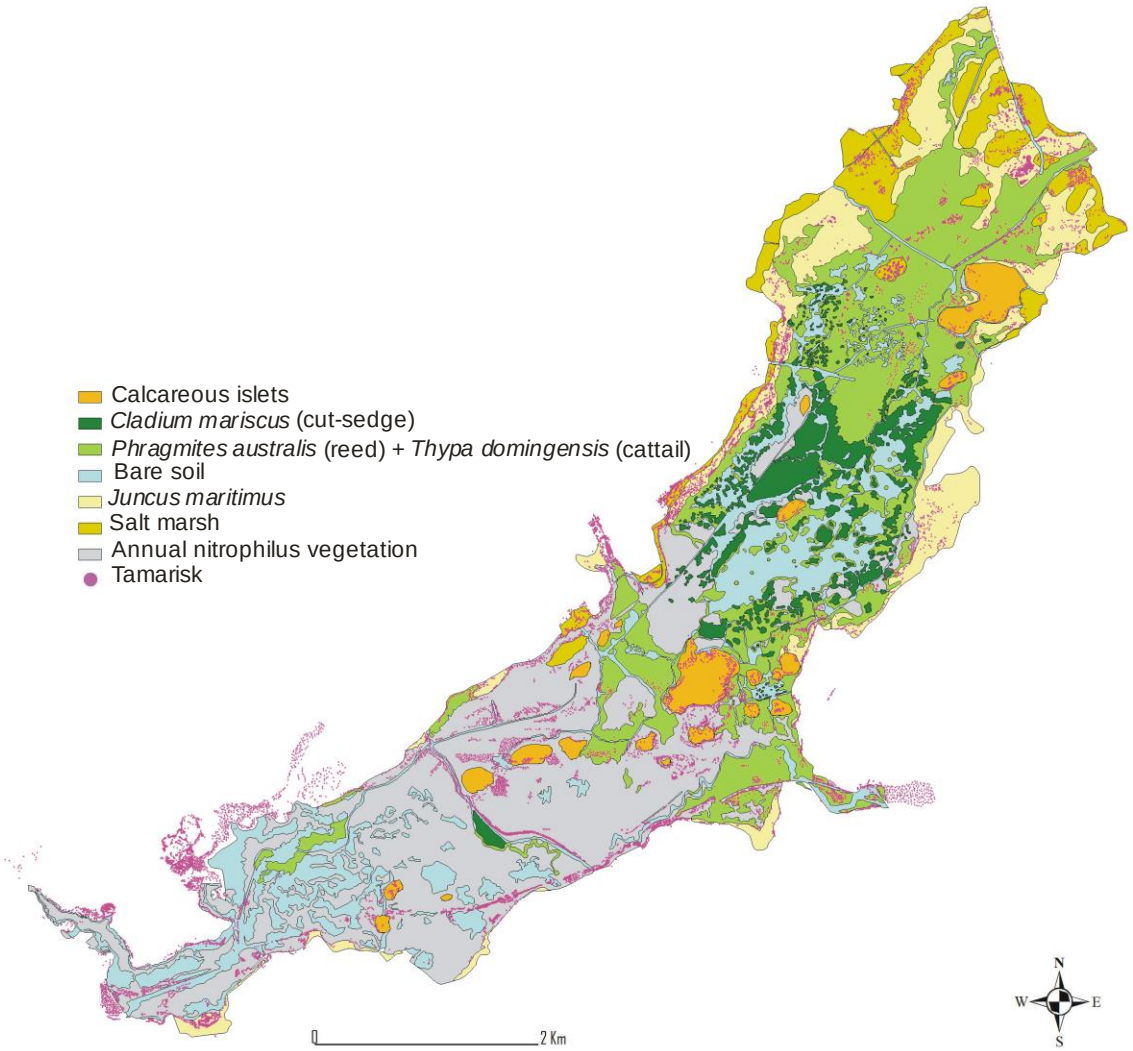

Fig. 4.4. Vegetation map of Las Tablas de Daimiel National Park (TDNP) in 2007 (modified from Cirujano et al., 2007).

The particular ecology of reed, a perennial rhizomatic plant with annual turnover rate, together with its anthropic management (i.e. reaping and cut-sedge sowing), has turned this species into a determinant factor conditioning both the structure and

physical-chemical properties of TDNP soils (Aguilera et al., 2011). Knowledge of its physical growth parameters becomes essential in order to assess the movement of water and solutes through the VZ (Pic. 4.1).

Picture 4.1. Dense young reed (*Phragmites australis*) stands with the presence of several *Tamarix canariensis* trees in the background.

Álvarez-Cobelas and Cirujano (2007) studied the responses of emergent vegetation to environmental factors in TDNP. They found out that growth rates of cut-sedge were higher at NE sites, ranging from 0.001 d^{-1} to 0.022 d^{-1}, whereas reed growth was similar at all sites, ranging between 0.001 d^{-1} and 0.045 d^{-1}. Sedimentary nutrients displayed significant relationships with plant growth rates. While *Cladium* growth rate was positively related with nitrogen, *Phragmites* growth rate was negatively related with the N:P ratio. *Typha* growth rate was negatively related with sedimentary nitrogen and phosphorus. Water level was weakly but positively related with growth rates of *Cladium* and *Typha*.

One of the most important results obtained by these authors is the opposite relation of cut-sedge and reed cover with average flooding in the preceding year, positive for the former and negative for the last (Álvarez-Cobelas and Cirujano, 2007; Cirujano et al., 2010). Besides that, there is a significant negative relationship between sedimentary phosphorus and cut-sedge biomass. On the contrary, reed biomass could be controlled by water level variability (positive relationship) as well as by averaged water level of the preceding year (negative relationship). Cattail biomass appeared to be related with sedimentary phosphorus (Álvarez-Cobelas and Cirujano, 2007).

During 2000, 2001, 2002 and 2008, both reed and cut-sedge attained their highest biomass at NE sites, coinciding with the shallower sites of the wetland and river discharge sites (Álvarez-Cobelas and Cirujano, 2007; Cirujano et al., 2010). The aboveground: belowground biomass ratio of these helophytes in TDNP is lower than in most wetlands, indicating the power of their root system. However, the ratio for reed increased from 1.24 in 2002 to 2.33 in 2008 (Cirujano et al., 2010). Aerial biomass of annual plant populations was negligible before 2006 but as a result of a heavy drought, they thrived later and peaked in 2007 and 2008. The relationship between above and belowground biomass in annual plants decreased, changing from 7.3 in 2007 to 0.61 in 2008.

Regarding nutrient content of major helophytes in TDNP, cut-sedge shows the highest percentages of carbon contents, reed the highest percentages of nitrogen contents and cattail the highest phosphorus ones (Cirujano et al., 2007).

Finally, helophyte decomposition was a slow process for *Cladium* and *Phragmites* in TDNP, with 50% of the initial biomass being decomposed after 1.5 years. There were no significant correlations between environmental variables and decomposition rates. An initial phase of leaching with the highest rates ($p < 0.05$) of mass loss and nutrients occurred for both plant species. Plant litter decaying rates were roughly an order of magnitude lower than nutrient release rates in both species. These results suggest that slow decomposition rates of emergent plant biomass increases organic matter

sedimentation and reduces water quality at TDNP (Sánchez-Carrillo et al., 2001; Cirujano et al., 2010). This fact is enhanced by the usual lack of outflows from the anthropized closed system, contributing to increase eutrophication.

CHAPTER 5

Materials and methods

This chapter provides a description of the different sampling and laboratory materials and methods used for data gathering. Statistical and hydrological tools for data analysis are also presented. To facilitate reading and identification of methods, the chapter has been subdivided in seven sections according to the main methodological areas: characterization of soil functional types, vadose zone chemistry, vadose zone physics, soil moisture monitoring, vadose zone water flow model, hydrology and hydrochemistry and meteorological data and. Vadose zone characterization is limited to the top aquifer layer of the multi-layer system which is essentially constituted by the Quaternary marshy-lacustrine sediments here defined as SFT (see sections 4.4 and 4.5).

All field sampling campaigns and laboratory analyses were undertaken throughout the period 2006-2010. Additional and complementary data from bibliographic sources is also conveniently described and referenced. Soil analytical determinations have been performed at the laboratories of the Department of Edaphology of the Complutense University of Madrid and of the Soil Science Centre of the Alterra Research Institute from Wageningen UR in the Netherlands, whereas hydrochemical water analyses have been carried out by the laboratory of hydrochemistry of the Geological Survey of Spain.

Due to the relevant role of TDNP peat soils for system dynamics, an independent intensive study focusing on the characteristics of this material regarding the presence of cracks and pipes and the occurrence of smouldering fires was conducted in 2009. Several specific field sampling campaigns and laboratory analyses on the physical and chemical properties of peat were performed. An important part of these results have been published in the book edited version of the Master thesis of Jiménez-Pinilla (2011). Therefore, for further information which has not been considered essential for this thesis the reader is referred to this publication.

Unless otherwise stated, the spreadsheet Microsoft Office Excel has been used for quantitative data management, analysis and representation. All maps have been elaborated with ArcGis 9.3 developed by ESRI.

5.1. Mapping of soil functional types

The concept of SFT of sedimentary materials regarding their hydraulic properties as constituents of the Quaternary VZ of TDNP was introduced in section 4.5. These functional types provide the basis for the particular analyses and discussions presented in this thesis. Their definition has been based on their specific hydraulic, morphometric and physic-chemical properties as described in sections 5.2 and 5.3.

The next basic step to be able to spatially contextualize the results of this thesis was to elaborate a map of the main distribution of these soil types in TDNP. The map has been based on the information provided by 61 descriptive columns up to 120 cm deep which were randomly sampled in January 2008 all over TDNP with an Eijkelkamp P1.01 auger (Fig. 5.1). Additionally, another 64 random profiles were described in N and NW areas throughout two sampling campaigns in September and December 2009 (Fig. 5.1). Complementary information provided by the map of sedimentary lithologies from Dominguez-Castro et al. (2006) and the lithological columns described in García-Hidalgo et al. (1995) has also been used.

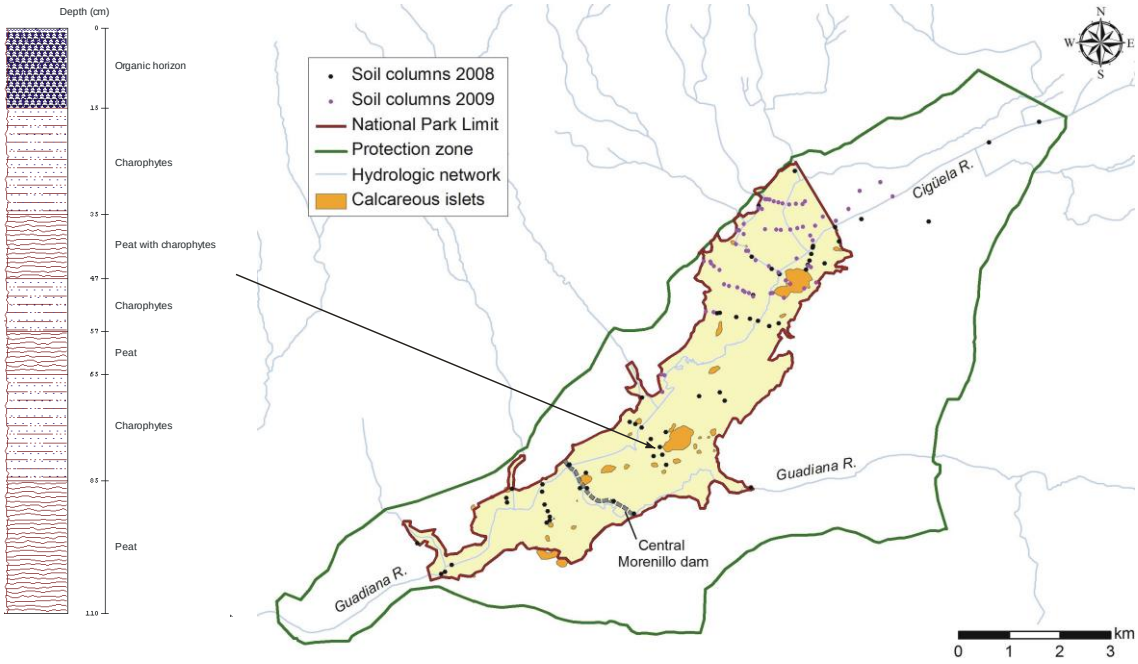

Fig. 5.1. Location of sampling points where soil columns were bored and described during 2008 and 2009 field campaigns in the Las Tablas de Daimiel National Park (TDNP) area. At the time of sampling, most rivers, ditches and streams of the hydrologic network were dry. An example of one of the descriptive columns with typical arrangement of sediments is shown on the left (all descriptive columns can be found in appendix A).

5.*2. Vadose zone chemistry*

This section describes the methodology used to characterize both the amount and distribution of mobile solutes stored in the VZ of TDNP that are readily available to be washed and transported to the groundwater by infiltrating waters. The relationship of these solutes to certain environmental factors is explored through the application of multivariate redundancy analysis. Moreover, the observations on soil chemistry have contributed to the definition of soil functional types.

5.2.1. Sampling and laboratory analyses

Sampling was carried out on July 2006 under dry soil conditions. A total of 111 disturbed soil samples were taken every 20 cm, from the topsoil to a maximum of 120 cm deep, in 22 points located along four transects, three transversal and one longitudinal (Fig. 5.2). Choice of sampling points was pseudo-random, conditioned by the limited accessibility to some inner areas of TDNP, but still ensuring independence of observations between them. The chosen transects allowed to obtain representative samples of the different soil types and the microtopographic variability. Special care has been taken to adequately represent variability in the two main directions, NE-SW and NW-SE, which define the flux of water and sediments in the Park.

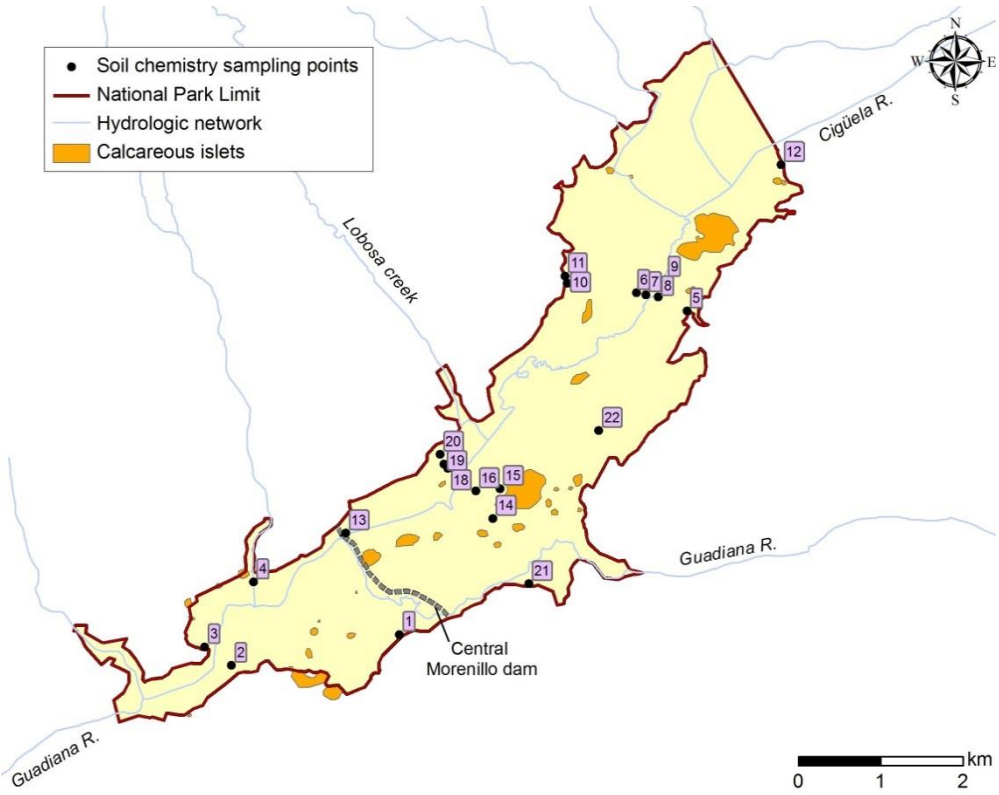

Fig. 5.2. Location of sampling points inside Las Tablas de Daimiel National Park (TDNP) for vadose zone chemical characterization. At the time of sampling in July 2006 dry conditions prevailed and the hydrologic network was virtually inactive. However, pseudo-random sampling points' arrangement accounts for variability associated to main water flux directions as well as soil types and microtopgraphic variations inside TDNP (see text for further discussion).

Samples were gathered with an Eijkelkamp P1.01 auger (Pic. 5.1). They were kept in plastic bags and air dried before their analytical processing. Unless otherwise stated all soil chemical analyses have been performed following ISRIC (International Soil Reference and Information Centre) procedures (Van Reeuwijk, 2002). Mobile soil solutes were determined in 1:5 soil-water extracts: sodium and potassium (atomic emission spectrophotometry), calcium, magnesium, sulfate, chloride, bicarbonate, nitrate, nitrite, ammonium, phosphate and silica (absortion spectrophotometry), carbonate (volumetry) and boron (ICP/AES). The electrical conductivity of the 1:5 soil-water extracts was measured by electrometry. In addition, the following complementary determinations were carried out on the solid matrix (Pic. 5.2): pH in 1:2.5 soil suspensions both in water and 1 M KCl solution (potentiometric determination), organic carbon (Walkley-Black method), nitrogen (Kjeldahl method), available phosphorus (Olsen method) and carbonates (Piper acid neutralization).

Picture 5.1. Eijkelkamp P1.01 auger used for soil sampling in Las Tablas de Daimiel National Park.

In February and April 2009, 19 samples were taken for specific peat chemistry analysis. They were subjected to the same analytical determinations as described in the previous paragraph, and also for cation exchange capacity and base saturation. These data was published by Jiménez-Pinilla (2011) and, although it has not been included in the multivariate analysis presented in this thesis, it will be mentioned when convenient.

Picture 5.2. Laboratory analyses for soil chemistry determinations: a) preparation of 1:5 soil-water extracts; b) total nitrogen determination through Kjeldahl distillation method; c) samples and spectrophotometer for available phosphorus determination through Olsen method; d) process of organic matter determination through Walkley-Black method with a semi-automatic agitator for titration.

5.2.2. Statistical analyses

The variables under study were subjected to a descriptive statistical analysis where mean, median, maximum, minimum, standard deviation, coefficients of variation, skewness and kurtosis were calculated. Relationships and associations between variables were assessed by means of Pearson correlation analysis.

On the other hand, the multiple regression approach "trend surface analysis" (TSA) was conducted to detect spatial trends in the data (Gittins, 1968 in Tiemeyer et al., 2007). The three possible pairwise combinations between spatial coordinates latitude-longitude-altitude were tested as model predictors. Both mean and median values of each of the 20 parameters analysed in each sampling point were used as dependent chemical variables.

One-way analysis of variance (ANOVA) was performed to evaluate significant differences between mean values of chemical variables at different depths. Prior to this, variables were tested in terms of their normality (Kolmogorov-Smirnov test) and homogeneity of variances across the levels of the factor (Levene's test). When F-test was significant at a 0.05 probability level, comparisons between the means were made using the least significance difference (LSD) and Tukey HSD multiple range tests.

Finally, in order to integrate all the information on spatial variability and relationships between soil chemical variables and environmental factors, a multivariate gradient analysis was carried out (Leps and Smilauer, 2003). The multivariate gradient analysis couples ordination and multiple regression techniques. The purpose of ordination is to find canonical axes that explain the maximum variability in the chemical composition of the samples. Unconstrained ordination or indirect gradient analysis seeks the variables that best explain the composition (and they are taken as ordination axes). On the other hand, in constrained ordination or direct gradient analysis, variability is only explained in terms of the measured environmental variables or factors. In the first case

ordination axes correspond to the directions of maximum variability in the dataset, while in the second one they represent the maximum variability that can be explained by the environmental factors. Both approaches are complementary. Through the indirect analysis the main variability in composition is obtained, while with the direct method only the variability associated to the environmental factors is considered.

According to the results of the gradient length analysis (Hill and Gauch, 1980) performed previously on the response dataset, a linear analysis model was selected instead of a unimodal one. Therefore, the methods used for unconstrained and constrained ordination were principal component analysis (PCA) and redundancy analysis (RDA), respectively. All PCA and RDA analyses were performed on the untransformed data, standardized and based on the correlation matrix. In the case of PCA, chemical variables were centred and standardized, while for RDA they were standardized by error variance. Additionally, two different Monte Carlo permutation tests were performed to evaluate the signification of ordination axes, one for just the first axis and the other one for all canonical axes together (sum of canonical eigenvalues). Also, two different kinds of permutations have been applied for each test: unconstrained and constrained for linear transects (see section 5.2.1).

The results of the ordination analysis were visualized by means of correlation biplots and triplots. These graphs allow representing correlations and associations among chemical variables, environmental factors and/or sampling points on the first two ordination axes.

All analyses and statistical tests were performed using CANOCO for Windows 4.5 (Leps and Smilauer, 2003), SPSS 12.0 (Pardo and Ruiz, 2001) and the application XLSTAT 2009.3.02 for Microsoft Excel developed by Addinsoft.

5.3. Vadose zone physics

Determination of TDNP soils' physical properties is essential to understand how water and solutes flow through them and, thus, to define the functional types which constitute the VZ of the top aquifer layer. Intensive field and laboratory work has allowed for the determination of several physical parameters: texture, bulk density, saturated hydraulic conductivity, infiltration curves, water repellency, capillary wetting rate, and water retention and hydraulic conductivity curves. All these information has provided the basis for building a VZ water flow model and analyse the peat-fire relation, which, in turn, constitute tools to support Park management.

Due to the large number of physical parameters considered in this research, this section has been subdivided into three subsections according to the main types of soil physical analyses.

5.3.1. Soil water repellency and wetting rate

Among the most common measurement techniques to quantify the degree of SWR described in Letey et al. (2000), the "water drop penetration time" (WDPT) test (Dekker and Jungerius, 1990; Bisdom et al., 1993; Dekker and Ritsema, 1994) has been chosen because it is simple, inexpensive and easy to perform in the field and the laboratory, while broadly determines the presence of SWR and how long it persists (Dekker et al., 2009). It involves placing droplets of distilled water onto the surface of a soil sample and recording the time for their complete infiltration (Pic. 5.3). An arbitrary WDPT threshold of 5 s has been generally used to distinguish between wettable and water repellent soils. Characterization of the degree and persistence of SWR in the laboratory has been performed according to the classification established by Dekker and Jungerius (1990) shown in Table 5.1.

Picture 5.3. Water drop penetration test (WDPT): water drop placed on top of dry peat material and recording of time for complete absorption.

The WDPT test was carried out in the field to determine "actual" SWR, as well as in the laboratory on both air-dried and oven-dried samples at different temperatures (25, 35, 45, 55, 65, 75 and 105 °C) to characterize "potential" SWR.

Table 5.1. Classes and degrees of soil water repellency based on the water drop penetration test (WDPT) as defined by Dekker and Jungerius (1990).

Class	Time for water drop penetration	Soil water repellency degree
1	< 5 s	Wettable
2	5–60 s	Slight
3	60–600 s	Strong
4	600–3600 s	Severe
5	>1 h	Extreme

The capillary wetting rate allows determining the influence of hydrophobicity on the ability of a given material to absorb water. Sealed field-moist samples taken in 100 cm^3 steel cylinders were kept in the laboratory at a constant temperature of 20 °C and a relative air humidity of 50-60%, for at least two days, to allow them to equilibrate with the ambient air humidity. Then the samples, within their steel cylinders, were subjected to a constant pressure head of -2.5 cm water applied at the bottom of the

sample. Samples were connected to a scale recording weight increment due to water absorption (Pic. 5.4). The experimental set-up was designed in such a way that water content increments of 0.2 vol% (≅ 0.2 g) were recorded until relatively constant water content was achieved over a period of one week (Dekker and Ritsema, 1996). In a similar way as Dekker et al. (1999) the experiment was sequentially repeated on the same samples after oven-drying them at different temperatures, 25 °C, 65 °C, and 105 °C, in order to investigate the influence of drying temperature on soil wetting rate.

Picture 5.4. Experimental setup for wetting rate determinations at the laboratory of the Soil Science Centre of the Alterra Research Institute in Wageningen.

Sampling for SWR characterization was carried out in two phases. In the first one in 2008 the objective was to determine the occurrence and degree of SWR in TDNP soil materials. The aim of the second one in 2009 was to investigate the seasonal influence on the hydrophobic properties of those materials that were found to be water repellent.

In May and June 2008 disturbed samples in plastic bags and replicate undisturbed samples in normalized 100 cm^3 steel cylinders (Eijkelkamp 07.01.53.NN) from different soil materials in depth were gathered in 5 randomly chosen points within TDNP (Pic. 5.5). A total of 29 disturbed and 31 undistubed samples were taken at 10 cm depth intervals from the topsoil to a maximum depth of 105 cm.

Picture 5.5. Collection of undisturbed soil samples in normalized 100 cm^3 steel cylinders (Eijkelkamp 07.01.53.NN) for soil water repellency analysis.

The steel cylinders were wrapped in plastic film and the plastic bags properly sealed and transported in boxes to the laboratories of the Soil Science Centre of the Alterra Research Institute in Wageningen, where SWR and wetting rate analyses were carried out throughout July, August and September 2008. Disturbed samples were splitted in two subsets where two kinds of actual and potential SWR determinations were performed with the WDPT test: i) one subset was left to air dry in a lab room at 20 °C and 35-65% for five weeks and gravimetric water content as percentage weight variation and SWR were periodically monitored; ii) the samples from the other subset were subsequently oven-dried at increasing temperatures (25, 35, 45, 55, 65, 75 and 105 °C) until constant weights were observed and gravimetric water contents and SWR conveniently assessed. The 100 cm^3 undisturbed samples were used for the wetting rate experiment as described above. Additionally, the bulk density of these samples could be collaterally determined after the last oven-drying at 105 °C.

The organic matter (OM) content of the disturbed samples was determined by loss on ignition (LOI). This was the analytical method available at the Alterra Soil Science laboratory at that moment. The principle of this method is that at sufficiently high temperatures typically ranging from 300 to 600 °C OM is combusted to ash and carbon dioxide, with the weight loss being proportional to the amount of OM in the sample (Konen et al., 2002; Sutherland, 1998; Heiri et al., 2001; Abella and Zimmer, 2007).

However, some authors have argued the inaccuracy of this method as soil composition (presence of clays, salts and organic carbon content) induces significant deviations of the values, particulary at low organic carbon (C_{org}) contents (Santisteban et al., 2004). Sieved samples (<2 mm) were oven-dried at 105 °C for 24 h and then weighed to measure moisture loss before LOI. The samples were then combusted at 450 °C for 16 h in a muffle furnace. This temperature selected for LOI was seen by Sutherland (1998), after a review of a variety of studies, as a trade-off between oxidation of OM without degradation of carbonates or significant modification of clays. LOI, expressed as percentage, was then calculated using the following equation:

$$LOI\ (\%) = ((DW_{105} - DW_{450}) / DW_{105}) * 100 \quad (1)$$

where DW_{105} and DW_{450} represent the dry weight (g) of the oven-dried sample at 105 °C and after combustion at 450 °C, respectively. Division of LOI by the conventional 'Von Bemmelen' factor of 1.724, which assumes 58% of OM is C_{org} (Broadbent, 1953) provides an estimate of C_{org}.

The seasonal effect on SWR was assessed in 2009 after two sampling campaigns, one in February and the other one in July. Initially, 100 points within TDNP areas dominated by organic materials were selected by simple random sampling. After in situ observation and description in depth using an Eijkelkamp P1.01 auger, 33 points were chosen for monitoring (Fig. 5.3). Each point was sampled at a given depth between 0 and 115 cm where target materials were found. On each sampling campaign, in situ determination of actual SWR by means of the WDPT test and collection of disturbed samples for laboratory analysis of potential SWR after oven-drying at 105 °C were carried out. Besides that, organic carbon was determined on the February samples through the Walkley-Black method.

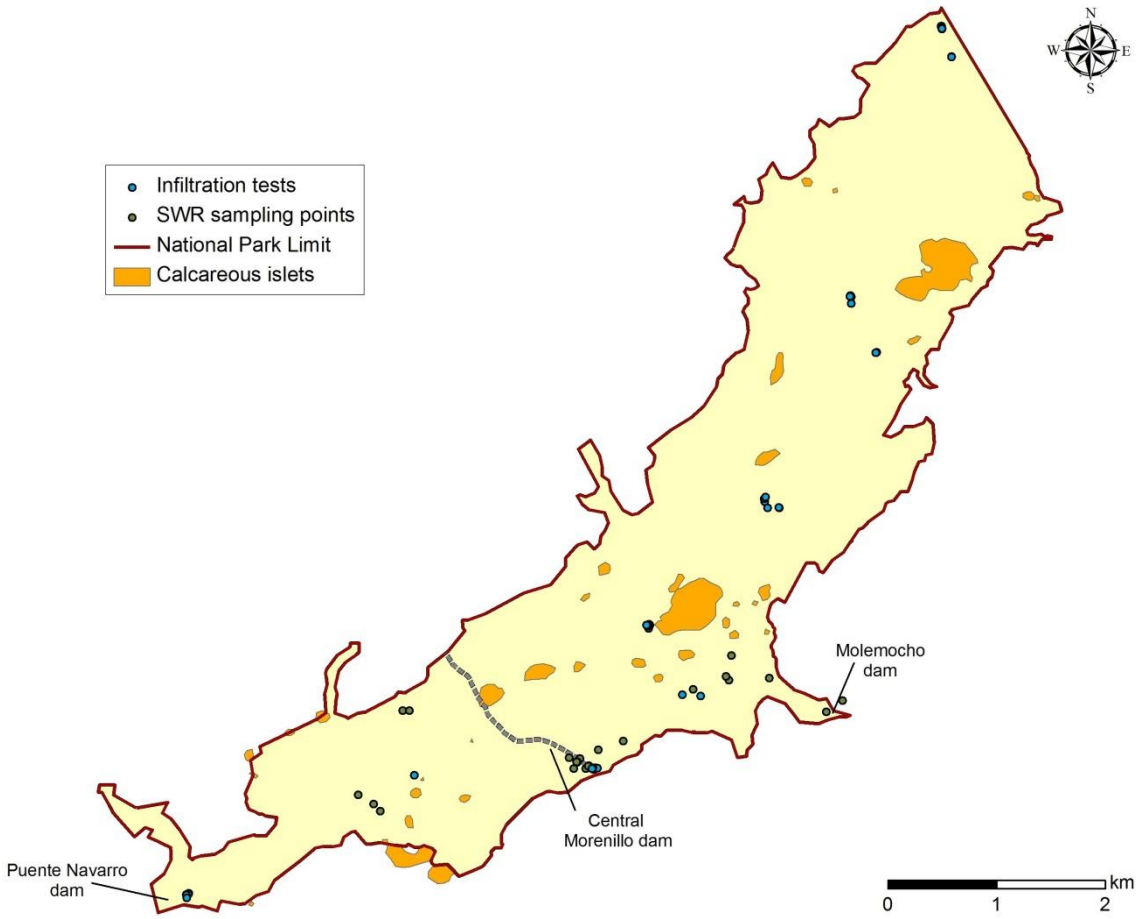

Fig. 5.3. Locations of infiltration tests carried out in 2008 and seasonal soil water repellency (SWR) monitoring sites in February and July 2009 within Las Tablas de Daimiel National Park (TDNP) limit. Several infiltration tests were performed in nearby sites in areas were major soil types were found. SWR sampling points are located in places dominated by organic materials.

5.3.2. Bulk density, soil hydraulic parameters and peat cracking

A total of 43 undisturbed soil cores of 100 cm^3 from the different soil materials were taken between April and May 2008. Average bulk density was determined by water loss weight (≅ volume) after drying overnight at 105 °C on at least three replicates per material. Average water retention of the soils at pF pressure points 0, 0.4, 1, 2, 2.3, 2.7, 3, 3.4 and 4.2 was determined on a minimum of 3 and a maximum of 5 replicates. Methods used for pF determination were: Eijkelkamp 08.01 sandbox for pF 0 to 2.0; Eijkelkamp 08.02 sand/kaolin box for pF 2.0 to 2.7; Eijkelkamp 08.03 pressure membrane apparatus for pF 3.0 to 4.2. Saturated hydraulic conductivity (K_s) was

measured with an Eijkelkamp 09.02 laboratory permeameter on either one or two replicates of each soil at constant varying heads between 0.4 and 1.9 cm (Pic. 5.6).

Additional determinations were carried out in the most widespread soil types in TDNP (charophyte layers and organic soils). Six undisturbed topsoil samples were collected in August 2008 in PVC cylinders of 10.3 cm diameter and 8.1 cm height. They were properly sealed with their lids, wrapped in plastic film and sent in boxes to the laboratories of the Soil Science Centre of the Alterra Research Institute in Wageningen. There the samples were slowly saturated from the bottom up for 72 hours (Pic. 5.7). The K_s was measured on the saturated samples using the constant head method as described by Stolte (1997). Immediately afterwards, the saturated samples were placed on an experimental setup for determination of water retention and hydraulic conductivity characteristics using Wind's evaporation method (Wind, 1968) as described in Wesseling et al. (2009). Weight loss due to evaporation is continuously monitored while 4 ceramic tensiometers monitor changes in soil water pressure at different depths in the range of -1000 cm to 0 cm (Pic. 5.8). Due to air entering the tensiometers at different pressure heads and other unexpected electronic problems, only partial hydraulic curves of these samples were finally available. The estimation of soil hydraulic parameters derived from these experiments is presented with the VZ water flow modelling approach (see section 5.5).

On the other hand, field observations on the characterisitcs of cracks and pipes in shrinking peats such as width, depth and interconnection were annotated throughout the studied period. Big hollows of decimetric thickness were often found in the subsoil. They apparently constitute the footprints of former peat fires (Moreno et al., 2012a).

Picture 5.6. Equipment for soil hydraulic parameters determinations: a) Eijkelkamp 08.01 sandbox for pF 0 to 2.0; b) Eijkelkamp 08.02 sand/kaolin box for pF 2.0 to 2.7; c) Eijkelkamp 08.03 pressure membrane apparatus for pF 3.0 to 4.2; d) Eijkelkamp 09.02 laboratory permeameter.

5.3.3. Infiltration

Topsoil infiltration curves of the different soil materials have been estimated through single-ring constant ponded head infiltration tests. A total of 49 infiltration tests (at least 6 per soil type) were performed throughout 2008 and 2009. Tests were carried out in randomly selected nearby locations within each dominant area (Fig. 5.3). Steel rings of 33 cm diameter and 40 cm height were used (Pic. 5.9). The imposed constant

head in the different tests varied between 10 cm and 12 cm. During the experiments elapsed times for each 1 cm head fall were recorded and water level restored to the constant head value until stable recordings were achieved.

Picture 5.7. a) Saturation of samples from the bottom up for 72 hours and b) experimental setup for saturated hydraulic determination as described by Stolte (1997) in the laboratory of Soil Science Centre of the Alterra Research Institute in Wageningen.

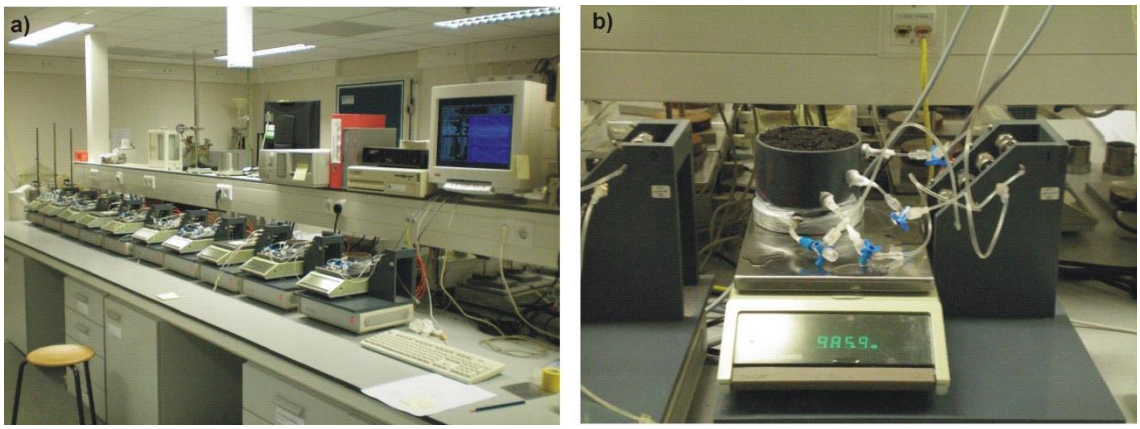

Picture 5.8. a) Experimental setup for determination of water retention and hydraulic conductivity characteristics using Wind's evaporation method (Wind, 1968) at the laboratory of Soil Science Centre of the Alterra Research Institute in Wageningen; b) detail of one of the samples in the Wind's evaporation method setup where weight loss due to evaporation is continuously monitored while 4 ceramic tensiometers monitor changes in soil water pressure at different depths in the range of -1000 cm to 0 cm.

Picture 5.9. Field works during constant head infiltration tests with steel rings in Las Tablas de Daimiel National Park.

Infiltration rates of each test were fitted to the Horton (Horton, 1940) and modified Kostiakov (Smith, 1972) empirical models. The main difference between these models is the kind of analytical function to be adjusted. Horton's model represents the infiltration process in time through an exponential equation:

$$f = f_c + (f_0 - f_c)^{-kt} \quad (2)$$

where f = infiltration capacity (mm h^{-1}); f_c = final infiltration capacity at the end of the infiltration test; f_0 = initial infiltration capacity; t = time (h); and k = fitting parameter representing the exponential decay constant (h^{-1}).

On contrary, the modified Kostiakov model uses a potential function as the best-fit equation for infiltration:

$$f = f_c + a\,t^{-b} \quad (3)$$

where *a* and *b* are empirical fitting parameters which rely on soil type, initial moisture content, rainfall rate, vegetative cover, etc. (Parhi et al., 2007).

Data from infiltration tests were also used to estimate saturated hydraulic conductivities according to the second method proposed by Wu et al (1999). This method was particularly developed to calculate K_s by best fit of a generalized solution to the infiltration curves that are measured by single-infiltrometers at relatively small constant ponded heads. It is based on the assumption that the last part of the infiltration event has reached steady state which corresponds to saturated conditions. Therefore, the last part of the accumulated infiltration curve is fitted to a linear equation and then K_s is calculated from:

$$K_s = \frac{A}{a * f} \quad (4)$$

where *A* is the slope of the linear regression; *a* is a dimensionless constant empirically determined to be equal to 0.9084; and *f* is a factor depending on the dimensions of the ring and the characteristics of the tested material which can be estimated by:

$$f = \left(\frac{H + 1/\alpha}{d + r/2}\right) + 1 \quad (5)$$

where *d* is the ring insertion depth; *r* is the radious of the ring infiltrometer; *H* is the ponded depth in the ring; and α a parameter depending on the soil material. For TDNP soils the following values of α suggested by Elrick and Reynolds (1992) have been used: α = 0.36 cm^{-1} for sandy and loamy sand textures, α = 0.04 cm^{-1} for clayey textures and the recommended value of α = 0.12 cm^{-1} for the rest of soils.

Estimation of fitting parameters in equations (2) and (3) was performed with SPSS 12.0 (Pardo and Ruiz, 2001).

5.4. Soil moisture and temperature monitoring

Soil moisture and temperature monitoring has supported soil physical determinations, smouldering peat fire characterization and VZ water flow modelling. A description of the different sampling campaigns and methods regarding these two variables is provided in the following paragraphs.

Both continous as well as discrete observations of soil water content were gathered throughout the studied period. Random soil profiles were sampled in May 2007 and June 2008 at 10 cm intervals to a maximum depth of 110 cm (Fig. 5.4). Samples were put into sealable plastic bags and transported to the laboratory for gravimetric determination of moisture content after overnight drying at 105 °C (Van Reeuwijk, 2002). Water content of randomly collected samples from peat and organic soils taken in February and July 2009 was also measured.

A superficial thermographic campaign was conducted in June 2009 using a Fluke Ti10 Thermal Imager, a fully radiometric infrared camera with a temperature measurement range between -20 °C and +250 °C and an accuracy of $\pm$ 2 °C.

On the other hand, a monitoring network of soil moisture and temperature in the upper levels of the VZ was installed in 2009. Instruments of Decagon Devices Inc. for continuous recording of soil moisture and temperature were installed in 12 monitoring points P01-P12 inside TDNP in April 2009 (Fig. 5.4). Each point was equipped with a datalogger (Em50 ECH2O) connected to two EC20 moisture sensors and three ECT temperature sensors (Pic. 5.10). The time interval for data recording was set in 15 minutes.

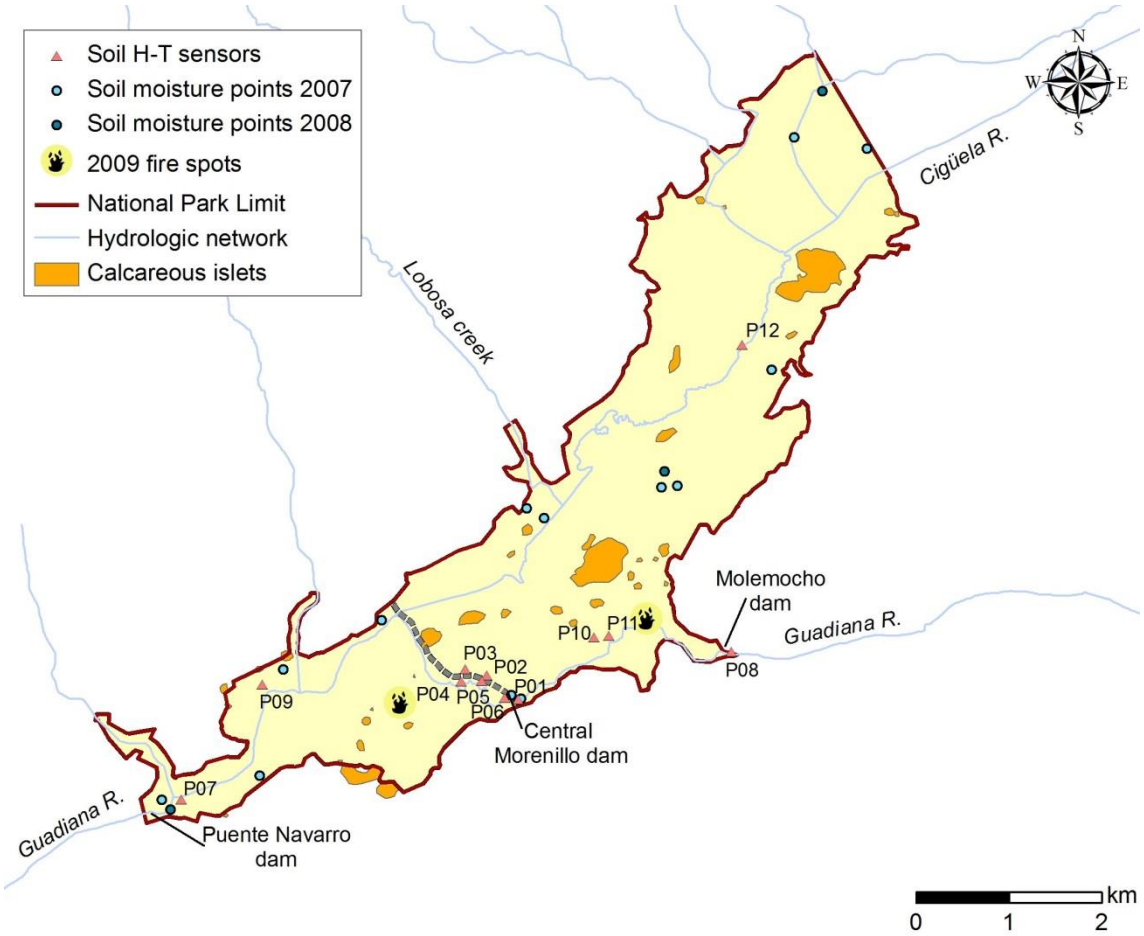

Fig. 5.4. Location of points inside Las Tablas de Daimiel National Park (TDNP) where random soil moisture profiles were sampled in depth in May 2007 and June 2008, respectively, and of the twelve locations (P01 to P12) where soil moisture (H) and temperature (T) sensors were installed in April 2009 for continuous monitoring. Locations of the spots where 2009 smouldering peat fires were first detected are also shown.

Table 5.2 shows the geographic location of each datalogger and the depth at which sensors were placed. Due to the variability in the sedimentary structure in TDNP depths at which sensors were installed varied from some points to others. Selected targets for soil moisture and temperature monitoring were preferably peats. A description of soil materials layout was noted at each point. Sensors were placed on the top surface layer and in deeper layers (Table 5.2). The deepest temperature sensors of dataloggers P01, P02, P03, P04, P06 and P07 were placed inside cavities to control inner air temperature. Therefore, the location of the sensors has provided information on the behaviour of both the material itself as well as the associated structures.

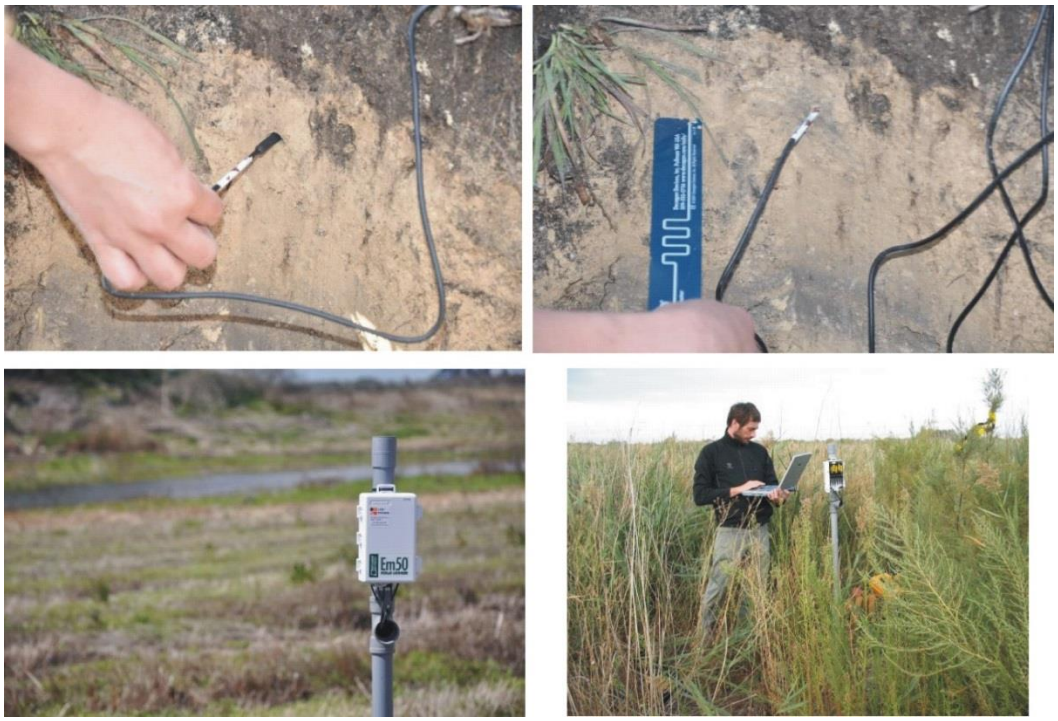

Picture 5.10. Soil moisture and temperature sensors installation and datalogging in Las Tablas de Daimiel National Park.

Table 5.2. Depth of temperature and moisture sensors at each monitoring point. GWL: groundwater level.

Datalogger identifier	Sensor depth (cm)				
	T1	T2	T3	H1	H2
P01	20	50	82	20	50
P02	20	50	100	20	50
P03	20	60	150	20	60
P04	20	61	120	20	61
P05	20	50	80	26	50
P06	20	30	100	22	35
P07	20	37	100	20	37
P08	20	50	65 (GWL)	20	50
P09	20	50	80	20	50
P10	20	50	80	20	50
P11	20	50	65 (GWL)	20	50
P12	20	50	80	20	50

5.5. Hydrology and Hydrochemistry

The subsurface hydrological and hydrochemical environment of TDNP has been extensively monitored in the period 2006-2010. Data on surface water and groundwater have been compiled and analysed to understand current hydrological behaviour and qualitative state of the TDNP system. Several hydrological and statistical tools have been applied for this purpose in order to develop a conceptual model of the dynamics of surface water-groundwater interactions. Due to limitations of accessibility and availability, most sampling points are located around TDNP margins. Nevertheless, the distribution of sampling points accounts for all the boundary conditions of the "closed" recharge system.

5.5.1. Sampling and laboratory analyses

The sampling network consists on 18 groundwater monitoring points (G) and 7 points for surface and ponding water (S) quality monitoring, located around the perimeter of TDNP (Fig. 5.5). Another point, named S-IW, located at a gauging station upstream from TDNP, in the Cigüela River, has been used to monitor incoming surface water to the Park. All groundwater sampling points were installed either in late 1970s and early 1980s by the Civil Engineering Service of Spain (SGOP) or by the Park Managing Authorities in the mid 1980s. Although available information on their construction characteristics is scarce (Table 5.3), the distribution of the sampling points around TDNP limits accounts for all the boundary conditions of the "closed" recharge system (Fig. 5.5). All surface water sampling points and 7 groundwater monitoring points (G-02, G-04, G-06, G-10, G-11, G-12 and G-13) were sampled regularly (approximately on a monthly basis) from April 2006 to October 2008. Besides this, surface water and groundwater samples from these points, except for S-5 and G-12, taken also by IGME in July 2003 and June 2004, have also been included. Point G-13 was dry most of the

time throughout the studied period and only 5 samples could be retrieved. The other 10 groundwater monitoring points belong to a complementary network and they were monitored at least twice a year in the same period, except for G-07, which was only sampled in September 2008 after construction by Park managers. Total depth of groundwater monitoring points is variable; they are supposed to be screened all through their length (García Rodríguez, 1996), except for G-06 and G-07 (Table 5.3). Lithostratigraphic columns of single points are only available for G-04, G-07, G-10 and G-11.

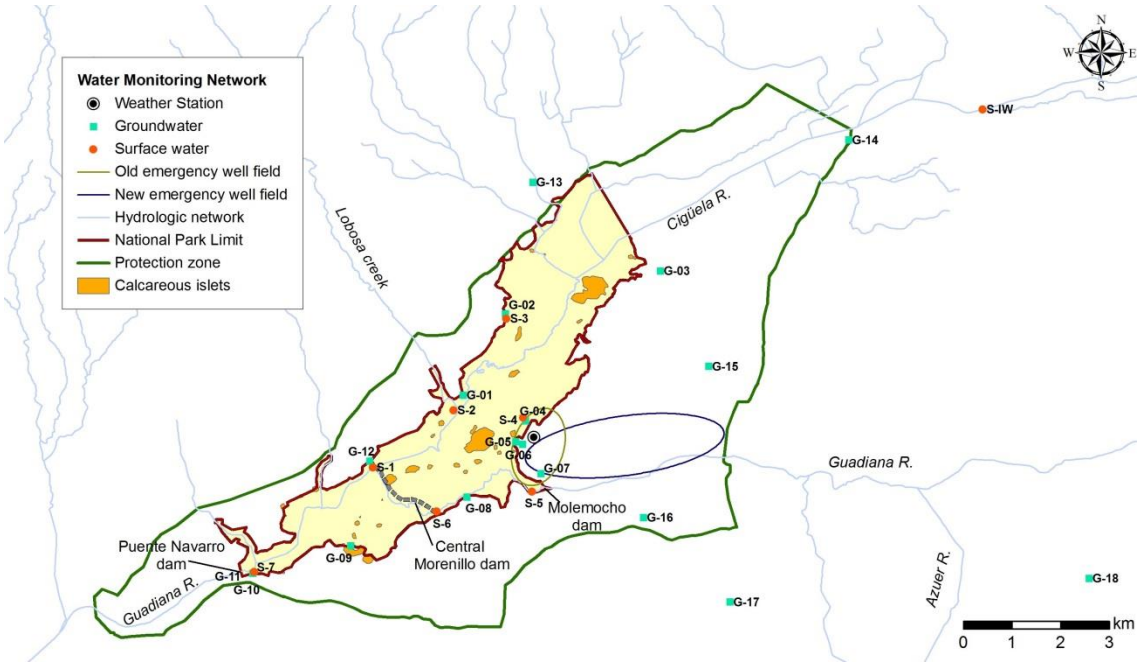

Fig. 5.5. Location of surface water and groundwater sampling points from the monitoring network in Las Tablas de Daimiel National Park (TDNP) area. Old and new emergency well field areas as well as the location of the weather station are also shown.

During each sampling campaign, depths to groundwater levels were measured from the casing top at each monitoring point and the water level in the Puente Navarro dam (close to S-7) was also registered. Surface and groundwater samples were taken in polyethylene bottles, filled to the brim, preserved at 4°C and delivered to the laboratory on the same day (Pic. 5.11). The pH and the electrical conductivity (EC) of the samples were measured both in the field and in the laboratory by electrometry.

Table 5.3. Characteristics of the groundwater monitoring points from the sampling network. Elevations of groundwater monitoring points have been taken from a digital elevation model (cell size 2 m x 2 m with ± 5 cm vertical resolution). Tubing depths have been measured with a probe. Lithol. Col.: availability of descriptive lithological column; y: yes; n: no; m: monthly; b: biannually; o: once.

Monitoring point	Elevation (masl)	Depth (m)	Fully screened	Lithol. Col.	Sampling interval
G-01	607.7	63	y	n	m
G-02	607.6	64	y	n	m
G-03	608.3	42	y	n	b
G-04	609.3	68	y	y	m
G-05	608.3	22	y	n	b
G-06	607.8	45	n	n	m
G-07	620.0	82	n	y	o
G-08	608.5	46	y	n	b
G-09	607.9	44	y	n	b
G-10	607.5	84	y	y	m
G-11	607.5	14	y	y	m
G-12	607.8	36	y	n	m
G-13	613.2	9.5	y	n	m
G-14	609.6	31	y	n	b
G-15	618.9	47	y	n	b
G-16	621.0	-	y	n	b
G-17	615.0	28	y	n	b
G-18	617.0	48	y	n	b

Subsequently, major and minor anions and cations (atomic emission spectrophotometry for sodium and potassium, ICP/AES for boron, ionic chromatography for bromide, and absorption spectrophotometry with continuous flow autoanalyzer for other elements), oxidability to potassium permanganate, heavy metals (atomic absorption spectrophotometry), and total organic nitrogen (Kjeldahl

method) and carbon (UNE-EN 1484 method) were determined at the laboratory of hydrochemistry of IGME.

Some complementary hydrochemical sampling campaigns were carried out throughout the studied period and the same parameters mentioned above determined on each sample. In March 2008, 19 surface and phreatic water points were sampled along a transect of the Cigüela River ditch (Castaño et al., 2011; Moreno et al., 2013). One of these points represents the old effluent from the wastewater treatment plant of Villarrubia de los Ojos (Fig. 2.2). Moreover, four samples from the Tajo-Segura transfer spread along the almost 300 km between the derivation point in Carrascosa (Cuenca) and TDNP were taken in May 2009.

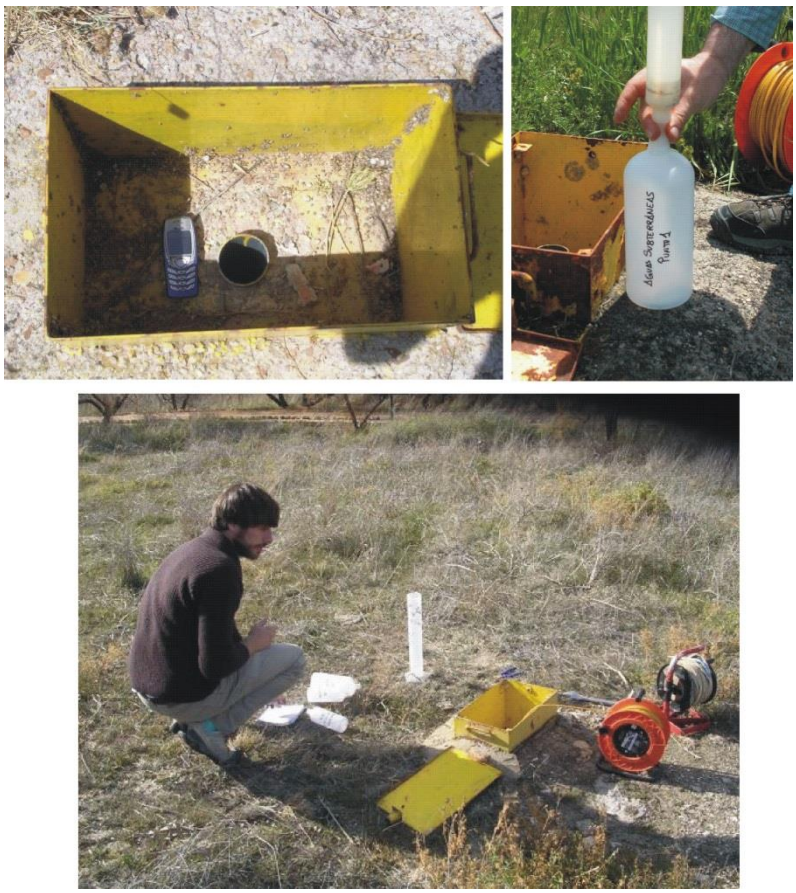

Picture 5.11. Detail of one of the groundwater monitoring points in Las Tablas de Daimiel National Park as well as groundwatwer sampling and groundwater level measurement.

In May 2008 and March 2010, samples were taken for analysis of the stable (^{2}H and ^{18}O) and radioactive (tritium) environmental isotopes of the water. The stable isotope ratios of water, $^{2}H/^{1}H$ and $^{18}O/^{16}O$, are expressed by convention as parts per thousand deviation relative to the standard VSMOW (Vienna Standard Mean Ocean Water). The widely used delta notation, $\delta^{2}H$ or $\delta^{18}O$ (‰), is defined as $(R_{SAMPLE}/R_{STANDARD}-1)\times 1000$, where R_{SAMPLE} and $R_{STANDARD}$ stand for the isotope ratios $^{2}H/^{1}H$ or $^{18}O/^{16}O$ of the sample and the standard, respectively. Stable isotopes were measured with a double entry isotope ratio mass spectrometer (IRMS) with analytical uncertainties of $\pm$ 0.2 ‰ for $\delta^{18}O$ and $\pm$ 1.5 ‰ for $\delta^{2}H$. The tritium radioisotope activity in water samples was determined by electrolytic enrichment and liquid scintillation counting. Tritium concentrations are expressed in tritium units (TU), where one TU corresponds to one tritium atom per 10^{18} hydrogen atoms, with a detection limit of 0.4 TU. All the isotopic analyses were performed at the laboratory of Isotopic Applications of CEDEX on the basis of the Collaborative Agreement for the Joint Laboratory IGME-CEDEX of Isotopic Hydrology.

Complementary time series data on monthly flooding surfaces in the period 1974-2010 and water transfers to the Park from the Tagus River in the period 1988-2010 have been provided by the TDNP Managing Authorities. Flooding areas have been continuously monitored on an approximately monthly basis since 1988, when the first water transfer was carried out, whereas earlier data were mostly estimated either through remote sensing (García Jiménez et al., 1992) or through multiple linear regression (Álvarez-Cobelas et al., 2001). A time series of groundwater levels in G-04 for the period 1974-2010 has been built with measured values and data provided IGME and Guadiana River Basin District Authority. Additionally, daily records between November 2007 and May 2009 from a sensor installed in G-04 have also been used. Information of isotopes in Ciudad Real rainfall has been taken from Díaz-Teijeiro et al. (2009). For comparison purposes, monthly groundwater level records for G-02, G-04, G-06, G-10 and G-11, ranging from December 1991 to June 1995, and water levels in the scale of the Puente Navarro dam in 1993 and 1994, have been taken from García Rodríguez (1996). Besides that, for the period 2009-2010, groundwater level data sets

for G-03, G-04, G-05, G-08, G-09, G-14 and G-15 have been completed with records available at the website of the Ministry of Rural and Marine Environment (MARM, 2011). Daily records for the period 2005-2010 from a sensor datalogger installed in G-08 have been also provided by the Guadiana River Basin District Authority.

5.5.2. Data analysis

A simple stepwise procedure for data analysis and hydrological characterization has been carried out:

i) General analysis of the hydrochemical characteristics of incoming surface water, ponding water and groundwater, using simple descriptive statistics to define general characteristics of sampling points.

ii) Grouping of groundwater monitoring points with homogenous hydrochemical behaviour. Clustering has been performed by means of hierarchical cluster analysis of the median, range and interquartile range values of the EC distribution in the groundwater monitoring points and the gauging station, using Euclidean distance and Ward's amalgamation method. The gauging station accounts for the variability associated to floods and freshets. The analysis has been based on the EC as it is the variable with the highest amount of observations and because this parameter reflects both the internal and external processes that determine the variability in groundwater composition, being directly related to the amount of total dissolved solids.

iii) Determination of response capacities of each group through the analysis of the interrelation between hydrochemistry and flooding by means of box-plots and Stiff diagrams.

iv) Study of the interaction between groundwater levels and flooding area to match hydrodynamic and hydrochemical responses of groundwater to flooding. The long-term temporal relationship between monthly groundwater level in a

representative monitoring point and flooding area has also been analysed through cross correlation.

v) Complementary analysis for validation of results with information provided by environmental isotopes of the water.

vi) Integration of hydrochemical, hydrodynamic, isotopic and flooding interrelations to define a conceptual model of zonal hydrological behaviour with the support of available lithostratigraphic information.

Bivariate relationships and associations between variables have been assessed by means of Pearson correlation analysis. All statistical analyses have been performed with the application XLSTAT 2009.3.02 for Microsoft Excel developed by Addinsoft. Finally, in order to avoid misuse of linear interpolation in time series, in the plots presented in this study, solid lines have been drawn between observations separated by time-lags under 3 months and dashed lines to a maximum of 6 months intervals.

For the statistical analyses, concentrations of parameters below their detection limit have been replaced by half of this value (Shumway et al., 2002).

5.6. Vadose zone water flow modelling with SWAP

All the information obtained with the methods described in the previous sections has been integrated to build up a water flow model in the functional types of the VZ which can support TDNP management by, for example, predicting critical soil moisture conditions resulting from system drying out. The approach is based on the one-dimensional field scale SWAP model (Soil-Water-Atmosphere-Plant), which simulates soil moisture movement in the VZ in interaction with vegetation development in shallow systems, where transport processes are predominantly vertical (Kroes et al., 2008). The input data for the model are soil physical properties, vegetation growth parameters, and daily meteorological conditions. Furthermore, the model allows

considering preferential flow through macropores such as shrinking cracks in peat or clay.

5.6.1. Model description

SWAP ver. 3.2 is a computer model that simulates transport of water, solutes and heat in the VZ in interaction with vegetation development. In the vertical direction the model domain reaches from a plane just above the canopy to a plane in the shallow groundwater. In this zone the transport processes are predominantly vertical, thus SWAP is a one-dimensional, vertically directed model (Kroes et al., 2008). The program is designed for integrated modeling of the Soil-Water-Atmosphere-Plant system. Transport processes at field scale level and during entire growing seasons are considered. The upper boundary conditions are defined by the soil surface with or without vegetation and are controlled by the rates of potential evapotranspiration, irrigation, precipitation, and interception. The lateral boundary simulates the interaction with surface water systems (not considered in this study). The bottom boundary is located in the unsaturated zone or in the upper part of the groundwater and describes the interaction with regional groundwater.

Gradients of the soil water potential induce soil water movement. Darcy's equation is commonly used to quantify these soil water fluxes. For one-dimensional vertical flow, Darcy's equation can be written as:

$$q = -K(h)\frac{\partial(h+z)}{\partial z} \qquad (6)$$

where q is soil water flux density (positive upward) (cm d^{-1}), $K(h)$ is hydraulic conductivity (cm d^{-1}), h is soil water pressure head (cm) and z is the vertical coordinate (cm), taken positively upward.

SWAP calculates soil water flow solving the Richards' equation numerically with an implicit, backward, finite difference scheme. The equation includes terms for root water extraction and macropore exchange:

$$\frac{\partial \theta}{\partial t} = \frac{\partial \left[K(h)\left(\frac{\partial h}{\partial z} + 1 \right) \right]}{\partial z} - S_a(h) - S_m(h) \tag{7}$$

where θ is the volumetric water content (cm^3 cm^{-3}); t is the time (d); $K(h)$ is the hydraulic conductivity (cm d^{-1}); h is the soil water pressure head (cm), assumed to be positive to simplify notation; z is the vertical coordinate (cm), taken positively upward; $S_a(h)$ is the soil water extraction rate by plant roots (d^{-1}); and $S_m(h)$ is the exchange rate with macropores (d^{-1}).

The soil hydraulic functions are described by the Mualem-van Genuchten relations (Mualem, 1976; van Genuchten, 1980), with a modification near saturation based on the introduction of a small minimum capillary height h_e as a cut-off point, as described by Ippisch et al. (2006):

$$\theta(h) = \theta_r + (\theta_s - \theta_r) S_e(h) \tag{8}$$

$$S_e(h) = \begin{cases} \frac{1}{S_c}\left[1 + (\alpha h)^n \right]^{-m} & h > h_e \\ 1 & h \le h_e \end{cases} \tag{9}$$

$$K(S_e) = \begin{cases} K_s S_e^{\,L} \left[\frac{1 - \left(1 - \left(S_e S_c \right)^{1/m} \right)^m}{1 - \left(1 - \left(S_c \right)^{1/m} \right)^m} \right]^2 & S_e < 1 \\ 1 & S_e \ge 1 \end{cases} \tag{10}$$

where θ_s is the saturated water content ($cm^3\ cm^{-3}$); θ_r is the residual water content in the very dry range ($cm^3\ cm^{-3}$); α (>0, in cm^{-1}), n (>1, dimensionless) and m (taken equal to 1-1/n) are empirical shape factors; S_e is the effective saturation and $S_c = [1+(\alpha h_e)^n]^{-m}$ is the saturation at the cut-off point in the classical van Genuchten model; K_s (cm d^{-1}) is the saturated hydraulic conductivity; L, (dimensionless) is an empirical shape coefficient.

Scaling of main drying and main wetting curves describe hysteresis in the retention function. Surface runoff is only considered when the height of water ponding on the soil surface exceeds a critical depth. In the simple crop growth module (used in this study) the measured leaf area index, crop height, and rooting depth are prescribed as a function of crop development stage. SWAP simulates root water uptake and actual transpiration according to the model proposed by Feddes et al. (1978), where root water uptake S_a is described as a function of the pressure head, h:

$$S_a(h) = \alpha(h) S_p = \alpha(h)\left(\frac{T_p}{z_r}\right) \tag{11}$$

being S_p the potential water extraction rate of the roots (d^{-1}); z_r (cm) the thickness of the root zone; T_p the potential transpiration rate (cm d^{-1}); and $\alpha(h)$ the dimensionless semiempirical reduction factor due to water stress, varying between 0 and 1. The shape of the function $\alpha(h)$ depends on four user defined critical values of h, which are related to crop type and to potential transpiration rates. Integration of $S_a(h)$ over the rooting depth yields the actual transpiration rate. If the simple crop module is chosen, the root depth and density, the leaf area index, and the crop height are specified by the user as a function of the crop development stage.

Macroporosity can be caused by shrinking and cracking of soil, by plant roots, by soil fauna, or by tillage operations. The predominant feature of macropore flow is that precipitation and flooding water with solutes are routed into macropores at the soil surface, bypassing the reactive unsaturated soil. This water is transported rapidly

downward and distributed throughout different depths in the soil or groundwater. In SWAP, the inflow, vertical transport, and distribution of water are based on the macropore geometry which is described by characterizing the volume according to the two main properties, vertical continuity and persistency (van Schaik et al., 2010). With respect to vertical continuity, the macropores are divided into two domains: (i) the Main Bypass (MB) flow domain, which is the network of continuous, horizontal interconnected macropores, and (ii) the internal catchment (IC) domain, the discontinuous macropores ending at different depths. The internal catchment domain causes infiltration of macropore water at different, relatively shallow depth. The distribution of macropore volume throughout both domains is obtained by analytical equations with four basic input parameters: the depth of the A horizon (Z_{ah}) and the depth of the IC domain (Z_{ic}), the volumetric proportion of the IC domain at the soil surface (P_{ic}), and a shape factor exponent (m). With respect to persistency, the volume of each of the domains consists of partly: (i) static macropore volume, representing macropores that are permanently present, and (ii) dynamic macropore volume, that is, shrinkage cracks.

For this study, the macropore SWAP module has been used to model water flow through the huge cracks that progressively developed on TDNP peat soils throughout the studied period (see section 6.6.3). According to Hendriks (2004), for peat soils three shrinkage stages can be distinguished (Fig. 5.6):

1. Near-normal shrinkage: volume reduction equals nearly moisture loss, little air enters the pores and the peat matrix remains close to saturation.
2. Subnormal shrinkage: upon drying moisture loss exceeds volume reduction, air enters the relatively large pores while the small pores in the organic fibres, that form the 'skeleton' around the larger pores, remain water-filled.
3. Supernormal shrinkage: volume reduction exceeds by far moisture loss, small pores are emptied and the skeleton collapses, so that air is driven out of the larger pores and the matrix reaches its final, smallest volume when the moisture content is zero.

On the saturation line shrinkage equals moisture loss and the soil aggregate remains saturated.

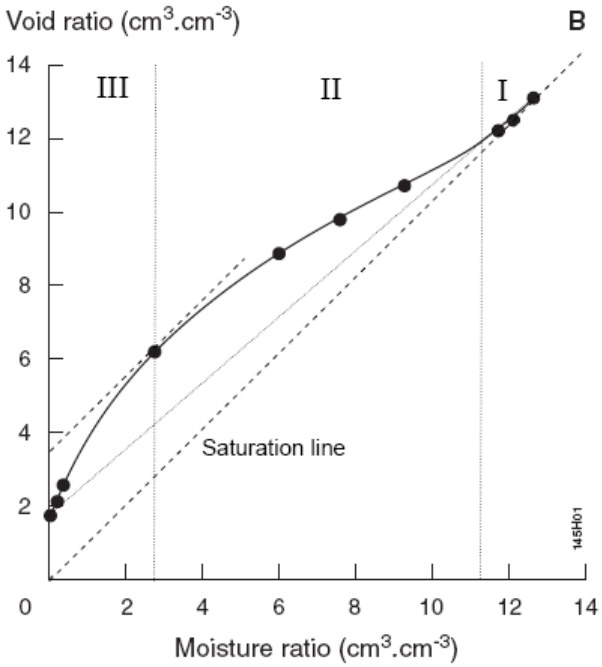

Fig. 5.6. Typical shrinkage characteristic of peat (after Hendriks, 2004), expressed as void ratio *e* (volume of pores / volume of solid phase) as a function of moisture ratio ϑ (volume of moisture / volume of solid phase), showing the three shrinkage stages: I Near-normal, II Subnormal, III Supernormal. Black dots are measurements while solid line is fit with Eq. (12).

SWAP uses the Hendriks' analytical equation to define the shrinkage curve of peat and peaty soils (Hendriks, 2004):

$$e(\vartheta)=\begin{cases} e_t\left[1+P\dfrac{\vartheta_t^{\alpha_H}(e^{-\beta\vartheta_t}-e^{-\beta})}{\vartheta_p^{\alpha_H}(e^{-\alpha_H}-e^{-\beta})}\right] & 0<\vartheta<\vartheta_a \\ e_t & \vartheta_a\le\vartheta<\vartheta_s \end{cases} \tag{12}$$

with:

$$e_t=e_0+(e_s-e_0)\frac{\vartheta}{\vartheta_s};\ e_s=\vartheta_s=\frac{\theta_s}{1-\theta_s} \tag{13}$$

$$\vartheta_t = \frac{\vartheta}{\vartheta_a};\ \vartheta_p = \frac{\alpha_H}{\beta} \quad 0 < \alpha_H < \beta \tag{14}$$

where e is the void ratio ($cm^3\ cm^{-3}$) which equals the ratio of pore volume to solid phase volume (1- θ_s) expressed as a function of the moisture ratio ϑ ($cm^3\ cm^{-3}$) of moisture volume to solid phase volume; e_s and ϑ_s are the void and the moisture ratio at saturation, respectively; e_0 is the void ratio at $\vartheta = 0$; ϑ_a is the moisture ratio at the transition of the near-normal shrinkage stage to the subnormal shrinkage stage, when air entry increases substantially; α_H, β and P are dimensionless shape fitting parameters.

5.6.2. Parameter estimation

K_s and θ_s (pF 0) were measured in the laboratory as described in section 5.3.2. In soil functional types were contradictory determinations of K_s were obtained due to the presence of secondary porosity in the sample, averaging with estimations through the Wu et al., (1999) method described in section 5.3.3., the H5 hierarchical pedotransfer function implemented in Rosetta ver. 1.2 (Schaap et al., 2001) and the Puckett point pedotransfer method in Soilpar ver. 2.00 (Acutis and Donatello, 2003) was carried out. The rest of the parameters for the water retention curve (θ_r, α, n and h_e) were fitted by nonlinear regression using sequential quadratic programming as optimization approach. Parameter L in the hydraulic conductivity function has often been given a physical interpretation as a pore-connectivity and tortuosity parameter normally assumed to be 0.5 (Mualem, 1976; van Genuchten, 1980, Simunek et al., 1998; Letts et al., 2000; Schwärzel et al., 2006; Vogel et al., 2001). However, an empirical approach by Schaap and Leij (2000) found that values of $L \leq -1$ are more suitable for fine textured soils as they cause a more gradual drop in conductivity than positive values. Nevertheless, parameter L shows low sensitivities in relation to soil water flow (van

Dam, 2000; Singh, 2005; Singh et al., 2010). Availability of conductivity measurements from the Wind evaporation method in major soil types (organic and charophytes) allowed for the fitting of *L*. This was done with the RETC ver. 6.02 computer program for describing the hydraulic properties of unsaturated soils (van Genuchten et al., 1991). The code uses a nonlinear least-squares optimization approach based on Marquardt's maximum neighbourhood method. For the remaining soils the values of *L* were either fixed to the usual 0.5 or to -1 (Schaap and Leij, 2000; Jhorar et al., 2004). Finally, the alpha parameter of the main wetting curve in case of hysteresis was approximated as 2α (Simunek et al., 1999).

The shrinking parameters of TDNP peat soils in Eq. (12) to (14) were estimated on the basis of the normalized curve (i.e. referenced to moisture ratio at saturation) of four fitted shrinking curves from a similar semi-decomposed Polish reed peat ranked as H5 in the von Post scale (appendix B). The von Post scale ranks peat decomposition on a scale of H1 to H10: H1 being pristine undecomposed fibrous peat and H10 being fully decomposed humified peat (Kechavarzi et al., 2010). However, the similarity between peat samples is relative and the Polish ones seem to have a lesser degree of decomposition than TDNP ones, as inferred from higher water contents at all matric potentials (appendix B). The estimated shape parameters α_H, β and *P* were those of the normalized curve, whereas the e_0 and ϑ_a values from the normalized curve were re-scaled multiplying them by the measured ϑ_s of TDNP peat samples. Water repellency of peat soils was taken into account in the calculation of sorptivity as a function of moisture content. Other physical input parameters related to macropore geometry, such as continuity, persistency and distribution in depth, as well as macropore water flow properties were initially estimated either through field observations or left as default values (appendix C).

5.6.3. Calibration and validation

Model calibrations have been performed within the period March 2007 - November 2009, during which extreme desiccation of TDNP took place leading to a smouldering peat fire in the summer of 2009. Due to the high heterogeneity of TDNP system, the model is intended to approximate the global average behaviour in typical soil profiles. Likewise in other previous SWAP models, it has been considered that the whole of the TDNP area may be represented by a collection of n sub-areas (Jhorar et al., 2004). In this case, n equals 10 and each sub-area is represented by a typical soil profile based on the arrangement of SFT. One different model has been carried out for each sub-area. Depth of soil profiles was determined by the minimum groundwater level along the period. Potential evapotranspiration was estimated by the Penman–Monteith equation, using daily weather data of solar radiation, air humidity, wind speed, and air temperature from the TDNP meteorological station, as well as vegetation characteristics such as minimum resistance, reflectance (albedo), and height. The characteristics of the most widespread plant species developed upon typical SFT profiles in TDNP during the sampling period (see section 4.7) were included in the different models: *Phragmites australis*, *Cochlearia glastifolia, Conya Canadensis*, *Tamarix canariensis* and *Juncus maritimus*. Physical growth parameters of these species for the simple crop module were either obtained from the literature or adapted from the additional crop data provided with the SWAP ver. 3.2 package (De Baets et al., 2007; Asaeda and Karunaratne, 2000; Hardej and Ozimek, 2002; Burba et al., 1999; Chun and Choi, 2009; Sala et al., 1996; Nagler et al., 2004; Lesica and Miles, 2001; Ladenburger et al., 2006; Sher et al., 2000). Two kinds of meteorological data files were tested on each model, one including daily rainfall amounts and the other detailed rainfall intensities which take into account actual amounts per time interval (see section 5.7). Bottom boundary conditions used were either averaged topographically corrected groundwater levels from the sampled groundwater monitoring points (see section 5.5) as a Dirichlet condition, or free drainage of soil profile (Nuemann condition) where the gradient of hydraulic head is assumed to be

equal to one at the bottom boundary (i.e. bottom flux is only provoked by gravity flow and the head pressure gradient equals zero), which sets bottom flux equal to the hydraulic conductivity of the lowest compartment:

$$\left[\frac{\partial(h+z)}{\partial z}\right]_{z=bot} = 1 \rightarrow q_{bot} = -K_n \quad (15)$$

The free drainage option is often applied for soil profiles with deep groundwater levels (Kroes et al., 2008). In peat soils preferential flow through shrinking cracks was simulated with the macropore flow module. Output files include yearly and daily water balances and daily values of state variables and fluxes at different depths.

In the same way as commonly used in other actual studies with SWAP, the soil water content in the soil profile (see section 5.4) has been used as calibration variable and the root mean squared error (RMSE) as criterion for evaluation of model performance (Singh et al., 2010; Sheikh and Van Loon, 2007; Scorza Júnior et al., 2010; Bonfante et al., 2010; van Schaik et al., 2010). The inclusion of hysteresis and frost in the models, as well as the adjustment of macropore geometry parameters in peats, was manually calibrated. In this sense, options and values of parameters were calibrated iteratively and separately within a chosen range according to field observations, while keeping the other parameters constant until the minimum RMSE criterion was met. This way, the sensitivity of model parameters could be evaluated at the same time (Hughes et al., 2010). On the basis of the literature review, where similar data and models where used, an upper bound for the RMSE of 0.1 cm^3 cm^{-3} has been chosen (Sheikh and Van Loon, 2007).

Model validation has been carried out by testing the model performance with the final values of the parameters obtained in the calibration on a partial dataset of the moisture sensors outside the calibration period. Model validations start the day after the last calibration day in May 2009 and end in either June or July 2009, before the steep decreases induced by extreme desiccation and smouldering fires were registered

by the sensors. The initial soil moisture condition was set to the values in depth provided by the sensors for the last calibration day.

5.6.4. Simulations

In order to assess the usefulness of the VZ water flow model as a support tool for Park management, SWAP simulations of soil water content in time have been carried out for a strong drainage scenario. As two of the main management concerns in TDNP are reed invasion and smouldering peat fires, model simulations have been focused on the estimation of suitable soil water conditions for the development of these problems. Therefore, simulations allow for determining the moment at which the critical soil water contents for optimal reed growth, reed die-back and risk of smouldering peat fires are reached under a typical extremely dry climatic context.

The critical soil water content values used in this study have been based on the literature of previous research on peat fires and *Phragmites australis* ecology. The gravimetric critical soil moisture condition for peat to start being combustible has been estimated in 125% in dry base (Rein et al., 2008; Reardon et al., 2007). Besides this, following Frandsen (1997), a 50% ignition probability has been estimated at a gravimetric moisture content of 60%.

Even though reed tolerates a wide range of flooding conditions, as reported in the review paper by Engloner (2009), four critical soil water contents can be identified in relation to its growth dynamics: optimal growth occurs at a soil water content around 96% of field capacity, normal growth above 67% of field capacity, deficient growth starts at 56% of field capacity, and mortality threshold is attained at approximately 25% of field capacity (Xie and Yang, 2009; Saltmarsh et al., 2006). After transformation of these values to the corresponding volumetric water contents on each TDNP soil

type, a 10% confidence interval has been defined for each critical value to account for estimation errors.

Synthetic daily weather data representing a series of dry hydrological years have been generated from historical observed records of the 20th century. As the weather records from the TDNP meteorological station are only available since 1982, the station 4121 from Ciudad Real (1920-present) has been used as the reference one for data generation (see section 5.7).

Simulations always start at the moment when flooding disappears and the saturated soil begins to desaturate. Therefore, the initial soil moisture condition is saturated soil profile or groundwater level set at 0 cm. No additional water inputs other than rain are considered. As no prescribed groundwater levels are available and the free drainage bottom boundary condition only applies with deep groundwater levels, for example deeper than 2 m (Sheikh and Van Loon, 2007), a flux controlled bottom boundary condition (i.e. Neumann condition) has been chosen for simulations. Bottom flux is formulated as an exponential function of groundwater levels (Massop and De Wit, 1994 in Kroes et al., 2008):

$$q_{bot} = ae^{(b|gwl|)} \quad (16)$$

Bottom flux q_{bot} (cm d^{-1}) at the start of a time step is calculated as a function of the groundwater level (*gwl*) of the previous time step. To determine empirical coefficients *a* (cm d^{-1}) and *b* (cm^{-1}), the optimization program "FitGwl" was used (Wesseling, 2012). The program calls SWAP with different parameter-values and finds the optimal set. Both the meteorological data (top boundary) and the soil physical characteristics of each soil layer are supposed to be known and the same period of data should be run for which measured groundwater levels are available. Therefore, FitGwl was run with the calibrated models resulting from the monitored periods (see section 5.6.3). The

selected goodness of fit statistic is the mean squared error normalized by the variance of the observed data (NMSE):

$$F = \frac{\sum_{i=1}^{N}\left(y_i^m - y_i^c\right)^2}{\sum_{i=1}^{N}\left(y_i^m - \mu^m\right)^2} \quad (17)$$

$$\mu^m = \frac{1}{N}\sum_{i=1}^{N} y_i^m \quad (18)$$

where *m* and *c* indicate measured and computed groundwater level values, respectively. The *F* statistic is dimensionless and a good performance is characterized by a value close to cero.

5.7. Weather data

Meteorological data is essential for hydrological studies and due to its transversal character for the different analyses performed in this thesis, it has been considered appropriate to specify the methodology for its gathering and processing in a separate section. In section 4.2 the need of narrowing the analysis of climatic series in the TDNP area to a time scale suitable for hydrological management and planning was stated. The following paragraphs describe the methods used for weather data construction and management.

Available meteorological data for the weather station 4112U (1982-2010), located inside TDNP (Fig. 5.5), and the station 4121 from Ciudad Real (1920-2010) have been provided by the Spanish Meteorology Agency (AEMET). Data included daily series of rainfall amount and minimum and maximum temperature. In the case of station 4121 data on wind speed, insolation duration and atmospheric pressure were also available

from 1961. Furthermore, TDNP Managing Authorities have provided series of 10 min interval records and daily averages for station 4112U in the period 2002-2009, including data on wind speed, solar radiation, relative air humidity, accumulated rainfall and maximum and average temperatures.

The Ciudad Real station is located at a distance of 25 km southwest from TDNP and compiles with the all the requirements described in FAO procedures (2006) to adequately represent the meteorological characteristics of the region: distance between stations < 50 km; identical atmospheric mechanisms determining precipitation and cloudiness; homogeneous physiography in the region. Similarity between rainfall and temperature records of both stations on daily, monthly and annual basis has been recently reported by Santisteban and Mediavilla (2012a).

Required weather data files for water flow modelling with SWAP (see section 5.6) are shown in Figure 5.7. In order to calculate potential evapotranspiration (ET_p) with the Penman-Monteith equation, daily data on maximum and minimum air temperature, solar radiation, vapour pressure and wind speed are required (Kroes et al., 2008; FAO, 2006). All these variables have been taken from the short time interval records provided by TDNP Managing Authorities for model calibration and validation in the period 2007-2009. Actual vapour pressure has been calculated from minimum temperature and maximum relative humidity according to the following equation (FAO, 2006):

$$e_a = 0.6108 * \exp\left[\frac{17.27 * T_{min}}{T_{min} + 237.3}\right] * \frac{HR_{max}}{100} \quad (19)$$

where e_a is the actual vapour pressure (kPa), T_{min} is the minimum temperature (°C) and HR_{max} is the maximum relative humidity (%).

Detailed rainfall data representing rainfall intensities per time interval (Fig. 5.7b) have been calculated from the available 10 min interval records.

a)

```
*****************************************************************************
* File name: Meteo_TD.007
* Contents: SWAP - Meteorological data of Tablas de Daimiel weather station
*****************************************************************************
* Comment area:
* Data starts in march 2007
*
*****************************************************************************
    Station   DD MM YYYY     RAD    Tmin    Tmax    HUM    WIND    RAIN   ETref
*             nr nr   nr    kJ/m2      C       C     kPa     m/s      mm      mm
*****************************************************************************
 'TD'    1    3    2007    19457.28    4.0    17.0    0.77    3.8    0.1    -99.9
 'TD'    2    3    2007    17876.16    3.0    18.0    0.72    3.0    0.1    -99.9
 'TD'    3    3    2007    18135.36    3.0    20.0    0.73    1.5    0.1    -99.9
 'TD'    4    3    2007    19025.28    1.0    22.0    0.62    2.7    0.1    -99.9
 'TD'    5    3    2007    19509.12    4.0    17.0    0.76    2.1    0.2    -99.9
 'TD'    6    3    2007    6246.72    2.0    13.0    0.65    2.5    0.0    -99.9
 'TD'    7    3    2007    16640.64    4.0    18.0    0.77    6.9    2.1    -99.9
 'TD'    8    3    2007    20390.40    6.0    15.0    0.59    5.8    0.0    -99.9
 'TD'    9    3    2007    18256.32    -1.0    17.0    0.49    2.0    0.0    -99.9
 'TD'    10    3    2007    17919.36    3.0    18.0    0.49    5.9    0.0    -99.9
 'TD'    11    3    2007    22412.16    2.0    16.0    0.51    3.1    0.0    -99.9
 'TD'    12    3    2007    21461.76    1.0    16.0    0.54    3.2    0.0    -99.9
 'TD'    13    3    2007    20520.00    4.0    17.0    0.72    5.4    0.0    -99.9
 'TD'    14    3    2007    21720.96    5.0    19.0    0.65    5.5    0.0    -99.9
```

b)

```
*****************************************************************************
* File name: Raindetail.007
* Contents:  Detailed rainfall input data
*****************************************************************************
* Comments: starting in March 2007
* 1. Input similar to tipping-bucket rain measurements:
*     t1   rainamount_1
*     t2   rainamount_2 (rain amount (mm) between t1 and t2)
* 2. In order to calculate the correct rainfall intensity, the first rainfall
*    record should be at or before the start of the simulation
*****************************************************************************

 Station     Day    Month    Year         Time        Amount
*              nr       nr      nr           d            mm
 'TD'     1     3     2007     0.000     0.0
 'TD'     1     3     2007     0.264     0.0
 'TD'     1     3     2007     0.271     0.1
 'TD'     2     3     2007     0.361     0.0
 'TD'     2     3     2007     0.368     0.1
 'TD'     3     3     2007     0.188     0.0
 'TD'     3     3     2007     0.194     0.1
 'TD'     4     3     2007     0.236     0.0
 'TD'     4     3     2007     0.243     0.1
 'TD'     5     3     2007     0.028     0.1
 'TD'     5     3     2007     0.250     0.0
 'TD'     5     3     2007     0.257     0.1
 'TD'     7     3     2007     0.486     2.1
 'TD'     26     3     2007     0.701     0.0
 'TD'     26     3     2007     0.743     0.6
 'TD'     27     3     2007     0.299     0.0
```

Fig. 5.7. Format of input weather data files for SWAP vadose zone water flow model a) basic daily weather data and b) detailed rainfall data representing rainfall intensities per time interval. RAD: solar radiation; T_{min}: minimum temperature; T_{max}: maximum temperature; HUM: air vapour pressure; WIND: wind speed; RAIN: rainfall amount; ET_{ref}: reference evapotranspiration.

For soil water flow simulations under typical regional drying scenarios (see section 5.6.4), the longer time series from the 4121 Ciudad Real station has been used. Wet, normal and dry hydrological years have been defined according to the distribution of annual rainfall amounts in the period 1920-2010: wet years as those with a total rainfall above the third quartile; normal years as those with a total rainfall between the first and third quartiles; and dry years with a total rainfall below the first quartile.

Then, a synthetic drying series of daily meteorological data has been built taking the mean values of the historical records of dry cycles. However, no data on relative air humidity is included in the Ciudad Real station series and records on wind speed and insolation were only available from 1961. For this reason, two approaches have been followed for daily ET_p estimation in model simulations:

a) Penman-Monteith using available data to estimate air humidity and solar radiation by means of the following equations (FAO, 2006):

$$e_a = 0.6108 * \exp\left[\frac{17.27*(T_{min}-2)}{(T_{min}-2)+237.3}\right] \quad (20)$$

where T_{min}-2 is an standard correction to approximate the dew point temperature in arid regions where air is not saturated yet at the minimum temperature (FAO, 2006).

$$R_s = \left(0.25 + 0.50\frac{n}{N}\right)R_a \quad (21)$$

where R_s is solar radiation (MJ m^{-2} d^{-1}); n accounts for actual duration of daily insolation (h); N is the maximum possible insolation duration (h); and R_a is the extraterrestrial radiation (MJ m^{-2} d^{-1}). N and R_a are calculated with the following equations:

$$N = \frac{24}{\pi}\omega_s \quad (22)$$

$$R_a = \frac{24*60}{\pi}G_{sc}d_r\left[\omega_s \sin(\varphi)\sin(\delta) + \cos(\varphi)\cos(\delta)\sin(\omega_s)\right] \quad (23)$$

being G_{sc} the solar constant (0.082 MJ m^{-2} min^{-1}); d_r the inverse relative Earth-Sun distance (dimensionless), calculated as a cosine function of the year date number (starting the count in January 1st); φ the latitude (rad); δ the solar declination (rad), calculated as a sine function of the year date number; and ω_s the radiation angle at sunset calculated as arccos[-tan(φ)tan(δ)].

b) ET_p estimated as the product of the reference evapotranspiration (ET_{ref}) by a crop factor (K_c) or a soil factor (K_{soil}) in case of bare soil. K_c values as a function of development stage for each vegetation type have been taken from reference tables in FAO (2006), whereas K_{soil} has been set to 1.15 to account for the increase in the ET_p due to the smaller albedo of a wet soil and the chance of having heat stored in the soil surface from previous dry periods (FAO, 2006). Daily ET_{ref} has been estimated through the Hargreaves equation (Hargreaves and Samani, 1985):

$$ET_{ref} = 0.0023\left(T_{mean} + 17.8\right)\left(T_{\max} - T_{\min}\right)^{0.5} R_a \quad (24)$$

$$ET_p = K_{c(soil)} ET_{ref} \quad (25)$$

where T_{mean} and $T_{\max}$ are the mean and maximum temperatures, respectively.

CHAPTER 6

Results and discussion

6.1. Soil functional types and spatial distribution

Four main soil materials have been defined on the basis of soil physical-chemical analyses and field observations (Aguilera et al., 2009a): charophyte layers (unconsolidated carbonated sediments biologically produced), clay, fluvial silt (fluvial deposits in rivers, ditches and drains) and organic (high OM content). These materials describe the recent sedimentary record (Holocene) and their average stratigraphic layout can be interpreted as the transition from a fluvial stage to a marshy-lacustrine stage (see section 4.4).

Picture 6.1. a) Samples of the different soil functional types (SFT) defined in Las Tablas de Daimiel National Park (TDNP). From left to right: clay, fluvial silt, peat, organic and undisturbed charophytes. From b) to e) different typical arrangement of SFT in the TDNP area.

The physical-chemical properties of each soil type are mainly determined by the parent material but other factors, basically anthropization (drainage, compacting) and edaphization, can be as important or even more than the former. Edaphization starts from the moment the "tablas" dry out and the soil development processes begin. The response of each soil material to anthropization is variable, the most extreme case being represented by dry peat combustion. Therefore, the defined soil units (SFT) also take into account the degrees of materials alteration and evolution (Table 6.1).

Three different types of charophyte layers have been further distinguished: i) undisturbed light coloured material, located in flat areas without vegetation and frequently flooded; ii) edaphized brownish-ochre charophytes, with a lesser degree of compacting and a greater OM content mainly originated on reed decomposition; iii) saline white charophytes, in clayey northern and western areas. Among organic soils, peat is the most relevant one from an environmental management point of view. Large areas where alternations of charophytes and peat layers occur have been considered independently, although the measurement of their physical properties has been carried out separately. Peat and charophyte layers are tabular levels which laterally overlap showing the transition between subenvironments with different depths of ponding water. These levels are sporadically crossed by nutrient rich fluvial silts that have filled up ditches and drains. Another kind of organic soil showing different physical-chemical properties than peat has also been described within peat and peat-charophytes alternations areas (Pic. 6.1).

Due to endorheic processes, salt efflorescences and salt crusts are locally present, being generally associated with strong seasonal changes in water level (Cirujano et al., 1996), but their marginal distribution is not significant enough to consider them as a separate SFT. Finally, the eastern border of TDNP shows some topographically elevated areas, constituted by different Tertiary and Quaternary deposits, which are never flooded and, thus, have not been considered in the study (edge zone).

Table 6.1. Main soil materials indentifed in the TDNP environment and soil functional types (SFT) defined based on their physical-chemical hydraulic properties as water and solute transmitters and storage in the Quaternary vadose zone underneath the Park.

Main soil materials	Soil functional types (SFT)
Charophyte layers	Undisturbed charophytes Edaphized charophytes Saline charophytes
Clay	Clay
Fluvial silt	Silt Peaty silt
Organic	Peat Organic

The map of the average distribution of SFT as constituents of the first meter of the VZ is shown in Figure 6.1. The basic 61 soil columns sampled in January 2008 to support map creation are presented in appendix A. The additional 64 columns sampled in 2009 in the northern TDNP area have been used as complementary information and have not been digitalized (appendix A). Top saline clayey and efflorescence materials are dominant in the NW, carbonated undisturbed charophyte layers in the main central flooding area, whereas peat rich materials expand throughout southern areas (Aguilera et al., 2009a; Aguilera et al., 2011; Moreno et al., 2010). In general, charophytes are widespread in the western area of TDNP (lacustrine environment), and peats in the eastern area (marshy environment), indicating higher water depth and oxygenation to the W (García-Hidalgo et al., 1995).

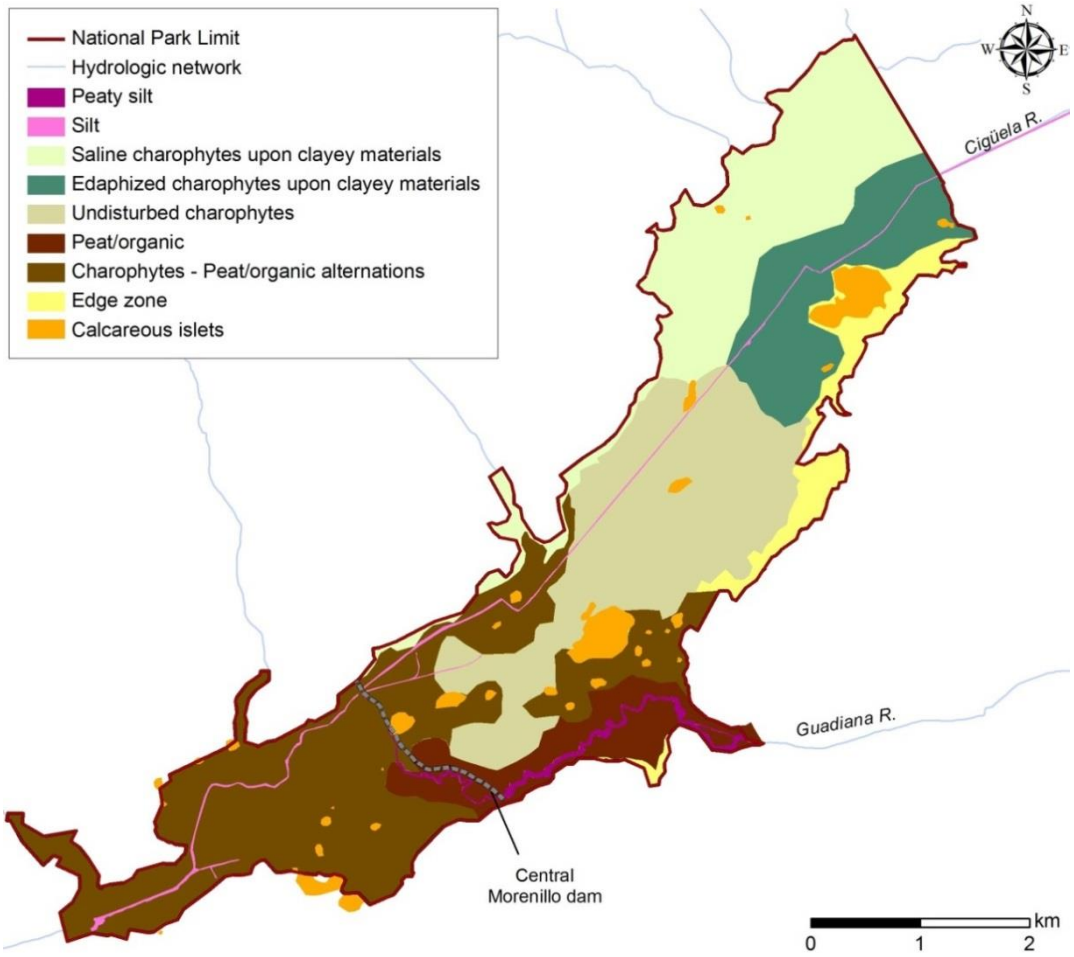

Fig. 6.1. Spatial distribution of soil functional types (SFT) within Las Tablas de Daimiel National Park (TDNP) according to the classification shown in Table 6.1.

The distribution of SFT is highly conditioned by the surface hydrologic network. It can be seen how the clayey northern area is further subdivided into two domains by the Cigüela River ditch, one saline on the right margin and the other one organic rich on the left margin. Longer and deeper floods take place on the left margin of the river due to its topographically lower elevation, supporting macrophyte development and OM accumulation in the topsoil. On contrary, higher areas in the northern right margin receive lesser amounts of flooding water and, thus, evaporation is a stronger controlling factor. Besides that, salt dissolution from saline clayey soils enhances salt concentration in the topsoil. Silty textured deposits accumulate in ditches and riverbeds as a normal depositional feature in fluvial environments. Less decomposed peat layers are dominant in the area of influence of the Guadiana River and peaty silts

are found in the Guadiana riverbed (ditch). This is mainly due to permanent and carbonated nature of the discharged groundwaters that used to slowly flow through it, contributing to increased vegetation growth and decay under anoxic conditions.

6.2. Vadose zone chemical characterization

The results presented in this section were published in an article in Geoderma (Aguilera et al., 2011). Although multivariate analysis techniques have recently become common tools in soil science (Vestin et al., 2006; González et al., 2007; Tiemeyer et al., 2007; Momtaz et al., 2009; Visconti et al., 2009), the application of redundancy analysis to explain variability in soil chemistry in terms of easily measurable environmental factors represents a pioneer approach. Besides, almost no data regarding soil chemistry in TDNP have been reported yet. Only one study has been found in which high resolution geochemical composition of a single 187 cm core in the northern inlet area is analysed (Santisteban et al., 2004). The complete dataset of soil chemical determinations in sampled points can be found in appendix D.

6.2.1. General chemical composition

Descriptive statistics for soil chemical variables are shown in Table 6.2. The average concentrations (mg l^{-1}) of major cations and anions for all soil-water extracts decrease as follows: calcium > magnesium > sodium > potassium and sulfate > chloride > bicarbonate > nitrate. The first three cations and the first two anions are the most abundant in salt affected soils (Schawb, 2000 in Visconti et al., 2009). The fact that sodium concentrations are larger than those of potassium is especially indicative of this affection (Bohn et al., 2001). Moreover, average electrical conductivities are over 3,000 µS cm^{-1}. High sulfate concentrations are due to the weathering and dissolution

of gypsic lithologies and to the prevailing oxidant conditions, while calcium comes from both, gypsum and carbonate dissolution.

The soil pH in KCl solution is an indicator of the potential acidity of soils. For the analysed soils values of this parameter are only slightly lower than those obtained for the pH in water. This is due to the abundance of alkaline cations (calcium and magnesium) in the exchange complex (Bohn et al., 2001) together with the pH-buffering effect exerted by the lithologically and biologically originated carbonates (mean value of 48.9%).

The observed coefficients of variation (CV) indicate very large variability in the data with the exception of pH and calcium. Variability is particularly high in the case of nutrients and minor elements. Similar results were obtained by Visconti et al. (2009) in saturation extracts from calcareous soils. This dispersion is related to the higher values found in the upper soil layers. In these cases, the use of medians instead of means as representative values of soil profiles is recommended (Zhang et al., 2008; Wang et al., 2009b). Medians can be considered less biased measurements of centralization when attempting to describe datasets with large variability.

Table 6.2. Chemical composition of 1:5 soil-water extracts and soil matrix samples (n = 111) from Las Tablas de Daimiel National Park (TDNP). Mean values in depth and overall descriptive statistics for each chemical parameter are shown. a: minimum; b: maximum; c: standard deviation; d: coefficient of variation; e: electrical conductivity; f: soil pH in water; g: soil pH in KCl solution; h: organic carbon; i: total Kjeldahl nitrogen; j: available phosphorus; k: carbonates expressed as

	Mean in depth													
Depth (cm)	0-20	20-40	40-60	60-80	80-100	100-120	Min[a]	Max[b]	Mean	Median	SD[c]	CV[d] (%)	Skewness	Kurtosis
Na^+ (mg l^{-1})	214	162	139	158	151	76	5	1185	163	123	170	104.3	2.8	11.8
K^+ (mg l^{-1})[m]	21	12	9	10	9	6	2	53	12	10	9	71.0	1.6	3.8
Ca^{2+} (mg l^{-1})	515	537	511	506	490	545	140	710	513	535	97	19.0	-2.0	4.6
Mg^{2+} (mg l^{-1})	284	250	222	246	239	140	13	1242	245	208	204	83.1	2.2	6.4
SO_4^{2-} (mg l^{-1})	1985	1963	1884	1948	1888	1780	285	5100	1930	1900	696	36.1	1.2	4.4
Cl^- (mg l^{-1})	483	384	307	339	343	118	6	2380	365	268	417	114.2	2.2	5.9
HCO_3^- (mg l^{-1})[m]	81.4	67.6	62.5	63.6	56.5	49.3	31.0	138.0	66.0	62.0	24.3	36.8	0.7	-0.1
NO_3^- (mg l^{-1})[m]	61.5	38.1	22.5	26.4	17.1	15.3	< 0.5	270.0	32.9	18.0	42.2	128.3	2.7	9.5
NO_2^- (mg l^{-1})	1.01	0.51	0.75	0.21	0.08	0.19	< 0.05	12.20	0.51	0.06	1.62	317.9	4.6	25.1
NH_4^+ (mg l^{-1})	0.94	0.89	1.23	1.70	0.93	0.61	< 0.05	8.50	1.13	0.52	1.65	146.0	2.3	6.1
PO_4^{3-} (mg l^{-1})[m]	0.32	0.27	< 0.04	0.02	0.02	< 0.04	< 0.04	2.54	0.12	< 0.04	0.37	302.9	4.2	19.7
SiO_2 (mg l^{-1})[m]	10.2	6.3	6.0	5.9	5.4	10.2	1.4	27.1	6.9	5.4	5.0	73.2	1.8	3.7
B (µg l^{-1})	139	121	17	74	75	< 50	< 50	737	83	0	158	190.2	1.9	3.1

Table 6.2. Continuation

Depth (cm)	Mean in depth						Min[a]	Max[b]	Mean	Median	SD[c]	CV[d] (%)	Skewness	Kurtosis
	0-20	20-40	40-60	60-80	80-100	100-120								
EC (µS cm^{-1})[e]	3998	3599	3424	3630	3473	2717	838	12090	3603	3280	1712	47.5	2.0	6.4
pH (H_2O)[f]	7.8	8.0	8.1	8.1	8.2	7.9	6.9	9.4	8.0	7.9	0.5	6.2	0.5	-0.1
pH (KCl)[g]	7.5	7.7	7.9	7.8	7.9	7.5	6.7	9.3	7.8	7.6	0.5	7.0	0.7	-0.2
C_{org} (%)[h,m]	6.1	4.7	2.9	3.5	3.3	1.9	0.1	22.1	4.1	3.1	3.9	94.7	1.8	4.9
Total N (%)[i,m]	0.56	0.40	0.27	0.34	0.28	0.23	0.04	1.21	0.37	0.27	0.29	79.2	1.0	0.1
P (mg kg^{-1})[j,m]	28	13	8	9	9	5	< 1	110	13	7	19	142.9	3.0	10.7
$CaCO_3$ (%)[k]	46.7	48.9	52.6	48.8	48.1	44.3	8.1	90.4	48.9	45.3	23.8	48.7	0.1	-1.3
C/N[l]	6.3	6.4	5.6	5.3	5.5	6.0	0.9	11.1	5.8	6.1	1.9	33.1	-0.2	0.2

All variables except for calcium show positive skewness due to the presence of large values. This indicates an either natural or anthropogenic enrichment (Zhang et al., 2008) of the topsoil. Agreeing again with the results from Visconti et al. (2009), pH and carbonates are the less asymmetric variables, showing a uniform distribution in depth. This was also reported by González et al. (2007) for another area of calcareous Fluvisols in central Spain. The absence of normality in the data, pointed out by the observed asymmetry together with the high kurtosis coefficients, was corroborated through the Kolmogorov-Smirnov test. Only bicarbonate and carbonates show approximately normal distributions. Given the huge soil system heterogeneity and the complex interactions among determinant factors, the no-normality in the distribution of physical-chemical properties is more the rule than the exception, as confirmed by other researchers (Young et al., 1999; Tiemeyer et al., 2007; Zhang et al., 2008; Momtaz et al., 2009; Visconti et al., 2009). This general absence of normality and symmetry is partially overcome, mainly the second one, through the logarithmic transformation of the data (Tiemeyer et al., 2007; Zhang et al., 2008; Momtaz et al., 2009; Visconti et al., 2009; Wang et al., 2009b).

The accumulation of nutrients (potassium, nitrate, phosphate, organic carbon, total nitrogen, and available phosphorus) in the topsoil was statistically proven by means of a one-way ANOVA taking the depth intervals as the factor (Table 6.2). Although ANOVA is robust against deviations from normality, the variables must be symmetrically distributed (Pardo and Ruiz, 2001). For this reason, the analysis was performed on the logarithmic transformation of the data, which also verifies the assumption of homogeneity of variances. Multiple range comparison tests (LSD and Tukey HSD) confirmed that significant statistical differences only exist between mean values in the topsoil (0-20 cm) and mean values in the other depth intervals. In this sense, depth is a key factor in delimiting the soil's aeration zone, where evaporation rates are highest and OM oxidation takes place with the subsequent release of inorganic forms. Nutrient accumulation in the upper soil layer with a sharp decrease in depth has been observed in different natural (Takii and Fukui, 1996; Vestin et al., 2006)

and anthropized (González et al., 2007; Tiemeyer et al., 2007; Esteller et al., 2009) environments.

Box-plots in Figure 6.2 show the distribution in depth of nutrients and pH. The decrease in soluble nutrient content with depth is coupled to a smooth increase in soil pH. This latter parameter shows a relatively homogeneous distribution along the profile and slightly basic values, as observed by González et al. (2007) and Miralles et al. (2009) in other Spanish regions. Soil pH in water ranges between 7.5 and 8.5, which is exactly the typical range for calcareous soils where pH is usually controlled by $CaCO_3$ dissolution (Bohn et al., 2001). Nitrate and potassium concentrations in the topsoil, varying between 0-200 mg l^{-1} and 6-53 mg l^{-1}, respectively, can be considered as very high for natural soils (Cobertera, 1993). Median values in this layer (49 mg l^{-1} for nitrate and 19.5 mg l^{-1} for potassium) are half of those found by Visconti et al. (2009) in saturation extracts from fertirrigated soils in the SE of Spain (99.2 mg l^{-1} for nitrate and 35.1 mg l^{-1} for potassium). Even though many empirical equations have been developed to predict the properties of saturation extracts, primarily electrical conductivity, from the properties of 1:5 soil-water extracts, there are not universally valid equations relating concentrations from both methods (Visconti et al., 2010). However it can be assumed that they would be higher in saturation extracts than in soil-water solution as found by the same authors for electrical conductivities. At the same time, nitrate concentrations are in the same order of magnitude as those obtained by Esteller et al. (2009) in vacuumed water from soils treated with biosolids and compost. Phosphate concentrations in aqueous extracts from topsoil layers range between 0 and 1.6 mg l^{-1} (median equals 0.2 mg l^{-1}) and are similar to those observed by the same authors in soils amended with organic wastes. On the other hand, ammonium concentrations in the topsoil are quite low due to oxidation processes (Carter, 1997 in Esteller et al., 2009), and they increase with depth as the environment becomes less oxidant.

Organic carbon content is particularly high in the first 20 cm of the soil profile (0.9 to 14% and median of 5.7%), as well as total nitrogen (0.1 to 1.2% and median of 0.5%)

and, to a lesser extent, available phosphorus (0 to 109.9 mg kg^{-1} and median of 19.7 mg kg^{-1}). Median values of these three variables are considered as "very high" for natural soils (Cobertera, 1993). When comparing these results to other researches worldwide, it can be drawn that nutrient content in TDNP topsoils is similar to that in organic soils of other disturbed wetlands (Koerselman et al., 1993; Mesnage et al., 2002; Aldous et al., 2005; Tiemeyer et al., 2007; Zhang et al., 2008), and often higher than that in agricultural or forest areas (González et al., 2007; Esteller et al., 2009; Fernández et al., 2009; Lamparter et al., 2009; Miralles et al., 2009; Momtaz et al., 2009; Romanyà and Rovira, 2009; Wang et al., 2009a,b).

The concentrations of available phosphorus in the soil are much higher than those of inorganic phosphorus in the aqueous extracts (Table 6.2). Available phosphorus concentration is strongly regulated by chemical sorption processes and it is enhanced by drainage conditions in the topsoil (Olila et al., 1997; Reddy and DeLaune, 2008). Large carbonates and calcium amounts together with the slightly basic pH condition inorganic phosphorus sorption onto calcium carbonate surfaces, either through calcium phosphate formation or through carbonate displacement by hydrogen phosphate anions (Olila et al., 1997; Bohn et al., 2001; Reddy and DeLaune, 2008). Another relevant mechanism for inorganic phosphorus retention would be the sorption to organic compounds. Low phosphorus concentrations in the soil-solution can be also explained by the fact that calcium phosphate is hardly soluble at pH values over 8 (Lindsay and Moreno in Bohn et al., 2001).

Available phosphorus decrease in depth is very sharp. This variable also displays large dispersion towards extreme values with a CV of 143% and a skewness coefficient of 3 (Table 6.2). Organic carbon and associated total nitrogen decrease more gradually in depth. This fact was also observed by Esteller et al. (2009) and Niedermeier and Robinson (2009), although in the former case the decrease in available phosphorus concentration was gradual too. On the other hand, in the Mediterranean carbonated materials analysed by González et al. (2007) the decrease in organic carbon and total nitrogen in the first 75 cm of the soil profile was very noticeable. This is due to the fact

that in calcareous soils the OM accumulation horizon is very thin, given the large mineralization rates. However, TDNP soils have accumulated large amounts of OM during past reducing conditions. Finally, the organic carbon to total nitrogen ratio (C/N) keeps median values between 5 and 6, when the typical value for balanced microbial activity is around 10 (Bohn et al., 2001; Reddy and DeLaune, 2008). This indicates a mineralization trend in TDNP soils supported by dry conditions.

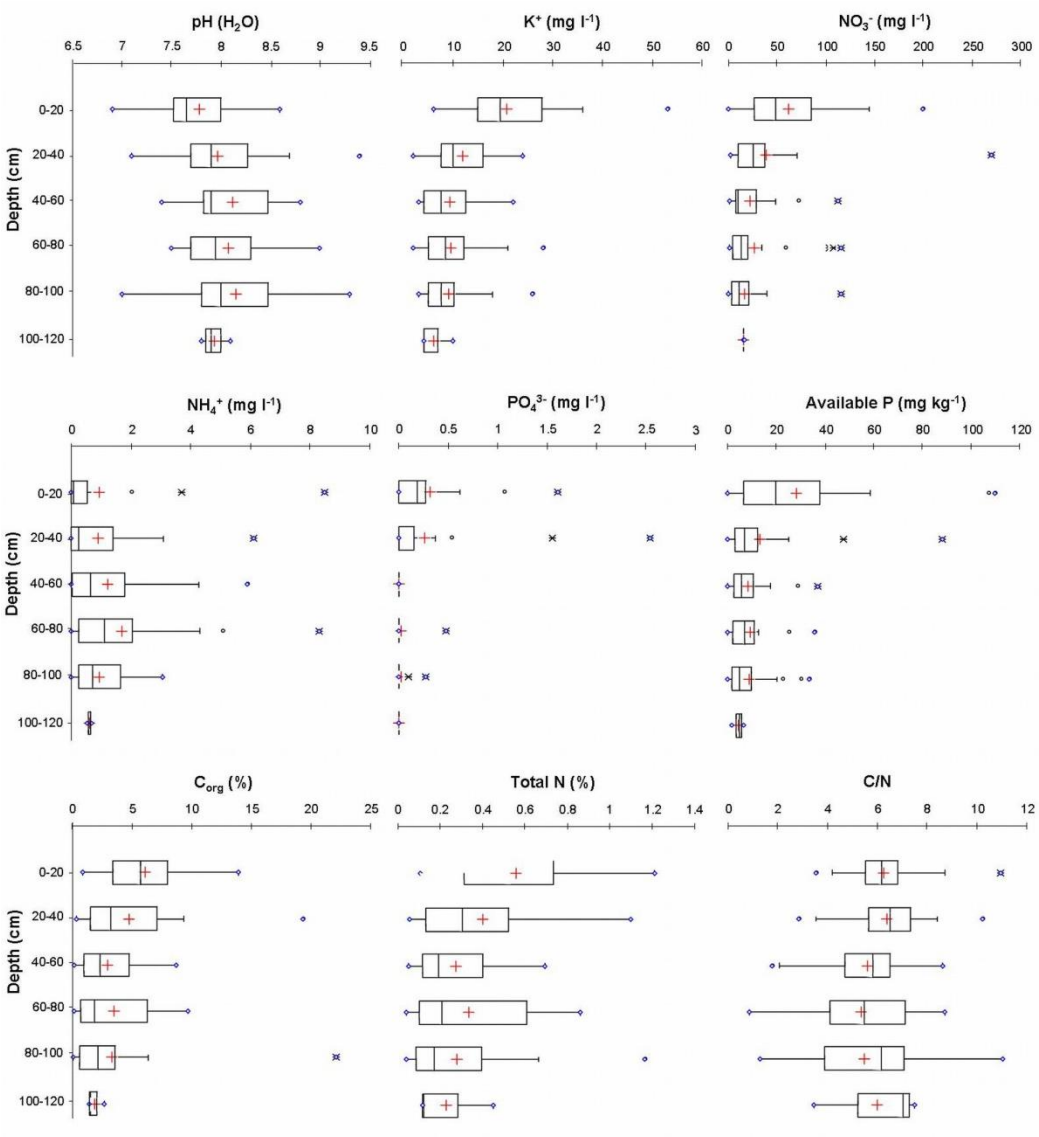

Fig. 6.2. Box-plots showing the distribution in depth of: soil pH in water (pH (H_2O)), water soluble nutrients in 1:5 soil-water extracts (K^+, NO_3^-, NH_4^+ and PO_4^{3-}), available phosphorus, organic carbon (C_{org}), total Kjeldahl nitrogen, and organic carbon-total nitrogen ratio (C/N) from the sampled soils (n = 111). Boxes lenghts represent the interquartile range, the line inside the median and the cross the mean. Straight lines from the box extend to minimum and maximum non outlier values.

6.2.2. Correlation analysis

Table 6.3 shows the results from bivariate correlation analysis. High correlations are found among major anions and cations in the soil-water extracts, on one side, and among nutrients on the other. Calcium is the cation showing the lowest correlation with the other major anions and cations (r<0.60) and, therefore, with the electrical conductivity (r=0.39; p<0.001). This indicates a lower concentration of this cation in highly saline points, where magnesium and sodium dominate, as their correlation coefficients with chloride and conductivity are greater than 0.90 (p<0.001). As in the calcareous soils filled with Quaternary silts and clays studied by Visconti et al. (2009), the highest correlation is found between sodium and chloride (r=0.97 against r=0.92 in these authors' research).

In the case of nutrients, significant positive correlations among all of them are observed (except for potassium). The outstanding co-appearance of nitrate and phosphate in the extracts from the different soil samples (r=0.68; p<0.001)) is worth mentioning. The high correlation between organic carbon and total nitrogen (r=0.92; p<0.001) suggests the predominance of organic forms of nitrogen (González et al., 2007). This strong linear association between both parameters is usually reported in soil chemistry studies (González et al., 2007; Tiemeyer et al., 2007; Fernández et al., 2009; Miralles et al., 2009; Wang et al., 2009a). On the other hand, available phosphorus shows a weaker though significant correlation with organic carbon (r=0.28; p<0.01) and total nitrogen (r=0.34; p<0.001). The strong significant relationship between nitrate in the extract and organic carbon (r=0.74; p<0.001) and total nitrogen (r=0.63; p<0.001) in the soil matrix corroborates the large contribution of OM mineralization to the release of inorganic forms in the system, something usual in organic soils from drained wetlands (Olde Venterink et al., 2002).

Table 6.3. Bivariate Pearson correlation coefficients for soil chemical variables both in 1:5 soil-water extracts and the soil matrix. Bold characters indicate significant correlation at the 0.05 probability level (2-tailed); * indicate significant correlation at the 0.01 probability level (2-tailed); ** indicate significant correlation at the 0.001 probability level (2-tailed).

	Na^+	K^+	Ca^{2+}	Mg^{2+}	SO_4^{2-}	Cl^-	HCO_3^-	NO_3^-	NO_2^-	NH_4^+	PO_4^{3-}	SiO_2	B	EC	pH (H_2O)	pH (KCl)	C_{org}	Total N	P	CO_3^{2-}
K^+	**0.72****																			
Ca^{2+}	**0.26***	0.17																		
Mg^{2+}	**0.95****	**0.68****	**0.28***																	
SO_4^{2-}	**0.87****	**0.65****	**0.56****	**0.93****																
Cl^-	**0.97****	**0.66****	**0.28***	**0.96****	**0.86****															
HCO_3^-	-0.08	0.04	**-0.24**	-0.09	-0.18	-0.13														
NO_3^-	**0.25***	**0.27***	**0.21**	**0.23**	**0.20**	**0.23**	**0.53****													
NO_2^-	-0.06	0.00	0.00	-0.07	-0.06	-0.07	**0.26***	0.08												
NH_4^+	-0.02	-0.12	0.05	-0.01	0.00	-0.01	0.18	0.02	-0.14											
PO_4^{3-}	0.16	0.16	0.16	0.13	0.11	0.18	**0.32****	**0.68****	-0.09	-0.03										
SiO_2	-0.12	**0.21**	-0.05	-0.11	-0.08	-0.16	0.18	0.18	0.04	-0.03	0.15									
B	0.08	**0.29***	0.06	0.11	0.13	0.05	**0.35****	**0.29***	-0.08	0.11	**0.23**	**0.22**								
EC	**0.96****	**0.67****	**0.39****	**0.95****	**0.91****	**0.95****	-0.12	**0.23**	-0.03	0.02	0.14	-0.15	0.06							
pH (H_2O)	**0.34****	0.18	0.14	**0.35****	**0.35****	**0.36****	**-0.69****	**-0.51****	-0.17	-0.11	**-0.38****	**-0.28***	**-0.34****	**0.37****						
pH (KCl)	**0.36****	**0.20**	0.10	**0.35****	**0.34****	**0.37****	**-0.66****	**-0.48****	-0.15	-0.12	**-0.35****	**-0.32****	**-0.32****	**0.37****	**0.98****					
C_{org}	0.07	0.11	0.02	0.06	0.02	0.05	**0.76****	**0.74****	0.11	0.02	**0.58****	0.17	**0.51****	0.03	**-0.76****	**-0.73****				
Total N	-0.01	0.08	-0.09	-0.01	-0.07	-0.03	**0.78****	**0.63****	0.11	0.05	**0.46****	**0.25***	**0.41****	-0.06	**-0.77****	**-0.75****	**0.92****			
P	-0.07	**0.21**	-0.10	-0.09	-0.13	-0.09	**0.26***	0.09	0.00	-0.12	0.09	**0.37****	**0.19**	-0.09	**-0.34****	**-0.36****	**0.28***	**0.34****		
$CaCO_3$	**-0.29***	**-0.29***	**-0.39****	**-0.32****	**-0.43****	**-0.31****	**0.51****	0.04	0.18	**0.22**	-0.10	-0.13	-0.11	**-0.33****	**-0.36****	**-0.35****	0.17	**0.22**	0.14	
C/N	0.02	0.12	0.00	0.06	0.03	0.00	**0.53****	**0.52****	0.14	0.15	**0.38****	0.14	**0.34****	0.02	**-0.59****	**-0.56****	**0.62****	**0.42****	0.18	**0.36****

Another interesting relationship was detected between organic carbon and bicarbonate (r=0.76; p<0.001). Very similar correlation coefficients were also found in the calcareous soils studied by González et al. (2007) and in the saturation extracts from Visconti et al. (2009). Agreeing with González et al. (2007), this relationship is due to the reaction of the CO_2 generated during microbial degradation of organic material with soil water, through the process of carbonation, typical of alkaline soils (Bohn et al., 2001; Reddy and DeLaune, 2008; Karberg et al., 2005):

$$CO_{2(aq)} + H_2O \leftrightarrow H_2CO_3 \leftrightarrow HCO_3^-{}_{(aq)} + H^+_{(aq)} \quad (26)$$

Soil pH (H_2O) is positively correlated with major ions in the extract and, therefore, with electrical conductivity. On the other hand, it is negatively correlated with nutrients, especially with organic carbon (r=-0.76; p<0.001) and total nitrogen (r=-0.77; p<0.001). OM displays a pH-buffering capacity in alkaline soils, contributing to keep pH values not too basic (Bohn et al., 2001). Beside this, both products from OM decomposition and organic compounds released by microbial activity provide with further acidity, thus increasing mineral alteration. This explains the observed relation between acidity and OM content, comparable to that found in other works (Zhang et al., 2008; Miralles et al., 2009).

The process of carbonation is also responsible for the negative significant correlation between pH (H_2O) and bicarbonate concentration in aqueous extracts (r=-0.69; p<0.001). As the content of soil OM increases, microbial activity is enhanced and so is the carbon dioxide release. As a consequence, the chemical equilibrium in the carbonation reaction (Eq. 26) is shifted towards the formation of bicarbonate and acidity is increased. Initial alkalinity in the topsoil is partially neutralized (Fig. 6.2) as this layer registers the highest root and microbial respiration given the greater oxygen availability in the soil pores.

Three chemical variables, pH (KCl), C/N and nitrite, were excluded from the statistical analyses described below. The first one, pH (KCl), lacks of added relevant information

for the study due to its strong linear relation with pH (H_2O). In the case of C/N, it is a synthetic variable generated upon the values obtained for two other variables. Finally, NO_2^- concentrations are quite low, often close to the experimental detection limit, so that analytical quantifications of this parameter suffer from high uncertainty. Therefore, the spatial distribution of 18 variables will be statistically analysed in 22 sampling points.

6.2.3. Trend surface analysis (TSA)

TSA did not detect generalized spatial variation trends in the variables. When taking longitude and latitude as predictors and the median values of the chemical parameters on each soil profile as dependent variables, none of the regression models showed a goodness of fit over 50% (R^2>0.5). Nevertheless, when considering the mean values in soil profiles, calcium and pH increased their coefficient of determination to 0.57 and 0.55, respectively. This is due to the fact that the distribution of these variables is more homogeneous along soil profiles. Including the topographic elevation as independent variable together with latitude improved the results for four variables: pH (R^2_{mean}=0.71), sodium (R^2_{median}=0.52), available phosphorus (R^2_{median}=0.69) and boron (R^2_{median}=0.80). Even though these are just a few variables from a big pool, these results indicate the existence of latitudinal and topographical patterns of variation in the distribution of soil pH, phosphorus and salinity. Multivariate analysis will allow for a deeper exploration of this issue.

TSA has provided very little information with respect to the spatial distribution of soil chemical variables. Other researches such as Tiemeyer et al. (2007) did detect spatial trends but the working scale was significantly smaller (<85 ha against 2000 ha in TDNP) and the system more homogeneous (only peat material).

6.2.4. Multivariate analysis

The contribution of an ordination analysis can be measured by means of their eigenvalues (λ_i). The first two axes of the PCA account for 59% (λ_1=0.328, λ_2=0.262) of the total variance for 18 chemical variables in 111 samples (Fig. 6.3). Correlations can be estimated by perpendicularly projecting the arrow tips of the other species onto a particular species arrow (Leps and Smilauer, 2003). Three different chemical environments can be distinguished in TDNP soils: saline, organic (nutrients) and carbonated. The eigenvalues obtained show that both axes account for similar percentages of the total variability. The first one is defined by major cations and anions and the electrical conductivity (salinity), whereas the second axis is related to the nutrient content in both the extract and the solid matrix. The separation of calcium from the other saline ions is also observed. It is worth mentioning the association of both silica and boron with the organic environment. Soil development involves a steady loss of silicon through dissolution conditioned by processes related to the OM cycle and microbial activity (Bohn et al., 2001). Boron is an essential micronutrient for plants that in soils has both natural and anthropogenic origin. Much of the available soil boron is held rather tightly by soil organic material. Its availability decreases with increasing pH, with maximum adsorption at pH 7 to 9 (Bohn et al., 2001). As OM decomposition occurs boron is released with a portion being absorbed by plants, leached below the root zone area (especially in high rainfall/acid soil areas) or tied up (unavailable) under alkaline soil conditions (Muntean, 2010). Carbonated environments can be clearly differentiated from the other two groups, showing a slightly negative correlation with salts and a slightly positive one with OM. The already commented inverse relationship between soil pH and nutrient content is clearly depicted in the ordination diagram as well as the plot synthesizes the results obtained for the correlation analysis. In general, samples are homogeneously distributed around the origin of the coordinate system, except for a few of them showing extreme values in the first axis and some other with high scores in the second axis and average in the first one. Distance between points is a measure of their dissimilarity regarding

chemical composition. In this case the generalized proximity between samples is due to the fact that they have been taken in depth in the same soil profiles.

Some of the chemical variables could be removed from the analysis regarding colinearity issues (i.e. total nitrogen or major ions), allowing for the detection of key variables. However, the primary objective of this work is to find out how soil solutes are spatially related to each other and to the considered environmental factors, rather than the isolation of single key variables as a standard multivariate procedure. Therefore, percentages of explained variability might be slightly overestimated and should be only considered as approximated values, but resulting outcomes regarding associations and relationships between variables and factors will be perfectly accurate and comparable among tests.

The unconstrained variability explained by the PCA (59%) can be compared to the 64.4% observed by Visconti et al. (2009) taking into account that they analysed 13 variables in saturation extracts from more homogeneous calcareous soils. Actually, the first axis (44%) of their study was also highly correlated with extract's salinity (electrical conductivity and ions). At the same time, their second axis (20.4%) correlated with alkalinity and nutrients (nitrite and dissolved organic carbon) and, thus, with OM oxidation and subsequent dissolution of carbonate minerals described above. When compared to the results obtained by Miralles et al. (2009), mainly for soils developed under Mediterranean forest areas, it can be observed how organic carbon is in both cases a key variable accounting for a large percentage of total soil chemistry variability. The two first axes in the PCA carried out by Vestin et al. (2006) explained 54% of chemical and mineralogical variability in alkaline and non-alkaline soils under coniferous forests in higher latitudes. Finally, Momtaz et al. (2009) performed a factor analysis on 7 soil properties for piedmont, levee and lowland landforms in Iran. Their results showed percentages of explained variation between 60% and 78%, agreeing with this study in TDNP in both the inverse relationship between pH (H_2O) and organic carbon and the clear distinction between surface and deeper samples.

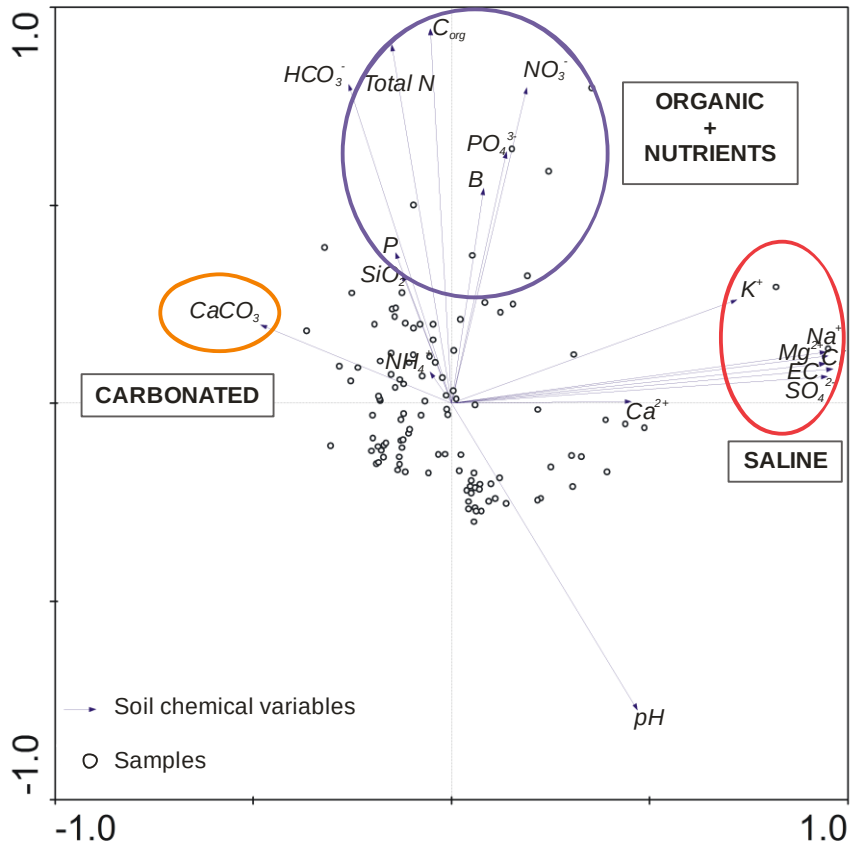

Fig. 6.3. Ordination diagrams from the correlation-based indirect gradient analysis (Principal Component Analysis, PCA). Variability explained by the first two axes (correlation biplot) of the distribution of 18 chemical variables in 1:5 soil-water extracts and the soil matrix of 111 soil samples is represented.

On the other hand, four environmental factors have been considered for the RDA analysis; soil type, depth, microtopography and position regarding the central Morenillo dam (Table 6.4). In general, soil type, depth and microtopography, are intimately related to soil physical-chemical properties (Koerselman et al., 1993; Takii and Fukui, 1996; Bohn et al., 2001; Eimers et al., 2003; Tiemeyer et al., 2007; Zhang et al., 2008; Esteller et al., 2009; Miralles et al., 2009; Momtaz et al., 2009; Wang et al., 2009a,b). Soil physical properties such as texture, structure, porosity, density and hydraulic conductivity, are closely related to the chemical ones. Microrelief is a crucial factor for water distribution in the topsoil and, therefore, for the evaporation and physical-chemical reactions that take place in this layer. Central Morenillo dam allows for keeping higher and longer flooding events in the northern zone of the TDNP. This area is more influenced by external water inputs and, therefore, it registers the highest

sedimentation rates (Sánchez-Carrillo et al., 2001). Furthermore, the considered environmental factors are also susceptible to be modified by certain activities performed within the anthropic management of this degraded wetland: use of heavy farm machinery for reed reaping or cut-sedge sowing, construction of ditches and fire breaks, works for peat fires extinction, and artificial flooding with either groundwater or treated wastewater.

Five different kinds of soil profiles were defined according to the distribution of SFT; five homogeneous intervals of topographic variation in the surface were derived from a digital elevation model (cell size 2x2 m with $\pm$ 5 cm vertical resolution); finally, position regarding the dam is an anthropogenic factor that considers points located upstream (Tablas zone) or downstream (Cañas zone) the dam (Fig. 2.1). Table 6.4 shows the combination of levels of these factors at each sampling point. Most soil profiles are located in areas with a microtopographic variation in the range between 595.5 and 596 m, being edaphized charophyte layers and alternation of peat and charophyte layers the dominant SFT.

Based on the global results presented in section 6.2.1, it was decided to carry out two different redundancy analyses, one for topsoil samples (0-20 cm) where larger amounts of solutes accumulate (Table 6.2), and the other one for the median values of each variable in each sampling point, as this is the parameter which better describes the chemical composition in soil profiles. The variation explained by the principal component analyses carried out separately for topsoil and whole profiles described by their median values is, respectively, 57.3% and 61.4%. In both cases most variability is controlled by the first axis (λ_1). The percentages are quite similar to the 59% of the global PCA including all the 111 samples. This guarantees the suitability of these two redundancy analyses and proves the robustness of the analysis only based on 22 samples.

Table 6.4. Factor levels from the environmental variables considered for the multivariate soil chemical analysis on each sampling location.

Sampling point	Location	Microtopography (masl)	Soil type
1	Cañas zone	594.9-595.5	Fluvial silts
2	Cañas zone	595.5-596	Charophytes-Peat alternations
3	Cañas zone	594.9-595.5	Edaphized charophytes
4	Cañas zone	594.9-595.5	Charophytes-Peat alternations
5	Tablas zone	595.5-596	Edaphized charophytes
6	Tablas zone	595.5-596	Edaphized charophytes
7	Tablas zone	595.5-596	Edaphized charophytes
8	Tablas zone	595.5-596	Edaphized charophytes
9	Tablas zone	595.5-596	Edaphized charophytes
10	Tablas zone	596-596.5	Saline charophytes
11	Tablas zone	596-596.5	Saline charophytes
12	Tablas zone	> 596.5	Saline charophytes
13	Tablas zone	< 594.9	Fluvial silts
14	Tablas zone	595.5-596	Charophytes-Peat alternations
15	Tablas zone	595.5-596	Edaphized charophytes
16	Tablas zone	595.5-596	Undisturbed charophytes
17	Tablas zone	594.9-595.5	Fluvial silts
18	Tablas zone	595.5-596	Charophytes-Peat alternations
19	Tablas zone	594.9-595.5	Saline charophytes
20	Tablas zone	> 596.5	Charophytes-Peat alternations
21	Tablas zone	596-596.5	Charophytes-Peat alternations
22	Tablas zone	596-596.5	Undisturbed charophytes

The first two ordination axes in the RDA for median values in soil profiles account for 40.9% of the variance in the data, mainly concentrated in the first axis (λ_1=0.340, λ_2=0.069). This is equivalent to a 71.3% of the unconstrained variability explained by

the medians PCA. The Monte Carlo tests based on 999 permutations have proven the significance of both the first canonical axis (p=0.048) and all canonical axes together (p=0.020).

By using centered values all the information concerning the entire soil profile is integrated. The ordination diagram (Fig. 6.4) shows the association of the first axis with the microtopography factor. The perpendicular projection of sample points and centroids of qualitative environmental variables (i.e. soil type) onto the overlying arrow of a particular quantitative variable can be used to approximate the abundance or value of this variable in individual samples or classes. The predicted increase occurs in the direction indicated by the arrow. Sample points or centroids projecting near the origin are predicted to correspond to samples or classes with average value of the particular quantitative variable close to that of the entire data set (Leps and Smilauer, 2003).

In relation to microtopography, higher areas are positively correlated with salinity and pH (high scores in the first axis). They are represented by saline charophyte layers (samples 10, 11, 12 and 19) which accumulate the largest amounts of typically saline ions (magnesium, sodium, chloride and sulfate). Salts seem to have accumulated upon charophytes influenced by flooding of Cigüela River saline waters, evaporation, lithological weathering and shallow groundwater levels. With an average EC of 5723 µS cm^{-1} and a sodium adsorption ratio (SAR) below 15% (range 1.00% to 6.75%), saline charophytes can be classified as *saline* soils (Bohn et al., 2001).

On the other hand, OM and nutrients and, to a lesser extent, carbonates tend to accumulate in lower areas (negative scores in the first axis). Soil salinity and water soluble nutrients are linked to the northern sector of TDNP (Tablas zone), whereas lower areas downstream from the central dam (Cañas zone) are linked to carbonated soils and OM (Figs. 2.1, 5.2 and 6.1). Soil nutrients are mainly associated with fluvial silts (samples 1, 13 and 17) and also, especially in the case of water soluble nitrate,

with edaphized charophytes and charophytes-peat alternations, where the former predominate (Figs. 5.2 and 6.1).

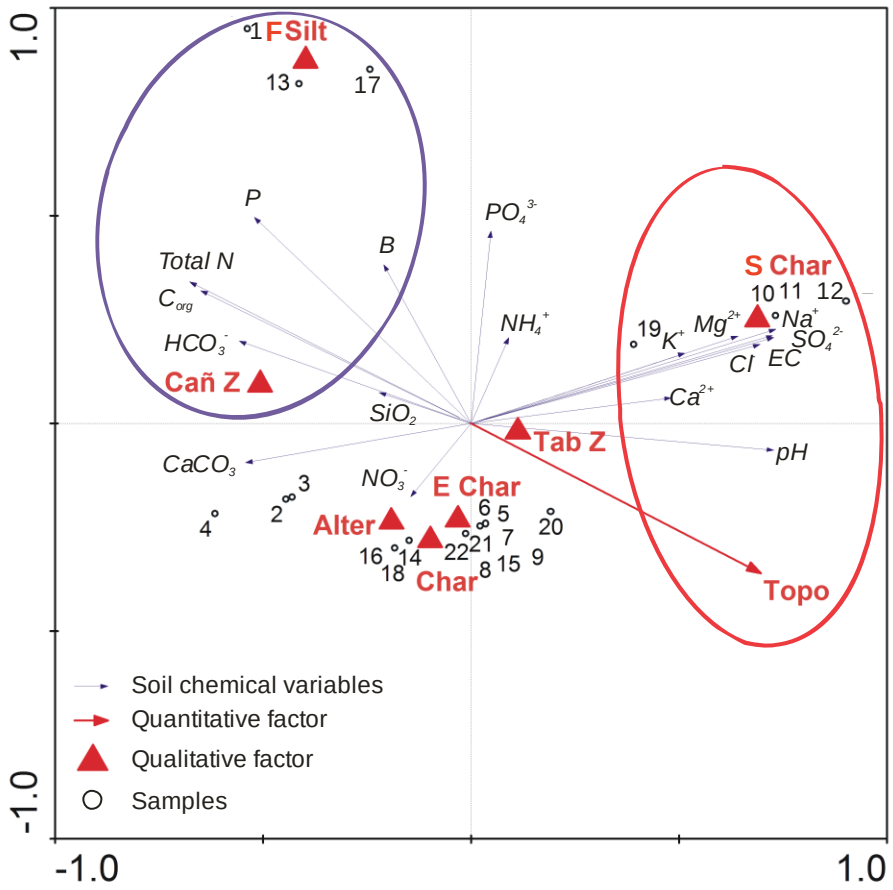

Fig. 6.4. Ordination diagrams from the correlation-based direct gradient analysis (Redundancy Analysis, RDA). Variability explained by the first two axes (correlation triplot) of the relationship between median values of soil chemical variables in 1:5 soil-water extracts and the soil matrix and environmental factors (soil type and depth, microtopography and position regarding the central Morenillo dam) for the 22 sampling points (Fig. 5.2). Topo: microtopography; F Silt: fluvial silts; S Char: saline charophytes; E Char: edaphized charophytes; Char: undisturbed charophytes; Alter: charophytes-peat alternations; Tab Z: Tablas zone; Cañ Z: Cañas zone.

The RDA for the topsoil layer explains 37.3% of the variance in the data and, again, the first axis controls most of the variability (λ_1=0.309, λ_2=0.064). This represents a 70.8% of the total variability explained by the PCA of topsoil samples. Both the first canonical axis and all the canonical axes together are significant (p=0.020).

The separation of salts from nutrients along the first axis points out a clear dichotomy in the upper soil layer: saline samples show low nutrient contents and vice versa (Fig. 6.5). High scores in the first axis are linked to saline samples from higher areas (10, 11, 12, 19) located in the northern and western side of the Park (Fig. 5.2). By contrast, negative values belong to soils in western (5, 6, 7, 8, 9) and central (13, 15, 17, 20, 21) areas where OM and nutrients accumulate. The north-south gradient in the settling out of mineral and organic sediments is related to the main surface water flux direction inside TDNP. Edaphized charophytes accumulate more nutrients in the topsoil than fluvial silts, especially in the extract. This can be explained by the fact that these edaphized charophytes are located in areas with abundant vegetation, mainly reed (Figs. 4.4 and 6.1), and the data precisely belong to the root zone (Takii and Fukui, 1996).

Reed is a perennial rhizomatic plant which has an annual turnover rate and the below-ground biomass is of the same order of magnitude or even higher than the above-ground biomass. Therefore, it is likely that reed constitutes one of the main sources of OM and nutrients to the environment through debris decomposition and mineralization (Takii and Fukui, 1996; Sánchez-Carrillo and Álvarez-Cobelas, 2001; Mesnage et al, 2002). Sánchez-Carrillo et al. (2001) reported a linear relationship between reed cover and OM sedimentation rate in TDNP with a R^2 of 0.78 ($p<0.004$). This hypothesis, together with the rapid process of OM mineralization in the topsoil discussed above, seems to indicate the occurrence of a cyclic process with a positive feedback: nutrient accumulation, associated with high mineralization rates, supports again the development of the primary source, reed. The net effect from the relation between plant productivity and decomposition is debris accumulation (Sánchez-Carrillo et al., 2001). This fact is in agreement with the review by Brisson and Chazarenc (2009) of the efficiency of wetland macrophyte species on nutrients and pollutants removal. Reed is the second most researched species but it is only highly efficient on the removal of nitrogen compounds (nitrate and ammonium) which, in turn, will return to the environment in organic form.

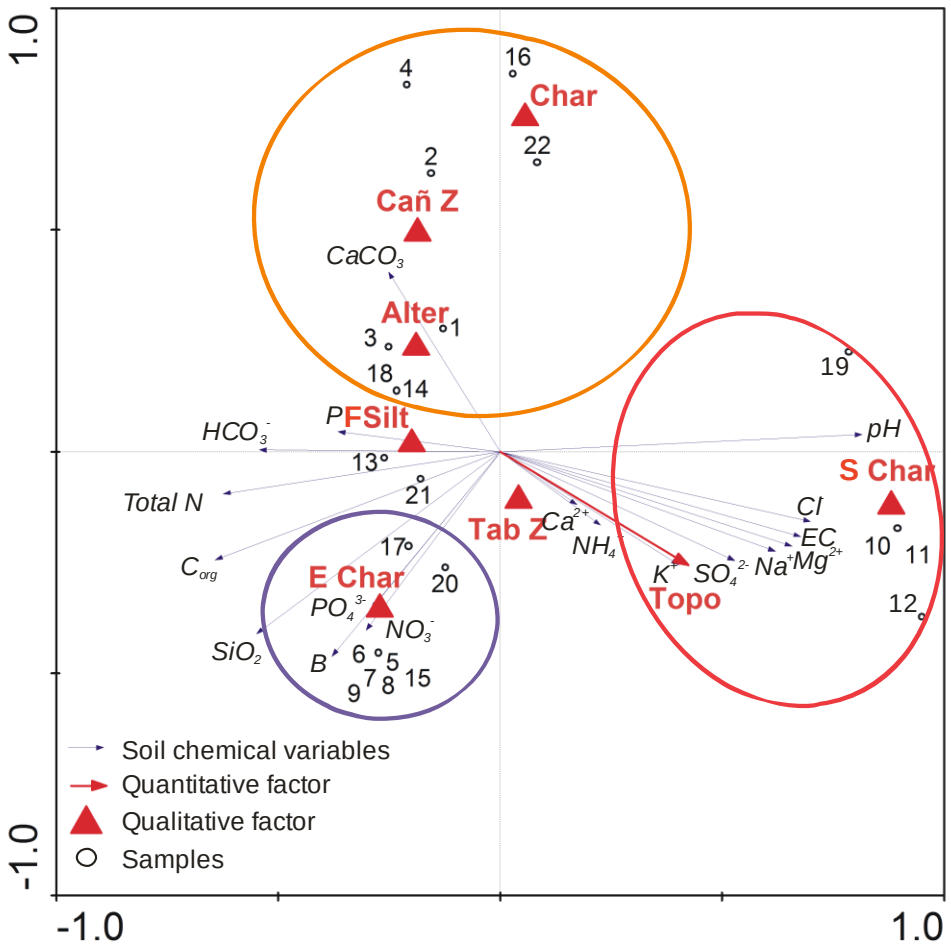

Fig. 6.5. Ordination diagrams from the correlation-based direct gradient analysis (Redundancy Analysis, RDA). Variability explained by the first two axes (correlation triplot) of the relationship between chemical variables in 1:5 soil-water extracts and the soil matrix and environmental factors (soil type and depth, microtopography and position regarding the central Morenillo dam) for the surface samples (0-20 cm) of 22 sampling points (Fig. 5.2). Topo: microtopography; F Silt: fluvial silts; S Char: saline charophytes; E Char: edaphized charophytes; Char: undisturbed charophytes; Alter: charophytes-peat alternations; Tab Z: Tablas zone; Cañ Z: Cañas zone.

The second canonical axis is defined by the position regarding the central Morenillo dam. Positive values correspond to the southern carbonated Cañas zone where charophyte layers dominate (Fig. 6.1), whereas the negative ones correspond to the vaster Tablas zone, where both salts and nutrients are present. In this case, the microtopographic factor has a lesser weight due to the generalized accumulation of solutes in topsoil.

Both RDA models manage to explain about 71% of the total unconstrained variance accounted for by the PCA. This emphasizes the relevance of the environmental factors considered.

6.2.5. Summary and conclusions on VZ chemistry

The vadose zone in TDNP is a carbonated environment with high salinity and large topsoil nutrient accumulation. Median electrical conductivity in soil-water extracts of soil profiles is 3,280 $\mu S\ cm^{-1}$ and median organic matter content in the soil matrix is 5.33%. Nutrient content in the first 20 cm of the soil profile is similar to that in organic soils of other altered wetland areas worldwide and higher than the average for agricultural or forest areas. This nutrient surplus allows classifying TDNP as an eutrophic system. Correlation analysis has indentified organic matter mineralization as a controlling factor on VZ chemistry during drying conditions.

Principal component analysis accounts for 59% of total observed variability in soil chemical composition and allows to distinguish three different environments: saline, carbonated and organic where most nutrients accumulate. Organic carbon is a key variable accounting for a large percentage of total soil chemistry variability. An approximately 40% out of the 59% is explained in terms of the four environmental factors considered: soil type, depth, microtopography and position regarding the central dam. The multivariate model associates saline samples with higher topographical areas and the organic ones with lower zones. Salinity and nutrients are more likely to accumulate upstream from the dam, whereas downstream the environment is dominated by carbonates.

The redundancy analysis carried out for the median values of chemical properties in each soil profile points out the existence of two types of homogeneous soil profiles in depth: saline charophytes as representatives of saline environments and fluvial silts as

OM and nutrients accumulators. On the other hand, the redundancy analysis for the topsoil shows that surface nutrient accumulation is controlled by reed dynamics in areas where edaphized charophytes predominate (Fig. 6.1).

The results agree with the geochemical interpretation of environmental changes in the wetland for the last 3,000 years argued in Santisteban and Mediavilla (2012b) through the analysis of a 1 m core. They identify three major facies from bottom to top: gypsum-rich muds and sands, organic matter rich muds and charophytes muds and sands. Transitions between facies are mainly controlled by flooding conditions and helophyte vegetation.

The trend surface analysis does not detect significant patterns of variation associated to spatial coordinates due to the high heterogeneity of the study site revealed by the redundancy analysis.

6.3. Vadose zone physical characterization

The classification of SFT has been mainly based on the physical analyses performed on TDNP soil materials. In this section results on soil physical properties during drying conditions are already presented according to this classification.

6.3.1. Soil physical properties

Table 6.5 shows the average bulk density (BD), texture, OM content and degree of water repellency of the different SFT defined in section 6.1. All raw measured data is presented in appendix E. Most soils are fine textured (silt loam) as expected for typical floodplain wetland soils (Lindbo and Richardson, 2001; Reddy and DeLaune, 2008).

Only peat and edaphized charophytes show a high sand fraction. A large sand fraction (71.7%) was also reported by Gebhardt et al (2012) for a less decomposed fibrous sedge peat. In general, lower bulk densities correspond to those materials that show higher OM contents, being that of peat (0.18 g cm^{-3}) considerably smaller that the rest. Results on TDNP peats texture, bulk density and OM content point out to a semi-fibrous peat that can be ranked as H5-H6 in the von Post scale (Kechavarzi et al., 2010; Gebhardt et al., 2012).

Measured saturated hydraulic conductivities of organic SFT are much higher than those of other soil types. The extremely large K_s values observed for TDNP peats can be explained by the highly developed secondary porosity (i.e. cracks) together with the huge swelling capacity. A relative decreasing trend on K_s values is observed with increasing bulk densities. Lower densities and higher OM contents in peat, organic soil, peaty silt and edaphized charophytes determine a less compact structure which enhances the water transmissivity capacity of these materials. Nevertheless, larger K_s variability in these SFT is observed. This will be discussed in the next section.

6.3.2. Infiltration curves and capacities

The most recent hydrological studies in the anthropized semiarid wetland area have been focused on the estimation of the different components of the water budget in order to determine water requirements for suitable flooding conditions (García Rodríguez, 1996; Sánchez-Carrillo et al., 2004; Castaño et al., 2008; Sánchez-Carrillo and Álvarez-Cobelas, 2010; Navarro et al., 2012). As argued in section 4.3, authors agree on the major relevance of the infiltration term. However, no data on infiltration from dry soils has been published yet. The results of the infiltration tests presented below constitute the first approximation to in situ unsaturated water dynamics on drained SFT.

Table 6.5. Main average physical properties of TDNP soil functional types. BD: bulk density; K_s: saturated hydraulic conductivity both measured in the laboratory and inferred from infiltration tests; OM: organic matter. Values in brackets represent standard deviations.

Soil type	BD ($g\ cm^{-3}$)	K_s lab ($cm\ d^{-1}$)	K_s infiltration ($cm\ d^{-1}$)	OM (%)	Sand (%)	Silt (%)	Clay (%)	Texture	Water repellency (field/lab)
Undisturbed charophytes	0.76 (0.14)	84 (11)	171 (126)	6.0	34	57.7	8.3	Silt loam	No/No
Edaphized charophytes	0.66 (0.05)	527 (263)	826 (378)	12.0	52.9	39.2	7.9	Sandy Loam	Yes/Slight
Saline charophytes	0.56	1687 (942)	-	2.1	26.1	67.9	6	Silt loam	No/No
Clay	1.30 (0.09)	148 (17)	99 (105)	3.5	12.3	68.1	19.6	Silt loam	No/No
Silt	0.91 (0.30)	38 (2)	292 (128)	9.5	17.6	67.9	14.5	Silt loam	No/No
Peat	0.18 (0.04)	22161 (9009)	996 (149)	50.1	88.1	0.0	11.9	Loamy sand	Yes/Severe-Extreme
Organic	0.52 (0.06)	588 (176)	-	33.0	-	-	-	-	No/No
Peaty silt	0.77 (0.02)	4664 (2560)	857 (525)	53.1	15.1	61	23.9	Silt loam	No/No

An example of infiltration curve for each SFT is shown in Figure 6.6. The remaining curves have been included in appendix E. Due to the strong degree of heterogeneity and irregularities observed within some soil types (i.e. peat), once the infiltration speed of the field test seemed to have stabilized, it was decided to stop it for at least 10 minutes allowing for the infiltration of remaining water in the cylinder and then restart it to check that a constant infiltration capacity had actually been achieved (Fig. 6.6e,f). In some cases unavoidable problems such as water unavailability forced interrumption of infiltration tests for longer times (Fig. 6.6g). Most curves show an irregular distribution of small peaks and valleys of infiltration rates in time (Fig. 6.6, appendix E). This is likely due to the effect of secondary porosity as well as the random arrangement of SFT layers with varying permeability.

The goodness of fit of both Horton and Kostiakov models has been quite satisfactory. All tests show R^2 values over 0.6 and over 0.8 in 82% of the cases. However, Kostiakov's model does not give realistic estimates of the final infiltration capacity f_c, particularly in those tests in which a fast decrease of the initial infiltration speed is observed, yielding null or even negative values of this parameter (Fig. 6.6, appendix E). According to Mbagwu (1994) this model is more suitable to simulate horizontal flux where the gravity effect is negligible, but not for systems where gravity driven vertical flux is dominant. Due to hydraulic gradient inversion, a vertical downward flux had been assumed for the TDNP system (see section 3.2). Infiltration results seem to corroborate this assumption.

Final infiltration capacities of TDNP soil functional types derived from Horton models are represented in Figure 6.7. According to Klute (1965), the observed f_c values for the different materials lay between moderately and very fast. The lowest capacities correspond to clayey materials with an average value of 159 cm d^{-1}, whereas peats reach up to over 2,000 cm d^{-1}. Peaty silts and edaphized charophytes show median and average values over 1,000 cm d^{-1}. Singular water transmission properties of each SFT are evidenced by the different shapes of the infiltration curves and f_c box-plots. Relatively large variabilities within SFT reflect small scale heterogeneity given the

spatial proximity between test locations (Fig. 5.3). Similarly as observed in laboratory K_s determinations, the highest f_c average values and variability belong to the soil types with higher OM content: peat, peaty silt and edaphized charophytes (Table 6.5). This is due to the fact that infiltration capacity of peat and other organic materials is strongly influenced by their desiccation state. When dry, peat tends to be hydrophobic and water retention is hindered (see section 6.3.3). Moreover, extensive development of cracks and hollows in the subsoil support faster infiltration through preferential flow paths (see section 6.6.3). As expected, clay materials show the lowest infiltration capacities. Another remarkable observation is that the lowest variability corresponds to those SFT with higher bulk density (Table 6.5). Denser materials are also the most compact, showing less number of hollows and, thus, more homogeneous from a structural point of view.

On the other hand, Figure 6.8 shows one of the fitted curves for K_s estimation from infiltration data following the method proposed by Wu et al (1999). In all cases linear fitting of the last part of the accumulated infiltration curve has yielded R^2 values over 0.99 (appendix E). Average K_s values are higher than those determined in the laboratory for charophytes and silt SFT and lower for peat, peaty silt and clay (Table 6.5). The main reason is that the last ones are shrinking soils and the small samples (100 cm^3) used for the laboratory permeameter are highly conditioned by the random effect of secondary porosity and at the same time they are not influenced by underlying materials as they are under field conditions.

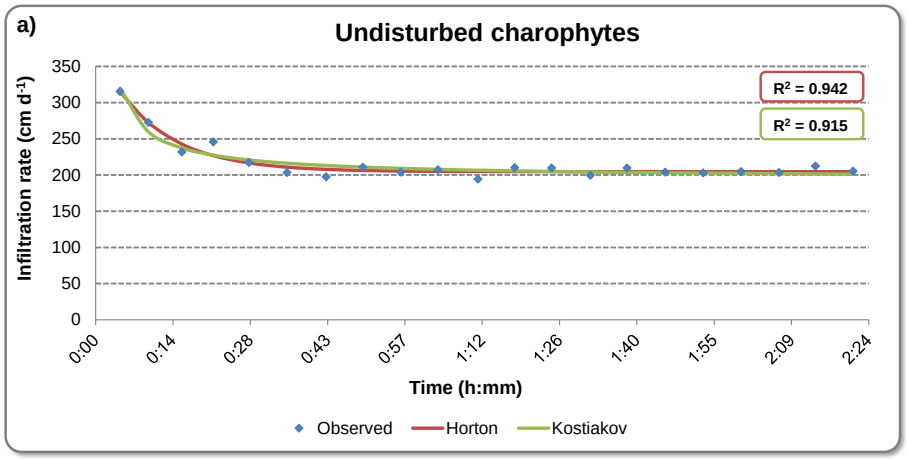
a)
Undisturbed charophytes
Infiltration rate (cm d-1)
350
300
250
200
150
100
50
0
0:00
0:14
0:28
0:43
0:57
1:12
1:26
1:40
1:55
2:09
2:24
Time (h:mm)
R² = 0.942
R² = 0.915
Observed
Horton
Kostiakov

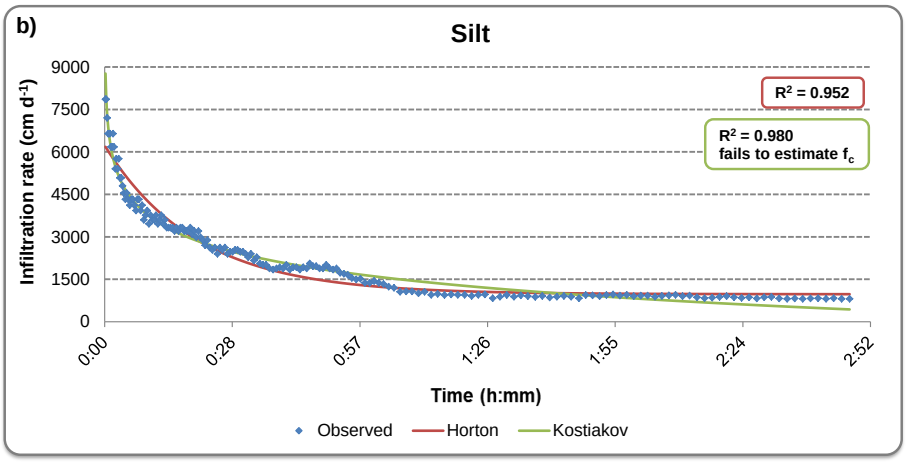
b)
Silt
Infiltration rate (cm d-1)
9000
7500
6000
4500
3000
1500
0
0:00
0:28
0:57
1:26
1:55
2:24
2:52
Time (h:mm)
R² = 0.952
R² = 0.980
fails to estimate fc
Observed
Horton
Kostiakov

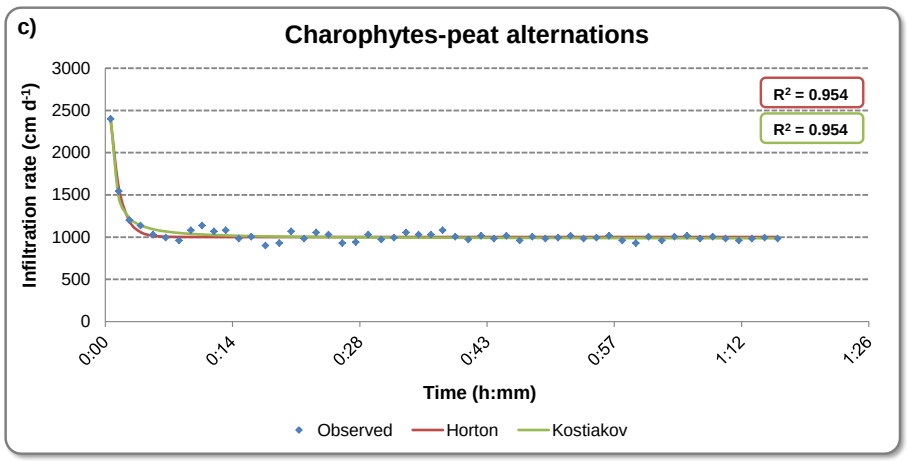
c)
Charophytes-peat alternations
Infiltration rate (cm d-1)
3000
2500
2000
1500
1000
500
0
0:00
0:14
0:28
0:43
0:57
1:12
1:26
Time (h:mm)
R² = 0.954
R² = 0.954
Observed
Horton
Kostiakov

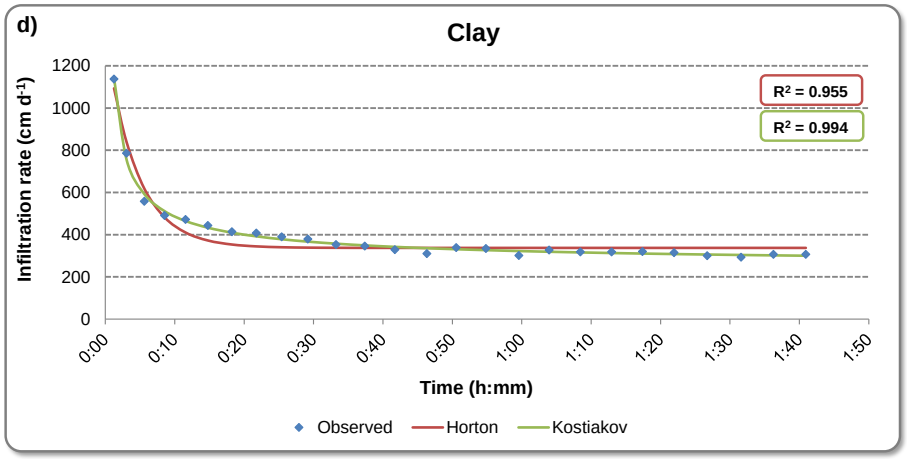
d)
Clay
Infiltration rate (cm d-1)
1200
1000
800
600
400
200
0
0:00
0:10
0:20
0:30
0:40
0:50
1:00
1:10
1:20
1:30
1:40
1:50
Time (h:mm)
R² = 0.955
R² = 0.994
Observed
Horton
Kostiakov

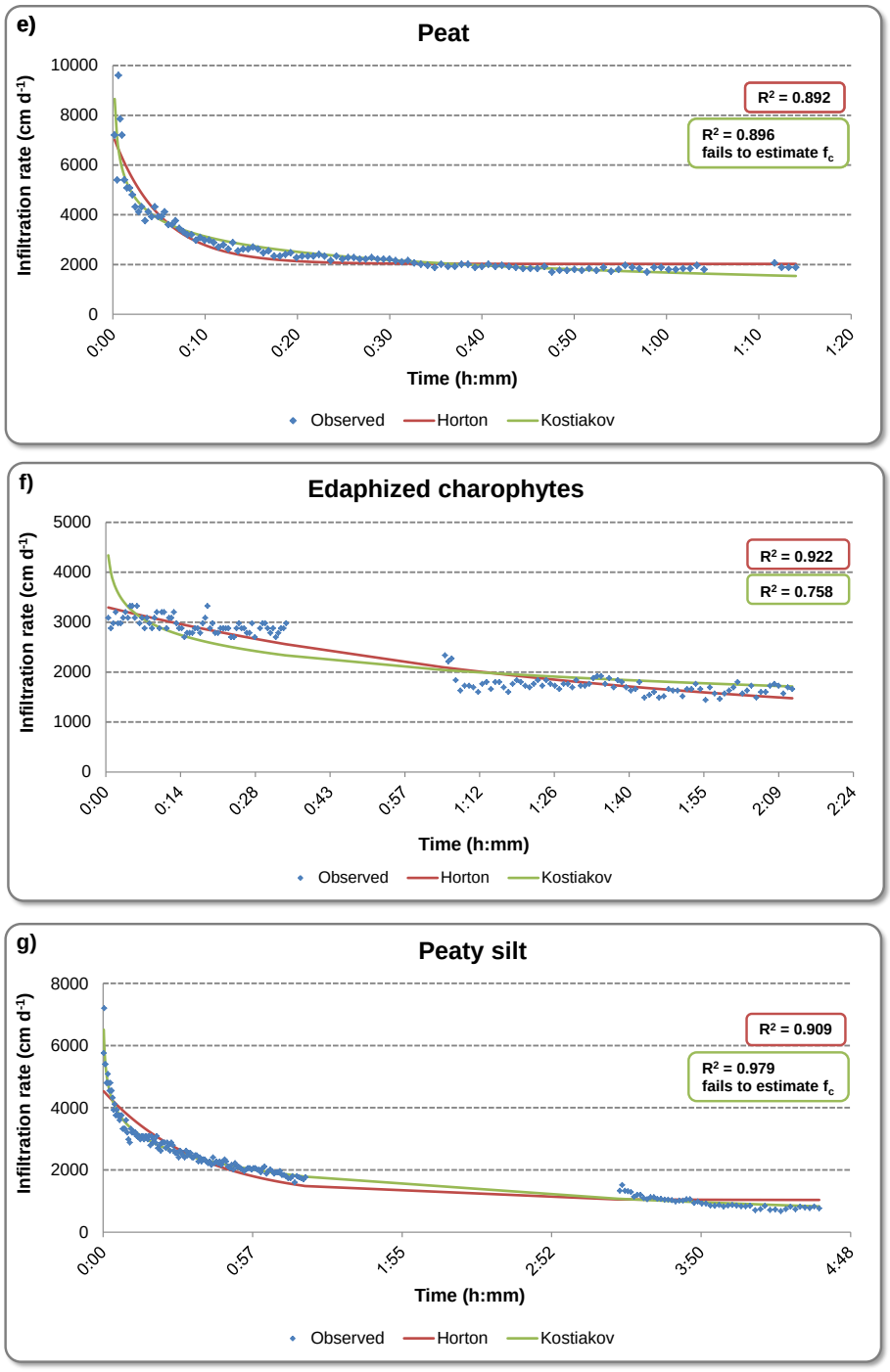

Fig. 6.6. Infiltration rates from constant-head infiltration tests on different soil functional types in Las Tablas de Daimiel National Park (TDNP). Fitted curves to the empirical Horton and Kostiakov models and goodness of fit (R^2 values) are shown. Discontinuities in observed data are either due to planned interruptions to check for stabilization (e and f) or to water unavailability and other unavoidable problems that arose at the moment tests were carried out (g).

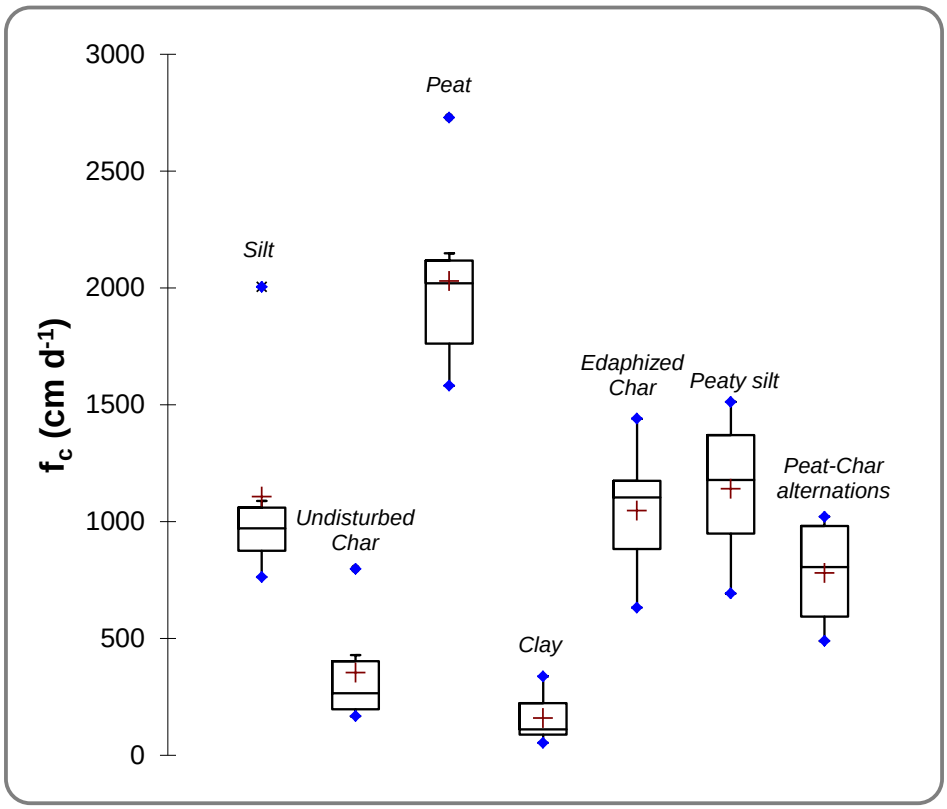

Fig. 6.7. Box-plots of the distribution of final infiltration capacities (f_c) of the different soil functional types of Las Tablas de Daimiel National Park (TDNP) estimated through Horton empirical models derived from infiltration tests. Boxes heights represent the interquartile range, the line inside the median and the cross the mean. Straight lines from the box extend to minimum and maximum non outlier values.

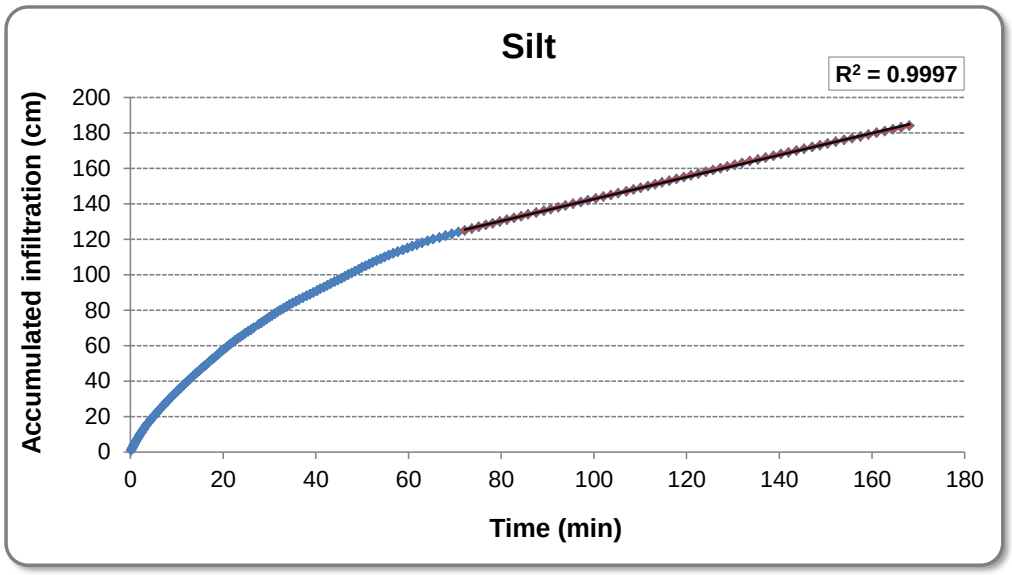

Fig. 6.8. Example of linear fitting to the last part of the accumulated infiltration curve for saturated hydraulic (K_s) estimation following the procedure proposed by Wu et al. (1999) on a silt soil functional type of Las Tablas de Daimiel National Park (TDNP). Red dots represent the last part of the curve and the solid line the best linear fit. The rest of curves have been included in appendix E.

6.3.3. Hydrophobicity of TDNP soils

The initial phase of potential SWR characterization in TDNP soils on oven and air-dried samples evidenced that water repellency only occurred in SFT with significant OM content (peat and edaphized charophytes). Figure 6.9 shows the results of the hydrophobicity analyses for these two functional types. Topsoil peat samples (10-15 cm and 20-25 cm) show extreme actual SWR (class 5) under initial field sampling conditions. Unexpectedly, SWR of peat samples decreased after oven-drying at temperatures in the range 25-55 °C. However, SWR rose again after oven-drying at 65 °C and became extreme from 75 °C at all sampling depths.

Air drying conditions on peat samples up to 40 cm deep increased the initial either absent or slight degree of SWR (classes 1 and 2) to severe (class 4) after the first 5 days. Subsequently, the degree decreased to strong (class 3) and kept constant until the end of the experiment. The deepest samples, less influenced by the plant rooting system, were not affected by air drying and SWR remained in a constant strong or slight degree throughout the analysis.

On the other hand, edaphized charophytes only showed slight SWR in the topsoil layer (0-10 cm) when oven-dried at temperatures above 55 °C. Air drying, however, caused the development of slight SWR in this topsoil layer since the beginning of the experiment, and after the first 20 days on the 10-20 cm and 20-30 cm samples. It is noteworthy how charophytes turn water repellent when edaphized and their OM content increases, supporting their separation as different SFT with different hydraulic properties. However, the average OM content of edaphized charophytes is much lower than that of peat and other organic soils (Table 6.5). In charophytes, which are mainly composed by carbonates, the SWR property is conferred by the organic compounds released by reed plants that coat the inorganic fraction. The highly hydrophobic nature of the organic compounds released by *Phragmites* spp. plants was pointed out by Jaramillo (2006) in his review work. Processes of charophytes edaphization, supported

by OM contribution from higher levels inducing the development of hydrophobic qualities in these soil materials, are accelerated by wetland desiccation.

As reported by other authors, the results indicate that the development of SWR is not only influenced by intrinsic soil properties but by drying conditions as well (see section 2.5). There is a recent scientific discussion regarding the reliability of assessing SWR in "artificially" dried samples in the lab, where completely different conditions (i.e. evaporation, humidity, biological activity, wind, etc) from those observed under prolonged "real" drought conditions in the field appear to produce or create some quite different repellency responses (Doerr et al., 2002; Ziogas et al., 2005; Taümer et al., 2005; Diehl and Schaumann, 2007; Dekker et al., 2009). In the particular case of TDNP the determination of "potential" SWR in the lab was supported by the superficial thermographic campaign in June 2009 (see section 5.4) which revealed that during summer topsoil temperatures reach values between 65 °C and 85 °C, particularly in dark materials such as peat and organic soils. These high temperatures completely dry the soil matrix in a similar way as an oven would, inducing extreme SWR and maximum risk of combustibility. Nevertheless, field SWR characterization becomes essential before drawing any further conclusions.

The 2009 field campaign gave new insights on the in situ SWR characteristics and seasonal effects (i.e. soil moisture condition) in TDNP soils. Sampling focused on the organic SFT which had showed water repellency in the lab and out of the 33 monitored points, 26 corresponded to peat dominated areas and the other 8 to edaphized charophytes and organic soils. The results of SWR measurements are summarized in Figure 6.10. Under humid field conditions, only a low number of unprocessed peat samples exhibited water repellency (4 out of 26 peat samples). These measurements were performed on February, when the average moisture content of peat was relatively high (30% in volume). However, a remarkable proportion of the wettable peat samples (62%) became water repellent after drying at 105 °C. As observed in Figure 6.10, peats with higher OM contents tend to display higher degrees of water repellency. A threshold value around 45% OM content can be defined, below which

TDNP peats are wettable and above which they turn water repellent. Among the group of charophytes and organic soils, only 1 sample of edaphized charophytes with high organic matter content showed in situ SWR in February.

Soil water content and field SWR variations between February and July 2009 are shown in Figure 6.11. In situ SWR in both seasons was observed in two samples of this subset, one of edaphized charophytes and one of peat. Under dry environmental conditions in July, 5 peat samples became water repellent. These samples showed relatively sharp decreases in their water content between both sampling campaigns. The shaded band corresponds to the critical soil water content range (9-22%) estimated for TDNP peats according to field and laboratory observations. Peat becomes hydrophobic at water contents within or below this range.

However, 2 peat samples that showed in situ SWR in February were not repellent in July. Volumetric water content of one of these samples increased from 16% in February to 47% in July, whereas the other one remained almost constant around 15%. Both samples showed large organic matter contents over 50%. These observations might be due to small scale heterogeneity as the samples were not taken in the same exact location in both periods (centimetric variability). Sampling atmospheric conditions have also been reported to affect field SWR determinations (Doerr et al., 2002). Furthermore, irregular wetting patterns in peat areas during 2009 were enhanced by the strong development of cracks and pipes.

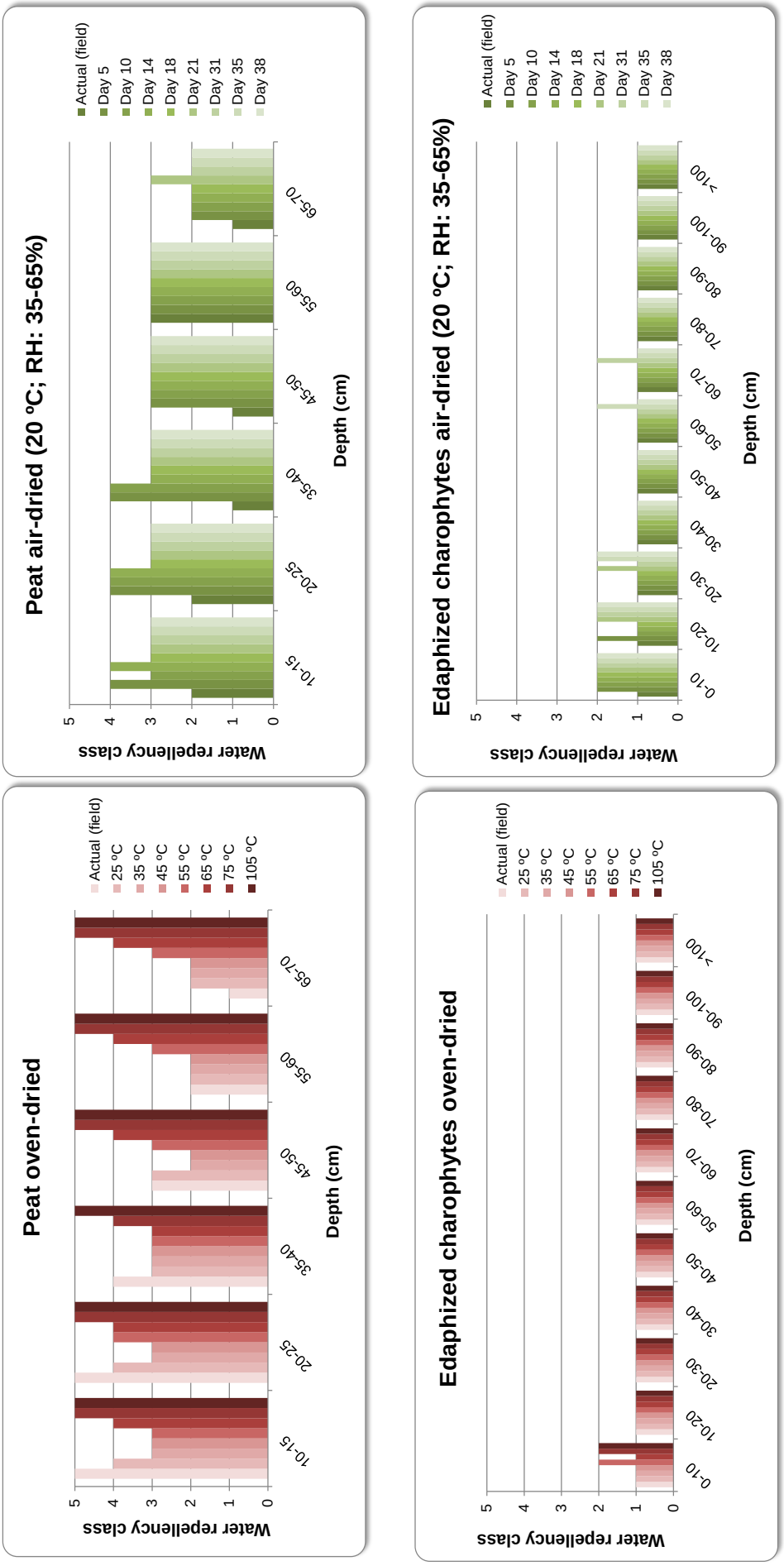

Fig. 6.9. Potential soil water repellency (SWR) characterization in peat and edaphized charophytes soils from Las Tablas de Daimiel National Park (TDNP). For each soil type, SWR degrees (classes as defined by Dekker and Jungerius, 1990were assessed on samples gathered in depth in random soil profiles through two different methods: oven-drying at increasing temperatures (red gradated bars) and air-drying in the laboratory for several days (green gradated bars) under controlled room air temperature and relative humidity (RH).

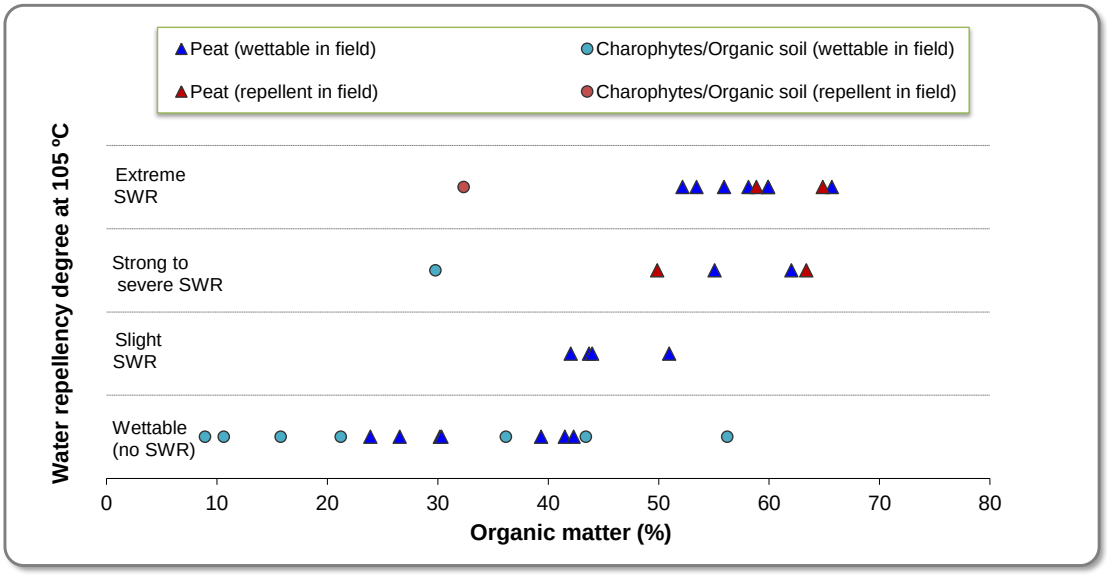

Fig. 6.10. Actual and potential soil ater repellency (SWR) degree against organic matter content (%) in random samples from different depths of organic soil functional types (SFT) from Las Tablas de Daimiel National Park (TDNP). Potential SWR degrees in the laboratory have been estimated by means of the Water Drop Penetration Test (WDPT): wettable (< 5 s), slight WR (5-60 s), strong to severe WR (60-3600 s) and extreme WR (> 3600 s). Actual SWR determined in the field in February 2009 only distinguishes between wettable (< 5 s, blue) and repellent (> 5 s, red) samples. Peat samples (triangles); charophytes and organic soils samples (circles).

On the other hand, the actual effect of SWR on the water absorption capacity of TDNP soils was studied through the capillary wetting rate experiment. The most noticeable differences have been observed between topsoil samples of different SFT (Fig. 6.12). Under field conditions, maximum wetting rate of non repellent soils such as clay, silt and undisturbed charophytes is reached within the first 10 hours of experiment. This time is considerably reduced when the test is carried out on oven-dried samples. Silt is the SFT that can uptake the highest water volumes, which is in agreement with its water retention properties (see section 6.7.1). The parallel behaviour of undisturbed charophytes and silt appears to be related to their common silty textural nature (Table 6.5). On contrary, peat, in spite of showing the highest measured θ_s exceeding 75 vol% (see Table 6.8 in section 6.7.1), is unable to absorb water volumes above 20% and requires longer times to reach constant levels. This is due to water repellency and when it becomes extreme, after drying at 105 °C, peat capillary water absorption capacity is completely hindered.

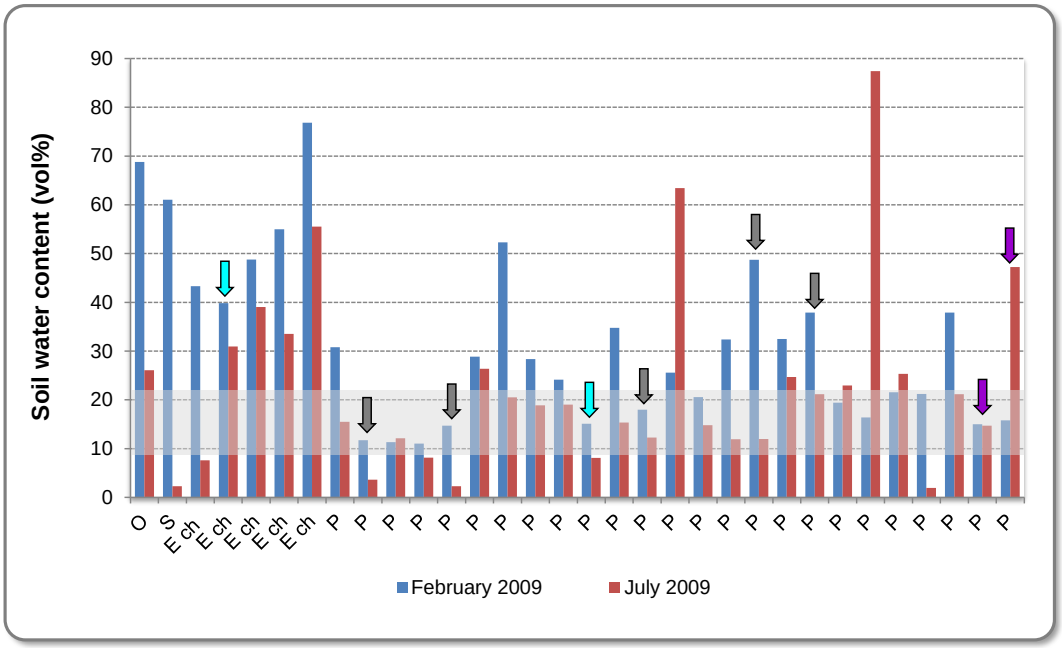

Fig. 6.11. Seasonal soil water content and actual soil water repellency variations in random samples from different depths of organic soil functional types (SFT) from Las Tablas de Daimiel National Park (TDNP): P (peat), E ch (edaphized charophytes), O (organic) and S (silt). Turquoise arrows represent soil samples that were water repellent in the field both in February and July; dark grey arrows indicate samples that were not water repellent in February but became repellent in July; purple arrows identify those samples that showed soil water repellency in February but not in July. The shaded band corresponds to the estimated critical soil water content range (9-22%) for TDNP peats to become soil water repellent.

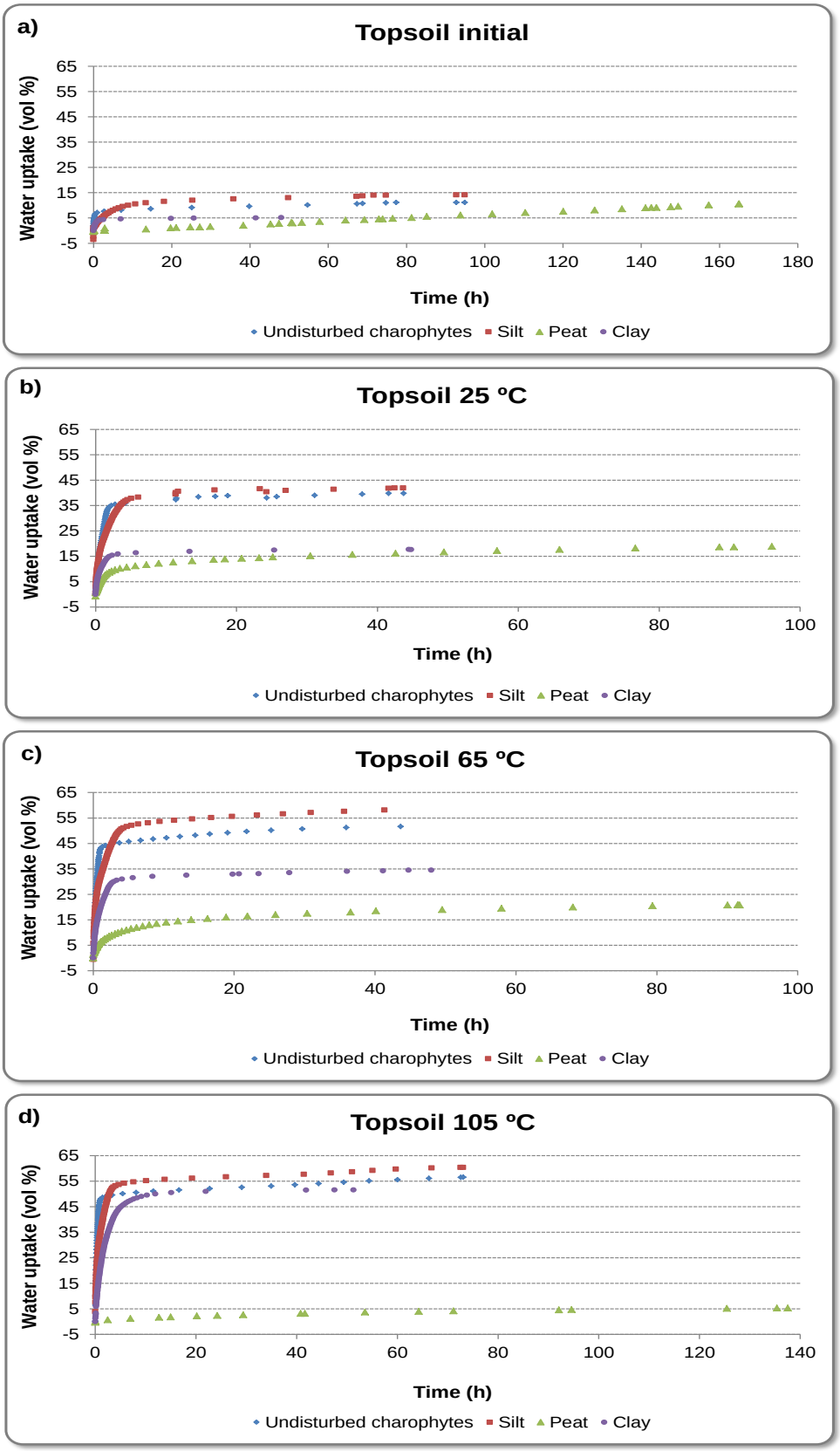

Fig. 6.12. Capillary wetting rate curves of topsoil samples of different soil functional types (SFT) from Las Tablas de Daimiel National Park (TDNP). The experiment was carried out on the field-moist samples (a) and then successively repeated after oven-drying at increasing temperatures (b, c and d).

6.3.4. Summary and conclusions on VZ physics

The SFT physical properties reflect large and small scale heterogeneity. A wide range of bulk densities, saturated hydraulic conductivities and infiltration capacities have been observed. SFT textures, however, show a more homogenous distribution of fined grained materials (silt loam) typical of wetland areas.

In general, lower bulk densities are associated to higher saturated hydraulic conductivities, infiltration capacities and organic matter contents. Lower densities and higher organic matter contents in peat, organic soil, peaty silt and edaphized charophytes determine a less compact structure which enhances the water transmissivity capacity of these materials. Extremely large K_s values measured for TDNP peats [$(2.2. \pm 0.9)\cdot 10^4$. cm d^{-1}]) are conditioned by highly developed secondary porosity and huge swelling capacity.

Infiltration curves have been successfully fitted to Horton's and Kostiakov's models (R^2 above 0.6 in all cases and over 0.8 in 82% of the cases). The lowest capacities correspond to clayey materials with an average value of 159 cm d^{-1}, whereas peats reach up to over 2,000 cm d^{-1}. However, Kostiakov's model does not give realistic estimates of the final infiltration capacity in those tests in which a fast decrease of the initial infiltration speed is observed. The underlying reason is the suitability of this model to simulate horizontal infiltration fluxes where the gravity effect is negligible (Mbagwu, 1994), which is not the case of systems such as TDNP where gravity driven vertical flux is dominant due to hydraulic gradient inversion.

The analyses of SWR in TDNP soils have identified peat and edaphized charophytes as the only water repellent SFT. The amount and type of organic matter, as well as the soil water content have been targeted as the main conditioning factors. For TDNP peats, a threshold value around 45% OM content can be defined, below which they are wettable and above which they turn water repellent. The SFT classified as organic soil

does not show SWR. As reported by other authors for different kinds of soils (Wallis and Horne, 1992 in Doerr et al., 2000; Valat et al., 1991; Ellies et al., 2005; Hurra and Schaumann, 2006), the underlying reason seems to be the quality of their organic matter, as these soils are either flooded, bare or covered by annual vegetation, but not by reed beds like edaphized charophytes. In general, edaphized charophytes show a slight degree of water repellency. However, peat soils develop extreme SWR after complete drying at 105 °C, a laboratory condition no too far from reality given the high temperatures and smouldering combustion observed in the field. However, SWR studies need to be complemented with in-situ measurements to take into account actual field conditions and seasonal influence. In this sense, most peat field samples did not show SWR under humid winter conditions whereas 20% became water repellent in July. These results allowed defining a critical volumetric soil water content range between 9% and 22% for SWR development in TDNP peats. SWR on dry peat soils strongly hampers their water absorption capacity as revealed by the wetting rate experiment, being unable to absorb water volumes above 20%.

6.4. Soil moisture and temperature

The soil moisture status is a variable of great importance to understand the behaviour of the VZ. Nevertheless, it has been used as calibration variable in the water flow model presented in section 6.7. Both soil moisture and temperature, together with organic carbon, are key variables in smouldering fires (Grishin et al., 2006; Rein et al., 2008; Rein, 2009).

The sensor network installed in TDNP soils (Fig. 5.4) has allowed for continuous monitoring of temperature and moisture variations at different depths from mid April 2009 until December 2009. Soil profiles of the 12 monitoring points described in situ in April 2009 are represented in Figure 6.13. In general, the arrangement of SFT shows high heterogeneity, even when comparing near soil profiles. This is due to natural

historic flood and drought cycles in TDNP (Gil-García et al., 2007; Santisteban and Mediavilla, 2012b) that strongly modify the emergent vegetation development and, particularly, the growth of charophytes.

Profiles P01 and P10 are mainly constituted by peat while the rest represent alternations with charophytes or other organic materials. Soil profile P01 shows peaty layers of more than two meters thick. This kind of soil profile can only be found in certain areas around the Guadiana riverbed (Fig. 6.1) and, thus, it just accounts for a very small percentage of total outcropping peatlands in the Park.

Profiles P02, P03 and P04 are typical representatives of the most usual distribution of peat: thin layers, generally between 0.1 and 0.5 m, alternating with charophyte layers. Profile P02 showed an impenetrable layer of hard dry compact grey peaty material between 60 and 80 cm deep. This kind of material was often found in peat dominated areas throughout TDNP during different field sampling campaigns under dry conditions. It likely represents peat layers that burnt in former fires.

On the other hand, profiles P06 to P11 show higher lithological heterogeneity with peat layers of variable thickness appearing at different depths. In two of these points (P08 and P11) shallow groundwater levels were observed at 65 cm deep. This fact is likely related to their proximity to the Guadiana River ditch (Fig. 5.4). Profiles P05 and P09 are the only ones where peat layers were not present, the former entirely constituted by organic soil and the last dominated by charophytes. Finally, P12, located in the northern area, shows a thick clay layer underneath the peat.

It is also worth mentioning that in profiles P03, P04, P06 and P07 between 65 and 80 cm deep, cavities ranging from 0.5 to 1 m deep were observed. These cavities are highly relevant from the water transmission and air circulation point of view, as will be discussed in section 6.6.

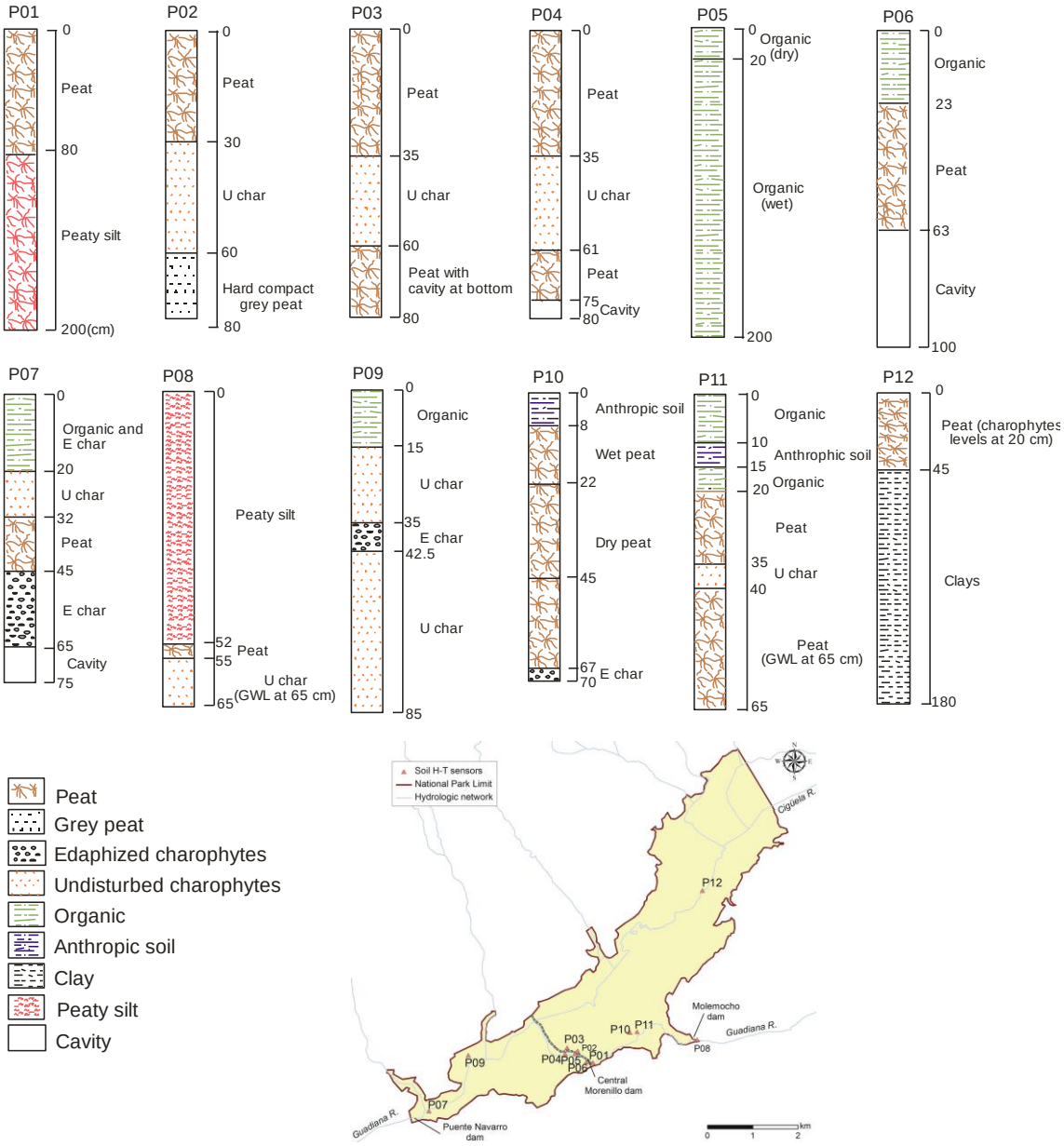

Fig. 6.13. Descriptive soil profiles with the arrangement of soil functional types (SFT) layers in depth in the twelve locations inside Las Tablas de Daimiel National Park (TDNP) where soil moisture and temperature sensors for continuous monitoring were installed (see Fig. 5.4).

Figure 6.14 shows the soil moisture and temperature response recorded by the sensors. The general trend through the warm season (April to June) is a gradual temperature increase coupled to a soil moisture decrease. Gaps and negative values in sensor recordings are likely due to disconnections from the soil matrix as cracks and hollows developed. In spite of material heterogeneity, all plots show a temperature

decrease in depth until the end of the summer. Colder meteorological conditions from then on induced sharper temperature decreases near the soil surface (sensor T1) and temperatures become higher in deeper layers (sensors T2 and T3). The particular case of P03 is linked to the 2009 smouldering fire and is further discussed in section 6.6.4.

The shallowest temperature sensor (T1) placed at 20 cm from the surface in all points reflect daily thermal oscillations. Sensors T2, placed around 50 cm deep, show in most cases a soft relatively linear temperature increase in time. The deepest temperature sensors (T3) located inside cavities (P01, P02, P03, P04, P06 and P07) do not show significant variations, in exception of P01, where daily thermal oscillations began to be registered by this sensor from the end of May. This fact can be explained by a significant increase of the cavity were it was placed. Both the highest and lowest temperatures have been recorded in shallow peat in P02, with values exceding 35 °C by the end of the 2009 summer season and droping to around 4 °C at the end of November.

On the other hand, deeper soil moisture sensors (H2) globally registered higher water contents than the shallower ones (H1), independently from the soil material. These expected observations are related to higher evaporation levels near the surface. In peat dominated areas around the central Morenillo dam, moisture differences are sharper in those points where peat showed and advanced stage of desiccation (P04, P05 and P06). For saturated conditions in P08 and P11 (groundwater level at 65 cm deep), higher and constant soil water contents are observed in both sensors.

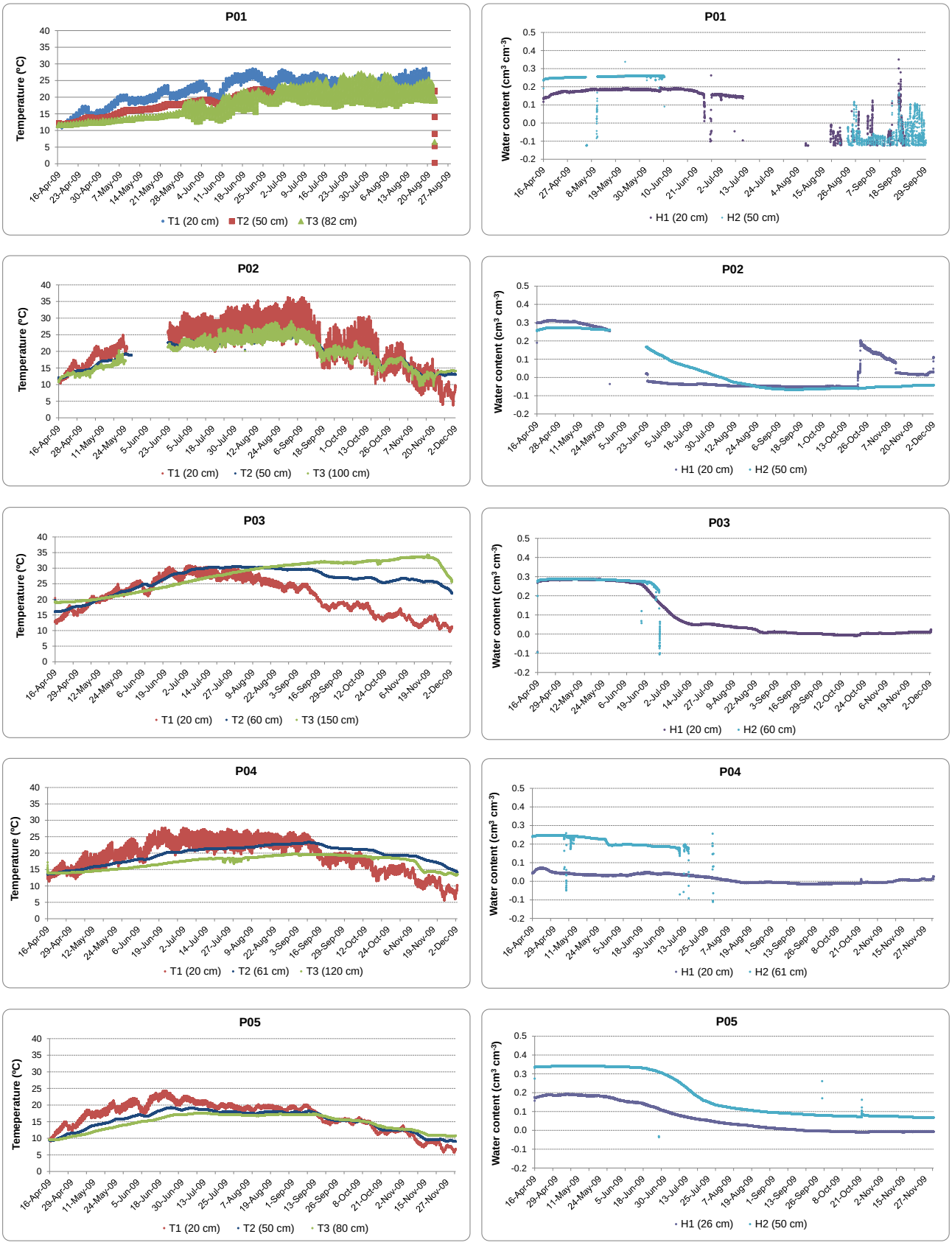

Fig. 6.14. In depth soil temperature and moisture patterns recorded by moisture (H) and temperature (T) sensors in each of the twelve monitoring points (Figs. 5.4 and 6.13) between April and December 2009. GWL: groundwater level.

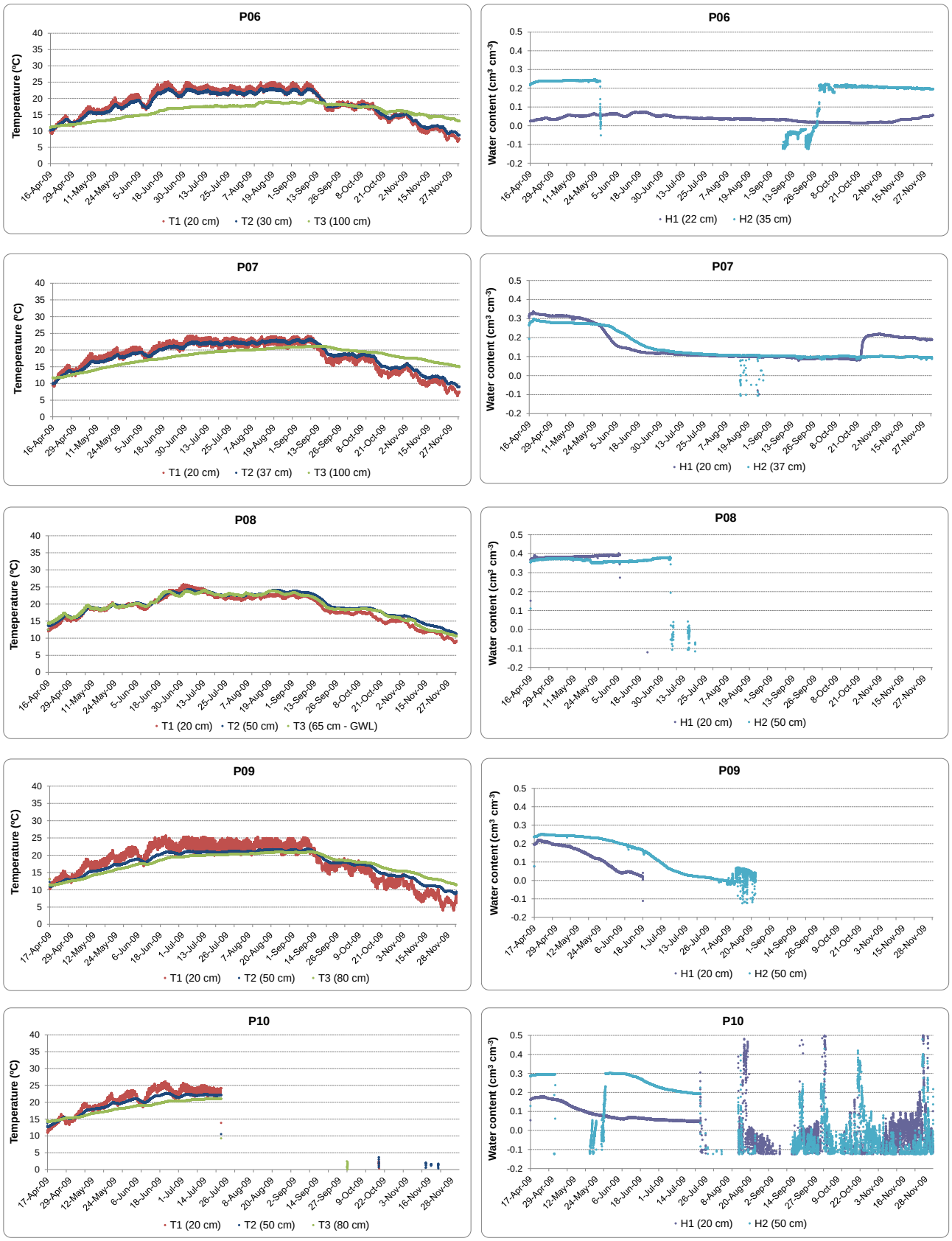

Fig. 6.14. Continuation.

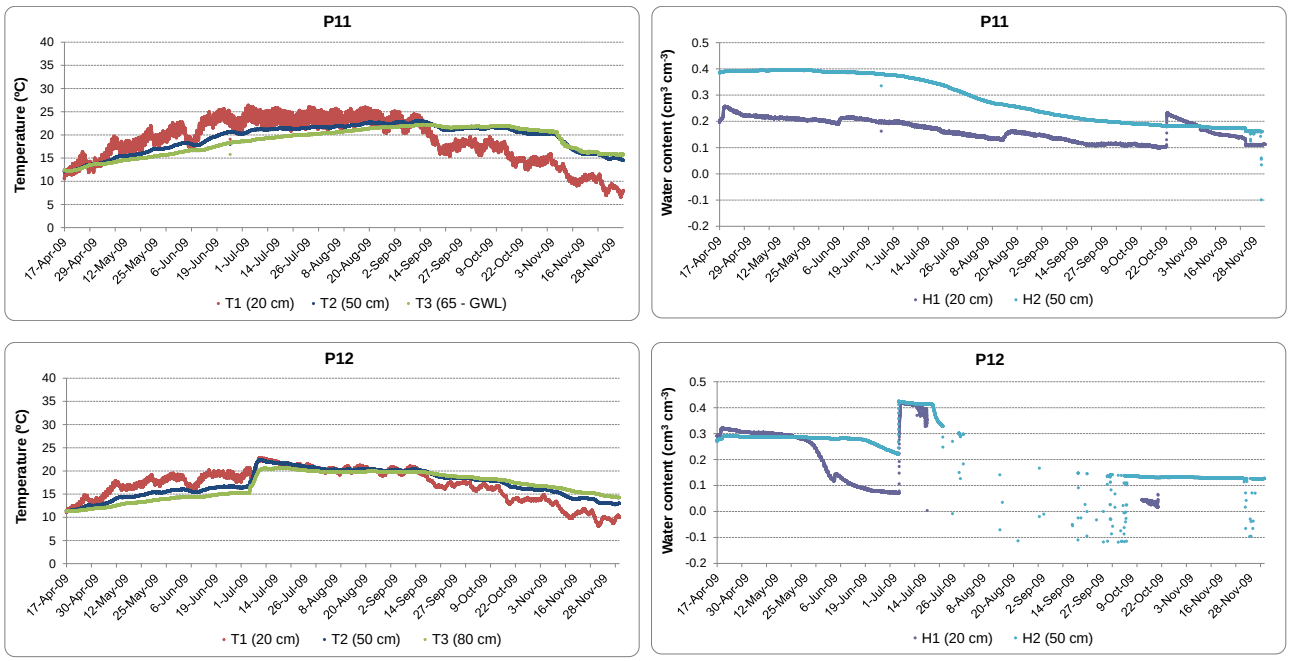

Fig. 6.14. Continuation.

The monitoring point in the northern TDNP area (P12) is the only one which registered the inflow of the 2009 water transfer (Fig. 6.14). This transfer had a very low performance (Fig. 4.2), and only the northern inlet area was slightly flooded. Soil water content in the deepest H2 sensor placed in clay peaked to values close to the 0.49 $cm^3\ cm^{-3}$ θ_s value found for this material (see Table 6.8 and Fig. 6.29 in section 6.7.1). The graph shows the seasonal temperature increase mentioned above and the topsoil peat moisture decrease (H1: 20 cm) to almost complete drying out. The deepest sensor (H2: 50 cm) placed in clay registered a much softer and slower soil moisture decline. Immediate response following the arrival of the transferred water is observed: temperature and soil moisture increase and homogenization in all sensors. A very sharp soil moisture increase was recorded by the peat sensor, corroborating the high absorption capacity of this material when excess water is available. However, soil moisture decrease starts rapidly after a few days (sooner in the topsoil peat) as surface flooding disappears.

In general, charophytes show higher water contents than peats due to prevailing drainage conditions. However, peat is a warmer material with temperatures exceeding those of charophytes in around 2 °C during the coldest months. Peat temperatures in depth are also 3-4 °C higher than in other materials during warmer months. Higher temperature in topsoil peat is due to its dark colour which enhances the absorption solar radiation, the main source for soil heat (Brady and Raymond, 1996). Higher temperature in deeper peat can be explained by the intensive microbial activity supported by this organic material (Guerrero, 1985), which causes oxygen consumption and temperature increase (Brady and Raymond, 1996). Furthermore, low soil moisture enhances temperature increase as the heating capacity of water is higher than that of rocks.

6.5. Hydrological and hydrochemical environment: conceptual model of SW-GW interactions

The results presented in this section regarding TDNP surface water and groundwater hydrochemical environments and SW-GW interactions have been recently published in an article in Hydrogeology Journal (Aguilera et al., 2013). The dynamics of SW-GW interactions under varying flooding conditions in the complex multi-layer aquifer system around the TDNP area are discussed. In order to tackle the complexity and heterogeneity of the area and the lack of detailed geological and hydrogeological data, a simple approach combining the hydrochemical, hydrodynamical and isotopic dataset through clustering techniques and long-term time series analysis has been applied (see section 5.6.2). This has allowed, for the first time, to delve into the dynamic and zoned behaviour of the system under extreme drying and flooding conditions, interrelating both local and regional scales. A conceptual model of TDNP hydrological behaviour, involving both spatial and temporal considerations in SW-GW interactions, is proposed. The model is based on the interrelation between flooding, groundwater

level and hydrochemistry, and takes into account factors derived from lithostratigraphic layout and system anthropization.

6.5.1. Hydrochemistry

The sampling period 2003-2010 represents a desiccation process in the wetland until an extraordinary wet period slightly supported by a small water transfer at the beginning of 2010 manage to re-flood the whole area. In 2009 TDNP dried out completely and a smouldering peat fire took place (Moreno et al., 2010, 2012b). This desiccation process is reflected in the hydrochemical characteristics of the samples, where large solute concentrations and variability are observed (Table 6.6). In both surface water and groundwater, variables show wide dispersion, particularly in surface water, as it is subjected to different origins (water transfer, rainfall, wastewater, freshet and groundwater) and higher evaporation rates. In a recent work by Castaño et al. (2011), using the isotopic composition of precipitation as input, they estimated an evaporation rate of 25% in incoming water through the Cigüela ditch and of 45% in re-evaporated water table samples. The system of dams inside TDNP increases ponding water residence time and enhances infiltration, thus, conditioning evaporative processes that increase water salinity (de la Losa et al., 2012).

Due to the large hydrochemical variability, highly conditioned by anthropic factors, a comparative multivariate statistical analysis on the data of single monitoring points such as that performed for VZ chemistry (see section 6.2) has not been considered useful. The whole unprocessed hydrochemical dataset has been included in appendix F.

6.5.1.1. Surface water

The hydrochemistry of surface water, both ponding water and inflow water, shows very large variability in all parameters, except for pH, with coefficients of variation ranging from 14% to 200%. Therefore, similarly as for VZ chemistry, median values are more representative than mean values to describe average characteristics (see section 6.2.1). The median EC values are between 3,000-5,000 μS cm^{-1}, except for the outlet point S-7 where average salinity exceeds 11,000 μS cm^{-1}. The relatively high salinity observed in ponding water, particularly in points located on the right (north) margin, results from the combination of evaporation and shallowness, and salt dissolution from saline clayey soils (Aguilera et al. 2011; Castaño et al., 2011; Jolly et al. 2008).

One general spatial distinctive feature can be outlined: higher EC values and dispersion in the northwestern area (S-1, S-2 and S-3), and relatively lower in the eastern side (S-4, S-5 and S-6) and inflowing water at the gauging station in the Cigüela River (S-IW). The pH values are quite homogeneous and slightly basic in all sampling points, with the highest median values being reported at inlet point (7.8 in S-IW) and the lowest at the outlet (7.0 in S-7). Besides this, median TOC concentrations in ponding water are, in general, higher than the average for surface water (5-6 mg l^{-1}, Rodríguez Vidal, 2003). In fact, the correlation coefficient between pH and TOC in ponding water is -0.48 ($p<0.0001$) and, therefore, redox processes associated to organic matter might be the cause of the slight acidification along TDNP. The fact that the lowest TOC concentrations are found in the inflow water reflects the important internal loading of organic matter and eutrophic conditions in TDNP reported in previous studies (see section 6.2; Sánchez-Carrillo and Álvarez-Cobelas, 2001; Sánchez-Carrillo et al., 2001). The sampling points S-5 and S-6, with lower salinity and dispersion, represent the flow through the Guadiana ditch of the groundwater that is pumped from wells such as G-07 to artificially flood the eastern area of the Park during dry periods (Fig. 5.5). The outlet point at the Puente Navarro dam (S-7) shows the highest values of all parameters. In this point water remained for a longer time during the drying out of the

Park in 2007-2009 and, thus, more samples (n=28) could be taken reflecting the concentration process due to evaporation.

On the other hand, the global NO_3^- concentrations in surface water are relatively low (medians below 8 mg l^{-1}). Opposite to organic carbon, the highest nitrate median values are attained at the inflow point and at S-5 (fed by groundwater), suggesting that the main source of NO_3^- to the hydrological system is external (Berzas et al., 2000; Rebollo, 2007; Sánchez-Carrillo and Álvarez-Cobelas, 2001).

6.5.1.2. Groundwater

Variability is lower in groundwater than in surface water, as almost half of the CV values for major variables such as EC and SO_4^{2-} are below 10% (Table 6.6). The highest salinity levels (median > 9,000 μS cm^{-1}) can be found upstream of the central dam, both in the NW area (G-01 and G-02) and in the northeastern side (G-03, G-04, G-05 and G-06). However, this group of extremely saline points shows different dispersion patterns: higher EC and SO_4^{2-} variability in G-03, G-04 and G-05, with CV values ranging from 21% to 32%, than in G-01, G-02 and G-06, where CV values range from 4% to 8% The lowest salinities correspond to G-12, G-15, G-17 and G-18, with median and average values below 2,000 μS cm^{-1}. The first three, located east from TDNP limits (Fig. 5.5), represent the quality of the regional Tertiary aquifer in the pumping areas.

Groundwater nitrate concentrations are higher than in surface water, with the highest values again in the northern area (G-01 and G-02, Fig. 5.5), and in groundwater monitoring points located further away from TDNP limits which are influenced by fertilized irrigation areas. These findings, together with the observations in surface water, point to agriculture as a primary source of nitrate in the water system. Nevertheless, internal loading through organic matter oxidation must also be taken

into account (see section 6.2). Further $^{15}N/^{14}N$ and $^{18}O/^{16}O$ isotopic analyses should be performed to determine nitrate sources to the TDNP system.

The largest average TOC concentrations are found in G-04, G-05 and G-11 (medians above 9 mg l^{-1}), indicating a close interrelation with surface water given the significant presence of TOC in most ponding water samples and that usual concentrations in unpolluted groundwater are around 1 mg l^{-1} (Rodríguez Vidal, 2003). Given that infiltration is a dominant process and that the organic carbon concentration in the first meter of the VZ is quite high (see section 6.2.1), the source of TOC in groundwater is necessarily linked to the surface environment, as observed in other semiarid floodplains (Valett et al., 2005). Similarly as in surface water, pH is very constant and homogeneous, with median values slightly lower and closer to neutrality. However, some of the lowest median pH values also correspond to G-03, G-04, G-05 and G-11. These facts strongly suggest an influence of organic matter degradation and bacterial respiration in infiltrating surface water through the VZ on these groundwater monitoring points (see section 6.2.2). Besides these, strong smells were always recorded in G-11, indicating anaerobic organic matter degradation.

Point G-08, located between S-5 and S-6 (Fig. 5.5), seems to be influenced by the infiltration of the groundwater pumped from the emergency wells and poured into the Guadiana ditch, as pointed out by the similarity with the hydrochemical composition of S-5 and S-6.

The differences in Ca^{2+} concentrations between sampling points are less pronounced due to its presence in both gypsic and carbonated media, which enhances the dynamism of this cation from the point of view of geochemical dissolution-precipitation equilibrium. The values and homogeneity in groundwater calcium concentrations are in agreement with those observed in SFT constituting the VZ (see section 6.2.1), corroborating the controlling effect of lithology. Nevertheless, it is noteworthy that the highest Ca^{2+} concentrations in groundwater, apart from saline G-

01 and G-02, are, again, observed in G-03, G-04, G-05 and G-11, where values are similar (slightly higher) to the concentrations found in surface water.

The hydrochemical study reflects the high degree of system heterogeneity further increased by human intervention. Footprints of degradation are increased salinity and nutrient loading to the groundwater system.

Table 6.6. Descriptive statistics of physical-chemical variables in surface and groundwater sampling points from the monitoring network in the period 2003-2010. Electrical conductivity (EC) and pH values correspond to laboratory determinations. SD: standard deviation; n: number of samples; CV: coefficient of variation.

			EC (µS cm^{-1})							SO_4^{2-} (mg l^{-1})						
			n	Min	Max	Median	Mean	SD	CV	n	Min	Max	Median	Mean	SD	CV
Groundwater		G-01	11	12604	16284	15383	15012	1219	0.08	11	3900	5350	4620	4749	402	0.08
		G-02	31	12233	15114	13774	13716	565	0.04	31	2500	3840	3500	3509	233	0.07
		G-03	7	3024	10924	9725	8583	2782	0.32	7	592	2800	2300	2143	681	0.32
		G-04	32	3690	13174	10584	9866	2052	0.21	32	1200	4150	3300	3252	670	0.21
		G-05	7	3690	13284	12494	11350	3154	0.28	7	1422	4220	3800	3535	878	0.25
		G-06	31	9033	12143	10633	10513	737	0.07	31	2840	3700	3300	3295	215	0.07
		G-07	1			2563	2563			1			730	730		
		G-08	5	3333	3924	3553	3634	239	0.07	5	980	1250	1160	1142	89	0.08
		G-09	7	1692	3094	2334	2219	485	0.22	7	336	628	390	445	116	0.26
		G-10	28	3864	4723	4269	4269	194	0.05	28	1020	1460	1186	1175	94	0.08
		G-11	30	2440	7795	7088	6929	892	0.13	30	960	3100	2750	2662	398	0.15
		G-12	24	1340	5910	1704	1891	879	0.46	24	190	2520	262	361	453	1.25
		G-13	4	3770	5544	4814	4736	773	0.16	4	1240	1910	1655	1615	281	0.17
		G-14	7	4773	6510	5024	5378	668	0.12	7	1930	2500	2080	2151	213	0.10
		G-15	7	1430	1659	1574	1550	85	0.05	7	464	570	508	522	34	0.07
		G-17	5	1244	2314	1695	1681	377	0.22	5	306	608	420	416	110	0.26
		G-18	6	613	703	677	671	30	0.04	6	78	92	87	86	4	0.05
Surface Water	Ponding water	S-1	5	1406	16994	3904	7518	5821	0.77	5	664	8650	1510	3235	2943	0.91
		S-2	10	1362	17103	4864	6692	4228	0.63	10	664	4050	1615	1891	861	0.46
		S-3	3	4264	26385	4614	11754	10346	0.88	3	1580	8900	1870	4117	3384	0.82
		S-4	5	1413	5895	3824	3804	1432	0.38	5	656	1810	1540	1429	413	0.29
		S-5	21	1050	3513	2973	2908	522	0.18	21	446	1240	1080	1001	179	0.18
		S-6	13	1410	5003	3444	3496	851	0.24	13	668	2060	1300	1388	370	0.27
		S-7	28	1406	145621	11739	18074	25653	1.42	28	652	48000	4995	6762	8361	1.24
	Inflow water	S-IW	6	1487	5045	3559	3406	1135	0.33	6	732	1920	1485	1347	412	0.31

Table 6.6. Continuation

			Ca^{2+} (mg l^{-1})							pH						
			n	Min	Max	Median	Mean	SD	CV	n	Min	Max	Median	Mean	SD	CV
Groundwater		G-01	11	520	860	590	624	99	0.16	11	7.0	8.0	7.3	7.5	0.3	0.04
		G-02	31	600	980	712	720	76	0.11	31	6.8	7.9	7.2	7.3	0.3	0.05
		G-03	7	250	780	640	593	155	0.26	7	6.3	7.5	6.8	6.9	0.4	0.06
		G-04	32	292	760	655	636	98	0.15	32	6.6	7.8	7.2	7.2	0.4	0.05
		G-05	7	380	760	640	593	114	0.19	7	7.0	8.0	7.2	7.4	0.4	0.05
		G-06	31	370	698	570	558	65	0.12	31	6.8	7.8	7.3	7.4	0.3	0.04
		G-07	1			220	220			1			7.5	7.5		
		G-08	5	260	390	322	323	43	0.13	5	7.2	7.8	7.3	7.4	0.2	0.03
		G-09	7	122	252	152	173	46	0.26	7	5.2	7.7	7.2	7.0	0.8	0.11
		G-10	28	340	529	394	408	48	0.12	28	6.5	7.6	6.9	7.0	0.3	0.05
		G-11	30	334	870	755	749	96	0.13	30	6.5	8.0	6.8	7.0	0.4	0.06
		G-12	24	61	630	125	144	106	0.74	24	6.5	7.9	7.0	7.1	0.4	0.06
		G-13	4	429	631	515	523	82	0.16	4	7.2	7.9	7.3	7.4	0.3	0.04
		G-14	7	420	651	492	513	83	0.16	7	6.8	8.0	7.3	7.4	0.4	0.06
		G-15	7	168	216	188	191	18	0.09	7	7.4	8.1	7.5	7.6	0.3	0.03
		G-17	5	132	242	166	176	37	0.21	5	7.1	7.9	7.2	7.4	0.3	0.04
		G-18	6	62	100	81	83	12	0.14	6	7.3	8.0	7.4	7.6	0.2	0.03
Surface Water	Ponding water	S-1	5	240	1790	542	788	557	0.71	5	7.0	7.7	7.5	7.4	0.2	0.03
		S-2	10	236	790	481	533	178	0.33	10	7.1	8.0	7.7	7.6	0.3	0.04
		S-3	3	467	650	641	586	84	0.14	3	7.0	7.7	7.5	7.4	0.3	0.04
		S-4	5	246	518	430	416	95	0.23	5	6.9	7.9	7.5	7.4	0.4	0.05
		S-5	21	146	392	310	313	60	0.19	21	7.0	7.9	7.5	7.5	0.2	0.03
		S-6	13	240	604	384	414	106	0.26	13	6.9	7.8	7.4	7.4	0.3	0.04
		S-7	28	242	1600	940	937	361	0.39	28	6.1	8.0	7.0	7.1	0.5	0.06
	Inflow water	S-IW	6	250	496	418	386	94	0.24	6	7.2	7.9	7.8	7.7	0.2	0.03

Table 6.6. Continuation.

			NO_3^- (mg l^{-1})							TOC (mg l^{-1})						
			n	Min	Max	Median	Mean	SD	CV	n	Min	Max	Median	Mean	SD	CV
Groundwater		G-01	11	24.0	47.0	33.0	33.3	7.8	0.23	11	2.0	8.2	6.0	5.7	1.7	0.30
		G-02	31	1.0	92.0	66.0	65.3	15.1	0.23	29	3.4	29.8	4.2	5.4	4.7	0.88
		G-03	7	3.0	70.0	4.0	17.3	23.8	1.38	7	1.8	5.5	3.2	3.1	1.1	0.36
		G-04	32	0.3	9.0	1.0	1.6	1.8	1.17	30	6.0	50.2	10.6	11.4	7.4	0.64
		G-05	7	0.3	6.0	1.0	1.8	1.9	1.08	7	3.2	14.2	9.2	9.2	3.1	0.33
		G-06	31	0.3	24.0	6.0	9.5	7.5	0.79	29	3.5	13.0	7.1	7.6	1.9	0.26
		G-07	1			20.0	20.0			1			1.1	1.1		
		G-08	5	1.0	38.0	14.0	15.6	12.6	0.81	5	3.2	16.0	3.6	6.6	4.9	0.74
		G-09	7	0.3	64.0	0.3	9.6	22.2	2.32	7	2.1	20.2	3.0	5.6	6.0	1.07
		G-10	28	3.0	23.0	5.5	6.4	3.8	0.59	28	0.3	9.5	4.3	4.4	1.6	0.35
		G-11	30	1.0	41.0	28.0	25.9	9.3	0.36	30	7.2	40.4	29.9	28.7	6.2	0.22
		G-12	24	1.0	7.0	4.0	3.7	1.5	0.40	23	0.3	5.0	1.1	1.2	0.9	0.76
		G-13	4	16.0	40.0	26.5	27.3	10.8	0.40	2	0.3	0.8	0.5	0.5	0.3	0.50
		G-14	7	48.0	330.0	98.0	126.0	86.0	0.68	7	1.5	16.6	2.8	5.4	5.2	0.96
		G-15	7	29.0	39.0	31.0	32.1	3.0	0.09	7	1.0	3.5	1.7	2.0	0.9	0.44
		G-17	5	30.0	37.0	32.0	33.2	2.8	0.08	5	0.3	2.8	1.6	1.7	0.8	0.50
		G-18	6	23.0	27.0	24.0	24.2	1.3	0.06	6	0.3	2.2	0.9	1.0	0.7	0.70
Surface Water	Ponding water	S-1	5	0.3	24.0	0.3	5.2	9.4	1.83	3	5.9	99.9	52.1	52.6	38.3	0.73
		S-2	10	0.3	18.0	0.6	4.0	5.6	1.40	8	6.8	43.5	17.7	21.0	11.0	0.52
		S-3	3	1.0	30.0	2.0	11.0	13.4	1.22	1			353.6	353.6		
		S-4	5	0.3	14.0	0.3	3.0	5.5	1.83	3	7.7	37.2	36.2	27.0	13.7	0.51
		S-5	21	0.3	26.0	8.0	9.3	6.7	0.72	20	1.5	16.8	4.7	5.3	2.9	0.54
		S-6	13	0.3	26.0	3.0	5.4	6.8	1.26	12	5.1	24.9	7.3	10.2	6.3	0.62
		S-7	27	0.3	50.0	1.0	13.7	17.1	1.25	27	5.4	414.4	75.6	104.5	97.0	0.93
	Inflow water	S-IW	6	0.3	34.0	11.0	11.9	11.2	0.94	4	3.9	9.4	6.3	6.5	2.2	0.34

6.5.2. The interrelation between hydrochemistry and flooding

Five groups of groundwater monitoring points have been indentified at a small dissimilarity level based on the results provided by the hierarchical cluster analysis of the EC distributions (Fig. 6.15a). Box-plots diagrams of available EC data from each point in the period 2003-2010 represent the variability of their composition (Fig. 6.15b). The first group, showing little spread, includes the monitoring points representative of the deeper layers of the Tertiary aquifer (G-15, G-17 and G-18) and three points of the southern area of TDNP (G-08, G-09 and G-10). The second group is constituted by two groundwater monitoring points located in the northern area (G-13 and G-14) together with the surface incoming water (S-IW), therefore apparently associated with flooding and freshet events. The third group represents the irregular behaviour of two singular points (G-11 and G-12) which show opposite hydrochemical response against flooding. The fourth group is made up by highly saline points with low variability (G-01, G-02 and G-06). The last group is constituted by the most variable groundwater monitoring points (G-03, G-04 and G-05) which show a dynamic behaviour in their composition: saline groundwater under drying conditions and response to incoming surface water during flooding events. To be discussed further is the particularly remarkable difference in behaviour between points located close to each other, such as G-04 and G-06, and G-10 and G-11 (Fig. 5.5).

The dynamic behaviour of the TDNP hydrological system becomes evident when comparing the hydrochemical characteristics in two different periods by means of Stiff diagrams of both surface water and groundwater (Fig. 6.16). A first overview of the plots depicts a global dominance of sulphate-magnesium hydrochemical facies under drying conditions in May 2008 and a shift to sulphate-calcium facies in March 2010 after reflooding took place following heavy rainfalls in the whole catchment basin. Missing diagrams in Fig. 6.16a,b are due to the fact that either monitoring points were respectively dry or could not be accessed at the depicted sampling times.

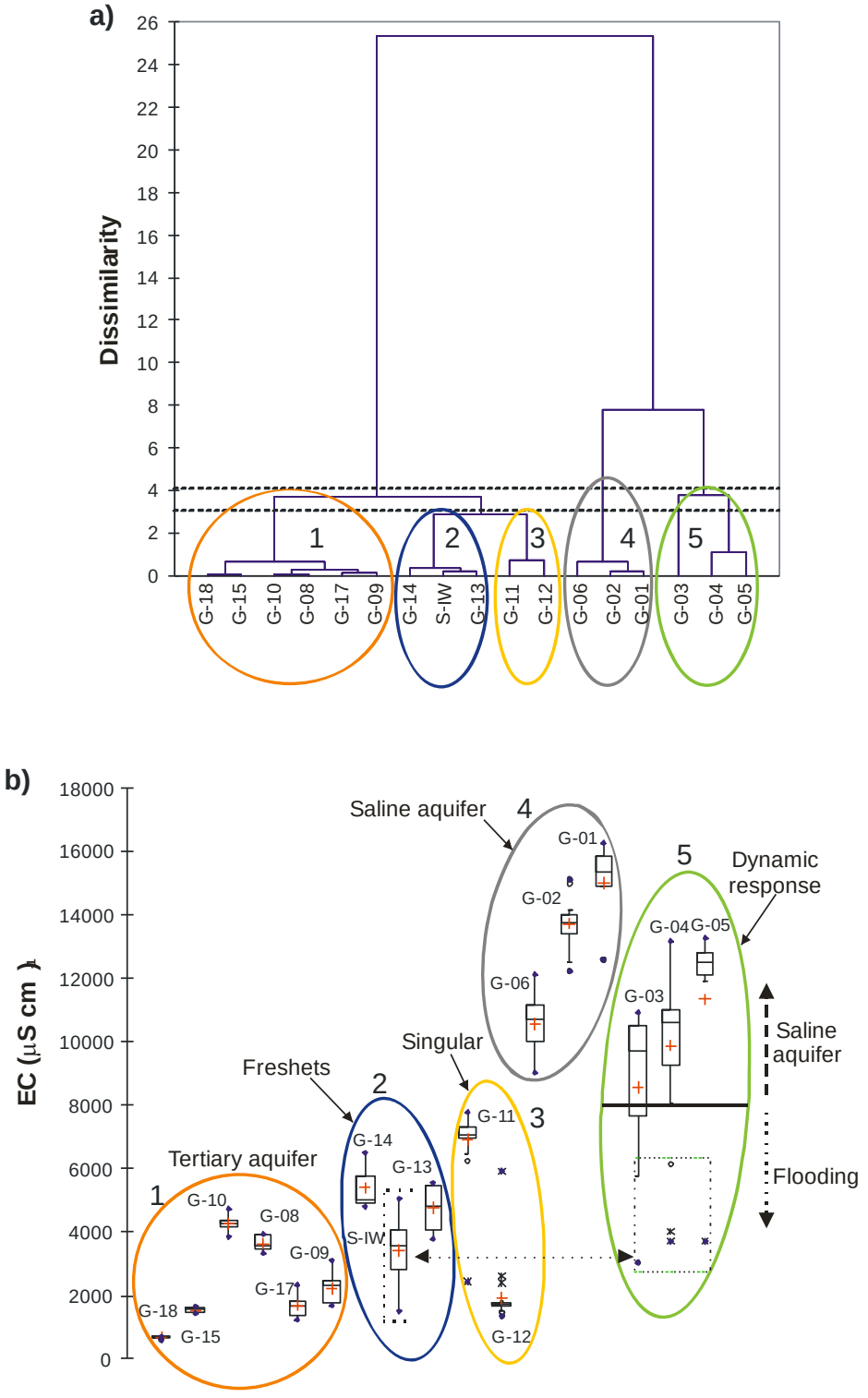

Fig. 6.15. a) Dendrogram from the hierarchical cluster analysis of median, range and interquartile ranges of the distribution of electrical conductivity (EC) in the groundwater monitoring points and the gauging station (S-IW) in Las Tablas de Daimiel National Park area (Fig. 5.5). Dashed lines represent dissimilarity levels 3 and 4. b) Box plots of the EC values in the sampling points of the five groups defined through the cluster analysis in the period 2003-2010. The horizontal dotted line with arrows represents the association between small EC values in groundwater monitoring points from group 5 and flooding events monitored at S-IW.

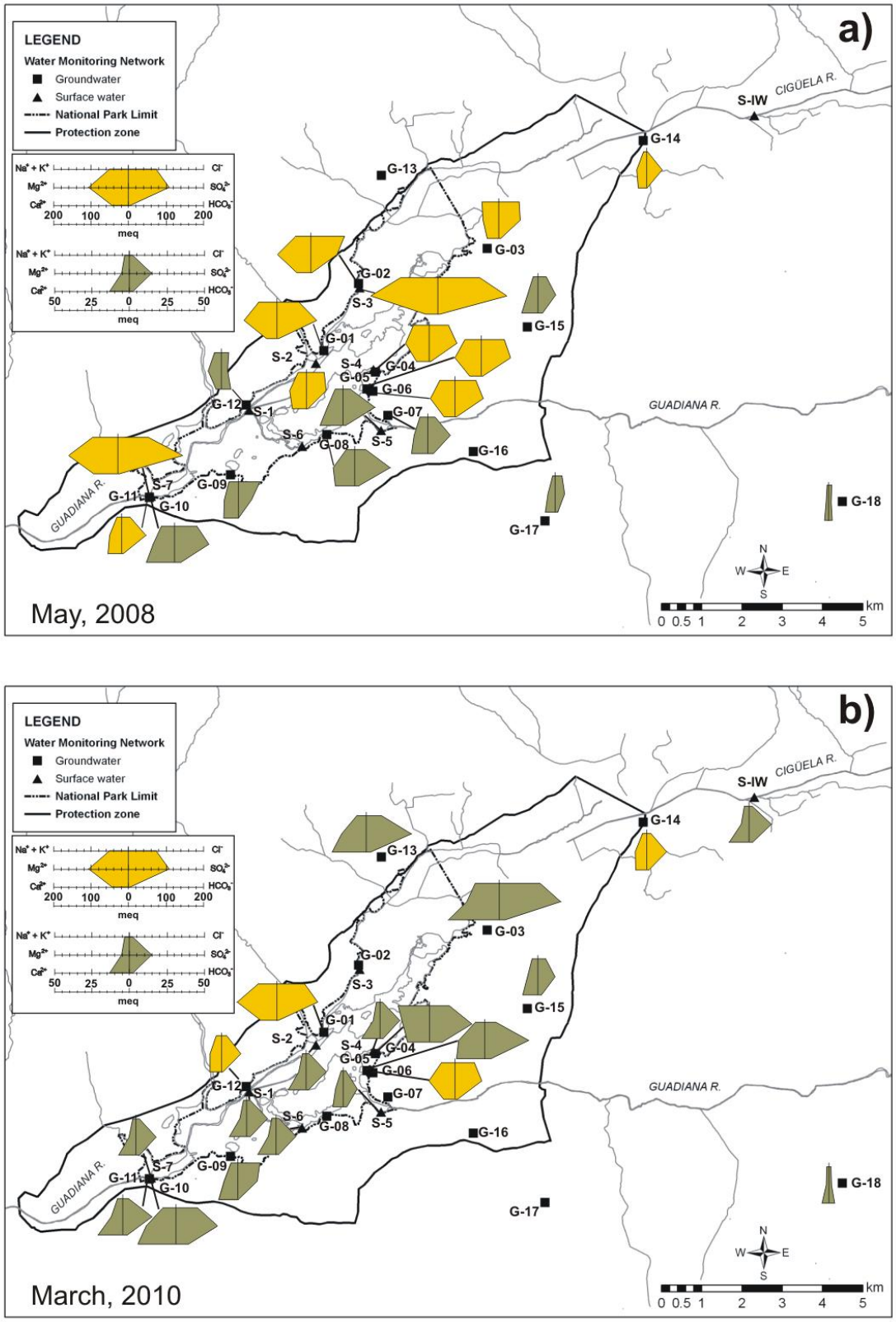

Fig. 6.16. Stiff diagrams of surface water and groundwater sampling points in Las Tablas de Daimiel National Park (TDNP) area under a) drying conditions in May 2008, and b) flooding conditions in March 2010. Note, the yellow and green Stiff diagrams represent different concentration scales.

The Stiff diagrams in May 2008 show the concentrated and salinized conditions in most ponding and groundwater sampling points in the TDNP environment. The 2010 flooding homogenises the quality of surface water as similar Stiff diagrams can be observed for ponding water and incoming water samples, whereas groundwater monitoring points of groups 3 and 5 show the clearest response (Fig. 6.16b). The diagrams of group 5 groundwater monitoring points (G-03, G-04 and G-05) show a notable mixture of saline groundwater with flooding freshwater recharge (Fig. 6.16b). On the other hand, points of group 2, which EC variability was associated to that of S-IW (Fig. 6.15), show a remobilisation effect on groundwater due to rainfall and freshet recharge. The Stiff diagrams from groups 1 and 4 hardly differ between both periods.

6.5.3. The interrelation between groundwater level and flooding

A detailed analysis on the temporal interrelation between available historical records of groundwater level in G-04 (group 5) and both rainfall and flooding area is shown in Figures 6.17a and 6.17b, respectively. Monitoring point G-04 was chosen for two reasons: qualitative response to flooding (Figs. 6.15b and 6.16) and sampling point with more available data. The analysis of results will focus on the period 1988-2010, for which measured, rather than estimated, flood-related data are available. Particularly, this is the period that reflects the current conditions of absence of natural groundwater discharges and of anthropic management of TDNP, and where surface water levels are artificially maintained unless extraordinary wet periods, such as 1997-1998 and 2010-2011, occur. Nevertheless, during the 1980s, quasi-natural groundwater conditions still prevailed, as inferred by the small groundwater-level response to a small areal extent of flooding (Fig. 6.17b).

From the trends shown in Figure 6.17, it is clear that, since 1988, the oscillations of groundwater level have followed the fluctuations in the flooding area, which is highly conditioned by water transfers (Fig. 6.17b). In contrast, the groundwater level

association with rainfall is restricted to extreme rainfall events, such as those of 1997 and 2010, which caused a temporary "natural" flooding through freshets (Fig. 6.17a). The insignificance of direct rainfall recharge has also been observed in other semiarid floodplain wetlands such as the Okavango Delta (Wolski and Savanije, 2006).

The cross-correlation between the 1988-2010 time series of flooding area and groundwater level allows one to quantify the influence of the former on the latter. If a cut-off point of 0.4 is chosen for the correlation coefficient, the positive association between flooding and groundwater level can be set at around 3 months (Fig. 6.18). This means that the average effect of flooding on groundwater (i.e. rise of groundwater levels) would disappear after 3 months.

When the hydrographs of groundwater monitoring points representative of the defined groups are plotted against the flooding area, some particular features arise (Fig. 6.19): i) both flooding-area and groundwater-level peaks are highly dependent on water transfers through the Cigüela River; ii) greater groundwater level response to small flooding events, such as the late spring freshet and summer water transfer in 2007, is found in points located upstream from the central dam, like G-02 (group 4) and G-04 (group 5), as in these cases the area downstream of the dam often remains dry; iii) inefficient water transfers, like that in the late spring of 2009 where just 0.75 hm^3 out of 20 hm^3 reached TDNP, only induce groundwater-level response in areas around the Cigüela ditch, like at G-14 (Fig. 5.5); iv) points from group 1 with deeper groundwater levels (see G-10, G-15, G-17 and G-18 in Table 6.7) are influenced by pumping cycles in southeastern irrigation areas; v) there is a global groundwater level response to full flooding in 2010.

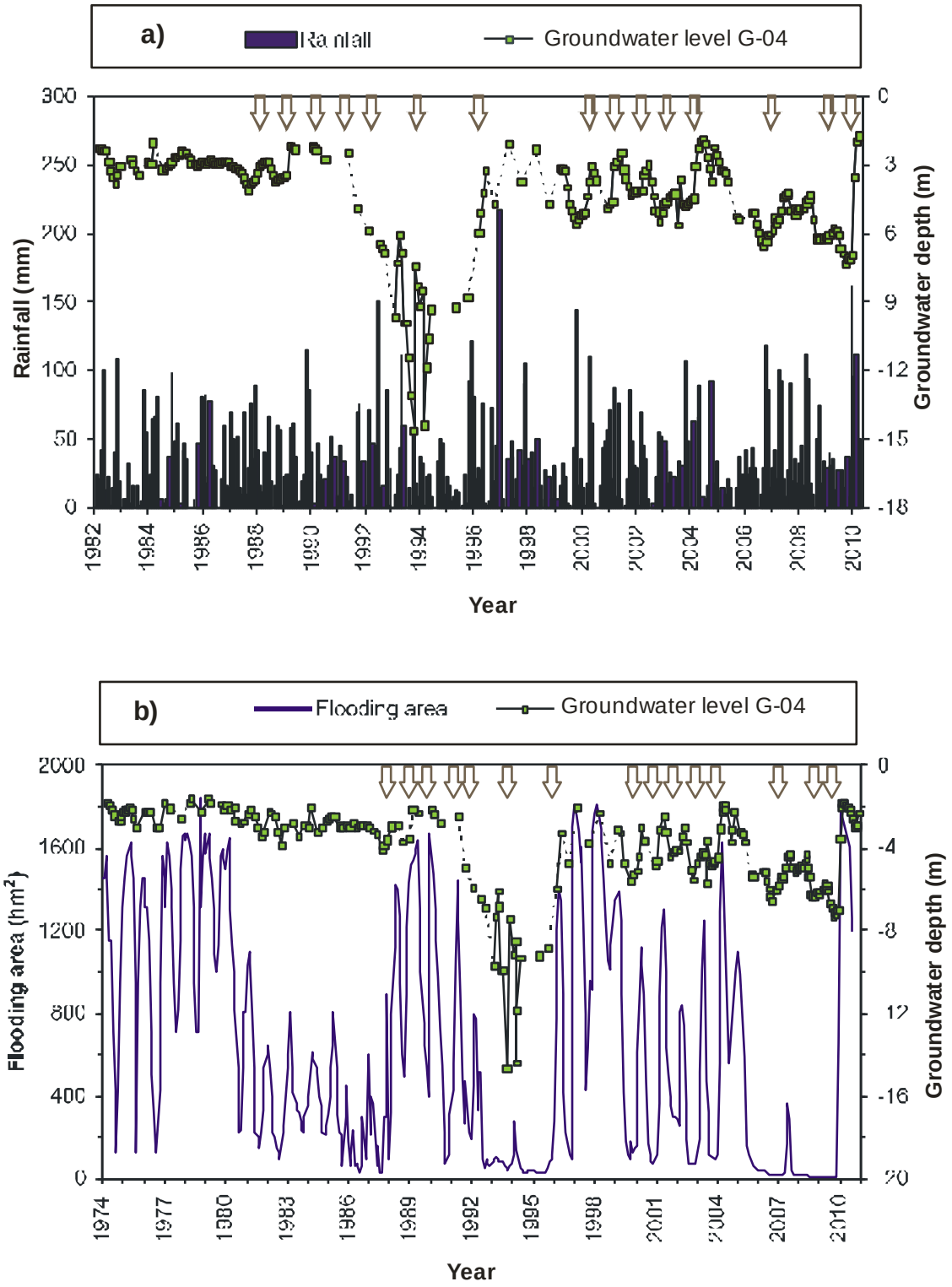

Fig. 6.17. Historical records of the groundwater level in a representative groundwater sampling point (G-04) against a) monthly rainfall and b) flooding area in Las Tablas de Daimiel National Park (TDNP). Arrows represent water transfers operations to TDNP.

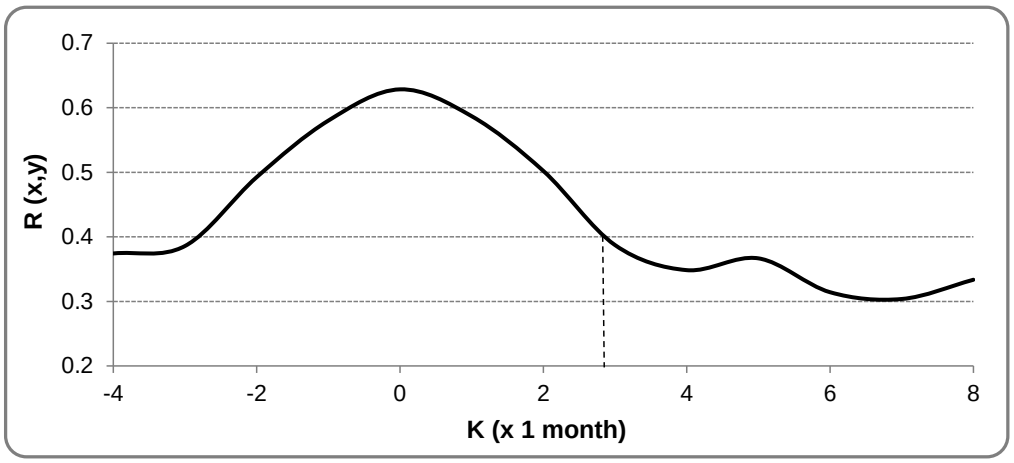

Fig. 6.18. Cross-correlogram between the time series of flooding area and groundwater-level depth in groundwater sampling point G-04 in the period 1988-2010. *R*(x,y) is the correlation coefficient and *K* is the time-lag in months.

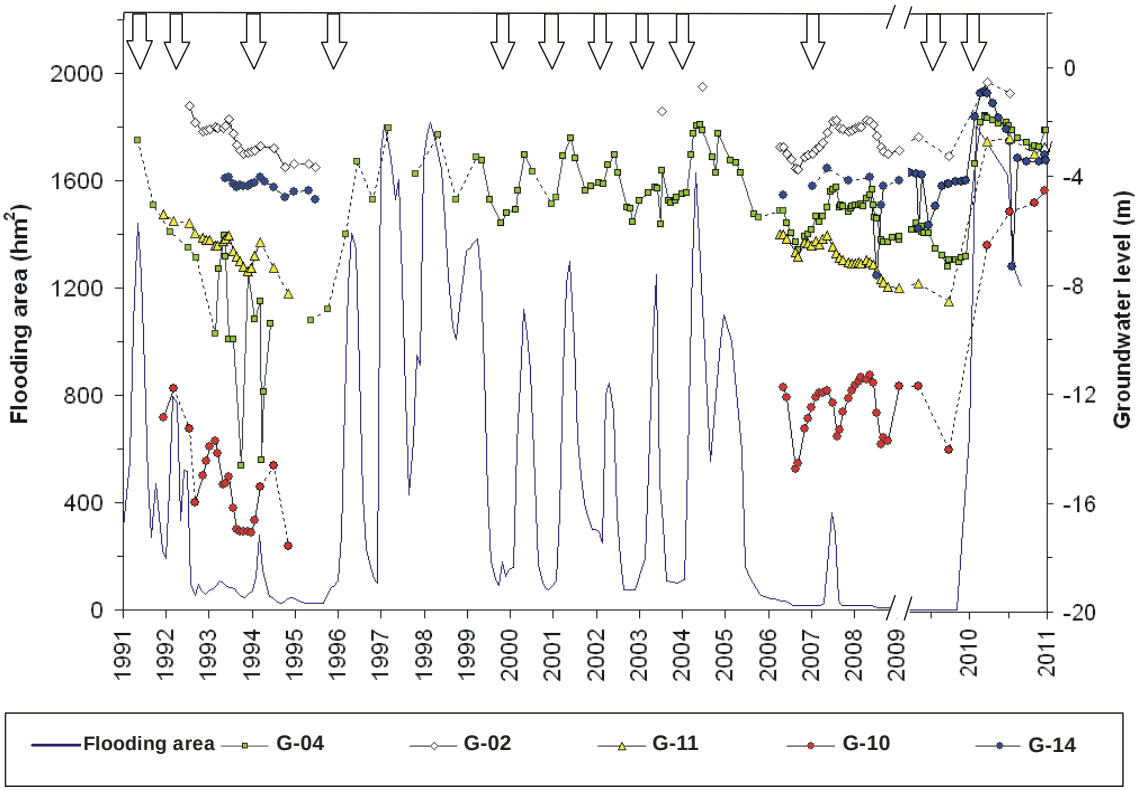

Fig. 6.19. Measured and bibliographic (García Rodríguez 1996; MARM, 2011) groundwater levels in representative groundwater sampling points of clustered groups (Fig. 6.15) for the period 1991-2010. Arrows represent water transfers to Las Tablas de Daimiel National Park (TDNP). Note that the temporal scale has been widened from 2009 onwards to facilitate the visualization of points.

Therefore, the grouping of points based on their hydrochemical characteristics is not entirely reflected in their hydrodynamic ones. Groundwater level response in points around TDNP is conditioned by the retaining effect of the central dam and the pumps from emergency wells (Fig. 5.5), which allow, respectively, for higher levels in points from groups 4 and 5, located upstream from the dam, and for stronger oscillations in the eastern side where pumps concentrate (Fig. 6.19, Table 6.7).

Table 6.7. Descriptive statistics of measured groundwater levels in points of the monitoring network (Fig. 5.5) in the period 2003-2010; SD: standard deviation; n: number of samples; CV: coefficient of variation.

	Depth to groundwater (m)						
Location	n	Min	Max	Median	Mean	SD	CV
G-01	18	-4.0	-0.6	-2.6	-2.5	0.8	0.32
G-02	36	-3.6	-0.5	-2.4	-2.4	0.7	0.31
G-03	15	-5.6	-1.7	-5.0	-4.6	1.1	0.23
G-04	51	-7.2	-1.8	-5.1	-5.0	1.3	0.25
G-05	15	-6.3	-1.4	-5.3	-4.5	1.6	0.35
G-06	36	-8.1	-2.6	-6.5	-6.3	1.3	0.20
G-07	1			-27.8	-27.8		
G-08	12	-8.2	-1.6	-6.3	-5.9	1.5	0.26
G-09	14	-6.9	-1.0	-5.7	-4.8	2.0	0.42
G-10	34	-14.7	-4.5	-12.0	-11.7	2.5	0.21
G-11	36	-8.6	-2.6	-6.8	-6.4	1.4	0.22
G-12	32	-5.2	-0.7	-4.0	-3.7	1.0	0.28
G-13	5	-8.2	-4.6	-7.2	-6.8	1.3	0.19
G-14	14	-7.6	-0.9	-4.1	-4.1	1.4	0.35
G-15	14	-30.9	-14.3	-29.1	-26.6	5.7	0.21
G-16	2	-17.6	-14.4	-16.0	-16.0	1.6	0.10
G-17	10	-24.0	-8.8	-22.2	-20.0	5.4	0.27
G-18	11	-32.0	-18.3	-30.3	-27.7	5.2	0.19

6.5.4. The interrelation between groundwater level and hydrochemistry

A closer look at the interrelation between groundwater level and EC in G-04 shows that the global hydrochemical response follows the hydrodynamic one almost immediately, as defined by the inverse temporal changes in Figure 6.20. In fact, the correlation coefficient for both variables is -0.72 ($p<0.0001$). When low-salinity surface-water inputs occur, the increase in groundwater level due to infiltration is coupled to a decrease in EC (periods 2 and 4). However, when drainage conditions prevail (drying periods 1 and 3), groundwater level drawdown promotes groundwater concentration and salinization towards those of the NW area.

The particular case of the Puente Navarro dam has been studied in detail as shown in Figure 6.21. The parallel changes of water-level elevations in the dam's surface water and in the groundwater monitoring point G-11 (Fig. 6.21) indicate that the former represents the top limit of the saturated zone (García Rodríguez, 1996). The existence of a connection between the water in the dam and in the aquifer is supported by the TOC evolution in S-7 and G-11 from April 2006 to April 2007 (flooded conditions in the dam), where a decrease in S-7 is coupled to an increase in G-11. This would explain the fast evolution of groundwater composition in G-11 towards the characteristics of surface water after full flooding in 2010 (Fig. 6.16b). During drier periods when the dam is almost empty and only small phreatic ponds remain (May 2007 to June 2008), the water-level limit of the saturated zone becomes closer to the level in G-11 as suggested by parallel evolution of TOC. The deeper groundwater levels and different hydrochemical composition observed in the nearby groundwater sampling point G-10 (Table 6.7, Fig. 6.19), point to the behaviour of the materials near the dam and G-11 being that of materials hosting a perched water table. The existence of perched water tables has been recently confirmed by two other studies, one with the data of four boreholes 8 to 12 m deep drilled in the left margin area of TDNP (Castaño et al., 2013), and another one on the Cigüela ditch in the northern inlet area (Moreno et al., 2013).

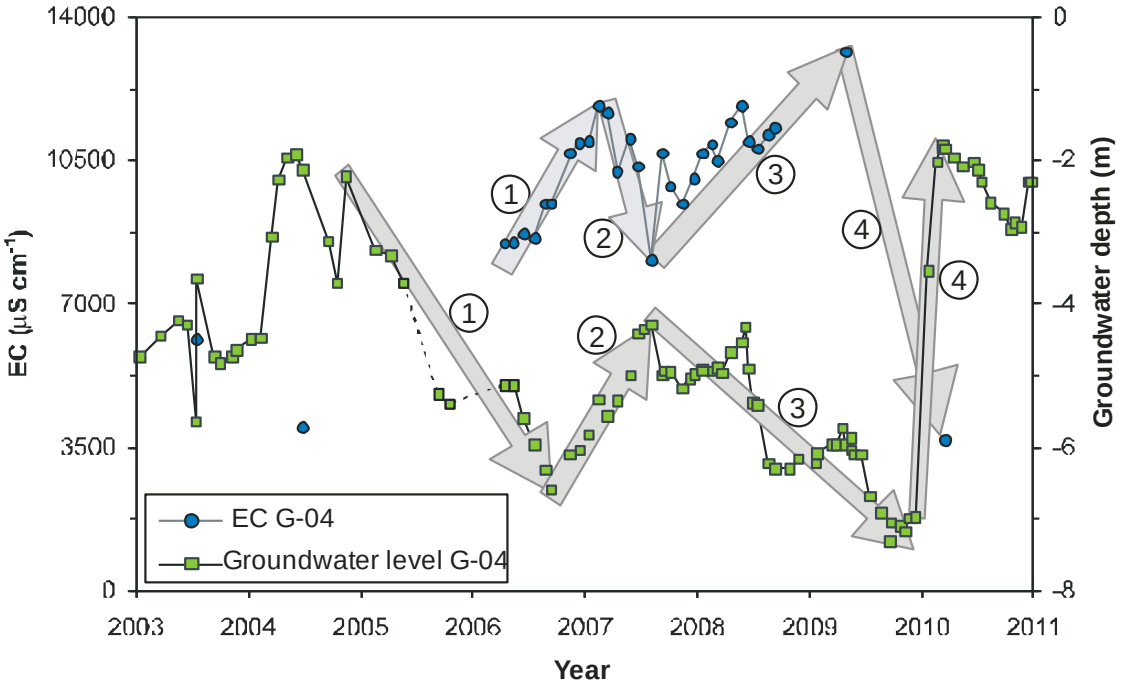

Fig. 6.20. Groundwater level and electrical conductivity (EC) in groundwater sampling point G-04 during the sampling period 2003-2010. Circled numbers indicate analysed drying and flooding subperiods of interrelation between both variables which are further discussed in the text.

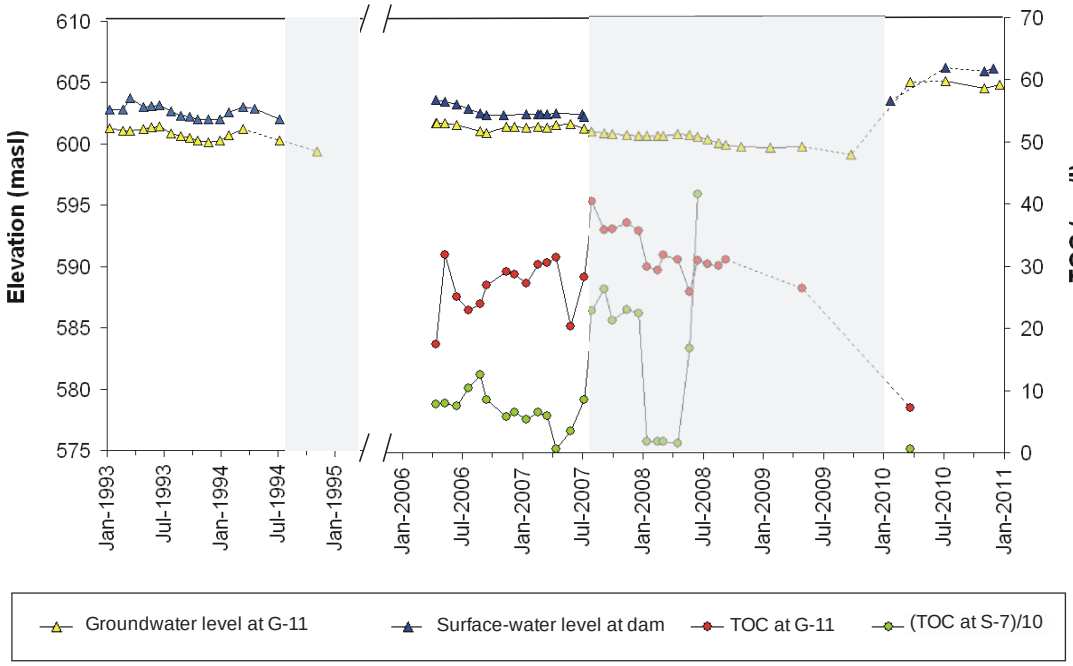

Fig. 6.21. Surface-water and groundwater-level elevations at the Puente Navarro dam (S-7) and groundwater sampling point G-11, respectively. Data for the period 1993-1994 (left) have been taken from García Rodríguez (1996). Throughout the sampled period 2006-2010 (right), measured total organic carbon (TOC) concentrations are also shown. Note that TOC concentrations in S-7 have been divided by 10 for scaling purposes. Grey bands indicate periods when the water level in the dam remained below the bottom of the scale post.

6.5.5. Isotopic analyses

A first global overview of the stable isotopic compositions of single groundwater samples suggests that the aquifer recharge represents different evaporation stages, according to the regional evaporation line (Castaño et al., 2011) both under drying (Fig. 6.22a) and flooding conditions (Fig. 6.22b). Isotopic composition of recharge comes from rainfall with some evaporation prior to or during infiltration in ponds or streams.

The composition of the samples from groups 1 and 4 under drying conditions in May 2008 (Figs. 6.22a and 6.23a) is almost the same as the composition following flooding and rainfall recharge in March 2010 (Figs. 6.22b and 6.23b). The lighter $\delta^{2}H$ and $\delta^{18}O$ composition of the samples from group 1, representative of the deeper layers of the Tertiary aquifer (G-15, G-17 and G-18), lies below the local evaporation line (LEL) and is equivalent to slightly evaporated rainfall water from higher far-off recharge areas. Tritium concentrations of these samples remain at a constant value below 1 TU in both sampling periods (Fig. 6.23), indicating the "old" nature of the groundwater (before 1960), or, more unlikely, a mixture of older rainfall recharge water with a small proportion of recent recharge water (Vallejos et al., 2002; Plata, 2006). Samples from G-01 and G-02 (group 4) show a similar constant pattern but slightly higher evaporation and tritium values are found (0.7-1.6 TU). Local recharge processes conditioned by the top low-permeability clayey Quaternary materials (García Rodríguez, 1996, Aguilera et al., 2009b) would explain the higher evaporation and still low interaction with present rainfall or ponding recharge in the NW area. The samples from other points of these two groups (G-06, G-09 and G-10), all located in the left margin of TDNP, are much more evaporated and show a wide range of higher tritium concentrations (> 4 TU) indicative of a more recent recharge process. Overall, a generalized scarce renewal of the water is inferred from the constant pattern in the observations.

On the other hand, the isotopic composition of surface water samples under flooded conditions is homogeneous and equals that of S-IW (Figs. 6.22b and 6.23b). When surface inputs cease or water renewal is decreased, the waters start to evaporate and lie along the local evaporation line (Fig. 6.22a). Tritium concentrations are in the same order of magnitude as current rainfall, except for S-5 in May 2008, which represents pumped groundwater (Fig. 6.23a). Besides this, the isotopic observations for S-5 and G-08 support the interaction inferred from the hydrochemical analysis (Table 6.6, Fig. 6.16a), suggesting a strong influence of evaporated recharge from S-5 on the groundwater in G-08 (Figs. 6.22a and 6.23a).

The isotopic composition of G-14 (group 2) is very similar to that of S-IW, supporting the interrelation with surface water in the Cigüela ditch and with the regional recharge signal. The values of G-13 in March 2010, showing the lightest composition and tritium values below 4 TU (Figs. 6.22b and 6.23b), suggest a mixing of old groundwater with hillslope and freshet recharge.

The samples from G-03, G-04 and G-05 (group 5) and G-11 (group 3) follow the pattern of fast infiltrating surface water. When low evaporation is observed in surface waters, groundwater in these points show the same isotopic composition (Fig. 6.22b), which is consistent with the recharge process occurring quickly and without time for significant evaporation to occur as observed in other wetland areas (Harvey et al., 2002 in Harvey and McCormick, 2009). However, under drying conditions, they show the footprint of the different evaporation stages as surface water does (Fig. 6.22a). The highest evaporation is observed in G-11, due to its association with surface water in the dam (S-7). This information is also supported by the tritium concentrations found in groundwater samples from these points. In this region, groundwater tritium contents in the range of 3-6 TU are indicative of water originated in precipitation after 1982 (Plata, 2006). Higher concentrations are indicative of an "artificial" origin from the Tagus water transfers which carry effluents from a nuclear plant (Plata, 2006).

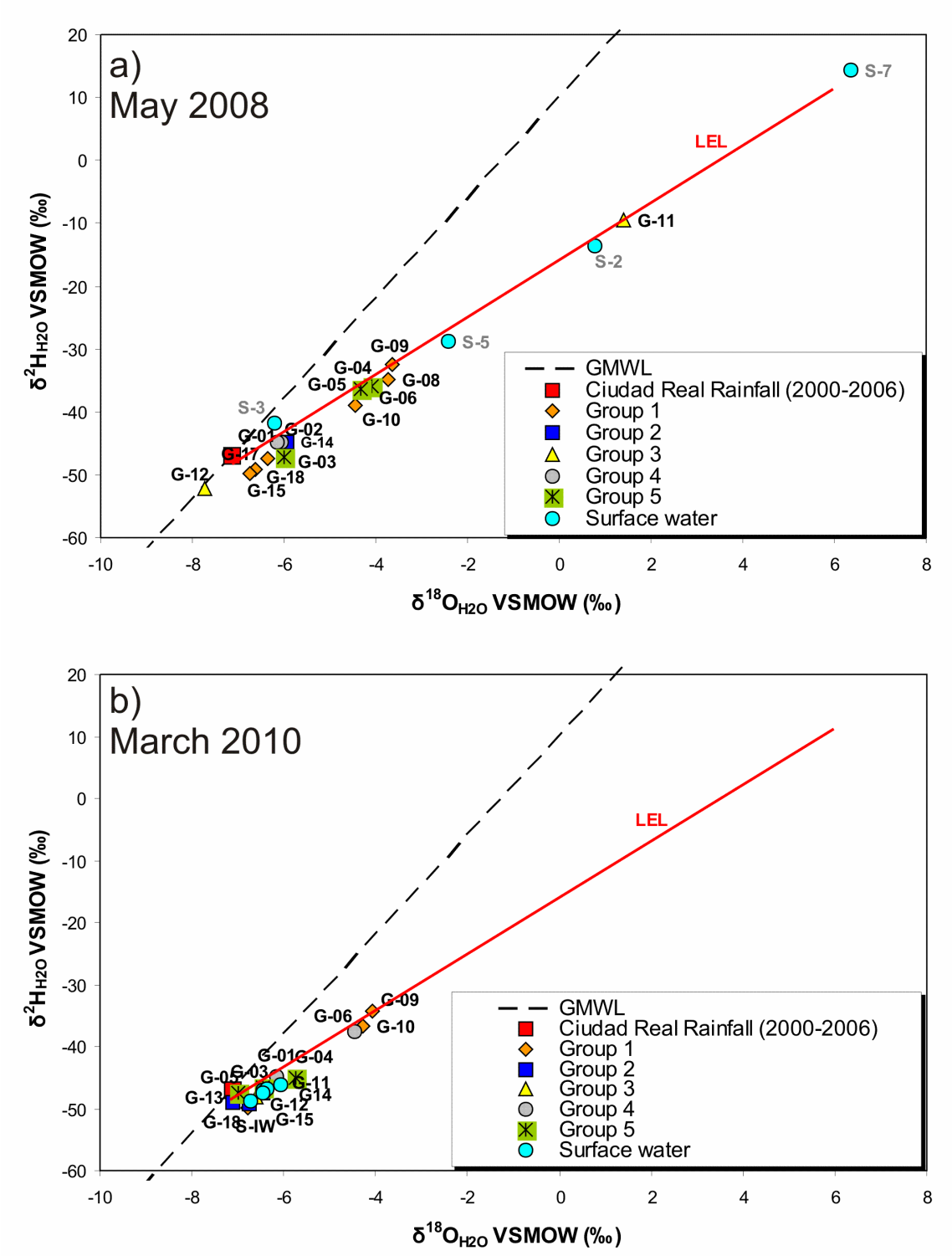

Fig. 6.22. $\delta^2H/\delta^{18}O$ ratios for Las Tablas de Daimiel National Park (TDNP) surface and groundwater samples under a) drying (May 2008) and b) flooding (March 2010) conditions. Groups refer to the hydrochemical cluster of groundwater sampling points (Fig. 6.15); GMWL: global meteoric water line (Craig, 1961); LEL: local evaporation line (Castaño et al., 2011); Ciudad Real rainfall weighted average for the period 2000-2006 has been taken from Díaz-Teijeiro et al. (2009).

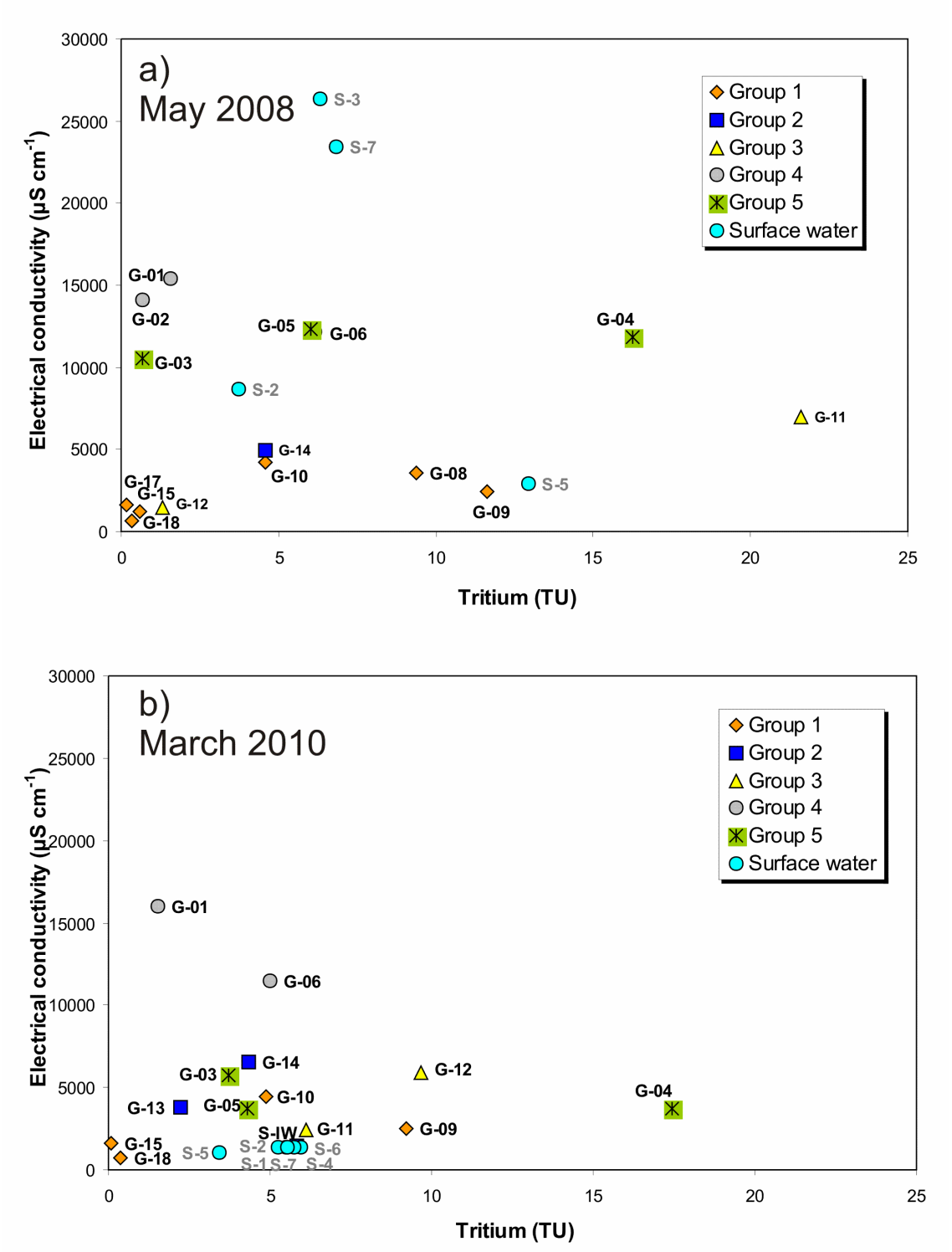

Fig. 6.23. Tritium concentrations against electrical conductivity for Las Tablas de Daimiel National Park (TDNP) surface and groundwater samples under a) drying (May 2008) and b) flooding (March 2010) conditions. Groups refer to the hydrochemical cluster of groundwater sampling points (Fig. 6.15).

Summarizing, the information provided by the isotopic analyses seems to be consistent with the hydrochemical cluster described in section 6.5.2 as different isotopic signals can be indentified for the different groups.

6.5.6. Conceptual hydrological model

6.5.6.1. Spatial distribution

The proposed conceptual model of the spatial distribution of SW-GW hydrological behaviour of TDNP is outlined in Figure 6.24. Under drying conditions, five zones can be distinguished (Fig. 6.24a):

i) In the northern inlet area, groundwater from sampling points clustered to hydrochemical group 2 is highly influenced by surface and subsurface processes in the alluvial deposits of the Cigüela River (i.e. S-IW) and surrounding hillslopes (Fig. 5.5), as supported by the isotopic (Figs. 22 and 23), hydrochemical (Fig. 6.15) and hydrodynamic (Fig. 6.19) analyses.

ii) A generalized saline surface and subsurface environment, more extreme in the right margin, is observed upstream of the central dam and is represented by hydrochemical groups 4 and 5 (Table 6.6, Figs. 6.15 and 6.16a). According to isotopic analyses (Figs. 22a and 23a), recent recharge that has undergone strong evaporation and recirculation in the emergency wells area is observed in the eastern side (G-04, G-05 and G-06) while moderately evaporated older recharge is reflected elsewhere (G-01, G-02 and G-03). Besides that, groundwater levels in the whole area are globally shallower (Table 6.7) and show parallel changes over time (Fig. 6.19).

iii) The area of influence of the water pumped from the emergency wells to the Guadiana ditch which infiltrates along the way (S-5, G-08 and S-6).

iv) Points located downstream of the central dam (G-09, G-10, G-11, G-12 and S-7) corresponding to hydrochemical groups 1 and 3, which show less salinity (Table 6.6, Figs. 6.15b and 6.16a), except for S-7, and similar groundwater level changes over time, except for G-10 (data not shown). However, the hydrochemical and hydrodynamic behaviour of single monitoring points in this area is highly variable (Figs. 6.15b, 6.16a, 6.22a and 6.23a) and should be considered separately.

v) The regional Tertiary aquifer, characterized by "old" very slightly evaporated groundwater that is moving further east from the TDNP limits (G-15, G-17 and G-18).

This zoning under drying conditions is consistent with vadose chemical analyses where high accumulation of salts and nutrients were found upstream of the central dam (see section 6.2).

The dynamic and variable behaviour of the system becomes evident following flooding recharge (Fig. 6.24b). A global hydrodynamic response (i.e. increase of groundwater levels) is observed (Fig. 6.19) after the entire TDNP area is flooded (Figs. 6.16b, 6.22b and 6.23b). Immediate hydrochemical and isotopic response is also observed in points from groups 2, 3 and 5, but not in points from groups 1 and 4 (Figs. 6.15b, 6.16b, 6.20, 6.22b and 6.23b). Hence, there is a substantial change of surface-subsurface interaction and spatial zoning compared with drying conditions. In G-03, G-04, G-05 and G-11 the effect is a decrease of ionic concentrations due to the mixing of saline groundwater with low conductivity flooding water. However, in the western G-12, and also in G-14 in the north, increased salinity after flooding can be explained by remobilisation of saline groundwater due to an increase of the groundwater flow, as well as leaching of saline soils in the recharge process.

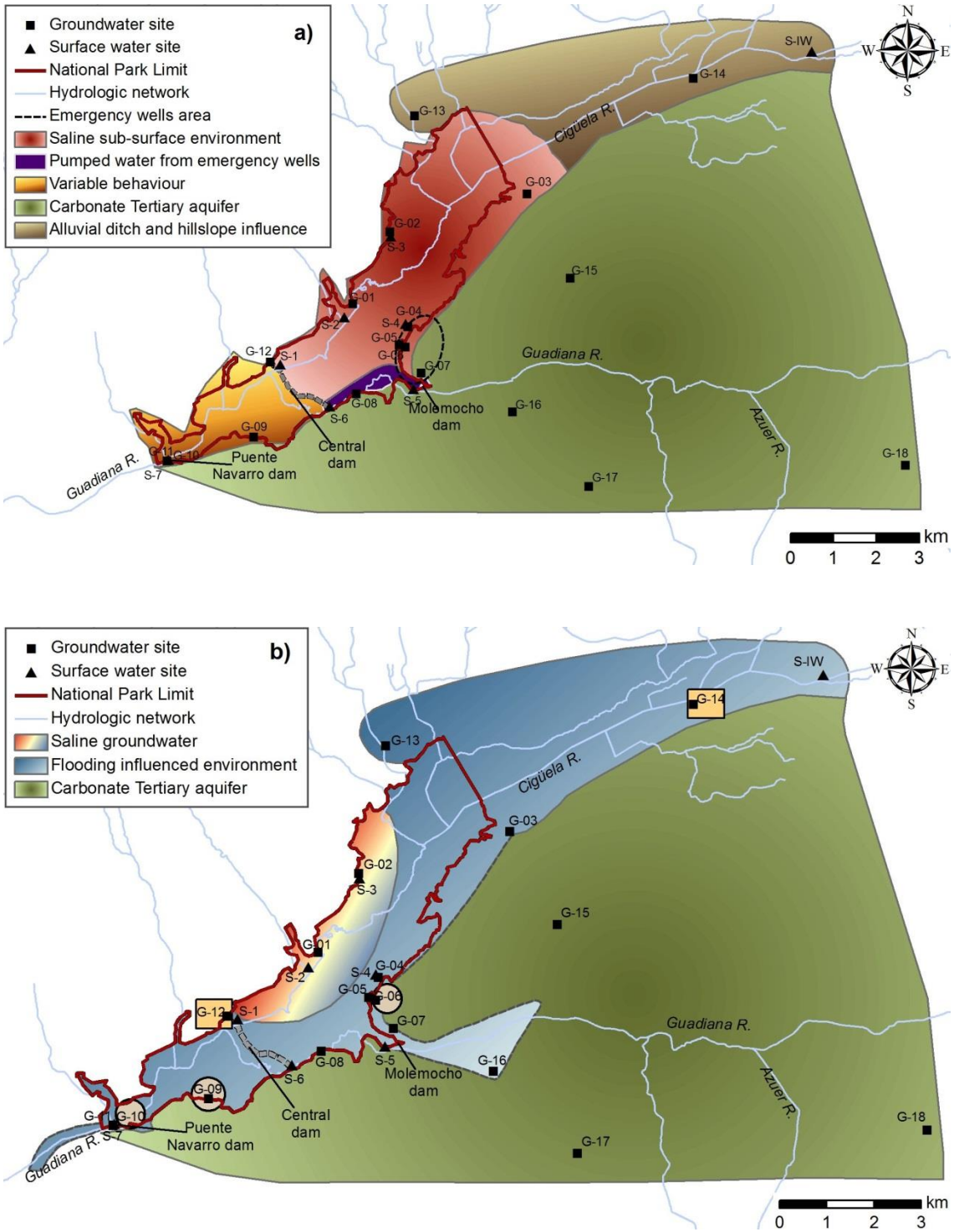

Fig. 6.24. Conceptual model of hydrological behaviour and surface water (SW)–groundwater (GW) interaction in the Las Tablas de Daimiel National Park (TDNP) area under a) drying and b) flooding conditions; circled groundwater sampling points in the left margin of TDNP show no significant hydrochemical or isotopic response to flooding; squared groundwater sampling points show increased salinity after rainfall and freshet flooding; dashed lines indicate extended areas of flooding influence in the left margin of TDNP and around the inlet and outlet points of the Guadiana River.

In spite of the lack of knowledge regarding local geological and hydrogeological variability, available lithostratigraphic information from individual groundwater monitoring points, boreholes and hydrogeological profiles around TDNP (García Rodríguez, 1996; MARM, 2011) indicates a general W-E transition underneath the Park from Miocene-Pliocene clay and marl to thick layers of Miocene-Pliocene limestone and marl with varying degrees of karstification, with gypsum lenses appearing randomly at various depths in the entire area, particularly in the north. These geological features, mainly karstification, would explain the higher response capacity and interaction with flooding surface water through infiltration shown by groundwater monitoring points located along the left margin of TDNP. This interaction was also supported by the large TOC concentrations observed in both surface water and groundwater (see section 6.5.1).

Regarding the degree of SW-GW interaction, as depicted by the isotopic analyses (Figs. 6.22 and 6.23), the shallow groundwater in the left margin of TDNP (G-03, G-04, G-05, G-06, G-08, G-09 and G-11) has varying higher tritium content than the right margin (G-01 and G-02), indicating that surface water recharge processes are highly local, as reported for other wetlands (Sikdar and Sahu, 2009). Overlying low-permeability materials in the NW area hinder SW-GW interactions and, thus, groundwater renewal. The hydrodynamic response to flooding in this area would be associated with a piston effect of lateral displacement of groundwater by flooding and rainfall recharge. Very low tritium contents and depleted $\delta^2H/\delta^{18}O$ ratios in both periods in deep groundwater monitoring points located east from TDNP (G-15, G-17 and G-18) suggest fast infiltration in distant eastern recharge areas (i.e. regional flow) and long residence times (i.e. residual flow). The lower salinity and small hydrochemical variation observed in these points indicate a disconnection with the TDNP system. Only at places closer to the southern TDNP limit, where the deep aquifer shows relatively higher tritium contents (G-10), is a possible mixing of groundwater of shallow (G-11) and deep aquifer layers likely to occur. The singular behaviour of points G-06 and G-09 from groups 1 and 4, respectively, is likely due to unknown characteristics of pipe construction and screening depths.

6.5.6.2. Functioning of SW-GW interactions in the left margin of TDNP

Once the spatial patterns of hydrological behaviours have shown that SW-GW interactions mainly occur in the left margin area of TDNP, a detailed analysis focusing on the vertical relationships of different aquifer layers has been performed based on the presented results and bibliographic data gathered for points G-04, G-10 and G-11.

Point G-04 shows an opposite hydrodynamic and hydrochemical response (Fig. 6.20). Its lithological column shows outcropping Miocene limestone, marls and clay to a depth of 32 m followed by Miocene gypsum and clay to approximately 80 m deep. During drying periods, the left margin of TDNP suffers higher drawdown of groundwater levels due to: i) groundwater pumping for agricultural purposes in the whole Mancha Occidental aquifer system; ii) increased pumping from the surrounding emergency wells to keep minimum flooding levels, as happened in the beginning of the 1990s (Figs. 5.5 and 6.17b); iii) downward groundwater drainage from upper permeable layers in the multi-layer aquifer as a result of groundwater level drawdown. As a consequence, decreasing water flux and increasingly evaporated recharge during drying periods brings about recharge water's quality homogenisation and stabilization with the marly gypsum-rich lithology of the semi-permeable layers (stages 1 and 3 in Fig. 6.20).

On the other hand, during flooding events, fast infiltration through the highly permeable carbonate materials induces a fast recovery of groundwater levels (Figs. 6.17b and 6.19) and mixing and replacement of the saline stagnant groundwater with low electrical-conductivity freshwater (Figs. 6.16b and 6.20). The cross-correlation analysis of flooding area and groundwater level time series has shown that, under current anthropized conditions, the significant hydrodynamic response in G-04 lasts for 3 months (Fig. 6.18). After this time, which would be shorter without the retention effect of the central dam, saturation of the different aquifer layers might have been attained. Then, in the absence of new inputs, drainage from permeable layers through

semi-permeable ones is predominant. The isotopic composition of G-04 under drying and flooded conditions is in accordance with the mentioned process, as evaporated recharge water is immediately mixed with depleted infiltrating surface water following flooding (Fig. 6.22).

Real field evidence for the described processes is found at the outlet area of the Puente Navarro dam (Fig. 5.5), which can be used as a down-scaled example of the current behaviour of TDNP's left margin area, in that it is controlled by infiltration in a multi-layer aquifer system. The dam represents the top limit of the saturated zone of a perched water table monitored at point G-11 (Fig. 6.21). During drying conditions (2006-2008), small ponds remain and highly polluted eutrophicated conditions and pollutant concentration due to evaporation are observed (see S-7 in Table 6.6, Figs. 6.16a, 6.21, 6.22a and 6.23a).

In spite of G-10 being located only 5 m away from G-11, it shows entirely different hydrodynamic, hydrochemical and isotopic characteristics (Table 6.6, Figs. 6.15, 6.16, 6.19, 6.22 and 6.23). The only basic difference between points G-10 and G-11 is their active depth, 14 m and 84 m, respectively (Table 5.3), and, thus, the different layers bored by G-10 and not by G-11 below 14 m deep. The available description shows an alternation of limestone and marly limestone to an approximate depth of 3.5 m, followed by a thick dominance of Tertiary marls with thin intercalations of sand, sandstone and limestone to a depth of 77 m.

Perched water table in G-11 (group 3) conditions an immediate hydrodynamic, hydrochemical and isotopic response to flooding (Figs. 6.16, 6.21, 6.22 and 6.23). Point G-10 was clustered to group 1 of constant hydrochemical behaviour and, due to its depth, it can be considered as representative of the deeper layers of the regional Tertiary aquifer in the area. However, the isotopic composition of this point indicates an evaporated recharge later than 1982 (Plata, 2006), pointing to influence of the infiltration of evaporated ponding water in TDNP through the different Miocene levels. Furthermore, tritium content in G-10 remains quite constant, with similar values to

that of surface water, indicating that the recharge takes place basically during periods of freshets (Fig. 6.23). Under drying conditions, the groundwater level in G-10, which is highly influenced by pumps from southern irrigation areas, is 5-10 m lower than in G-11 (Fig. 6.19, Table 6.7). These evidences support that a downward water flux from the perched level through semi-permeable layers is developed, conditioning a slow delayed recharge of deeper Miocene layers, in a similar way as observed by different researchers in other wetland systems (Sikdar and Sahu, 2009; Rudolph et al., 2005).

After the first two months of re-flooded conditions, the difference between the groundwater levels in G-11 and G-10 was reduced to less than 4 m and, although not significant, slight increases in major cation and anion concentrations in G-10 were observed (Fig. 6.16). This implies that a mixing of the displaced saline and polluted groundwater from perched G-11 with the upwelling groundwater from the regional Tertiary aquifer is likely to occur. Actually, after 3 years of permanent flooding, the groundwater level difference has been reduced to less than half a meter by the beginning of the spring in 2013 (Silvino Castaño, IGME, personal communication, 2013). Moreover, isotopic results prove that there is no significant mixture of groundwater of different layers through the pipe.

A simplified conceptual diagram of the described processes in the left margin of TDNP is shown in Figure 6.25. Under natural conditions (A), all layers of a multi-layer aquifer system would be saturated and the regional aquifer would discharge good quality groundwater into the TDNP wetland area. Degradation and anthropization have strongly modified system dynamics, inverting hydraulic gradients and turning TDNP into an efficient artificial recharge pond. During drying periods (B and C), drainage of overlaying highly permeable aquifer layers (i.e. karstified limestone) through semi-permeable materials, and increased pumping from emergency (in TDNP) and irrigation wells (in eastern areas), promote sharp drawdowns of groundwater levels and separation of different aquifer levels through semi-permeable aquitards (Castaño et al., 2013). Hence, the regional flow is somehow disconnected from the local recharge flow and is likely to be predominantly horizontal towards the main pumping irrigation

areas in the SE and SW, as similarly observed by Rudolph et al. (2005) in a headwater lagoon system in Mexico.

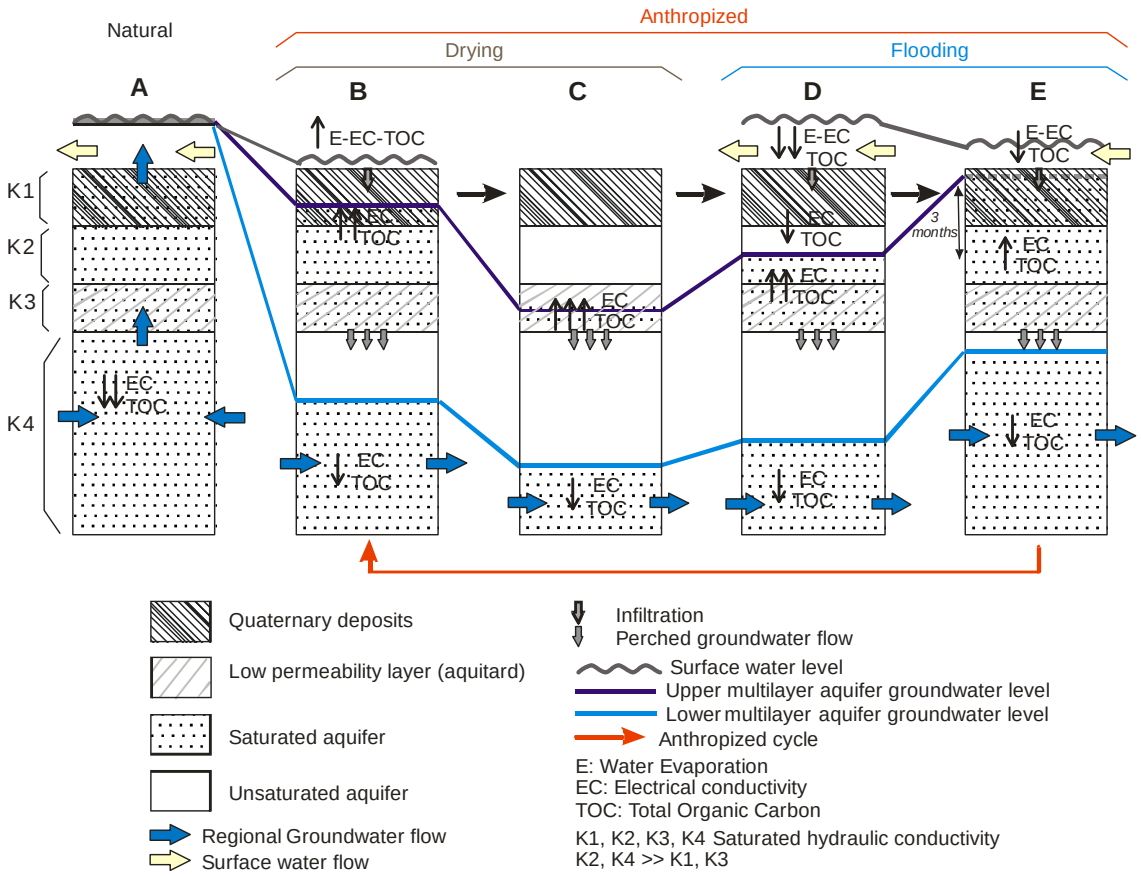

Fig. 6.25. Schematic conceptual diagram of the surface water-groundwater interactions through the multi-layer aquifer system in the left margin area of Las Tablas de Daimiel National Park (TDNP). Upward and downward black arrows preceding E, EC and TOC indicate increasing or decreasing trends. See the text for further discussion of the different stages A-E.

A big impoverishment of groundwater quality in the top layers occurs due to management practices and lithology (B), as low-quality artificially-maintained ponding water (i.e. pumped groundwater, water transfers) infiltrates through saline nutrient-rich sediments (Aguilera et al., 2011). A slow percolation through semi-permeable layers is developed towards deeper more permeable levels connected to the regional flow (Castaño et al., 2013), in a similar way as found by Sikdar and Shau (2009) in a wetland system in India. Over time, due to the water exchange between the surface

and subsurface, the layer with originally high quality fresh groundwater near the top of the aquifer is progressively replaced by contaminated water from the surface (C), as also observed by Rudolph et al. (2005). It is uncertain how long contaminants will be stored in groundwater before being transformed or discharged back.

Subsequent flooding events with low electrical conductivity surface water cause fast infiltration and re-saturation of top karstified permeable layers, displacing the stored poor quality groundwater (D). The recovery of groundwater levels is also very fast and some time after re-flooding takes place, re-saturation of the different aquifer layers might be attained (3 months in the case of one representative groundwater monitoring point) and groundwater from the deeper layers mixes with the displaced saline and nutrient rich groundwater (E). Upon subsequent drying, due to increased hydraulic gradients towards pumping areas, the risk of pollution spread is enhanced.

6.5.7. Summary and conclusions on hydrology and hydrochemistry

The results emphasize the consequences of both direct and indirect anthropization on the semiarid hydrological system of TDNP. Salinization and increased nutrient content in groundwater are the hydrochemical footprints of degradation and inversion of the groundwater flow which transformed the wetland into an artificial recharge area for a highly heterogeneous multi-layer aquifer system. As found by Crosbie et al. (2009) for semiarid floodplain wetlands of the lower River Murray basin in SE Australia, the repeated occurrence of the drying and wetting cycles leads to soil salinization, particularly in terminal wetlands such as TDNP. Salinity in TDNP has been usually linked to the incoming water through the Cigüela River (Álvarez-Cobelas et al., 2001; Berzas et al., 2000; Cirujano et al., 1996). However, given the results presented here, at least for groundwater, lithology seems to be a more important factor which strongly conditions groundwater salinization following freshets. Salinity in the upper system is also conditioned by evaporation (Castaño et al., 2011).

Large hydrochemical variability is observed, particularly in surface water, accounting for the different sources and processes involved. Median values of electrical conductivity in surface water range between 2,973 and 11,739 μS cm^{-1}, and in groundwater between 677 and 15,383 μS cm^{-1}. This variability seems to be conditioned by local factors in the recharge brought about by the characteristics of the "edge" geology (i.e. material heterogeinity, lithological changes, variable Tertiary-Quaternary contacts) and the anthropic management of the system (i.e. groundwater pumping and recirculation, disturbance of the physical environment).

Groundwater level oscillations follow fluctuations in the flooding area, which is highly conditioned by water transfers. In contrast, the groundwater level association with rainfall is restricted to extreme rainfall events which cause a temporary "natural" flooding through freshets. The cross-correlation between the 1988-2010 time series of flooding area and groundwater level in a representative groundwater monitoring has showed that the positive association between flooding and groundwater level (i.e. rise of groundwater levels) can be set at around 3 months.

Groundwater level response in points around TDNP is conditioned by the retaining effect of the central dam and the pumps from emergency wells (Fig. 5.5), which allow for higher levels in areas upstream from the dam and for stronger oscillations in the eastern side, respectively.

The existence of perched water tables has been evidenced from the case of the Puente Navarro outlet dam, where two adjacent groundwater monitoring points with different bored depths show entirely different characteristics, and confirmed by two recent studies in other TDNP areas (Castaño et al., 2013; Moreno et al., 2013). One point is hydrodynamically and hydrochemically connected to the surface water in the dam, which therefore represents the top limit of the saturated zone. However, the other nearby sampling point, showing deeper groundwater levels and different hydrochemical composition, can be considered as representative of the deeper layers of the regional Tertiary aquifer in the area. These findings support the initial

hypothesis that due to hydraulic gradient inversion and wetland disconnection the system behaves as a disconnected multi-layer aquifer system (see section 3.2).

Isotopic analyses show highly local aquifer recharge processes representing different evaporation stages.

According to hydrochemical, hydrodynamic and isotopic analyses 5 hydrological environments have been distinguished under dry conditions (Fig. 6.24a): i) northern inlet area, where groundwater is highly influenced by surface and subsurface processes in the alluvial deposits of the Cigüela River and surrounding hillslopes; ii) a generalized saline surface and subsurface environment, more extreme in the right margin, is observed upstream from the central dam; iii) the area of influence of the water pumped from the emergency wells to the Guadiana ditch which infiltrates along the way; iv) a less saline but highly variable groundwater environment downstream from the central dam; v) the regional Tertiary aquifer, characterized by "old" very slightly evaporated groundwater as moving further east from the TDNP limits.

The dynamic and variable behaviour of the system becomes evident following flooding recharge. A global hydrodynamic response is observed (Fig. 6.24b). Besides this, varying immediate hydrochemical and isotopic responses in different areas appear to be mainly conditioned by lithological features.

A conceptual model which is meant to be an integrated subsurface approximation to the current hydrological functioning of the anthropized wetland is proposed (Fig. 6.25). Relevant SW-GW interactions are mainly localized in the left margin of TDNP, as confirmed by fast response capacities to extraordinary flooding observed in the hydrochemical, hydrodynamical and isotopic data. During drying periods, small intermittent artificial and/or low flow natural floods are followed by infiltration of remaining stagnant evaporated and poor quality ponding water into saline low permeability layers. The presence of highly permeable Holocene (i.e. cracked peat) and Tertiary (i.e. karstified limestone) materials in the top layers enhance SW-GW

interaction. Field evidence of perched flow of groundwater to deeper layers through semi-permeable aquitards (Castaño et al., 2013) indicates the risk of pollution spread to other groundwater bodies, as these deeper layers are connected to the regional groundwater flows towards the main irrigation areas. Increased groundwater levels after flooding could produce re-saturation of the different aquifer layers in a relatively short time (i.e. 3 months), thus, enhancing the mixing of displaced saline polluted groundwater with the rising better quality groundwater of the lower layers. In this sense, the lateral continuity of the semi-permeable aquitard units is a controlling factor in the potential long-term impacts of infiltrating surface waters on the groundwater quality and further studies are needed to determine the possible existence of "stratigraphic shortcuts" for pollutants (Rudolph et al., 2005; Sikdar and Sahu 2009).

According to dominant SW-GW interactions, the anthropized TDNP can be classified as a losing wetland (sometimes connected and sometimes disconnected), as ponding water recharges the underlying aquifer (Jolly et al., 2008). Other major semiarid wetlands such as the Okavango Delta (Wolski and Savanije, 2006) and the Prairie Potholes (Winter, 1999) also behave as net recharge areas. The results also point out the need to redefine traditional hydrological zonings of TDNP based on flooding patterns in the Cigüela and Guadiana Rivers (Aranda et al., 1993; Álvarez-Cobelas et al., 2001; Berzas et al., 2000; Cirujano et al., 1996; Sánchez-Carrillo et al., 2001; Sánchez-Carrillo and Álvarez-Cobelas, 2001) towards a NW-SE scope regarding infiltration and groundwater flow characteristics in a multi-layer aquifer system.

The presented approach has proved to be useful for assessment of hydrological behaviour and SW-GW interactions in a semiarid wetland area. Moreover, similar approaches with the initial use of simplified conceptual models are currently being followed by other researchers worldwide (Crosbie et al., 2009; Harvey and McCormick, 2009; Hughes et al., 2010; Marimuthu et al., 2005; Rodríguez-Rodríguez et al., 2007; Sikdar and Sahu, 2009; Somay et al., 2008; Staes et al., 2009). The results will provide a basis for both future research and for the development of more complete hydrological

models, in a similar way as once had to be done for other well-known systems such as the Okavango Delta (McCarthy et al., 1998). However, further in situ knowledge of the local geology is still pre-required before any complex modelling approach is attempted. The relative simplicity of the employed methodology allows for its application in other similar complex groundwater linked wetlands in semiarid areas as long as sufficient basic data and monitoring are available.

6.6. Specific analysis of TDNP peats and smouldering fire

The specific study on peats physical-chemical properties conditioning their combustibility, based on the 2009 smouldering fires, has been published in a special issue of the journal Fire Techonology (Moreno et al., 2010). Determination of peat properties, particularly their morphology, water repellency and genesis of cracks and pipes, together with the continuous monitoring of soil moisture and temperature, has been basic to understand the origin and the mechanism of peat fire propagation. This has enabled to propose and establish preventive measures for fire control.

6.6.1. The 2009 smouldering fire

The first signs of 2009 smouldering fires were smoke columns observed in the southern Cañas zone of TDNP on August 29th (Figs. 2.1 and 5.4). The Cañas was a wide area covered by dense vegetation and with neither vehicle nor pedestrian tracks. These weak plumes were visible to the naked eye due to water condensation in the smoke during the cooler night time, more pronounced by the end of the summer (Pic. 20a,b). Probably the fire had been active for a long time but could not be sighted until that day. On the other hand, two flaming fires took place just 50 m away from the Park limit in the Molemocho mill area (Fig. 5.4). The origin of these fires is unknown, but

they occurred in areas with heavy traffic of agricultural machinery. The first fire started on July 25th and the second one on September 27th. The burnt areas were 0.2 and 0.4 km^2, respectively. These fires propagated through the peaty silts in the Guadiana ditch to the underlying peats and provoked a serious smouldering fire still active in December 2009 (Pic. 6.2c,d). The fire in this area did not cross the TDNP limit and spread inside because the permanent artificially-flooded Molemocho zone acted as a barrier.

6.6.2. Fire related properties of TDNP soils

As expected, peat and peaty silt exhibit the highest organic matter contents among the different TDNP soil types (see Table 6.5 in section 6.3). However, the average value of 50.1% organic matter content is relatively low for peats. This can be explained taking into account that peaty levels frequently contain intercalated thin layers of carbonates deposited during periods of higher rainfall than that corresponding to organic matter deposition. In zones of the Guadiana River with thick peat layers (see profile P01 in Fig. 6.13), the organic matter contents are much higher, between 51 and 71% (Fig. 6.10, appendix B).

On the other hand, it has been stated that carbonate deposits (charophyte layers) are frequently affected by edaphization processes. Thus, a big portion of TDNP soils show higher organic matter contents than those in the surroundings (Aguilera et al., 2009a). Materials classified as organic soils usually contain a large fraction of edaphized superficial charophytes deposits, with large organic matter contents (mean value of 33%). Sometimes, especially when found in surface horizons, these materials may have enough vegetal remains to be able to burn and propagate the fire at least superficially. This effect has been observed in the fire started in the limit of the Park.

Picture 6.2. a-b) Smoke columns observed through peat cracks in the 2009 smouldering fire inside las Tablas de Daimiel National Park (TDNP); c-d) Smoke columns from the 2009 smouldering peat and peaty silt fire in the Guadiana River ditch area outside the TDNP limit caused by flaming fires that started in nearby areas related to agricultural activities.

One noteworthy property of peat is its low bulk density when comparing with mineral soils (Table 6.5). Average bulk density in TDNP peats is 0.18 g cm^{-3}. Organic soils are the second less dense material with an average value of 0.52 g cm^{-3}, almost three times that for peat. The low densities of peats are due to their huge primary porosity which for Spanish peatlands ranges from 52% to 92% depending on their moisture status (Guerrero, 1989) and for British temperate peatlands from 72% to 92% (Dawson, 2006). This property allows them to absorb higher amounts of water and also to burn easily when dry. Average bulk density of pure undisturbed charophytes is 0.76 g cm^{-3} which, compared to calcium carbonate density (2.7 g cm^{-3}), proves that this material is very porous as well, being capable to absorb more than twice its own weight in water.

In relation to fire risk in TDNP under dry conditions, peats represent the best fuel material as they combine large values of organic matter content and porosity. The desiccation process decreases peat total porosity making it shrink (Guerrero, 1989) and giving rise to the formation of cracks and hollows which constitute preferential flow paths for both air and infiltrating waters. This process, together with the development of a permanent non-saturated VZ, further cause ground subsidence (Jiménez-Pinilla, 2011).

6.6.3. Distribution of cracks and hollows

The total peat outcropping surface in TDNP is around 1.5 km^2 (Fig. 6.1). Nevertheless, this extension is not a good indicator of the total peat content of the soil matrix. It must be also taken into account the special arrangement of sediments.

The existence of pipes in peatlands has been described focusing on their influence on the water flux (Holden and Burt, 2002). In the same way that these pipes may contribute to hydrological flux under wet conditions, under dry conditions they constitute preferential flow paths for air so that they support the maintenance and propagation of smouldering peat fires and for smoke evacuation (Rein et al., 2008).

As stated in the previous section, the presence of cavities was detected mainly in those areas with large peat contents. Hollows were occasionally observed during a sampling campaign in 2006. In another sampling campaign carried out three years later, cavities were found in almost 50% of all auger holes drilled. Surface cracks were first detected in small number in 2007. Cracks number and extension grew exponentially from 2008 and especially during summer 2009. Plain and easily accessible sampling areas, that used to exist one year before, became very dangerous to explore, as the soil cracks reached up to half meter wide and two meters depth (Pic. 6.3). However, on the contrary to other authors' research (Holden and Burt, 2002), neither spatial

distribution pattern nor preferential orientation in the system of cracks was observed, and many of them seemed to come from the collapse of the hollows observed in 2006.

Picture 6.3. a) Surface cracks in the central Morenillo dam in Las Tablas de Daimiel National Park (TDNP) in 2009; b) large interconnected peat crack system inside TDNP in 2009; c) peat crack development inside TDNP in 2008; d-e) other dangerous side effects caused by peat cracks.

Although no topographic measurements have been taken, the existence of numerous sinkhole shaped collapses of several tens of meters in diameter were quite visible in the areas where the biggest cracks had appeared. High soil temperatures and low water contents accelerate physical-chemical processes promoting the formation of new hollows and the progressive development of existing ones. Before the 1980s, when the area was completely flooded, the hollows network dimension was probably very small.

6.6.4. Moisture and temperature monitoring in soil profiles

The fact that TDNP peat soils show water repellency is quite relevant. In relation to smouldering fires, the peats tendency to develop SWR after being dried (see section 6.3.3) might produce that peaty material close to pipes where hot smoke circulates becomes hydrophobic. SWR on peat surface constitutes a barrier to water penetration into the peat mass. In these conditions, incoming water will tend to rapidly drain off the system by preferential flow paths. As peat wetting is hindered, progressive drying of peat masses is enhanced with the subsequent increased combustion risk. This way, when the 2009 smouldering fire was active in TDNP, typically moderate rainfalls from autumn to spring (average precipitation about 40 mm mo^{-1}) were not expected to be sufficient to put out the fire naturally. These foreseeable scarce rainfalls were expected to move as surface or sub-surface runoff around the big masses of peat, without wetting the inner parts.

In the same way as for soil water repellency (see section 6.3.3), soil water content and organic fraction are the main controlling properties for smouldering fires ignition and spread (Frandsen, 1987). In this sense, the smouldering ignition limit of peat moss mixed with water and mineral soil depends on the mixture's moisture and inorganic content (Frandsen, 1987). The ignition limit can be approximated in two dimensions by a straight line extending from 110.0% (dry weight base) on the moisture axis (ordinate) to 81.5% on the inorganic axis (abscissa) (Frandsen, 1987). Successful ignitions are accomplished only within the triangle bounded by the axes and the ignition limit. Fransden (1997) extended his previous studies testing field samples from different materials (sedge, white spruce, pine duff, etc). In this second work Fransden expressed the results as ignition probabilities, so that land managers can determine the probability of smouldering ignition of organic soils based on the values of the inorganic and moisture contents. Moisture content controls peat ignition being a moisture value below 125 ± 10% in dry base required (Rein et al., 2008; Reardon et al., 2007). Besides this, the depth and the area affected in case of fire will also be dictated by the

moisture distribution in peat layers. These authors argue that if field soil moisture in shallow peat layers is below 115% in dry base, then the fire danger would be high, if between 115% and 135% the danger would be intermediate, and for moistures above 135% the fire danger would be low.

In Figure 6.26 a Frandsen diagram shows the moisture and inorganic content of the TDNP samples taken in April and September 2009. It is striking that only 7 out of the total 37 samples show moisture contents above 115% in dry base. This means that the fire risk in TDNP was already extreme some months before the first fire detections. It can be observed in the graph how already in April, a usually rainy month when there should be no problem of moisture lack in the soil, a large amount of samples, particularly those with higher organic content, lay inside the bounded area of high ignition risk. It can also be seen that after a very dry summer the situation turns dramatic and all the samples with inorganic content above 50% fall inside the ignition limit zone. There are some samples, corresponding to those areas that are artificially flooded during the whole year, that remain outside the ignition triangle, both in April and September.

Although it was not its primary objective, the soil moisture and temperature monitoring network has also provided relevant information regarding smouldering fire management and prevention inside TDNP. The moisture and temperature records corresponding to the dataloggers in P03 and P05 (Table 5.2) are shown in Figure 6.27. The distance between them was 240 m (Fig. 5.4). The moisture and temperature trend recorded in P05, which was located on an organic soil (Fig. 6.13), agrees with the expected behaviour under normal conditions. The most superficial sensor, at 20 cm deep (T1), shows the typical short-time (daily) temperature oscillations (Fig. 6.27a). In the deepest sensor, at 80 cm deep, changes are controlled by seasonal patterns and the effect of daily oscillations disappears. Soil moisture behaves in a classic way for this kind of soils showing a sharp decrease in the beginning of the summer and no recovery even after first November rains.

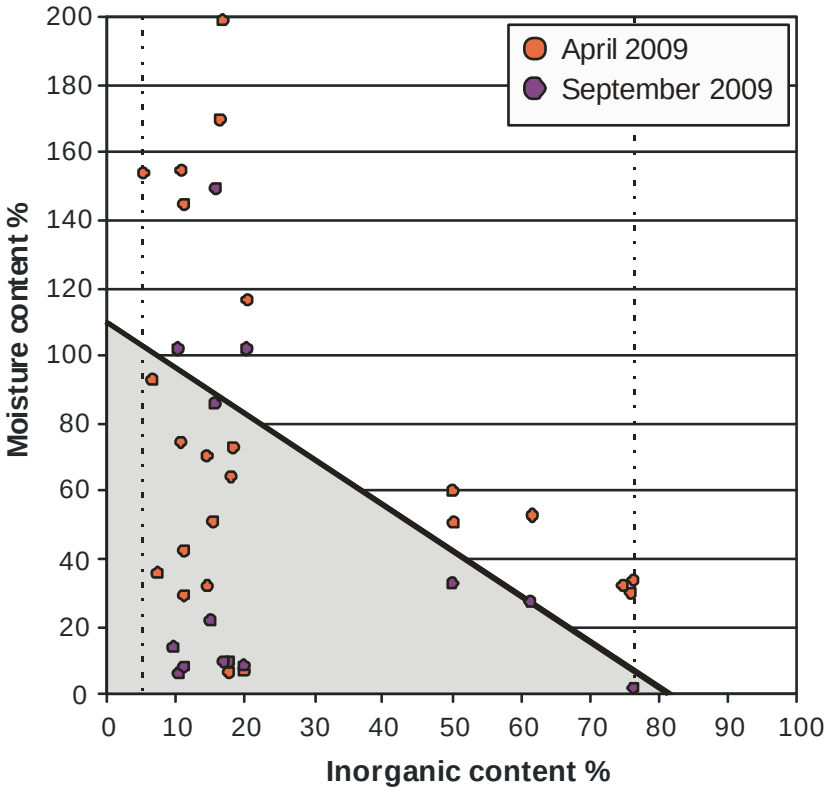

Fig. 6.26. Frandsen's diagram of Las Tablas de Daimiel National Park (TDNP) soils ignition limit as a function of inorganic and moisture contents before and after fire detection in summer 2009 (adapted from Frandsen, 1987). Successful ignitions are accomplished only within the shaded triangle bounded by the axes and the dark solid line. Vertical dotted lines represent minimum and maximum inorganic contents found in TDNP samples.

The smouldering fire detected in the Cañas area (Figs. 2.1 and 5.4) was about 540 m away from the point where datalogger P03 was installed (Fig. 5.4). Soil moisture records in P03 behave in a similar way as in P05, although the summer decrease is even sharper (Fig. 6.27b). The superficial temperature sensor also shows a similar pattern as in P05 but not the deeper sensors. Sensor T3, placed at 150 cm deep inside a crack, shows a continuous and almost constant temperature increase until November, when it abruptly decreases. It seems that hot smoke reached this sensor through the pipes' network. The smoke flow ceased when this network was disconnected by excavators during the fire extinction work (see section 6.6.5 below) and then the recorded temperature decreased. Sensor T2, at 60 cm deep, shows a constant temperature increase due to both seasonal effects and heat transfer from the

hot smoke circulating through the pipes where T3 is installed. It begins to cool down in August and in the same way as T3, a sharp decrease starts by the end of November.

From the analysis and comparison of records from P03 and P05 it can be deduced that: i) pipes' network is interconnected and capable to transfer air, heat and probably the fire over very long distances; ii) the effects of the flux of hot smoke have to be further studied, as this smoke probably desiccates the peat along the pipes supporting its ignition, and could offer preferential directions of spread; iii) the fire control work by means of soil mechanical digging up and compacting (see section 6.6.5 below) was effective and its effects measurable over long distances.

6.6.5. Fire-fighting and fire control

As typically moderate rainfalls from autumn to spring were not expected to be effective in putting out the fire naturally (see previous section), the action planned was to re-flood TDNP with a sufficient volume of transferred water. The best period selected for doing this was during autumn/winter, under suitable soil moisture conditions and minimum evapotranspiration. While waiting for this water transfer, a series of temporary palliative measures aimed to stop fire propagation were taken. One of the main fire control actions consisted on mechanical digging up and compacting of those areas where smoking cracks or pipes have been detected (Pic. 6.4). Additionally, the area where the first smoke columns were observed (Cañas zone) was locally flooded through continuous 3,000 m^3 d^{-1} water flow from nearby wells.

In Figure 6.28, an outline of the soil physical response following TDNP desiccation, smouldering fire and fire control actions is shown. The typical sediments arrangement in the TDNP is depicted in figure Fig. 6.28a. Some small shrinkage cracks that develop naturally during dry periods can also be observed. The consequences of the extreme lack of water from 2004 to 2009 are shown in Fig. 28b: development of big cracks and

hollows and peat combustion. Subsequent mechanical treatment of the soil for fire control using heavy machinery caused the disturbance of the soil structure: cracks and hollows were filled and materials were mixed and compacted (Fig. 28c).

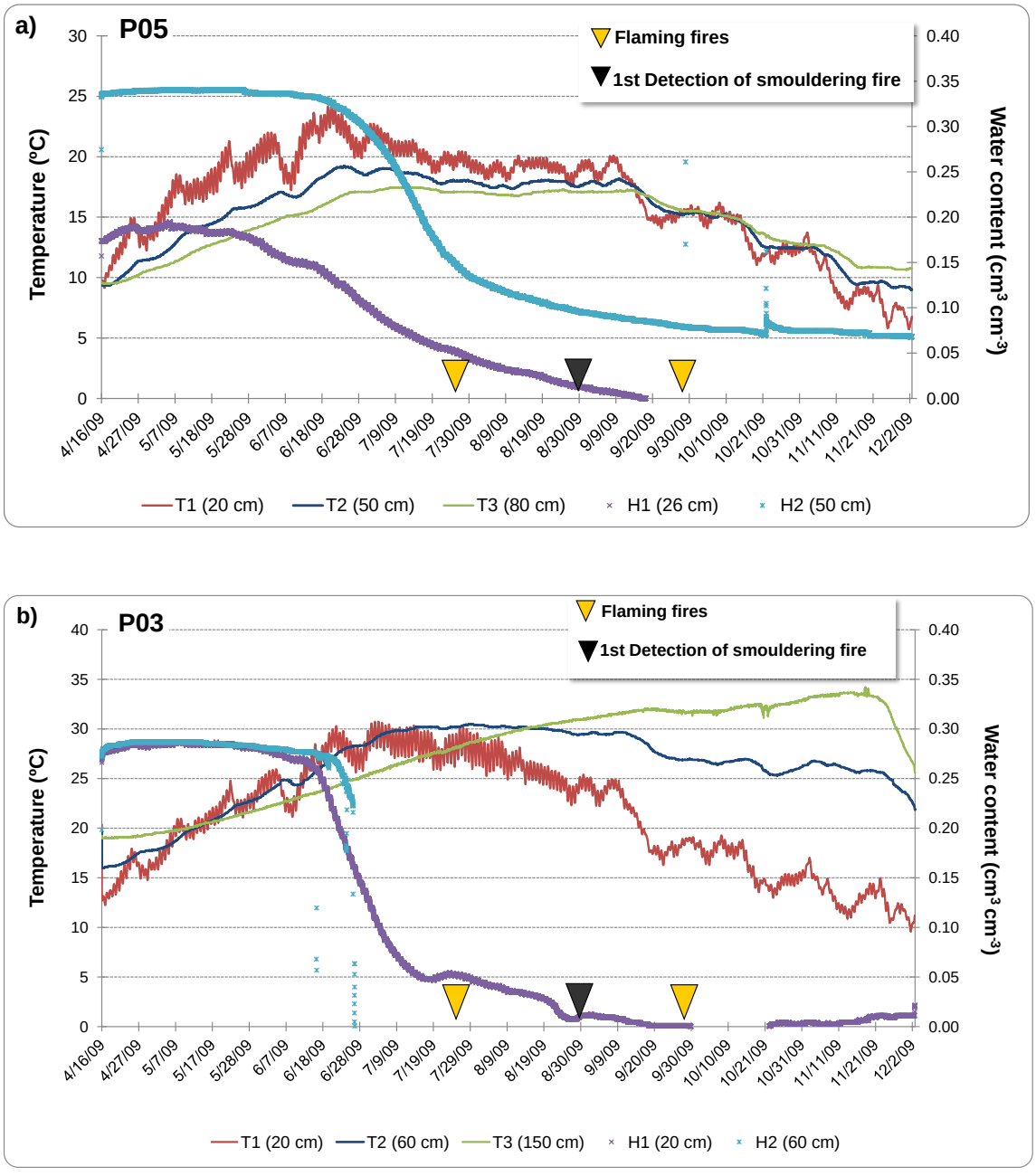

Fig. 6.27. Moisture and temperature response in sensors of a) P05 and b) P03 monitoring points inside Las Tablas de Daimiel National Park (Table 5.2; Figs. 5.4 and 6.13). First detection moments of flaming and smouldering fires are also shown.

Picture 6.4. Soil mechanical digging up and compacting works against smouldering peat fire propagation inside Las Tablas de Daimiel National Park in 2009.

Soil mechanical disturbance can fight against fire propagation by means of three concurrent effects (Fig. 28c): a) material compacting that prevents air circulation and oxygen input to the system; b) disruption of continuity in peat pipes and cracks; c) breakage of continuity in peat layers making it more difficult for the ignition front to propagate through the peat mass. Soil mechanical disturbance was applied against both the inner and outer TDNP smouldering fires.

On January 9th 2010 water from a 20 hm^3 transfer started to flood the Park. Flooding through water transfer was planned to be only undertaken inside TDNP. Finally, the water transfer was not completed because of the exceptionally heavy and continuous precipitations that fell in the region from December 2009 to February 2010. Thanks to these torrential rains, the entire TDNP was inundated. Fire was considered to be extinguished by this flooding as the whole system was submerged below a more than 1 m water sheet.

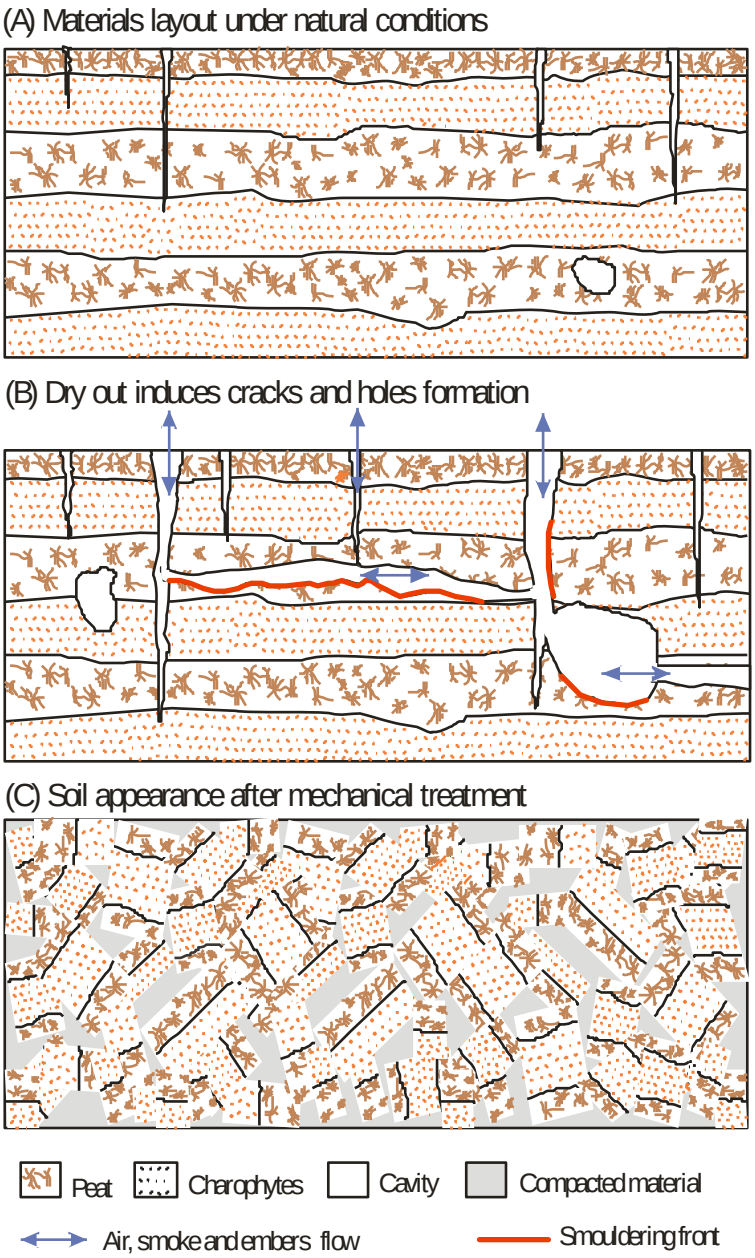

Fig. 6.28. Schematic representation of the effects on soil's physical structure derived from system dry out and soil mechanic treatment for smouldering fire control in Las Tablas de Daimiel National Park (TDNP).

6.6.6. Summary and conclusions on peat fires

The detailed knowledge about TDNP soil characteristics and VZ structure has been fundamental when attempting to propose and establish preventive measures for fire

control. The most remarkable experimental results reported in this section include the description of those soil characteristics reported in section 6.3 which are fire related, peat masses distribution, cracks and hollows development, and soil moisture and temperature records collected before and during the 2009 fires.

TDNP peats are the best fuel material in the area due to the combination of moderate to high organic matter contents (average value of 50.1% and maximum values ranging from 51 to 71%) with low bulk densities due to large primary porosity (0.18 g cm^{-3}) and water repellency development when dry. Furthermore, peats with higher organic matter contents tend to display higher degrees of water repellency (see Fig. 6.10 in section 6.3.3).

The desiccation process decreases peat total porosity making it shrink and giving rise to cracks and hollows which constitute preferential flow paths for both air and infiltrating waters. Cracks number, dimension and extension grew exponentially from 2008 and especially during summer 2009, reaching up to half meter wide and two meters depth. High soil temperatures and low water contents accelerate physical-chemical processes promoting the formation of new hollows and the progressive development of existing ones. Peat shrinking and non-saturated conditions are also the main cause of soil subsidence (Jiménez-Pinilla, 2011).

Soil water content and organic fraction are the main controlling properties for smouldering fires ignition and spread. According to Frandsen's diagram (1987), successful ignitions are accomplished at moisture content below 110.0% in dry weight base, and inorganic content below 81.5%. Most TDNP samples fell within this range before the 2009 fire started (Fig. 6.26). Nevertheless, a global critical moisture value of 125 ± 10% in dry base for peat to start being combustible is widely acknowledged (Rein et al., 2008; Reardon et al., 2007).

Continuous soil moisture and temperature monitoring is recommended as indicator of potential combustion and auto-ignition fire risk. Sensors for soil moisture and

temperature monitoring showed that the 2009 fire was transmitted through the underground peat pipes over long distances, being even able to flow below engineering structures such as the central Morenillo dam (Pic. 6.3a). However, this monitoring has not been useful as alert system for an already active fire. The punctual character of this method makes it limited to the situations where the fire seat is close enough to the sensing point. Also, subtle temperature variations require longer records and numerous control points to allow the fire heating being distinguished from the noise and other effects different from fire.

The presence of active smoke columns is a late warning for fire detection. First columns were visible with the decrease in early morning atmospheric temperatures by the end of August but the starting moment remains unknown. The fact that the development of cracks and hollows in these peats has been very fast, especially during 2009, highlight the need for future researches to get to know the dimensions and spatial distribution of the pipes' system as soon as it is developing during a system dry out.

The fire control measures undertaken before the complete flooding of the Park such as mechanical compacting were effective but only had a palliative character.

Typical natural precipitations (around 350-450 mm y^{-1} mainly distributed between autumn and spring) are considered insufficient to wet the peat. The pipe's network and the high hydrophobicity of peats do not allow natural moderate rainfall to sufficiently wet the soil as runoff is concentrated on preferential flow paths. However, exceptionally intense and continuous precipitations can lead to an unexpected natural inundation of TDNP, as occurred. The particular arrangement of sediments in the TDNP VZ allows the existence of perched water tables. This contributes to the fast spread of the water sheet along the Park.

6.7. Vadose zone water flow model and simulations

Determination of SFT water retention and hydraulic conductivity parameters has allowed for calibration of VZ water flow models during drainage conditions. Special attention has been given to peat shrinking characteristics to account for macropore flow dynamics. Models are presented as a tool to support Park management and predict the development of soil moisture conditions suitable for reed overgrowth and/or peat combustion risk.

6.7.1. Soil hydraulic properties

Measured and estimated values of SFT water retention and hydraulic conductivity parameters used for water flow modelling with SWAP are shown in Table 6.8 (see section 5.6.2). The water retention parameters values appear in the same range reported for typical fine-textured (Schaap and Leij, 2000; Wösten and van Genuchten, 1988; Wösten et al., 1999; van Genuchten et al., 1991; Yates et al., 1989; Wösten et al., 2001 in Kroes et al., 2008; Ippisch et al., 2006; Parker et al., 1985; Sarwar et al., 2000; Wöhling et al., 2008) and organic peat soils (Wösten et al., 2001 in Kroes et al., 2008; Gnatowski et al., 2010; Kechavarzi et al., 2010; Weiss et al., 1988; Olszta and Kowalski, 1996; Schwärzel et al., 2006; Letts et al., 2000). However, except for peat, θ_s and θ_r water contents in TDNP wetland soils are usually higher than those reported in the literature, particularly for θ_s. Except for clay, water content at saturation of the different SFT lie in a narrow range between 0.65 and 0.75 cm^3 cm^{-3} indicating their high water absorption capacities (Table 6.8). A clear distinction can be made between organic and non organic SFT regarding their residual water contents, an order of magnitude higher for the former. This is in agreement with the water retention capacity of soil organic matter.

The results show a higher degree of reliability in the estimation of water retention curve parameters than those of the hydraulic conductivity curve (*L*). This is due to the irregular and scattered behaviour of *K(h)* measurements recorded with the Wind evaporation method compared to those of $\theta(h)$ (see figures in appendix E). Difficulties in fitting hydraulic conductivity curves are widely acknowledged by soil scientists (Schaap and Leij, 2000; van Genuchten, 1980; Schaap et al., 2001; Olszta and Kowalski, 1996; Yates et al., 1989; Gnatowski et al., 2010). The use of measured instead of fitted K_s values appears as an added difficulty due to extremely large values, but it was decided to stick to the original physically-based Mualem's definition of this parameter. Nevertheless, resulting *L* values are in the expected order of magnitude for fine textured soils reported by Schaap and Leij (2000).

Special attention has been given to peat hydraulic parameters. Although, as stated above, resulting values are comparable to those reported in other works, θ_s and θ_r values in TDNP peats are generally lower whereas α is higher. Sensitivity of the hydrualic functions to variations in the hydraulic parameters differs depending on target soil type and fitting procedures (Simunek et al, 1998; Oliver and Smetten, 2005). However, in the case of peat, moisture retention characteristic and hydraulic conductivity function depend on the botanical origin and the degree of peat decomposition (Gnatowski et al., 2010). These factors are highly dependent on climatic environmental conditions. In this sense, most peat studies refer to higher latitude peatlands whereas comparative information from semiarid regions is absent. Future specific research on physical properties of peatlands in warmer areas is, therefore, fundamental.

The shape of SFT fitted water retention curves (Fig. 6.29) is in accordance with their textural classification or organic nature (Table 6.5). A clear distinction can be observed between charophyte rich soils, which have a bigger sand fraction and show higher water content variations at pF values ranging from near saturation (1) to permanent wilting point (4.2), and other organic or finer textured soils where water is more strongly retained at increasing matric potentials.

Table 6.8. Average estimates of soil hydraulic parameters used for SWAP modelling. All parameters are defined in section 5.6.

	Water retention						Hydraulic conductivity		
Soil type	θ_s ($cm^3\ cm^{-3}$)	θ_r ($cm^3\ cm^{-3}$)	α (cm^{-1})	n	h_e (cm)	R^2	K_s ($cm\ d^{-1}$)	L	R^2
Undisturbed charophytes	0.723	0.054	0.012	1.649	0.794	0.995	84	-1.361	0.522
Edaphized charophytes	0.715	0.133	0.003	1.983	0.010	0.979	527	-1.0	-
Saline charophytes	0.721	0.023	0.030	1.503	2.215	0.997	84	-1.0	-
Clay	0.487	0.090	0.028	1.206	0	0.957	48	-1.0	-
Silt	0.674	0.156	0.007	1.524	0.010	0.994	38	0.5	-
Peat	0.752	0.192	0.227	1.497	0.898	0.995	1000	-1.435	0.500
Organic	0.735	0.190	0.109	1.331	0.730	0.994	588	-1.816	0.585
Peaty silt	0.654	0.127	0.054	1.256	0	0.886	443	0.5	-

Another interesting feature that can be inferred from the shape of the pF curves is the pore size distribution (Eijkelkamp, 2005). Pores of similar size will be emptied at the same matric potential. The more homogenous the pore size distribution, the faster the drop in soil moisture content upon a small decrease in matric potential, and the flatter the slope of the pF curve. The steeper the slope, the more gradual is the emptying of soil pores and the more heterogeneous the pore size distribution. Therefore, according to the plots in Figure 6.29, charophyte-rich soils would have a more homogenous pore size distribution than other finer textured and organic-rich SFT in TDNP. Flattering in the peat curve is likely induced by large secondary porosity due to shrinking and cracking.

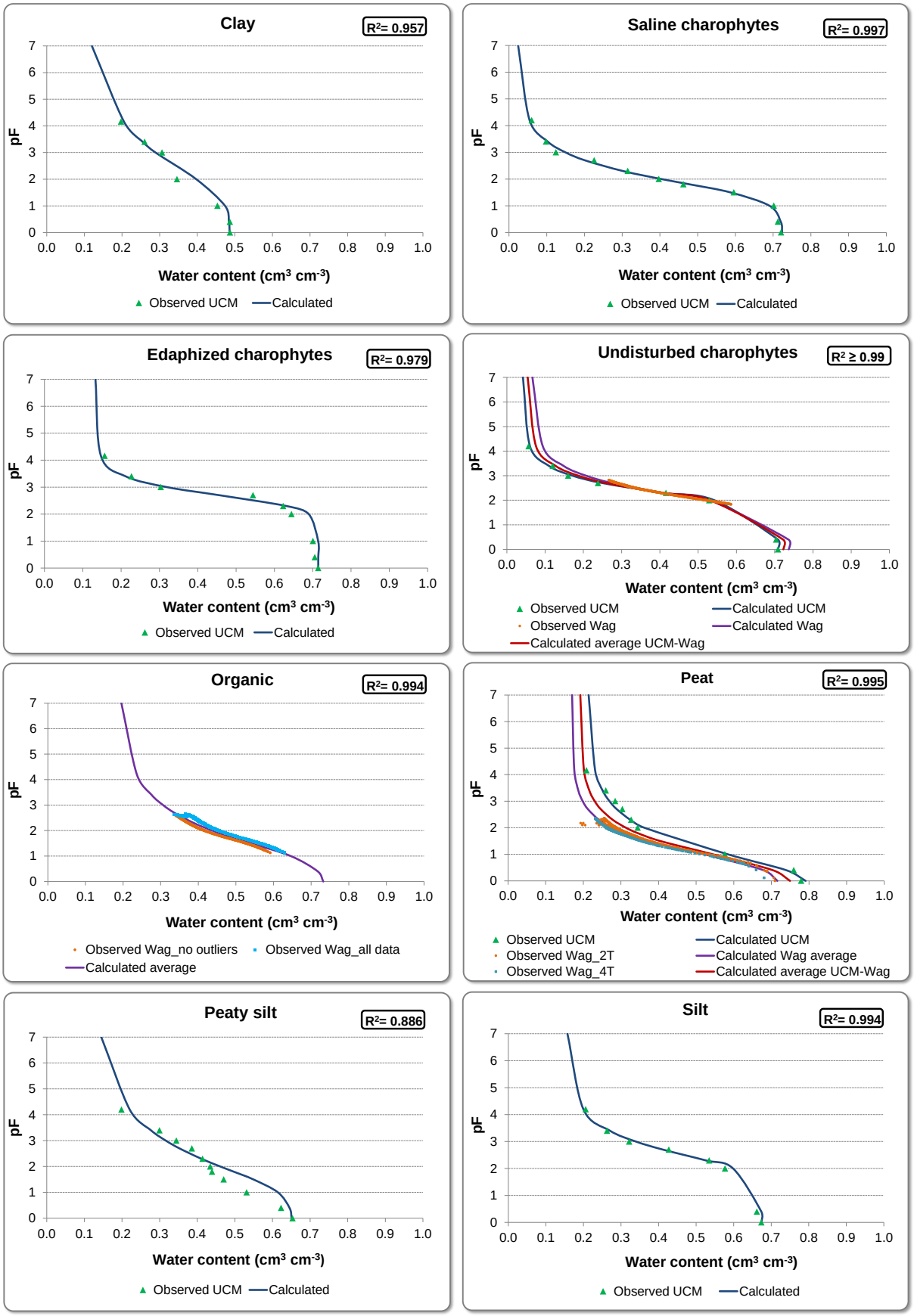

Fig. 6.29. Water rentention characteristics and fitted curves of the different soil functional types (SFT) in Las Tablas de Daimiel National Park. Green observed data correspond to determinations with the sandbox, sand/kaolin and pressure membrane apparatus in the laboratory of the Department of Edaphology at the Complutense University of Madrid (UCM). In the case of undisturbed charophytes, peat and organic soils measurements from the Wind evaporation method performed in the laboratory of the Alterra Soil Research Centre in Wageningen (Wag) with different combinations of available data (orange and blue) from up to four tensiometers (T) as well as average fits derived have been included. Overall goodnss of fit for each SFT is expressed in terms of the R^2 values.

It is worth mentioning that in the case of peat and undisturbed charophytes, pF curves obtained through different methods in different laboratories and with different samples (sandbox, sand/kaolin and pressure membrane apparatus in UCM, and Wind evaporation method in Wageningen) are very similar to each other. This is a proof of the reliability of the measurements and an indication that general SFT hydraulic patterns have been captured within a dominantly heterogeneous environment.

6.7.2. Shrinking characteristics of TDNP peat soils

The soil matrix of peat soils shrinks upon drying as a result of drainage and evapotranspiration. Vertical shrinkage causes subsidence of the soil surface whereas horizontal shrinkage causes the soil to crack (Hendriks, 2004). These phenomena have been observed in situ in TDNP peat soils during the drying monitored period (see section 6.6).

Parameters for describing the shrinking curve of TDNP peats are shown in Table 6.9. The estimated shrinking curve for TDNP peat shows almost no near-normal shrinkage stage (ϑ_s = 3.53, ϑ_a = 3.49) where the peat matrix remains close to saturation (Fig. 6.30). This fact was also reported by Dawson (2006) for different lowland agricultural peat soils in England, suggesting that the air-entry point occurs quite rapidly after drainage begins. According to the estimated h_e value for TDNP peats, air-entry appears to occur at less than -1 cm water potential (Table 6.8). The curve continues with a typical subnormal stage and a wide supernormal shrinking stage starting approximately at a moisture ratio of 1 $cm^3\ cm^{-3}$ and void ration of 2.2 $cm^3\ cm^{-3}$ (Fig. 6.30). This last fact is in accordance with field observations of big cracks and hollows which can only develop when volume reduction exceeds by far moisture loss and the skeleton collapses.

Table 6.9. Estimated parameters of Las Tablas de Daimiel National Park (TDNP) peat shrinking curve. Parameters are defined in section 5.6.

e_0 ($cm^3\ cm^{-3}$)	ϑ_s ($cm^3\ cm^{-3}$)	ϑ_a ($cm^3\ cm^{-3}$)	α_H	β	P
0.60	3.53	3.49	0.76	3.084	0.539

It has to be taken into account that the presented shrinking curve is a rough estimation from a normalized curve from a relatively similar semi-decomposed peat (see section 5.6.2). Furthermore, similarity is restricted to the specific samples, as the degree of peat decomposition varies, among other factors, with soil depth (Dawson, 2006; Kechavarzi et al., 2010). In addition, pedogenic alterations due to intensive drainage and land management lead to a greater degradation of the soil structure in the upper soil layers. Less decomposed peats appear to have a higher propensity to shrink under increasing water potentials (Kechavarzi et al., 2010; Gebhardt et al. 2012). In this sense, estimated e_0 and ϑ_s parameters for the TDNP peat shrinking curve are lower than those obtained by Kechavarzi et al. (2010) and Gebhardt et al. (2012) for other Northern European fibrous peats. Nevertheless, lower water retention properties and OM content of TDNP peat samples indicate a higher degree of decomposition than that of the reference Polish reed peat or those analysed in the mentioned researches (Kechavarzi et al., 2010). These authors argue that decomposition and humification result in the degradation of the soil structure and in a decrease in water storage, water transmission and water retention, all three processes observed in TDNP peats thruought the PhD research period.

In the same way as for hydrualic properties, comparative results on the shrinking characteristics of peat soils in Mediterranean semiarid regions have not been found in the literature. Therefore, more accurate knowledge on TDNP peat shrinking characteristics would require actual determinations of void and moisture ratios on peat samples of different soil layers.

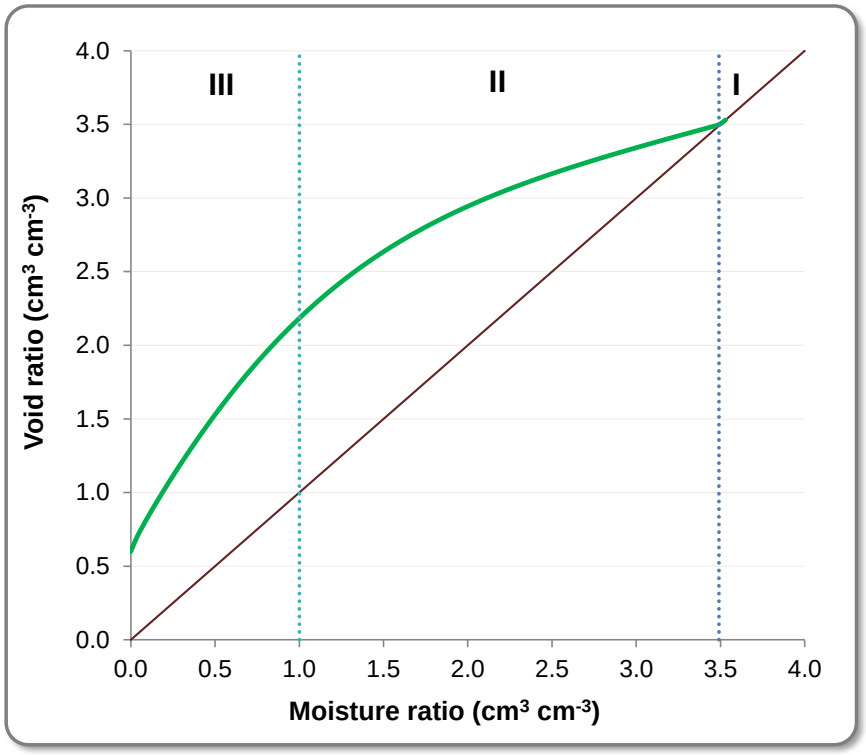

Fig. 6.30. Estimated shrinking curve (green) for Las Tablas de Daimiel National Park (TDNP) peat. The shrinkage charactersitc is expressed as void ratio (volume of pores / volume of solid phase) as a function of moisture ratio (volume of moisture / volume of solid phase), showing the three shrinkage stages: I Near-normal, II Subnormal, III Supernormal (after Hendriks, 2004). The solid line represents the saturation line.

6.7.3. Soil profiles

Typical soil profiles that represent the arrangement of SFT in the whole TDNP area are depicted in Figure 6.31. These profiles correspond to the average distribution in depth of soil materials in the spatial domains defined in the SFT map (Fig. 6.1). Nevertheless, the SFT map represents the general zonal distribution of dominant materials at the top of the VZ (i.e. from soil surface to 1 meter deep) whereas these soil profiles are meant to represent the SFT distribution in the whole Quaternary VZ. As the maximum drilling depth of sampled soil columns was 120 cm, the definition of soil profiles below this depth has been based on the random field observations (i.e. mechanical digging up for peat fire extinction, water pipe construction in TDNP limits, etc) and reviewed literature (García Rodríguez, 1996; García-Hidalgo et al., 1995; Domínguez-Castro et

al., 2006). At the bottom of all profiles a low permeability silt or clay layer which supports perched conditions in the shallow TDNP groundwater system has been set.

Profiles I to III represent arrangement of silty layers in the Guadiana and Cigüela ditches and in the Puente Navarro dam. Profiles IV to VI depict the typical soil structure in charophyte rich areas: edaphized and saline charophytes overlying clay in the northern left and right margins of the Cigüela ditch, respectively, and the thick layers of undisturbed charophytes in the main central flooding areas. Profile VII accounts for the typical distribution in peat dominated areas, whereas profiles VIII to X represent different arrangements of alternations of peat and organic materials layers with charophytes layers around and downstream the central Morenillo dam.

6.7.4. Model calibration and validation

After a long and tedious process of unknown parameter estimation through trial and error, SWAP models for the soil profiles described in the previous section were calibrated and validated. Given that the models were intended to approximate the global average behaviour in typical soil profiles of the heteregoneous system and not to give exact soil water content estimations (a much larger sensor network all over TDNP for continuous monitoring would be required for this), quite successful fittings have been achieved. Except for the undisturbed charophytes model, RMSE values of calculated water contents against recorded sensor data at different depths are far below the considered upper bound of 0.1 $cm^3 cm^{-3}$ (Table 6.10).

Table 6.10 also shows the main characteristics of the most relevant models where continuous water content measurements (i.e. data from soil moisture sensors) were available. The inclusion of hysteresis of soil water retention curve and reduced soil water flow due to frost globally improved model performance, except for peat profiles. Additional rainfall intensity data (detailed rainfall amounts per time interval) was also

suitable for most models. Free drainage bottom boundary condition in fluvial silt models reflects a strong downward gravity-driven hydraulic gradient and the connection of ditches with deeper aquifer layers

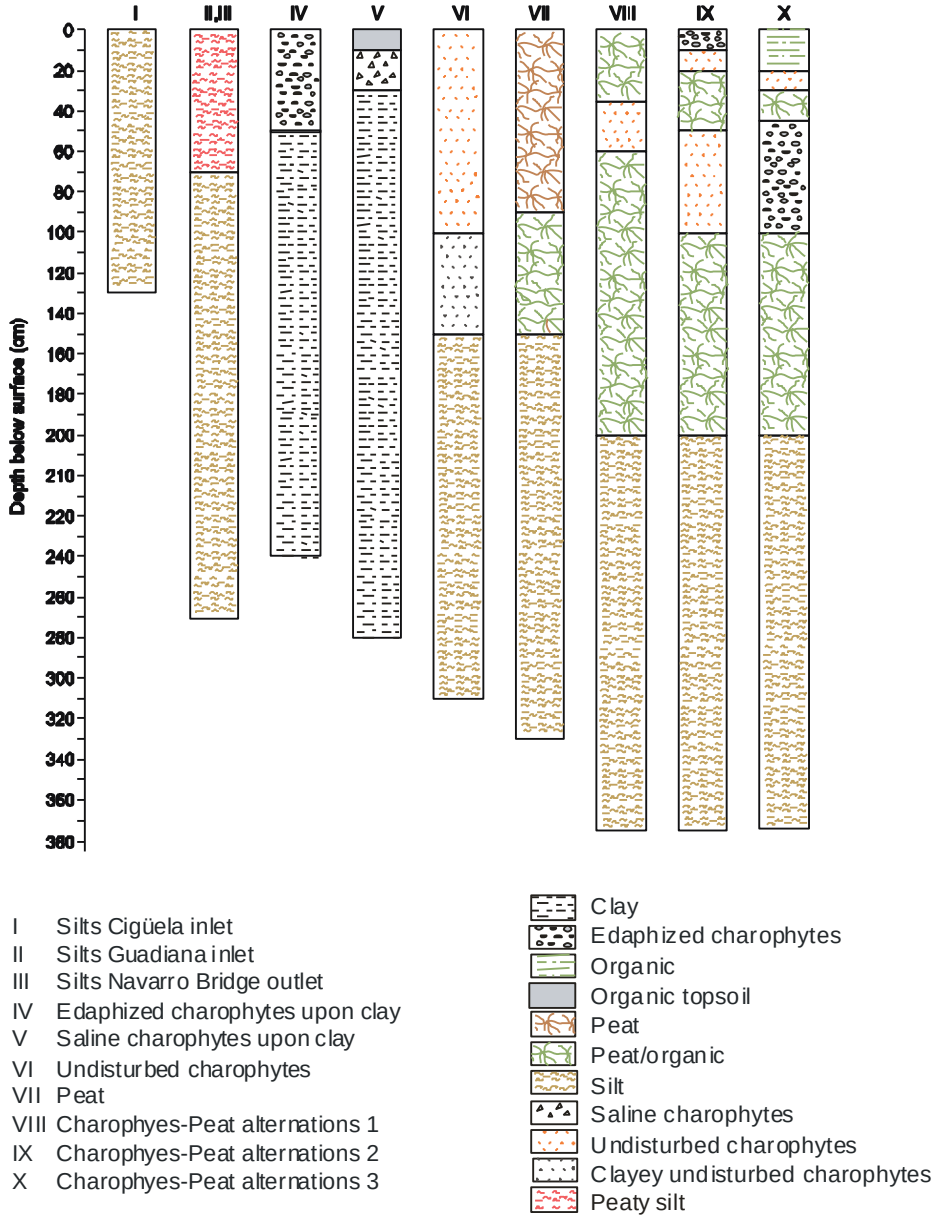

Fig. 6.31. Soil profiles used for vadose zone water flow modelling with SWAP describing the typical distribution in depth of soil functional types (SFT) in Las Tablas de Daimiel National Park area.

Table 6.10. Summary of main calibration and validation options and goodness of fit in vadose zone water flow models carried out with SWAP for typical soil profiles of Las Tablas de Daimiel National Park. Cal: calibration; Val: validation; BBC: bottom boundary condition; IMC: initial soil moisture condition; *: root mean squared errors of calculated values against continuous sensor data in model calibration.

Main SFT	Profile N°	Cal	Val	BBC	IMC	Vegetation	RMSE* ($cm^3\ cm^{-3}$)
Fluvial silt	II	1/3/2007-20/5/2009	21/5/2009-5/7/2009	Free draing.	GWL	*Bare soil*	0.024
Edaphized charophytes	IV	1/3/2007-25/5/2009	26/5/2009-2/7/2009	GWL (monthly)	GWL	*Phragmites australis*	0.007
Saline charophytes	V	1/3/2007-25/5/2009	26/5/2009-2/7/2009	GWL (monthly)	GWL	*Tamarix canariensis / Juncus maritimus*	0.007/ 0.041
Undisturb. charophytes	VI	1/6/2007-18/5/2009	19/5/2009-8/6/2009	GWL (daily records from G-04 sensor)	Pressure head in depth	*Bare soil*	0.195
Peat	VII	1/3/2007-26/5/2009	27/5/2009-1/7/2009	GWL (daily records from G-08 sensor)	GWL	*Cochlearia glastifolia, Conya Canadensis*	0.029
Peat-charophytes alternations	VIII	1/3/2007-22/5/2009	23/5/2009-1/7/2009	GWL (monthly)	GWL	*Cochlearia glastifolia, Conya Canadensis*	0.036
Peat-charophytes alternations	X	1/3/2007-10/5/2009	11/5/2009-31/5/2009	GWL (monthly)	GWL	*Phragmites australis*	0.028

Calibration-validation plots for the most representative soil profiles are shown in Figure 6.32 (the remaining ones have been included in appendix G). In general, all models show satisfactory results except for the undisturbed charophytes one where soil water content appears to be overestimated, although the soil moisture trend is reproduced. Different soil layouts and parameter configurations were tested but no improvements could be achieved. It is quite surprising given the fact that undisturbed charophytes show very homogeneous structure and hydraulic properties as inferred from field and laboratory observations. Besides this, the distribution in depth of this typical soil profile was one of the best known and same as for the peat model, it could be calibrated with a long time series of daily groundwater levels (Table 6.10). However, the groundwater level and, thus, soil water status, in the modelled area was influenced by occasional water pumps from the nearby emergency wells area throughout the monitored period, as well as by the effect of the 2007 spring freshet and small summer water transfer. That is the reason why model calibration was started in June 2007.

The most likely underlying reason for the large discrepancies between recorded and calculated water contents for this SFT is the prescribed groundwater levels, which are conditioned by the retaining effect of the central Morenillo dam (Castaño et al., 2012a,b). Moisture sensor monitoring point P09 used to calibrate the undisturbed charophytes model is located some distance downstream from the dam (Fig. 5.4), where the average groundwater level is deeper than in the target “tablazo” area upstream (Fig. 6.1). The average difference in groundwater levels between both areas in periods not influenced by external factors is around 130 cm. In fact, when a SWAP trial was run with the whole groundwater level dataset lowered by 1 m, the match between sensor measurements and simulated values improved significantly.

Fig. 6.32a: Peaty silt (soil profile II)

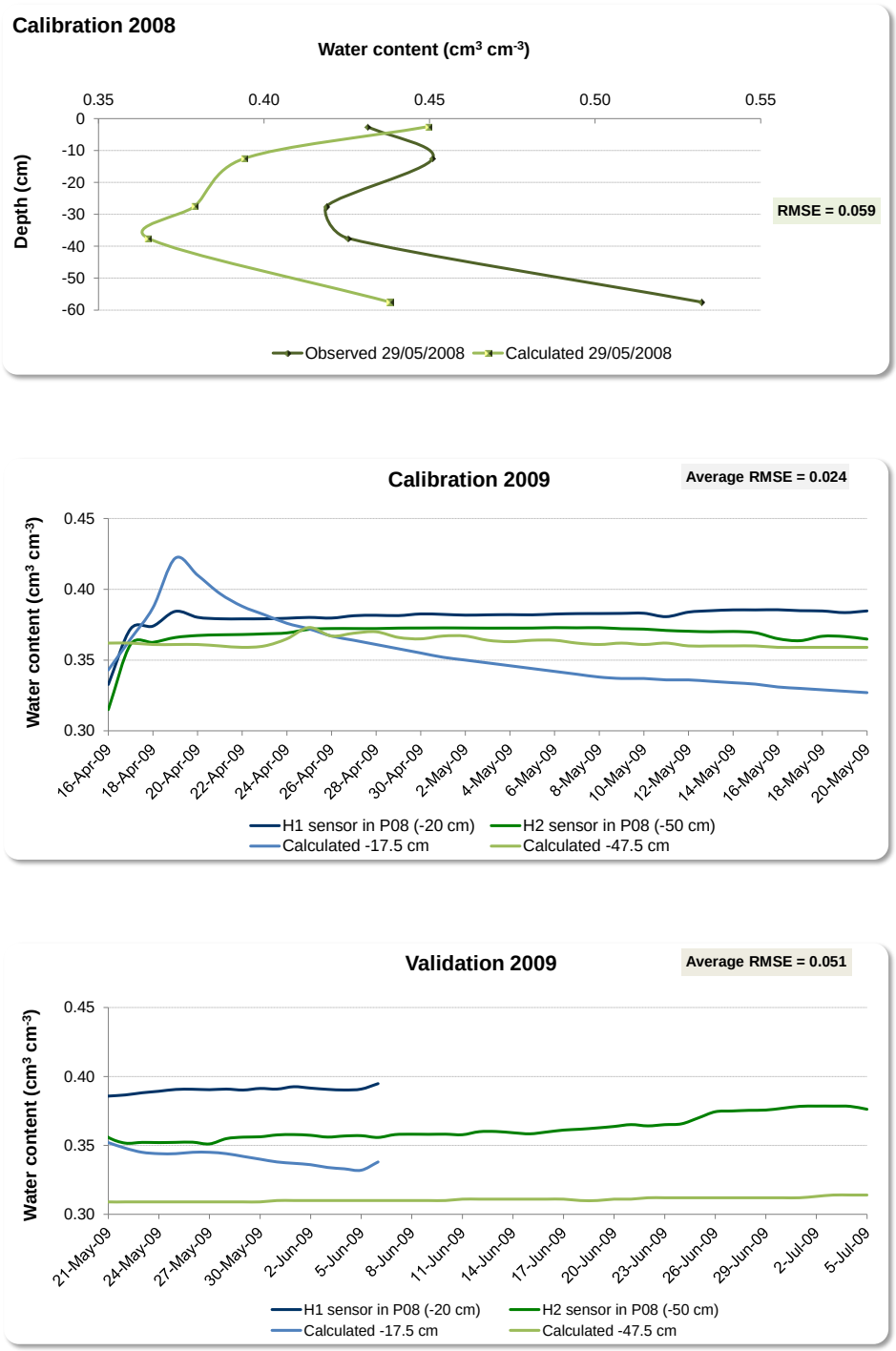

Fig. 6.32. a-g) Calibration and validation plots of SWAP vadose zone water flow models for typical soil profiles in Las Tablas de Daimiel National Park (Fig. 6.31, Table 6.10). Both discrete and continuous soil water content observations with moisture sensors (Fig. 5.4) within the period 2007-2009 are plotted against calculated values with SWAP. Note scale differences in soil water content axes. Average goodness of fit for each calibration and validation is represented by means of the root mean squared error (RMSE). Calibration and validation plots for soil profiles I, III and IX have been included in appendix G.

Fig. 6.32b: Edaphized charophytes overlying clay (soil profile IV)

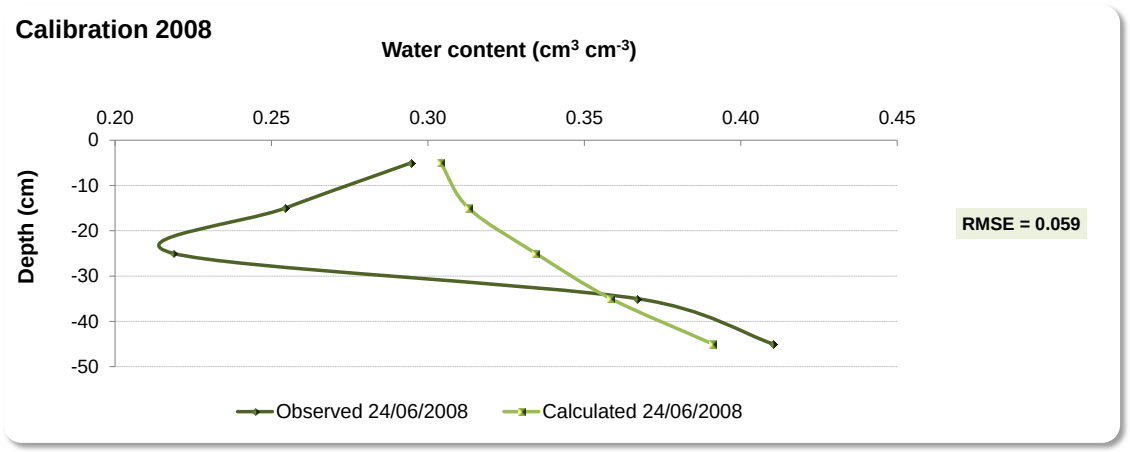

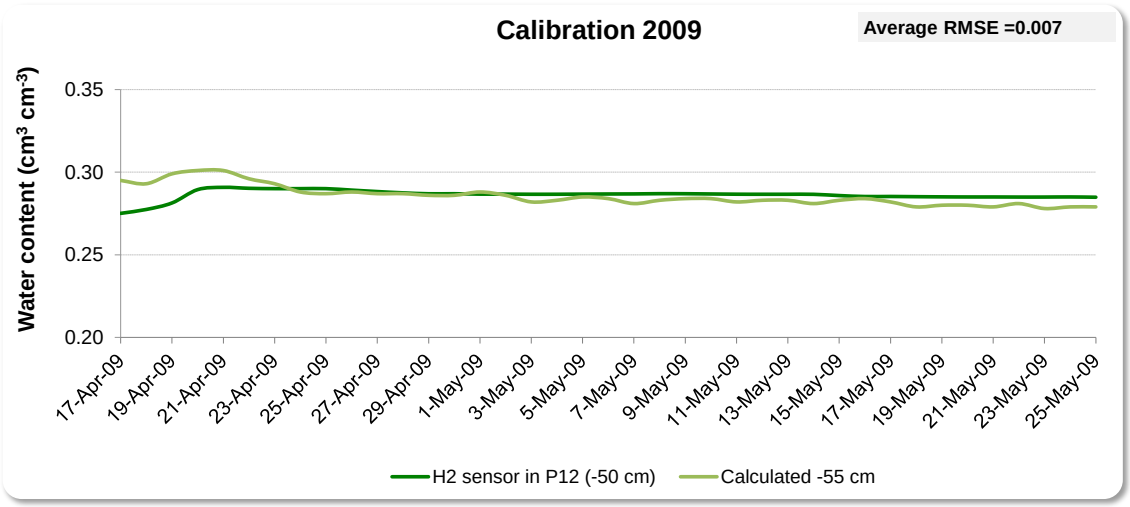

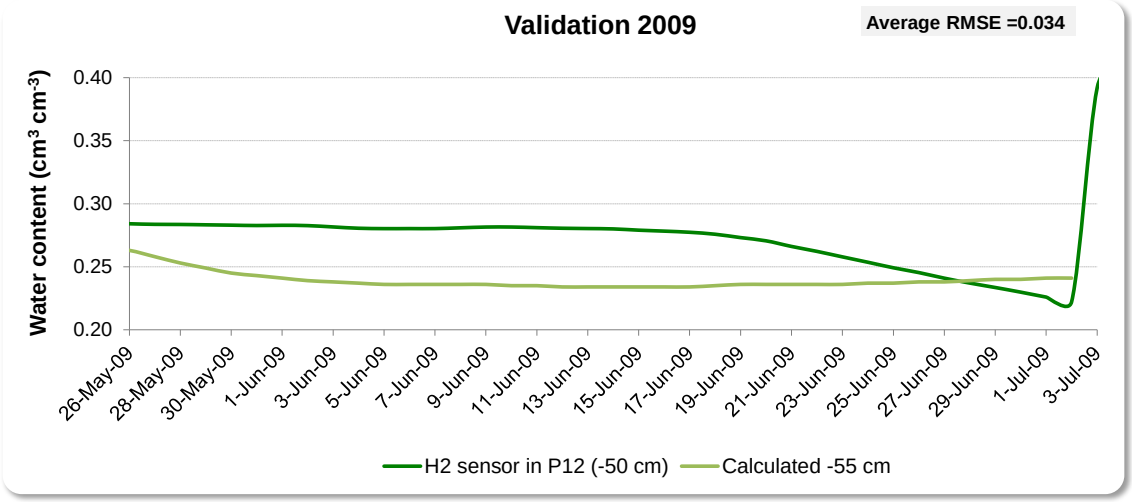

Fig. 6.32c: Saline charophytes overlying clay (soil profile V)

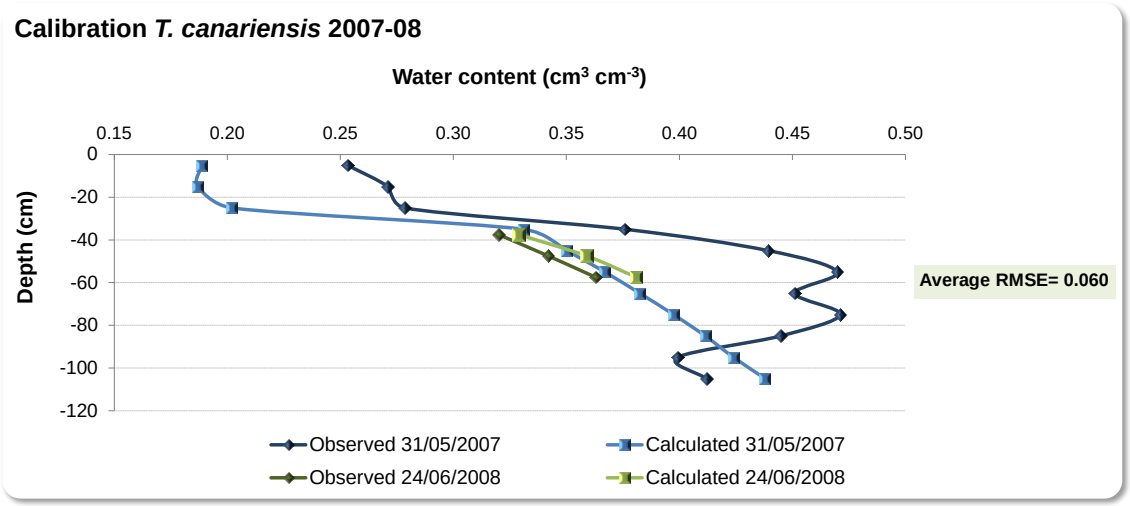

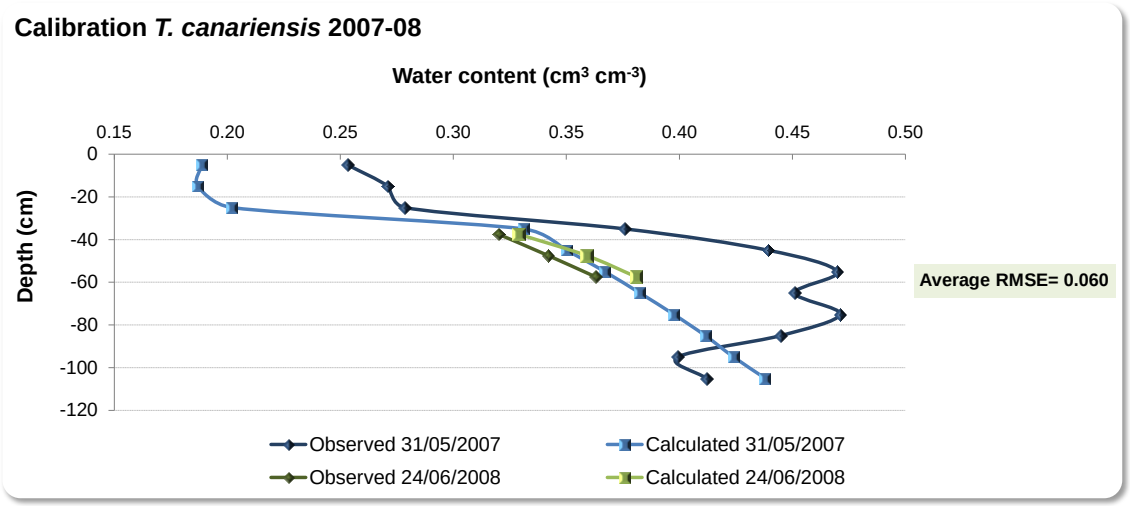

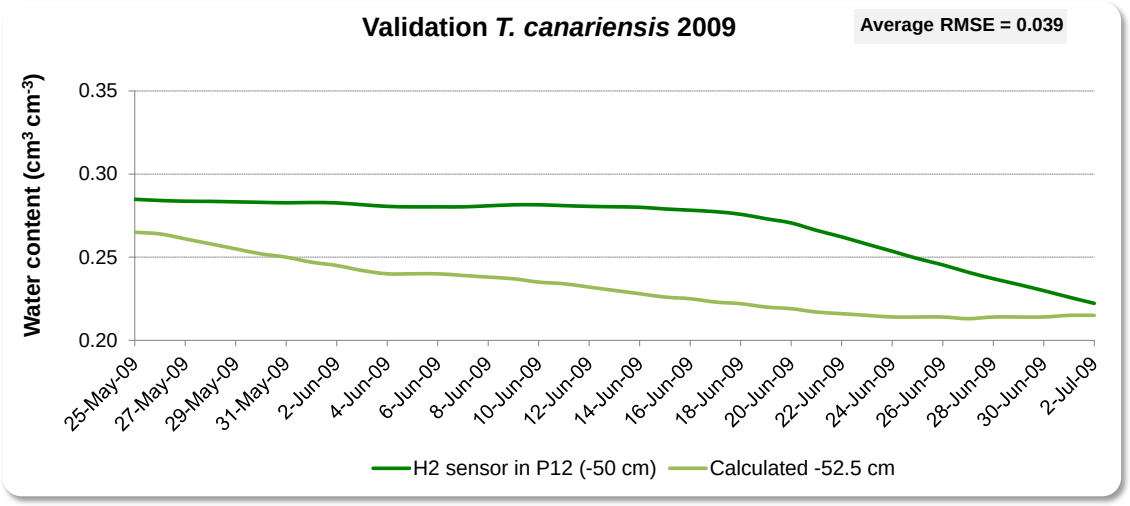

Fig. 6.32d: Undisturbed charophytes (soil profile VI)

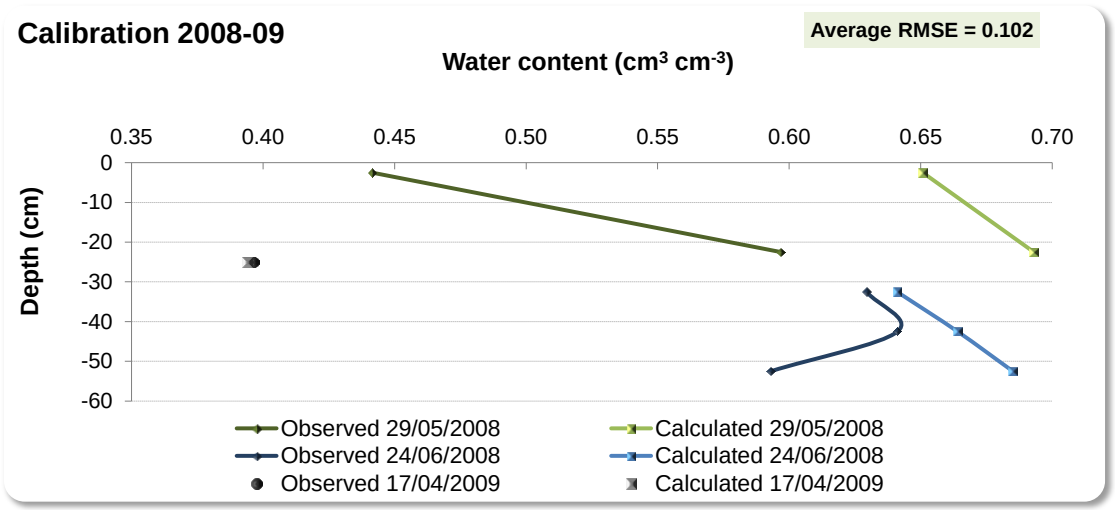

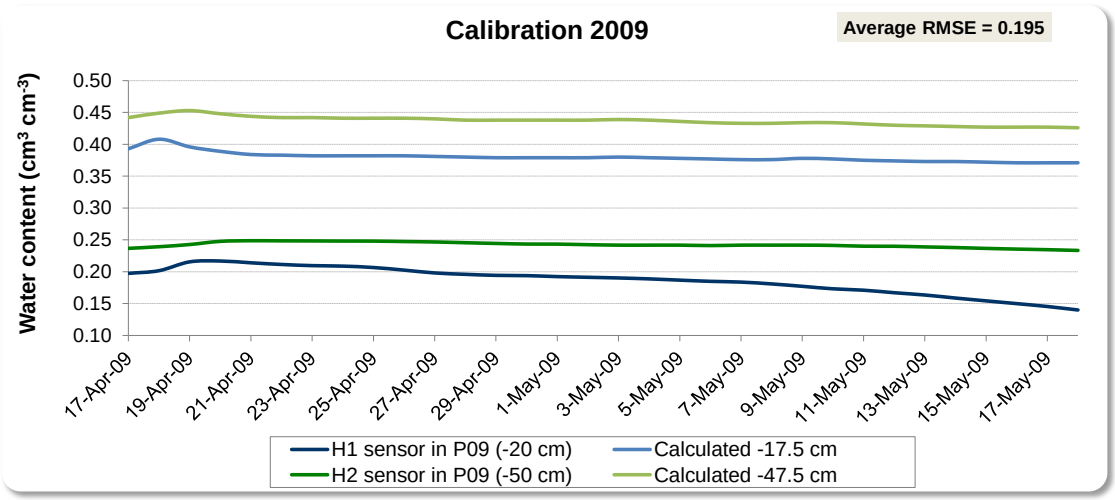

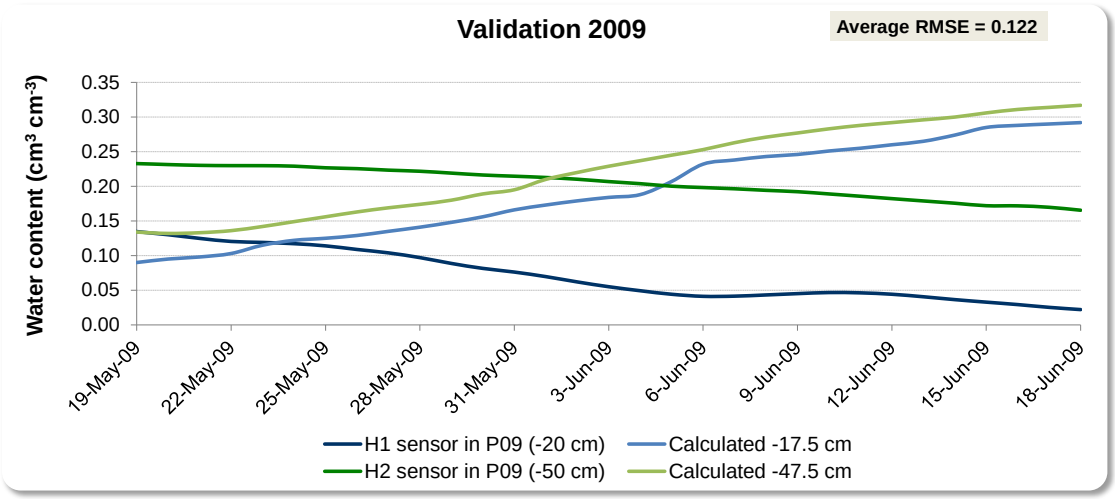

Fig. 6.32e: Peat (soil profile VII)

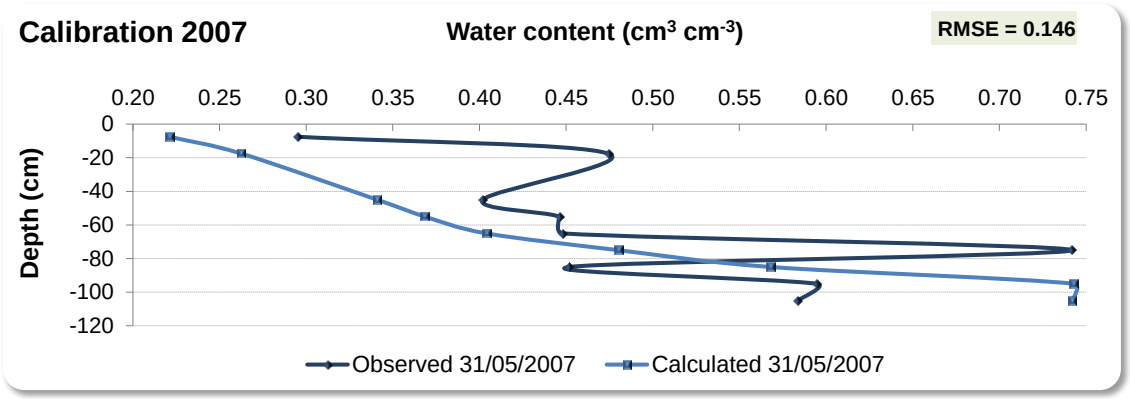

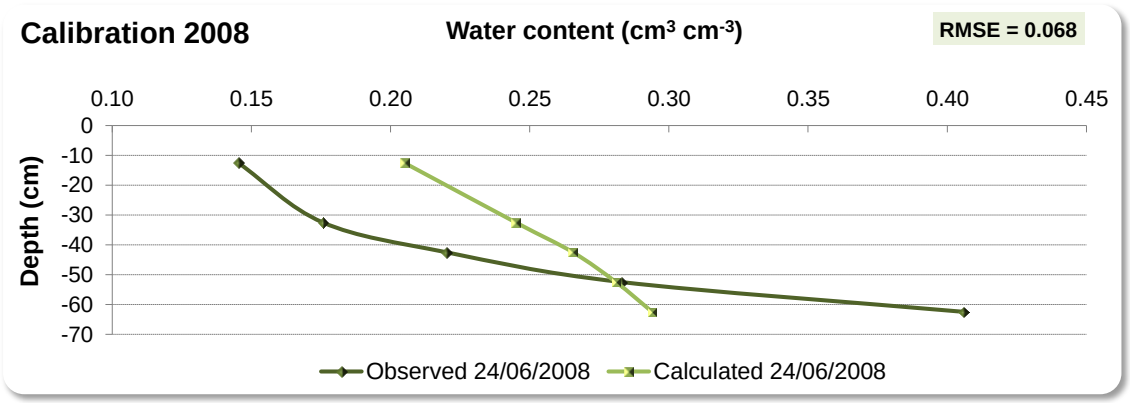

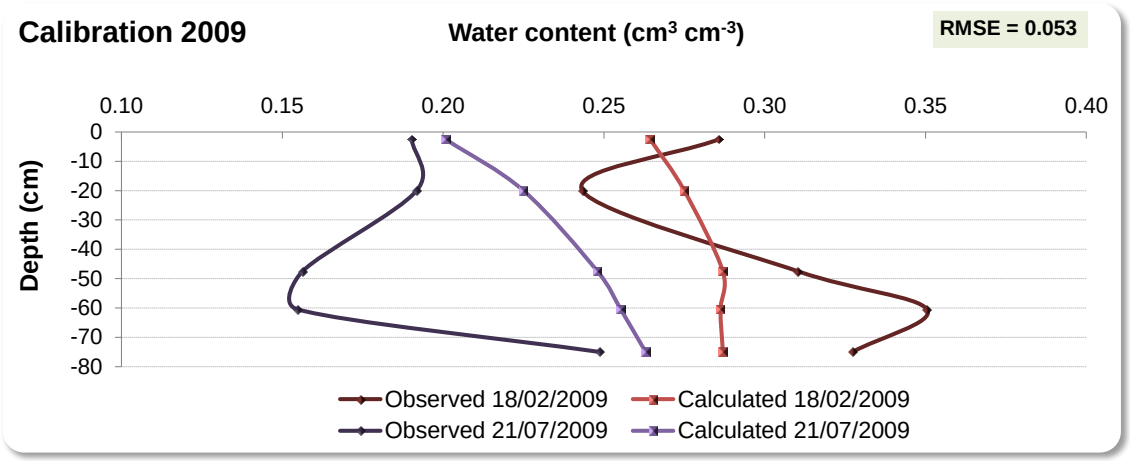

Fig. 6.32e: Continuation.

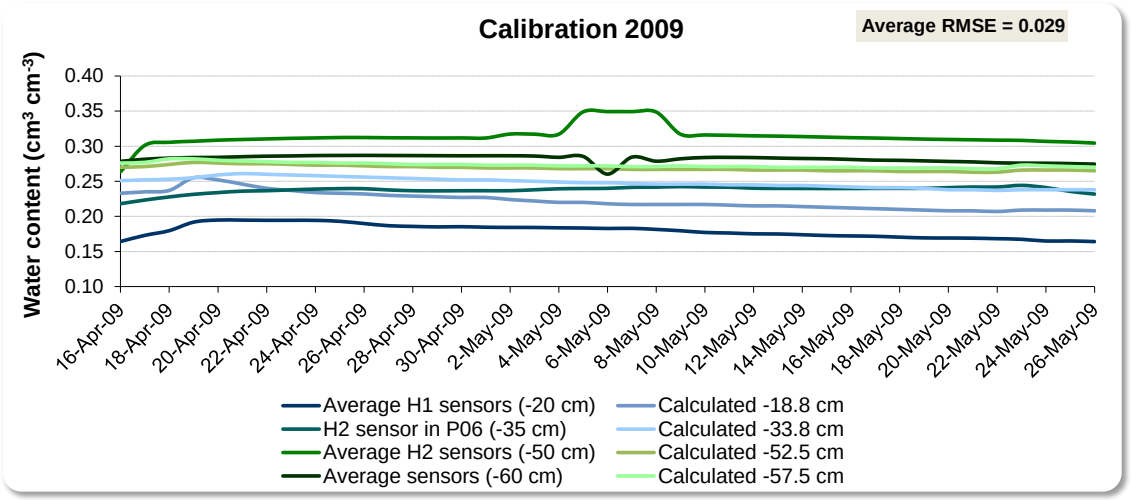

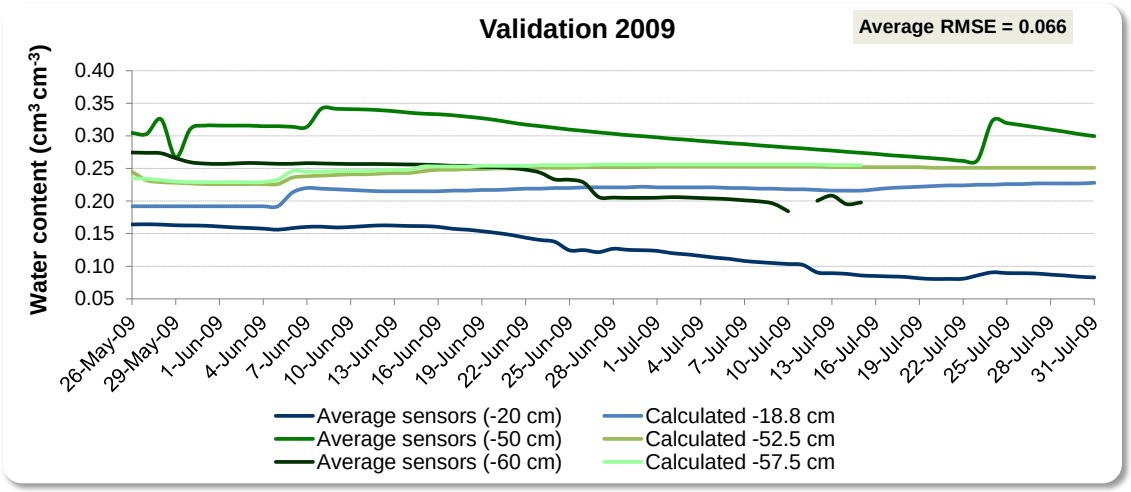

Fig. 6.32f: Charophytes-Peat alternations (soil profile VIII)

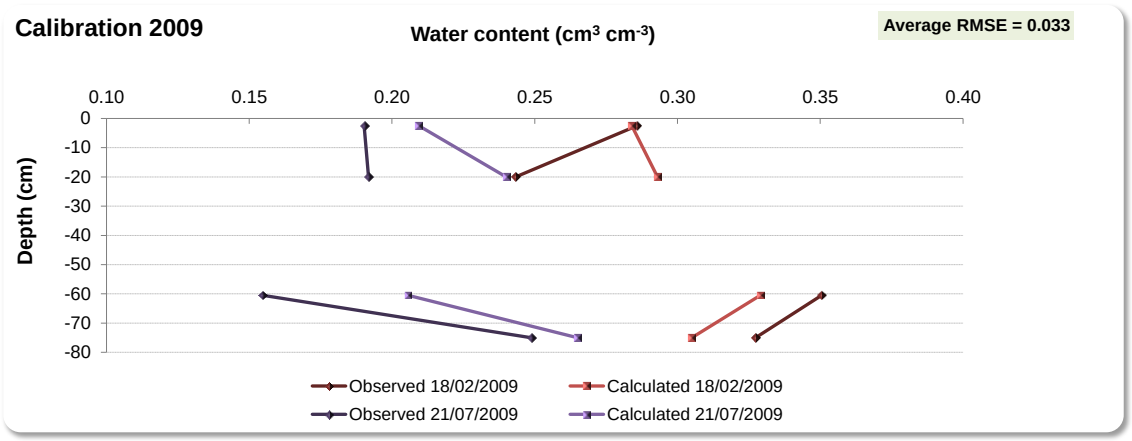

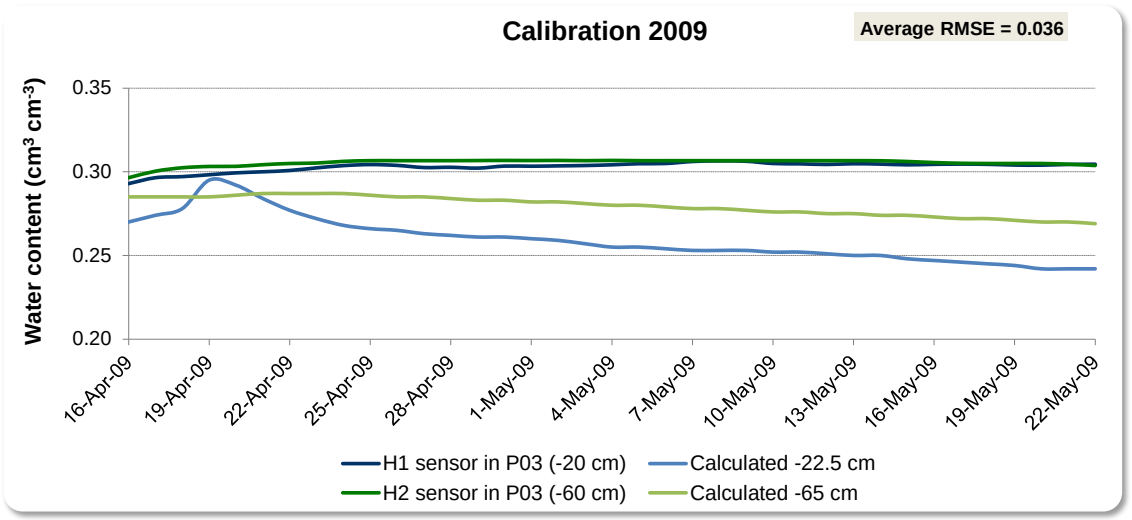

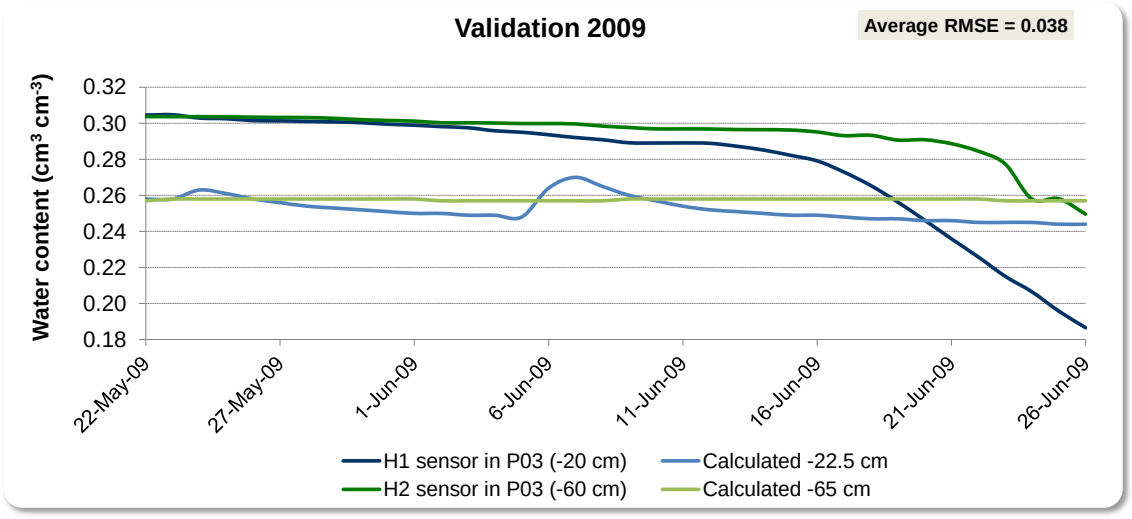

Fig. 6.32g: Charophytes-Peat alternations (soil profile X)

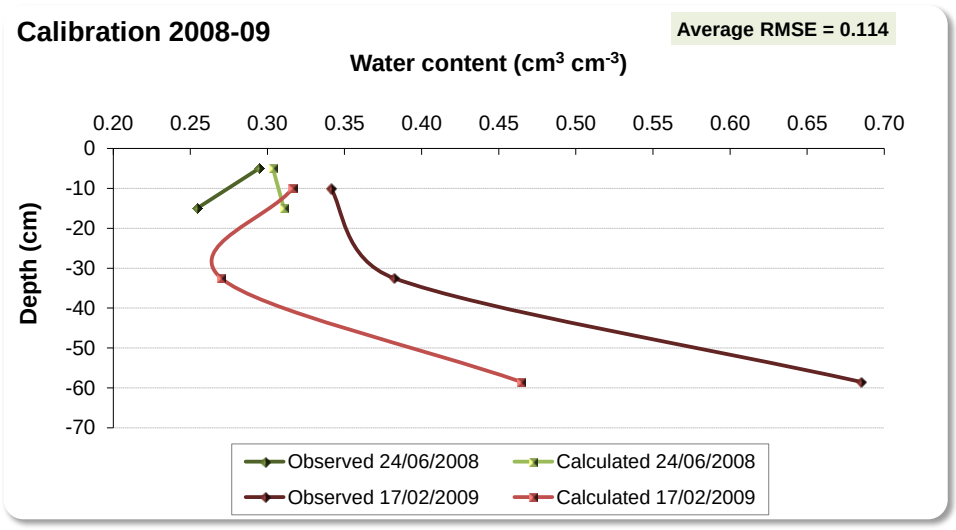

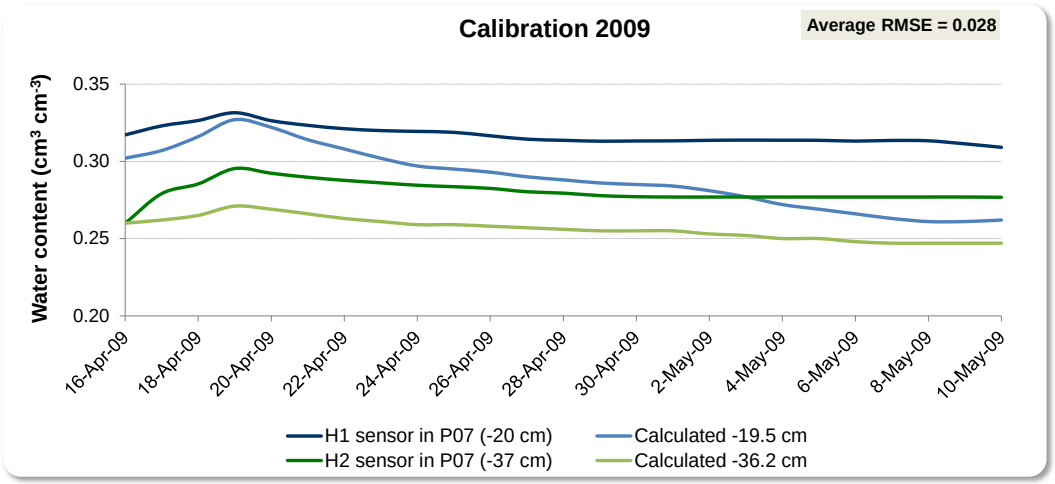

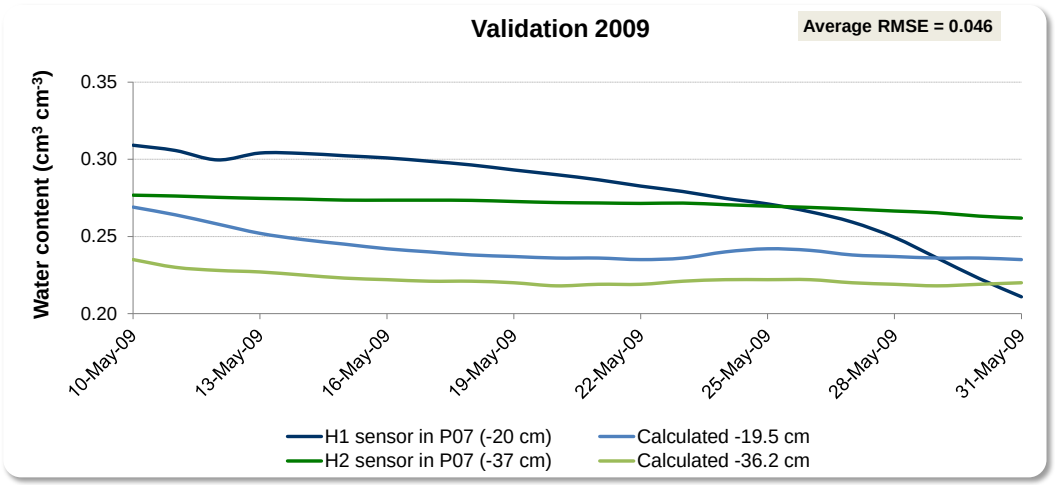

6.7.5. Drainage scenario simulations

6.7.5.1. Climatic analysis

As reported by Santisteban and Mediavilla (2012a), Figure 6.33 shows that there is a global good correspondence between Ciudad Real and TDNP rainfall data (R^2_{annual}=0.77; $R^2_{monthly}$=0.90),. Therefore, the analysis of the long-term series of Ciudad Real seems reasonably extendable to TDNP and missing monthly data in the series of 4112U (01/1987-03/1988 and 01/1989-03/1990 in Fig. 6.17a) have been estimated by linear regression with the records from station 4121.

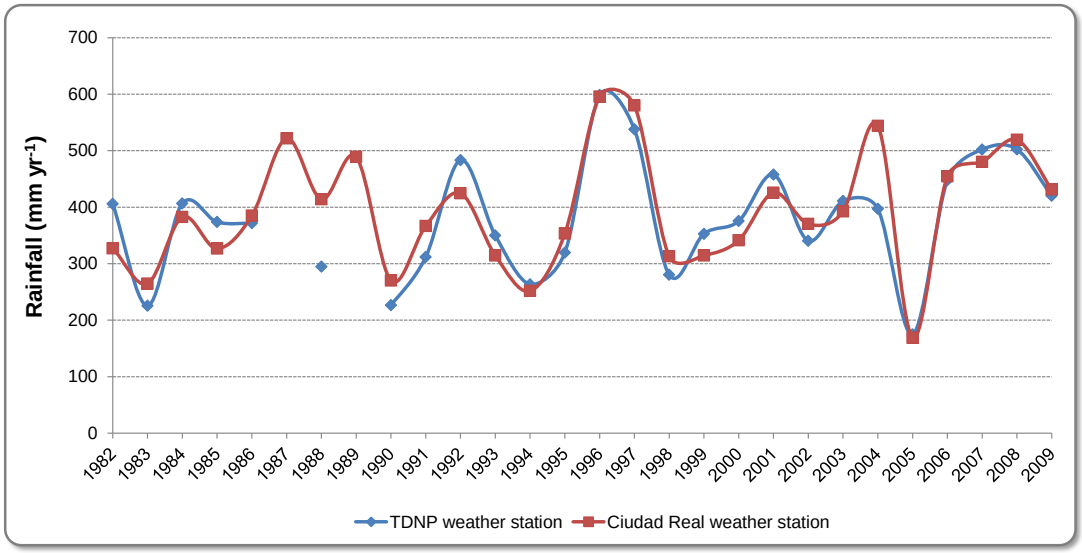

Fig. 6.33. Annual rainfall data recorded in the Las Tablas de Daimiel National Park (TDNP) and Ciudad Real weather stations for the period 1982-2009.

Based on the quartile distribution of available annual rainfall data in the Ciudad Real weather station series (see section 5.7), wet years have been defined as hydrological years with a total rainfall above 475 mm, normal years as those with a total rainfall between 334 mm and 475 mm, and dry years with a total rainfall below 334 mm (Fig.

6.34). It can be observed that 2-year and 3-year dry and wet cycles are recurrent in the series, whereas normal cycles are generally longer and more widespread throughout the analysed 90-year period. Among drying cycles two distinct patterns are found: increasing trends (1930/31-1932/33 and 2004/05-2005/06) and decreasing trends (1952/53-1953/54, 1981/82-1983/84 and 1992/93-1994/95).

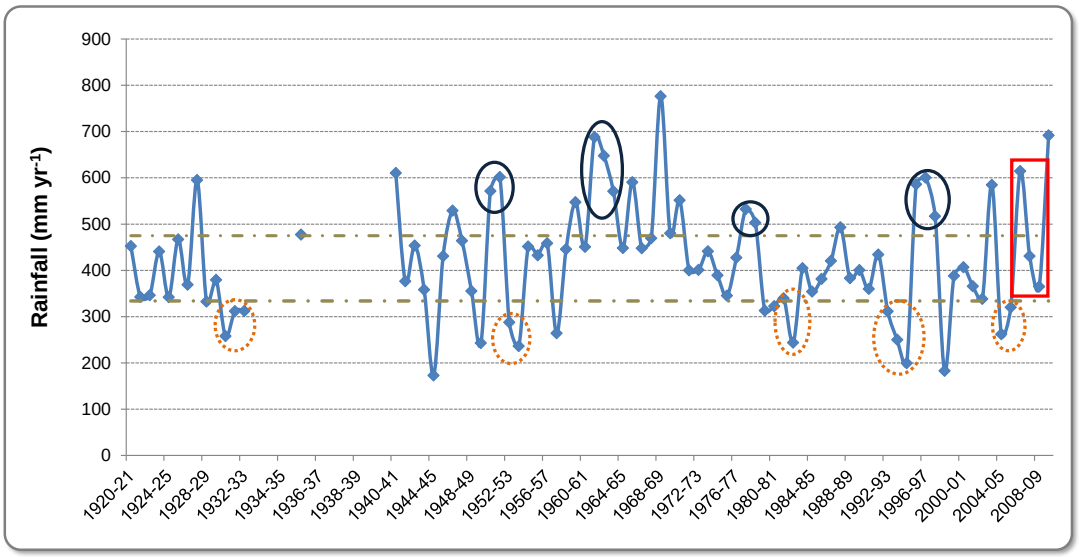

Fig. 6.34. Total rainfall amounts recorded in the 4121 Ciudad Real weather station, located 25 km southwest from Las Tablas de Daimiel National Park, for the series of hydrological years between 1920-21 and 2008-09. Horizontal dashed lines represent the cut-off rainfall amounts for subdivision in wet (>475 mm), average and dry (<334 mm) hydrological years based on the quartile distribution of total rainfall amounts in the series. Dark solid and orange dashed circles represent 2 and 3-year wet and dry cycles, respectively; the red rectangle indicates the period monitored in this thesis.

For simulation purposes of a drying management scenario, 2-year decreasing trends have been chosen as basic weather data for synthetic series construction: 1952/53-1953/54, 1981/82-1983/84 and 1992/93-1993/94 (only the first two years of the 3-year dry cycle). This decision has been based on their higher abundance, time scale suitability for management planning, and worst case scenario conditions representation. The daily synthetic series has been built taken the mean values of meteorological variables of all the first and second hydrological years, respectively. Estimation of missing data required for the SWAP model for ET_p calculation has been carried out as described in section 5.7.

6.7.5.2. Simulations

In recent years the SWAP model has been successfully employed to evaluate management options with respect to field scale water (including groundwater level simulations) and solute movement (van Dam et al., 2008; Dawson, 2006; Martínez et al., 2008; Jhorar, 2002; Kelleners et al., 1999; Bonfante et al., 2010, 2011; Cirkel et al., 2010; Droogers et al., 2008; Sarwar et al., 2000; Singh et al., 2010; van Schaik et al., 2010). Therefore, this tool can be used for simulating different hydrological management scenarios in degraded wetlands such as TDNP.

Once models were calibrated-validated, typical SFT profiles VI and VII were chosen for drainage scenario simulations (Fig. 6.31). The first one corresponds to the main flooding area were undisturbed charophytes accumulate. Reed seed-rhizome banks in these soils induce macrophyte overgrowth and invasion when the system starts to dry out (Álvarez-Cobelas et al., 2001; Álvarez-Cobelas and Cirujano, 2007; Cirujano et al., 2010). Soil profile VII is the representative of peat dominated areas which are susceptible of burning during drainage episodes (Moreno et al., 2010).

Before simulations could be performed, the functional relationship between bottom flux and groundwater level had to be set as bottom boundary condition for each soil profile (see section 5.6.4). Optimizations carried out with the FitGwl application yielded excellent results with values of the *F* goodness of fit statistic (NMSE) close to 0 (Fig. 6.35).

On the other hand, critical soil water contents for reed growth dynamics and peat combustion risk were calculated on the basis of undisturbed charophytes and peat hydraulic characteristics (see section 5.6.4). Soil water contents at field capacity have been taken from water retention curves at pF 2 (Fig. 6.29) and gravimetric soil moistures have been transformed to volumetric water contents multiplying by the corresponding bulk density (Table 6.5). The resulting values are presented in Table

6.11. It is remarkable that critical soil water contents regarding peat combustion almost coincide with those determined as the range of critical water contents for peat to become water repellent (0.09-0.22 cm^3 cm^{-3}, Fig. 6.11).

Table 6.11. Estimated critical soil water contents for reed growth dynamics and peat combustion risk in Las Tablas de Daimiel National Park (TDNP) undisturbed charophytes and peat soil functional types.

		Critical water content (cm^3 cm^{-3})	
		Undisturbed charophytes	Peat
Reed growth	Optimal	0.51	0.30
	Normal	0.36	0.21
	Deficient	0.30	0.17
	Mortality threshold	0.13	0.08
Peat combustion	Combustible		0.225
	Ignition probability = 0.5		0.108

With the estimated empirical coefficients *a* and *b* from the exponential relation between bottom flux and groundwater level and the synthetic weather data series for a two-hydrological years dry cycle (see section 6.7), simulations of soil water content in time were performed. Different approaches were tested for each soil profile to take into account different management scenarios as well as model performance regarding different parameter configurations. These included all combinations of ET_p calculation methods (Penman-Monteith or ET_{ref}), vegetation type, use of crop (soil) factor K_c (K_{soil}) or crop height, and development or not of macropores in peat soils. When ET_{ref} is chosen only K_c or K_{soil} can be used for soil water flow modeling as ET_p equals ET_{ref} by the corresponding factor (Eq. 25). Table 6.12 shows the literature based estimation of K_c, K_{soil} and plant height values as a function of development stage which in SWAP is considered to range between 0 and 2. Nevertheless, values for K_c represent average non-stressed growth conditions in sub-humid climates (FAO, 2006).

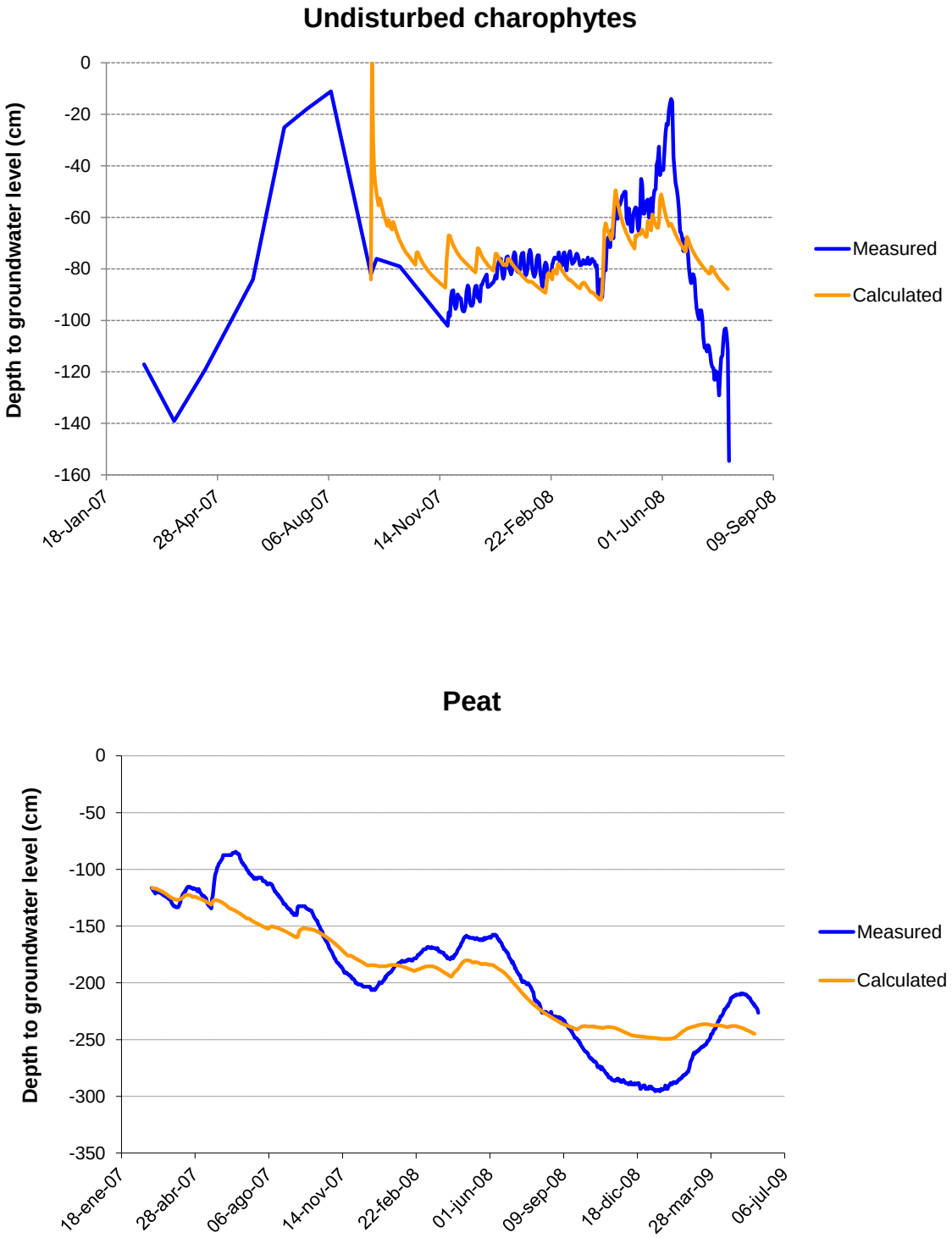

Fig. 6.35. Measured and optimized groundwater levels through the FitGwl application run with undisturbed charophytes and peat SWAP models for optimization of the functional relantionship between bottom flux and groundwater level defined in Eq. (16) to be set as bottom boundary conditions in simulations. Optimized values of *a*, *b* parameters as well as the *F* goodness of fit statistic (Eqs. 17 and 18) are shown.

Table 6.12. Estimated values of crop (K_c) and soil (K_{soil}) factors and plant height, as a function of plant development stage, for ET_P calculation in SWAP simulations (FAO, 2006). Parameters are described in section 5.7.

Vegetation	Development stage (0-2)	K_c	Height (cm)	K_{soil}
Bare soil	0-2			1.15
Reed (*Phragmites asutralis*)	0-1.3	0.90	100	
	1.3-1.8	1.20	150	
	1.8-2	0.70	200	
Annual nitrophilous (*Conya Canadensis, Cochlearia glastifolia*)	0-0.6	1.05	30	
	0.6-1.7	1.10	130	
	1.7-2	1.10	150	

Simulation plots depicted in Figures 6.36 and 6.37 show the soil water content evolution at different depths in the soil profiles together with the lines representing critical soil water contents for reed growth dynamics and peat combustion risk. Accuracy in ET_p estimations can be inferred from the similarity between Penman-Monteith and ET_{ref} plots. The only significant differences are found at higher depths, where faster decreases in soil water contents in Penman-Monteith simulations compared to ET_{ref} ones are observed. Therefore, although in the case data on relative air humidity, wind speed and solar radiation were not available, simulation results would still be consistent, especially for the topsoil.

The activation of the macropore flow module in peat simulations has a significant effect in deeper layers of the soil profile (i.e. below 50 cm), particularly under bare soil conditions, where a faster decrease in soil water content is observed (Figs. 6.37b,d). The sharpest soil water content decreases are found in simulations with vegetation cover (Figs. 6.37e-j). The worst desiccation scenario appears when plant height instead of crop factor is considered (Figs. 6.37g,h,j).

Regarding reed growth in flooding areas dominated by charophyte sedimentation, all simulations show that optimal topsoil water content for reed growth is reached around the first summer (Fig. 6.36). This means that reed overgrowth and invasion under dry conditions would peak 9-10 months after flooding ceased. Under bare soil conditions, soil water content along the rooting depth of the profile (estimated around 50 cm) remains above the normal growth critical value during the whole simulated period (Figs. 6.36a,b), indicating that reed overgrowth is prone to occur at anytime during the drying out. Therefore, simulations considering a reed cover seem to be more realistic.

Reed growth is limited under permanent ponding layer over 4 cm deep (Fernández González et al., 2004). As simulations start when flooding has just disappeared and sprouts from rhizomes develop around April (Fernández González et al., 2004), vegetation emergence has been set to the 1st of April of the first hydrological year. In all reed simulations excluding the one considering plant height, soil water contents along the rooting depth remain between optimal and normal critical values until the second summer when topsoil moisture status falls to deficient growth levels (Figs. 6.36c,d). However when reed height as function of development stage is taken into account, the shape of the moisture curves changes drastically. A fast sharp soil water content drawdown at all rooting depths takes place during the first summer reaching the deficient growth critical value by the beginning of autumn (Fig. 6.36e). From then, soil water contents progressively decrease until the mortality threshold critical value in the topsoil is reached by the beginning of the second summer and reed dieback would start.

Large heights and, thus, plant cover, reached by reed beds cause a significant increase in the ET_p term during dry periods, as reported by Sánchez-Carrillo et al. (2004), conditioning a faster soil drying out. Since plant height is a measurable parameter corroborated with in situ observations it might be even more reliable than the averaged tabulated crop factor values, which, as stated above, represent optimal growing conditions in sub-humid climates (FAO, 2006).

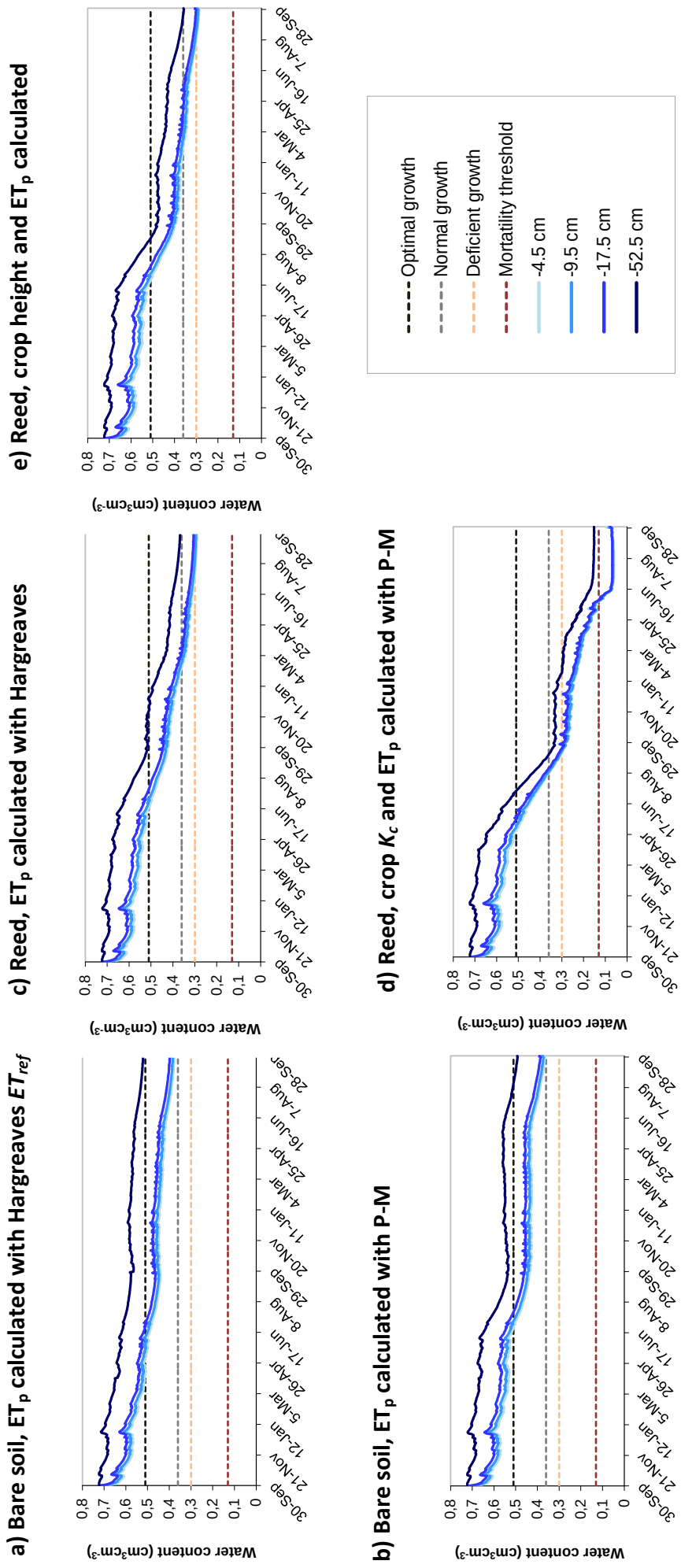

Fig. 6.36. SWAP simulations of soil water content at different depths in undisturbed charophytes dominated areas (typical soil profile VI in Fig. 6.31) in Las Tablas de Daimiel National Park under a 2-hydrological year drainage scenario. Horizontal dotted lines reflect critical soil water contents for reed growth dynamics (Table 6.11). Each plot a-e) represents a different combination of vegetation type and development (Table 6.12) as well as potential evapotranspiration (ET_p) calculation method. ET_{ref}: reference evapotranspiration; P-M: Penman-Monteith.

On the other hand, peat simulations under bare soil conditions show that soil water content in the profile would remain above critical levels during the entire period (Figs. 6.37a-d). This means, again, that reed overgrowth is ensured at some point during the drying out. A gradual soil water content decrease showing an asymptotic behaviour around the critical optimal reed growth value is observed at all depths. As mentioned above, the activation of macropore flow has a significant effect in deeper layers of the soil profile where soil moisture loss is accelerated.

In peat simulations with vegetation soil water content decreases are sharper, particularly when plant height is considered (Figs. 6.37e-j). In these models the final asymptotic trend is towards the critical soil water content for peat combustibility. However, soil water content decrease in peat is limited to the residual moisture content parameter (ϑ_r) which equals 0.192 (Table 6.8). This is a physical parameter which only considers drying by suction pressure, but not by extreme heat such as temperatures reached in dry topsoil TDNP peats in summer (over 80°C as measured with a thermographic camera). Under these extreme circumstances, it is highly likely that peat shrinking and cracking can induce material desiccation below this residual value. Therefore, on simulations where soil moisture reaches the ϑ_r value and remains constant a further drawdown could be expected and critical soil water contents of 0.5 ignition probability and/or deficient reed growth attained. This would be the case of the topsoil by the second summer in all plant models. The worst scenario, represented by simulations of peat soil covered by reed beds, plant height used, with and without macropore flow, shows that extreme drying in the first 20 cm of the soil profile is already reached during the first summer (Figs. 6.37g,h). Then it recovers a little bit during autumn and winter, but falls again to the ϑ_r value in early spring and remains almost constant until the end of simulation, when the soil water content at 52.5 cm deep also drops near this value.

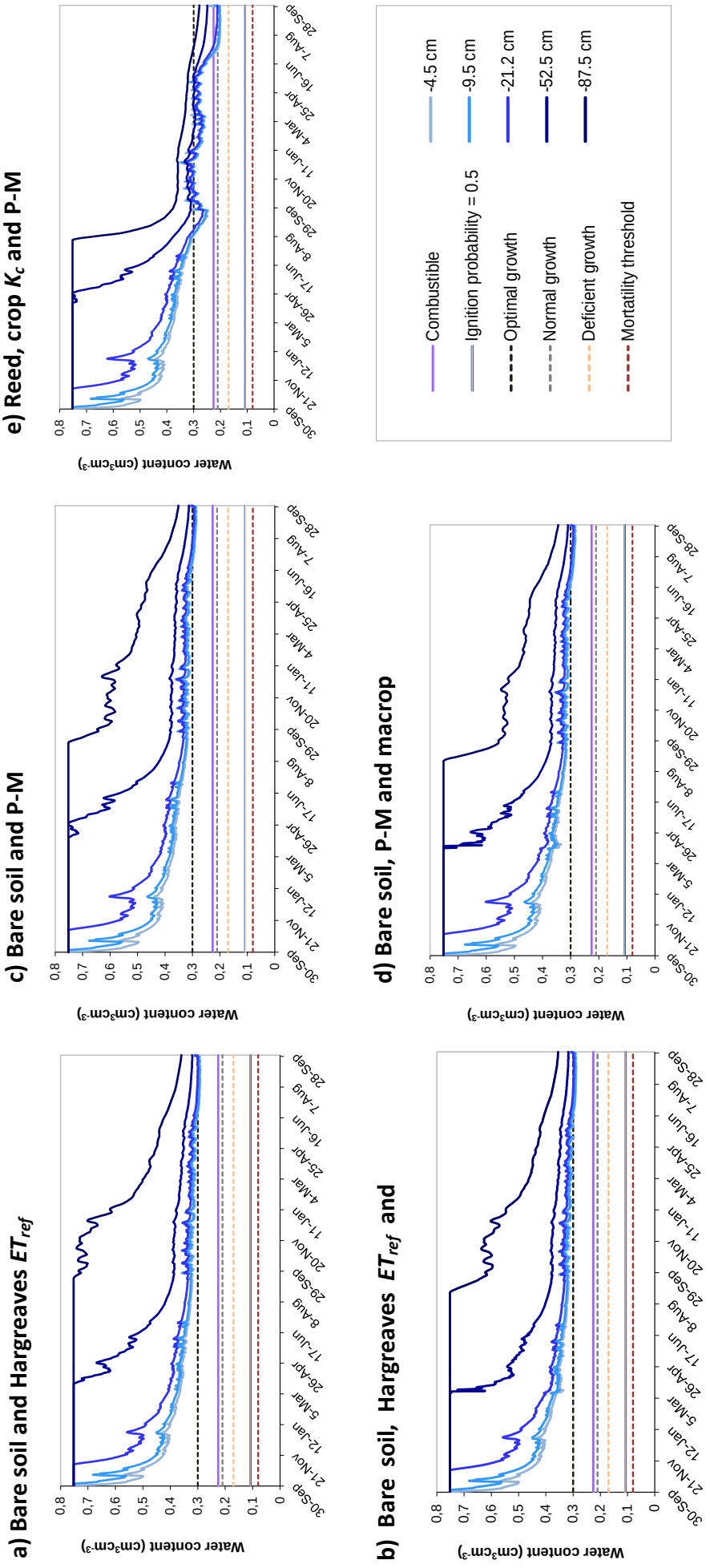

Fig. 6.37. SWAP simulations of soil water content at different depths in peat dominated areas (typical soil profile VII in Fig. 6.31) in Las Tablas de Daimiel National Park under a 2-hydrological year drainage scenario. Horizontal solid and dotted lines reflect critical soil water contents for peat combustion risk and reed growth dynamics, respectively (Table 6.11). Each plot a-j) represents a different combination of vegetation type and development (Table 6.12), potential evapotranspiration (ET_p) calculation method and activation or not of macropore flow module. ET_{ref}: reference evapotranspiration; P-M: Penman-Monteith; K_c: crop factor; macrop: macropores.

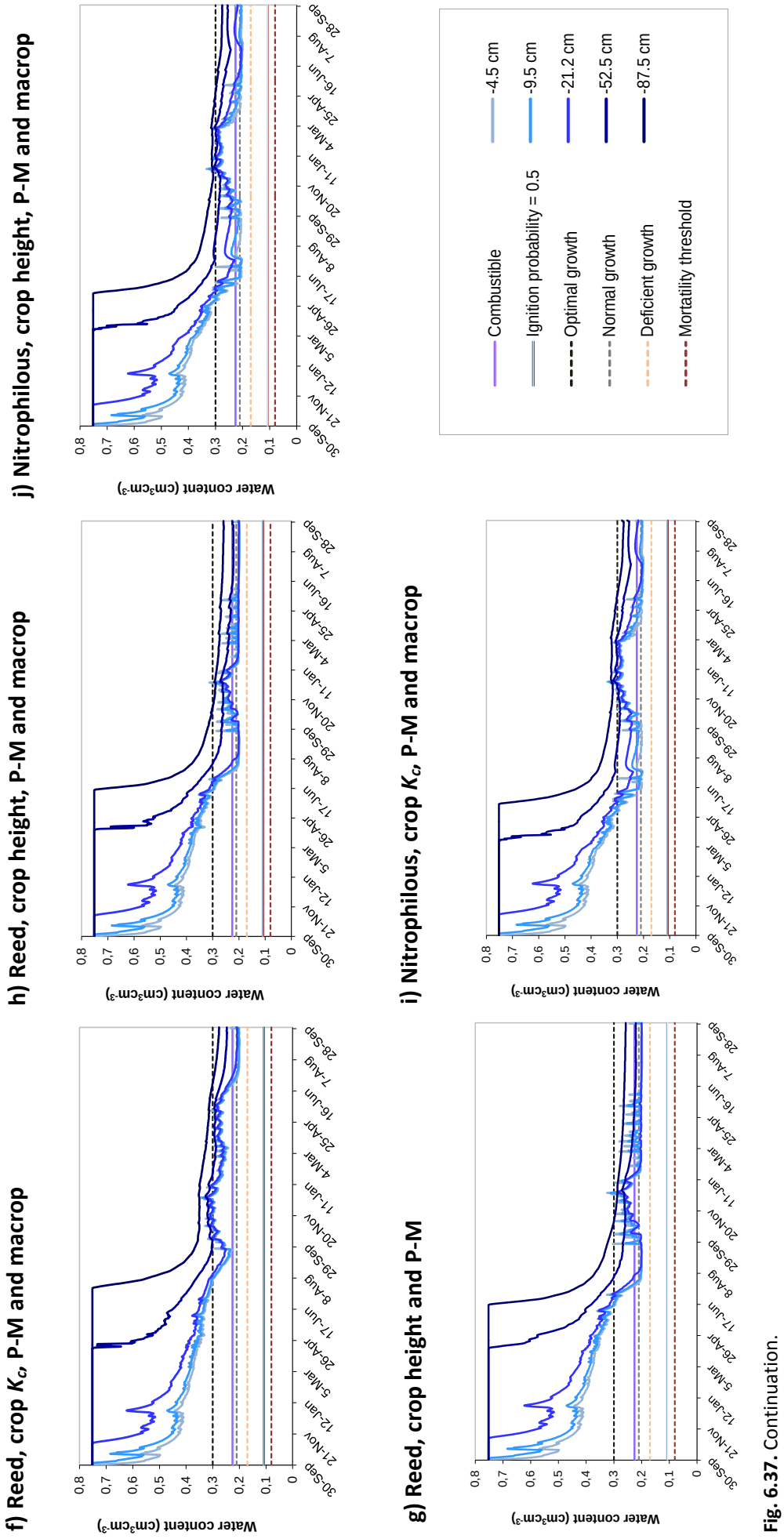

Fig. 6.37. Continuation.

6.7.6. Summary and conclusions on TDNP VZ water flow model

Water retention parameters (θ_s, θ_r, n, α and h_e) of TDNP soils have been successfully estimated with high goodness of fit (R^2>0.88). The shape of water retention curves is in accordance with the textural classification or organic nature of SFT. A clear distinction can be observed between charophyte-rich soils, which have a bigger sand fraction and show higher water content variations in the 1-4.2 pF range, and other organic or finer textured soils where water is strongly held. This implies a more homogenous pore size distribution of charophyte-rich soils against other finer textured and organic-rich SFT in TDNP.

On the other hand, higher uncertainity is involved in hydraulic conductivity parameters (K_s and L) estimations. Method sensitivity and sample heterogeneity (i.e. secondary porosity) condition large variability in the measurements and, thus, in the estimates. Nevertheless, resulting L values are in the expected order of magnitude for fine textured soils reported by Schaap and Leij (2000).

Peat shrinking upon drying causes cracking and subsidence. The parameters describing the shrinking characteristics of TDNP peats have been derived from those measured on other similar peat materials. The resulting shrinking curve shows a narrow near-normal shrinkage stage, followed by a typical subnormal stage and a wide supernormal shrinking stage. This last fact is in agreement with field observations of big cracks and hollows that can only develop when volume reduction exceeds by far moisture loss and the skeleton collapses.

Ten typical soil profiles representing the arrangement in depth of SFT in different TDNP areas have been defined for VZ water flow modelling with SWAP. These profiles extend through the whole thickness of the Quaternary VZ and, thus, some assumptions based on random observations and reviewed literature had to be made for their description below the maximum drilling depth of sampled soil columns (120 cm).

Assumptions made for the description in depth of characteristic soil profiles seem relatively accurate given the outcome of the calibration processes. Except for the undisturbed charophytes model, RMSE of calculated water contents versus sensor records at different depths are under 0.05 cm^3 cm^{-3}, far below the considered upper bound of 0.1 cm^3 cm^{-3}. In the case of undisturbed charophytes, one of the most homogeneous and well-known soil materials, the discrepancies between measured and calculated water contents seem to mainly arise from the different average groundwater level in the area of sensor location and in the area represented by the model, and to a lesser extent by occasional external influences from pumps in the emergency wells area, freshets and water transfers throughout the monitored period.

The VZ water flow model has been presented as management tool capable of simulating the development of critical soil water contents for reed growth dynamics and peat combustion risk on a typical 2-year drainage scenario. Simulations were carried out on the typical soil profiles of the two most relevant and widespread SFT in TDNP: undisturbed charophytes and peat. The functional relationship between bottom flux and groundwater level to be used as the bottom boundary condition in simulations was successfully fitted through the FitGwl application (Wesseling, 2013). Critical soil water contents were calculated on the basis of undisturbed charophytes and peat hydraulic properties. A noteworthy observation is that critical soil water contents regarding peat combustion (0.11-0.23 cm^3 cm^{-3}) are very similar to those determined as the range of critical water contents for peat to become water repellent (0.09-0.22 cm^3 cm^{-3}). This observation strengthens the reliability of the results presented in this thesis.

Different approaches were tested for each soil profile to take into account different management scenarios as well as model performance regarding different parameter configurations. These included all combinations of ET_p calculation methods (Penman-Monteith or ET_{ref}), vegetation type, use of crop (soil) factor K_c (K_{soil}) or crop height, and development or not of macropores in peat soils. Accuracy in ET_p estimations can be inferred from the similarity between Penman-Monteith and ET_{ref} plots. The activation

of the macropore flow module in peat simulations had a significant effect in deeper layers of the soil profile (i.e. below 50 cm), particularly under bare soil conditions, where a faster decrease in soil water content has been observed. The sharpest soil water content decreases have been found in simulations with vegetation cover. The worst desiccation scenario appears when plant height instead of crop factor is considered.

All simulations on undisturbed charophytes indicate suitable soil water conditions for reed overgrowth. The optimal topsoil water content for reed growth would be reached by the first summer, this is, 9-10 months after flooding ceased. In all reed simulations excluding the one considering plant height, soil water contents along the rooting depth remained between optimal and normal critical values until the second summer when topsoil moisture status fell to deficient growth levels. However, when reed height as function of development stage was considered in the model, steeper soil water content decreases were observed at all depths, deficient growth being attained in the first summer and mortality threshold in the second. Large heights reached by reed beds during its annual cycle cause a significant increase in model ET_p calculations, conditioning a faster soil drying out.

On the other hand, peat simulations also showed the development of suitable conditions for reed overgrowth. Sharper soil water content decreases have been observed in simulations with vegetation, particularly when plant height was considered, and a final asymptotic trend towards the critical soil water content for peat combustibility reached. However, as peat drying out is limited to the physical, suction pressure-based, residual moisture content parameter, actual desiccation caused by extreme heat during the summer season coupled to peat shrinking and cracking might not be accounted for in the model. Therefore, on simulations where soil moisture reached the ϑ_r value and remained constant a further soil water content decrease could be actually occurring and critical soil water contents of 0.5 ignition probability and/or deficient reed growth attained.

CHAPTER 7

Synthesis. Environmental and management implications

At present TDNP has remained completely flooded for almost four years, since the beginning of 2010. Flooded conditions have been sustained by continuous inflowing water through ditched riverbeds allowed by water released from upstream reservoirs. This prolonged situation has recently led to the resurrection of some of the so-called "Ojillos" springs along the Guadiana River, which had been dried since the mid 1980s, causing, for the first time in almost 30 years, groundwater discharge inflow through the Molemocho mill. As hold by the conceptual model of SW-GW interactions presented in section 6.5.6.2, this means that partial re-saturation of the different levels of the multi-layer aquifer system has been attained. Surely, this is a proof of the dynamism of the TDNP hydrological system and its capability for natural recovery. Indeed this means good news for the wetland ecosystem and Park managers, but even though one battle has been won, the war is not over yet.

The extraordinary situation has to confront the anthropized reality. The wet climatic cycle will not last forever and farmers are already starting to claim an increase in pumping rights thinking that the Mancha Occidental aquifer system is now "recovered". However, as pointed out by the results presented in this thesis, TDNP hydrological equilibrium is very sensitive and complex, and it is highly conditioned by hydrodynamic disturbances. In fact, recent measurements indicate that TDNP is still a recharge area in spite of the increase of groundwater levels and the appearance of groundwater discharge areas in the Guadiana riverbed (Castaño et al., 2013). The changeable and contradictory socio-political environment is at the same time the giver and taker, the protector and destroyer of the TDNP's identity. Although nature's auto-regulation and buffering capacities could provide restoration in spite of semiarid conditions, past 50-year history shows that human actions and impacts would keep that from happening. Unless, of course, a deep change in the "social mind" and the local, regional and even global human role in the planet takes place.

While this philosophical reflection awaits for the evolution of contemporaneous history to be further revealed, the presented PhD dissertation is a contribution for the understanding of the current behaviour of the anthropized TDNP system. The study

has focused on a drying period and the findings aim to support Park management under adverse circumstances. In this section, environmental and management implications derived from physical-chemical environment characterization are discussed. Furthermore, the validity of some of the methods and results as management tools is also argued.

7.1. Qualitative implications

The chemical studies performed (surface water, vadose zone and groundwater) show, particularly through the organic carbon contents, that, during drainage conditions, there is an active downward nutrient transport from inflowing surface water to the groundwater through the vadose zone.

During drying periods, evaporation, salt dissolution from saline soils, low quality inflows (i.e. wastewater, pumped groundwater) and internal organic matter loading condition high salinity and solute content in scarce occasional ponding water. Extremely high infiltration rates and saturated hydraulic conductivities in dry SFT (see section 6.3.2) bring about a strong downward gradient transporting water and solutes through the VZ towards groundwater. Results on VZ chemistry reveal some issues concerning the interaction of infiltrating water with the soil matrix. A strong nutrient accumulation (absorption) in the topsoil (0-20 cm) has been observed. Approximate median electrical conductivity, organic carbon, total nitrogen, available phosphorus and leachable nitrate contents in this layer are 4,000 $\mu S\ cm^{-1}$, 6%, 0.5%, 20 mg kg^{-1} and 50 mg l^{-1}, respectively. Furthermore, salinity, soil organic carbon and total nitrogen remain quite high in depth. Nutrients have both external (phosphorus, organic carbon) as well as internal (nitrate, organic carbon) origins. External inputs take place through inflowing surface waters whereas internal ones mainly come from plant organic matter accumulation and mineralization. The hydrochemical interaction between surface water and shallow groundwater through the soil matrix has been evidenced by TOC

distributions in the Puente Navarro dam outlet area and infiltration from the Guadiana ditch (see section 6.5) as well as in the Cigüela ditch inlet area (Moreno et al., 2013). Organic matter oxidation by microbial activity leading to increased acidity through decarbonation-carbonation reactions is evidenced in the whole surface water-VZ-groundwater system during system dry outs. As for other nutrients, such as nitrate and phosphorus, results point out to a well-developed buffering absorption capacity of TDNP soils and ecosystem recycling (plants, microorganisms) during drying conditions. On contrary, generalized salinity in all studied environments (surface water, VZ and groundwater) appears to be controlled by lithological and evaporative processes.

The analysis of the data presented in section 6.2 regarding nutrient content of TDNP soils proves a clear spatial association between soil organic matter and nutrient content in depth, particularly phosphorus, with the surface water drainage network (fluvial silts in riverbeds and ditches). This indicates that occasional flooding through freshets or transfers has side-effects, representing a primary source of nutrients to TDNP soils. This has been confirmed by the hydrochemical analyses of the effluent of the Villarrubia de los Ojos wastewater treatment along the Cigüela ditch (Moreno et al., 2013; Fig. 2.2). Moreover, the fact that the Park is located at the downstream edge of the Upper Guadiana basin, where agricultural practices are quite intense, has to be taken into account. Even though the hydrologic network remains inactive for long periods, occasional water inflows carrying considerable loads of particles from lithological weathering as well as wastewater, agricultural and even industrial spills occur (Moreno et al., 2013). The accumulation of phosphorus coming from nonpoint source pollution in ditches and lower areas is indeed a generalized process in basins (Reddy and DeLaune, 2008). The implications of these phenomena are enhanced as the silty nutrient-rich material filling up the ditches gives rise to perched water tables underneath TDNP as “bank storage” processes (Silvino Castaño, IGME, personal communication, 2012). This perched levels store shallow polluted groundwater which percolates to deeper aquifer layers (see sections 6.5 and 6.7).

As reported by Reddy and DeLaune (2008) drainage conditions are reflected by the predominance of oxidized forms of nitrogen and sulphur (nitrate, sulphate), which is the case of TDNP soils during drying periods. In general, the major fraction of soil organic matter is very insoluble and, therefore, only a very little amount is leached towards the groundwater (Bohn et al., 2001). The main mechanism for soil organic matter removal is oxidation through microbial degradation. When moderate nitrate loadings enter the system, they can be managed by plants and microorganisms or retained by the soil matrix, reducing the dissolved fraction that percolates towards the groundwater (Bohn et al., 2001). Dry TDNP peats, for example, show high cation exchange capacity over 30 cmol+ kg^{-1} (Jiménez-Pinilla, 2011). This would mean that peat is an efficient natural buffer, but the exchange complex is controlled by Ca^{2+} and soluble nitrate concentrations up to 440 mg l^{-1} have been measured (Jiménez-Pinilla, 2011). Therefore, large nitrate concentrations and infiltration rates observed in TDNP soils clearly pose a risk of groundwater pollution.

Soil and water nutrient overabundance allows classifying TDNP as an eutrophic system. In the case of the phosphorus stored in organic soils, it is during the initial phases of the rewetting process when conditions are most favourable for its release as the system shifts to reducing conditions (Koerselman et al., 1993; Olila et al., 1997; Olde et al., 2002; Aldous et al., 2005; Reddy and DeLaune, 2008; Niedermeier and Robinson, 2009). These conditions are also suitable for organic carbon and ammonia mobilization and subsequent risk of leaching towards the groundwater level (Zak and Gelbrecht, 2007). According to Koerselman et al. (1993), the release and mobilization of peat sorbed nutrients (N and P), especially P, are enhanced if the quality of flooding water is poor. In this sense, incoming waters through the Cigüela River or those usually pumped from the aquifer often have very low qualities when they reach TDNP. This issue is particularly relevant as the largest amounts of phosphorus in the Park accumulate in the fluvial silts of the ditch network which are connected to deeper aquifer layers.

Aldous et al. (2005) suggest keeping soil saturated conditions to minimize the amount of phosphorus released from recently rewetted wetland soils, whereas Olila et al. (1997) propose the addition of chemical amendments to counteract the initial release effect. Zak and Gelbrecht (2007) recommend the removal of the most decomposed peat layer to limit nutrient mobilization. However, topsoil removal does not seem advisable in TDNP, unless flooding is undertaken immediately and permanently, because the high organic matter contents observed in depth will lead to a new oxidation and nutrient release process as they turn into the new aeration zone. Furthermore, higher organic matter oxidation rates brought about by drainage conditions not only support the release of soil nutrients but also of CO_2, thus contributing to the reversal of system's function as a carbon sink (Rodríguez-Murillo et al., 2011; Sánchez-Andrés et al., 2010b).

In a spatial context, the VZ chemical multivariate analysis identified three major soil environments in TDNP: saline, organic (nutrients) and carbonated. A large percentage of the chemical variability is associated with four environmental factors (soil type, depth, microtopography and position regarding the central dam). These factors are susceptible of being altered by certain activities performed within the anthropic management of the wetland during drying periods such as use of heavy farm machinery for reed reaping, cut-sedge sowing, construction of fire breaks, works for peat fires extinction, or artificial flooding with either groundwater or treated wastewater (Fig. 2.2). The multivariate model associates saline soils (i.e. saline charophyte layers and clay) with higher topographical areas and the organic ones (i.e. fluvial silt and charophytes-peat alternations) with lower zones. Salinity and nutrients are more likely to accumulate upstream from the dam, whereas downstream the environment is dominated by carbonates (Aguilera et al., 2011). Edaphized charophytes accumulate higher amounts of soluble nutrients in the topsoil than fluvial silts.

The map of soil functional types (Fig. 6.1) shows that the major organic and nutrient accumulator types lie on the left TDNP margin, where the highest degree of SW-GW

has been observed (Aguilera et al., 2013). This implies a higher risk of solute mobilization and transport according to the processes described above. Therefore, entrance of heavy machinery inside TDNP should be restricted and their tracks controlled, as they mainly operate in these left margin areas. Tractors modify soil physical (i.e. structure, compaction, see Fig. 6.28) and geomorphological properties (i.e. microtopography) as well as the nutrient balance. Although soil compacting may reduce infiltration rates, their random activity and soil's structure disruption develop new preferential flowpaths for water and solutes. Furthermore, reed cover remove could accelerate soil physical degradation due to increased soil exposure and decreased root system bonding effect. Hence, properties of soils as water and solute transmitters are altered, conditioning surface water-groundwater interactions and the risk of pollution spread.

On the other hand, flooding with high salinity groundwater from emergency wells has been a usual practice during water shortage periods. The possibility of flooding a bigger area with treated wastewaters during extremely drying periods has also been considered through the REGATA plan (Sánchez-Carrillo et al., 2010). Both measures enhance the process of soil salinization and the above mentioned risk of nutrient mobilization through the VZ. Furthermore, flooding with pumped groundwater is an expensive measure which also induces local depletion of groundwater levels, thus, increasing the downward vertical hydraulic gradient. This fact enhances infiltration and recirculation of the poured water. At the same time, the chemical quality of soil and water is deteriorated through this process of recirculation as saline groundwater is used. Nevertheless, this process will change from now on as the new emergency well area is located further away from TDNP limits (Fig. 2.2) and less saline groundwater will be used. This will modify water quality in flooded areas as well as in the aquifer inducing changes in chemical and, perhaps, ecological equilibriums.

7.2. Quantitative implications

The most relevant physical properties of dry TDNP soils indicate extremely high water transmissivities as shown by infiltration tests and saturated hydraulic conductivity determinations, particularly in organic SFT, in which lower bulk densities and higher organic matter contents determine a less compact structure. Average infiltration rates on dry peat, peaty silts and edaphized charophytes exceed 1,000 cm d^{-1} whereas average laboratory saturated hydraulic conductivities exceed 500 cm d^{-1} in all organic SFT, reaching up to over 4,000 cm d^{-1} and 22,000 cm d^{-1} in peaty silt and peat, respectively (Table 6.5). This is due to their highly developed secondary porosity upon shrinking and cracking caused by desiccation. In the case of peat, strong soil water repellency and limited wetting capacity worsens the negative hydraulic effect caused by drainage (i.e. soil physical degradation). Threshold values of 45% organic matter content and 9-22 vol% critical soil water content range have been determined for soil water repellency development in TDNP peats. This means that peats with higher organic matter contents and/or with water contents below or within this range become water repellent. These facts condition that peat, in spite of showing the highest water retention properties (Fig. 6.29), show lower water contents than charophytes during a system dry out, as observed in soil moisture sensors records (see section 6.4).

Although a first aproximation has been made to characterize the physical properites of TDNP peats, further research is still needed to accurately measure specific shrinking and hydraulic characteristics based on organic matter origin and composition as well as degree of decomposition. Nevertheless, there is a generalized lack of knowledge of Mediterranean semiarid peatlands as inferred from the reviewed literature.

Implications of SFT physical characterization and spatial distribution during a drying period are not quite encouraging. As stated above, average infiltration rates in left margin areas and downstream from the central dam increase several orders of

magnitude in respect to the values reported for flooded conditions (Castaño, 2004; Castaño et al., 2008; Navarro et al., 2011, 2012). High infiltration rates appear as the main cause for the sharp fluctuations observed in both flooding area and groundwater levels, particularly in E-SE TDNP areas (García Rodríguez, 1996; Castaño, 2004; Aguilera et al., 2013; Castaño et al., 2012a,b). In situ field evidence of fast surface water loss was observed in 2008. Pumped groundwater poured over the peaty silts in the Guadiana ditch around the Molemocho dam mill infiltrated straight away and a sink-effect was observed in areas of preferential flow. Surface water-groundwater connection in the Guadiana ditch area has been corroborated by hydrochemic and isotopic analyses in surface water and a groundwater monitoring point (see section 6.5).

On the other hand, flooding area is not the only relevant feature regarding the quantitative state of TDNP, which is the major concern for Park managers. During drying periods, soil water content arises as the controlling factor for reed overgrowth and expansion, and for peat combustibility. The VZ water flow model presented in section 6.7 has proved to be a valuable management tool for hydrological planning in drainage scenarios. For example, TDNP managers could easily predict when critical soil water contents for reed overgrowth or peat combustion risk would be reached under different climatic hypotheses once flooded area has disappeared during a system dry out. As models for the different SFT have already been calibrated and their parameters set, all that is needed to carry out a simulation in charophytes or peat dominated environments is a series of daily basic meteorological data (being rainfall amount and minimum, mean and maximum temperatures the minimum required).

According to the simulation examples presented in this thesis representing a typical two-hydrological year dry climatic cycle in the semiarid region, invasion of reed sprouts from the seed-rhizome bank stored in TDNP soils is inevitable (section 6.7.5). Starting from saturated conditions, a soil moisture status between optimal and normal growth critical soil water contents would develop between the first and the second summer in both charophytes dominated floodable areas as well as peat areas. For both SFT, the

sharpest soil water content decreases have been found in simulations with vegetation cover. The worst desiccation scenario appears when plant height as function of development stage is considered, due to its strong influence on evapotranspiration processes during drying periods (Sánchez-Carrillo et al., 2004).

Regarding peat combustibility, the macropore flow has a significant effect in deeper layers of the soil profile where soil moisture loss is accelerated. In models with vegetation cover, critical soil water contents for combustibility are already attained by the first summer, and critical values of 0.5 ignition probability could be expected in the topsoil and even up to 50 cm deep by the second summer.

A sensor network for soil moisture and temperature monitoring has proved to be useful in determining the influence of environmental and anthropic factors in the VZ during dry periods. For example, underground cracks and hollows development, rise of groundwater levels and surface water inflows arrival and influence on the soil moisture status can be detected and monitored in real time. However, the discrete character of this tool limits its applicability: how many sensors and where should they be installed? Although the physical environment is well-known by Park managers and technical staff and the map of SFT (Fig. 6.1) contributes to delimit target areas, the extreme small-scale heterogeneity that arises during drying periods makes it difficult to rely on a few devices alone to represent ongoing processes that are prone to take place. Nevertheless, the complementary use of simulations and sensor network can be a powerful tool for management during system drying outs. Sensors can help to keep track of events and/or predictions related to simulations although this seems difficult due to system's dynamism.

7.3. Peat fires implications

The process of peat cracking, compacting and subsidence caused by desiccation and oxidation (Mesnage et al., 2002; Aldous et al., 2005; Zak and Gelbrecht, 2007) is the most striking representative of soil disturbance and degradation in TDNP. Fast development of huge cracks and hollows (diameter of tens of centimetres and average depths ranging between 2 and 3 m) was observed through the dry period 2006-2009, leading to spontaneous process of peat smouldering combustion which started in August 2009. Subsequent soil mechanical treatment for fire control using heavy machinery caused soil's structure disturbance: cracks and hollows were filled and materials were mixed and compacted (Moreno et al., 2010). Nevertheless, fire control works by means of soil mechanical digging up and compacting were effective and the effects measurable over long distances.

There are both chemical and physical implications of smouldering peat fires. Foreseeable consequences of peat combustion include an even higher risk of lixiviation of inorganic forms and electrical conductivity rise (Rein et al., 2008; Dikici and Yilmaz, 2006; Pic. 7.1). These facts could have influenced the sharp immediate electrical conductivity rise registered in groundwater monitoring point G-04 following reflooding in the beginning of 2010 (Castaño et al., 2012b). Although in this study groundwater remobilisation in both the saturated and unsaturated zones is pointed out as the main controlling factor for groundwater temperature and electrical conductivity rise, it is possible that post-fire effects mentioned above could have contributed to these observations through lateral subsurface water displacement from burned peat dominated areas. TDNP damming would support lateral water flow after reflooding (Castaño et al., 2012b).

Picture 7.1. Sulphur deposits following peat combustion in 2009 in the Guadiana River ditch next to the Molemocho dam inlet area to Las Tablas de Daimiel Nationla Park.

From a global perspective, although TDNP is an active carbon sink, smouldering fires destroy a long term, recalcitrant carbon store (Rein, 2010), and the final balance could well represent a carbon source, even in the middle-long term (Rodríguez-Murillo et al., 2011). From a physical point of view, fire causes soil's structure disturbance towards increased bulk density and decreased porosity and aggregate stability (Giovannini and Lucchesi, 1997), although the latter has been also found to increase following fire in a pine forest (Fox et al., 2007). Besides this, soil is expected to become more hydrophobic (DeBano, 2000b; Doerr et al., 2000; Fox et al., 2007) and reduce its water retention capacity up to 40% (Aguilera et al., 2011).

The irreversible fire-induced modification of soil's physical-chemical structure brings about the disappearance of the substrate that supports a large fraction of wetland's biodiversity. If the ecological, environmental and landscape functions of TDNP are to be maintained, the prevention of new fires is an essential issue. As pointed out in the previous sections, the TDNP area is also a source of groundwater pollution, this fact being aggravated by the fires. Managing an efficient prevention is very difficult given that it is impossible to keep the Park under constant natural flooding conditions. The following measures are proposed:

1. Guaranteeing minimum soil water content in the Park for preventing combustion processes. The only way to do so is keeping a minimum external water supply. A soil moisture and temperature monitoring network allows detecting when the introduction of water in the system becomes essential (i.e. development of critical soil water contents for peat combustibility).
2. Trying to avoid surface fires by any means as they can be transmitted to even relatively wet peats. For that it is necessary to control or even forbid the stubble burning within a protection perimeter around the Park.
3. Sealing any superficial hollow which might connect the pipes' network to the atmosphere. This way the circulation of air through the deep network will be prevented. This circulation supports peat desiccation, supplies oxygen to the system and allows for the release of the gases produced in the combustion process.
4. Increase knowledge of TDNP peats properties in order to build up a dynamic model of crack and pipe development.

Continuous soil moisture and temperature monitoring is recommended as indicator of potential combustion and auto-ignition fire risk but it is not useful as alert system for an already active fire. The fire control measures undertaken in 2009 before the complete flooding of the Park such as mechanical compacting were effective but only had a palliative character as only full flooding could stop smouldering combustion.

7.4. Hydrological implications

Along 2012 a new permanent dam has been built in the Cigüela ditch in the northern inlet area, and in 2013 a provisional artificial "recharge pond" has been created in the Guadiana riverbed. This means that now the whole TDNP is closed, as all inlet and outlet points are dammed. During extraordinary flooded conditions, the area becomes a system of connected reservoirs where hydrological conditions are artificially

regulated (Castaño et al., 2012b). Upon drainage, TDNP fully operates as an artificial recharge system with optimal performance in the left margin area as a consequence of higher permeability of underlying materials and increased hydraulic gradients supported by higher pumping rates. Dam-closing of the system avoiding surface water outflow conditions internal nutrient and organic matter accumulation (Sánchez-Carrillo and Álvarez-Cobelas, 2001; Sánchez-Carrillo et al., 2001). Considering that the system also receives wastewater inflows (Fig. 2.2), the functioning of TDNP can be compared to that of a constructed wetland for wastewater treatment.

Although in the very unlikely case that a "self-sustaining" hydrology (i.e. aquifer restoration, approximation of natural hydroperiod and flood frequency patterns through artificial water resource management) is re-established in TDNP, restoration to its "natural" conditions will still be impossible (Angeler et al., 2010) as it now constitutes as "disturbed natural system" (see section 2.3). Climate change will further increase the uncertainty regarding rehabilitation outcomes (Harris et al., 2006), particularly considering the increased aridity predicted for the Mediterranean region (Gao and Giorgi, 2008; Abouabdillah et al., 2010).

In general, hydrology is the key to wetland persistence and conservation (Richter et al., 1996; Rodríguez-Rodríguez, 2007; Rodríguez-Rodríguez et al., 2007; Shaffer et al., 1999; Somay and Filiz, 2003; Sánchez-Carrillo and Álvarez-Cobelas, 2010; Zedler, 2000). Furthermore, the effect of SW-GW interactions has been recently acknowledged as an essential issue to understand the hydrology of different wetland systems worldwide (Acreman and Miller, 2006; Carol et al., 2011; Harvey and McCormick, 2009; Jolly et al., 2008; Kaplan and Muñoz-Carpena, 2011; Kazezyilmaz-Alhan et al., 2007; McCarthy, 2006; Rodríguez-Rodríguez, 2007; Rudolph et al., 2005; Sikdar and Sahu, 2009; van der Kamp and Hayashi, 2009; Wolski and Savenije, 2006).

The hydrochemic, hydrodynamic and isotopic analyses leading to the conceptual model of SW-GW interactions presented in section 6.5 have shown the dynamic behaviour of the system following flooding. Fast infiltration of renewed ponding water

homogenizes the quality of surface water and groundwater in "interactive" left margin areas. The VZ constituted by SFT is saturated and at some point all aquifer layers might be as well re-saturated, conditioning groundwater mixing and, upon subsequent drying, the risk of water and solute transport towards pumping areas. As pointed out in section 7.1, there is a big chance of nutrient release from SFT following re-flooding. What happens then with all the nutrients stored in the VZ? Which amount can be released? How fast? Further analysis need to be performed to give a precise answer to this question.

As pointed out by the results presented in this study and argued by other authors, the lack of dynamic surface-subsurface interaction (Harvey et al., 2007; Sophocleous, 2002; Kazezyılmaz-Alhan et al., 2007; Jolly et al., 2008) and distributed spatial considerations (Carol et al., 2011; Krause and Bronstert, 2004), might pose a serious source of error and uncertainty to existing hydrological models of TDNP (EPTISA, 1986; García Rodríguez, 1996; Sánchez-Carrillo and Álvarez-Cobelas, 2010; Navarro et al., 2011). Furthermore, the spatial and temporal variability of the hydrological parameters is, in turn, the crucial information Park managers need (Hughes et al., 2010).

Current global demand for numerical quantitative hydrological and hydrogeological models of wetlands (Hattermann et al., 2008; Gusyev and Haitjema, 2011; Kazezyılmaz-Alhan et al., 2007; Bauer et al., 2006; Boswell and Olyphant, 2007; Wolski et al., 2006) is widely met by means of user-friendly and powerful computational tools (Trepel et al., 2000; Wang et al., 2010). Inverse methods for optimal parameter estimation make model convergence quite achievable with even small amounts of input data. However, uncertainty analysis of parameter estimations is quite difficult to assess when available information is scarce (Pappenberger and Beven, 2006; Hughes et al., 2010; Kazezyılmaz-Alhan et al., 2007; Staes et al., 2009; Bauer et al., 2006), and highly heterogeneous and irregular systems such as semiarid wetlands require detailed local spatial and temporal knowledge of the physical environment for successful estimations of involved processes (i.e. aquifer layering and interconnection,

infiltration, evapotranspiration). Moreover, there is a need for more dynamic and sophisticated models that account explicitly for the effect of surface water-groundwater interactions such as the WETSAND model (Kazezyılmaz-Alhan et al., 2007), where these interactions are combined with nutrient transport, or box-type models such as FEUWAnet (Dall'O' et al., 2001). Management models must also be flexible enough to cope with new environmental data as they emerge over time.

The output of the SWAP unsaturated flow model used in this study could be also coupled to nutrient transport models. However, in small scale areas, previous accurate knowledge of local geology becomes extremely relevant in determining both the hydrodynamic as well as the hydrochemical characteristics (Carol et al., 2011; Litaor et al., 2008; Hughes et al., 2010; Trepel et al., 2000; Sophocleous, 2002; Andersen, 2004; Sikdar and Sahu, 2009; Somay and Filiz, 2003; Devito et al., 1996; O'Drsicoll and Parizek, 2008; Rogers and Dreiss, 1995). The results of many hydrological studies that have given low attention to these features (Conan et al., 2003; Cooper et al., 1998; Drexler et al., 1999; Owen, 1995; Wang et al., 2010) might be questioned.

In TDNP it is crucial to develop a detailed 3D hydrogeological map, especially from the eastern side, to thoroughly assess the dynamics of the multi-layer aquifer under current anthropized conditions. The use of tracers and remote sensing to delimit hydrogeological compartments and connectivity is also advisable (Becker, 2006; Melendez-Pastor et al., 2010; Powell et al., 2008). In this sense, the research team constituted by Koch, Schmid and Gumuzzio has been quite prolific during the past decade in determining spatial patterns of TDNP characteristics linked to wetland degradation, mainly those related to soil surface and vegetation, through remote sensing (see references in Chapter 9).

When still some key features such as geology or hydrogeology remain partially unknown, development of simple conceptual models of hydrological behaviour such as the one proposed here, based on basic information (i.e. flooding area, groundwater levels and basic hydrochemical information), might be appropriate to determine

specific areas or variables which need to be accurately studied and monitored in order to develop a reliable quantitative management tool (Hughes et al., 2010; Larsen et al., 2007; Patten et al., 2008). Therefore, for any future hydrological modelling of TDNP intended to support management practices the outcome of the conceptual model presented in this study should be taken into account. The relative simplicity of the employed methodology allows for its application in other similar complex groundwater linked wetlands in semiarid areas where detailed knowledge of local geology is still absent, as long as sufficient basic data and monitoring are available.

7.5. Summary of environmental and management implications

During drying periods, the combination of large surface water and soil nutrient and organic matter contents with high water transmissivity capacities in the VZ of the left TDNP margin, conditions groundwater pollution, as inferred from hydrological and hydrochemical analyses. The anthropic management of TDNP (soil compacting by heavy machinery, recirculation of low quality groundwater, reed reaping, water transfers or smouldering fire extinction) increases the risk of releasing stored nutrients. As organic soils are widespread in the left TDNP margin area, it is likely that increased SW-GW interactions in this area are enhanced by soil physical degradation. Preferential flow paths through peat cracks and hollows in S and SE areas constitute freeways for water and solute transport (Moreno et al., 2010; Aguilera et al., 2013). Fluvial silts in ditches, which store large amounts of nutrients and organic matter, as well as low permeability Tertiary levels, hold perched poor-quality groundwater levels connected to deeper layers.

The closing effect of the dams and the functioning of the system as an artificial recharge pond causes that the overall effect of management measures during drying periods is solute accumulation in the VZ. Thus, the chemical quality of soil and water is deteriorated and system salinization and eutrophication is enhanced. Besides this, the

extent of SW-GW interactions condition a higher risk that groundwater pollution is spread through the groundwater flow that percolates from TDNP to deeper aquifer layers and meets the regional flow towards pumping irrigation areas. Further research on local geological characteristics (i.e. geophysical studies) and hydrological and hydrochemical dynamics in flooding periods is still required in order to build more accurate flux and transport hydrological models.

Increased understanding of the TDNP physical-chemical environment has allowed for the development of tools to support Park management during a system dry out. The classification and mapping of SFT involves in itself an enhancement of current knowledge of the physical environment and will contribute to management actions planning. It has allowed to delimit areas showing homogeneous behaviour and, thus, modelling time as well as monitoring systems expenses can be optimized.

Vadose zone water flow simulations under different management scenarios can, for example, help to foresee the development of soil moisture conditions suitable for reed overgrowth and peat combustion risk. The diagram in Figure 6.38 shows how this tool can be implemented to support management and decision making. This way, management actions could be less dependent on improvisation and their impact to the physical system minimized. Modelling can be complemented with a monitoring network of soil moisture and temperature sensors at different depths. With these sensors underground cracks and hollows development or surface water inflows arrival could be also detected and monitored in real time. However, due to its discrete nature and the large degree of spatial heterogeneity, sensors alone are insufficient to make decisions on whether when and where certain management actions should be undertaken.

The huge amount of compiled data on soil-water physical-chemical properties is in itself a valuable management tool. Qualitative and quantitative characteristics of drying processes in the Park can be used as input data for different eco-hydrological modelling approaches suitable for managing needs. For example, soil and water

chemical data (appendices II and IX) can be used as a basis for transport modelling when more accurate information on geological and hydrogeological characteristics is available.

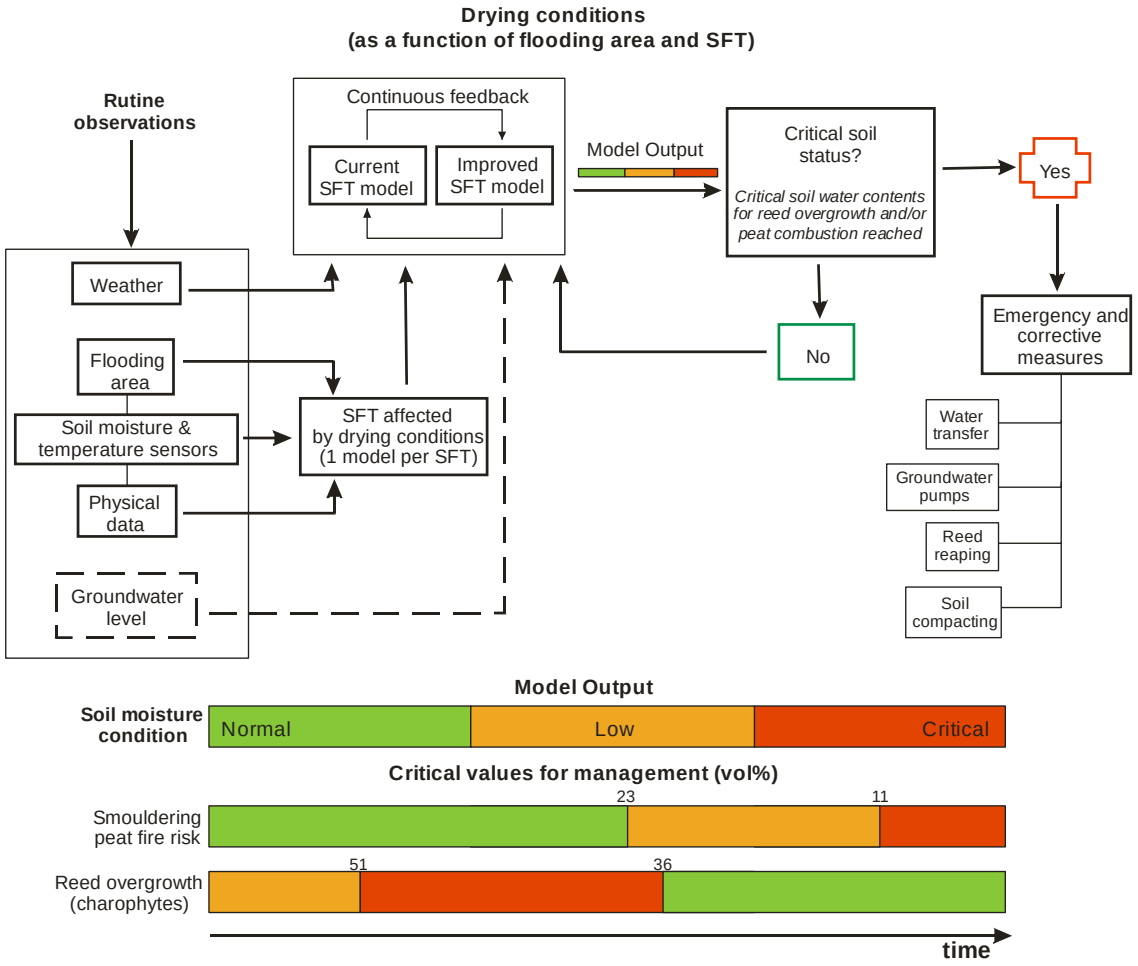

Fig. 6.38. Diagram of vadose zone water flow modelling implementantion as a support tool for Las Tablas de Daimiel National Park (TDNP) management. Soil functional types (SFT) affected by drying conditions can be monitored by Park staff through routine observations of flooding area, soil temperature and moisture sensors and other physical data such as cracks development. Target SFT are modelled with the only input requirement of a series of basic meterological data according to predicted drying patterns. Model outputs allow determining time patterns for the development of critical soil moisture conditions for reed overgrowth or peat combustion rik and, thus, management measures can be planned ahead. If no critical conditions are expected feedback modelling can be carried out with new input data to improve model predictions.

Finally, although impacts derived from system management have been evidenced, there is still a need to quantify their influence and degree of disturbance on soil-water physical-chemical properties.

To summarize, the two main objectives defined in chapter 3 have been successfully achieved through an integrated methodological approach of VZ and SW-GW study tackling with system complexity, heterogeneity and lack of geological and hydrogeological knowledge. Hopefully, the information provided in this research will contribute to support and enhance management actions in Las Tablas de Daimiel National Park.

CHAPTER 8

Conclusions

In order to accomplish the objectives presented in chapter 3, it has been necessary to delve into the knowledge of the TDNP local physical environment: VZ physics and chemistry, surface water-groundwater interactions, VZ water flow, peat specific properties, etc. With this information it has been possible to derive management implications and to develop tools to support environmental management of the anthropized wetland area.

The main conclusions regarding characterization of the physical-chemical environment (section 3.1.1.) can be summarised as:

8.1. Soil functional types

- Physical-analyses have allowed to identify four main TDNP soil materials as constituents of the VZ: charophyte layers, organic, fluvial silt and clay.
- The main soil materials have been further subdivided into eight units or subtypes named "soil functional types" (SFT), which take into account specific hydraulic properties conditioned by the degree of alteration and evolution. These units are: undisturbed charophytes, edaphized charophytes, saline charophytes, clay, silt, organic silt, peat and organic.
- Novel information on the characteristics and spatial distribution of SFT supports Park management.

8.2. Vadose zone chemistry

- The VZ is a carbonated environment with high salinity and significant topsoil nutrient accumulation, which allows classifying TDNP as an eutrophic system.

- Approximate topsoil median electrical conductivity, organic carbon, total nitrogen, available phosphorus and leachable nitrate contents are 4,000 μS cm^{-1}, 6%, 0.5%, 20 mg kg^{-1} and 50 mg l^{-1}, respectively.
- Median electrical conductivity in soil-water extracts of soil profiles is 3,280 μS cm^{-1}, and median organic matter content in the soil matrix is 5.33%. Large variability in nutrient distribution is observed.
- Topsoil solutes content is similar to that in organic soils of other disturbed wetland areas worldwide and higher than the average for agricultural or forest areas.
- During drying conditions, organic matter mineralization becomes a controlling factor on VZ chemistry.
- Principal component analysis (PCA) accounts for 59% of total observed variability in soil chemical composition and allows distinguishing three different environments: saline, carbonated and organic, where most nutrients accumulate.
- Organic carbon is a key variable accounting for a large percentage of total soil chemistry variability.
- Redundancy analysis (RDA) shows that around 40% of the variability can be explained in terms of four human-influenced environmental factors: soil type, depth, microtopography and position regarding the central dam.
- Saline soils are associated with higher topographical areas and organic soils with lower zones. Salinity and nutrients are more likely to accumulate upstream from the central dam whereas downstream carbonate environment is dominant.
- Saline charophytes are representative of saline environments and fluvial silts as OM and nutrients accumulators. Furthermore, surface nutrient accumulation is controlled by reed dynamics in areas where edaphized charophytes predominate.
- Soil nutrients are prone to be realeased upon flooding events and management actions.

8.3. Vadose zone physics

- Physical properties of SFT show large variability reflecting high system heterogeneity.
- Lower bulk densities in organic SFT are associated to higher saturated hydraulic conductivities, infiltration capacities and organic matter contents, conditioning a less compact structure which enhances water transmissivity capacities.
- TDNP peats show extremely high K_s values [$(2.22 \pm 0.9)\cdot10^4$ cm d^{-1}] due to secondary porosity and swelling capacity.
- Infiltration curves from field tests have been successfully fitted to Horton's empirical model (R^2>0.8 in most cases). Extremely high average infiltration capacities in dry SFT range between 159 cm d^{-1} in clay to over 2,000 cm d^{-1} in peat, with all organic materials exceeding 1,000 cm d^{-1}.
- Kostiakov's infiltration model, more suitable to simulate horizontal fluxes, failed to give realistic estimates of the final infiltration capacity, thus, corroborating the initial assumption of predominant vertical downward flux due to hydraulic gradient inversion.
- Extremely large water transmissivity capacities in dominant SFT in the left margin area of TDNP condition a higher degree of SW-GW interactions.
- Only two organic SFT (peat and edapizhed charophytes) show "actual" (in situ) and "potential" (laboratory) soil water repellency conditioned by amount and type of organic matter, soil water content and drying conditions.
- Edaphized charophytes show a slight degree of soil water repellency.
- Peats develop extreme soil water repellency after oven-drying at 105 °C, a laboratory condition not far from reality given the high topsoil temperatures observed in the field.
- Field monitoring showed that most peat samples were not repellent under humid winter conditions, but 23% became repellent in summer, thus, preferential flow through cracks is enhanced.

- A threshold 45% organic matter content and 9-22 vol% critical soil water content range have been defined for soil water repellency development in TDNP peats: peat materials with higher organic matter contents and/or with water contents below or within this range become water repellent.
- The capillary wetting capacity of dry peat is extremely low compared to that of other SFT, being unable to absorb water volumes above 20%.
- During drying conditions, charophytes show higher water contents than peat, but the last is a warmer material than the former.
- Water retention parameters of TDNP SFT have been successfully estimated (R^2>0.88).
- A more homogenous pore size distribution of charophyte-rich soils against other finer textured and organic-rich SFT in TDNP is inferred from the shape of water retention curves.
- Peat shrinking characteristics have been estimated from those measured on other similar peat materials. Although results are in agreement with field observations and macropore flow modelling, further research on Mediterranean semiarid peatlands is still required.
- One-dimensional VZ water flow models haven successfully calibrated with SWAP on ten typical soil profiles representing the arrangement in depth of SFT in different TDNP areas (RMSE<0.05 cm^3 cm^{-3}).
- Simulations on a typical 2-year drainage scenario showed that development of soil moisture conditions for reed overgrowth (36-51 vol% in charophytes and 21-30 vol% in peat) and peat combustion risk (below 23 vol%) are expected.
- Models can be used as tools for Park management during drainage conditions.

8.4. Peat and fire

- TDNP peats are the best fuel material in the area due to the combination of moderate to high organic matter contents (average value of 50.1% and maximum values ranging from 51 to 71%) with low bulk densities (0.18 g cm^{-3}) due to large porosity and water repellency development when dry.
- The desiccation process decreases peat total porosity making it shrink and giving rise to cracks and hollows which constitute preferential flow paths for both air and infiltrating waters.
- High soil temperatures and low water contents promote exponential increase in cracks and hollows number, dimension and extension in short time (i.e. less than one year), reaching up to half meter wide and two meters deep.
- Peat shrinking and non-saturated conditions are also the main cause of soil subsidence during the monitored period.
- Soil water content and organic fraction are the main controlling properties for smouldering fires ignition and spread.
- According to TDNP samples and Frandsen's diagram, successful ignitions are accomplished at a moisture content below 110.0% in dry weight base (20% in volumetric base), and inorganic content below 81.5%.
- Sensors for soil moisture and temperature monitoring showed that the 2009 fire was transmitted through the underground peat pipes over long distances, being even able to flow underneath engineering structures such as the central Morenillo dam.
- Due to soil water repellency and preferential flow through cracks, normal rainfalls in the area are not expected to be sufficient to fully wet the peat and put out smouldering fires naturally.
- Fire irreversibly modifies soil physical properties, increasing the risk of solute mobilisation and, thus, groundwater pollution.

- Continuous soil moisture and temperature monitoring is recommended to support other prevention tools so as to indicate potential combustion and auto-ignition fire risk, but it is not useful as alert system for an already active fire.

8.5. Hydrology and hydrochemistry

- As for VZ, groundwater salinization and increased nutrient content in groundwater are the hydrochemical footprints of degradation and hydraulic gradient inversion.
- Median values of electrical conductivity in surface water range between 2,973 and 11,739 $\mu S\ cm^{-1}$, and in groundwater between 677 and 15,383 $\mu S\ cm^{-1}$.
- Median TOC concentrations in some groundwater monitoring points reach over 9 $mg\ l^{-1}$.
- Lithology and evaporation appear as the main controlling factors for groundwater salinization.
- Large hydrochemical variability is observed, particularly in surface water, accounting for the different sources and processes involved. Variability seems to be conditioned by local factors in the recharge water and residence time in ponds brought about by "edge" geology characteristics (i.e. lithological changes, "bank storage" processes in adjacent materials to the wetland area) and by anthropic management (i.e. groundwater pumping and recirculation, physical environment disturbance, damming, etc).
- Groundwater level oscillations follow fluctuations in the flooding area whereas association to rainfall is restricted to extreme events which cause a temporary "natural" flooding.
- Cross-correlation analysis on a 22-year time series shows that the positive association between flooding and groundwater level in a representative

monitoring point (i.e. rise of groundwater levels) lasts for approximately 3 months.

- Groundwater level response in points around TDNP is conditioned by the retaining effect of the central dam and the pumps from emergency wells.
- The initial hypothesis of disconnected multi-layer aquifer system behaviour has been evidenced by hydrochemic, hydrodynamic and isotopic analyses.
- Upon drying conditions, perched water table conditions near the surface develop and flow of groundwater to deeper layers through semi-permeable aquitards takes place.
- Isotopic analyses evidence local aquifer recharge processes representing different evaporation stages.
- Five hydrological environments have been distinguished under drying conditions: i) northern inlet area, where groundwater is highly influenced by surface and subsurface processes in the alluvial deposits of the Cigüela River and surrounding hillslopes; ii) a saline surface and subsurface environment, more extreme in the right margin, upstream from the central dam; iii) the area of influence of the infiltration of groundwater pumped from the emergency wells to the Guadiana ditch; iv) a less saline but highly variable groundwater environment downstream from the central dam; v) the regional Tertiary aquifer, characterized by "old" very slightly evaporated groundwater as moving further east from TDNP limits.
- The hydrological system is dynamic: upon flooding a global hydrodynamic response is observed whereas hydrochemical responses appear to be mainly conditioned by lithological features and soil degradation, particularly in the left TDNP margin area.
- During extraordinary flooded conditions, the area becomes a system of connected reservoirs where hydrological conditions are artificially regulated. Upon drainage TDNP fully operates as an artificial recharge system with optimal performance in the left margin area.

- A conceptual model of the dynamics of SW-GW interactions in the "active" left margin area is proposed. The model points out the risk of pollution spread from shallow aquifer layers underneath TDNP to deeper layers connected to the regional groundwater flows towards the main irrigation areas,
- Extraordinary rainfall amounts and re-flooded conditions since the end of 2010 have allowed for partial re-saturation of aquifer levels and a near-natural hydrological behaviour of the system.

8.6. Future research and recommendations

This research contribution has allowed for an improved understanding of the soil-water system response of a disturbed semiarid protected wetland area through an integrated methodological approach. Nevertheless, further scientific work is still needed to narrow uncertainity. Some guidelines are listed below:

- Improve geological and hydrogeological knowledge at the TDNP scale in order to enhance hydrological models.
- Determine the potential effect of flooding events on soil-water pollution.
- Couple output of SWAP water flow model to a nutrient transport model to assess mobility of nutrients stored in the VZ.
- Carry out a more exhaustive study on peat properties to narrow and improve estimations on critical soil water contents and shrinking characteristics.
- There is also a need for future researches to get to know the dimensions and spatial distribution of the pipes' system as soon as it is developing during a system dry out.
- Quantify the effect of anthropic impacts (i.e. tractors) on soil properties.

- Consideration of presented data and tools such as VZ water flow models for future management in order to improve effectiveness and minimize environmental impacts.

CHAPTER 9

References

Abella SR, Zimmer BW (2007) Estimating Organic Carbon from Loss-On-Ignition in Northern Arizona Forest Soils. Soil Sci Soc Am J 71(2):545-550

Abouabdillah A, Oueslati O, De Girolamo AM, Porto AL (2010) Modeling the impact of climate change in a mediterranean catchment (Merguellil, Tunisia). Fresen Environ Bull 59:2334-2347

Acreman MC, Miller F (2006) Hydrological impact assessment of wetlands. In: Proccedings of the International Symposium on Groundwater Sustainability (ISGWAS). Alicante, pp 225-255

Acutis M, Donatelli M (2003) SOILPAR 2.00: software to estimate soil hydrological parameters and functions. Geoderma 18:373-377

Aguilera H, Castaño S, Moreno L, Jiménez-Hernández ME, de la Losa A (2013) Model of hydrological behaviour of the anthropized semiarid wetland of Las Tablas de Daimiel National Park (Spain) based on surface water-groundwater interactions. Hydrogeol J 21:623-641

Aguilera H, Moreno L, Castaño S, Jiménez-Hernández ME, de la Losa A (2009a) Contenido y distribución espacial de nutrientes móviles en la zona no saturada en el Parque Nacional de las Tablas de Daimiel (Nutrient content and spatial distribution in the unsaturated zone at the Las Tablas de Daimiel National Park). Bol Geol Min 120(3):393–408

Aguilera H, Moreno L, Jiménez-Hernández ME, Castaño S, de la Losa A (2011) Management implications inferred from the multivariate analysis of vadose zone chemical variables in Las Tablas de Daimiel National Park (Spain). Geoderma 162:365-377

Aguilera H, Moreno L, Jiménez-Hernández ME, de la Losa A, Castaño S (2009b) Propiedades físicas e hidráulicas de la ZNS en el Parque Nacional de Las Tablas de Daimiel (Physical and hydraulic properties of the UZ in Las Tablas de Daimiel National Park). In: Silva O, Carrera J (eds) Estudios de la zona no saturada del suelo, Vol. IX-ZNS'09. CIMNE, Barcelona, pp 51-58

Aldaya MM, Martínez-Santos P, Llamas MR (2010) Incorporating the Water Footprint and Virtual Water into Policy: Reflections from the Mancha Occidental Region, Spain. Water Resour Res 24:941-958

Aldous A, McCormick P, Ferguson C, Graham S, Craft C (2005) Hydrologic regime controls soil phosphorus fluxes in restoration and undisturbed wetlands. Restor Ecol 13(2):341-347

Álvarez-Cobelas M, Cirujano S (2007) Multilevel responses of emergent vegetation to environmental factors in a semiarid floodplain. Aquat Bot 87:49-60

Álvarez-Cobelas M, Cirujano S, Sánchez-Carrillo S (2001) Hydrological and botanical man-made changes in the Spanish wetland of Las Tablas de Daimiel. Biol Conserv 97:89-98

Álvarez-Cobelas M, Rojo C, Angeler DG (2005) Mediterranean limnology: current status, gaps and the future. J Limnol 64:13-29

Álvarez-Cobelas M, Sánchez-Carrillo S, Cirujano S (2007) Strong site effects dictate nutrient patterns in a Mediterranean floodplain. Wetlands 27:326-336

Álvarez-Cobelas M, Sánchez-Carrillo S, Cirujano S, Angeler DG (2008) Long-term changes in spatial patterns of emergent vegetation in a Mediterranean floodplain: natural versus anthropogenic constraints. Plant Ecol 194:257-271

Álvarez-Cobelas M, Sánchez-Carrillo S, Cirujano S, Angeler DG (2010) A story of the wetland water quality deterioration: salinization, pollution, eutrophication and siltation. In: Sánchez-Carrillo S, Angeler DG (eds) Ecology of Threatened Semi-Arid Wetlands: Long-Term Research in Las Tablas de Daimiel. Springer Science+Business Media B.V., pp 109-133

Amezaga JM, Santamaría L (2000) Wetland Connectedness and Policy Fragmentation: Steps Towards a Sustainable European Wetland Policy. Phys Chem Earth (B) 25:635-640

Andersen HE (2004) Hydrology and nitrogen balance of a seasonally inundated Danish floodplain wetland. Hydrol Process 18:415-434

Angeler DG, Álvarez-Cobelas M, Rojo C, Sánchez-Carrillo S (2010) Phytoplankton community similarity in a semiarid floodplain under contrasting hydrological connectivity regimes. Ecol Res 25:513-520

Angeler DG, Chow-Fraser P, Hanson MA, Sánchez-Carrillo S, Zimmer KD (2003) Biomanipulation: a useful tool for freshwater wetland mitigation. Freshwater Biol 48:2203-2213

Angeler DG, Sánchez-Carrillo S (2010) Synthesis: The Past, Present and Future of Las Tablas de Daimiel. In: Sánchez-Carrillo S, Angeler DG (eds) Ecology of Threatened Semi-Arid Wetlands: Long-Term Research in Las Tablas de Daimiel. Springer Science+Business Media B.V., pp 257-277

Angeler DG, Sánchez-Carrillo S, García G, Álvarez-Cobelas M (2001) The influence of Procambarus clarkii (Cambaridae, Decapoda) on water quality and sediment characteritics in a Spanish floodplain wetland. Hydrobiologia 464:89-98

Aranda G, García J, Martín-Montalvo JM (1993) Evolución de la calidad de las aguas en el P.N. de Las Tablas de Daimiel (Ciudad Real) durante el periodo comprendido desde 1988 a 1993 (Evolution of water quality in Las Tablas de Daimiel National Park in the period 1988-1993). Ecología 7:503-519

Asaeda T, Karunaratne S (2000) Dynamic modeling of the growth of Phragmites australis: model description. Aquat Bot 67:301-318

Bauer P, Gumbricht T, Kinzelbach W (2006) A regional coupled surface water/groundwater model of the Okavango Delta, Botswana. Water Resour Res 42(4), W04403

Berzas JJ, García LF, Rodríguez RC (1999) Determination of lead in waters and sediments from the wetland Tablas de Daimiel National Park (Spain). Fresen J Anal Chem 364:732-736

Berzas JJ, García LF, Rodríguez RC, Martín-Álvarez PJ (2000) Evolution of the water quality of a managed natural wetland: Tablas de Daimiel National Park (Spain). Water Res 34:3161-3170

Biebighauser TR (2007) Wetland drainage, restoration, and repair. The University Press of Kentucky, Kentucky

Bisdom EBA, Dekker LW, Schoute JFT (1993) Water repellency of size fractions from sandy soils and relationships with organic material and soil structure. Geoderma 56:105-118

Blanco-Canqui H, Lal R (2009) Extent of soil water repellency under long-term no-till soils. Geoderma 149:171-180

Bohn HL, McNeal BL, O'Connor GA (2001) Soil chemistry. 3rd ed. John Wiley & Sons,

Inc, New York

Bonfante A, Basile A, Acutis M, De Mascellis R, Manna P, Perego A, Terribile F (2010) SWAP, CropSyst and MACRO comparison in two contrasting soils cropped with maize in Northern Italy. Agr Water Manage 97:1051-1062

Bonfante A, Basile A, Manna P, Terribile F (2011) Use of Physically Based Models to Evaluate USDA Soil Moisture Classes. Soil Sci Soc Am J 75:181-191

Boswell JS, Olyphant GA (2007) Modeling the hydrologic response of groundwater dominated wetlands to transient boundary conditions: Implications for wetland restoration. J Hydrol 332:467-476

Brady NC, Raymond RW (1996) The nature and properties of soils. Prentice Hall. International Editions, USA

Brisson J, Chazarenc F (2009). Maximizing pollutant removal in constructed wetlands: Should we pay more attention to macrophyte species selection. Sci Total Environ 407:3923-3930

Broadbent FE (1953) The soil organic fraction. Adv Agron 5:153-183

Buczko U, Bens O, Durner W (2006) Spatial and temporal variability of water repellency in a sandy soil contaminated with tar oil and heavy metals. J Contam Hydrol 88:249-268

Burba GG, Verma SB, Kim J (1999) Surface energy fluxes of Phragmites australis in a prairie wetland. Agr Forest Meteorol 94:31-51

Cammeraat LH, Willott SJ, Compton SG, Incoll LD (2002) The effects of ants' nests on the physical, chemical and hydrological properties of a rangeland soil in semi-arid Spain. Geoderma 105:1-20

Carol ES, Kruse EE, Pousa JL (2011) Influence of the geologic and geomorphologic characteristics and of crab burrows on the interrelation between surface water and groundwater in an estuarine coastal wetland. J Hydrol 403:234-241

Castaño S (2004) Estudio metodológico para el cálculo de la infiltración en el vaso de las Tablas de Daimiel: validación de resultados (Methodological study to calculate water infiltration from Las Tablas de Daimiel: validation of results) Ph.D. thesis, Complutense University of Madrid, Madrid

Castaño S, Díaz-Teijeiro MF, Rodríguez-Arévalo J, Moreno L, Aguilera H, de la Losa A, Jiménez-Hernández ME (2011) Characterization of evaporation in "Las Tablas de Daimiel" National Park using stable istopes of water. In: Otero N, Soler A, Audí C (eds) 9th International Symposium on Applied Isotope Geochemistry (AIG-9). CIMNE, Tarragona, p 47

Castaño S, Martínez-Santos P, Martínez-Alfaro PE (2008) Evaluating infiltration losses in a Mediterranean wetland: Las Tablas de Daimiel National Park, Spain. Hydrol Process 22:5048-5053

Castaño S, Moreno L, Aguilera H, de la Losa A, Jiménez-Hernández ME (2012a) Las aguas subrerráneas en el entorno del Parque Nacional de Las Tablas de Daimiel (Groundwater in the Las Tablas de Daimiel National Park environment). In: Mediavilla (ed) Las Tablas de Daimiel: agua y sedimentos. Medio Ambiente Series, 14. Instituto Geológico y Minero de España, Madrid, pp 59-86

Castaño S, Moreno L, Aguilera H, de la Losa A, Jiménez-Hernández ME (2012b) Antropización del Parque Nacional de Daimiel: una visión desde la perspectiva del ciclo hídrico (Daimiel National Park anthropization: as seen from the

hydrological cycle perspective). In: Mediavilla (ed) Las Tablas de Daimiel: agua y sedimentos. Medio Ambiente, 14. Instituto Geológico y Minero de España, Madrid, pp 259-269

Castaño S, Mediavilla R, Santisteban JI, de la Losa A, Martínez-Santos (2013) Aportación al conocimiento del comportamiento hidrogeológico del límite Terciario-Cuaternario en el entorno del Parque Nacional de las Tablas de Daimiel (Contribution to the knowledge of the hydrogeological behaviour of Tertiary-Quaternary boundary in the vicinity of Las Tablas de Daimiel National Park). Geogaceta (in press)

Cerdà A, Doerr SH (2007) Soil wettability, runoff and erodibility of major dry-Mediterranean land use types on calcareous soils. Hydrol Process 21: 2325-2336

Chun YM, Choi YD (2009) Expansion of Phragmites australis (Cav.) Trin. ex Steud. (Common Reed) into Typha spp. (Cattail) Wetlands in Northwestern Indiana, USA. J Plant Biol 52:220-228

Cirkel DG, Witte JPM, van der Zee SEATM (2010) Estimating seepage intensities from groundwater level time series by inverse modelling: A sensitivity analysis on wet meadow scenarios. J Hydrol 385:132-142

Cirujano S (1996) Bentos vegetal, flora y vegetación superior (Vegetal benthos, flora and superior vegetation). In: Álvarez-Cobelas M, Cirujano S (eds) Las Tablas de Daimiel: Ecología Acuática y sociedad. Ministerio de Medio Ambiente, Madrid, pp 129-139

Cirujano S, Álvarez-Cobelas M, Ruíz de la Hermosa C (2010) Analysis of applied environmental management strategies for wetland conservation during the last 30 years: a local history. In: Sánchez-Carrillo S, Angeler DG (eds) Ecology of Threatened Semi-Arid Wetlands: Long-Term Research in Las Tablas de Daimiel. Springer Science+Business Media B.V., pp 229-237

Cirujano S, Álvarez-Cobelas M, Sánchez-Andrés R (2010) Macrophyte ecology and its long-term dynamics. In: Sánchez-Carrillo S, Angeler DG (eds) Ecology of Threatened Semi-Arid Wetlands: Long-Term Research in Las Tablas de Daimiel. Springer Science+Business Media B.V., pp 175-195

Cirujano S, Álvarez-Cobelas MA, Soriano O, Alonso JM, Moreno M, López E, Ortiz MJ (2007) Seguimiento y monitoreo en el P.N. Las Tablas de Daimiel (2003-2007) [Control and monitoring of Las Tablas de Daimiel National Park]. Estudios Europeos de Medio Ambiente S.L. (EINTAM) and Las Tablas de Daimiel National Park, report

Cirujano S, Casado C, Bernues M, Camargo JA (1996) Ecological study of Las Tablas de Daimiel National Park (Ciudad Real, Central Spain): Differences in water physico-chemistry and vegetation between 1974 and 1989. Biol Conserv 75:211-215

Cobertera E (1993) Edafología aplicada. Cátedra, Madrid

Conan C, de Marsily G, Bouraoui F, Bidoglio G (2003) A long-term hydrological modelling of the Upper Guadiana river basin (Spain). Phys Chem Earth, Parts A/B/C 28:193-200

Contreras S, Cantón Y, Solé-Benet A (2008) Sieving crusts and macrofaunal activity control soil water repellency in semiarid environments: Evidences from SE

Spain. Geoderma 145:252-258

Cooper DJ, MacDonald LH, Wenger SK, Woods SW (1998) Hydrologic restoration of a fen in Rocky Mountain National Park, Colorado, USA. Wetlands 18:335-345

Costanza R, d'Arge R, de Groot R, Farber S, Grasso M, Hannon B, Limburg K, Naeem S, O'Neill RV, Paruelo J, Raskin RG, Sutton P and Van den Belt M (1997) The value of the world's ecosystem services and natural capital. Nature 387:253-260

Craig H (1961) Isotopic variations in meteoric waters. Science, New Series 133:1702-1703

Crosbie RS, McEwan KL, Jolly ID, Holland KL, Lamontagne S, Moe KG, Simmons CT (2009) Salinization risk in semi-arid floodplain wetlands subjected to engineered wetting and drying cycles. Hydrol Process 23:3440-3452

Cruces J, Martínez Cortina L (2000) La Mancha Húmeda. Explotación intensiva de las aguas subterráneas en la cuenca alta del río Guadiana (The wet La Mancha. Intensive groundwater exploitation in the Upper Gudiana basin). Papeles del Proyecto Aguas Subterráneas, Serie A, n°3. Fundación Marcelino Botín, Santander

D'Auria G, Barón-Rodríguez MM, Durbán-Vicente AA, Moya A, Rojo C, Latorre A, Rodrigo MA (2010) Unravelling the bacterial diversity found in the semi-arid Tablas de Daimiel National Park wetland (central Spain). Aquat Microb Ecol 59:33-44

Dall'O' M, Kluge W, Bartels F (2001) FEUWAnet: a multi-box water level and lateral exchange model for riparian wetlands. J Hydrol 250:40-62

Dawson Q (2006) Low-lying agricultural peatland sustainability under managed water regimes. Ph.D. thesis, Cranfield University, Silsoe

De Baets S, Poesen J, Knapen A, Barberá GG, Navarro JA (2007) Root characteristics of representative Mediterranean plant species and their erosion-reducing potential during concentrated runoff. Plant Soil 294:169-183

de la Horra JL (1996) El medio edáfico (The edaphic environment). In: Álvarez-Cobelas M, Cirujano S (eds) Las Tablas de Daimiel: Ecología Acuática y sociedad. Ministerio de Medio Ambiente, Madrid, pp 35-46

de la Losa A, Aguilera H, Jiménez-Hernández ME, Castaño S, Moreno L (2012) Hidrología e hidroquímica (Hydrology and hydrochemistry). In: Mediavilla (ed) Las Tablas de Daimiel: agua y sedimentos. Medio Ambiente Series, 14. Instituto Geológico y Minero de España, Madrid, pp 87-124

DeBano LF (1981) Water repellent soils: a state-of-the-art. United States Department of Agriculture, Forest Service, General Technical Report PSW-46. Berkeley, California 21

DeBano LF (2000) The role of fire and soil heating on water repellency in wildland environments: a review. J Hydrol 231-232:195-206

DeBano LF (2000) Water repellency in soils: a historical overview. J Hydrol 231-232:4-32

Dekker LW, Doerr SH, Oostindie K, Ziogas AK, Ritsema CJ (2001) Water Repellency and Critical Soil Water Content in a Dune Sand. Soil Sci Soc Am J 65:1667-1674

Dekker LW, Jungerius PD (1990) Water repellency in the dunes with special reference to the Netherlands. Catena Suppl 18:73-183.

Dekker LW, Oostindie K, Ritsema CJ (2005) Exponential increase of publications related

to soil water repellency. Aust J Soil Res 43:403-441

Dekker LW, Ritsema CJ (1996) Variation in water content and wetting patterns in Dutch water repellent peaty clay and clayey peat soils. Catena 28:89-105

Dekker LW, Ritsema CJ, Oostindie K, Moore D, Wesseling JG (2009) Methods for determining soil water repellency on field-moist samples. Water Resour Res 45(4):W00D33

Dekker LW, Ritsema CJ, Wendroth O, Jarvis N, Oostindie K, Pohl W, Larsson M, Gaudet JP (1999) Moisture distributions and wetting rates of soils at experimental fields in the Netherlands , France , Sweden and Germany. J Hydrol 215:4-22

Devito KJ, Hill AR, Roulet N (1996) Groundwater-surface water interactions in headwater forested wetlands of the Canadian Shield. J Hydrol 181:127-147

Díaz-Teijeiro MF, Rodríguez-Arévalo J, Castaño S (2009) La Red Española de Vigilancia de Isótopos en la Precipitación (REVIP): distribución isotópica espacial y aportación al conocimiento del ciclo hidrológico (The Spanish Network for Surveillance of Isotopes in Precipitation: spatial isotopic distribution and contribution to the knowledge of the hydrological cycle). Ingeniería Civil 155:87-97

Diehl D, Schaumann GE (2007) The nature of wetting on urban soil samples: wetting kinetics and evaporation assessed from sessile drop shape. Hydrol Process 21:2255-2265

Dikici H, Yilmaz CH (2006) Peat fire effects on some properties of an artificially drained peatland. J Environ Qual 35:866-870

Doerr SH, Dekker LW, Ritsema CJ, Shakesby RA, Bryant R (2002) Water repellency of soils: the influence of ambient relative humidity. Soil Sci Soc Am J 66: 401-405

Doerr SH, Shakesby R, Walsh RPD (2000) Soil water repellency: its causes, characteristics and hydro-geomorphological significance. Earth-Sci Rev 51:33-65

Doerr SH, Shakesby RA, Walsh RPD (2000) Soil water repellency: its causes, characteristics and hydro-geomorphological significance. Earth-Sci Rev 51:33–65.

Doerr SH, Thomas AD (2000) The role of soil moisture in controlling water repellency: new evidence from forest soils in Portugal. J Hydrol 231-232:134-147

Domínguez-Castro F, Santisteban JI, Barriendos M, Mediavilla R (2008) Reconstruction of drought episodes for central Spain from rogation ceremonies recorded at the Toledo Cathedral from 1506 to 1900: A methodological approach. Global Planet Change 63:230-242

Domínguez-Castro F, Santisteban JI, Mediavilla R, Dean WE, López-Pamo E, Gil-García MJ, Ruiz-Zapata MB (2006) Environmental and geochemical record of human-induced changes in C storage during the last millennium in a temperate wetland (Las Tablas de Daimiel National Park, central Spain) Tellus 58:573-585

Dorado-Valiño M, Valdeolmillos Rodríguez A, Ruiz-Zapata MB, Gil-García MJ, de Bustamante Gutiérrez I (2002) Climatic changes since the Late-glacial/Holocene transition in La Mancha Plain (South-central Iberian Peninsula, Spain) and their incidence on Las Tablas de Daimiel marshlands. Quatern Int 93-94:73-84

Drexler JZ, Bedford BL, DeGaetano AT, Siegel DI (1999) Quantification of water budget and nutrient loading in a small peatland. J Am Water Resour Assoc 35:753-769

Droogers P, Van A (2008) Quantifying the impact of model inaccuracy in climate change impact assessment studies using an agro-hydrological model. Hydrol Earth Syst Sci 12:1-10

Eijkelkamp (2005) Operating instructions for 08.01 sandbox. Report 880299

Eimers MC, Dillon PJ, Schiff SL, Jeffries DS (2003) The effects of drying and re-wetting and increased temperature on sulphate release from upland and wetland material. Soil Biol Biogeochem 35:1663-1673

Ellis A, Ramírez C, Mac Donald R (2005) Organic matter and wetting capacity distribution in aggregates of Chilean soils. Catena 59:69-78

Elrick DE, Reynolds WD (1992) Infiltration from constant-head well permeameters and infiltrometers. In: Topp CG et al (eds) Advances in measurement of soil physical properties: Bringing theory into practice. SSSA Spec. Publ. 30 SSSA, Madison, WI, pp 1-24

Engloner AI (2009) Structure, growth dynamics and biomass of reed (Phragmites australis) - A review. Flora 204:331-346

EPTISA (1986) Estudio de viabilidad de un Plan de regeneración hídrica en el Parque Nacional de las Tablas de Daimiel (Ciudad Real) [Viability study of a hydrological regeneration Plan in the Las Tablas de Daimiel National Park (Ciudad Real). Estudios y Proyectos técnicos Industriales, S.A., Vol. I, report

Esnaola JM (1991) Análisis de las aportaciones superficiales al Parque Nacional de las Tablas de Daimiel y su influencia en la evolución hidrogeológica del ecosistema (Analysis of surface water contributions to Las Tablas de Daimiel National Park and their influence on the hydrogeological evolution of the ecosystem). Ph.D. thesis, Complutense University of Madrid, Madrid

Esteller MV, Martínez-Valdés H, Garrido S, Uribe Q (2009) Nitrate and phosphate leaching in a Phaeozem soil treated with biosolids, composted biosolids and inorganic fertilizers. Waste Manage 29:1936-1944

FAO (2006) Evapotranspiración del cultivo. Guías para la determinación de los requerimientos de agua de los cultivos (Crop evapotranspiration. Guidelines for the determination of water requirements) Estudio FAO Riego y Drenaje N° 56

Feddes RA, Kowalik PJ, Zaradny H (1978) Simulation of field water use and crop yield. Simulation Monographs. Pudoc, Wageningen

Fernández González J, Beascoechea EM, Muñoz JM, Curt Fernández de la Mora MD (2004) Manual Fitodepuración. Filtros de macrofitas en flotación (Phytodepuration manual. Bouyant macrophytes filtres) Fernández-González (ed) Ayuntamiento de Lorca, Universidad Politécnica de Madrid, Fundación Global Nature, Obra Social (eds), Madrid

Fernández JM, Plaza C, García-Gil JC, Polo A (2009) Biochemical properties and barley yield in a semiarid Mediterranean soil amended with two kinds of sewage sludge. Appl Soil Ecol 42:18-24

Fox DM, Darboux F, Carrega P (2007) Effects of fire-induced water repellency on soil aggregate stability, splash erosion, and saturated hydraulic conductivity for different size fractions. Hydrol Process 21:2377-2384

Frandsen WH (1987) The influence of moisture and mineral soil on the combustion limits of smoldering forest duff. Can J For Res 17:1540-1544

Frandsen WH (1997) Ignition probability of organic soils. Can J For Res 27: 1471-1477

Gao X, Giorgi F (2008) Increased aridity in the Mediterranean region under greenhouse gas forcing estimated from high resolution simulations with a regional climate model. Global Planet Change 62:195-209

García Jiménez MA, López-Camacho B, Montesinos S (1992) Aplicación de la teledetección al conocimiento hidrológico de la cuenca Alta del Guadiana (Remote sensing application to the hydrologic knowledge of the Upper Guadiana basin). In: Hidrogeología y Recursos Hidraúlicos (V Simposio de Hidrogeología). Alicante, 17:591-600

García Rodríguez M, Llamas MR (1993) Cambios paisajísticos en el Alto Guadiana causados por la explotación intensiva e incontrolada de aguas subterráneas (Intensive groundwater exploitation induced landscape changes at the Upper Guadiana basin). Actas de las VI Jornadas sobre el Paisaje. Segovia, pp 91-102

García Rodríguez M (1996) Hidrogeología de las Tablas de Daimiel y de los ojos del Guadiana: bases hidrogeológicas para una clasificación funcional de humedales ribereños (Hydrogeology of Las Tablas de Daimiel and the ojos del Guadiana: hydrogeological basis for a functional classification of riparian wetlands). Ph.D. thesis, Complutense University of Madrid, Madrid

García-Hidalgo JF, Temiño J, de Bustamante I, Segura M (1995) Evolución sedimentaria reciente de las Tablas de Daimiel (Ciudad Real) [Recent sedimentary evolution in Las Tablas de Daimiel (Ciudad Real)]. Geogaceta 18:87-89

Garkaklis MJ, Bradley JS, Wooller RD (2000) Digging by vertebrates as an activity promoting the development of water-repellent patches in sub-surface soil. J Arid Environ 45:35-42

Gebhardt S, Fleige H, Horn R (2012) Anisotropic shrinkage of mineral and organic soils and its impact on soil hydraulic properties. Soil Till Res 125:96-104

Gerakis A, Kalburtji K (1998) Agricultural activities affecting the functions and values of Ramsar wetland sites of Greece. Agr Ecosyst Environ 70:119-128

Gil-García MJ, Ruiz-Zapata MB, Santisteban JI, Mediavilla R, López-Pamo E, Dabrio CJ (2007) Late holocene environments in Las Tablas de Daimiel (south central Iberian peninsula, Spain). Veg Hist Archaeobot 16:241-250

Giovannini G, Lucchesi S (1997) Modifications induced in soil physico-chemical parameters by experimental fires at different intensities. Soil Sci 162(7):479-486

Gnatowski T, Szatylowicz J, Brandyk T, Kechavarzi C (2010) Hydraulic properties of fen peat soils in Poland. Geoderma 154:188-195

Goebel M, Bachmann J, Woche SK, Fischer WR, Horton R (2004) Water Potential and Aggregate Size Effects on Contact Angle and Surface Energy. Soil Sci Soc Am J 68:383-393

González C, Quintana JR, Moreno L, Vázquez A, Lafuente AL, Romero A (2007) Applying multivariate methods to soil-solution interactions in carbonate media. Geoderma 137:352-359

González Monterrubio JM (1992) Análisis hidrogeológico de la sobreexplotación y protección de humedales en la Ley de Aguas de 1985 (Hydrogeological analysis of the overexploitation and protection of wetlands in the 1985 Water Law) Ph.D. thesis, Complutense University of Madrid, Madrid

González-Pelayo O, Andreu V, Campo J, Gimeno-García E, Rubio JL (2006) Hydrological

properties of a Mediterranean soil burned with different fire intensities. Catena 68:186-193

González-Pérez JA, González-Vila FJ, Almendros G, Knicker H (2004) The effect of fire on soil organic matter-a review. Environ Int 30:855-870

Graber ER, Ben-Arie O, Wallach R (2006) Effect of sample disturbance on soil water repellency determination in sandy soils. Geoderma 136:11-19

Grishin AM, Golovanov AN, Sukov YV, Preis YI (2006). Experimental study of peat ignition and combustion. J Eng Phys Thermophys 79(3):563-568

Guerrero F (1985) Estudio de las aguas de turberas españolas (Spanish peatland water study). Instituto Nacional de Investigaciones Agrarias. Ministerio de agricultura, Pesca y Alimentación, Madrid

Guerrero F (1989) Estudio de las propiedades físicas y químicas de algunas turbas españolas y su posible aprovechamiento agrícola (Study of physical-chemical properties of some Spanish peats and their possible agricultural use). Instituto Nacional de Investigaciones Agrarias. Ministerio de agricultura, Pesca y Alimentación, Madrid

Gusyev MA, Haitjema HM (2011) Modeling flow in wetlands and underlying aquifers using a discharge potential formulation. J Hydrol 408:91-99

Hallett PD, Baumgartl T, Young IM (2001) Subcritical water repellency of aggregates from a range of soil management practices. Soil Sci Soc Am J 65:184-190

Hardej M, Ozimek T (2002) The effect of sewage sludge flooding on growth and morphometric parameters of Phragmites australis (Cav.) Trin. ex Steudel. Ecol Eng 18:343-350

Hargreaves GH, Samani ZA (1985) Reference crop evapotranspiration from temperature. Appl Eng Agric 1(2):96-99

Harper RJ, McKissock I, Gilkes RJ, Carter DJ, Blackwell PS (2000) A multivariate framework for interpreting the effects of soil properties, soil management and landuse on water repellency. J Hydrol 231-232:371-383

Harris JA, Hobbs RJ, Higgs E, Aronson J (2006) Ecological restoration and global climate change. Restor Ecol 14:170-176

Harvey FE, Ayers JF, Gosselin DC (2007) Ground water dependence of endangered ecosystems: Nebraska's eastern saline wetlands. Ground water 45:736-752

Harvey JW, McCormick PV (2009) Groundwater's significance to changing hydrology, water chemistry, and biological communities of a floodplain ecosystem, Everglades, South Florida, USA. Hydrogeol J 17:185-201

Hattermann FF, Krysanova V, Hesse C (2008) Modelling wetland processes in regional applications. Hydrol Sci J 53:1001-1012

Heiri O, Lotter AF, Lemcke G (2001) Loss on ignition as a method for estimating organic and carbonate content in sediments: reproducibility and comparability of results. J Paleolimnol 25:101-110

Hendriks RFA (2004). An analytical equation for describing the shrinkage characteristics of peat soils . In: Päivänen J (ed) Wise use of Peatlands. Proceedings of the 12th International Peat Congress. Tampere, Finland

Hill MO, Gauch HG (1980) Detrended correspondence analysis, an improved ordination technique. Vegetatio 42:47-58

Holden J, Burt TP (2002) Piping and pipeflow in a deep peat catchment. Catena 48:163-

199
Horton RE (1940) An approach toward a physical interpretation of infiltration capacity. Soil Sci Soc Am J 5:399-417
Hubbert KR, Preisler HK, Wohlgemuth PM, Graham RC, Narog MG (2006) Prescribed burning effects on soil physical properties and soil water repellency in a steep chaparral watershed, southern California, USA. Geoderma 130:284-298
Hughes DA, Kapangaziwiri E, Baker K (2010) Initial evaluation of a simple coupled surface and ground water hydrological model to assess sustainable ground water abstractions at the regional scale. Hydrol Res 41:1-12
Hurra J, Schaumann G (2006) Properties of soil organic matter and aqueous extracts of actually water repellent and wettable soil samples. Geoderma 132:222-239
Instituto Tecnológico GeoMinero de España, ITGE (1988) Mapa geológico de España 1:50.000. Hoja 760 (19-30): Daimiel [Geological map of Spain 1:50.000. Sheet 760 (19-30): Daimiel]. Second series, 1st edn. Servicio de publicaciones MIE, Madrid
INYPSA (1990) Estudio de seguimiento de los resultados del plan de regeneración hídrica del Parque Nacional de Las Tablas de Daimiel (Monitoring study on the performance of the hydrological regeneration plan of Las Tablas de Daimiel National Park). Ministerio de Agricultura, Pesca y Alimentación, ICONA, Madrid
Ippisch O, Vogel HJ, Bastian P (2006) Validity limits for the van Genuchten-Mualem model and implications for parameter estimation and numerical simulation. Adv Water Resour 29:1780-1789
ITGE (1980) Informe hidrogeológico sobre la captación de agua subterránea para el abastecimiento de Daimiel (Ciudad Real) [Hydrogeological report on groundwater collection for Daimiel (Ciudad Real) supply]. Internal report
IUSS Working Group WRB (2007) World Reference Base for Soil Resources 2006, first update 2007. World Soil Resources Reports No. 103. FAO, Rome
Jaramillo DF (2006) Repelencia al agua en suelos: una síntesis (Water repellency in soils: a synthesis) Rev Acad Colomb Cienc 30 (115):215-232
Jaramillo DF, Dekker LW, Ritsema CJ, Hendrickx JMH (2000) Occurrence of soil water repellency in arid and humid environments. J Hydrol 231-232:105-111
Jhorar RK, van Dam JC, Bastiaanssen WGM, Feddes RA (2004) Calibration of effective soil hydraulic parameters of heterogeneous soil profiles. J Hydrol 285:233-247
Jhorar RK (2002) Estimation of soil hydraulic parameters for water management studies in semi-arid zones. Ph.D. thesis, Wageningen University, Wageningen
Jia Z, Luo W (2009) A modified climate diagram displaying net water requirements of wetlands in arid and semi-arid regions. Agr Water Manage 96:1339-1343
Jiménez-Pinilla (2011) Estudio de las turbas en el Parque Nacional de Las Tablas de Daimiel. Editorial Académica Española, ISBN: 3846563226.
Johnston CA (1994) Cumulative impacts to wetlands. Wetlands 14:49-55
Jolly ID, McEwan KL, Holland KL (2008) A review of groundwater-surface water interactions in arid/semi-arid wetlands and the consequences of salinity for wetland ecology. Ecohydrology 1:43-58
Joosten H, Clark D (2002) Wise use of mires and peatlands. Background and Principles Including a Framework for Decision Making. International Mire Conservation Group and International Peat Society (ed), Saarijärvi, Finland.

Kaplan D, Muñoz-Carpena R (2011) Complementary effects of surface water and groundwater on soil moisture dynamics in a degraded coastal floodplain forest. J Hydrol 398:221-234

Kazezyilmaz-Alhan CM, Medina MA, Richardson CJ (2007) A wetland hydrology and water quality model incorporating surface water/groundwater interactions. Water Resour Res 43(4), W04434

Kechavarzi C, Dawson Q, Leeds-Harrison PB (2010) Physical properties of low-lying agricultural peat soils in England. Geoderma 154:196-202

Keizer JJ, Doerr SH, Malvar MC, Ferreira AJD, Pereira VMFG (2007) Temporal and spatial variations in topsoil water repellency throughout a crop-rotation cycle on sandy soil in north-central Portugal. Hydrol Process 21:2317-2324

Kelleners TJ, Beekma J, Chaudhry MR (1999) Spatially variable soil hydraulic properties for simulation of field-scale solute transport in the unsaturated zone. Geoderma 92:199-215

Kingsford RT (2000) Ecological impacts of dams, water diversions and river management on floodplain wetlands in Australia. Austral Ecol 25:109-127

Klute A (1965) Laboratory measurement of hydraulic conductivity of saturated soil. In: Black CA et al. (eds). Methods of soil analysis, part I. Physical and Mineralogical properties, including statistics of measurement and sampling. American Society and Agronomy, Inc. Publ. Madison, WI, pp 210-221

Koch M, Schimd T, Gumuzzio J (2008) Multisensor study of soil and wetland degradation in semi-arid Mediterranean ecosystems. IEEE Geosci Remote S 147:10-17

Koch M, Schmid T, Reyes M, Gumuzzio J (2012) Evaluating Full Polarimetric C- and L-Band Data for Mapping Wetland Conditions in a Semi-Arid Environment in Central Spain. IEEE J-STARS 5(3):1033-1044

Koerselman W, Van Kerkhoven M, Verhoeven J (1993) Release of inorganic N, P and K in peat soils; effect of temperature, water chemistry and water level. Biogeochem 20:63-81

Konen ME, Jacobs PM, Burras CL, Talaga BJ, Mason JA (2002) Equations for Predicting Soil Organic Carbon Using Loss-on-Ignition. Soil Sci Soc Am J 66:1878-1881

Krause S, Bronstert A (2004) Approximation of Groundwater - Surface Water – Interactions in a Mesoscale Lowland River Catchment. Hydrology: Science & Practice for the 21st Century, vol. 2, British Hydrological Society

Krause S, Heathwaite AL, Miller F, Hulme P, Crowe A (2007) Groundwater-Dependent Wetlands in the UK and Ireland: Controls, Functioning and Assessing the Likelihood of Damage from Human Activities. Water Resour Manag 21:2015-2025

Kroes JG, van Dam JC, Groenendijk P, Hendriks RFA, Jacobs CMJ (2008) SWAP version 3.2. Theory description and user manual. Alterra Report1649(02), Alterra, Wageningen

Ladenburger CG, Hild AL, Kazmer DJ, Munn LC (2006) Soil salinity patterns in Tamarix invasions in the Bighorn Basin, Wyoming, USA. J Arid Environ 65:111-128

Lamparter A, Bachmann J, Goebel MO, Woche SK (2009) Carbon mineralization in soil: Impact of wetting-drying, aggregation and water repellency. Geoderma 150(3-4):324-333

Larsen LG, Harvye JW, Crimaldi JP (2007) A delicate balance: ecohydrological feedbacks governing landscape morphology in a lotic peatland. Ecol Monogr 77:591-614

Leps J, Smilauer P (2003) Multivariate analysis of ecological data using CANOCO. Cambridge University Press, Cambridge

Lesica P, Miles S (2001) Tamarisk growth at the northern margin of its naturalized range in Montana, USA. Wetlands 21(2):240-246

Letey J, Carrillo MLK, Pang XP (2000) Approaches to characterize the degree of water repellency. J Hydrol 231-232:61-65

Letts MG, Roulet NT, Comer NT (2000) Parametrization of peatland hydraulic properties for the Canadian Land Surface Scheme. Atmos Ocean 38(1):141-160

Lewis SA, Robichaud PR, Frazier BE, Wu JQ, Laes DYM (2008) Using hyperspectral imagery to predict post-wildfire soil water repellency. Geomorphology 95:192-205

Lindbo DL, Richardson JL (2001) Hydric Soils and Wetlands in Riverine Systems. In: Richardson JL, Vepraskas MJ (eds) Wetland soils. Genesis, hydrology, landscapes and classification. Lewis Publishers, Boca Raton, Florida

Litaor MI, Eshel G, Reichmann O, Shenker M (2006) Hydrological Control of Phosphorus Mobility in Altered Wetland Soils. Soil Sci Soc Am J 70:1975-1982

Litaor MI, Eshel G, Sade R, Rimmer A, Shenker M (2008) Hydrogeological characterization of an altered wetland. J Hydrol 349:333-349

Llamas MR (1988) Conflicts between wetland conservation and groundwater exploitation: Two case histories in Spain. Environ Geol Water Sci. 11:241-251

López-Camacho B, De Bustamante I, Dorado-Valiño M, Arauzo M (1996) El entorno de Las Tablas: Hidrología (The Las Tablas environment: Hydrology). In: Álvarez-Cobelas M, Cirujano S (eds) Las Tablas de Daimiel. Ecología acuática y sociedad. Publications of the Autonomous Organism NATIONAL PARKS, Madrid, pp 57-63

Manzano M, Borja F, Montes C (2002) Metodología de tipificación hidrológica de los humedales españoles con vistas a su valoración funcional y a su gestión. Aplicación a los humedales de Doñana (Methodology of hydrologic typification of Spanish wetlands for their functional valuation and management) Bol Geol Min 113:313-330

Marimuthu S, Reynolds DA, La Salle CLG (2005) A field study of hydraulic, geochemical and stable isotope relationships in a coastal wetlands system. J Hydrol 315:93-116

MARM (2011) Groundwater Resources in Spain. http://sig.marm.es/recursossub/ Accessed 15 Dec 2011

Martinez CJ, Campbell KL, Annable MD, Kiker GA (2008) An object-oriented hydrologic model for humid, shallow water-table environments. J Hydrol 351:368-381

Martínez Cortina L (2003) Marco hidrológico de la cuenca alta del Guadiana (Hydrologic framework of the Upper Guadiana basin). In: Coleto C, Martínez Cortina L, Llamas MR (eds) Conflictos entre el desarrollo de las aguas subterráneas y la conservación de los humedales: la cuenca alta del Guadiana. Fundación Marcelino Botín. Ediciones Mundi-Prensa, Madrid, pp 3-68

Martínez-Santos P, Castaño S, Santisteban JI, Martínez-Alfaro PE, Mediavilla R, López Pamo E (2004) Tendencias climáticas durante el último siglo (1904-2002) en el Parque Nacional de Las Tablas de Daimiel (Ciudad Real) [Climatic patterns at Las

Tablas de Daimiel National Park during the last century (1904-2002)]. Geo-Temas 6(5):129-132

Martínez-Santos P, de Stefano L, Llamas MR, Martínez-Alfaro PE (2008a) Wetland Restoration in the Mancha Occidental Aquifer, Spain: A Critical Perspective on Water, Agricultural, and Environmental Policies. Restor Ecol 16:511-521

Martínez-Santos P, Llamas MR, Martínez-Alfaro PE (2008b) Vulnerability assessment of groundwater resources: A modelling-based approach to the Mancha Occidental aquifer, Spain. Environ Modell Softw 23:1145-1162

Mataix-Solera J, Arcenegui V, Guerrero C, Mayoral AM, Morales J, González J, García-Orenes F, Gómez I (2007) Water repellency under different plant species in a calcareous forest soil in a semiarid Mediterranean environment. Hydrol Process 21:2300-2309

Mbagwu JSC (1994) Soil physical properties influencing the fitting parameters in Philip and Kostiakov infiltration models. International Centre for Theoretical Physics, IC/94/97 Internal Report, Trieste

McCarthy TS (2006) Groundwater in the wetlands of the Okavango Delta, Botswana, and its contribution to the structure and function of the ecosystem. J Hydrol 320:264-282

McCarthy TS, Bloem A, Larkin PA (1998) Observations on the hydrology and geohydrology of the Okavango Delta. S Afr J Geol 101:101-117

Mediavilla R, Sabtisteban JI, Gil-García MJ, Ruiz-Zapata MB, Castaño S, Mediato JF (2011) El registro sedimentario del Parque Nacional de Las Tablas de Daimiel durante el Holoceno (The Holocene sedimentary record of Las Tablas de Daimiel National Park). In: Programa y resumen de las comunicaciones del XIX Bienal de la Real Sociedad Española de Historia Natural, "Paleoambientes del Cuaternario", Toledo, p 16

Mejías M, López Gutiérrez J, Martínez Cortina L (2012) Características hidrogeológicas y evolución piezométrica de la Mancha Occidental. Influencia del periodo húmedo 2009-2011 (Hydrogeological characteristics and groundwater evolution of the Western La Mancha unit: the influence of the wet period 2009-2011). Bol Geol Min 123(2):91-108

Melendez-Pastor I, Navarro-Pedreño J, Gómez I, Koch M (2010) Detecting drought induced environmental changes in a Mediterranean wetland by remote sensing. Appl Geogr 30:254-262

Mesnage V, Bonneville S, Laignel B, Lefebvre D, Dupont JP, Mikes D (2002) Filling of a wetland (Seine estuary, France): natural eutrophication or anthropogenic process? A sedimentological and geochemical study of wetland organic sediments. Hydrobiol 475/476:423-435

Messerli B, Grosjean M, Hofer T, Núñez L, Pfister C (2000) From nature-dominated to human-dominated environmental changes. Quaternary Sci Rev 19:459-479

Miralles I, Ortega R, Almendros G, Sánchez-Marañón M, Soriano M (2009) Soil quality and organic carbon ratios in mountain agroecosystems of South-east Spain. Geoderma 150:120-128

Mitsch WJ, Gosselink JG (2000) Wetlands. Wiley, New York

Moiwo JP, Lu W, Zhao Y, Yang Y, Yang Y (2010) Impact of land use on distributed hydrological processes in the semi-arid wetland ecosystem of Western Jilin.

Hydrol Process 24:492-503

Momtaz HR, Jafarzadeh AA, Torabi H, Oustan Sh, Samadi A, Davatgar N, Gilkes RJ (2009) An assessment of the variation in soil properties within and between landform in the Amol region, Iran. Geoderma 149:10-18

Moreno L, Aguilera H, Jiménez-Hernández ME, de la Losa A, Jiménez-Pinilla P, Castaño S (2012a) La zona no saturada en el Parque Nacional de las Tablas de Daimiel. Caracterización física y química. Implicaciones desde la perspectiva de la gestión y conservación del parque (The unsaturated zone at Las Tablas de Daimiel National Park. Physical and Chemicals characterization. Implications from a management and conservation point of view). In: Mediavilla (ed) Las Tablas de Daimiel: agua y sedimentos. Medio Ambiente, 14. Instituto Geológico y Minero de España, Madrid, pp 230-258

Moreno L, Jiménez-Hernández ME (2012b) Coal and Peat Fires. A Global Perspective. Chapter 22. Las Tablas de Daimiel National Park and Guadiana River Peat Fires of Spain. 2012 Edited by Glenn B. Stracher, Anupma Prakash and Ellina V. Sokol. Elsevier B.V.

Moreno L, Castaño S, Jiménez ME, Aguilera H, de la Losa A (2007) Control del efecto de la inversión del flujo vertical (descarga a recarga) sobre la composición química del agua subterránea en el Parque Nacional de Las Tablas de Daimiel [Control of the effect of the vertical flux inversion (from discharge to recharge) on the chemical composition of groundwater in Las Tablas de Daimiel National Park]. Resúmenes del I Congreso Nacional sobre Cambio Global, Getafe, p 30

Moreno L, de la Losa A, Jiménez-Hernández ME, Aguilera H, Castaño S (2013) Influencia del zanjón del río Cigüela sobre el humedal del Parque Nacional de as Tablas de Daimiel (España) en periodo de sequía [Influence of the Cigüela River ditch on the wetland of Las Tablas de Daimiel National Park (Spain) in a period of drought]. Cuaternario y Geomorfología (in press)

Moreno L, Jiménez-Hernández ME, Aguilera H, Jiménez P, de la Losa A (2010) The 2009 Smouldering Peat Fire in Las Tablas de Daimiel National Park (Spain). Fire Technol 47:519-538

Mualem Y (1976) A new model for predicting the hydraulic conductivity of unsaturated porous media. Water Resour Res 12:513-522

Muntean DW. Boron, the overlooked essential element.
http://www.soilandplantlaboratory.com/pdf/articles/BoronOverlookedEssential.pdf. Accessed 21 Jan 2010

Nagler PL, Glenn EP, Thompson TL, Huete A (2004) Leaf area index and normalized difference vegetation index as predictors of canopy characteristics and light interception by riparian species on the Lower Colorado River. Agr Forest Meteorol 125:1-17

Navarro V, García B, Asensio L (2012) Characterization of the infiltration rate in Las Tablas de Daimiel National Park, Central Spain. Hydrol Process 26:367-378

Navarro V, García B, Sánchez D, Asensio L (2011) An evaluation of the application of treated sewage effluents in Las Tablas de Daimiel National Park, Central Spain. J Hydrol 401:53-64

Niedermeier A, Robinson JS (2007) Hydrological controls on soil redox dynamics in a peat-based, restored wetland. Geoderma 137:318-326

Niedermeier A, Robinson JS (2009) Phosphorus dynamics in the ditch system of a restored peat wetland. Agr Ecosyst Environ 131(3-4):161-169

O'Drsicoll MA, Parizek RR (2008) Geological controls on seasonal-pool hydroperiod in a karst setting. Wetlands 28:1004-1017

Olde Venterink H, Davidsson TE, Kiehl K, Leonardson L (2002) Impact of drying and re-wetting on N, P and K dynamics in a wetland soil. Plant Soil 243:119-130

Olila OG, Reddy KR, Suites DL (1997) Influence of draining on soil phosphorus forms and distribution in a constructed wetland. Ecol Eng 9:157-169

Oliver YM, Smettem KRJ (2005) Predicting water balance in a sandy soil: model sensitivity to the variability of measured saturated and near saturated hydraulic properties. Aust J Soil Res 43:87-96

Olszta W, Kowalski D (1996) Verification of the van Genuchten method of determination of the hydraulic conductivity of peat soils. Int Agrophys 10:83-87

Ortega-Mayagoitia E, Armengol X, Rojo C (2000) Structure and dynamics of zooplankton in a semi-arid wetland, the National Park Las Tablas de Daimiel (Spain). Wetlands 20:629-638

Owen CR (1995) Water budget and flow pattern in an urban wetland. J Hydrol 169:171-187

Page SE, Siegert F, Rieley JO, Boehm HDV, Jaya A, Limin S (2002) The amount of carbon released from peat and forest fires in Indonesia during 1997. Nature 420:61-65

Pappenberger F, Beven KJ (2006) Ignorance is bliss: Or seven reasons not to use uncertainty analysis. Water Resour Res 42:5302-5310

Pardo A, Ruiz MA (2001) SPSS 10.0. Guía para el análisis de datos (SPSS 10.0. Guide for data anlysis). Hispanoportuguesa SPSS, Madrid

Parhi P, Mishra S, Singh R (2007) A Modification to Kostiakov and Modified Kostiakov Infiltration Models. Water Resources Management 21:1973-1989

Parish F, Sirin A, Charman D, Joosten H, Minaeva T and Silvius M (eds) (2008) Assessment on peatlands, biodiversity and climate change. Global Environment Centre, Kuala Lumpur & Weatlands International, Wageningen

Parker JC, Kool JB, van Genuchten MT (1985) Determining soil hydraulic properties from one-step outflow experiments by parameter estimation: II. Experimental studies. Soil Sci Soc Am J 49:1354-1359

Pascual H (1976) Contribución al estudio ecológico de Las Tablas de Daimiel. I. La vegetación [Contribution to the ecological study of Las Tablas de Daimiel. I. Vegetation] Anales INIA 2:107–128

Patten DT, Rouse L, Stromberg JC (2008) Isolated spring wetlands in the Great Basin and Mojave deserts, USA: potential response of vegetation to groundwater withdrawal. Environ Manage 41:398-413

Pérez-González A (1996) El entorno de Las Tablas: Marco Geológico y Geomorfológico (The Las Tablas environment: Geological and Geomorphological framework). In: Álvarez-Cobelas M, Cirujano S (eds) Las Tablas de Daimiel: Ecología Acuática y sociedad. Ministerio de Medio Ambiente, Madrid, pp 31-35

Pfadenhauer J, Klötzli F (1996) Restoration experiments in middle European wet terrestrial ecosystems: an overview. Vegetatio 126:101-115

Phillips JD (1989) Fluvial sediment storage in wetlands. Water Resour Bull 25:867-873

Plata A (2006) Presente y futuro del tritio natural como herramienta de investigación

hidrológica (Present and future of natural tritium as a tool for hydrologic research). Ingeniería Civil 143:1-15

Reardon J, Hungerford R, Ryan K (2007) Factors affecting sustained smouldering in organic soils from pocosin and pond pine woodland wetlands. Int J Wildland Fire 16:107-118

Rebollo JJ (2007) Hydrological Modelling and Nutrient Transport to the "Las Tablas de Daimiel" Wetland. M.S. thesis, Department of Land and Water Resources Engineering. Royal Institute of Technology (KTH), Stockholm

Reddy KR, DeLaune RD (2008) Biogeochemistry of Wetlands: Science and Applications. CRC Press, Taylor & Francis Group, New York

Rein G (2009) Smouldering Combustion Phenomena in Science and Technology. Int Rev Chem Eng 1:3-18

Rein G, Cleaver N, Ashton C, Pironi P, Torero JL (2008) The severity of smouldering peat fires and damage to the forest soil. Catena 74:304-309

Riaza A, García-Melendez E, Súarez M, Hausold A, Beisl U, Van Der Werff H, Pascual L (2006) Mapping of semi-arid iron bearing red sands on emerged areas around lake marshes (Tablas de Daimiel, Spain) using hyperspectral DAIS 7915 spectrometer data. Ann Geophys 49(1):4565-4582

Richter BD, Baumgartner JV, Powell J, Braun DP (1996) A Method for Assessing Hydrologic Alteration within Ecosystems. Conserv Biol 10:1163-1174

Ritsema CJ, Dekker LW (1994) Soil moisture and dry bulk density patterns in bare dune sands. J Hydrol 154:107-131

Ritsema CJ, Dekker LW (1996) Water repellency and its role in forming preferred flow paths in soils. Aust J Soil Res 34:475-487

Rodríguez-Alleres M, Benito E, de Blas E (2007b) Extent and persistence of water repellency in north-western Spanish soils. Hydrol Process 21:2291-2299

Rodríguez-Alleres M, de Blas E, Benito E (2007a) Estimation of soil water repellency of different particle size fractions in relation with carbon content by different methods. Sci Total Environ 378:147-150

Rodríguez García J, Pérez-González A (1999) Clasificación geomorfológica de los humedales y fondos endorreicos de La Mancha centro – occidental (Geomorphologic classification of wetlands and endorheic basins of central – western La Mancha, Spain). Geogaceta 26:83-86

Rodríguez-Murillo JC, Almendros G, Knicker H (2011) Wetland soil organic matter composition in a Mediterranean semiarid wetland (Las Tablas de Daimiel, Central Spain): Insight into different carbon sequestration pathways. Org Geochem 42:762-773

Rodríguez-Rodríguez M (2007) Hydrogeology of ponds, pools, and playa-lakes of southern Spain. Wetlands 27:819-830

Rodríguez-Rodríguez M, Benavente J (2008) Definition of Wetland Typology for Hydro-morphological Elements Within the WFD. A Case Study from Southern Spain. Water Resour Manag 22:797-821

Rodríguez-Rodríguez M, Moral F, Benavente J (2007) Hydro-morphological characteristics and hydrogeological functioning of a wetland system: a case study in southern Spain. Environ Geol 52:1375-1386

Rodríguez Vidal FJ (2003) Procesos de potabilización del agua e influencia del

tratamiento de ozonización (Processes to make water drinkable and ozonation treatment influence). Ediciones Díaz de Santos, S.A., Madrid

Rogers DB, Dreiss SJ (1995) Saline Groundwater in Mono Basin, California. 1. Distribution. Water Resour Res 31:3131-3150

Rojo C, Barón-Rodríguez MM, Álvarez-Cobelas M, Rodrigo MA (2010) Sustained primary production with changing phytoplankton assemblages in a semiarid wetland. Hydrobiologia 639:55-62

Romanyà J, Rovira P (2009) Organic and inorganic P reserves in rain-fed and irrigated calcareous soils under long-term organic and conventional agriculture. Geoderma 151:378-386

Rudolph DL, Sultan R, Garfias J, McLaren RG (2005) Significance of enhanced infiltration due to groundwater extraction on the disappearance of a headwater lagoon system: Toluca Basin, Mexico. Hydrogeol J 14:115-130

Sáez-Royuela R (1977) Contribución al estudio ecológico de Las Tablas de Daimiel. III. Las aguas (1974-1975) [Contribution to the ecological study of Las Tablas de Daimiel. III. Water (1974-1975)]. Anales INIA, Serie Recursos Naturales 3:101-149

Sala A, Stanley D, Smith AD (1996) Water Use by Tamarix Ramosissima and Associated Phreatophytes in a Mojave Desert Floodplain. Ecol Appl 6(3):888-898

Saltmarsh A, Mauchamp A, Rambal S (2006) Contrasted effects of water limitation on leaf functions and growth of two emergent co-occurring plant species, Cladium mariscus and Phragmites australis. Aquat Bot 84:191-198

Sánchez-Andrés R, Sánchez-Carrillo S, Ortiz-Llorente MJ, Álvarez-Cobelas M, Cirujano S (2010b) Do changes in flood pulse duration disturb soil carbon dioxide emissions in semi-arid floodplains? Biogeochem 101:257-267

Sánchez-Andrés R, Viedma MO, Sánchez-Carrillo S (2010) The effects of anthropogenic stressors on wetland loss and habitat quality deterioration in the Upper Guadiana River basin: a long-term assessment (1970-2000). In: Sánchez-Carrillo S, Angeler DG (eds) Ecology of Threatened Semi-Arid Wetlands: Long-Term Research in Las Tablas de Daimiel. Springer Science+Business Media B.V., pp 85-107

Sánchez-Carrillo S, Álvarez-Cobelas M (2001) Nutrient dynamics and eutrophication patterns in a semi-arid wetland: the effects of fluctuating hydrology. Water Air Soil Poll 131:97-118

Sánchez-Carrillo S, Álvarez-Cobelas M (2010) Climate and Hydrologic Trends: Climate Change Versus Hydrologic Overexploitation as Determinants of the Fluctuating Wetland Hydrology. In: Sánchez-Carrillo S, Angeler DG (eds) Ecology of Threatened Semi-Arid Wetlands: Long-Term Research in Las Tablas de Daimiel. Springer Science+Business Media B.V., pp 45-83

Sánchez-Carrillo S, Álvarez-Cobelas M, Angeler DG (2001) Sedimentation in the semi-arid freshwater wetland Las Tablas de Daimiel (Spain). Wetlands 21:112-124

Sánchez-Carrillo S, Angeler DG, Cirujano S, Álvarez-Cobelas M (2010) The wetland, its catchment settings and socioeconomic relevance: an overview. In: Sánchez-Carrillo S, Angeler DG (eds) Ecology of Threatened Semi-Arid Wetlands: Long-Term Research in Las Tablas de Daimiel. Springer Science+Business Media B.V., pp 3-20

Sánchez-Carrillo S, Angeler DG, Sánchez-Andrés R, Álvarez-Cobelas M, Garatuza-Payán J (2004) Evapotranspiration in semi-arid wetlands: relationships between inundation and the macrophyte cover:open-water ratio. Adv Water Resour 27:643-655

Sánchez-Carrillo, S. and Angeler, D.G. (eds) (2010) Ecology of Threatened Semi-Arid Wetlands: Long-Term Research in Las Tablas de Daimiel. Springer Science+Business Media B.V.

Santisteban JI, Mediavilla R, López-Pamo E, Dabrio CJ, Ruiz-Zapata MB, Gil-García MJ, Castaño S. Martínez-Alfaro PE (2004) Loss on ignition: a qualitative or quantitative method for organic matter and carbonate mineral content in sediments? J Paleolimnol 32:287-299

Santisteban JI, Mediavilla R (2012a) Evolución de las temperaturas y las precipitaciones desde el siglo XIX (Temperature and precipitation patterns since the XIX century). In: Mediavilla (ed) Las Tablas de Daimiel: agua y sedimentos. Medio Ambiente Series, 14. Instituto Geológico y Minero de España, Madrid, pp 17-36

Santisteban JI, Mediavilla R (2012b) Evolución ambiental para los últimos 3000 años a partir de información geoquímica (Environmental changes for the last 3000 years derived from geochemical information). In: Mediavilla (ed) Las Tablas de Daimiel: agua y sedimentos. Medio Ambiente Series, 14. Instituto Geológico y Minero de España, Madrid, pp 187-206

Sarwar A, Bastiaanssen WGM, Boers TM , van Dam JC (2000) Evaluating drainage design parameters for the fourth drainage project, Pakistan by using SWAP Model: Part I- calibration. Irrig Drain Syst 14:257-280

Schaap MG, Leij FJ (1999) Improved prediction of unsaturated hydraulic conductivity with the Mualem-van Genuchten model. Soil Sci Soc Am J 64:843-851

Schaap MG, Leij FJ, Van Genuchten MT (2001) ROSETTA: a computer program for estimating soil hydraulic parameters with hierarchical pedotransfer functions. J Hydrol 251:163-176

Schmid T, Koch M, Gumuzzio J (2005) Multisensor approach to determine changes of wetland characteristics in semiarid environments (Central Spain). IEEE T Geosci Remote 43:2516-2525

Schmid T, Koch M, Gumuzzio J (2005) Multisensor approach to determine changes of wetland characteristics in semiarid environments (central Spain). IEEE T Geosci Remote 43(11):2516-2525

Schmid T, Koch M, Gumuzzio J, Mather PM (2004) A spectral library for a semi-arid wetland and its application to studies of wetland degradation using hyperspectral and multispectral data. Int J Remote Sens 25(13):2485-2496

Schwärzel K, Šimůnek J, Stoffregen H, Wessolek G, van Genuchten MT (2006) Estimation of the Unsaturated Hydraulic Conductivity of Peat Soils. Vadose Zone J 5:628-640

Scorza Júnior RP, da Silva JP, de O Rigitano (2010) Simulation of moisture profiles in a latossol in Dourados region, in the state of Mato Grosso Do Sul, Brazil. Eng Agric, Jaboticabal 30(1):22-32

Servicio Geológico de la Dirección General de Obras Hidráulicas, SGDGOH (1989) Estudio para la ordenación de extracciones del acuífero de la Mancha occidental (Study for the regulation of groundwater extractions in the Mancha

Occidental aquifer). Report 12/89 (unpublished)
Shaffer PW, Kentula ME, Gwin SE (1999) Characterization of wetland hydrology using hydrogeomorphic classification. Wetlands 19:490-504
Sheikh V, van Loon EE (2007) Comparing Performance and Parameterization of a One-Dimensional Unsaturated Zone Model across Scales. Vadose Zone J 6(3):638-650
Sher A, Marshall DL, Gilbert S (2000) Competition between Native Populus deltoides and Invasive Tamarix ramosissima and the Implications for Reestablishing Flooding Disturbance. Conserv Biol 14(6):1744-1754
Shumway RH, Azari RS, Kayhanian M (2002) Statistical approaches to estimating mean water quality concentrations with detection limits. Environ Sci Technol. 36:3345-3353
Sikdar PK, Sahu P (2009) Understanding wetland sub-surface hydrology using geologic and isotopic signatures. Hydrol Earth Syst Sci 13:1313-1323
Šimůnek J, Kodešová R, Gribb MM, van Genuchten MT (1999) Estimating hysteresis in the soil water retention function from cone permeameter experiments. Water Resour Res 35(5): 1329-1345
Šimůnek J, Wendroth O, van Genuchten MT (1998) Parameter estimation analysis of the evaporation method for determining soil hydraulic properties. Soil Sci Soc Am J 62:894-905
Singh R (2005) Water productivity analysis from field to regional scale: integration of crop and soil modelling, remote sensing and geographical information. Ph.D. thesis, Wageningen University, Wageningen
Singh UK, Ren L, Kang S (2010) Simulation of soil water in space and time using an agro-hydrological model and remote sensing techniques. Agr Water Manage 97:1210-1220
Smith RE (1972) The infiltration envelope: results from a theoretical infiltrometer. J Hydrol 17:1-21
Somay AM, Filiz S (2003) Hydrology, hydrogeology and hydrochemistry of wetlands: a case study in Izmir Bird Paradise, Turkey. Environ Geol 43:825-835
Somay AM, Gemici Ü, Filiz S (2008) Hydrogeochemical investigation of Küçük Menderes River coastal wetland, Selçuk–Izmir, Turkey. Environ Geol 55:149-164
Sonneveld MPW (2008) Soil water repellency in an old and young pasture in relation to N application. Soil Use Manage 24:310-317
Sophocleous M (2002) Interactions between groundwater and surface water: the state of the science. Hydrogeol J 10:52-67
Staes J, Rubarenzya MH, Meire P, Willems P (2009) Modelling hydrological effects of wetland restoration: a differentiated view. Water Sci Technol 59:433-441
Stolte J (1997) Determination of the saturated hydraulic conductivity using the constant head method. Manual for soil physical measurements, version 3. DLO, Winand Staring Centre, Wageningen
Stracher GB, Taylor TP (2004) Coal fires burning out of control around the world: thermodynamic recipe for environmental catastrophe. Int J Coal Geol 59:7-17
Sutherland RA (1998) Loss-on-ignition estimates of organic matter and relationships to organic carbon in fluvial bed sediments. Hydrobiologia 389:153-167
Sutula MA, Perez BC, Reyes E, Childers DL, Davis S, Day JW, Rudnick D, Sklar F (2003)

Factors affecting spatial and temporal variability in material exchange between the Southern Everglades wetlands and Florida Bay (USA). Estuar Coast Shelf S 57:757-781

Takii S, Fukui M (1996) Comparison of anaerobic mineralization processes in sediments between littoral reed and offshore sites in a shallow hypertrophic lake. Hydrobiol 319:37-45

Taümer K, Stoffregen H, Wessolek G (2005) Determination of repellency distribution using soil organic matter and water content. Geoderma 125:107-115

Thiere G, Milenkovski S, Lindgren P-E, Sahlén G, Berglund O, Weisner SEB (2009) Wetland creation in agricultural landscapes: Biodiversity benefits on local and regional scales. Biol Conserv 142:964-973

Tiemeyer B, Frings J, Kahle P, Köhne S, Lennartz B (2007) A comprehensive study of nutrient losses, soil properties and groundwater concentrations in a degraded peatland used as intensive meadow – Implications for re-wetting. J Hydrol 345: 80-101

Trepel M, Dall'O' M, Dal Cin L, De Wit M, Opitz S, Palmeri L, Persson J, Pieterse NM, Timmermann T, Bendoricchio G, Kluge W, Jørgensen S-E (2000) Models for wetland planning, design and management. EcoSys Bd 8:93-137

Tucker KA, Karnok KJ, Radcliffe DE, Landry GJr, Roncadori RW, Tan KH (1990) Localized dry spots as caused by hydrophobic sands on bentgrass greens. Agron J 82:549-555

United States Department of Agriculture (USDA) (2010) Keys to soil taxonomy, 11th edn

Valett HM, Baker MA, Morrice JA, Crawford CS, Molles MCJ, Dahm CN, Moyer DL, Thibault JR, Ellis LM (2005) Biogeochemical and Metabolic Responses to the Flood Pulse in a Semiarid Floodplain. Ecology 86:220-234

Vallejos A, Pulido-Bosch A, Molina L, Sánchez-Martos F, Gisbert J, Martín Rosales W (2002) Contribución del contenido en tritio a la identificación del origen del agua subterránea: Sierra de Gádor (Almería) (Contribution of the tritium content for the identification of groundwater origin: Gádor Range (Almería)) Geogaceta 31:83-85

van Dam JC (2000) Field-scale water flow and solute transport. SWAP model concepts, parameter estimation and case studies. Ph.D. thesis, Wageningen University, Wageningen

van der Kamp G, Hayashi M (2009) Groundwater-wetland ecosystem interaction in the semiarid glaciated plains of North America. Hydrogeol J 17:203-214

van Duren IC, Pegtel DM (2000) Nutrient limitations in wet, drained and rewetted fen meadows: evaluation of methods and results. Plant Soil 220:35-47

van Genuchten MT (1980) A closed form equation for predicting the hydraulic conductivity of unsaturated soils. Soil Sci Soc Am J 44:892-898

van Genuchten MT, Leij FJ, Yates SR (1991) The RETC code for quantifying the hydraulic functions of unsaturated soils. U.S. Salinity Laboratory, Riverside, California

van Reeuwijk LP (2002) Procedures for Soil Analysis. 6th ed. ISRIC (Internacional Soil Reference and Information Centre), Wageningen.

van Schaik NLMB, Hendriks RFA, van Dam JC (2010) Parameterization of Macropore Flow Using Dye-Tracer Infiltration Patterns in the SWAP Model. Vadose Zone J

9:95-106

Verheijen FGA, Cammeraat LH (2007) The association between three dominant shrub species and water repellent soils along a range of soil moisture contents in semi-arid Spain. Hydrol Process 21:2310-2316

Vestin JLK, Nambu K, van Hess PAW, Bylund D, Lundström US (2006) The influence of alkaline and non-alkaline parent material on soil chemistry. Geoderma 135: 97-106

Visconti F, de Paz JM, Rubio JL (2009) Principal component analysis of chemical properties of soil saturation extracts from an irrigated Mediterranean area: Implications for calcite equilibrium in soil solutions. Geoderma 151:407-416

Visconti F, de Paz JM, Rubio JL (2010) What information does the electrical conductivity of soil water extracts of 1 to 5 ratio (w/v) provide for soil salinity assessment of agricultural irrigated lands? Geoderma 154:387-397

Vogel T, van Genuchten MT, Cislerova M (2000) Effect of the shape of the soil hydraulic functions near saturation on variably-saturated flow predictions. Adv Water Resour 24:133-144

Wallach R, Graber ER (2007) Infiltration into effluent irrigation-induced repellent soils and the dependence of repellency on ambient relative humidity. Hydrol Process 21:2346-2355

Wang M, Qin D, Lu C, Li Y (2010) Modeling Anthropogenic Impacts and Hydrological Processes on a Wetland in China. Water Resour Manag 24:2743-2757

Wang Y, Zhang X, Huang C (2009a) Spatial variability of soil total nitrogen and soil total phosphorus under different land uses in a small watershed on the Loess Plateau, China. Geoderma 150:141-149

Wang Y, Zhang X, Zhang J, Li S (2009b) Spatial variability of soil organic carbon in a watershed on the Loess Plateau. Pedosphere 19(4):486-495

Weiss R, Alm J, Laiho R, Laine J (1998) Modeling moisture retention in peat soils. Soil Sci Soc Am J 62:305-313

Wesseling JG (2013) FitGWL: a software tool to find the bottom boundary condition of SWAP that minimizes the difference between measured and calculated groundwater levels. Report. Alterra, Wageningen (In prep)

Wesseling JG, Stoof CR, Ritsema CJ, Oostindie K, Dekker LW (2009) The effect of soil texture and organic amendment on the hydrological behaviour of coarse-textured soils. Soil Use Manage 25:274-283

Wind GP (1968) Capillary conductivity data estimated by a simple method. In: Rijtema PE, Wassink H (eds) Water in the unsaturated zone. Proc Wageningen Symp, June 1966. Vol. 1. IASAH, Gentbrugge, pp 19-23

Winter TC (1999) Relation of streams, lakes, and wetlands to groundwater flow systems. Hydrol Process 7:28-45

Wöhling T, Vrugt JA, Barkle GF (2008) Comparison of Three Multiobjective Optimization Algorithms for Inverse Modeling of Vadose Zone Hydraulic Properties. Soil Sci Soc Am J 72:305-319

Wolski P, Savenije HHG (2006) Dynamics of floodplain-island groundwater flow in the Okavango Delta, Botswana. J Hydrol 320:283-301

Wolski P, Savenije HHG, Murray-Hudson M, Gumbricht T (2006) Modelling of the flooding in the Okavango Delta, Botswana, using a hybrid reservoir-GIS model. J

Hydrol 331:58-72

Wösten JHM, Lilly A, Nemes A, Le Bas C (1999) Development and use of a database of hydraulic properties of European soils. Geoderma 90:169-185

Wösten JHM, van Genuchten MT (1988) Using texture and other soil properties to predict the unsaturated soil hydraulic functions. Soil Sci Soc Am J 52:1762-1770

Wu L, Pan L, Mitchell J, Sanden B (1999) Measuring Saturated Hydraulic Conductivity using a Generalized Solution for Single-Ring Infiltrometers. Soil Sci Soc Am J 63:788-792

Xie T, Yang Z (2009) Effects of water stress on photosynthetic parameters of Phragmites australis in estuarine wetland of Yellow River Delta. Ying yong sheng tai xue bao = The journal of applied ecology 20(3):562-568

Yates SR, van Genuchten MT, Leij FJ (1989) Analysis of predicted hydraulic conductivities using RETC. In: van Genuchten MT, Leij FJ (eds) Proceedings of the International Workshop on Indirect Methods for Estimating the Hydraulic Properties of Unsaturated Soils, Riverside, California, pp 273-283

Young FJ, Hammer RD, Larsen D (1999) Frequency distribution of soil properties on a loess-mantled Missouri watershed. Soil Sci Soc Am J 63: 178-185

Zak D, Gelbrecht J (2007) The mobilisation of phosphorus, organic carbon and ammonium in the initial stage of fen rewetting (a case study from NE Germany). Biogeochem 85:141-151

Zedler JB (2000) Progress in wetland restoration ecology. Tree 15:402-407

Zedler JB, Kercher S (2005) Wetland Resources: Status, Trends, Ecosystem Services, and Restorability. Annu Rev Env Resour 30:39-74

Zhang C, Fay D, McGrath D, Grennan E, Carton OT (2008) Statistical analyses of geochemical variables in soils of Ireland. Geoderma 146:378-390

Zhao R, Chen Y, Zhou H, Li Y, Qian Y, Zhang L (2009) Assessment of wetland fragmentation in the Tarim River basin, western China. Environ Geol 57:455-464

Ziogas AK, Dekker LW, Oostindie K, Ritsema CJ (2005) Soil water repellency in north-eastern Greece with adverse effects of drying on the persistence. Aust J Soil Res 43:281-289

Zorrilla P, Carmona G, De la Hera Á, Varela-Ortega C, Martínez-Santos P, Bromley J, Jorgen Henriksen H (2010) Evaluation of bayesian networks as a tool for participatory water resources management: application to the Upper Guadiana basin in Spain. Ecol Soc 15(3)

APPENDIX A

Soil profiles

A.1. Descriptive columns from random soil profiles sampled in January 2008 in Las Tablas de Daimiel National Park

POINT 1

X (UTM)= 446147
Y (UTM)= 4338718

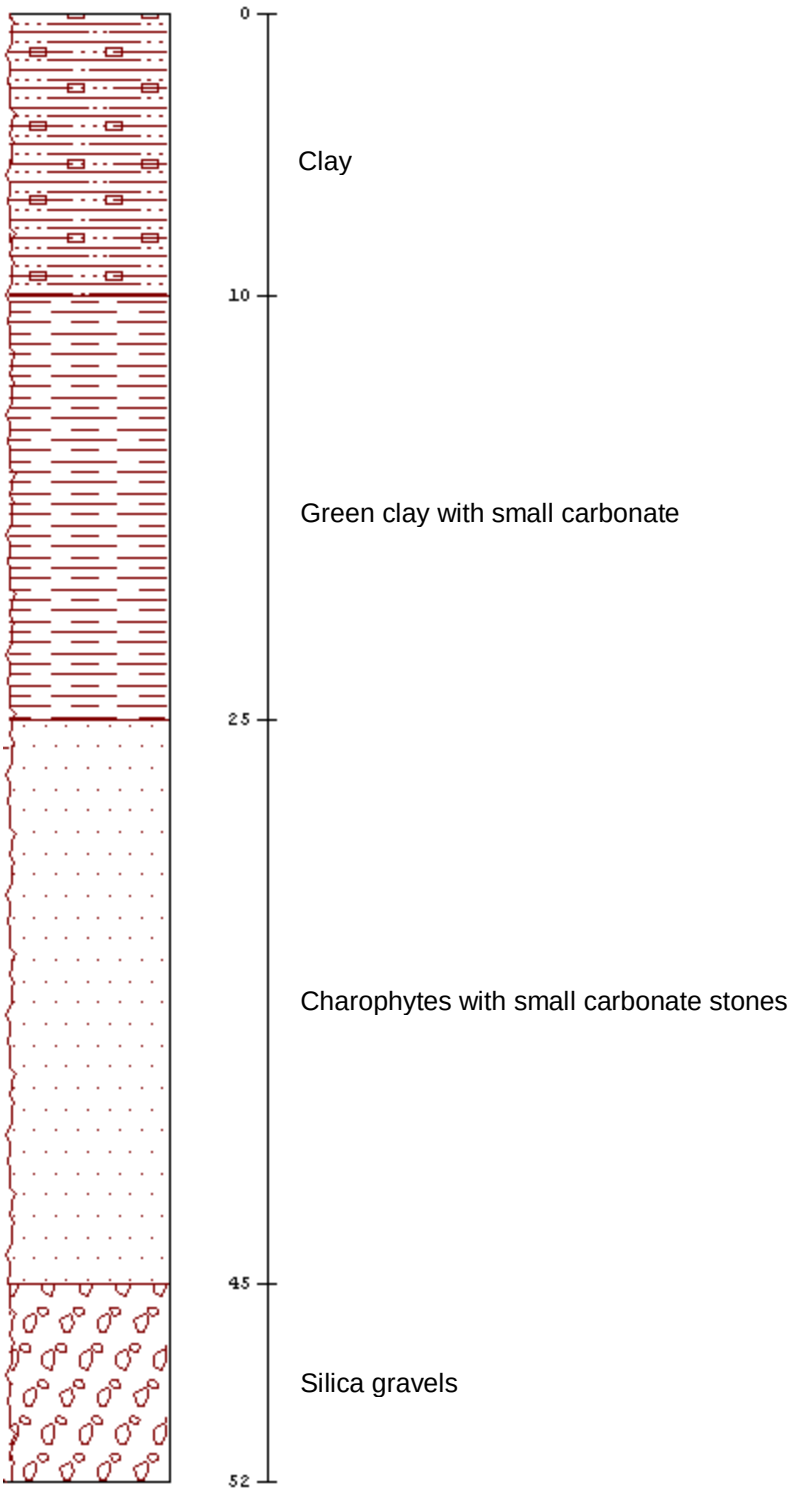

POINT 2

X= 445162
Y= 4338310

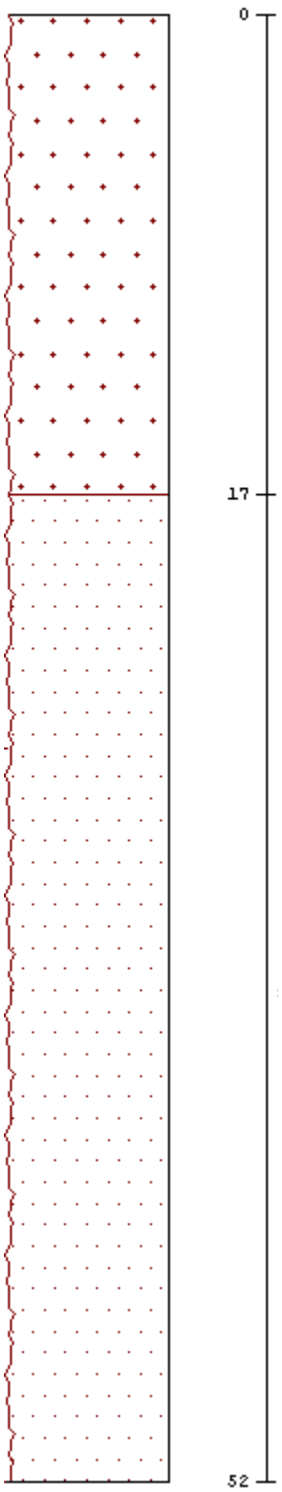

Disturbed grey sands with carbonate pebbles

Silica sands mixed with fluvial silts and charophytes matrix

POINT 3

X= 443969
Y= 4336736

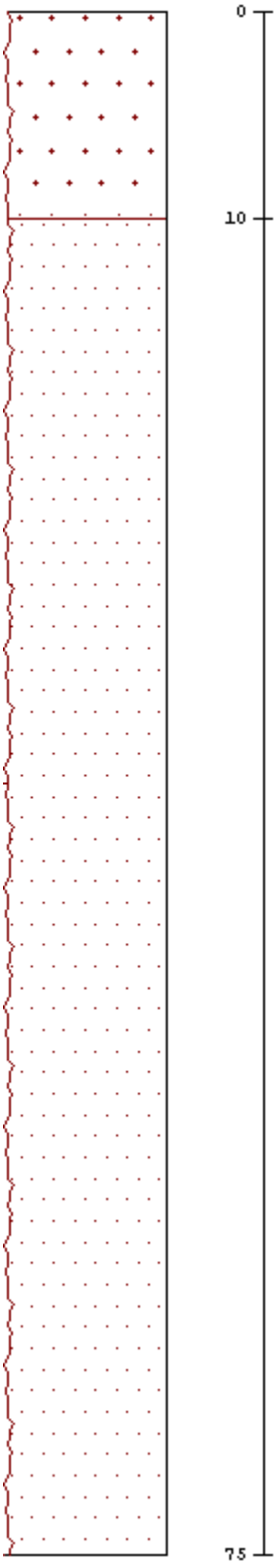

Disturbed grey sands

Very thin sand with charophytes and silica inclusions, and silty-clayey matrix

POINT 4

X= 442644
Y= 4336785

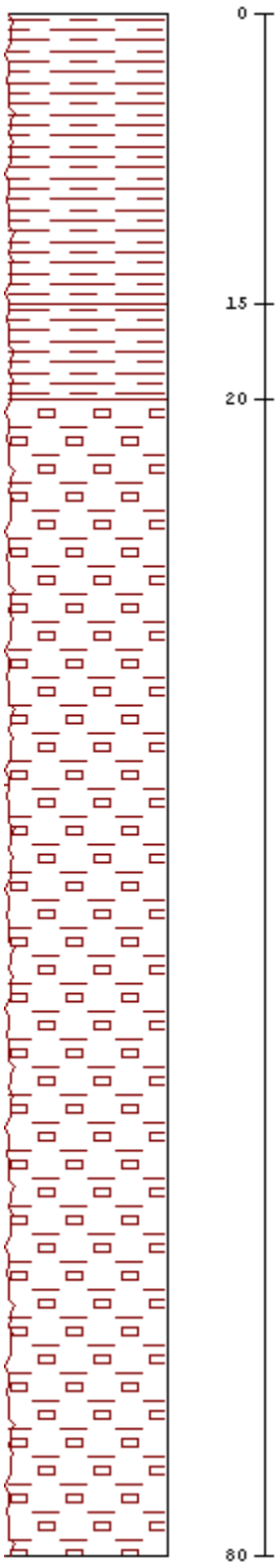

Disturbed green clay

Green clay with oxidized ochre

Green clay with salts

POINT 5

X= 442200
Y= 4336340

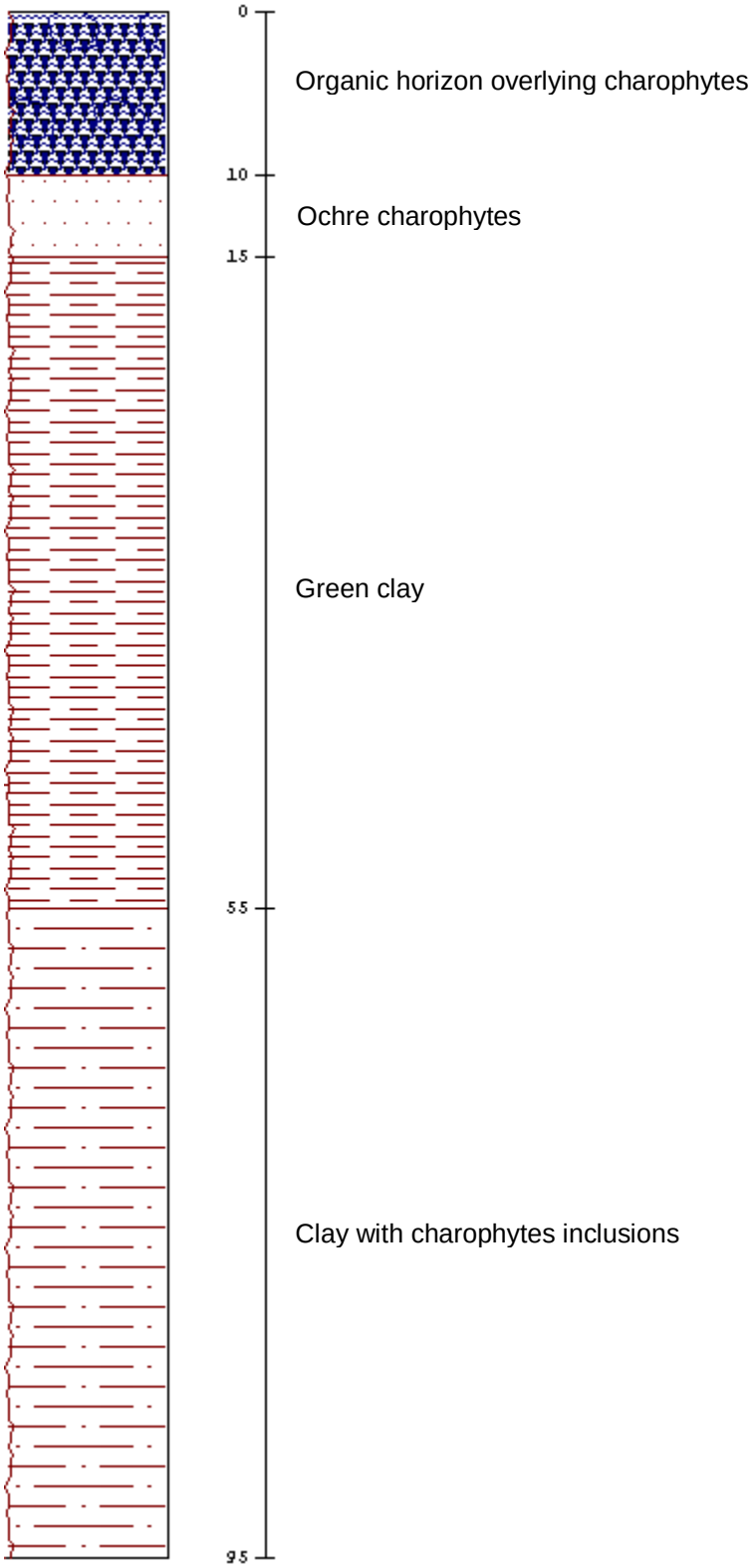

POINT 6

X= 442121
Y= 4336624

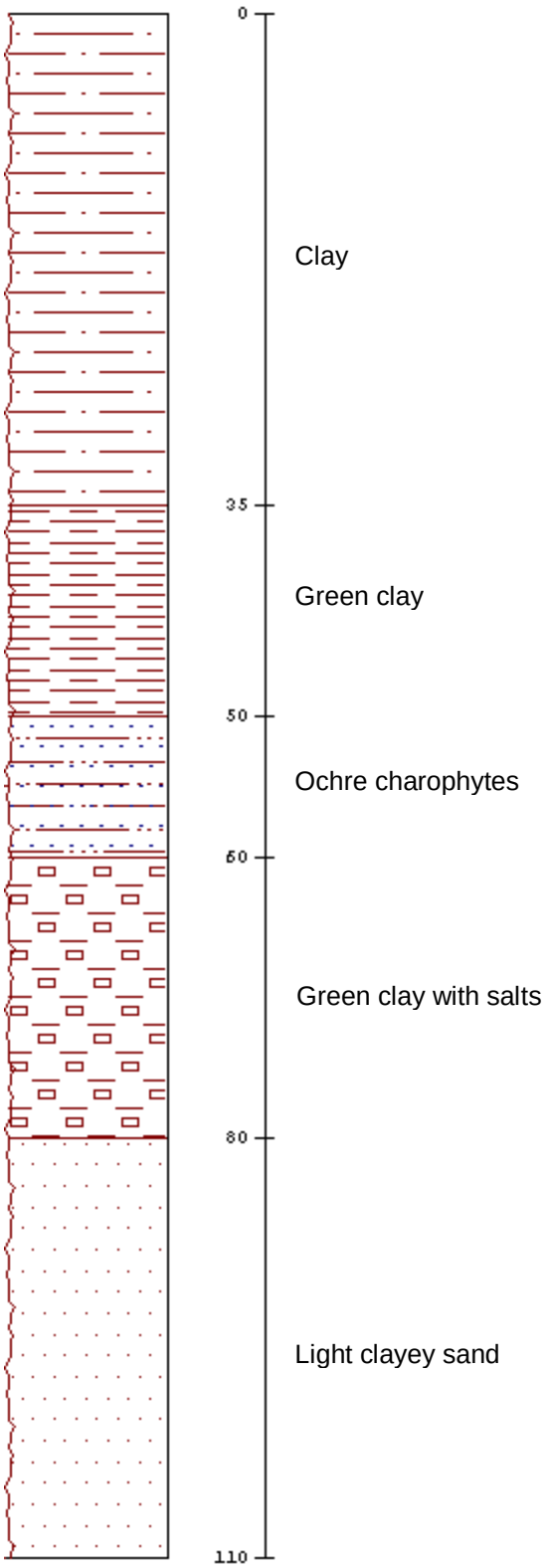

POINT 7

X= 441918
Y= 4335906

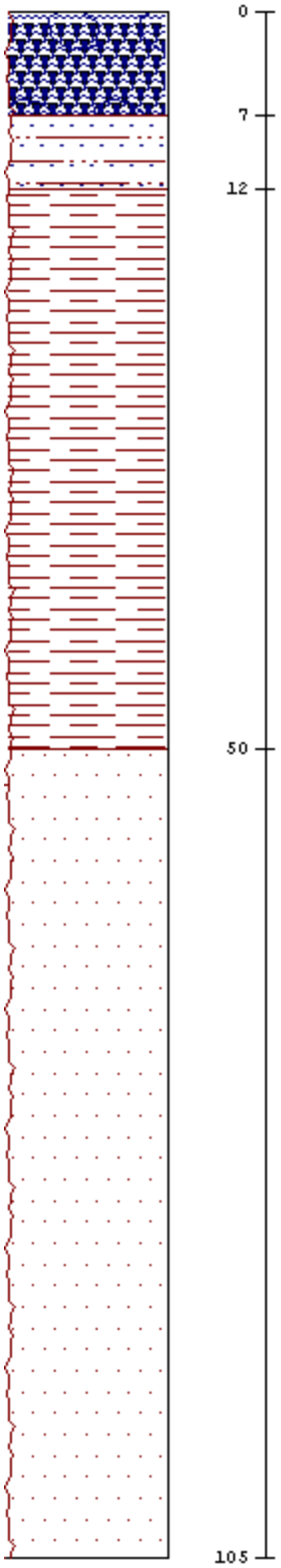

POINT 8

X= 441546
Y= 4335781

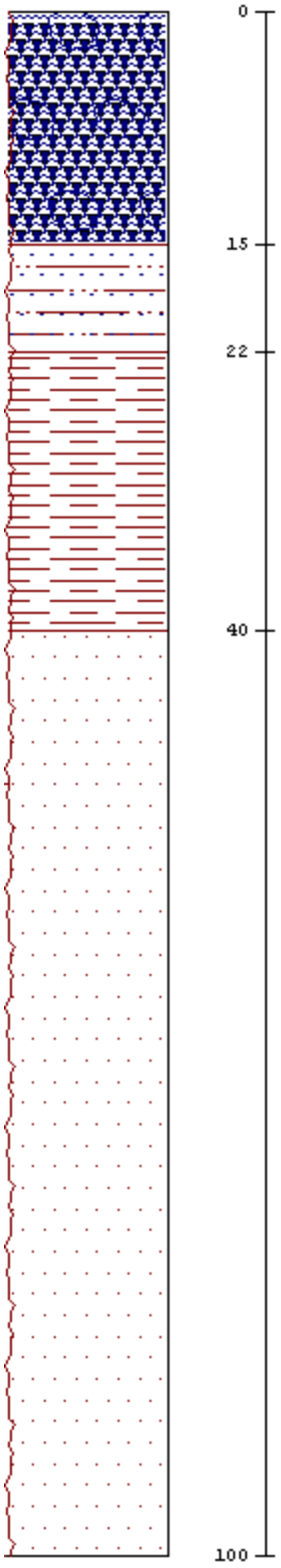

Charophytes and green clay overlaid by organic horizon

Charophytes

Green clay

Sand with quartzite and oxidation footprints

POINT 9

X= 441583
Y= 4335878

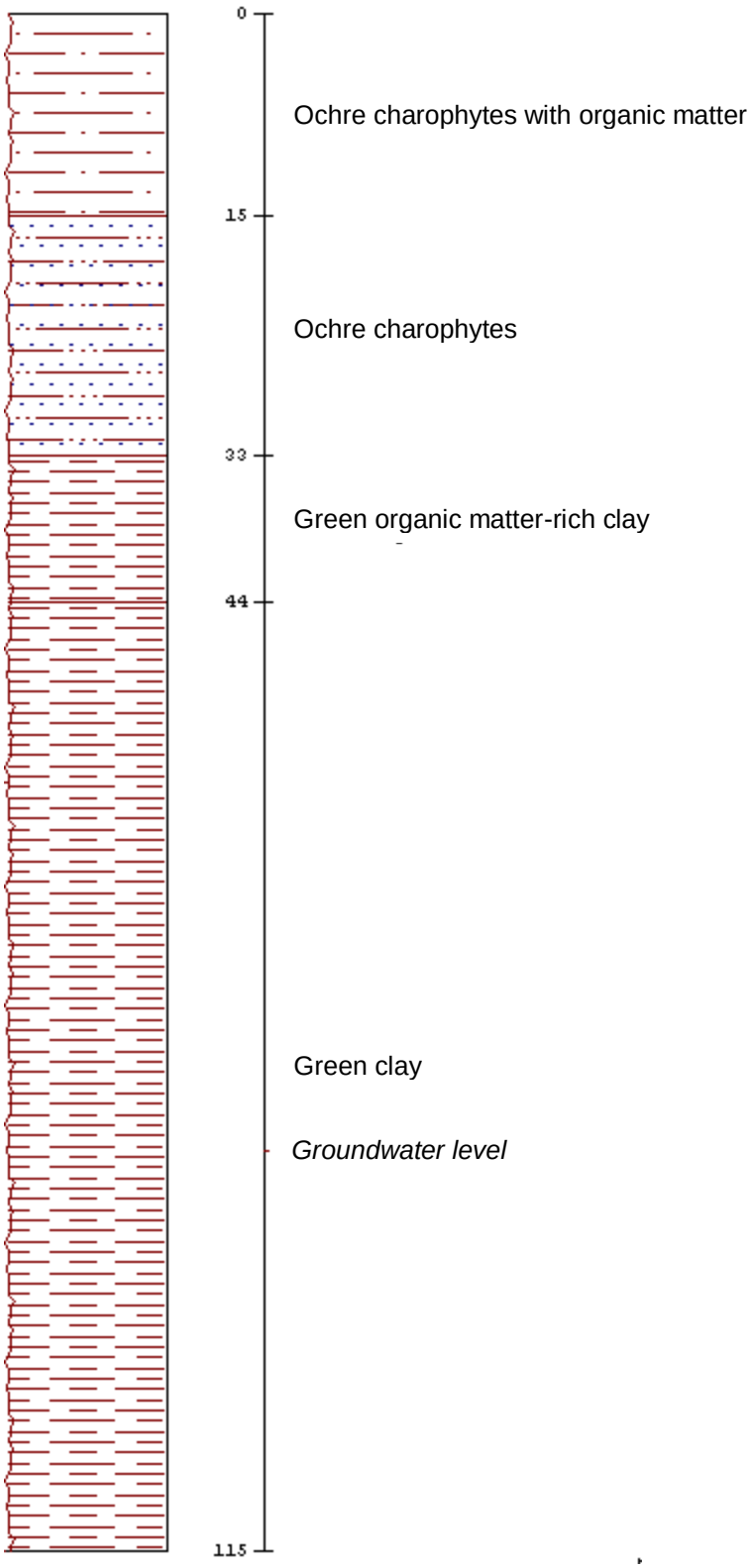

POINT 10

X= 441615
Y= 4335963

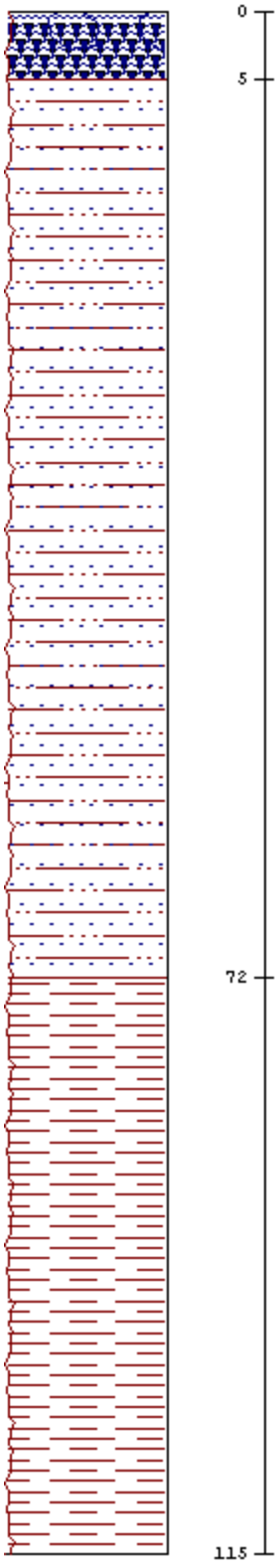

Organic horizon

Charophytes

Green clay with oxidation footprints from 95 cm

POINT 11

X= 441651
Y= 4336095

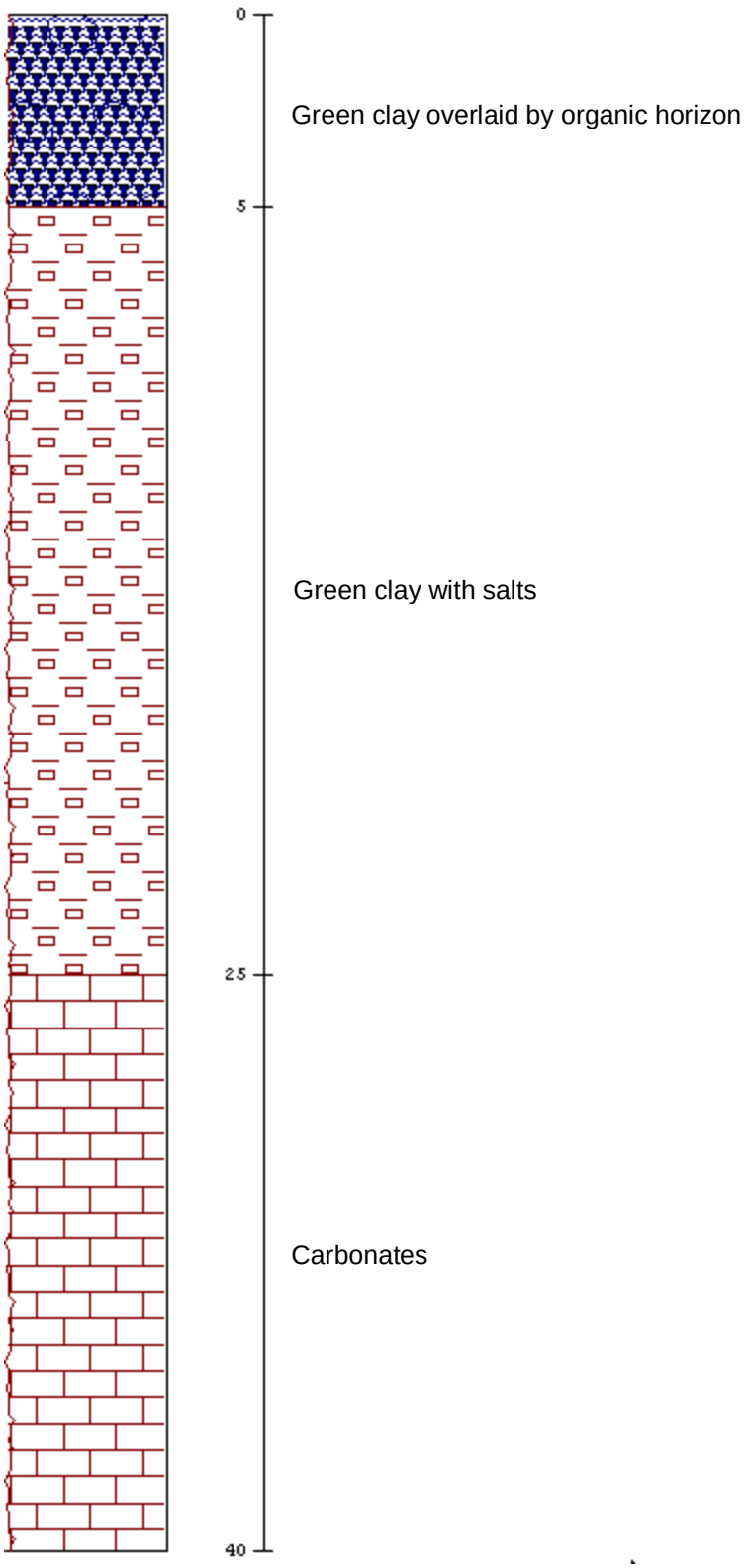

POINT 12

X= 441682
Y= 4336221

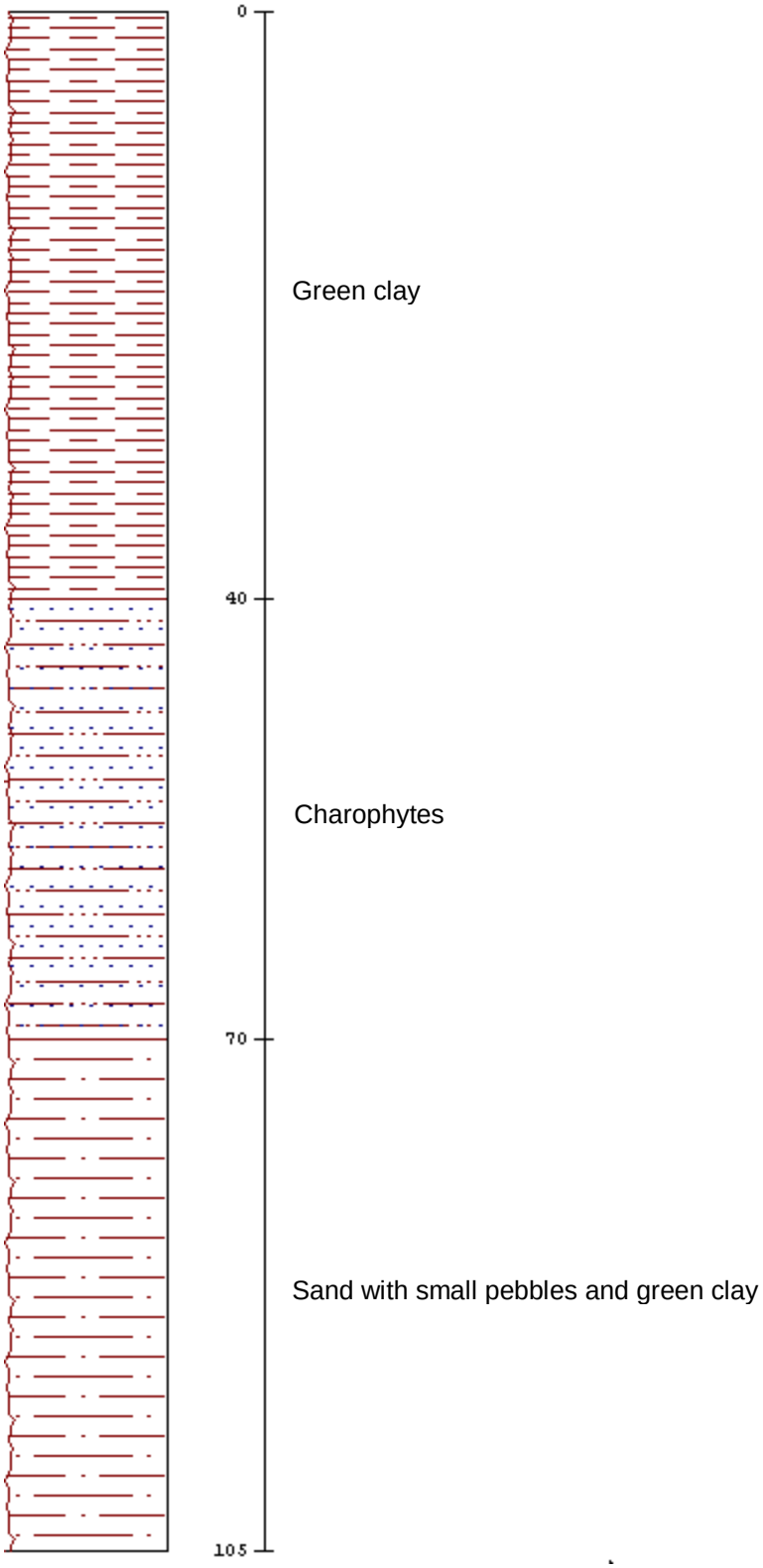

POINT 13

X= 441684
Y= 4336253

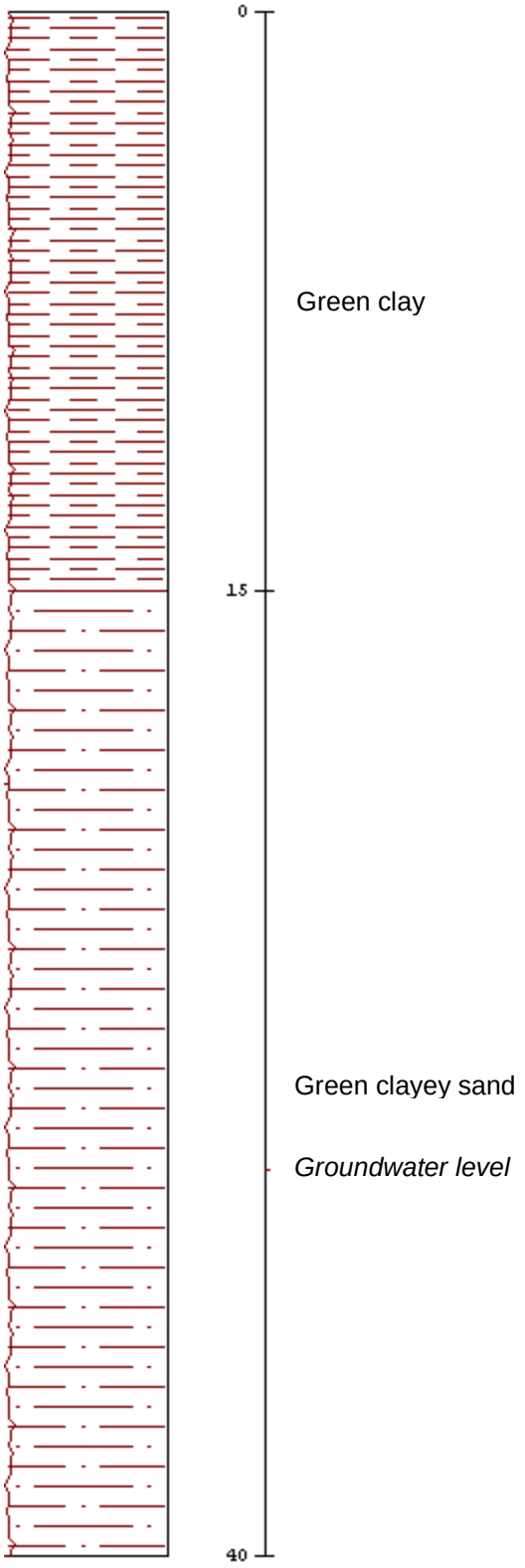

POINT 14

X= 434340
Y= 4329745

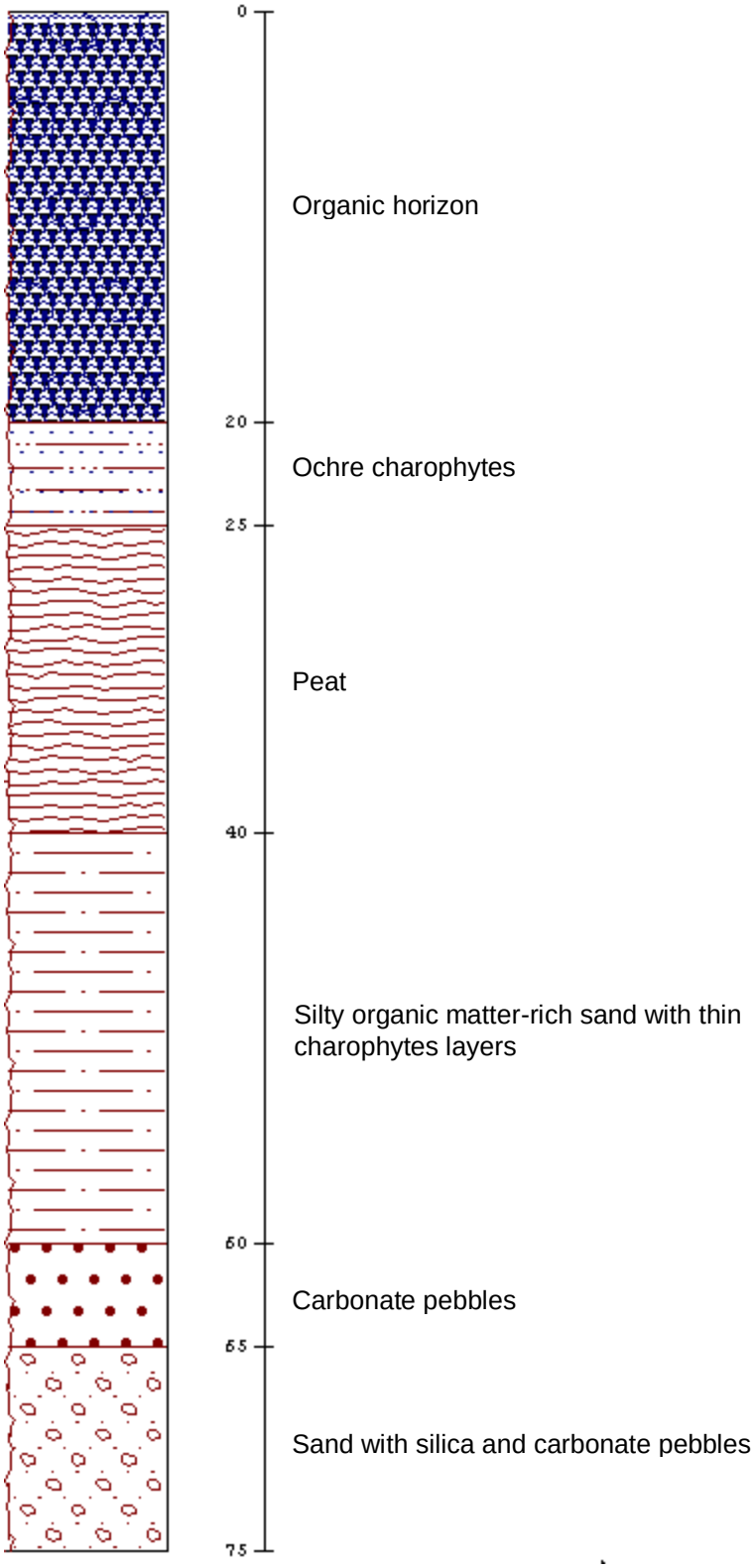

POINT 15

X= 434417
Y= 4329787

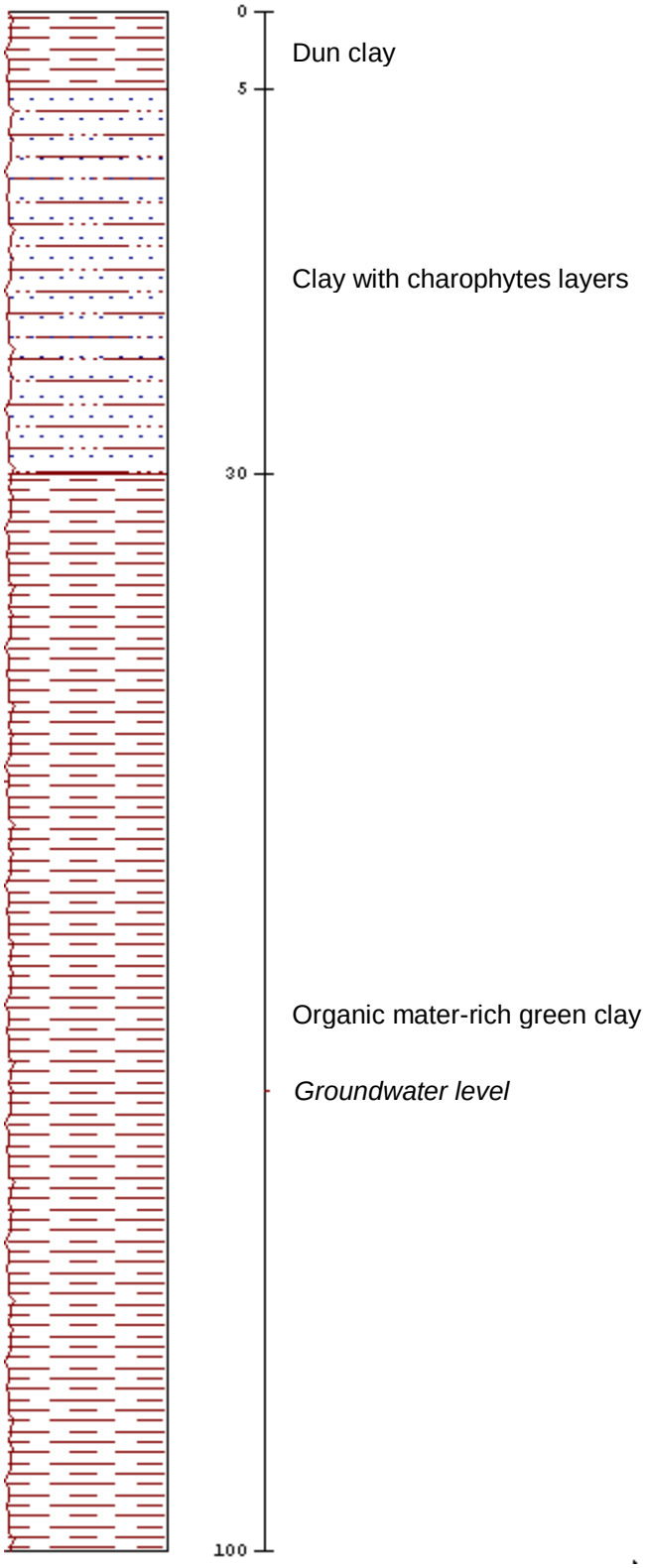

POINT 16

X= 438144
Y= 4330940

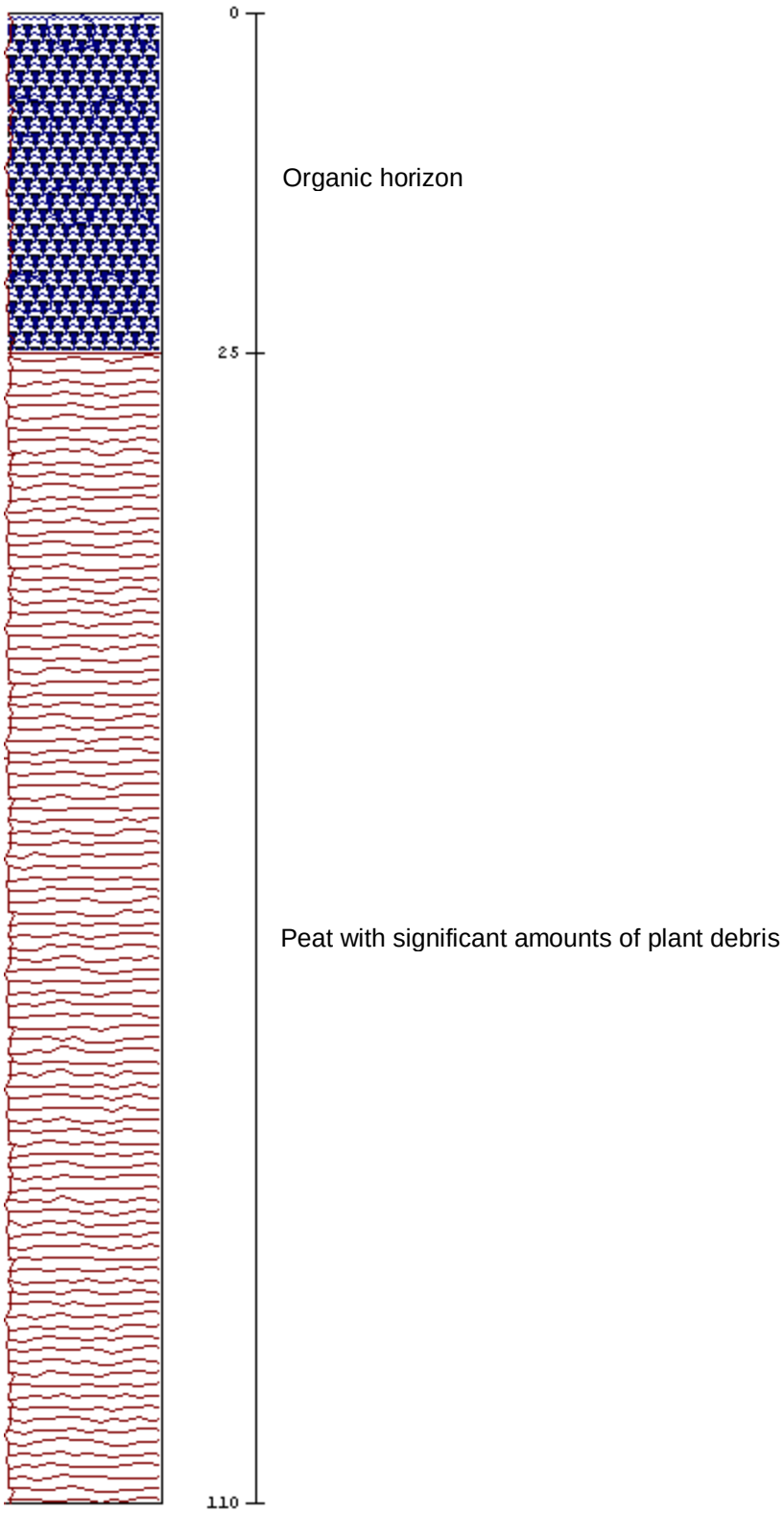

POINT 17

X= 437745
Y= 4331189

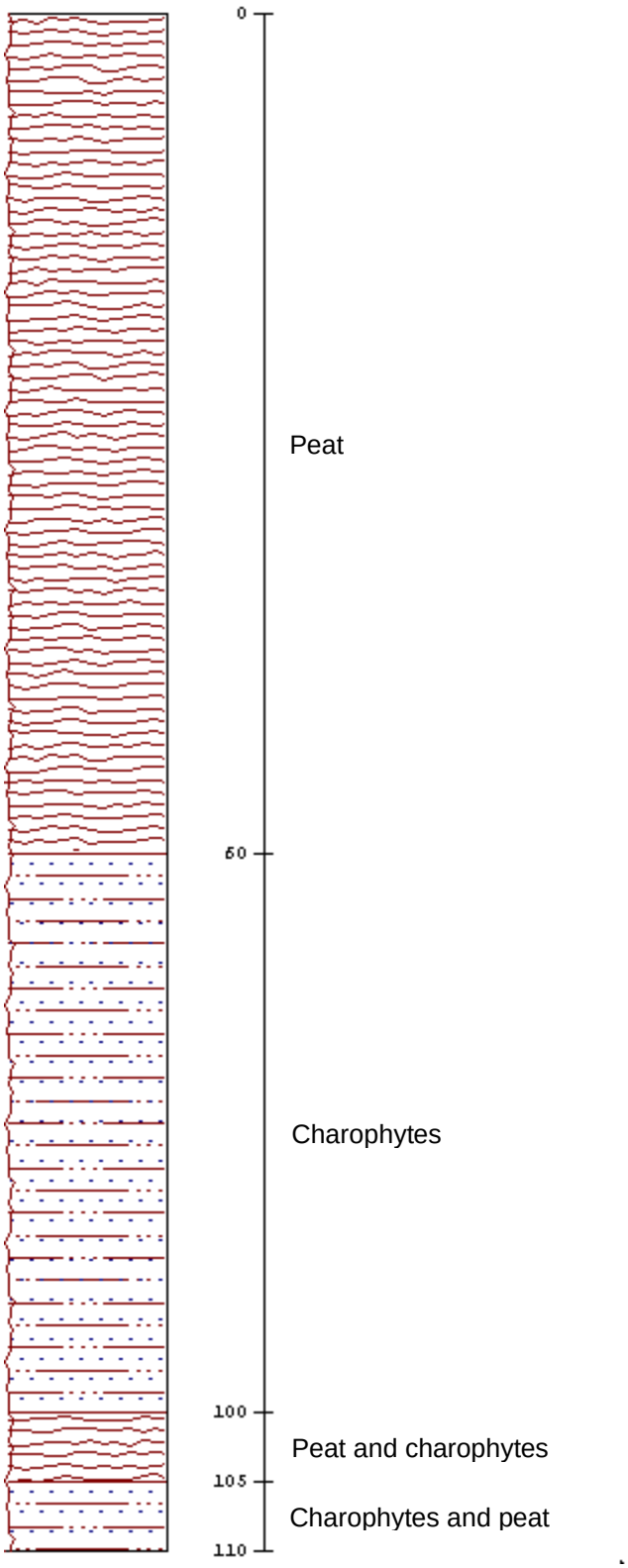

POINT 18

X= 440453
Y= 4331459

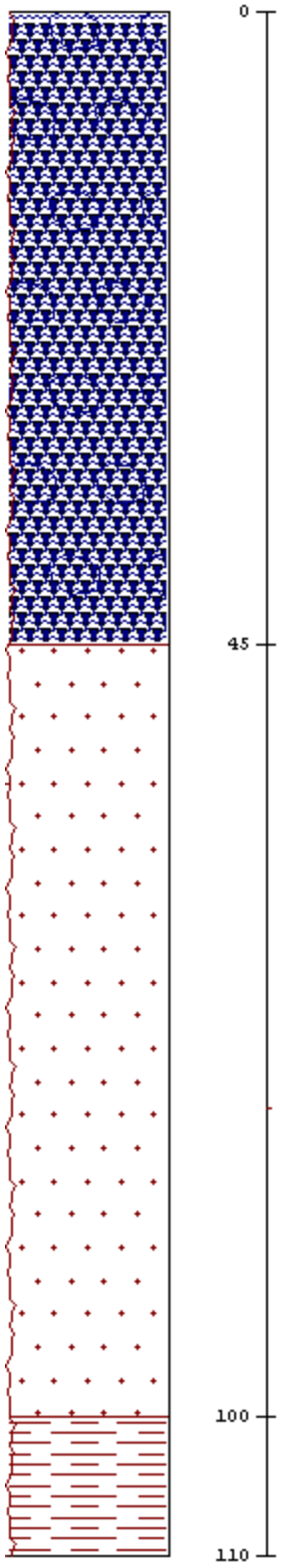

POINT 19

X= 439934
Y= 4333183

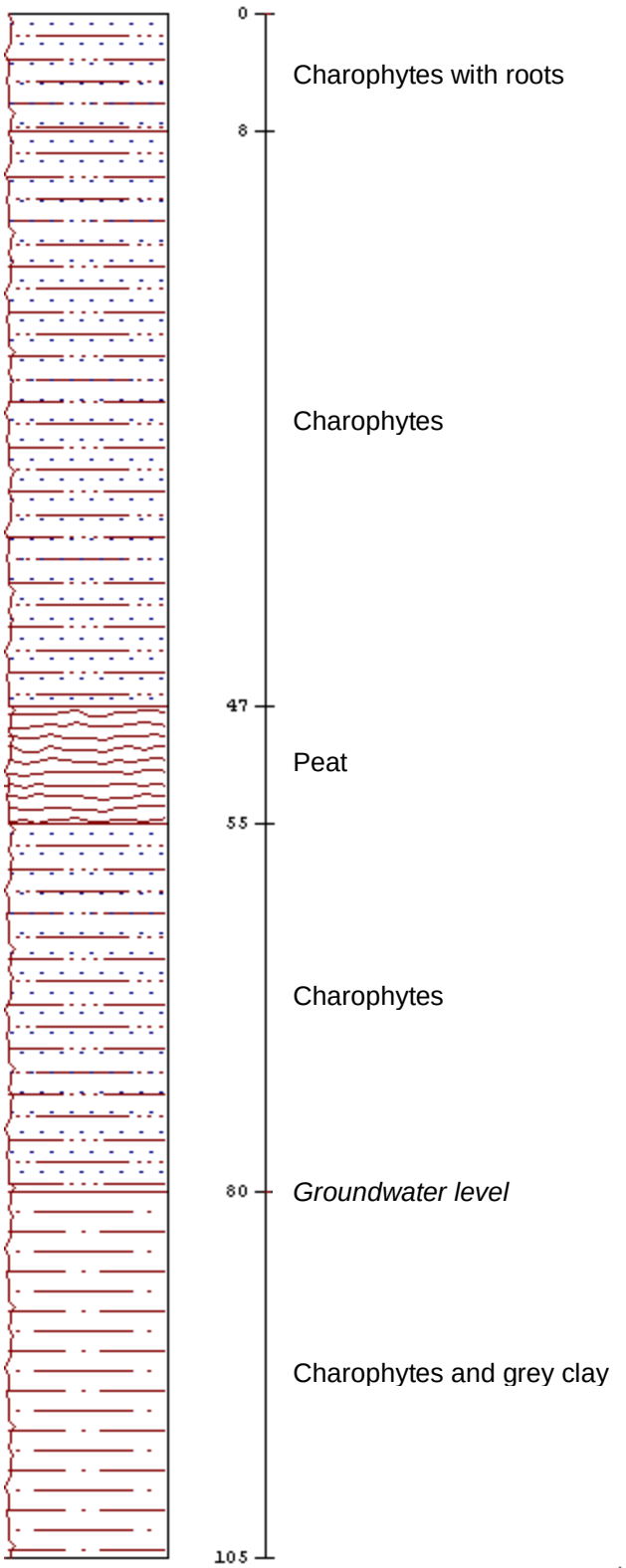

POINT 20

X= 439840
Y= 4333348

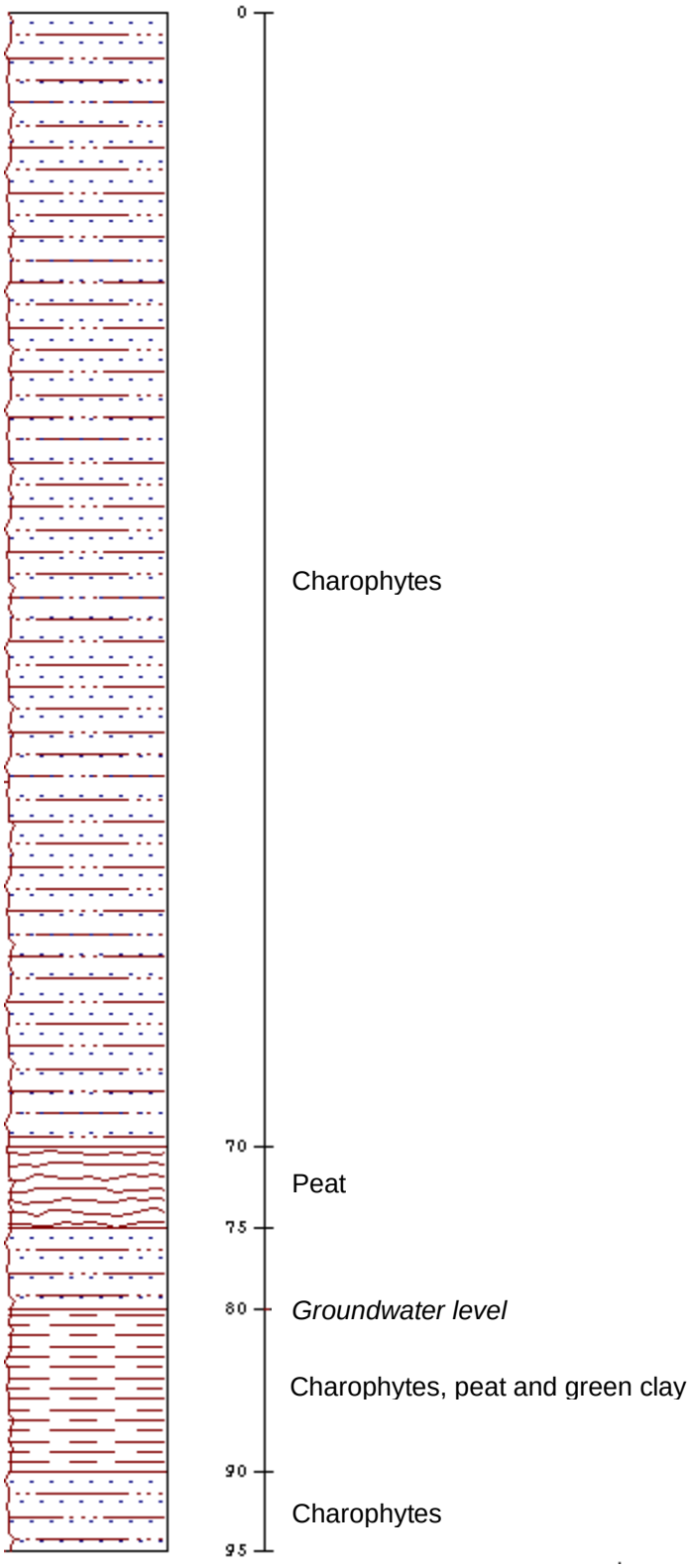

POINT 21

X= 441011
Y= 4334714

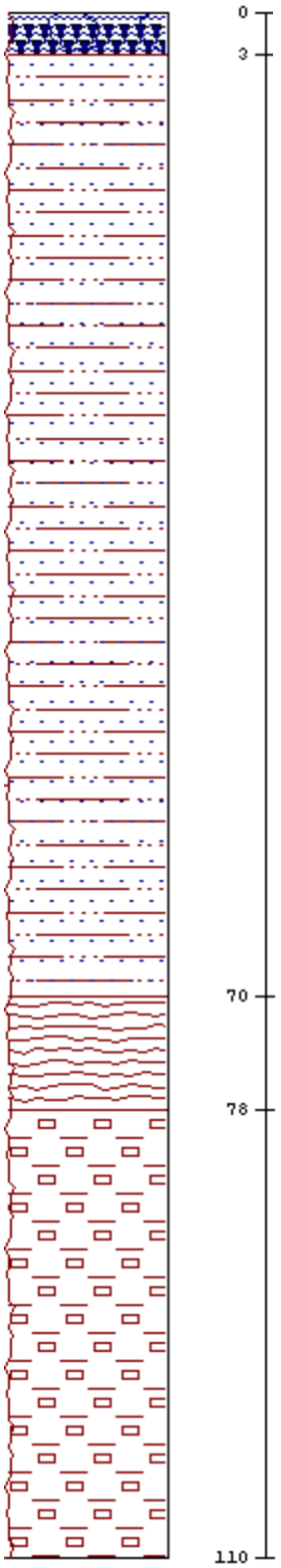

POINT 22

X= 440825
Y= 4334662

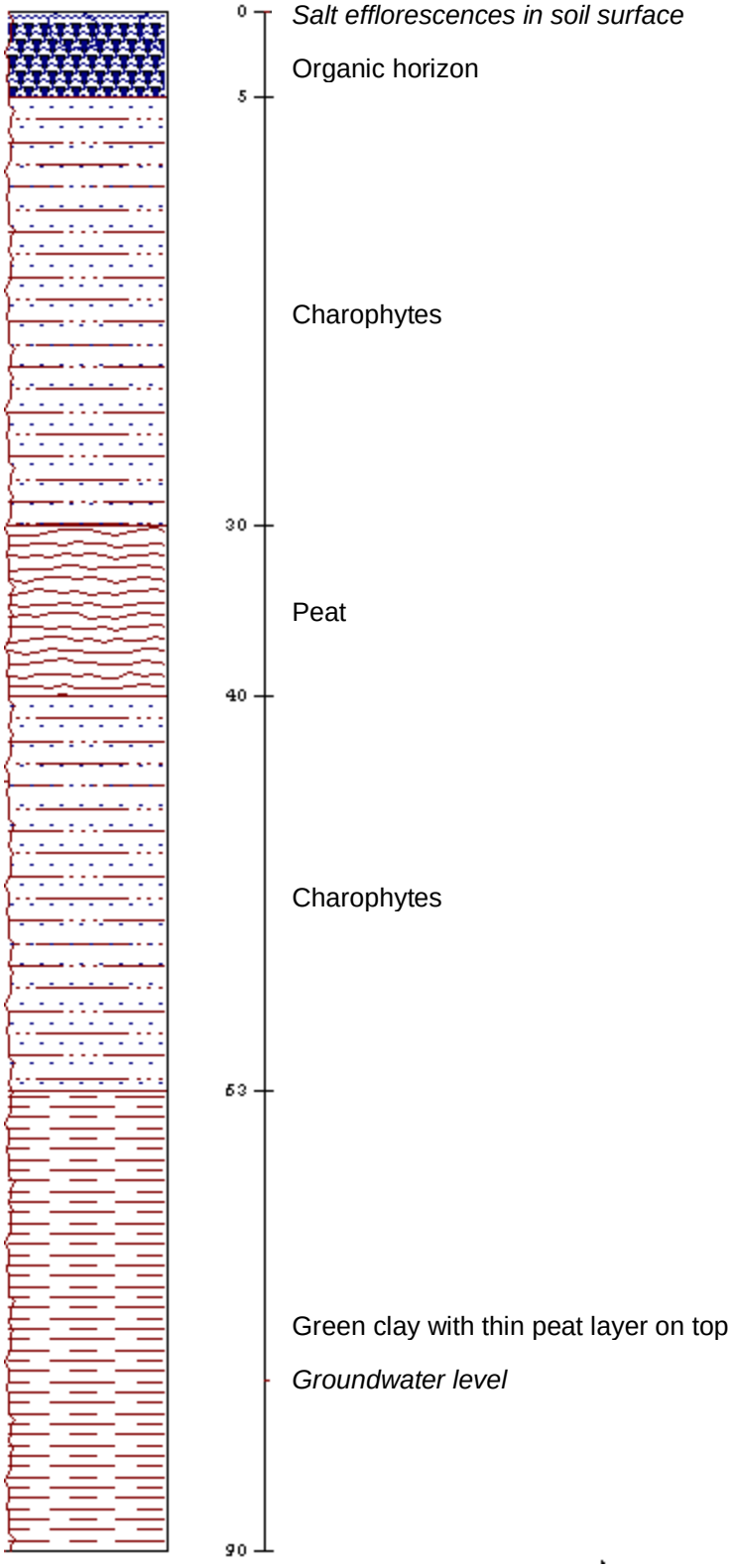

POINT 23

X= 440592
Y= 4334765

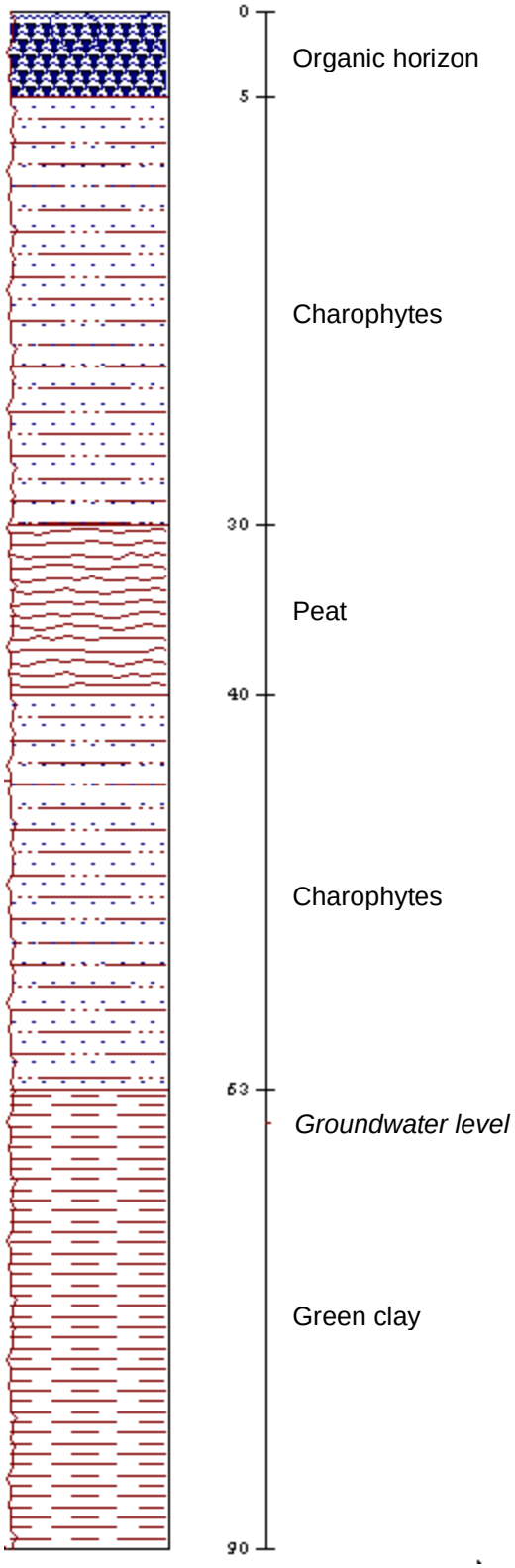

POINT 24

X= 440434
Y= 4334807

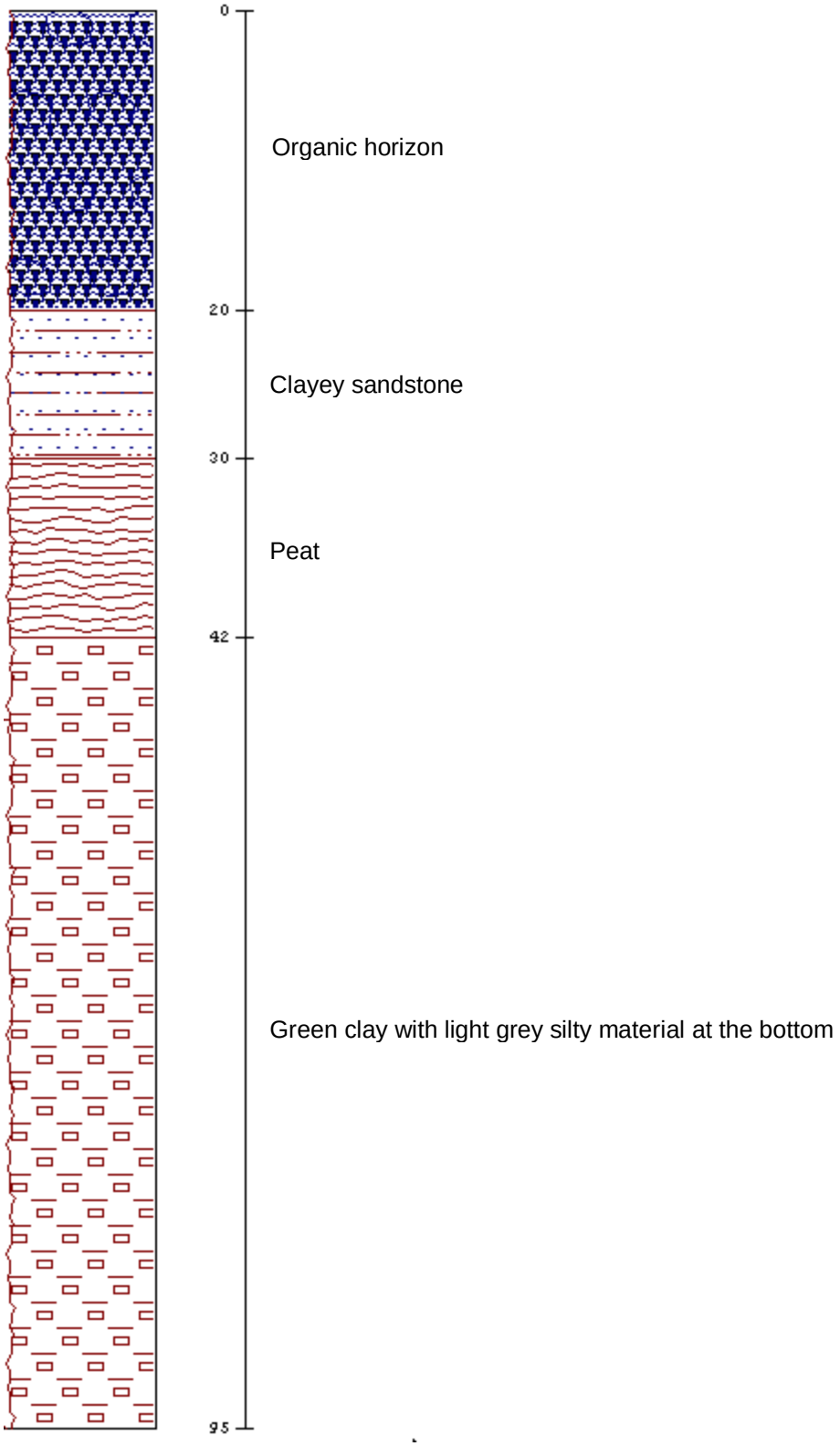

POINT 25

X= 441020
Y= 4335695

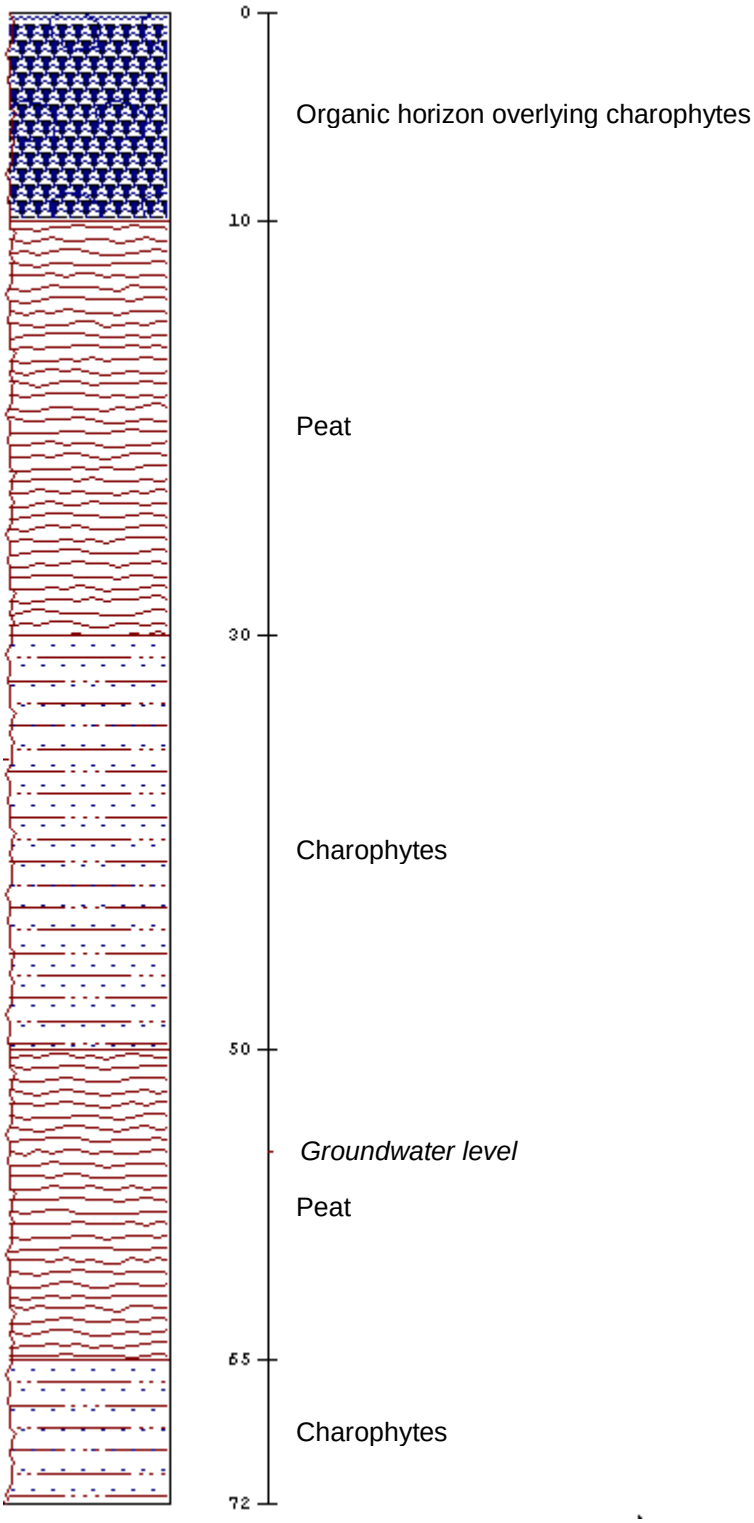

POINT 26

X= 441329
Y= 4337741

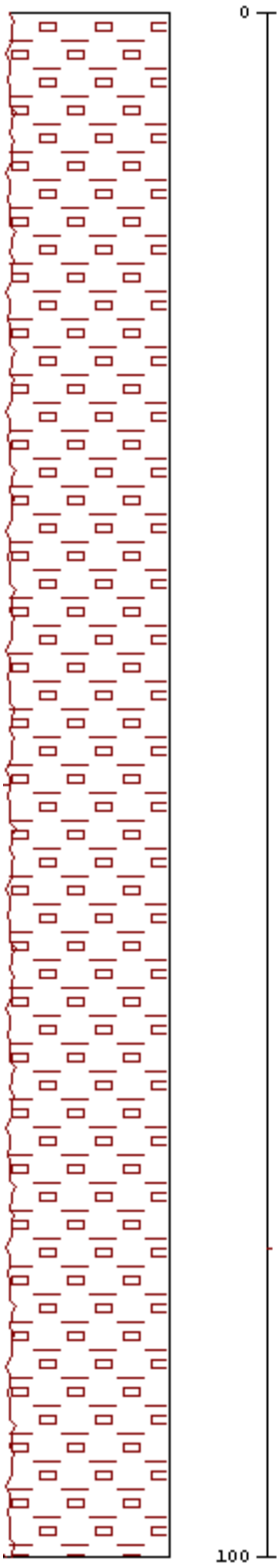

Green clay with salts and oxidation footprints

Lower salt content

POINT 27

X= 440608
Y= 4337049

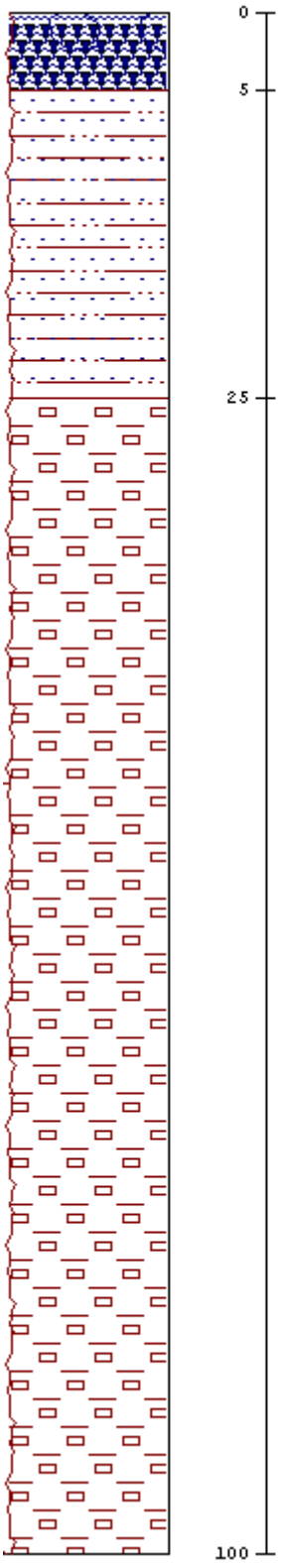

Organic horizon

Charophytes

Green clay with salts and oxidation footprints, and thin charophytes layers

POINT 28

X= 440164
Y= 4334844

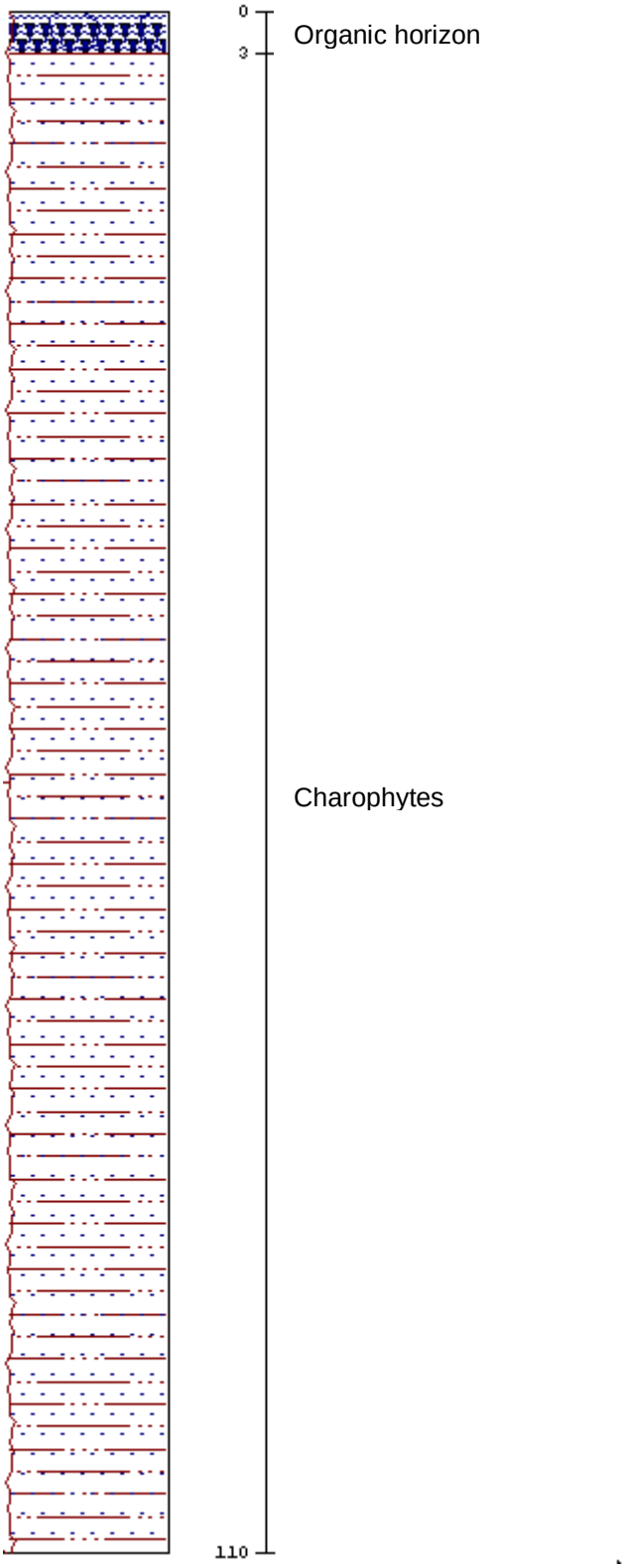

POINT 29

X= 439837
Y= 4334922

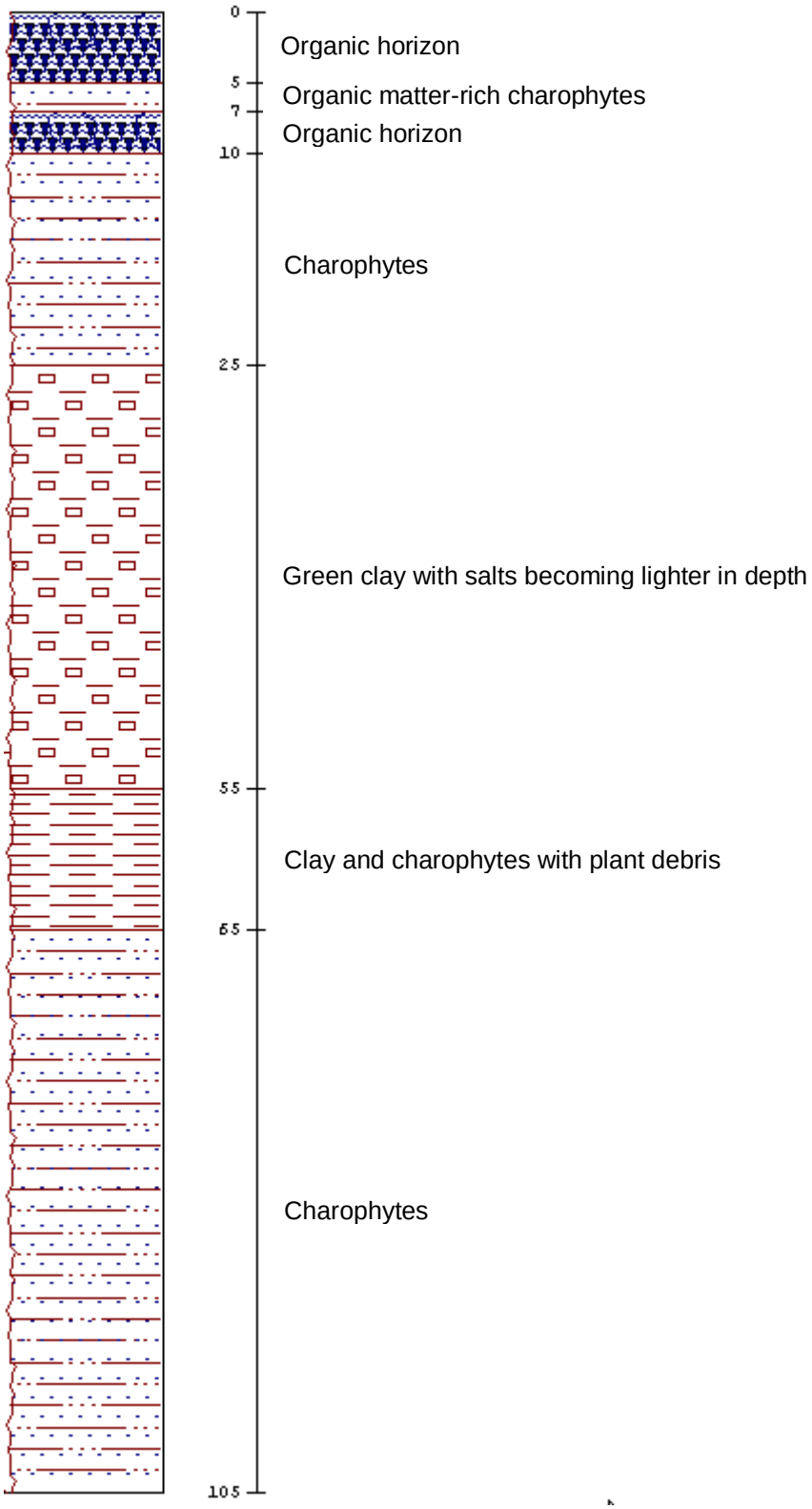

POINT 30

X= 439781
Y= 4334921

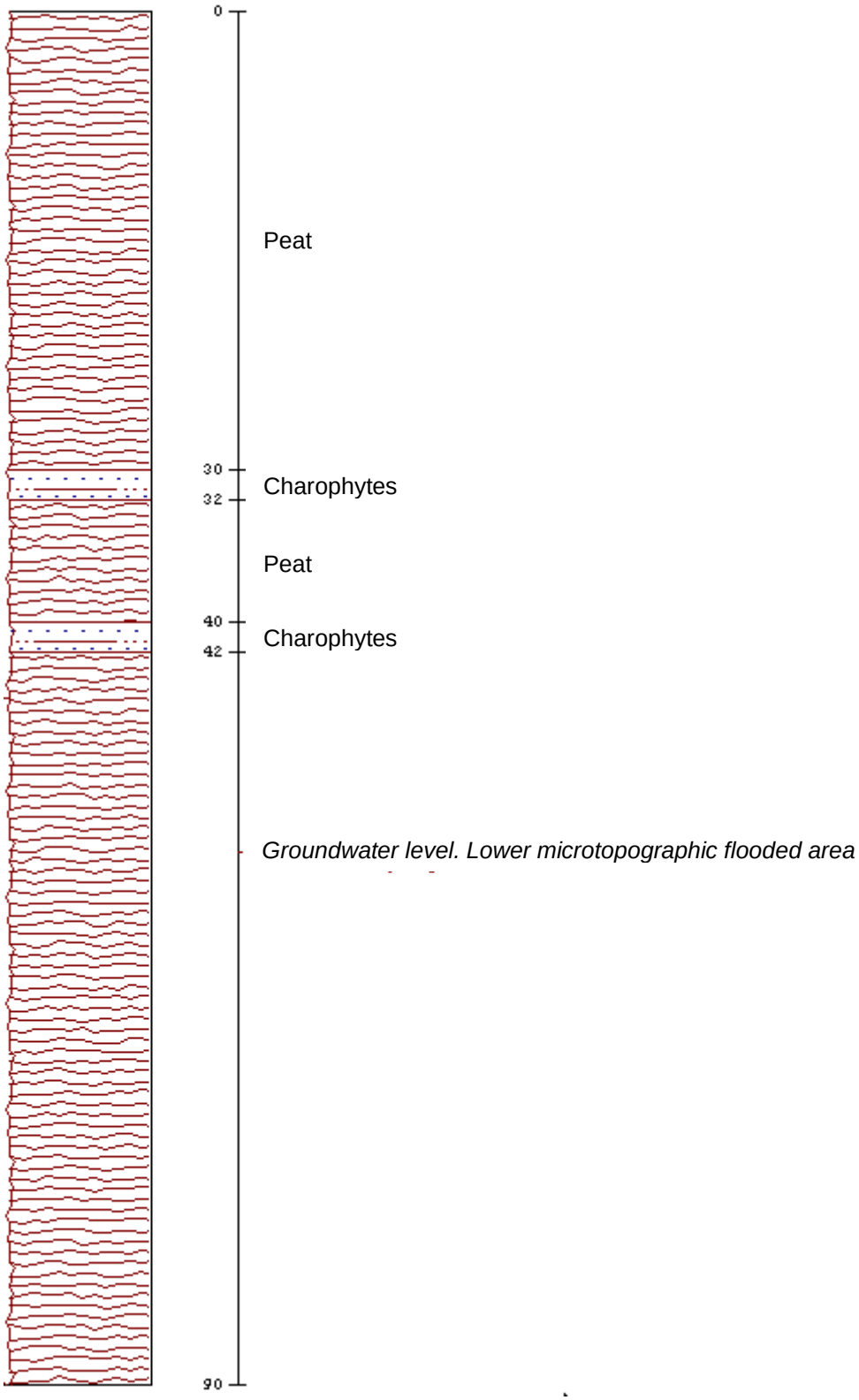

POINT 31

X= 438301
Y= 4333247

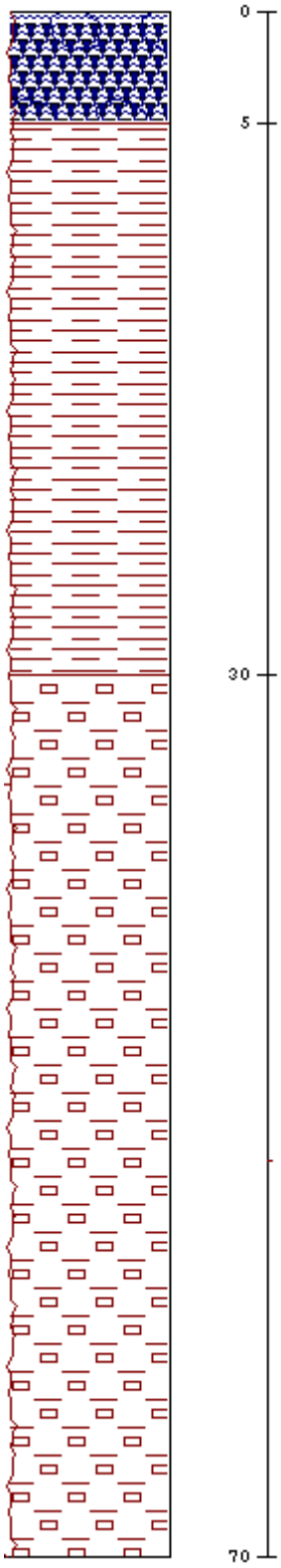

Organic horizon

Dark clay with significant amounts of plant debris

Green clay with salts

Groundwater level

POINT 32

X= 436861
Y= 4331901

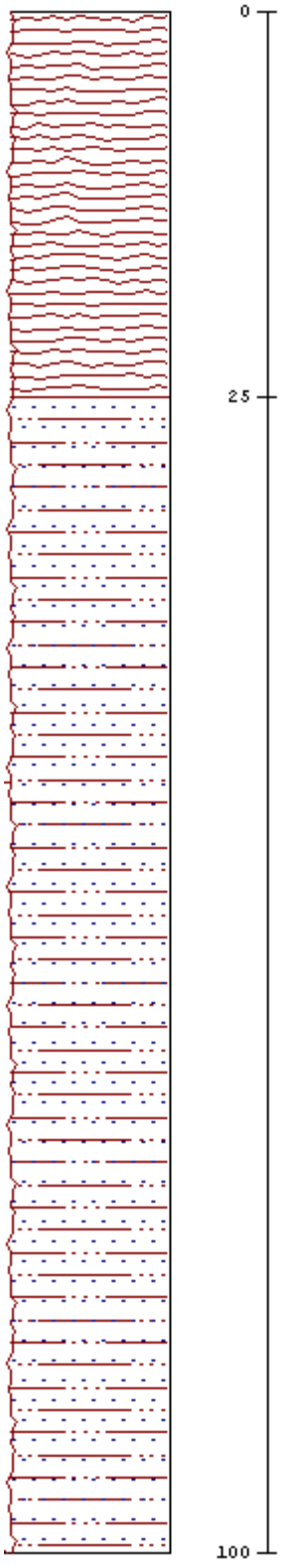

Peat

Charophytes with salts and ochre oxidized areas. High organic matter content at the bottom

POINT 33

X= 436875
Y= 4331917

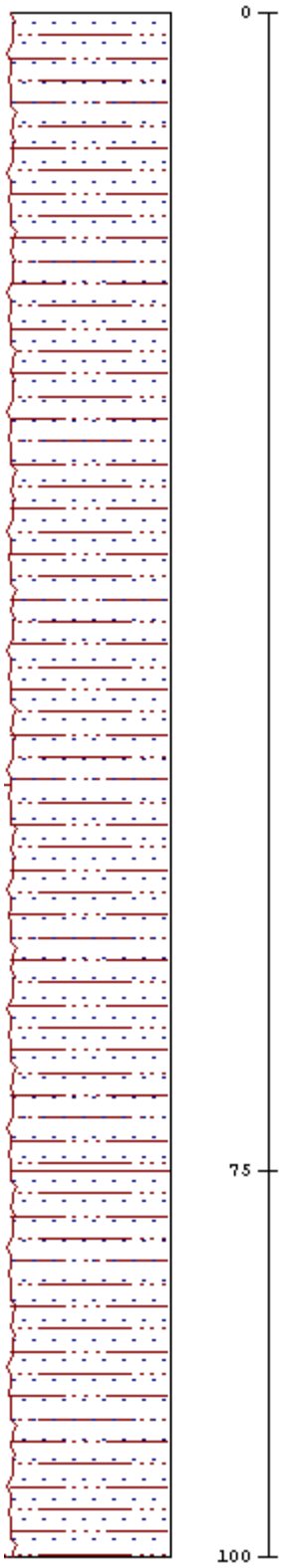

Ochre charophytes with clay and organic matter

Clayey ochre charophytes

POINT 34

X= 435734
Y= 4331434

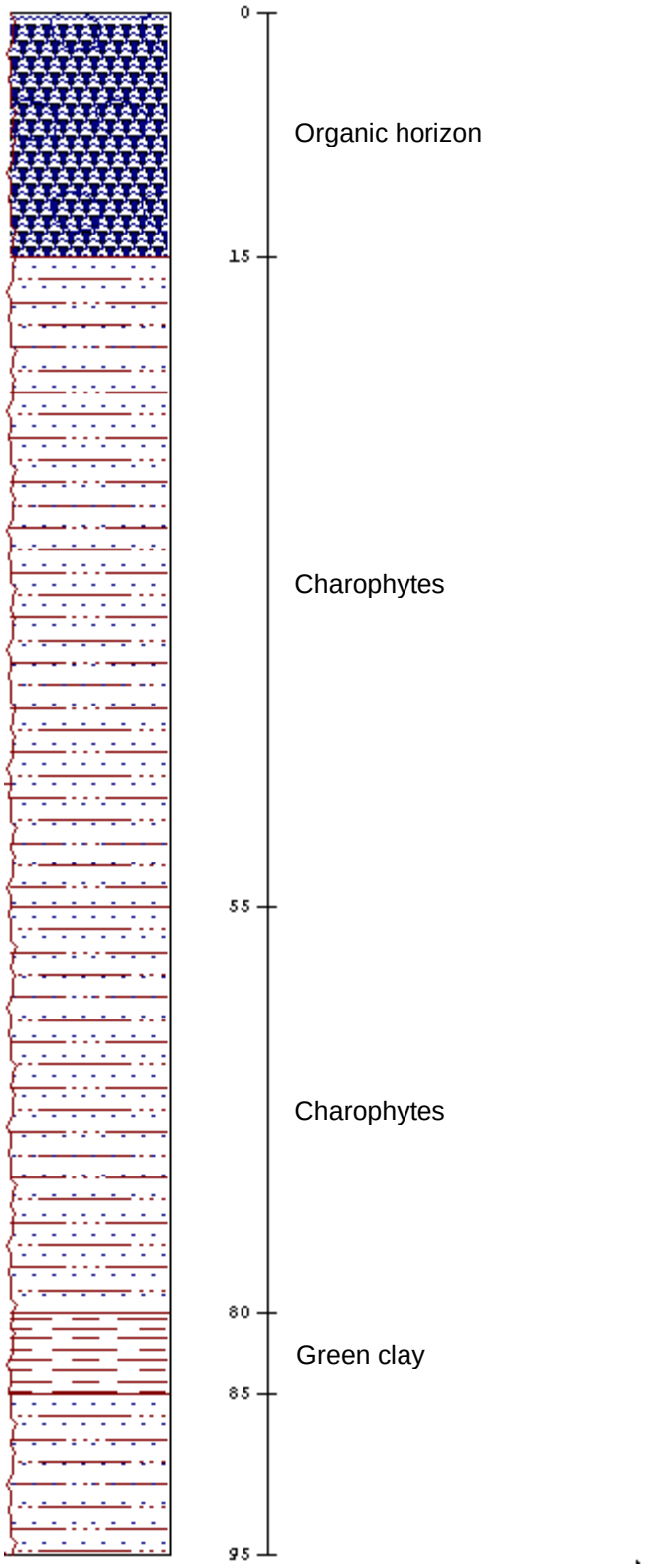

POINT 35

X= 433870
Y= 4330350

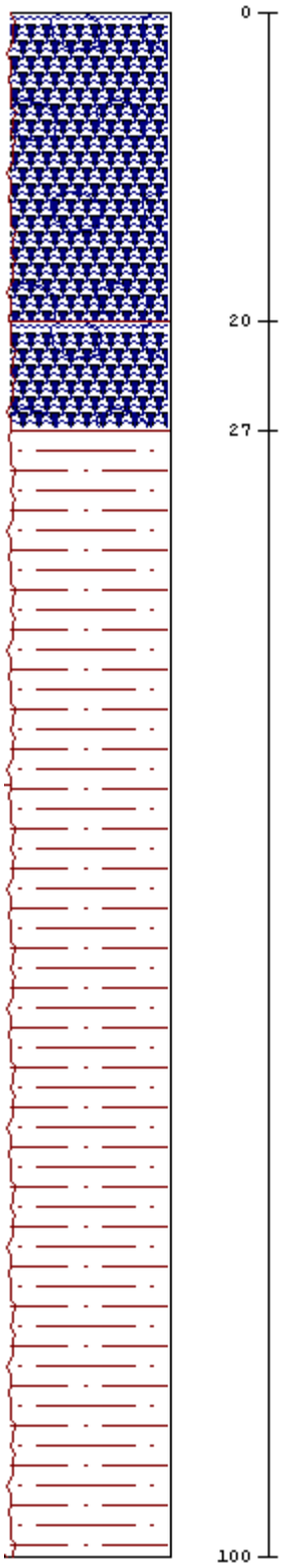

Organic horizon

Organic horizon with white concretions and carbonate pebbles

Green silt with salt?, calcareous pebbles and organic matter. Silt becomes brown in depth due to oxidation

POINT 36

X= 435628
Y= 4331250

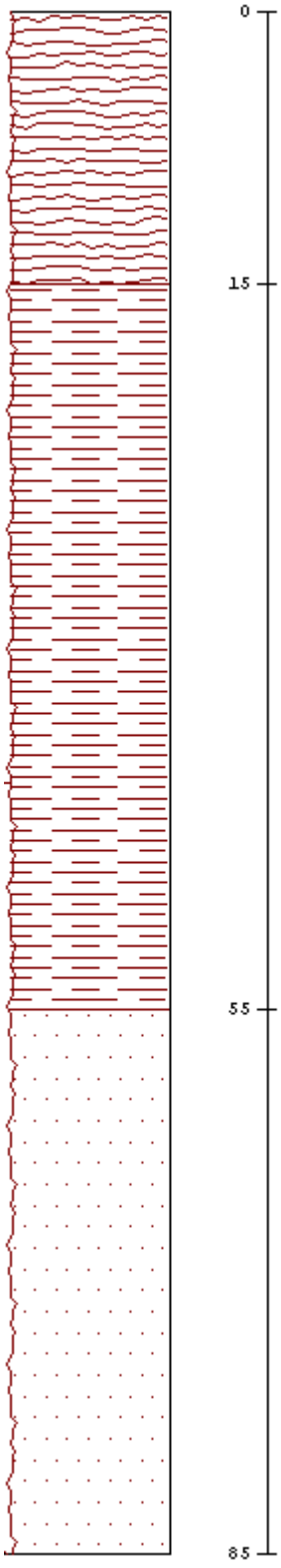

Peat

Green clay with small pebbles and ochre oxidized areas which are dominant from 45 cm deep

Brown silty sands with white areas and small carbonate pebbles

POINT 37

X= 435643
Y= 4331160

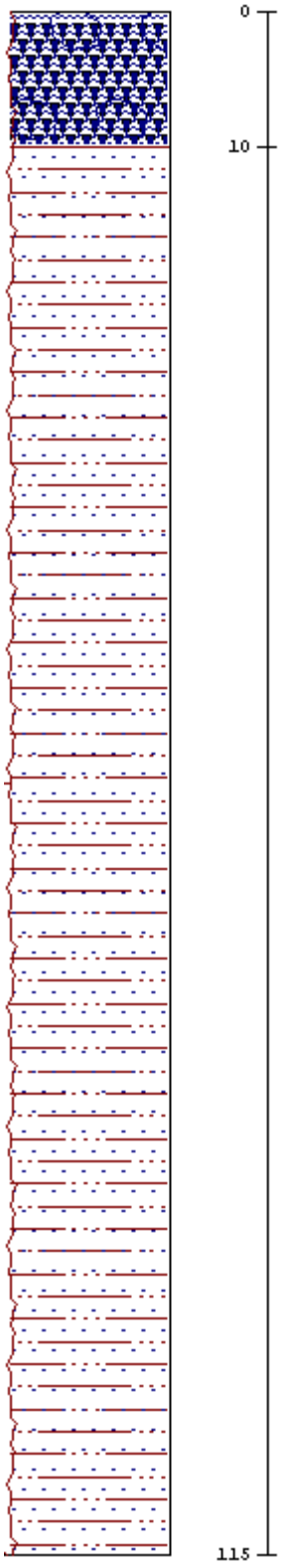

Organic horizon

Dark charophytes on top turning progressively lighter and becoming white from 45 cm deep

POINT 38

X= 4356485
Y= 4330807

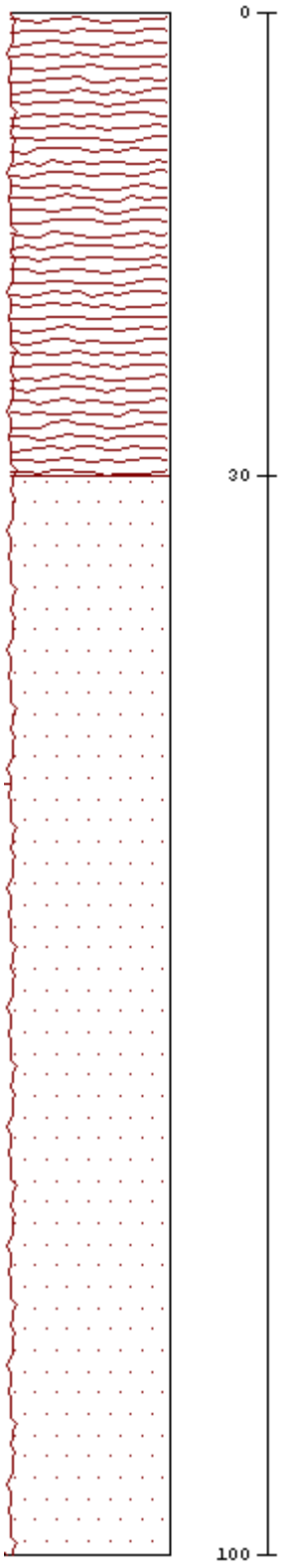

Peat with small carbonate pebbles and some clay

Sandy material from charophytes and white carbonates with brown silty matrix. Increasing charophytes content at the bottom, from 50 cm deep

POINT 39

X= 436487
Y= 4330879

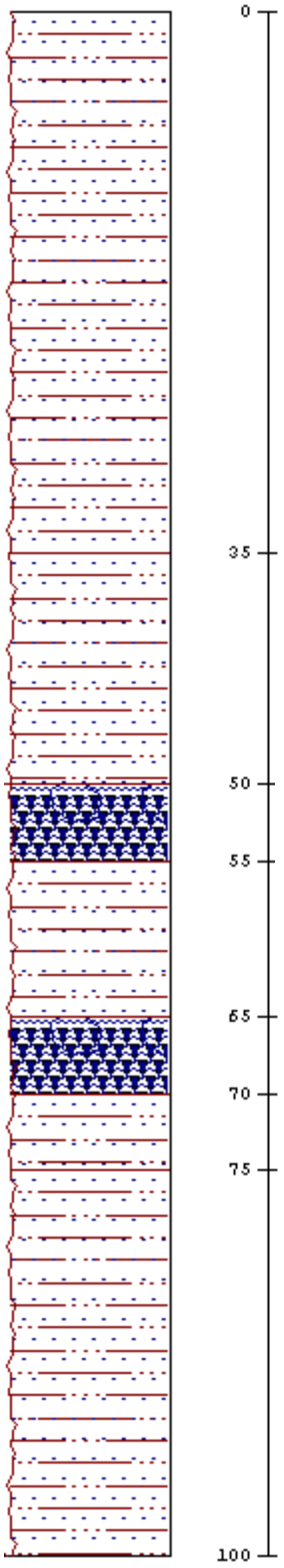

POINT 40

X= 436442
Y= 4330988

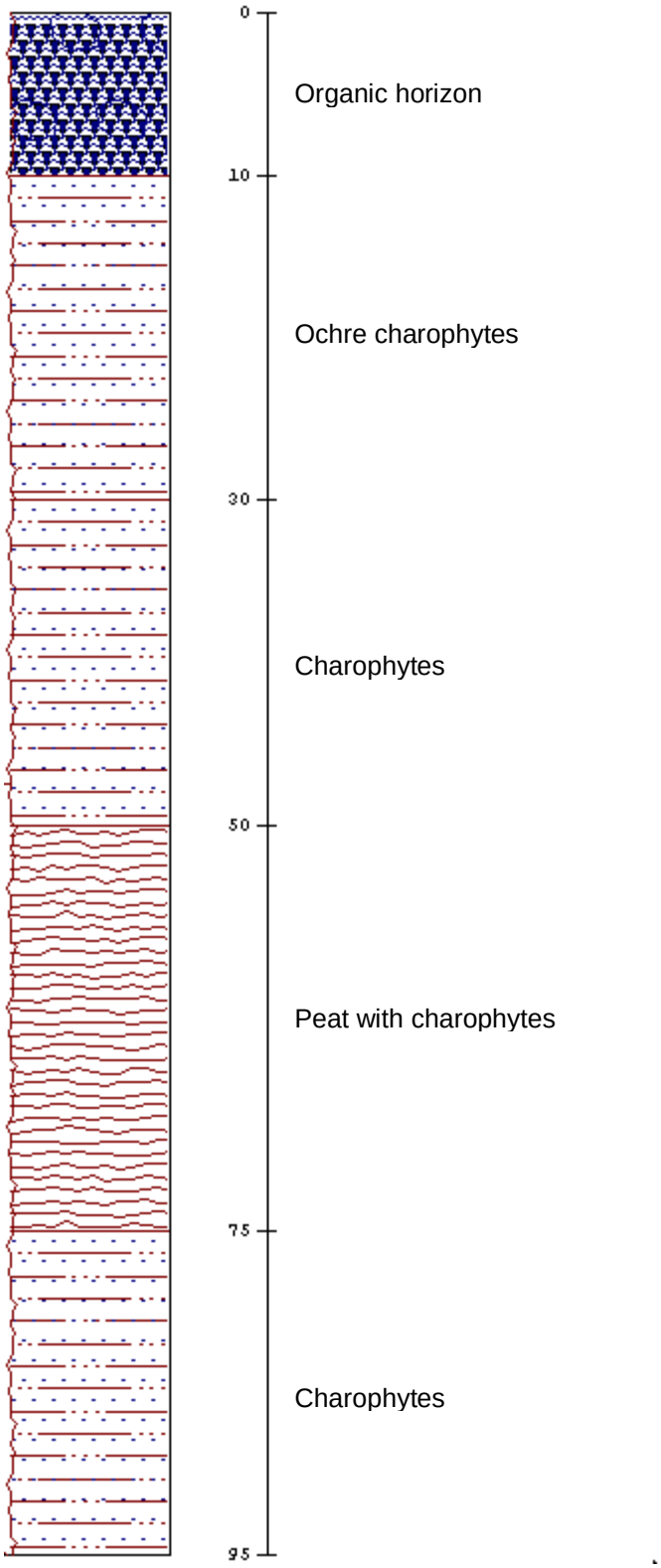

POINT 41

X= 436380
Y= 4331119

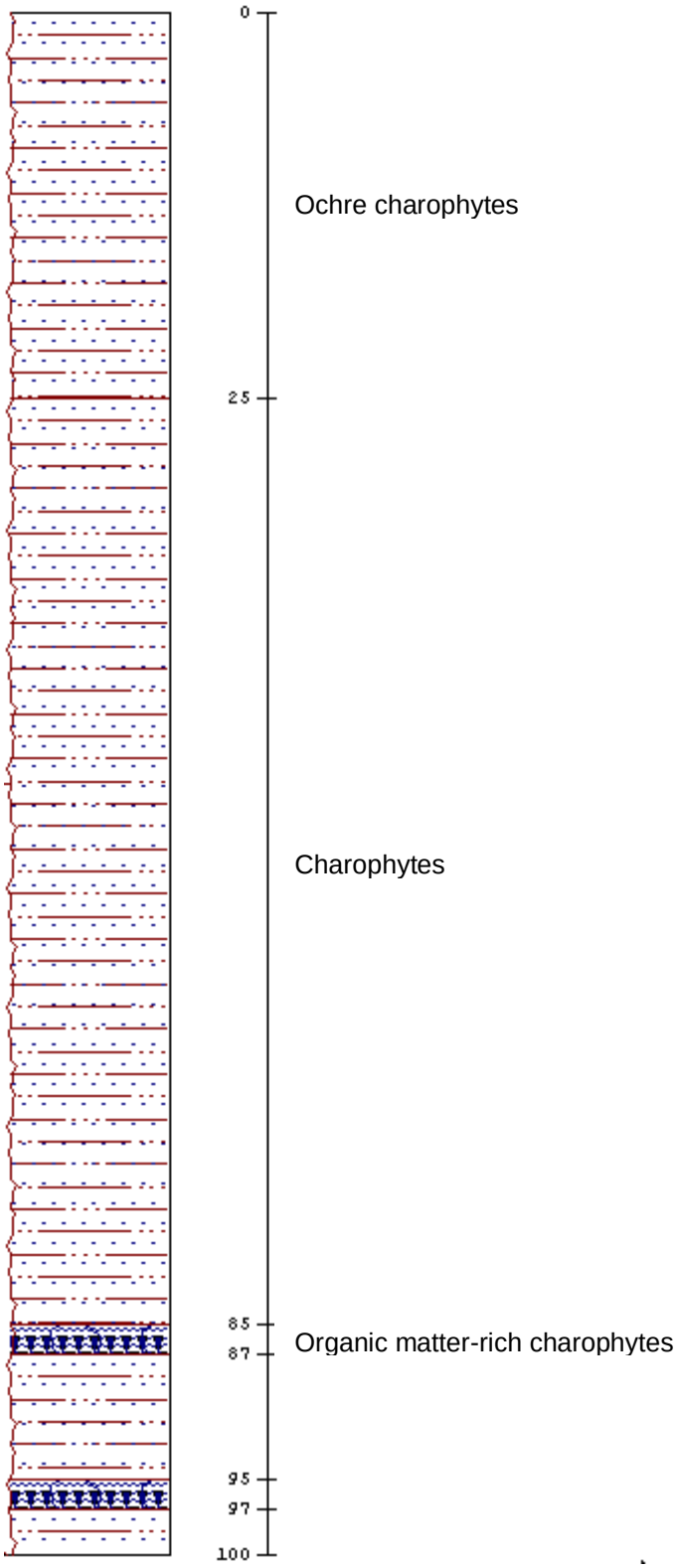

POINT 42

X= 436334
Y= 4331376

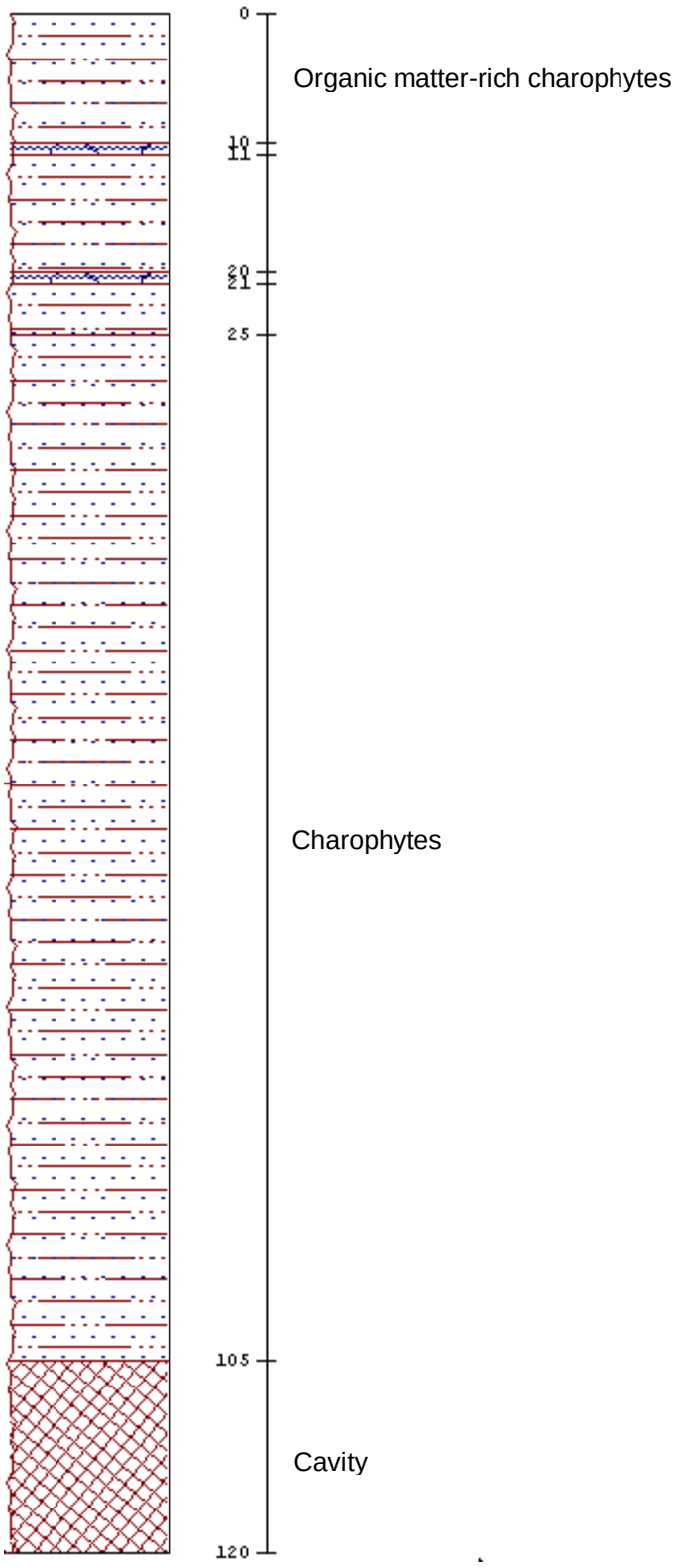

POINT 43

X= 436342
Y= 4331524

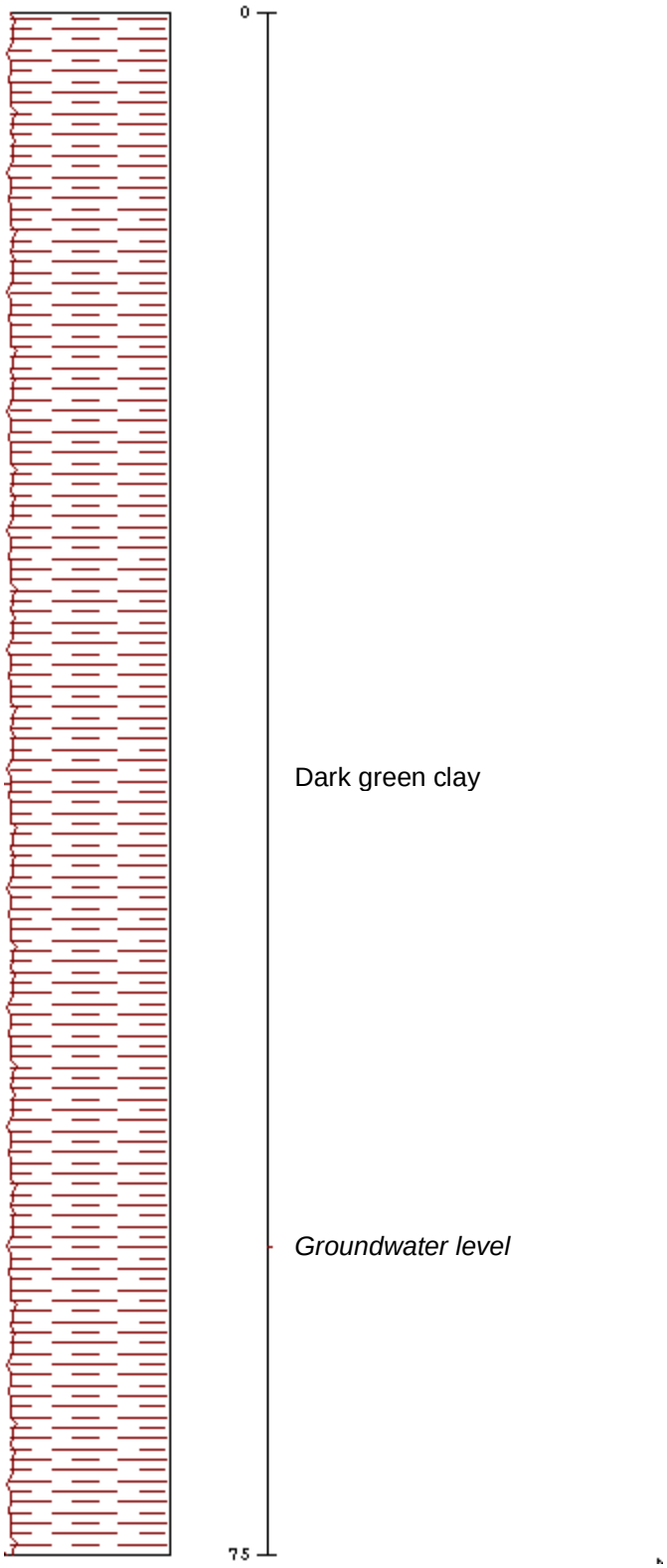

POINT 44

X= 437197
Y= 4331747

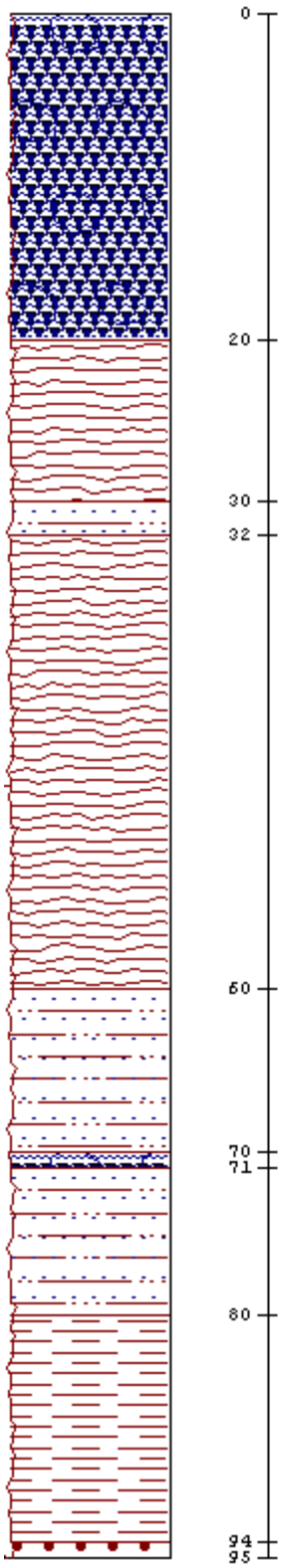

Organic horizon

Peat with thin charophytes layer between 30 and 32 cm deep

Organic matter-rich charophytes

Green clay with oxides. Carbonate pebbles at the bottom

POINT 45

X= 437218
Y= 4331448

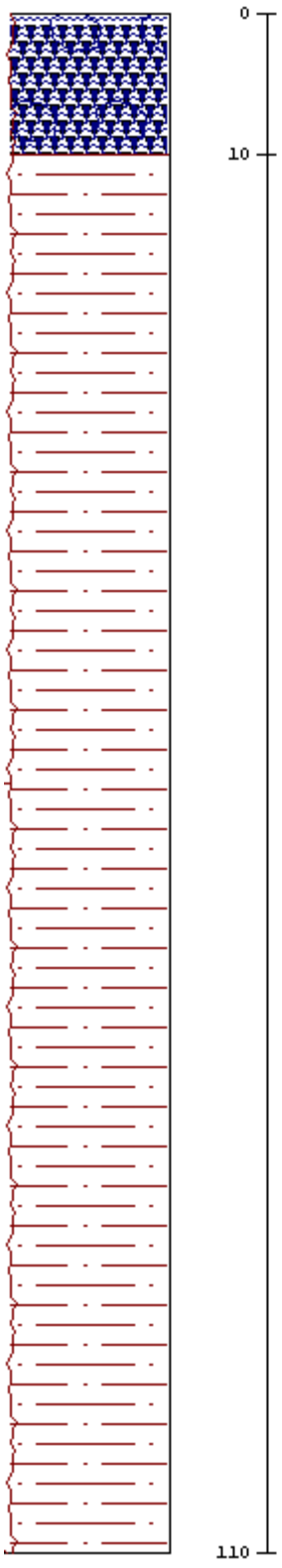

POINT 46

X= 437080
Y= 4331446

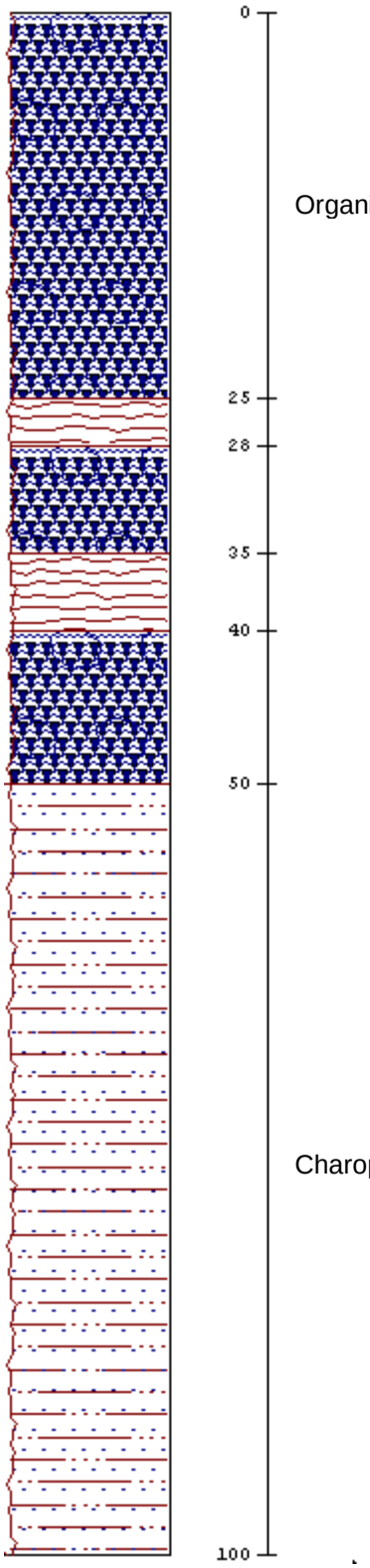

POINT 47

X= 438780
Y= 4331910

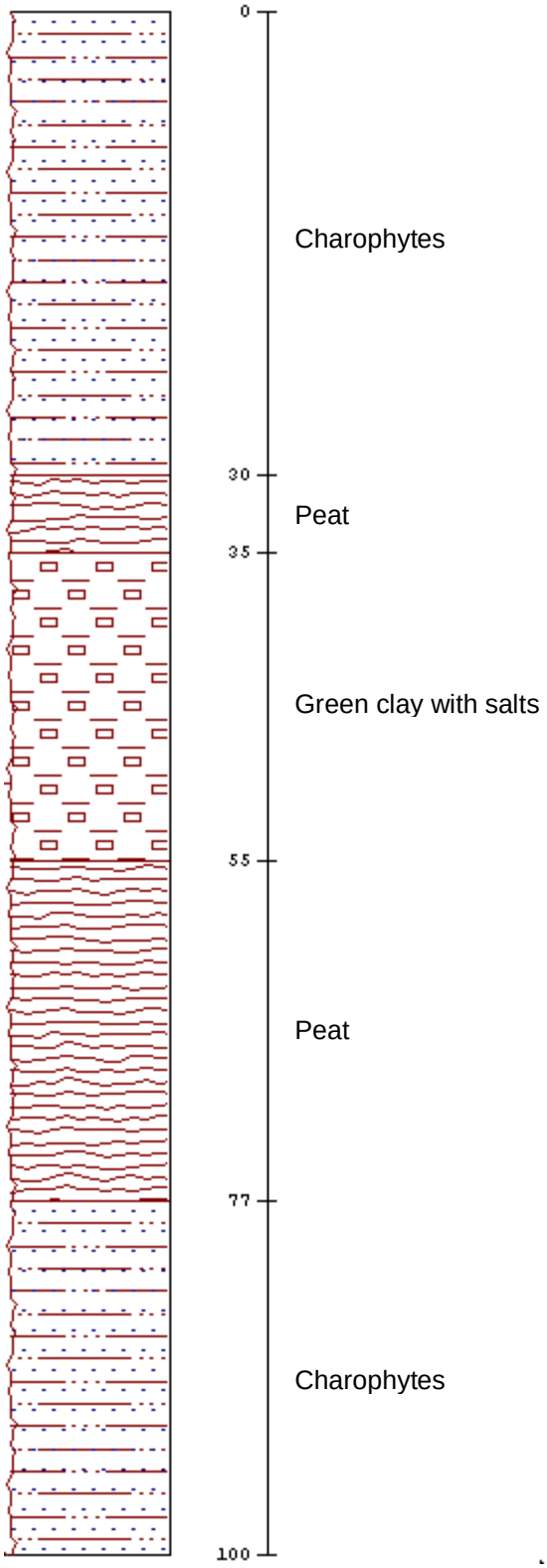

POINT 48

X= 438705
Y= 4332110

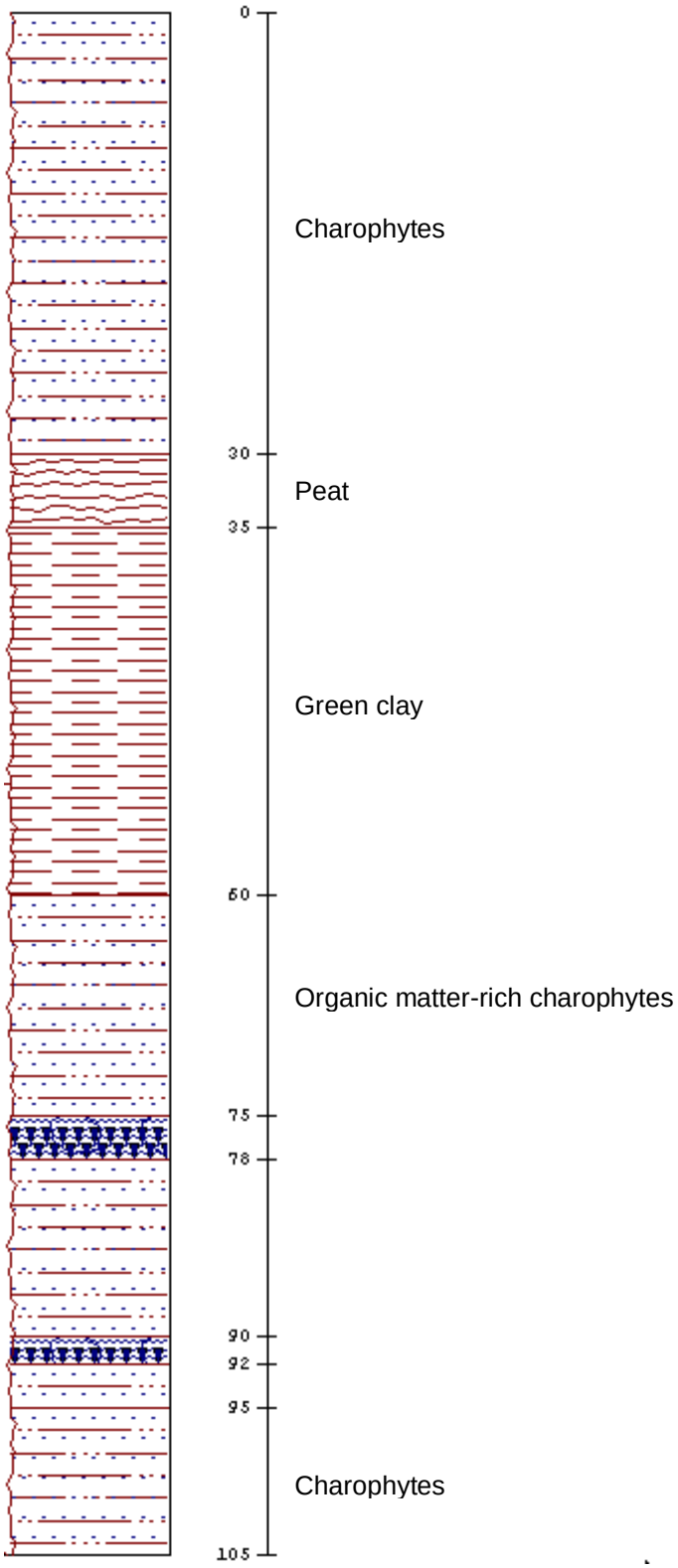

POINT 49

X= 438654
Y= 4332262

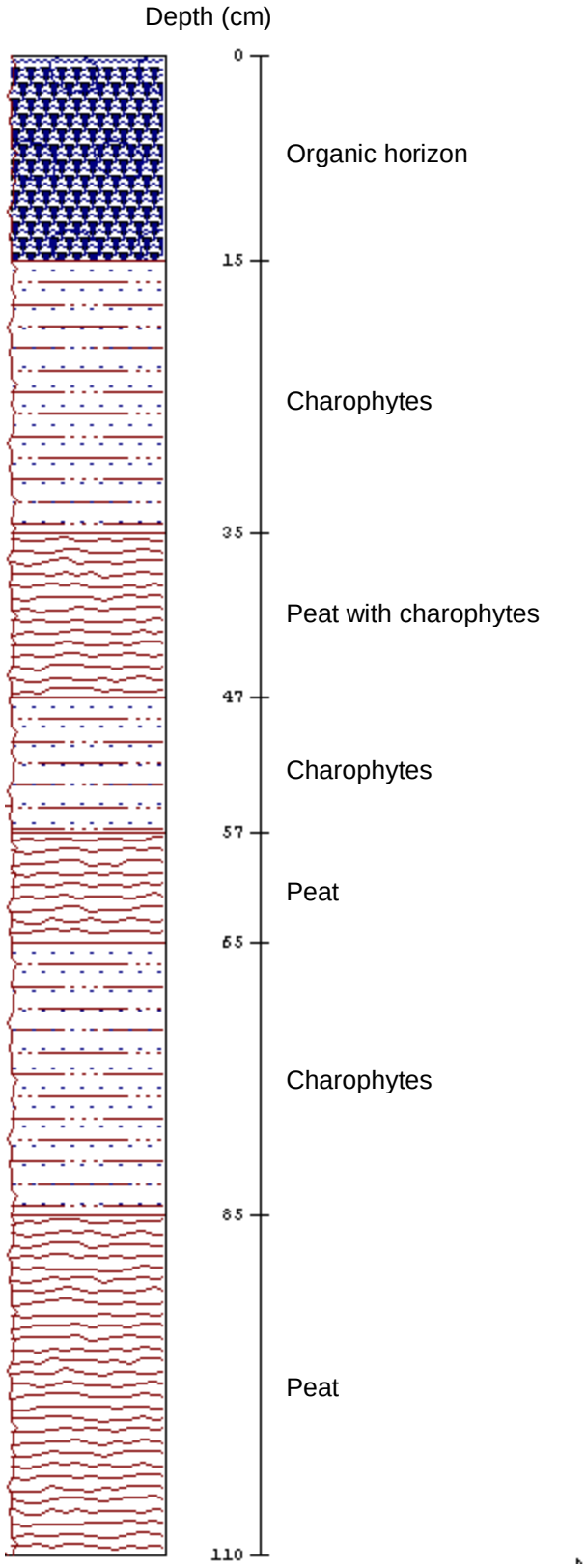

POINT 50

X= 438480
Y= 4332418

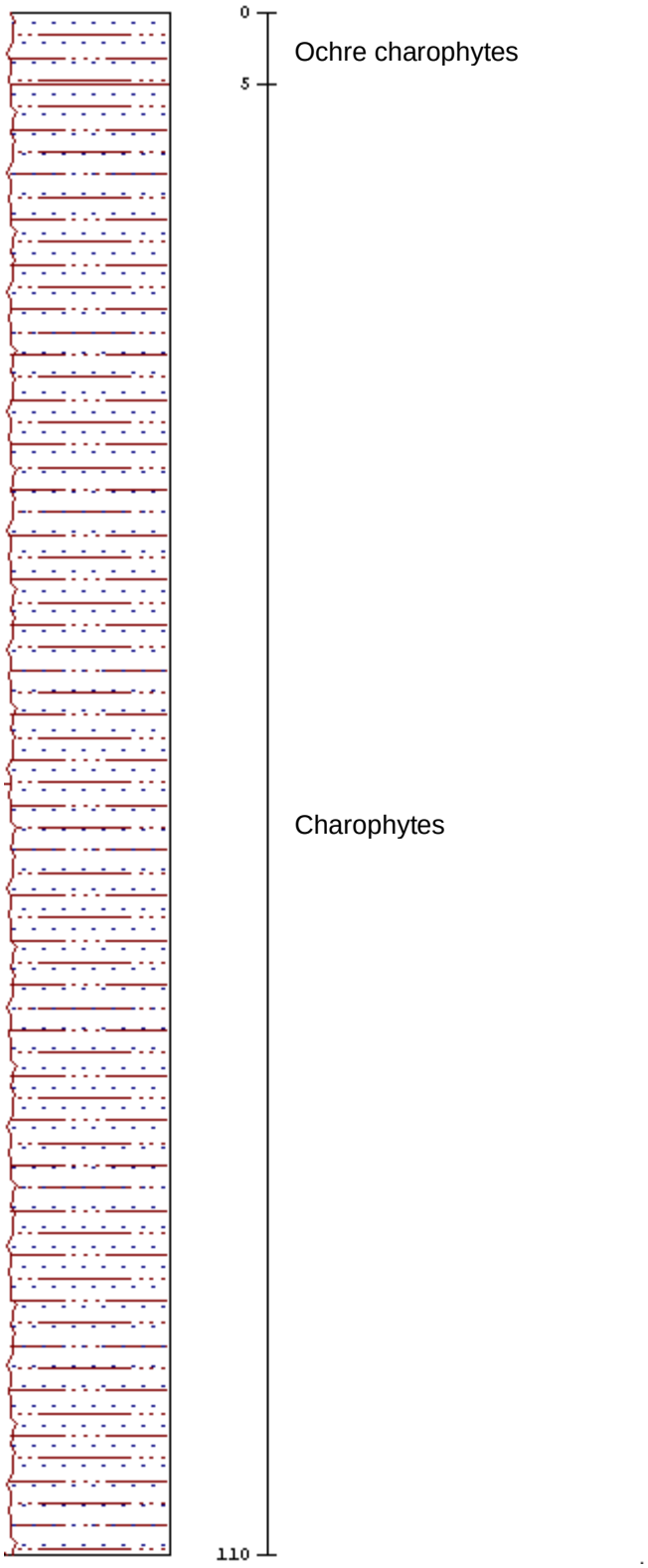

POINT 51

X= 438294
Y= 4332646

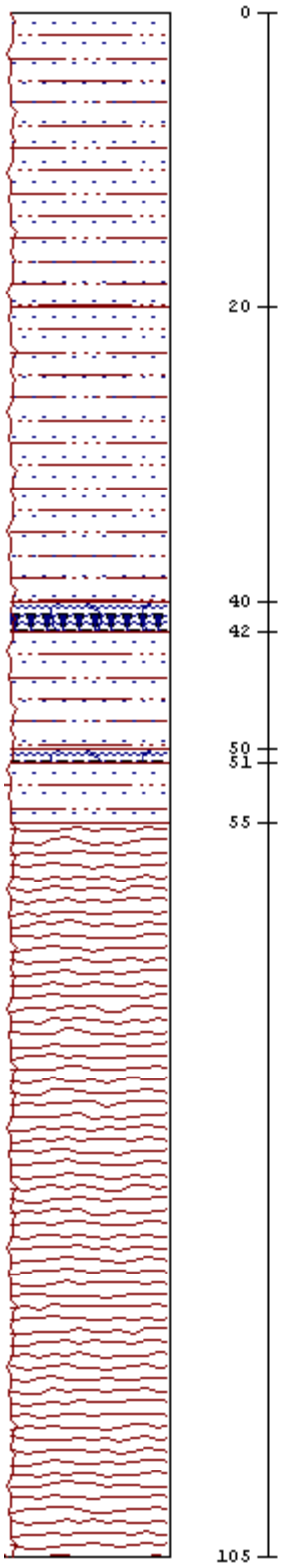

Ochre charophytes

Charophytes (organic matter-rich at 40-42 cm deep)

Peat

POINT 52

X= 438171
Y= 4332716

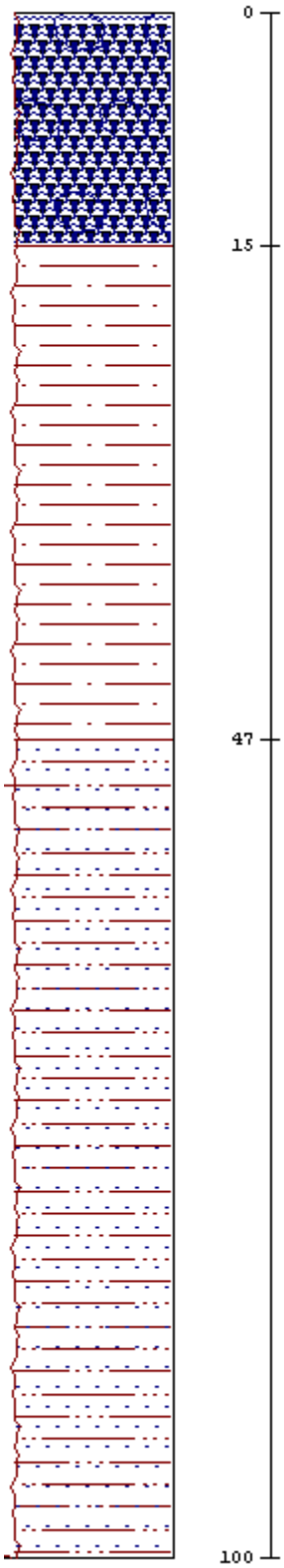

Organic horizon

Brown and green charophytes-rich silt, with salts and organic matter (it could be charophytes-clay alternations)

Charophytes with white powdery areas

POINT 53

X= 438063
Y= 4332560

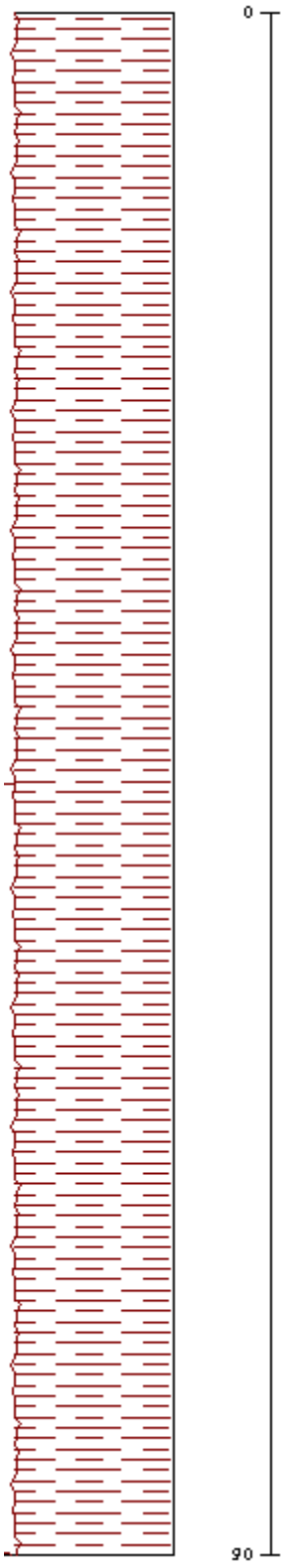

Green clay with plant debris and oxidation areas

POINT 54

X= 438774
Y= 4332560

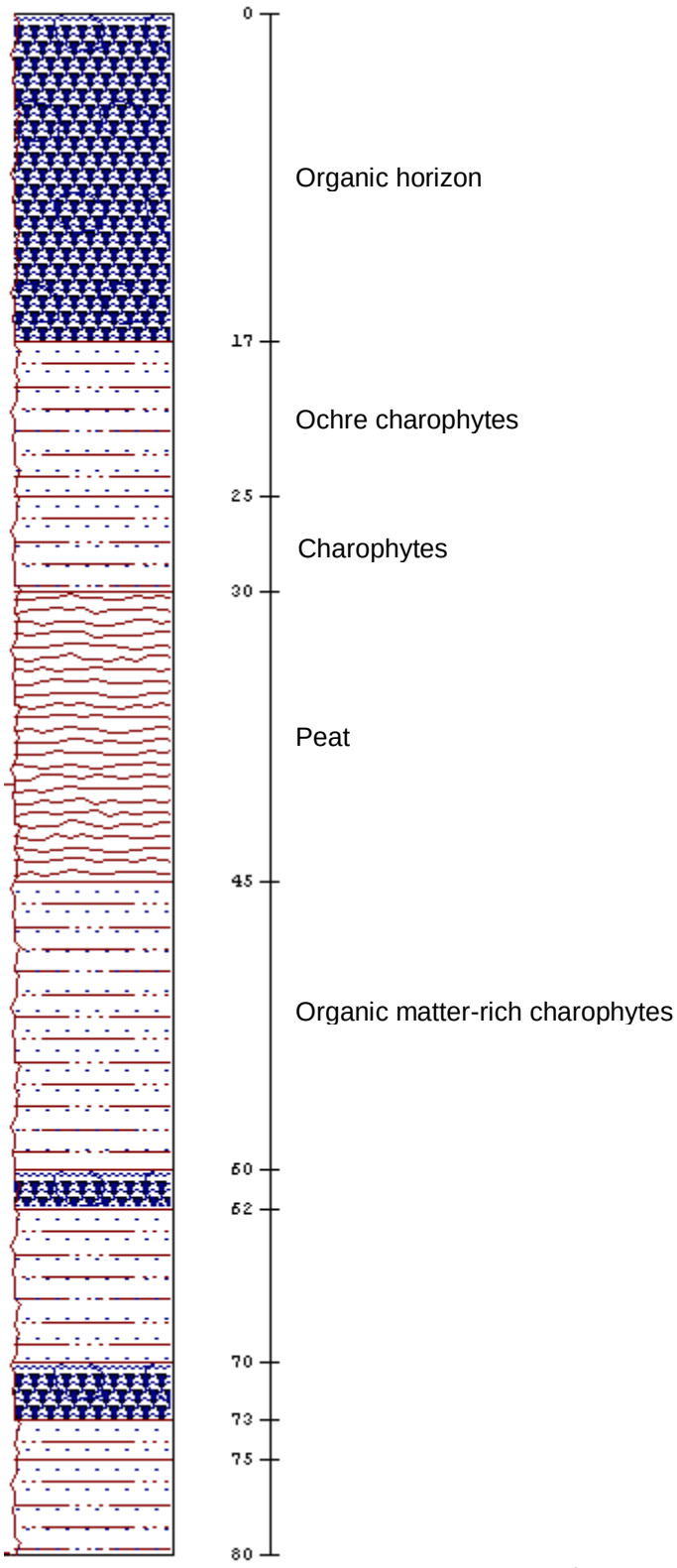

POINT 55

X= 438531
Y= 4332079

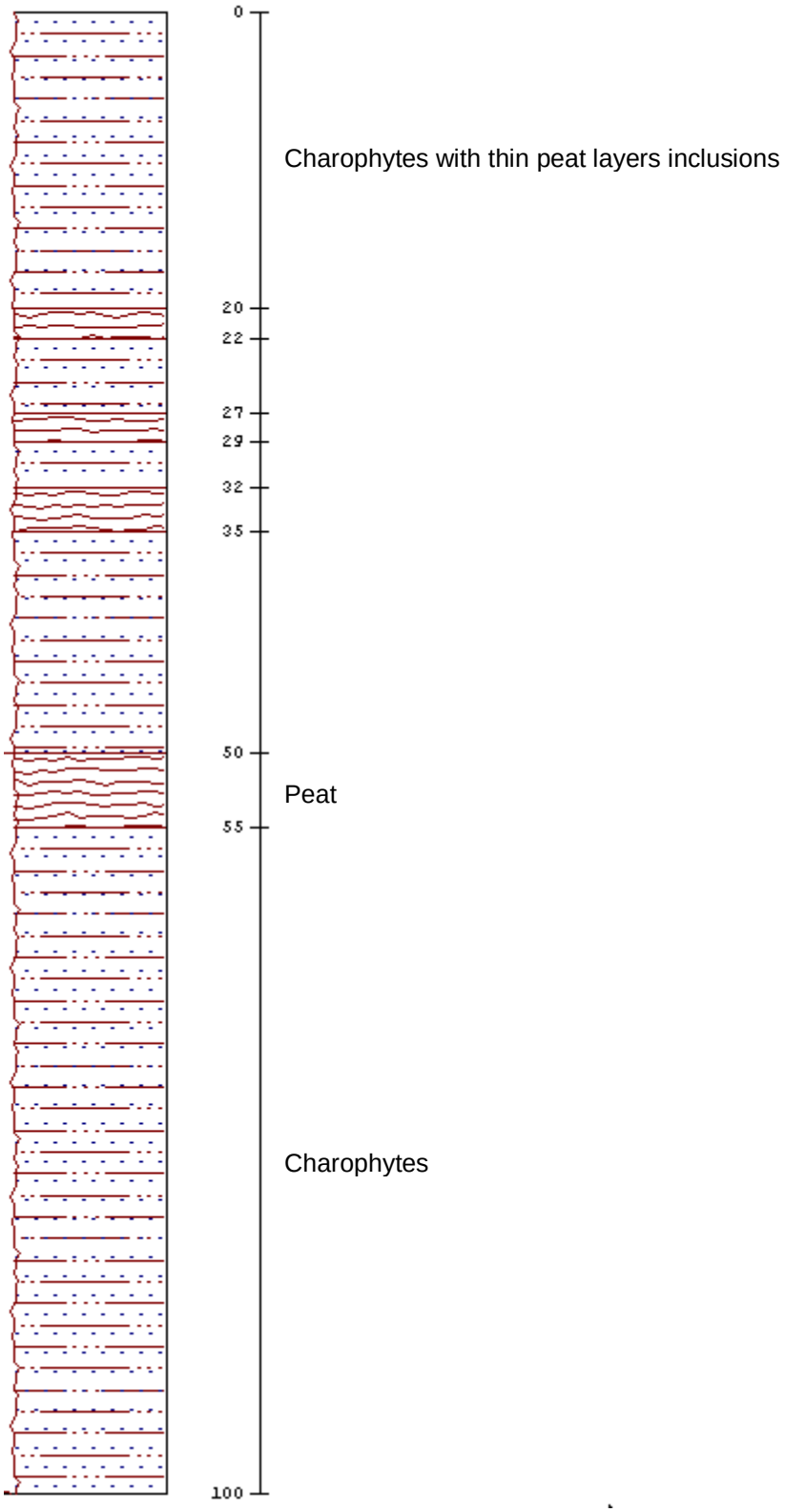

POINT 56

X= 440466
Y= 4336036

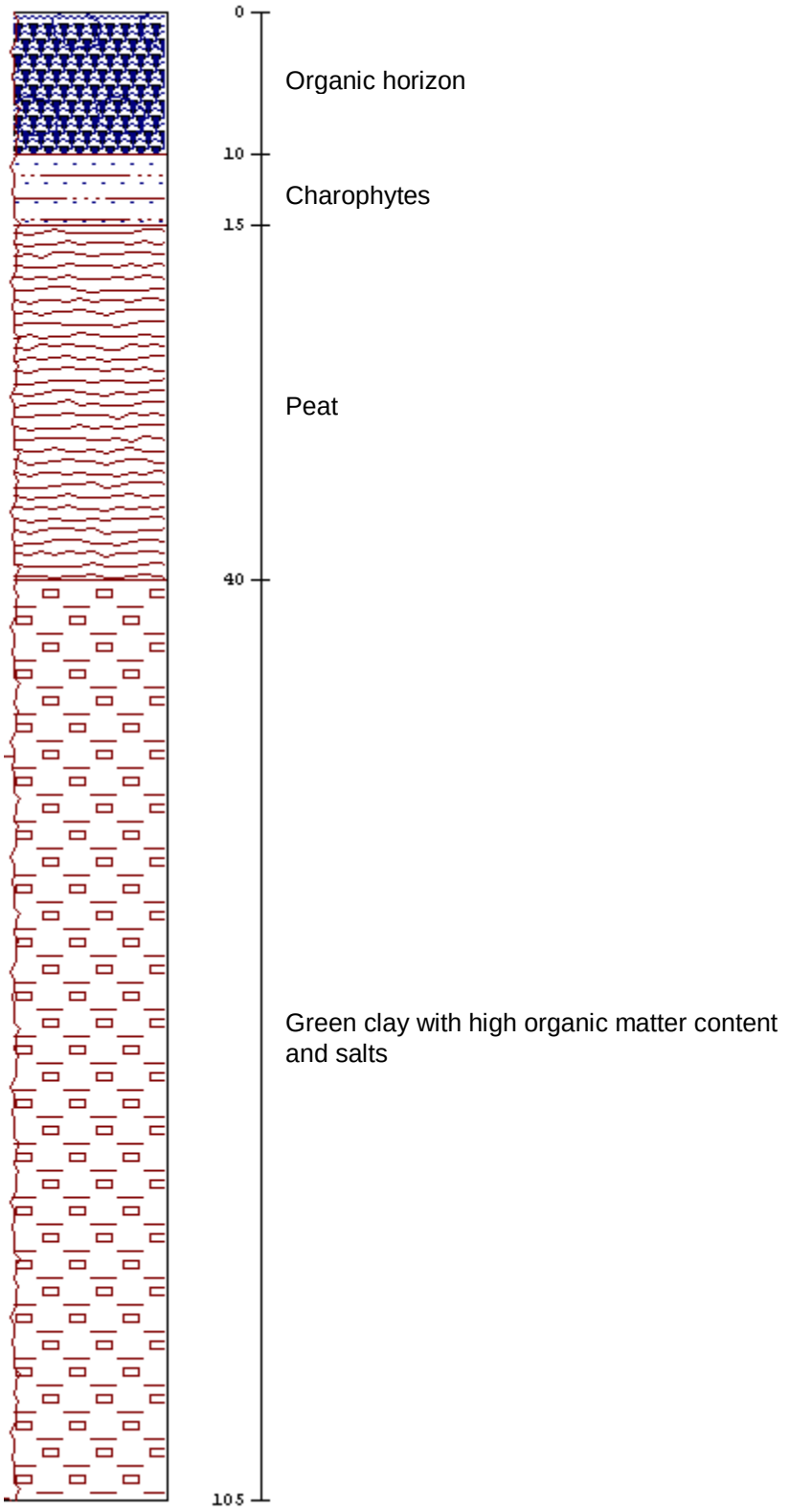

POINT 57

X= 440868
Y= 4335798

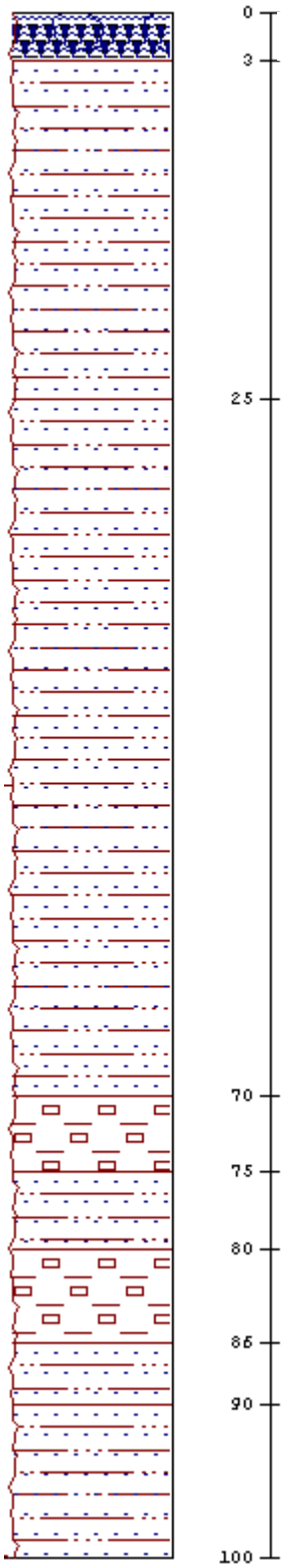

Organic horizon

Ochre charophytes

Charophytes with green clay and salts becoming more clayey and lighter at the bottom

Charophytes with light clay

POINT 58

X= 440498
Y= 4335281

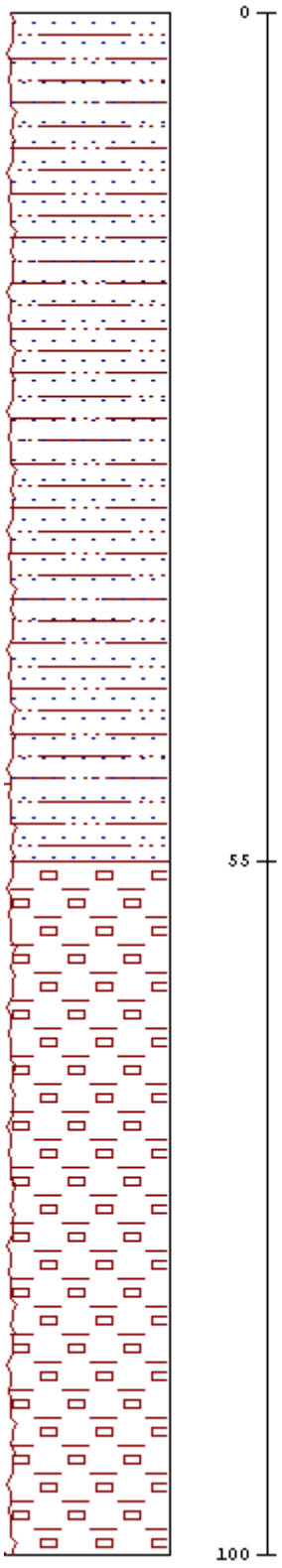

Ochre charophytes

Green clay with salts and charophytes

POINT 59

X= 439433
Y= 4333269

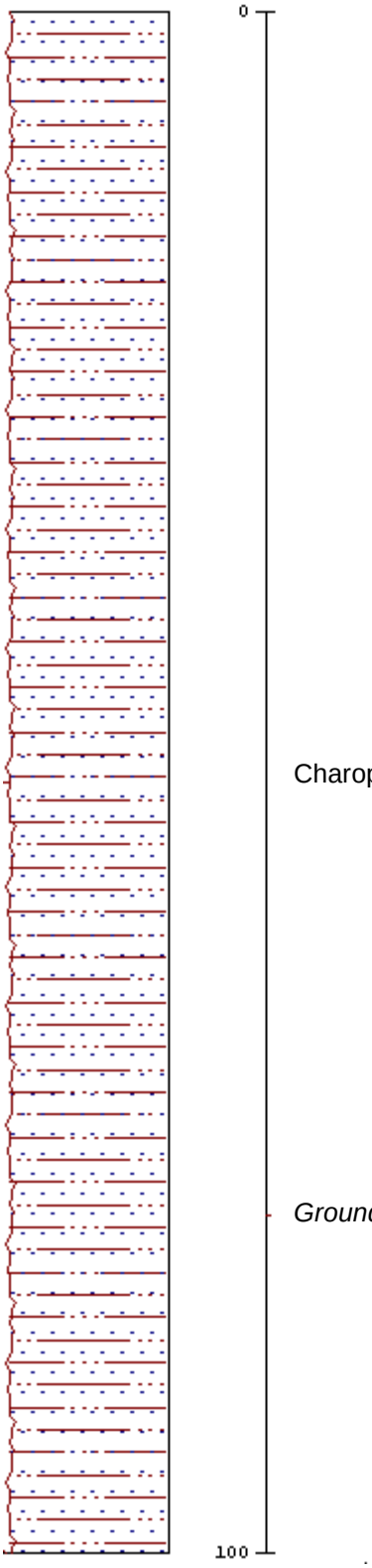

POINT 60

X= 436421
Y= 4330763

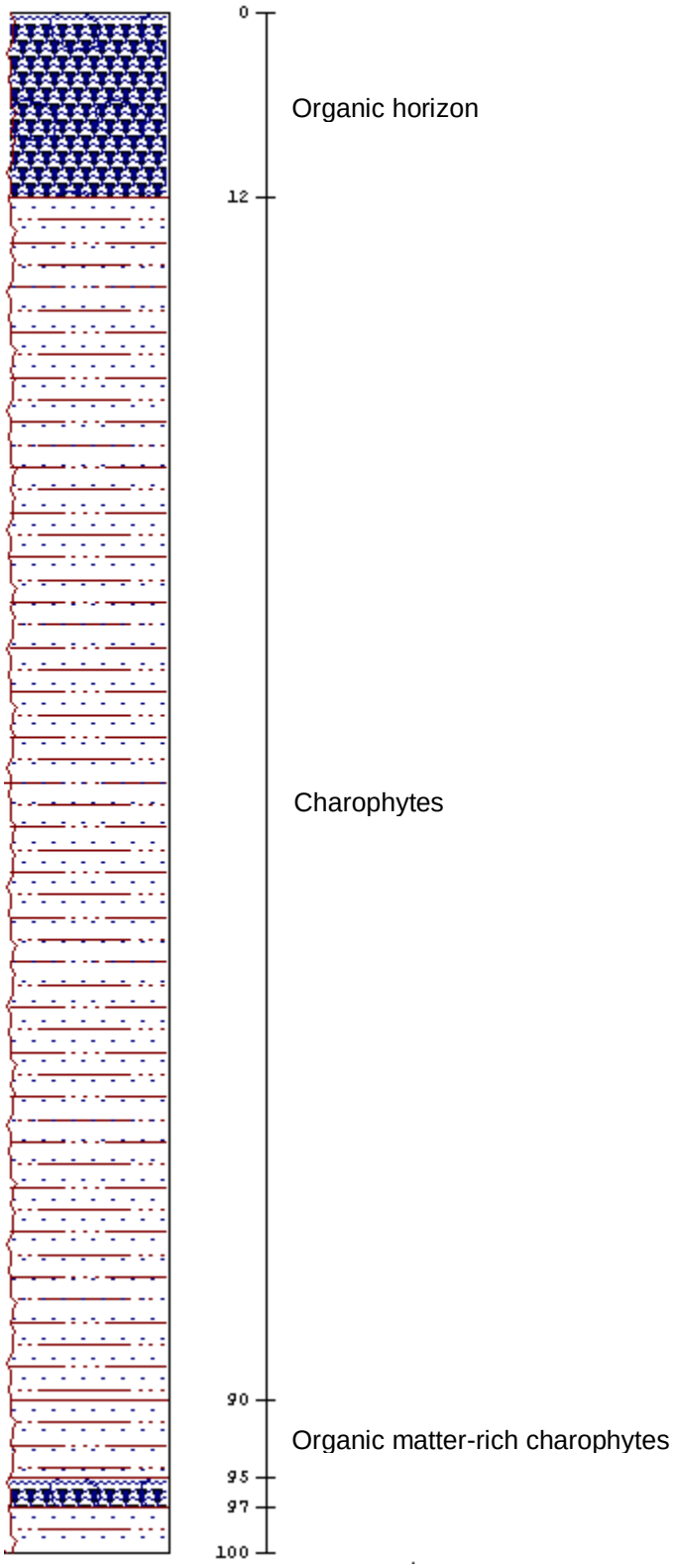

POINT 61

X= 434548
Y= 4329920

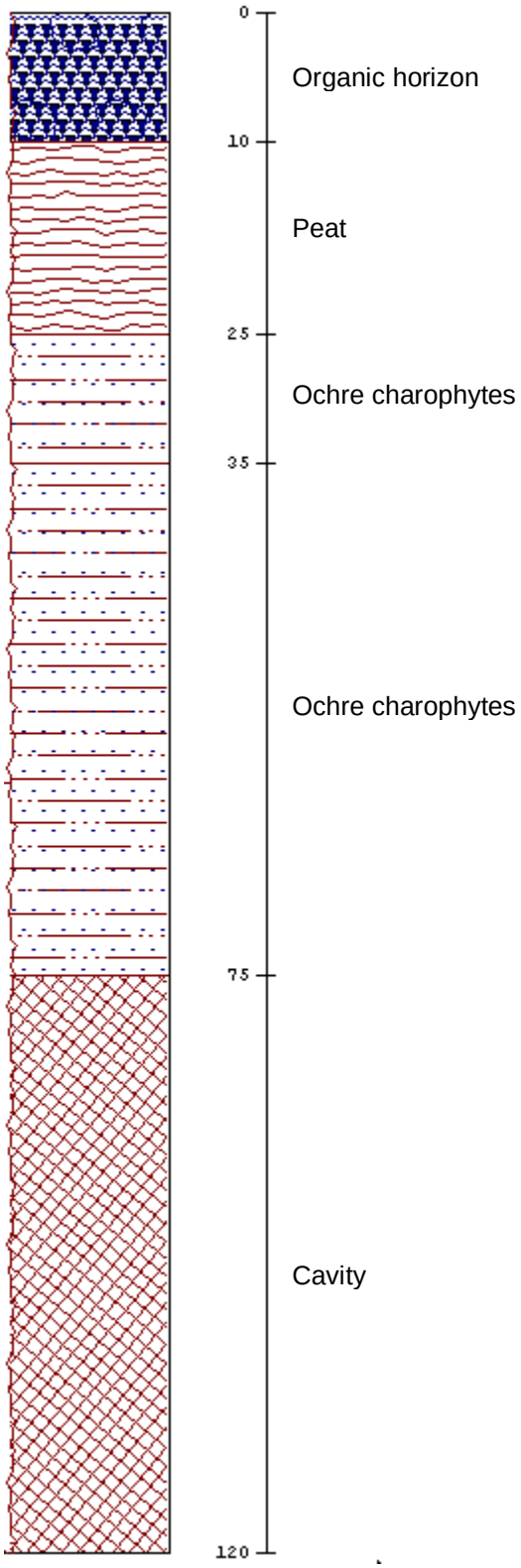

A.2. Additional random soil profiles sampled in 2009 in N and NW areas of Las Tablas de Daimiel National Park for soil functional type characterization and mapping.

Sampling point	X_UTM	Y_UTM	Depth (cm)	Soil type	Observations
1	440604	4337007	0-15	saline charophytes	
			15-	clay	
2	440669	4336988	0-40	saline charophytes upon undisturbed charophytes	
			40-	clay	
3	440175	4336561	0-30	brown-reddish sand	
4	440217	4336562	0-20	sandy edaphic material	deepest material looked like gypsum but it was not plastic
			20-30	saline charophytes	
			50-	sandy-clayey material	
5	440309	4336490	0-5	edaphized charophytes	
			5-50	saline white charophytes	
			50-	clay	
6	439565	4334954	0-50	edaphized charophytes	
			50-	clay	
7	439718	4334936	0-40	edaphized charophytes	
			40-	dark clay	
8	438684	4333699	0-70	undisturbed charophytes	
9	438746	4333688	0-30	undisturbed charophytes	
			30-40	peat	
			40-70	undisturbed charophytes	
10	438702	4333355	0-40	undisturbed charophytes with small stones	
11	441575	4335861	0-60	edaphized	

				charophytes	
			60-	clay	
12	441358	4336007	0-50	edaphized charophytes	
			50-	clay	
13	441640	4335830	0-70	edaphized charophytes	
			70-	wet clayey silt	
14	441670	4336367	0-65	edaphized charophytes	
			65-	clay	
15	441623	4336464	0-10	mix of organic soil and charophytes	elevated tamarisk area
			10-	clay	
16	441723	4336655	0-50	undisturbed charophytes	
			50-	clay	
17	441523	4337138	0-15	edaphized charophytes	
			15-40	saline charophytes	
			40-	clay	
18	443248	4337235	0-20	brown charophytes	between Cigüela ditch and tamarisk area. Brown charophytes could be either saline or edaphized
			20-	clay	
19	443009	4337517	0-35	wet saline charophytes	shallow groundwater level
			35-	wet silty charophytes	
20	442601	4337345	0-13	brown charophytes	brown charophytes could be either saline or edaphized
			13-30	saline charophytes	
21	442376	4336989	0-20	edaphized charophytes	northeastern edge area, reed and tamarisk vegetation
			20-35	clay	
22	442132	4336751	0-20	edaphized charophytes	next to Cigüela ditch
			20-82	edaphized charophytes and wet clayey silt	
23	441872	4336834	0-15	brown charophytes	tamarisk area with no reed
			15-	clay	
24	440737	4337181	0-5	organic soil	

			5-15	clay	
			15-30	saline charophytes	
			30-	clay	
25	440821	4337173	0-70	edaphized charophytes	lower microtopographic area with small reed plants
			70-	clay	
26	440772	4337177	0-10	peaty organic soil	elevated microtopographic area next to point 25
			10-45	saline charophytes and clay	
			45-	clay	
27	440908	4337142	0-20	edaphized charophytes	elevated microtopographic area with dense reed bed
			20-45	dry saline charophytes with clay	
			45-	clay	
28	440998	4337117	0-30	edaphized charophytes	lower microtopographic area with old reed bed
			30-60	mix of edaphized and saline charophytes	
			60-	clay	
29	441078	4337095	0-5	edaphic soil	elevated microtopographic area at the edge of reed bed
			5-15	clay	
			15-20	wet saline charophytes	
			20-35	clay	
30	441212	4337078	0-15	edaphized charophytes	
			15-40	saline charophytes	
			40-	clay	
31	441344	4337090	0-5	edaphized charophytes	
			5-32	clayey saline charophytes becoming wetter in depth	
32	441473	4337080	0-10	organic soil and edaphized charophytes	
			10-16	clay	
			16-20	undisturbed charophytes	
			20-38	clay	
33	441479	4336631	0-13	edaphized	reed bed

				charophytes	
			13-29	clay	
			29-52	edaphized charophytes	
			52-	clay	
34	441370	4336608	0-20	very wet clayey saline charophytes	no vegetation, very compact material
35	441232	4336577	0-3	organic soil and edaphized charophytes	herbaceous vegetation
			3-7	undisturbed and saline charophytes	
			7-46	very wet clayey saline charophytes becoming drier and whiter in depth	
36	441044	4336574	0-25	edaphized charophytes	reed dominated area
			25-32	clay	
			32-63	edaphized charophytes	
			63-	clay	
37	440955	4336579	0-14	edaphized charophytes	dense reed bed in elevated position
			14-68	edaphized charophytes becoming more saline in depth	
38	440733	4336582	0-15	organic soil and edaphized charophytes	outside reed bed
			15-23	clay	
			23-46	brown charophytes	
			46-	clay	
39	440312	4336689	0-6	organic soil and edaphized charophytes	
			6-19	silty clayey material	
			19-34	dry highly compact saline charophytes	
40	440158	4336291	0-5	organic soil	
			5-38	clayey saline charophytes	

			38-	clay	
41	440357	4336159	0-30	organic soil and edaphized charophytes	old reed bed area next to firebreak
			30-36	saline charophytes mixed with edaphized charophytes	
			36-67	dry highly compact saline charophytes	
42	440397	4336155	0-15	organic soil and edaphized charophytes	reed bed area next to firebreak
			15-67	saline charophytes becoming whiter in depth	
			67-	clay	
43	440548	4335970	0-45	edaphized charophytes	old reed bed area next to firebreak
			45-80	saline charophytes	
			80-	clay	
44	440808	4335854	0-5	organic soil and edaphized charophytes	
			5-74	mix of edaphized and saline charophytes	
			74-	white saline charophytes	
45	440997	4335728	0-	fluvial silt	Cigüela ditch in Algeciras islet area
46	441232	4335496	0-8	organic soil	TDNP limit, tamarisk area
			8-15	mix of charophytes and clay	
			15-	clay with charophytes	
47	441142	4335568	15	edaphized charophytes	mix of tamarisk and reed
			15-30	clay and saline charophytes	
			30-	clay	
48	441739	4335530	0-10	edaphized charophytes	
			10-20	clayey edaphized charophytes	

			20-40	saline charophytes	
			40-	saline silica sand	
49	441507	4335407	0-5	edaphized charophytes	tamarisk area
			5-35	saline charophytes	
			35-	clay	
50	441108	4335223	0-10	organic soil	elevated microtopographic area
			10-44	clayey saline charophytes	
			44-	clay	
51	440885	4335316	0-5	organic soil	
			5-30	clayey saline charophytes	
			30-	clay	
52	440845	4335309	0-10	organic soil	lower microtopographic area with reed and cut-sedge vegetation
			10-53	edaphized charophytes	
			53-	saline charophytes more compact and clayey in depth	
53	440496	4335247	0-20	peat	
			20-30	edaphized charophytes	
			30-	clay	
54	440411	4335318	0-20	peat	reed bed
			20-90	edaphized charophytes	
			90-	clay	
55	440329	4335342	0-25	edaphized charophytes	lower microtopographic area
			25-33	saline charophytes	
			33-48	clayey saline charophytes	
			48-	clay	
56	440296	4335370	0-23	edaphized charophytes	
			23-30	compact saline charophytes	
			30-	clay	
57	440186	4335430	0-26	edaphized charophytes	
			26-62	compact saline charophytes	
58	440017	4335460	0-20	peat	
			20-56	clayey saline charophytes	

			56-	clay	
59	439922	4335491	0-5	organic soil	
			5-30	edaphized charophytes	
			30-	mix of edaphized and saline charophytes	
60	439651	4335944	0-10	organic soil	
			10-15	clay	
			15-35	clayey saline charophytes	
			35-	clay	
61	439667	4335908	0-20	organic soil and edaphized charophytes	reed bed area
			20-40	clayey saline charophytes	
			40-62	dry saline charophytes	
			62-	clay	
62	439723	4335853	0-30	organic soil and edaphized charophytes	
			30-74	mix of saline and edaphized charophytes	
			74-	clay	
63	439834	4335775	0-33	organic soil and edaphized charophytes	
			33-77	mix of edaphized and saline charophytes	
			77-	clay	
64	439519	4335947	0-6	organic soil	
			6-30	wet clayey saline charophytes	
			30-	dry compact clay	

APPENDIX B

Peat characteristics

B.1. Shrinking characteristics of Polish reed peat

Average properties of Polish peat		
Ash content (%)	Bulk density (g cm^{-3})	Degree of decomposition
14.4	0.187	H5

	S1	S2	S3
pF	Water content (cm^3 cm^{-3})		
0	0.8698	0.871	0.8712
0.4	0.8581	0.8631	0.8615
1	0.8382	0.8458	0.8443
1.5	0.7456	0.7536	0.7587
1.7	0.7085	0.7165	0.7195
2	0.6467	0.6575	0.6572
2.3	0.5992	0.6053	0.607
2.7	0.5083	0.5388	0.5203
3	0.4835	0.5194	0.4982
3.4	0.3801	0.4014	0.401
4.2	0.3248	0.3367	0.349

Measurements		Fit S1		Fit S1	
Curve S1		Curve 1		Curve 1	
Moisture	Void	Mois ratio	Void ratio	Mois ratio	Void ratio
9.2604	9.3231	0	1.8658	4.743	7.5309
9.0076	9.1534	0.093	2.1165	4.836	7.5841
8.7624	9.0947	0.186	2.3135	4.929	7.636
8.2188	8.9614	0.279	2.4968	5.022	7.6865
7.9256	8.8893	0.372	2.6719	5.115	7.7358
7.4831	8.7080	0.465	2.8411	5.208	7.7838
5.1851	7.5945	0.558	3.0056	5.301	7.8307
5.0461	7.5444	0.651	3.1659	5.394	7.8763
4.8438	7.4165	0.744	3.3226	5.487	7.9209
4.5025	7.2530	0.837	3.4757	5.58	7.9644
4.1461	7.0282	0.93	3.6256	5.673	8.0068
3.7466	6.8231	1.023	3.7723	5.766	8.0482
3.3522	6.5702	1.116	3.9159	5.859	8.0886
3.1525	6.4292	1.209	4.0565	5.952	8.1282
2.9654	6.2506	1.302	4.1942	6.045	8.1668
2.7581	6.0807	1.395	4.3288	6.138	8.2045
2.5483	5.8418	1.488	4.4606	6.231	8.2414
2.3941	5.6791	1.581	4.5896	6.324	8.2775
2.2146	5.4857	1.674	4.7156	6.417	8.3128
1.9416	5.1619	1.767	4.8389	6.51	8.3474
1.7014	4.8547	1.86	4.9594	6.603	8.3812
1.4713	4.4938	1.953	5.0772	6.696	8.4144
1.1098	3.8680	2.046	5.1922	6.789	8.4469
0	1.8658	2.139	5.3046	6.882	8.4788
		2.232	5.4143	6.975	8.51
		2.325	5.5214	7.068	8.5407
		2.418	5.626	7.161	8.5709
		2.511	5.728	7.254	8.6005
		2.604	5.8275	7.347	8.6296
		2.697	5.9246	7.44	8.6582
		2.79	6.0192	7.533	8.6863
		2.883	6.1115	7.626	8.714
		2.976	6.2015	7.719	8.7413
		3.069	6.2892	7.812	8.7682
		3.162	6.3746	7.905	8.7947
		3.255	6.4579	7.998	8.8208
		3.348	6.539	8.091	8.8466
		3.441	6.618	8.184	8.8721
		3.534	6.695	8.277	8.8972
		3.627	6.77	8.37	8.9221
		3.72	6.843	8.463	8.9466
		3.813	6.9142	8.556	8.971
		3.906	6.9834	8.649	8.995
		3.999	7.0509	8.742	9.0189
		4.092	7.1166	8.835	9.0425
		4.185	7.1806	8.928	9.0659
		4.278	7.2429	9.021	9.0891
		4.371	7.3035	9.114	9.1513
		4.464	7.3626	9.207	9.2257
		4.557	7.4202	9.3	9.3
		4.65	7.4763		

Void0	1.87
MoisA	9.04
Alfa	0.75
Beta	2.75
P	0.48
R^2	0.9975
RMSE	0.01662

0.000	1.866
9.260	9.323

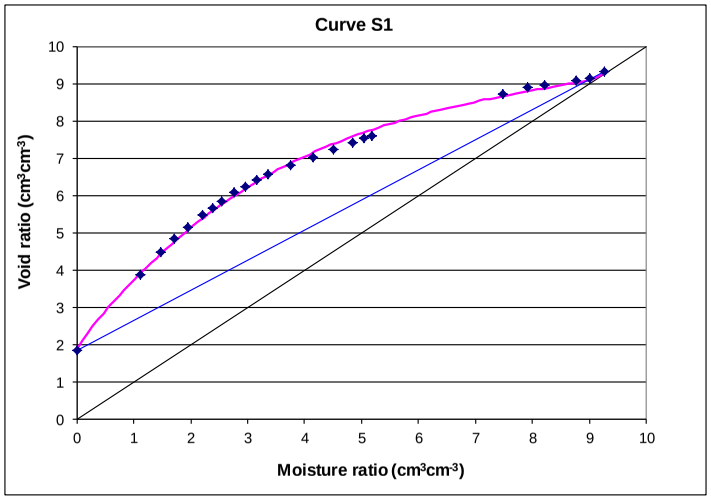

Measurements		Fit S2		Fit S2	
Curve S2		Curve 2		Curve 2	
Moisture	Void	Mois ratio	Void ratio	Mois ratio	Void ratio
8.2482	8.3146	0	1.4887	4.2066	6.6911
7.8799	8.1703	0.0825	1.6616	4.2891	6.7342
7.4617	8.0423	0.165	1.8293	4.3716	6.7762
6.6973	7.8040	0.2474	1.9949	4.454	6.8172
6.2071	7.5609	0.3299	2.1586	4.5365	6.8572
5.5894	7.2605	0.4124	2.3203	4.619	6.8963
3.1688	5.9995	0.4949	2.4799	4.7015	6.9345
2.9750	5.8445	0.5774	2.6372	4.784	6.9719
2.7451	5.6513	0.6599	2.792	4.8665	7.0085
2.4238	5.2636	0.7423	2.9442	4.9489	7.0445
2.1164	5.0513	0.8248	3.0935	5.0314	7.0798
1.7397	4.5990	0.9073	3.2399	5.1139	7.1144
1.4018	4.1092	0.9898	3.3832	5.1964	7.1485
1.2357	3.8490	1.0723	3.5234	5.2789	7.1821
1.1000	3.6084	1.1548	3.6604	5.3613	7.2152
0.9753	3.3966	1.2372	3.794	5.4438	7.2478
0.7842	3.0251	1.320	3.9244	5.5263	7.2801
0.6734	2.8055	1.4022	4.0515	5.6088	7.312
0.5737	2.5956	1.4847	4.1751	5.6913	7.3435
0.4408	2.3252	1.5672	4.2955	5.7738	7.3747
0.3660	2.1736	1.6496	4.4124	5.8562	7.4057
0.2248	1.8913	1.7321	4.5261	5.9387	7.4364
0.0000	1.4887	1.8146	4.6364	6.0212	7.467
		1.8971	4.7435	6.1037	7.4973
		1.9796	4.8474	6.1862	7.5275
		2.0621	4.9481	6.2687	7.5575
		2.1445	5.0457	6.3511	7.5875
		2.227	5.1402	6.4336	7.6173
		2.3095	5.2318	6.5161	7.6471
		2.392	5.3204	6.5986	7.6769
		2.4745	5.4062	6.6811	7.7066
		2.557	5.4892	6.7635	7.7363
		2.6394	5.5696	6.846	7.766
		2.7219	5.6473	6.9285	7.7957
		2.8044	5.7225	7.011	7.8255
		2.8869	5.7952	7.0935	7.8553
		2.9694	5.8656	7.176	7.8852
		3.0518	5.9337	7.2584	7.9152
		3.1343	5.9996	7.3409	7.9452
		3.2168	6.0633	7.4234	7.9754
		3.2993	6.125	7.5059	8.0056
		3.3818	6.1848	7.5884	8.036
		3.4643	6.2426	7.6709	8.0665
		3.5467	6.2987	7.7533	8.0971
		3.6292	6.353	7.8358	8.1279
		3.7117	6.4057	7.9183	8.1587
		3.7942	6.4568	8.0008	8.1898
		3.8767	6.5064	8.0833	8.221
		3.9591	6.5545	8.1657	8.2523
		4.0416	6.6013	8.2482	8.2838
		4.1241	6.6468		

Void0	1.49
MoisA	8.33
Alfa	0.96
Beta	4.03
P	0.56
R^2	0.9996
RMSE	0.0098

0.000	1.489
8.248	8.315

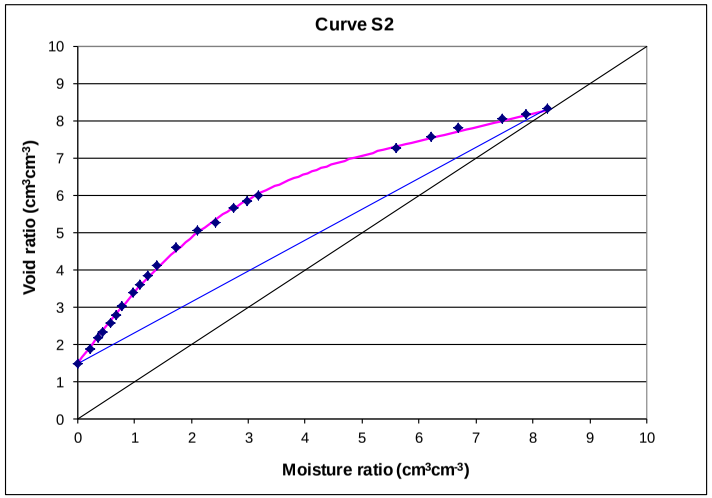

Measurements		Fit S3		Fit S3	
Curve S3		Curve 3		Curve 3	
Moisture	Void	Mois ratio	Void ratio	Mois ratio	Void ratio
8.1267	8.1699	0	1.39	4.1446	6.6229
7.8183	8.0311	0.0813	1.6147	4.2259	6.6701
7.5234	7.9882	0.1625	1.7943	4.3072	6.7159
6.8686	7.8188	0.2438	1.9626	4.3884	6.7606
6.4999	7.6521	0.3251	2.1244	4.4697	6.8041
6.0262	7.3911	0.4063	2.2815	4.551	6.8464
3.4742	6.1271	0.4876	2.4347	4.6322	6.8877
3.2753	5.9775	0.5689	2.5846	4.7135	6.9279
3.0339	5.7793	0.6501	2.7313	4.7948	6.9672
2.7278	5.5339	0.7314	2.875	4.876	7.0054
2.4596	5.2929	0.8127	3.0158	4.9573	7.0427
2.1021	4.9189	0.8939	3.1537	5.0386	7.0792
1.7535	4.5234	0.9752	3.2889	5.1198	7.1148
1.5859	4.2867	1.0565	3.4212	5.2011	7.1495
1.4362	4.0659	1.1377	3.5508	5.2824	7.1835
1.2999	3.8583	1.219	3.6775	5.3636	7.2168
1.1323	3.5637	1.300	3.8015	5.4449	7.2493
1.0004	3.3417	1.3815	3.9227	5.5262	7.2812
0.8820	3.1121	1.4628	4.0411	5.6074	7.3124
0.7054	2.7503	1.5441	4.1569	5.6887	7.343
0.5736	2.4828	1.6253	4.2698	5.77	7.373
0.4395	2.2239	1.7066	4.3801	5.8512	7.4024
0.3054	1.9596	1.7879	4.4877	5.9325	7.4314
0.0000	1.3946	1.8691	4.5926	6.0138	7.4598
		1.9504	4.6949	6.095	7.4877
		2.0317	4.7946	6.1763	7.5152
		2.1129	4.8918	6.2576	7.5422
		2.1942	4.9864	6.3388	7.5689
		2.2755	5.0786	6.4201	7.5951
		2.3568	5.1683	6.5014	7.621
		2.438	5.2556	6.5826	7.6466
		2.5193	5.3406	6.6639	7.6718
		2.6006	5.4233	6.7452	7.6968
		2.6818	5.5037	6.8264	7.7215
		2.7631	5.5819	6.9077	7.7459
		2.8444	5.658	6.989	7.77
		2.9256	5.7319	7.0703	7.794
		3.0069	5.8038	7.1515	7.8177
		3.0882	5.8737	7.2328	7.8412
		3.1694	5.9416	7.3141	7.8646
		3.2507	6.0076	7.3953	7.8878
		3.332	6.0718	7.4766	7.9108
		3.4132	6.1342	7.5579	7.9337
		3.4945	6.1948	7.6391	7.9565
		3.5758	6.2537	7.7204	7.9791
		3.657	6.311	7.8017	8.0017
		3.7383	6.3667	7.8829	8.0241
		3.8196	6.4209	7.9642	8.0465
		3.9008	6.4735	8.0455	8.0688
		3.9821	6.5247	8.1267	8.1267
		4.0634	6.5745		

Void0	**1.39**
MoisA	**8.06**
Alfa	**0.76**
Beta	**3.04**
P	**0.56**
R^2	**0.9992**
RMSE	**0.0131**

0.000	1.395
8.127	8.170

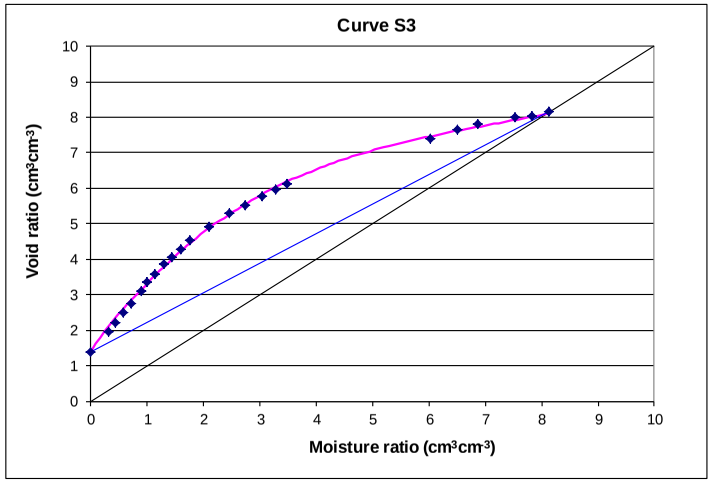

Measurements	
Curve S4	
Moisture	Void
8.6628	8.6628
8.2994	8.4850
7.9663	8.4340
7.3270	8.2451
6.9131	8.0609
6.2738	7.6594
3.3566	5.8276
3.1244	5.6224
2.8418	5.3740
2.4784	5.0208
2.1083	4.6250
1.7180	4.1362
1.3512	3.6359
1.1863	3.3600
1.0248	3.0978
0.9071	2.9100
0.6547	2.4365
0.5504	2.2306
0.4528	2.0494
0.3485	1.8596
0.2913	1.7728
0.2476	1.3757
0.0000	1.0166

Fit S4	
Curve 4	
Mois ratio	Void ratio
0	1.0166
0.0866	1.3084
0.1733	1.5018
0.2599	1.6793
0.3465	1.8485
0.4331	2.0125
0.5198	2.1723
0.6064	2.3287
0.693	2.482
0.7797	2.6323
0.8663	2.7798
0.9529	2.9246
1.0395	3.0666
1.1262	3.2059
1.2128	3.3424
1.2994	3.4763
1.386	3.6075
1.4727	3.7359
1.5593	3.8617
1.6459	3.9848
1.7326	4.1053
1.8192	4.2231
1.9058	4.3383
1.9924	4.451
2.0791	4.561
2.1657	4.6686
2.2523	4.7736
2.339	4.8762
2.4256	4.9764
2.5122	5.0742
2.5988	5.1697
2.6855	5.2628
2.7721	5.3538
2.8587	5.4425
2.9453	5.5291
3.032	5.6136
3.1186	5.696
3.2052	5.7765
3.2919	5.8549
3.3785	5.9315
3.4651	6.0062
3.5517	6.0791
3.6384	6.1502
3.725	6.2197
3.8116	6.2874
3.8983	6.3536
3.9849	6.4182
4.0715	6.4813
4.1581	6.5429
4.2448	6.603
4.3314	6.6618

Fit S4	
Curve 4	
Mois ratio	Void ratio
4.418	6.7193
4.5046	6.7755
4.5913	6.8304
4.6779	6.8842
4.7645	6.9367
4.8512	6.9882
4.9378	7.0386
5.0244	7.0879
5.111	7.1363
5.1977	7.1836
5.2843	7.2301
5.3709	7.2757
5.4576	7.3204
5.5442	7.3643
5.6308	7.4074
5.7174	7.4498
5.8041	7.4914
5.8907	7.5324
5.9773	7.5727
6.064	7.6123
6.1506	7.6514
6.2372	7.6899
6.3238	7.7279
6.4105	7.7653
6.4971	7.8022
6.5837	7.8387
6.6703	7.8748
6.757	7.9104
6.8436	7.9456
6.9302	7.9804
7.0169	8.0149
7.1035	8.0491
7.1901	8.0829
7.2767	8.1165
7.3634	8.1497
7.45	8.1827
7.5366	8.2155
7.6233	8.248
7.7099	8.2804
7.7965	8.3125
7.8831	8.3444
7.9698	8.3762
8.0564	8.4079
8.143	8.4394
8.2296	8.4707
8.3163	8.502
8.4029	8.5331
8.4895	8.5642
8.5762	8.5952
8.6628	8.6628

Void0	1.02
MoisA	8.59
Alfa	0.57
Beta	2.76
P	0.61
R^2	0.9991
RMSE	0.0163

0.000	1.017
8.663	8.663

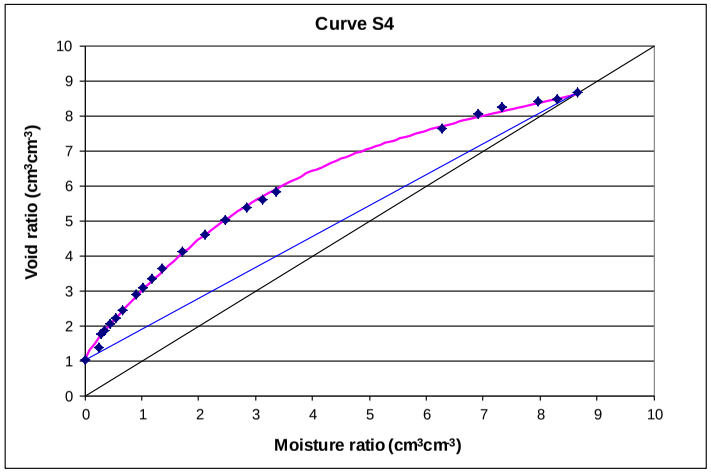

Fit normalized curves

Moisture	Void	Moisture	Void	Curves normalized Mois ratio	Void ratio	Curves normalized Mois ratio	Void ratio
1.00	1.01	0.80	0.94	0	0.17	0.51	0.8038
0.97	0.99	0.74	0.91	0.01	0.1969	0.52	0.8096
0.95	0.98	0.43	0.75	0.02	0.2185	0.53	0.8153
0.89	0.97	0.40	0.74	0.03	0.2387	0.54	0.8209
0.86	0.96	0.37	0.71	0.04	0.2582	0.55	0.8263
0.81	0.94	0.34	0.68	0.05	0.2772	0.56	0.8316
0.56	0.82	0.30	0.65	0.06	0.2956	0.57	0.8368
0.54	0.81	0.26	0.61	0.07	0.3137	0.58	0.8419
0.52	0.80	0.22	0.56	0.08	0.3314	0.59	0.8468
0.49	0.78	0.20	0.53	0.09	0.3488	0.6	0.8516
0.45	0.76	0.18	0.50	0.1	0.3658	0.61	0.8563
0.40	0.74	0.16	0.47	0.11	0.3824	0.62	0.861
0.36	0.71	0.14	0.44	0.12	0.3987	0.63	0.8655
0.34	0.69	0.12	0.41	0.13	0.4147	0.64	0.8699
0.32	0.67	0.11	0.38	0.14	0.4303	0.65	0.8743
0.30	0.66	0.09	0.34	0.15	0.4456	0.66	0.8785
0.28	0.63	0.07	0.31	0.160	0.4606	0.67	0.8827
0.26	0.61	0.05	0.27	0.17	0.4753	0.68	0.8868
0.24	0.59	0.04	0.24	0.18	0.4896	0.69	0.8908
0.21	0.56	0.00	0.17	0.19	0.5035	0.7	0.8948
0.18	0.52	1.00	1.00	0.2	0.5172	0.71	0.8987
0.16	0.49	0.96	0.98	0.21	0.5305	0.72	0.9025
0.12	0.42	0.92	0.97	0.22	0.5435	0.73	0.9062
0.00	0.20	0.85	0.95	0.23	0.5562	0.74	0.91
1.00	1.01	0.80	0.93	0.24	0.5686	0.75	0.9136
0.96	0.99	0.72	0.88	0.25	0.5807	0.76	0.9172
0.90	0.98	0.39	0.67	0.26	0.5924	0.77	0.9208
0.81	0.95	0.36	0.65	0.27	0.6039	0.78	0.9243
0.75	0.92	0.33	0.62	0.28	0.6151	0.79	0.9278
0.68	0.88	0.29	0.58	0.29	0.6259	0.8	0.9312
0.38	0.73	0.24	0.53	0.3	0.6365	0.81	0.9346
0.36	0.71	0.20	0.48	0.31	0.6468	0.82	0.9379
0.33	0.69	0.16	0.42	0.32	0.6569	0.83	0.9413
0.29	0.64	0.14	0.39	0.33	0.6666	0.84	0.9446
0.26	0.61	0.12	0.36	0.34	0.6761	0.85	0.9478
0.21	0.56	0.10	0.34	0.35	0.6854	0.86	0.9511
0.17	0.50	0.08	0.28	0.36	0.6944	0.87	0.9543
0.15	0.47	0.06	0.26	0.37	0.7032	0.88	0.9575
0.13	0.44	0.05	0.24	0.38	0.7117	0.89	0.9607
0.12	0.41	0.04	0.21	0.39	0.72	0.9	0.9638
0.10	0.37	0.03	0.20	0.4	0.728	0.91	0.967
0.08	0.34	0.03	0.16	0.41	0.7359	0.92	0.9701
0.07	0.31	0.00	0.12	0.42	0.7435	0.93	0.9732
0.05	0.28			0.43	0.751	0.94	0.9763
0.04	0.26			0.44	0.7582	0.95	0.9794
0.03	0.23			0.45	0.7652	0.96	0.9825
0.00	0.18			0.46	0.7721	0.97	0.9856
1.00	1.01			0.47	0.7788	0.98	0.9886
0.96	0.99			0.48	0.7853	0.99	0.9917
0.93	0.98			0.49	0.7916	1	1
0.85	0.96			0.5	0.7978		

		Averages of curves 1-4	
Void0	0.17	1.44	
MoisA	0.99	8.51	
Alfa	0.76	0.76	0.167158105
Beta	3.08	3.14	0.987195968
P	0.54	0.55	
R^2	0.9930	0.9989	
RMSE	0.0023	0.0140	

0.000	0.170		
1.000	1.000		8.618

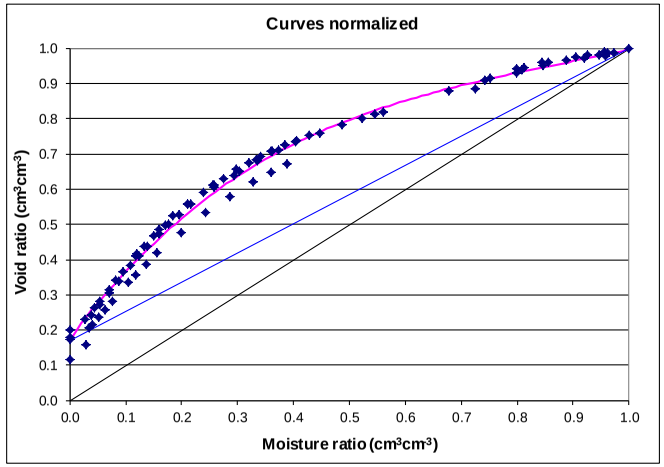

Composed curve for TDNP peat

Curve TDNP		Curve TDNP	
Mois ratio	Void ratio	Mois ratio	Void ratio
	0		
0	0.6		
0.0353	0.6952	1.8003	2.8339
0.0706	0.7716	1.8356	2.8544
0.1059	0.8433	1.8709	2.8745
0.1412	0.9123	1.9062	2.8941
0.1765	0.9792	1.9415	2.9131
0.2118	1.0446	1.9768	2.9318
0.2471	1.1085	2.0121	2.9499
0.2824	1.171	2.0474	2.9677
0.3177	1.2323	2.0827	2.9851
0.353	1.2923	2.118	3.0021
0.3883	1.3511	2.1533	3.0187
0.4236	1.4087	2.1886	3.0349
0.4589	1.465	2.2239	3.0508
0.4942	1.5202	2.2592	3.0664
0.5295	1.5742	2.2945	3.0817
0.565	1.627	2.3298	3.0967
0.6001	1.6786	2.3651	3.1114
0.6354	1.7291	2.4004	3.1259
0.6707	1.7783	2.4357	3.1401
0.706	1.8264	2.471	3.154
0.7413	1.8734	2.5063	3.1677
0.7766	1.9192	2.5416	3.1812
0.8119	1.9639	2.5769	3.1945
0.8472	2.0075	2.6122	3.2077
0.8825	2.0499	2.6475	3.2206
0.9178	2.0913	2.6828	3.2333
0.9531	2.1316	2.7181	3.2459
0.9884	2.1709	2.7534	3.2584
1.0237	2.2092	2.7887	3.2707
1.059	2.2464	2.824	3.2828
1.0943	2.2827	2.8593	3.2949
1.1296	2.3179	2.8946	3.3068
1.1649	2.3523	2.9299	3.3186
1.2002	2.3857	2.9652	3.3303
1.2355	2.4182	3.0005	3.3419
1.2708	2.4498	3.0358	3.3535
1.3061	2.4806	3.0711	3.3649
1.3414	2.5106	3.1064	3.3763
1.3767	2.5397	3.1417	3.3876
1.412	2.568	3.177	3.3989
1.4473	2.5956	3.2123	3.4101
1.4826	2.6224	3.2476	3.4212
1.5179	2.6485	3.2829	3.4323
1.5532	2.6739	3.3182	3.4434
1.5885	2.6986	3.3535	3.4544
1.6238	2.7227	3.3888	3.4654
1.6591	2.7461	3.4241	3.4764
1.6944	2.7689	3.4594	3.4873
1.7297	2.7911	3.4947	3.5007
1.765	2.8128	3.53	3.53

		F =	3.53
Void0	0.600	= F * value normalized curve	
MoisA	3.492	= F * value normalized curve	
Alfa	0.760		
Beta	3.084		
P	0.539		

0.000	0.600
3.527	3.527

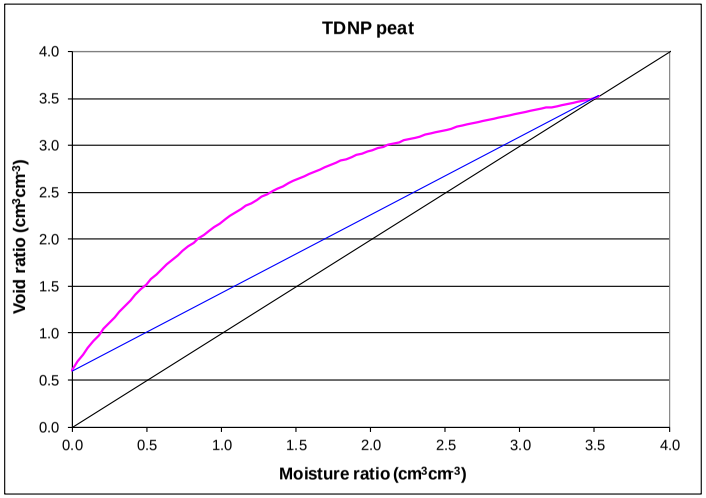

B.2. Organic matter content of Las Tablas de Daimiel National Park organic soils

Sample	X_UTM	Y_UTM	Depth (cm)	Soil functional type (SFT)	Average C_{org} (%)	Average OM (%)
1	440277	4331461	75 - 100	Edaphized charophytes	5.19	8.94
2	436110	4330614	0 - 20	Edaphized charophytes	6.18	10.65
3	436442	4331472	83 - 100	Edaphized charophytes	18.81	32.42
4	436379	4331471	0 - 10	Edaphized charophytes	21.03	36.25
5	438165	4330943	0 - 10	Organic soil	9.17	15.82
6	438086	4330963	0 - 20	Organic soil	17.04	29.38
7	437984	4330997	10 - 36	Organic soil	32.69	56.36
8	440277	4331461	50 - 75	Undisturbed charophytes	5.96	10.28
9	437954	4330940	0 - 20	Peat	12.34	21.28
10	436174	4330549	0 - 7	Peat	13.90	23.96
11	438064	4330940	50 - 58	Peat	15.45	26.63
12	436442	4331472	110 - 115	Peat	17.32	29.86
13	439379	4331751	0 - 5	Peat	17.56	30.28
14	440426	4331563	0 - 20	Peat	17.64	30.41
15	436856	4331826	68 - 72	Peat	22.47	38.73
16	438007	4331031	0 - 9	Peat	22.88	39.45
17	438089	4330966	10 - 30	Peat	24.13	41.61
18	437980	4331001	70 - 80	Peat	24.44	42.13
19	439752	4331771	20	Peat	24.60	42.41
20	439404	4331977	50 - 67	Peat	25.24	43.52
21	438090	4330966	20	Peat	25.40	43.80
22	438008	4331031	10 - 15	Peat	25.58	44.09
23	438952	4331615	45	Peat	29.00	50.00
24	435970	4330700	51 - 63	Peat	29.63	51.09
25	437980	4331001	30 - 50	Peat	30.33	52.29
26	437987	4331002	36 - 45	Peat	31.06	53.55
27	437984	4330997	36 - 43	Peat	31.67	54.60
28	438007	4331031	49 - 58	Peat	32.01	55.19
29	438177	4331110	45 - 50	Peat	32.52	56.07
30	439355	4331786	29 - 35.5	Peat	33.80	58.28
31	439050	4331666	21 - 29	Peat	34.21	58.99
32	437909	4331038	30 - 35	Peat	34.84	60.06
33	438009	4331031	45 - 56	Peat	36.06	62.17
34	439050	4331666	30	Peat	36.85	63.52
35	438408	4331192	27 - 38	Peat	37.72	65.03
36	438085	4330964	51 - 70	Peat	38.19	65.83
37	439050	4331666	11 - 21	Peat	41.24	71.10

APPENDIX C

SWAP input data file

C. Input data file for peat SWAP model

```
*******************************************************************************
**
* Filename: Peat.swp
* Contents: Main input data
*******************************************************************************
**
* Comment area:
*
* Case: Water flow model in Las Tablas de Daimiel National Park in central Spain

*******************************************************************************
**

*   The main input file .swp contains the following sections:
*         - General section
*         - Meteorology section
*         - Crop section
*         - Soil water section
*         - Lateral drainage section
*         - Bottom boundary section
*         - Heat flow section
*         - Solute transport section


*** GENERAL SECTION ***

*******************************************************************************
**
* Part 1: Environment

 PROJECT   = 'Tablas'          ! Project description, [A80]
 PATHWORK  = 'C:\Peat_run2_jan\'   ! Path to work folder, [A80]
 PATHATM   = 'C:\Peat_run2_jan\'   ! Path to folder with weather files, [A80]
 PATHCROP  = 'C:\Peat_run2_jan\'  ! Path to folder with crop files, [A80]
 PATHDRAIN = 'C:\Peat_run2_jan\'  ! Path to folder with drainage files, [A80]
 SWSCRE    = 1              ! Switch, display progression of simulation run:
                   !  SWSCRE = 0:  no display to screen
                   !  SWSCRE = 1:  display water balance to screen
                   !  SWSCRE = 2:  display daynumber to screen
 SWERROR   = 1           ! Switch for printing errors to screen [Y=1, N=0]
```

```
*******************************************************************************
**
*******************************************************************************
**
* Part 2: Simulation period
*
 TSTART  = 01-mar-2007 ! Start date of simulation run, give day-month-year, [dd-mmm-yyyy]
 TEND    = 26-may-2009 ! End   date of simulation run, give day-month-year, [dd-mmm-yyyy]
*******************************************************************************
**


*******************************************************************************
**
* Part 3: Output dates

* Number of output times during a day
 NPRINTDAY = 1      ! Number of output times during a day, [1..1000, I]

* If NPRINTDAY = 1, specify dates for output of state variables and fluxes
 SWMONTH = 0        ! Switch, output each month, [Y=1, N=0]

* If SWMONTH = 0, choose output interval and/or specific dates
 PERIOD = 1         ! Fixed output interval, ignore = 0, [0..366, I]
 SWRES  = 0         ! Switch, reset output interval counter each year, [Y=1, N=0]
 SWODAT = 0         ! Switch, extra output dates are given in table, [Y=1, N=0]

* If SWODAT = 1, list specific dates [dd-mmm-yyyy], maximum MAOUT dates:
 OUTDATINT =
 31-Jan-1980
 31-Dec-1982
* End of table

* Output times for overall water and solute balances in *.BAL and *.BLC file
* Output can be provided at a fixed date in a year or at different dates:
 SWYRVAR = 0        ! SWYRVAR = 0: each year output of balances at the same date
                    ! SWYRVAR = 1: output of balances at different dates

* If SWYRVAR = 0 specify fixed date:
 DATEFIX = 31 12    ! Specify day and month for output of yearly balances, [dd mm]

* If SWYRVAR = 1 specify all output dates [dd-mmm-yyyy], maximum MAOUT dates:
 OUTDAT =
 31-dec-1981
 31-dec-1982
* End of table
```

```
**********************************************************************
**
* Part 4: Output files

* General information
 OUTFIL   = 'Result' ! Generic file name of output files, [A16]
 SWHEADER = 0       ! Print header at the start of each balance period, [Y=1, N=0]

* Optional files
 SWVAP  = 1       ! Switch, output profiles of moisture, solute and temperature, [Y=1, N=0]
 SWBLC  = 1       ! Switch, output file with detailed yearly water balance, [Y=1, N=0]
 SWATE  = 1       ! Switch, output file with soil temperature profiles, [Y=1, N=0]
 SWBMA  = 1       ! Switch, output file with water fluxes, only for macropore flow, [Y=1, N=0]
 SWDRF  = 0       ! Switch, output of drainage fluxes, only for extended drainage, [Y=1, N=0]
 SWSWB  = 0       ! Switch, output surface water reservoir, only for extended drainage, [Y=1, N=0]

* Output for water quality models (PEARL, ANIMO) or other specific use (SWAFO to DZNEW)

* Optional output files
 SWAFO  = 0       ! Switch, output file with formatted hydrological data
                  ! SWAFO = 0: no output
                  ! SWAFO = 1: output to a file named *.AFO
                  ! SWAFO = 2: output to a file named *.BFO

 SWAUN  = 0       ! Switch, output file with unformatted hydrological data
                  ! SWAUN = 0: no output
                  ! SWAUN = 1: output to a file named *.AUN
                  ! SWAUN = 2: output to a file named *.BUN

* Critical deviation of water balance; in case of larger deviation, an error file is created
(*.DWB.CSV)
 CRITDEVMASBAL = 0.00001  ! Critical Deviation in water balance during PERIOD [0.0..1.0 cm, R]

* If SWAFO = 1 or 2, or SWAUN = 1 or 2: fine vertical discretization can be lumped
 SWDISCRVERT = 0   ! SWDISCRVERT = 0: no conversion
                   ! SWDISCRVERT = 1: convert vertical discretization,

* If SWDISCRVERT = 1 then specify:
 NUMNODNEW = 6    ! New number of nodes [1..macp, I, -]
* List thickness of each compartment, total thickness should correspond to Soil Water Section,
part 4
 DZNEW     = 1.0 1.0 1.0 1.0 1.0 1.0 1.0 1.0 1.0 1.0 2.5 2.5 2.5 2.5 2.5 2.5 2.5 2.5 5.0 5.0 5.0 5.0 5.0
5.0 5.0 5.0 5.0 10.0 10.0 10.0 10.0 10.0 10.0 10.0 10.0 10.0 10.0 10.0 10.0 10.0 10.0 10.0 10.0
10.0 25.0 25.0 25.0 25.0 25.0 25.0 25.0 25.0 ! thickness of compartments [1.0d-6...5.0d2, cm,
R]**********************************************************************
****
```

```
*** METEOROLOGY SECTION ***

************************************************************************
**
* General data

* File name
 METFIL = 'Meteo_TD'  ! File name of meteorological data without extension .YYY, [A200]
                ! Extension is equal to last 3 digits of year, e.g. 003 denotes year 2003

* Use of reference evapotranspiration data from meteorological file instead of basic data
 SWETR  =  0          ! Switch, use reference ET values of meteo file [Y=1, N=0]

* If SWETR = 0, specify:
 LAT    =   39.136      ! Latitude of meteo station, [-60..60 degrees, R, North = +]
 ALT    =   619.0       ! Altitude of meteo station, [-400..3000 m, R]
 ALTW   =   10.2         ! Altitude of wind speed measurement (10 m is default) [0..99 m, R]  Source
PNTD

* Use of detailed meteorological records for both ET and rainfall (< 1 day) in stead of daily values
 SWMETDETAIL = 0       ! Switch, use detailed meteorological records of both ET and rainfall [Y=1,
N=0]

* In case of detailed meteorological weather records (SWMETDETAIL = 1), specify:
 NMETDETAIL = 10       ! Number of weather data records per day, [1..96 -, I]

* In case of daily meteorological weather records (SWMETDETAIL = 0):
 SWETSINE = 0          ! Switch, distribute daily Tp and Ep according to sinus wave [Y=1, N=0] debería
usar esta option?

 SWRAIN =  3          ! Switch for use of actual rainfall intensity (only if SWMETDETAIL = 0):
                ! SWRAIN = 0: Use daily rainfall amounts
                ! SWRAIN = 1: Use daily rainfall amounts + mean intensity
                ! SWRAIN = 2: Use daily rainfall amounts + duration
                ! SWRAIN = 3: Use short time rainfall intensities, as supplied in separate file

* If SWRAIN = 1, then specify mean rainfall intensity RAINFLUX [0.d0..1000.d0 mm/d, R]
* as function of time TIME [0..366 d, R], maximum 30 records
  TIME    RAINFLUX
   1.0       20.0
 360.0       20.0
* End of table

* If SWRAIN = 3, then specify file name of file with detailed rainfall data
```

```
 RAINFIL = 'Raindetail'   ! File name of detailed rainfall data without extension .YYY, [A200]
                          ! Extension is equal to last 3 digits of year, e.g. 003 denotes year 2003
************************************************************************************
**


*** CROP SECTION ***

************************************************************************************
**
* Part 1: Crop rotation scheme during simulation period Sólo es posible un único crop por periodo,
es decir, dos especies no se pueden solapar en el tiempo (programa para granjeros)

* Specify information for each crop (maximum MACROP):
* CROPSTART  = date of crop emergence, [dd-mmm-yyyy]
* CROPEND    = date of crop harvest, [dd-mmm-yyyy]
* CROPNAME   = crop name, [A40]
* CROPFIL    = name of file with crop input parameters without extension .CRP, [A40]
* CROPTYPE   = type of crop model: simple = 1, detailed general = 2, detailed grass = 3

 CROPSTART     CROPEND      CROPNAME               CROPFIL        CROPTYPE
 01-mar-2007   15-jul-2007  'Cochlearia glastifolia'    'Cochlearia'    1
 16-jul-2007   30-nov-2007  'Conya canadensis'          'Conya'    1
 01-mar-2008   15-jul-2008  'Cochlearia glastifolia'    'Cochlearia'    1
 16-jul-2008   30-nov-2008  'Conya canadensis'          'Conya'    1
 01-mar-2009   26-may-2009  'Cochlearia glastifolia'    'Cochlearia'    1
* End of table
************************************************************************************
**


************************************************************************************
**
* Part 2: Fixed irrigation applications

* Switch for fixed irrigation applications
 SWIRFIX = 0    ! SWIRFIX = 0: no irrigation applications are prescribed
                ! SWIRFIX = 1: irrigation applications are prescribed

* If SWIRFIX = 1, specify:

* Switch for separate file with fixed irrigation applications
 SWIRGFIL  = 0  ! SWIRGFIL = 0: data are specified in the .swp file
                ! SWIRGFIL = 1: data are specified in a separate file

* If SWIRGFIL  = 0 specify information for each fixed irrigation event (max. MAIRG):
```

```
* IRDATE   = date of irrigation, [dd-mmm-yyyy]
* IRDEPTH  = amount of water, [0.0..100.0 cm, R]
* IRCONC   = concentration of irrigation water, [0.0..1000.0 mg/cm3, R]
* IRTYPE   = type of irrigation: sprinkling = 0, surface = 1

     IRDATE   IRDEPTH    IRCONC   IRTYPE
 05-jan-1980      0.5    1000.0       1
* end of table

* If SWIRGFIL  = 1, specify name of file with data of fixed irrigation applications:
  IRGFIL = 'testirri'     ! File name without extension .IRG [A16]
*************************************************************************
**


*** SOIL WATER SECTION ***

*************************************************************************
**
* Part 1: Initial soil moisture condition

 SWINCO = 2 ! Switch, type of initial soil moisture condition:
         ! 1 = pressure head as function of depth is input
         ! 2 = pressure head of each compartment is in hydrostatic equilibrium
         !     with initial groundwater level
         ! 3 = read final pressure heads from output of previous Swap simulation

* If SWINCO = 1, specify (maximum MACP):
* ZI = soil depth, [-10000..0 cm, R]
* H  = initial soil water pressure head, [-1.d10..1.d4 cm, R]

     ZI        H
-7.5      -1396.70826
-17.5     -40.6551012
-45.0     -61.6532472
-55.0     -33.60949568
-65.0     -32.75563833
-75.0     -0.358581752
-85.0     -31.21661319
-95.0     -9.06126665
-105.0     -10.3995084
* End of table

* If SWINCO = 2, specify:
  GWLI   = -116.400 ! Initial groundwater level, [-10000..100 cm, R]
```

```
* If SWINCO = 3, specify:
  INIFIL = 'result.end'   ! name of final with extension .END [a200]
******************************************************************************
**

******************************************************************************
**
* Part 2: Ponding, runoff and runon

* Ponding
  PONDMX  = 2.0  ! In case of ponding, minimum thickness for runoff, [0..1000 cm, R]

* Runoff
  RSRO    =  0.7 ! Drainage resistance for surface runoff [0.001..1.0 d, R]
  RSROEXP =  1.0 ! Exponent in drainage equation of surface runoff [0.1..10.0 -, R]

* Runon
* Specify whether runon data are provided in extra input file
  SWRUNON = 0  ! 0 = No input of runon data
               ! 1 = Runon data are provided in extra input file

* If SWRUNON = 1, specify name of file with runon input data
* This file may be an output *.inc file (with only 1 header) of a previous Swap-simulation
  RUFIL = 'runon.inc' ! File name with extension [A80]
******************************************************************************
**

******************************************************************************
**
* Part 3: Soil evaporation
*
  SWCFBS = 0   ! Switch for use of soil factor CFBS to calculate Epot from ETref
               ! 0 = CFBS is not used
               ! 1 = CFBS is used

* If SWCFBS = 1, specify soil factor CFBS:
  CFBS   = 1.0 ! Coefficient to derive Epot from ETref [0.1..1.5 -, R]
*
*
  SWREDU = 1   ! Switch, method for reduction of potential soil evaporation:
               ! 0 = reduction to maximum Darcy flux
               ! 1 = reduction to maximum Darcy flux and to maximum Black (1969)
               ! 2 = reduction to maximum Darcy flux and to maximum Bo/Str. (1986)
```

```
 COFRED = 0.35 ! Soil evaporation coefficient of Black, [0..1 cm/d1/2, R],
           ! or Boesten/Stroosnijder, [0..1 cm1/2, R]
 RSIGNI =  0.5 ! Minimum rainfall to reset method of Black [0..1 cm/d, R]
*******************************************************************************
**


*******************************************************************************
**
* Part 4: Vertical discretization of soil profile

* Specify the following data (maximum MACP lines):
* ISOILLAY = number of soil layer, start with 1 at soil surface, [1..MAHO, I]
* ISUBLAY  = number of sub layer, start with 1 at soil surface, [1..MACP, I]
* HSUBLAY  = height of sub layer, [0.0..1000.0 cm, R]
* HCOMP    = height of compartments in this layer, [0.0..1000.0 cm, R]
* NCOMP    = number of compartments in this layer (= HSUBLAY/HCOMP), [1..MACP, I]

 ISOILLAY ISUBLAY  HSUBLAY    HCOMP    NCOMP
    1      1       10.0      1.0      10
    1      2       40.0      2.5      16
    1      3       40.0      5.0       8
    2      4       60.0     10.0       6
    3      5      200.0     25.0       8
* end of table
*******************************************************************************
**


*******************************************************************************
**
* Part 5: Soil hydraulic functions

* Switch for Mualem - van Genuchten parameters or detailed tabels:
  SWSOPHY = 0   ! 0 = Mualem - van Genuchten parameters
            ! 1 = Detailed tables

* If SWSOPHY = 0, specify for each soil layer (maximum MAHO):
* ISOILLAY1 = number of soil layer, as defined in part 4 [1..MAHO, I]
* ORES   = Residual water content, [0..0.4 cm3/cm3, R]
* OSAT   = Saturated water content, [0..0.95 cm3/cm3, R]
* ALFA   = Shape parameter alfa of main drying curve, [0.0001..1 /cm, R]
* NPAR   = Shape parameter n, [1..4 -, R]
* KSAT   = Saturated vertical hydraulic conductivity, [1.d-5..1000 cm/d, R]
* LEXP   = Exponent in hydraulic conductivity function, [-25..25 -, R]
* ALFAW  = Alfa parameter of main wetting curve in case of hysteresis, [0.0001..1 /cm, R]
```

```
* H_ENPR = Air entry pressure head [-40.0..0.0 cm, R]

 ISOILLAY1  ORES   OSAT   ALFA   NPAR    KSAT    LEXP   ALFAW   H_ENPR
     1    0.192   0.752   0.227   1.497  1000.0   -1.435   0.454  0.000
     2    0.191   0.743   0.168   1.414   812.0   -1.626   0.336  0.000
     3    0.156   0.674   0.007   1.524   40.0    0.5    0.014   0.000
* --- end of table

* If SWSOPHY = 1, specify names of input files [A80] with soil hydraulic tables for each soil layer:
 FILENAMESOPHY = 'topsoil_sand_B2.csv', 'subsoil_sand_O2.csv'
**********************************************************************
**


**********************************************************************
**
* Part 6: Hysteresis of soil water retention function

* Switch for hysteresis: ! I think hysteresis is not working with macropore?
 SWHYST = 0   ! 0 = no hysteresis
          ! 1 = hysteresis, initial condition wetting
          ! 2 = hysteresis, initial condition drying

* If SWHYST = 1 or 2, specify:
 TAU = 0.2    ! Minimum pressure head difference to change wetting-drying, [0..1 cm, R]
**********************************************************************
**


**********************************************************************
**
* Part 7: Maximum rooting depth

 RDS   = 300.0     ! Maximum rooting depth allowed by the soil profile, [1..5000 cm, R]
**********************************************************************
**


**********************************************************************
**
* Part 8: Similar media scaling of soil hydraulic functions

 SWSCAL = 0 ! Switch for similar media scaling [Y=1, N=0]; no hysteresis is allowed
        ! in case of similar media scaling (SWHYST = 0)

* If SWSCAL = 1, specify:
```

```
 NSCALE = 3 ! Number of simulation runs, [1..MASCALE, I]

* Supply the scaling factors for each simulation run and each soil layer:

 RUN    SOIL1      SOIL2
  1     0.5        2.0
  2     1.0        1.0
  3     2.0        0.5
  4     1.0        1.0
  5     3.0        3.0
* End of table
*************************************************************************
**


*************************************************************************
**
* Part 9: Preferential flow due to macropores

 SWMACRO = 1     ! Switch for macropore flow, [0..2, I]:
            ! 0 = no macropore flow
            ! 1 = macropore flow

* If SwMacro = 1, specify parameters for macropore flow:
 Z_AH = -10.0 ! Depth bottom A-horizon [-1000..0 cm, R]
 Z_IC = -75.0 ! Depth bottom Internal Catchment (IC) domain [-1000..0 cm, R]
 Z_ST = -89.0 ! Depth bottom Static macropores [-1000..0 cm, R]
VlMpStSs = 0.15! Volume fraction of Static Macropores at Soil Surface [0..0.5 cm3/cm3, R]
PpIcSs = 0.99 ! Proportion of IC domain at Soil Surface [0..0.99 -, R]
NumSbDm = 3 ! Number of Sub-domains in IC domain [0..MaDm-2 -, I]
PowM = 7.5 ! Power M for frequency distrib. curve IC domain (OPTIONAL, default 1.0) [0..100 -, R]
RZah = 0.0 ! Fraction macropores ended at bottom A-horizon [OPTIONAL, default 0.0] [0..1 -, R]
SPoint = 1.0 ! Symmetry Point for freq. distr. curve [OPTIONAL, default 1.0] [0..1 -, R]
SwPowM = 0 ! Switch for double convex/concave freq. distr. curve (OPTIONAL, Y=1, N=0; default:
0) [0..1 -, I]
DiPoMi = 0.25 ! Minimal diameter soil polygons (shallow) [0.1..1000 cm, R]
DiPoMa = 4.0 ! Maximal diameter soil polygons (deep) [0.1..1000 cm, R]
ZDiPoMa = -150.0! Depth below which diameter polygons is max. (OPTIONAL, default 0.) [-1000..0
cm, R]


* Start of Tabel with shrinkage characteristics
* ISOILLAY3 = indicator (number) of soil layer, as defined in part 4 [1..MAHO, I]
* SWSoilShr = Switch for kind of soil for shrinkage curve: 0 = rigid, 1 = clay, 2 = peat [0..2 -, I]
* SWShrInp = Switch for determining shrinkage curve [1..2 -, I]: 1 = parameters of curve are given;
*                                        2 = typical points of curve given;
```

```
*                                   3 = (only peat) intersection points
*                                     of 3-straight-line-model given
* ThetCrMP = Threshold moisture content below which horizontal shrinkage [0..1 cm3/cm3, R] ! pag 145: 90-100% Osat = 0.95 * 0.752 = 0.714
* GeomFac = Geometry factor (3.0 = isotropic shrinkage), [0..100, R]! pag 145: usar 3.0
*
* ShrParA to ShrParE = parameters for describing shrinkage curves,
*          depending on combination of SWSoilShr and SwShrInp [-1000..1000, R]:
*       SWSoilShr = 0 : 0 variables required (all dummies)
*       SWSoilShr = 1, SwShrInp 1 = : 3 variables required (ShrParA to ShrParC) (rest dummies)
*       SWSoilShr = 1, SwShrInp 2 = : 2 variables required (ShrParA to ShrParB) (rest dummies)
*       SWSoilShr = 2, SwShrInp 1 = : 5 variables required (ShrParA to ShrParE)
*       SWSoilShr = 2, SwShrInp 2 = : 5 variables required (ShrParA to ShrParE)
*       SWSoilShr = 2, SwShrInp 3 = : 4 variables required (ShrParA to ShrParD) (rest dummy)


 ISOILLAY3  SWSoilShr  SwShrInp  ThetCrMP  GeomFac  ShrParA  ShrParB  ShrParC  ShrParD  ShrParE
   1         2          1        0.714      3.0     0.60     3.492    0.76     3.084    0.539  ! El 0.740 es el 95% del Osat de turbas (Emi)
   2         0          1        0.706      3.0     0.0      0.0      0.0      0.0      0.0
   3         0          1        0.640      3.0     0.0      0.0      0.0      0.0      0.0    ! El 0.640 es el 95% del Osat de limos
*End of Tabel with shrinkage characteristics

ZnCrAr = -5.0 ! Depth at which crack area of soil surface is calculated [-100..0 cm, R]; pag 145: usar -5.0
*************************************************************************
**
* Start of Tabel with sorptivity characteristics
* ISOILLAY4   = Indicator (number) of soil layer, as defined in part 4 [1..MAHO, I]
* SWSorp      = Switch for kind of sorptivity function [1..2 -, I]:
*           1 = calculated from hydraulic functions according to Parlange
*           2 = empirical function from measurements
* SorpFacParl = Factor for modifying Parlange function (OPTIONAL, default 1.0) [0..100 -, R]
* SorpMax     = Maximal sorptivity at theta residual [0..100 cm/d**0.5, R]
* SorpAlfa    = Fitting parameter for empirical sorptivity curve [-10..10 -, R]

 ISOILLAY4 SwSorp SorpFacParl SorpMax SorpAlfa
    1       1      0.33       0.0     0.0
    2       1      0.5        0.0     0.0
    3       1      1.0        5.0     0.0
*End of Tabel with sorptivity characteristics
*
 ShapeFacMp    = 1.0
 CritUndSatVol = 0.0 ! Critical value for under-saturation volume [0..10 -, R] 0.1 Default value.
```

```
*
 SwDrRap     = 0 ! Switch for simulating rapid drainage,[Y=1, N=0]
 RapDraResRef = 15. ! Reference rapid drainage resistance [0..1.E+10 /d, R]

RapDraReaExp = 2.0 ! Exponent for reaction rapid drainage to dynamic crack width [0..100 -, R]

 NumLevRapDra = 1 ! Number of drainage system connected to rapid drainage [1..NRLEVS, -, I]

* Threshold value for ponding (cm) on soil surface before overland flow into macropores starts
 PNDMXMP = 0.0 ! [0.0 .. 10.0, cm, R]

*************************************************************************
**
* Part 10: Snow and frost

* Snow
 SWSNOW = 0   ! Switch, calculate snow accumulation and melt, [Y=1, N=0]

* If SWSNOW = 1, specify:
 SNOWINCO = 22.0     ! Initial snow water equivalent, [0.0...1000.0 cm, R]
 TEPRRAIN = 2.0      ! Temperature above which all precipitation is rain,[ 0.0...5.0 ºC, R]
 TEPRSNOW = -2.0     ! Temperature below which all precipitation is snow,[-5.0...0.0 ºC, R]
 SNOWCOEF = 0.3      ! Snowmelt calibration factor, [0.0...10.0 -, R]

* Frost
 SWFROST = 0  ! Switch, in case of frost: reduce soil water flow, [Y=1, N=0] (sólo lo puedo usar si
meto datos de soil temperature y no vale con macroporos)

* If SWFROST = 1, then specify soil temperature to start end end flux-reduction
 tfroststa = 0.0     ! Soil temperature (ºC) where reduction of water fluxes starts [-10.0,5.0, oC, R];
0.0 is default value
 tfrostend = -1.0    ! Soil temperature (ºC) where reduction of water fluxes ends [-10.0,5.0, oC, R];
-1.0 is default value
*************************************************************************
**


*************************************************************************
**
* Part 11 Numerical solution of Richards' equation

 DTMIN       = 1.0d-6    ! Minimum timestep, [1.d-7..0.01 d, R]
 DTMAX       = 0.1       ! Maximum timestep, [ 0.01..0.5 d, R]  Si meto macroporo este valor tiene
que ser como mucho 0.1 (pag 138 manual)
 GWLCONV     = 100.0     ! Maximum dif. groundwater level between iterations, [1.d-5..1000 cm,
R]
```

```
 CritDevh1Cp    = 1.0d-2      ! Maximum relative difference in pressure heads per compartment,
[1.0d-10..0.1 -, R]
 CritDevh2Cp    = 1.0d-1      ! Maximum difference in pressure heads per compartment, [1.0d-
10..1.0 cm, R]
 CritDevPondDt = 1.0d-4     ! Maximum water balance error of ponding layer, [1.0d-6..0.1 cm, R]
 MaxIt        = 30        ! Maximum number of iteration cycles, [5..100 -, I]
 MaxBackTr    = 3         ! Maximum number of back track cycles within an iteration cycle, [1..10 -,I]

* Switch for mean of hydraulic conductivity, [1..4 -, I]:
* 1 = unweighted  arithmic mean; 2 = weighted  arithmic mean
* 3 = unweighted geometric mean; 4 = weighted geometric mean
 SWkmean = 2 ! Solo funciona (converge) con esta opción

* Switch for explicit/implicit solution Richards equation with hydraulic conductivity, [1..2 -, I]:
 SWkImpl = 0   ! 0 = explicit solution
           ! 1 = implicit solution
*******************************************************************************
**


*** LATERAL DRAINAGE SECTION ***

*******************************************************************************
**
* Specify whether lateral drainage to surface water should be included

 SWDRA = 0  ! Switch, simulation of lateral drainage:
         ! 0 = No simulation of drainage
         ! 1 = Simulation with basic drainage routine
         ! 2 = Simulation of drainage with surface water management

* If SWDRA = 1 or SWDRA = 2 specify name of file with drainage input data:
 DRFIL = 'Hupsel' ! File name with drainage input data without extension .DRA, [A16]
*******************************************************************************
**


*** BOTTOM BOUNDARY SECTION ***

*******************************************************************************
**
* Bottom boundary condition

 SWBBCFILE  = 0    ! Switch for file with bottom boundary conditions:
              ! SWBBCFILE = 0: data are specified in the .swp file
              ! SWBBCFILE = 1: data are specified in a separate file
```

* If SWBBCFILE = 1 specify name of file with bottom boundary conditions:
BBCFIL = ' ' ! File name without extension .BBC [A16]

* If SWBBCFILE = 0, select one of the following options: ! Which one I use with the perched groundwater table?
! 1 Prescribe groundwater level (disabled for macropore flow simulations) SI
! 2 Prescribe bottom flux
! 3 Calculate bottom flux from hydraulic head of deep aquifer
! 4 Calculate bottom flux as function of groundwater level
! 5 Prescribe soil water pressure head of bottom compartment
! 6 Bottom flux equals zero SI
! 7 Free drainage of soil profile SI
! 8 Free outflow at soil-air interface MAYBE

SWBOTB = 1 ! Switch for bottom boundary [1..8,-,I]

* Options 6,7 and 8 require no additional bottom input data
****
**

****
**
* SWBOTB = 1 Prescribe groundwater level

* specify DATE [dd-mmm-yyyy] and groundwater level [cm, -10000..1000, R]

DATE1 GWLEVEL ! (max. MABBC records)
28-Feb-2007 -116.400
1-Mar-2007 -116.817
2-Mar-2007 -117.483
3-Mar-2007 -118.067
4-Mar-2007 -118.400
5-Mar-2007 -120.233
6-Mar-2007 -119.650
7-Mar-2007 -117.983
8-Mar-2007 -119.900
9-Mar-2007 -120.400
10-Mar-2007 -120.567
11-Mar-2007 -120.567
12-Mar-2007 -120.567
13-Mar-2007 -121.233
14-Mar-2007 -121.567
15-Mar-2007 -121.567
16-Mar-2007 -121.983

17-Mar-2007 -122.733
18-Mar-2007 -123.067
19-Mar-2007 -122.317
20-Mar-2007 -123.733
21-Mar-2007 -124.233
22-Mar-2007 -125.483
23-Mar-2007 -125.400
24-Mar-2007 -125.817
25-Mar-2007 -126.400
26-Mar-2007 -127.650
27-Mar-2007 -129.150
28-Mar-2007 -129.900
29-Mar-2007 -131.317
30-Mar-2007 -132.317
31-Mar-2007 -132.150
1-Apr-2007 -132.067
2-Apr-2007 -132.900
3-Apr-2007 -133.400
4-Apr-2007 -133.400
5-Apr-2007 -133.400
6-Apr-2007 -132.650
7-Apr-2007 -130.733
8-Apr-2007 -128.233
9-Apr-2007 -125.400
10-Apr-2007 -123.983
11-Apr-2007 -122.733
12-Apr-2007 -121.233
13-Apr-2007 -120.650
14-Apr-2007 -119.317
15-Apr-2007 -118.483
16-Apr-2007 -117.067
17-Apr-2007 -116.067
18-Apr-2007 -115.483
19-Apr-2007 -115.233
20-Apr-2007 -115.233
21-Apr-2007 -115.483
22-Apr-2007 -116.067
23-Apr-2007 -116.400
24-Apr-2007 -116.483
25-Apr-2007 -116.567
26-Apr-2007 -116.400
27-Apr-2007 -116.733
28-Apr-2007 -117.400
29-Apr-2007 -117.483
30-Apr-2007 -117.233
1-May-2007 -117.733

2-May-2007 -117.400
3-May-2007 -117.650
4-May-2007 -119.400
5-May-2007 -120.233
6-May-2007 -121.400
7-May-2007 -122.233
8-May-2007 -123.067
9-May-2007 -123.400
10-May-2007 -123.650
11-May-2007 -124.400
12-May-2007 -125.150
13-May-2007 -125.567
14-May-2007 -127.817
15-May-2007 -129.733
16-May-2007 -130.817
17-May-2007 -131.983
18-May-2007 -132.400
19-May-2007 -133.233
20-May-2007 -132.983
21-May-2007 -126.233
22-May-2007 -122.650
23-May-2007 -116.317
24-May-2007 -110.983
25-May-2007 -106.067
26-May-2007 -102.983
27-May-2007 -100.650
28-May-2007 -98.233
29-May-2007 -96.733
30-May-2007 -95.150
31-May-2007 -93.983
...
* End of table
****
**

****
**
* SWBOTB = 2 Prescribe bottom flux

* Specify whether a sine or a table are used to prescribe the bottom flux:
SW2 = 2 ! 1 = sine function; 2 = table

* In case of sine function (SW2 = 1), specify:
SINAVE = 0.1 ! Average value of bottom flux, [-10..10 cm/d, R, + = upwards]
SINAMP = 0.05 ! Amplitude of bottom flux sine function, [-10..10 cm/d, R]

```
 SINMAX =  91.0  ! Time of the year with maximum bottom flux, [1..366 d, R]

* In case of table (SW2 = 2), specify date [dd-mmm-yyyy] and bottom flux QBOT2
* [-100..100 cm/d, R, positive = upwards]:

      DATE2     QBOT2         ! (maximum MABBC records)
 01-jan-1980      0.1
 30-jun-1980      0.2
 23-dec-1980     0.15
* End of table
*******************************************************************************
**


*******************************************************************************
**
* SWBOTB = 3    Calculate bottom flux from hydraulic head in deep aquifer

* Switch to suppress vertical hydraulic resistance between model bottom and groundwater level
 SWBOTB3RESVERT = 0 ! 0 = Include vertical hydraulic resistance
                    ! 1 = Suppress vertical hydraulic resistance

* Switch for numerical solution of bottom flux: 0 = explicit, 1 = implicit
 SWBOTB3IMPL = 0    ! 0 = explicit solution (choose always when SHAPE < 1.0)
                    ! 1 = implicit solution

* Specify:
 SHAPE  =   0.79  ! Shape factor to derive average groundwater level, [0.0..1.0 -, R]
 HDRAIN =  -110.0 ! Mean drain base to correct for average groundwater level, [-10000..0 cm, R]
 RIMLAY =   500.0 ! Vertical resistance of aquitard, [0..10000 d, R]

* Specify whether a sine function or a table are used to prescribe hydraulic head of deep aquifer:
 SW3    = 1       ! 1 = sine function;  2 = table

* In case of sine function (SW3  = 1), specify:
 AQAVE  =  -140.0 ! Average hydraulic head in underlaying aquifer, [-10000..1000 cm, R]
 AQAMP  =    20.0 ! Amplitude hydraulic head sinus wave, [0..1000 cm, R]
 AQTMAX =  120.0  ! First time of the year with maximum hydraulic head, [1..366 d, R]
 AQPER  =  365.0  ! Period hydraulic head sinus wave, [1..366 d, I]

* In case of table (SW3  = 2), specify date [dd-mmm-yyyy] and average hydraulic head
* HAQUIF in underlaying aquifer [-10000..1000 cm, R]:

      DATE3    HAQUIF         ! (maximum MABBC records)
 01-jan-1980     -95.0
 30-jun-1980    -110.0
```

```
 23-dec-1980     -70.0
* End of table

* An extra groundwater flux can be specified which is added to above specified flux
 SW4   = 1       ! 0 = no extra flux; 1 = include extra flux

* If SW4 = 1, specify date [dd-mmm-yyyy] and bottom flux QBOT4 [-100..100 cm/d, R,
* positive = upwards]:

      DATE4     QBOT4          ! (maximum MABBC records)
 01-jan-1980      1.0
 30-jun-1980     -0.15
 23-dec-1980      1.2
* End of table
*******************************************************************************
**


*******************************************************************************
**
* SWBOTB = 4     Calculate bottom flux as function of groundwater level

* Specify whether an exponential relation or a table is used to calculate the bottom flux
* from the groundwater level:
 SWQHBOT = 2      ! 1 = exponential relation;  2 = table

* In case of an exponential relation (SWQHBOT  = 1),
* specify coefficients of relation qbot = A exp (B*abs(groundwater level))
 COFQHA =  0.1  ! Coefficient A, [-100..100 cm/d, R]
 COFQHB =  0.5  ! Coefficient B  [-1..1 /cm, R]

* In case of a table (SWQHBOT  = 2),
* specify groundwaterlevel Htab [-10000..1000, cm, R]  and bottom flux QTAB [-100..100 cm/d, R]
* Htab is negative below the soil surface, Qtab is negative when flux is downward.
 HTAB   QTAB
 -0.1   -0.35
 -70.0  -0.05
-125.0  -0.01
*******************************************************************************
**


*******************************************************************************
**
* SWBOTB = 5     Prescribe soil water pressure head of bottom compartment
```

```
* Specify DATE [dd-mmm-yyyy] and bottom compartment pressure head HBOT5 [-1.d10..1000 cm,
R]:

      DATE5     HBOT5          ! (maximum MABBC records)
 01-jan-1980     -95.0
 30-jun-1980    -110.0
 23-dec-1980     -70.0
* End of table
*****************************************************************************
**


*** HEAT FLOW SECTION ***

*****************************************************************************
**
* Part 1: Specify whether simulation includes heat flow

 SWHEA  = 0 ! Switch for simulation of heat transport, [Y=1, N=0]
*****************************************************************************
**

*****************************************************************************
**
* Part 2: Heat flow calculation method

 SWCALT = 2     ! Switch for method: 1 = analytical method, 2 = numerical method
*****************************************************************************
**

*****************************************************************************
**
* Part 3: Analytical method

* If SWCALT = 1 specify the following heat parameters:
 TAMPLI = 10.0 ! Amplitude of annual temperature wave at soil surface, [0..50 C, R]
 TMEAN  = 15.0 ! Mean annual temperature at soil surface, [5..30 C, R]
 TIMREF = 90.0 ! Time in the year with top of sine temperature wave [1..366 d, R]
 DDAMP  = 50.0 ! Damping depth of temperature wave in soil, [0..500 cm, R]
*****************************************************************************
**

*****************************************************************************
**
* Part 4: Numerical method
```

```
* If SWCALT = 2 specify the following heat parameters:

* Specify for each soil type the soil texture (g/g mineral parts)
* and the organic matter content (g/g dry soil):

 ISOILLAY5  PSAND   PSILT   PCLAY   ORGMAT        ! (maximum MAHO records)
   1       0.88    0.00    0.12    0.462 ! Turba
   2       0.52    0.34    0.14    0.285 ! Mezcla Tu-Li
   3       0.18    0.68    0.14    0.109 ! Limos
* End of table

* If SWINCO = 1 or 2, list initial temperature TSOIL [-20..40 C, R] as function of
* soil depth ZH [-1.0d5..0 cm, R]:

    ZH    TSOIL   ! (maximum MACP records)
  -20.0     11.5   ! Uso temperatura inicial superficial la media del 16 abril de 2009 de sensores P-
1_turba 20 cm (11.5) o P-5_suelo org (9.6), de P-1 a 50 y 80 cm
  -50.0    12.0
  -80.0    11.7
* End of table

* Define top boundary condition:
 SwTopbHea = 1     ! 1 = use air temperature of meteo input file as top boundary
                   ! 2 = use measured top soil temperature as top boundary

* If SwTopbHea = 2, specify name of input file with soil surface temperatures
 TSOILFILE = 'Haarweg' ! File name without extension .TSS, [A16]

* Define bottom boundary condition:
 SwBotbHea = 1     ! 1 = no heat flux; 2 = prescribe bottom temperature

* If SwBotbHea = 2, specify a tabel with dates and temperatures at bottom boundary

 DATET          TBOT   ! (maximum MABBC records)
 01-jan-1980    -15.0
 30-jun-1980    -20.0
 23-dec-1980    -10.0
* End of table
*****************************************************************************
**


*** SOLUTE SECTION ***

*****************************************************************************
**
```

```
* Part 1: Specify whether simulation includes solute transport !

 SWSOLU = 0 ! Switch for simulation of solute transport, [Y=1, N=0]
******************************************************************************
**

******************************************************************************
**
* Part 2: Top boundary and initial condition

 CPRE = 0.003     ! Solute concentration in precipitation, [1..100 mg/cm3, R]  Es la concetracion media de Cl en CR-DSL2 expresada en mg/cm3, en mg/l el valor medio es 2.93 y al dividir entre 1000: 0.00293=0.003

* If SWINCO = 1 or 2, list initial solute concentration CML [1..1000 mg/cm3, R]
* as function of soil depth ZC [-10000..0 cm, R], max. MACP records:
    ZC      CML
  -10.0      1.37 ! conc media de Cl en clay charophytes entre 0-20 cm
  -30.0      0.71 ! conc media de Cl en clay charophytes entre 20-60 cm
  -80.0      0.78 ! conc media de Cl en clay charophytes entre 60-100 cm
* End of table
******************************************************************************
**

******************************************************************************
**
* Part 3: Miscellaneous parameters as function of soil depth

* Specify for each soil layer (maximum MAHO)
* ISOILLAY6 = number of soil layer, as defined in soil water section (part 4) [1..MAHO, I]
* LDIS     = dispersion length, [0..100 cm, R]
* KF       = Freundlich adsorption coefficient, [0..100 cm3/mg, R]
* BDENS    = dry soil bulk density, [500..3000 mg/cm3, R]
* DECPOT   = potential decomposition rate, [0..10 /d, R]

 ISOILLAY6      LDIS          KF       BDENS      DECPOT ! Como el Cl es conservativo la potential decompostion rate la mantengo en 0
    1        10.00   0.0001389    560.00     0.0 ! Valores tipicos de Ldis en campo están entre 5 y 20 cm (como los primeros 10 cm del perfil están menos consolidados y compactados pongo 10 cm de dispersión)
    2         7.00   0.0001378    650.00     0.0 ! Densidad aparente de ovas limpias no superfciales calculada como la media entre la de ovas salinas superficiales y ovas limpias
    3         5.00   0.0001378   1300.00     0.0
* End of Table
```

```
**********************************************************************
**

**********************************************************************
**
* Part 4: Diffusion constant and solute uptake by roots

 DDIF = 0.0    ! Molecular diffusion coefficient, [0..10 cm2/day, R]
 TSCF = 0.0    ! Relative uptake of solutes by roots, [0..10 -, R]
**********************************************************************
**

**********************************************************************
**
* Part 5: Adsorption

 SWSP = 0      ! Switch, consider solute adsorption, [Y=1, N=0]

* In case of adsorption (SWSP = 1), specify:
 FREXP = 0.9   ! Freundlich exponent, [0..10 -, R]
 CREF  = 1.0   ! Reference solute concentration for adsorption, [0..1000 mg/cm3, R]
**********************************************************************
**

**********************************************************************
**
* Part 6: Decomposition

 SWDC = 0      ! Switch, consideration of solute decomposition, [Y=1, N=0]

* In case of solute decomposition (SWDC = 1), specify:
 GAMPAR = 0.0  ! Factor reduction decomposition due to temperature, [0..0.5 /ºC, R]
 RTHETA = 0.3  ! Minimum water content for potential decomposition, [0..0.4 cm3/cm3, R]
 BEXP   = 0.7  ! Exponent in reduction decomposition due to dryness, [0..2 -, R]

* List the reduction of pot. decomposition for each soil type, [0..1 -, R]:

 ISOILLAY7  FDEPTH         ! (maximum MAHO records)
    1      1.00
    2      0.65
* End of table
**********************************************************************
**
```

```
*******************************************************************************
**
* Part 7: Solute residence in the saturated zone

 SWBR = 0      ! Switch, consider mixed reservoir of saturated zone [Y=1, N=0]

* Without mixed reservoir (SWBR = 0), specify:
 CDRAIN = 2.92   ! solute concentration in groundwater, [0..100 mg/cm3, R]

* In case of mixed reservoir (SWBR = 1), specify:
 DAQUIF = 110.0 ! Thickness saturated part of aquifer, [0..10000 cm, R]
 POROS  = 0.4   ! Porosity of aquifer, [0..0.6 -, R]
 KFSAT  = 0.2   ! Linear adsorption coefficient in aquifer, [0..100 cm3/mg, R]
 DECSAT = 1.0   ! Decomposition rate in aquifer, [0..10 /d, R]
 CDRAINI = 0.2  ! Initial solute concentration in groundwater, [0..100 mg/cm3, R]
*******************************************************************************
**

* End of the main input file .SWP!
```

APPENDIX D

Soil chemistry

D. Soil chemical data from random points sampled in Las Tablas de Daimiel National Park in July 2006

July 2006				1:5 soil-water extracts														1:2.5 soil suspensions		Solid soil matrix				
X (UTM)	Y (UTM)	Sampling point	cm Depth	Sample nº	mg l^{-1} Na	mg l^{-1} K	mg l^{-1} Ca	mg l^{-1} Mg	mg l^{-1} NH4	mg l^{-1} SO4	mg l^{-1} Cl	mg l^{-1} HCO3	mg l^{-1} CO3	mg l^{-1} NO3	mg l^{-1} NO2	mg l^{-1} P2O5	mg l^{-1} SiO2	mg l^{-1} B	µS cm^{-1} EC	pH (H_2O)	pH (KCl)	% OM	% N	mg Kg^{-1} P	% CaCO3	C/N
437539	4330679	1	0-20	1	22	9	344	86	0.08	1000	12	94	0	68	<0.05	0.16	11.7	<200	1986	7.6	7.2	15.94	1.21	37	57.8	8
437539	4330679	2	20-40	2	55	4	522	110	<0.05	1560	35	100	0	40	<0.05	0.23	4.1	<200	1966	7.5	7.2	15.18	0.99	12	65.8	9
437539	4330679	3	40-60	3	45	4	495	95	<0.05	1520	52	80	0	23	4.3	<0.04	4.7	<200	2590	7.6	7.4	9.05	0.40	10	72.9	13
437539	4330679	4	60-80	4	54	4	460	95	1.24	1380	90	65	0	16	0.12	<0.04	6.5	<200	2550	7.7	7.4	7.71	0.62	25	59.1	7
435495	4330302	5	60-80	5	45	5	432	81	1.72	1232	86	48	0	18	0.07	<0.04	3	<200	1999	7.7	7.5	3.45	0.16	6	88.2	13
435495	4330302	6	80-100	6	39	4	480	75	1.32	1344	73	45	0	12	0.1	<0.04	2	<200	2040	7.8	7.6	2.76	0.13	3	89.9	12
435495	4330302	7	0-20	7	128	18	540	216	<0.05	1880	246	95	0	94	0.05	<0.04	6.5	<200	3630	7.6	7.4	11.15	0.74	25	73.0	9
435495	4330302	8	20-40	8	99	14	470	176	<0.05	1580	150	115	0	66	<0.05	0.12	5.3	222	3060	7.3	7.1	16.16	0.79	8	67.9	12
435495	4330302	9	40-60	9	96	11	510	160	<0.05	1680	180	110	0	72	5.3	<0.04	6	<200	3160	7.4	7.1	15.07	0.69	10	62.9	13
435169	4330528	3	0-20	10	77	15	522	146	<0.05	1740	98	58	0	18	<0.05	0.18	11.8	<200	2980	7.6	7.3	9.02	0.56	110	27.1	9
435169	4330528	3	20-40	11	63	10	531	111	<0.05	1620	94	53	0	6	<0.05	<0.04	9.9	<200	2820	7.8	7.5	3.49	0.20	48	41.1	10
435169	4330528	3	40-60	12	40	8	504	91	<0.05	1500	63	54	0	5	<0.05	<0.04	8.2	<200	2590	7.9	7.6	1.29	0.10	29	46.8	8
435169	4330528	3	60-80	13	40	8	513	96	<0.05	1560	48	49	0	10	<0.05	<0.04	11.3	<200	2670	7.9	7.5	2.34	0.15	36	39.7	9
435169	4330528	3	80-100	14	30	7	504	82	0.05	1540	29	43	0	3	0.13	<0.04	12.4	<200	2480	7.9	7.5	0.96	0.07	30	32.9	8
435762	4331319	4	40-60	15	41	4	154	54	1.24	485	124	60	0	8	0.2	<0.04	3.3	<200	1261	7.9	7.8	4.85	0.28	6	85.8	10
435762	4331319	4	0-20	16	155	19	477	244	<0.05	1840	366	78	0	26	6.38	<0.04	6.6	<200	3820	7.9	7.6	7.92	0.43	6	71.3	11
435762	4331319	4	20-40	17	167	9	490	234	0.3	1800	386	84	0	24	5.6	<0.04	5.6	<200	3880	7.6	7.4	13.98	0.78	7	64.0	10
435762	4331319	4	60-80	18	49	4	236	92	2.16	740	112	89	0	18	<0.05	<0.04	1.7	204	1733	7.6	7.4	11.99	0.65	8	80.6	11
435762	4331319	4	80-100	19	48	6	220	82	0.93	715	101	64	0	22	<0.05	<0.04	6.1	200	1686	7.7	7.4	10.98	0.64	22	48.5	10
441037	4334611	5	20-40	20	107	16	550	150	0.62	1800	148	48	0	42	0.05	0.28	25.3	246	2990	8.2	8	2.14	0.11	<1	19.5	11
441037	4334611	5	40-60	21	93	14	521	168	0.52	1900	112	46	0	10	0.06	<0.04	27.11	<200	2890	8.3	8	1.67	0.11	2	21.7	9
441037	4334611	5	60-80	22	68	12	520	123	0.24	1660	66	47	0	10	0.08	<0.04	17.3	<200	2660	8.3	8	1.11	0.08	<1	15.8	8
441037	4334611	5	0-20	23	88	30	550	208	0.06	1940	92	69	0	110	<0.05	0.05	24.6	267	2270	8.0	7.7	6.69	0.31	4	31.7	12
440425	4334834	6	0-20	24	151	32	540	300	<0.05	2280	212	94	0	100	<0.05	0.19	12.9	654	3780	7.7	7.3	12.08	0.72	45	60.0	10
440425	4334834	6	60-80	25	159	15	553	280	0.97	2140	352	42	0	4	<0.05	<0.04	3.2	<200	3680	8.9	8.7	0.71	0.09	<1	24.7	4
440425	4334834	6	80-100	26	132	10	550	204	0.18	1920	270	32	0	3	<0.05	<0.04	2.5	<200	3330	9.1	8.9	0.50	0.09	<1	13.0	3
440425	4334834	6	20-40	27	369	24	560	668	<0.05	3550	808	67	0	71	0.06	0.07	5.1	290	4660	8.1	7.9	10.30	0.47	4	43.9	13
440425	4334834	6	40-60	28	303	22	520	512	0.85	3050	552	54	0	10	0.16	<0.04	4.6	<200	5370	8.8	8.5	2.10	0.14	2	38.8	9
440536	4334810	7	0-20	29	61	10	600	114	8.5	1940	11	80	0	49	0.1	0.13	10.5	524	2830	7.6	7.3	12.96	0.65	<1	19.9	12
440536	4334810	7	20-40	30	42	6	540	122	<0.05	1660	13	88	0	26	4.4	<0.04	5	214	2610	7.9	7.7	5.44	0.24	<1	45.2	13
440536	4334810	7	40-60	31	167	10	530	280	<0.05	2220	328	45	0	9	1.1	<0.04	5.4	<200	3830	8.7	8.6	2.96	0.15	<1	25.3	11
440536	4334810	7	60-80	32	157	9	520	264	1.04	2100	268	45	0	4	<0.05	<0.04	6.3	<200	3780	8.8	8.7	1.88	0.10	<1	28.3	10
440536	4334810	7	80-100	33	158	7	550	270	0.26	2100	349	35	0	2	0.1	<0.04	5.2	<200	3860	8.9	8.8	1.03	0.05	<1	18.5	11
440687	4334784	8	20-40	34	31	2	580	78	6.1	1500	61	76	0	30	0.23	1.16	3.5	<200	2500	7.7	7.4	5.58	0.22	7	70.5	14
440687	4334784	8	40-60	35	53	3	560	118	5.9	1620	95	97	0	112	0.44	<0.04	6.2	<200	2760	7.6	7.3	8.71	0.46	7	68.1	11
440687	4334784	8	60-80	36	56	5	600	104	8.3	1540	98	90	0	116	0.16	<0.04	7.8	205	2800	7.5	7.2	13.00	0.72	13	64.7	10
440687	4334784	8	0-20	37	65	10	549	142	0.2	1620	61	108	0	144	0.06	1.2	6.3	300	3080	6.9	6.7	23.49	0.72	4	34.7	19
440687	4334784	8	80-100	38	28	5	570	90	0.66	1740	24	48	0	26	0.21	<0.04	7.3	<200	2540	7.8	7.4	5.07	0.26	7	56.7	11
440687	4334784	8	100-120	39	21	4	600	59	0.54	1580	17	43	0	16	0.35	<0.04	5.7	<200	1900	7.9	7.4	2.57	0.12	5	43.4	13
440771	4334995	9	0-20	40	78	15	550	111	0.14	1540	97	105	0	74	12.2	<0.04	14.5	<200	2800	7.4	7.1	12.24	0.61	38	66.0	12
440771	4334995	9	20-40	41	34	3	497	75	2.29	1320	68	60	0	25	0.1	<0.04	7.2	<200	2280	7.7	7.3	7.29	0.37	12	78.1	11
440771	4334995	9	40-60	42	37	4	550	86	2.92	1480	61	84	0	31	0.16	<0.04	7.2	<200	2420	7.7	7.4	7.19	0.40	12	77.5	10
440771	4334995	9	60-80	43	42	4	550	102	4.3	1540	54	98	0	58	0.14	<0.04	9	<200	2550	7.7	7.3	9.51	0.57	12	73.2	10
440771	4334995	9	80-100	44	35	5	399	80	0.8	1160	53	51	0	40	0.32	<0.04	12.4	<200	2150	7.9	7.6	4.09	0.18	4	70.6	13
440771	4334995	9	100-120	45	33	4	580	78	0.7	1620	33	41	0	15	0.21	<0.04	9.2	<200	2600	8.1	7.7	2.50	0.12	2	51.0	12
439580	4334948	10	0-20	46	477	29	550	770	3.72	3000	1610	48	0	40	0.07	<0.04	5.6	<200	7980	8.5	8.2	3.35	0.18	6	30.0	11
439580	4334948	10	20-40	47	394	23	477	515	3.11	2550	924	45	0	30	0.09	0.07	4.7	<200	6420	8.7	8.3	2.42	0.12	6	25.8	12
439580	4334948	10	40-60	48	429	20	540	711	2.52	3250	1170	58	0	46	1.2	<0.04	7	<200	7240	8.5	8.1	4.31	0.18	18	37.4	14
439580	4334948	10	60-80	49	825	28	560	1242	1.37	5100	2010	75	0	104	0.06	0.36	10.1	337	10630	8.0	7.7	11.21	0.53	2	13.5	12
439580	4334948	10	80-100	50	451	26	530	792	1.78	3700	1160	57	0	19	0.19	0.07	4	<200	6640	8.4	8.2	5.38	0.24	3	28.5	13
439555	4335039	11	0-20	51	121	20	560	200	0.88	1940	283	43	0	<0.5	0.06	<0.04	3.7	<200	3410	8.5	8.5	1.55	0.11	3	11.1	8
439555	4335039	11	20-40	52	104	14	530	180	0.66	1960	172	41	0	2	0.08	<0.04	3.7	368	3040	8.3	8.2	0.65	0.06	2	10.9	7
439555	4335039	11	40-60	53	139	13	540	206	0.78	1940	270	40	0	1	0.08	<0.04	3.2	<200	3360	8.6	8.6	0.44	0.07	<1	16.3	4
439555	4335039	11	60-80	54	171	12	570	304	0.56	2360	440	48	0	1	0.08	<0.04	3.3	<200	4050	8.8	8.8	0.34	0.04	2	29.5	5
439555	4335039	11	80-100	55	192	11	610	336	0.28	2440	546	39	0	<0.5	<0.05	<0.04	3.3	<200	4360	8.9	8.7	0.29	0.04	4	44.2	4

July 2006					1:5 soil-water extracts															1:2.5 soil suspensions		Solid soil matrix				
X (UTM)	Y (UTM)	Sampling point	cm Depth	Sample nº	mg l^{-1} Na	mg l^{-1} K	mg l^{-1} Ca	mg l^{-1} Mg	mg l^{-1} NH4	mg l^{-1} SO4	mg l^{-1} Cl	mg l^{-1} HCO3	mg l^{-1} CO3	mg l^{-1} NO3	mg l^{-1} NO2	mg l^{-1} P2O5	mg l^{-1} SiO2	mg l^{-1} B	mS cm^{-1} EC	pH (H_2O)	pH (KCl)	% OM	% N	mg Kg^{-1} P	% CaCO3	C/N
442182	4336392	12	20-40	56	467	17	600	640	0.18	2900	1320	55	0	27	0.46	<0.04	2.8	<200	6690	9.4	9.3	2.09	0.13	2	63.0	10
442182	4336392	12	80-100	57	328	18	580	352	<0.05	2440	632	51	0	10	<0.05	<0.04	2.6	<200	4720	9.3	9.1	0.37	0.05	2	34.6	4
442182	4336392	12	0-20	58	1185	53	550	1084	2	4400	2380	70	0	88	0.65	0.21	5.9	<200	12090	8.6	8.5	4.42	0.24	7	58.9	11
442182	4336392	12	40-60	59	435	22	540	432	0.38	2600	864	34	0	18	<0.05	<0.04	2.4	<200	5970	8.8	8.8	0.96	0.07	<1	25.0	7
442182	4336392	12	60-80	60	363	21	520	328	0.32	2360	656	33	0	14	0.06	<0.04	2.3	<200	5160	9.0	8.9	0.56	0.06	3	30.9	6
436887	4331913	13	80-100	61	130	15	370	208	3.04	1580	260	76	0	4	0.11	<0.04	11.5	326	3060	7.8	7.7	9.70	0.45	33	71.1	13
436887	4331913	13	0-20	62	295	36	570	321	0.05	2240	628	85	0	28	<0.05	<0.04	10.6	218	4730	7.9	7.6	10.74	0.50	107	69.4	12
436887	4331913	13	20-40	63	171	19	531	321	<0.05	2180	374	76	0	23	<0.05	0.09	10.2	419	4200	7.9	7.6	12.37	0.50	88	65.9	14
436887	4331913	13	40-60	64	120	15	427	208	1.84	1720	216	68	0	7	<0.05	<0.04	8.5	375	3050	7.9	7.6	9.51	0.37	37	58.0	15
436887	4331913	13	60-80	65	133	17	500	244	3.98	1980	271	62	0	6	0.14	<0.04	11.4	332	3430	7.9	7.6	9.13	0.35	36	54.3	15
438676	4332089	14	0-20	66	16	7	140	40	<0.05	305	20	138	0	72	<0.05	0.14	11	<200	938	7.8	7.6	8.70	0.44	47	80.3	11
438676	4332089	14	20-40	67	66	9	275	98	<0.05	880	89	80	0	70	0.05	<0.04	4.3	<200	1892	7.6	7.4	11.51	0.53	18	73.9	13
438676	4332089	14	40-60	68	82	7	535	126	0.05	1600	133	75	0	48	<0.05	<0.04	4.8	<200	2850	7.6	7.3	10.50	0.55	12	68.9	11
438676	4332089	14	60-80	69	101	9	610	184	0.05	1940	170	68	0	108	<0.05	<0.04	6.8	<200	3210	7.5	7.2	15.87	0.69	9	39.2	13
438676	4332089	14	80-100	70	332	10	660	424	<0.05	2650	772	127	0	116	0.06	0.2	2.2	737	5300	7.0	6.7	38.08	1.16	12	25.3	19
438764	4332453	15	40-60	71	139	5	490	234	0.06	1820	359	84	0	41	3.2	<0.04	2.8	<200	3620	7.9	7.7	7.29	0.41	3	83.0	10
438764	4332453	15	60-80	72	117	6	470	230	<0.05	1920	286	86	0	34	3.4	<0.04	3	<200	3280	8.0	7.8	6.08	0.28	4	82.9	12
438764	4332453	15	80-100	73	112	5	430	212	1.74	1660	280	73	0	24	0.15	<0.04	2.6	<200	3170	8.0	7.8	5.28	0.27	2	85.6	11
438764	4332453	15	0-20	74	379	24	630	452	<0.05	2800	808	94	0	200	0.09	1.2	9.9	<200	5540	7.4	7.1	24.05	1.07	25	42.3	13
438764	4332453	15	20-40	75	445	16	710	508	<0.05	2750	1270	86	0	270	0.1	1.9	5.3	270	6560	7.1	6.9	33.33	1.10	12	20.7	18
438470	4332425	16	20-40	76	12	7	580	41	1.72	1460	9	62	0	17	0.05	<0.04	3.1	<200	1775	7.9	7.6	3.31	0.15	6	80.4	12
438470	4332425	16	40-60	77	15	7	550	52	2.2	1520	20	65	0	19	0.09	<0.04	2.7	<200	2330	7.9	7.6	3.37	0.17	6	85.0	11
438470	4332425	16	60-80	78	17	6	540	49	1.74	1440	18	55	0	15	0.11	<0.04	1.5	<200	2350	8.0	7.7	3.17	0.15	11	86.2	12
438470	4332425	16	80-100	79	14	6	504	51	1	1300	16	54	0	12	0.09	<0.04	1.4	246	2120	8.0	7.8	3.20	0.15	5	90.4	12
438470	4332425	16	0-20	80	15	15	620	64	0.06	1600	18	74	0	64	<0.05	0.15	5.2	<200	2480	7.5	7.3	8.07	0.31	12	62.3	15
438262	4332637	17	20-40	81	83	5	540	147	2	1760	188	61	0	8	<0.05	<0.04	10	<200	1578	7.7	7.4	5.67	0.37	25	38.6	9
438262	4332637	17	40-60	82	77	3	520	160	4.28	1700	182	87	0	9	0.07	<0.04	11.6	<200	3050	7.8	7.4	8.55	0.53	10	69.7	9
438262	4332637	17	60-80	83	123	5	530	222	5.08	1900	290	113	0	12	0.12	<0.04	7.4	271	3610	7.7	7.4	11.33	0.86	8	69.3	8
438262	4332637	17	0-20	84	294	6	640	352	0.09	2250	763	64	0	49	<0.05	0.46	21.4	<200	4900	7.6	7.2	14.04	0.79	59	45.3	10
438262	4332637	17	80-100	85	153	9	530	258	2.19	2080	334	82	0	18	0.08	<0.04	9.7	<200	3690	7.5	7.2	10.89	0.66	20	49.2	10
438128	4332699	18	60-80	86	143	9	560	214	0.54	1900	396	41	0	2	<0.05	<0.04	2.5	<200	3790	8.3	8.1	0.97	0.10	1	23.4	6
438128	4332699	18	80-100	87	147	8	520	255	0.48	2100	404	42	0	1	<0.05	<0.04	2.7	<200	3820	8.3	8.1	1.14	0.16	<1	21.1	4
438128	4332699	18	0-20	88	307	29	570	443	<0.05	2700	832	57	0	41	<0.05	0.36	12.1	371	3510	7.2	6.9	17.17	1.01	22	8.1	10
438128	4332699	18	20-40	89	277	22	600	412	<0.05	2650	740	54	0	25	<0.05	0.05	2.5	<200	4900	7.9	7.7	8.90	0.45	4	9.1	12
438128	4332699	18	40-60	90	152	10	570	226	1.31	2000	424	38	0	2	<0.05	<0.04	1.8	<200	3880	8.4	8.2	1.89	0.17	2	20.9	6
438078	4332749	19	0-20	91	410	20	600	492	0.56	2580	1190	43	0	22	0.09	<0.04	3.9	<200	6270	8.5	8.2	1.63	0.16	17	22.1	6
438078	4332749	19	20-40	92	168	10	560	234	0.33	2040	422	38	0	6	<0.05	<0.04	3.7	<200	4030	8.4	8.1	0.86	0.10	8	16.1	5
438078	4332749	19	40-60	93	179	10	592	280	0.32	2240	512	42	0	4	<0.05	<0.04	3.8	<200	4230	8.3	8.1	1.13	0.09	4	21.0	7
438078	4332749	19	60-80	94	174	11	540	240	1.16	2034	436	44	0	2	<0.05	<0.04	3.7	<200	4150	8.1	7.9	1.65	0.13	8	22.5	7
438078	4332749	19	80-100	95	171	12	530	238	1.64	1920	380	38	0	3	0.09	<0.04	4.1	<200	4010	8.2	7.9	1.31	0.10	8	22.1	7
438035	4332870	20	0-20	96	189	21	510	186	0.48	1860	410	62	0	20	2.4	<0.04	9.1	484	3940	8.0	7.7	2.90	0.24	11	16.9	7
438035	4332870	20	20-40	97	219	9	570	296	0.64	1920	720	36	0	3	<0.05	<0.04	2.9	275	4630	8.5	8.3	0.73	0.07	3	29.8	6
438035	4332870	20	40-60	98	203	4	540	292	0.07	1940	594	34	0	1	<0.05	<0.04	2.4	<200	2550	8.7	8.5	0.27	0.05	3	39.5	3
438035	4332870	20	60-80	99	197	3	510	280	0.07	1900	520	32	0	1	<0.05	<0.04	2.7	<200	4140	8.7	8.4	0.24	0.09	4	34.4	2
438035	4332870	20	80-100	100	196	3	510	268	<0.05	1960	532	31	0	1	<0.05	<0.04	2.8	<200	4170	8.7	8.5	0.22	0.06	<1	35.7	2
439115	4331295	21	0-20	101	5	24	152	13	0.05	285	12	129	0	32	<0.05	0.8	16.7	232	838	7.4	7.3	16.36	0.90	28	61.4	11
439115	4331295	21	20-40	102	11	13	590	85	0.06	1700	6	95	0	21	<0.05	0.4	12.8	364	2500	7.7	7.3	13.82	0.81	17	61.5	10
439115	4331295	21	40-60	103	35	3	580	113	0.05	1780	26	59	0	8	<0.05	<0.04	5.7	<200	2530	7.9	7.5	5.84	0.35	9	46.5	10
439115	4331295	21	60-80	104	33	2	380	100	<0.05	1220	43	51	0	6	<0.05	<0.04	5.2	<200	2030	7.9	7.5	3.19	0.26	5	37.6	7
439115	4331295	21	80-100	105	32	3	420	121	0.49	1480	28	58	0	5	<0.05	<0.04	6.5	<200	2230	7.9	7.4	4.90	0.38	8	40.5	7
439966	4333158	22	0-20	106	184	16	560	272	3.72	1940	484	102	0	14	<0.05	<0.04	4.1	<200	4150	8.1	7.9	5.57	0.33	11	78.7	10
439966	4333158	22	20-40	107	183	9	520	300	1.64	2040	456	67	0	6	0.05	<0.04	2.1	<200	4200	8.5	8.2	3.74	0.21	0	83.7	11
439966	4333158	22	40-60	108	174	7	480	284	1.72	1880	408	62	0	11	0.07	<0.04	2.1	<200	3800	8.4	8.2	3.70	0.21	3	87.1	10
439966	4333158	22	60-80	109	399	15	464	531	2.56	2900	756	118	0	21	<0.05	<0.04	3.8	270	5600	7.6	7.4	16.69	0.67	9	74.8	15
439966	4333158	22	80-100	110	301	10	326	380	1.84	1940	608	84	0	20	0.05	<0.04	6.3	<200	4080	8.0	7.8	8.66	0.43	9	82.5	12
439966	4333158	22	100-120	111	175	10	456	284	0.59	2140	304	64	0	15	<0.05	<0.04	15.7	<200	3650	7.8	7.5	4.59	0.45	7	38.6	6

APPENDIX E

Soil physics

E.1. Las Tablas de Daimiel National Park soil physical data

Soil Functional Type (SFT)	Texture	% sand	% silt	% clay
Silt (Puente Navarro dam)	Silt loam	17.6	67.94	14.46
Clay (cut-sedge dominated area)	Silt loam	11.5	74.87	13.63
Clay (bare soil)	Silt loam	13.16	61.22	25.62
Undisturbed charophytes	Silt loam	34	57.67	8.33
Saline charophytes (Casablanca)	Silt loam	26.19	67.88	5.93
Edaphized charophytes (reed beds)	Loam-Sandy loam	52.9	39.21	7.89
Peaty silt (Molemocho dam)	Silt loam	15.11	61	23.89
Peat (central Morenillo dam)	Loamy sand	88.09	0	11.91

Bulk density (g cm^{-3})

Undisturbed charophytes	Silt	Peat	Clay	Edaphized charophytes	Organic soil	Peaty silt
0.95	0.86	0.19	1.26	0.60	0.43	0.76
0.99	0.70	0.20	1.24	0.70	0.44	0.79
0.77	1.11	0.12	1.28	0.67	0.50	
0.70	1.09	0.15	1.31		0.52	
0.67	1.12	0.18	1.34		0.59	
0.67	1.23	0.13	1.48		0.51	
0.69	1.24	0.12	1.15		0.60	
0.60	1.14	0.24	1.35		0.57	
0.63	0.47	0.23	1.32			
0.82	0.55	0.19				
0.70	0.51	0.21				
0.70		0.19				
0.78		0.20				
0.88		0.14				
0.75		0.17				
0.75		0.15				
0.80		0.19				
0.80		0.22				
		0.22				

Wageningen lab (2008 samples)
UCM lab (2008 samples)
UCM lab (2009 samples)

Measured saturated hydraulic conductivity-K_s (cm d^{-1})

Undisturbed charophytes	Silt	Peat	Clay	Edaphized charophytes	Organic soil	Saline charophytes	Peaty silt
83	36	27502	159	748	748	1877	5867
82	38	28207	159	689	689	616	1819
86	41	27051	152	579	579	2914	7435
104	37	21206	124	295	295	1211	3279
76		6840		114	628	2621	7398
74				737		879	2186

Wageningen lab (2008 samples)
UCM lab (2008 samples)

Estimated saturated hydraulic conductivity-K_s (cm d^{-1})

Undisturbed charophytes	Silt	Peaty silt	Clay	Edaphized charophytes	Peat	Charophytes-peat alternations
90	257	1502	102	1450	1200	515
151	530	1505	98	950	1052	273
198	140	417	27	614	891	388
411	269	323	37	356	862	561
78	261	616	28	936	1123	567
96	294	777	302	648	850	315

	Organic carbon (C_{org}) and organic matter (OM) content (%)					
	2008			2009		
	C_{org} IGME lab (LOI), n=1	C_{org} Wageningen lab (LOI)	C_{org} UCM lab (Walkley-Black)	C_{org} (Walkley-Black)	Weighted average C_{org}	Average OM
Silt	4.73	3.96 (n=6)	6.22 (n=14)		5.50	9.47
Clay	3.38		1.97 (n=23)	2.55 (n=1)	2.05	3.53
Undisturbed charophytes	4.55	3.03 (n=6)	3.39 (n=11)	5.96 (n=1)	3.47	5.97
Saline charophytes	3.76		0.93 (n=8)		1.24	2.14
Edaphized charophytes	10.90	4.42 (n=11)	6.98 (n=14)	12.80 (n=4)	6.95	11.95
Peat	36.20	45.79 (n=6)		26.66 (n=44)	29.10	50.05
Organic soil				19.17 (n=6)	19.17	32.97
Peaty silt	30.87				30.87	53.09

E.2. Infiltration

In this appendix, plots for field infiltration tests and K_s estimation through the method proposed by Wu et al. (1999) are shown for 43 out of the 49 tests carried out in Las Tablas de Daimiel National Park. The other 6 have been discarded for not being representative either due to problems during test performance or abnormal measurements recording.

E.2.1. Infiltrations tests

Undisturbed charophytes

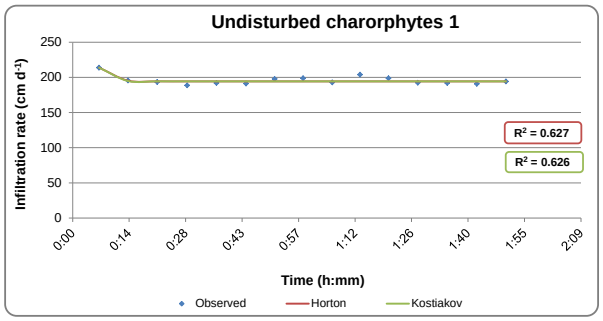

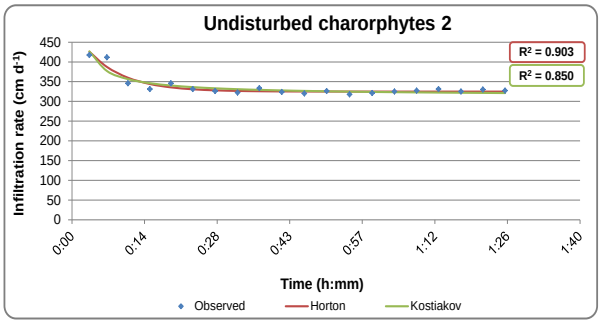

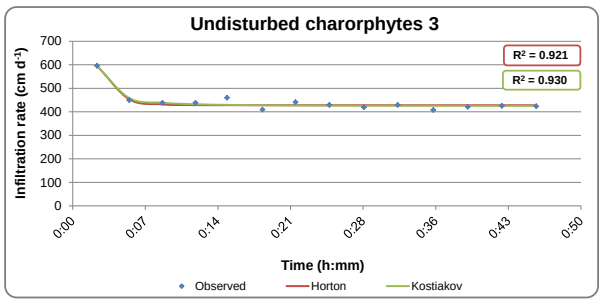

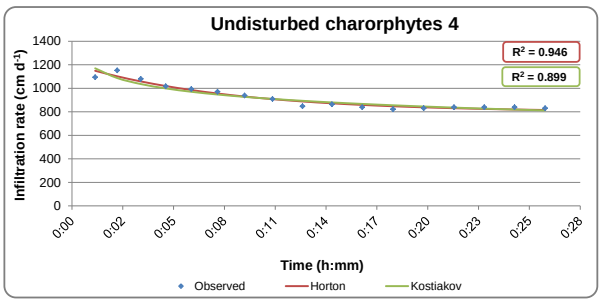

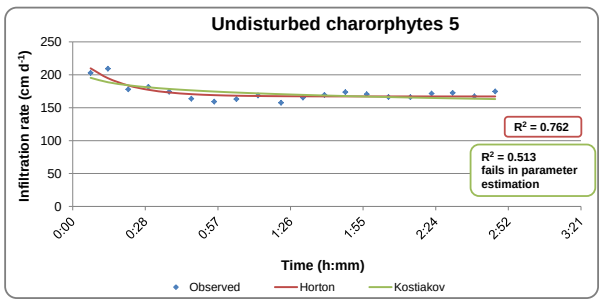

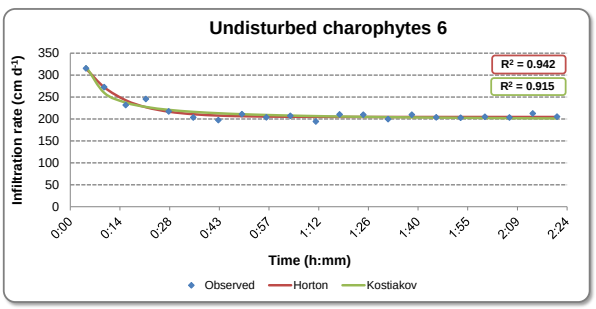

Silt

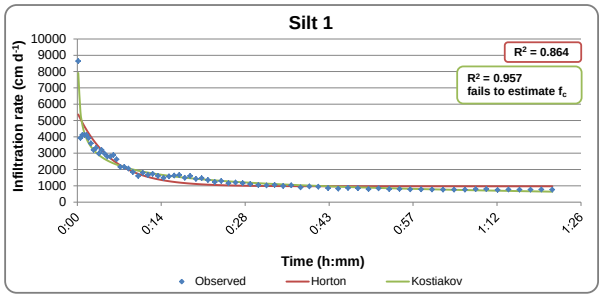
Silt 1
Infiltration rate (cm d⁻¹)
10000
9000
8000
7000
6000
5000
4000
3000
2000
1000
0
0:00
0:14
0:28
0:43
0:57
1:12
1:26
Time (h:mm)
R² = 0.864
R² = 0.957
fails to estimate fc
Observed
Horton
Kostiakov

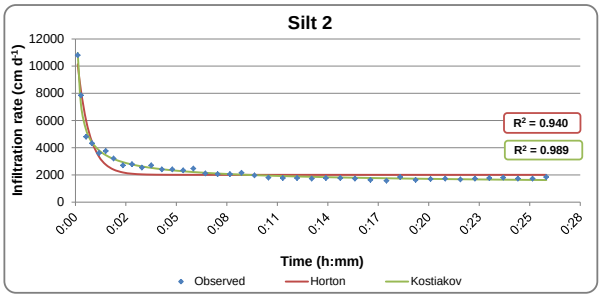
Silt 2
Infiltration rate (cm d⁻¹)
12000
10000
8000
6000
4000
2000
0
0:00
0:02
0:05
0:08
0:11
0:14
0:17
0:20
0:23
0:25
0:28
Time (h:mm)
R² = 0.940
R² = 0.989
Observed
Horton
Kostiakov

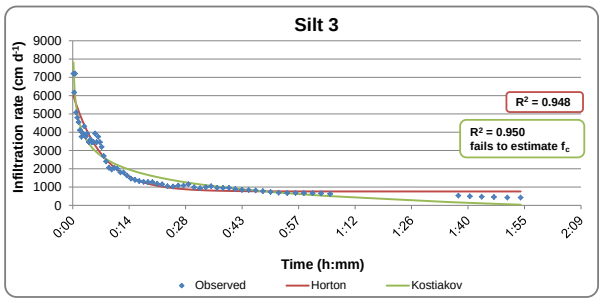
Silt 3
Infiltration rate (cm d⁻¹)
9000
8000
7000
6000
5000
4000
3000
2000
1000
0
0:00
0:14
0:28
0:43
0:57
1:12
1:26
1:40
1:55
2:09
Time (h:mm)
R² = 0.948
R² = 0.950
fails to estimate fc
Observed
Horton
Kostiakov

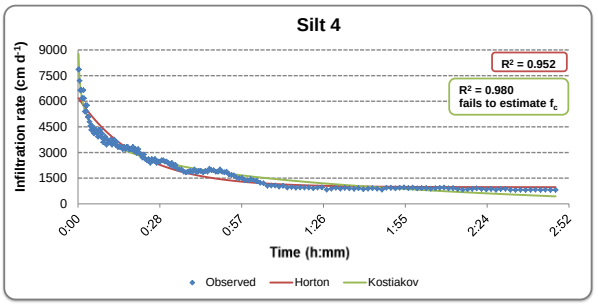
Silt 4
Infiltration rate (cm d⁻¹)
9000
7500
6000
4500
3000
1500
0
0:00
0:28
0:57
1:26
1:55
2:24
2:52
Time (h:mm)
R² = 0.952
R² = 0.980
fails to estimate fc
Observed
Horton
Kostiakov

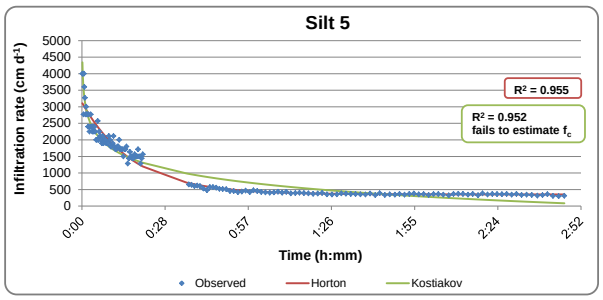
Silt 5
Infiltration rate (cm d⁻¹)
5000
4500
4000
3500
3000
2500
2000
1500
1000
500
0
0:00
0:28
0:57
1:26
1:55
2:24
2:52
Time (h:mm)
R² = 0.955
R² = 0.952
fails to estimate fc
Observed
Horton
Kostiakov

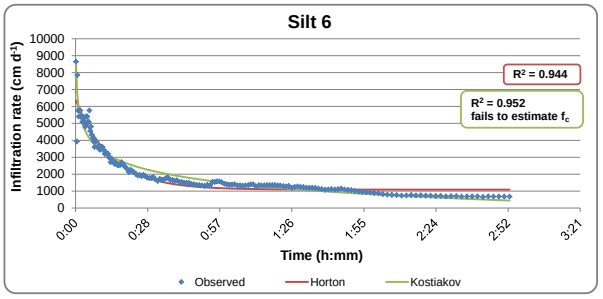
Silt 6
Infiltration rate (cm d⁻¹)
10000
9000
8000
7000
6000
5000
4000
3000
2000
1000
0
0:00
0:28
0:57
1:26
1:55
2:24
2:52
3:21
Time (h:mm)
R² = 0.944
R² = 0.952
fails to estimate fc
Observed
Horton
Kostiakov

Peat

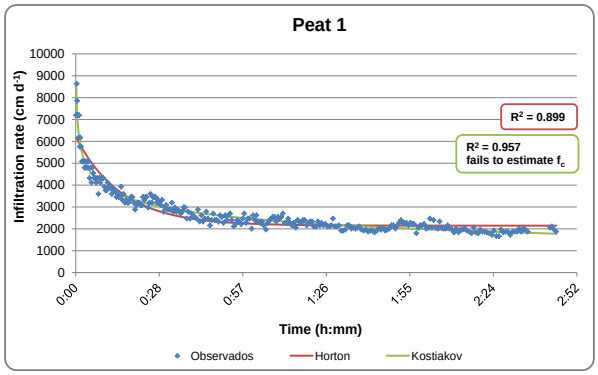
Peat 1
Infiltration rate (cm d-1)
10000
9000
8000
7000
6000
5000
4000
3000
2000
1000
0
0:00
0:28
0:57
1:26
1:55
2:24
2:52
Time (h:mm)
R² = 0.899
R² = 0.957
fails to estimate fc
Observados
Horton
Kostiakov

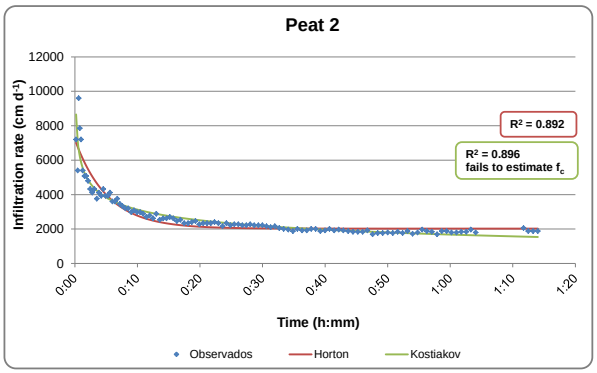
Peat 2
Infiltration rate (cm d-1)
12000
10000
8000
6000
4000
2000
0
0:00
0:10
0:20
0:30
0:40
0:50
1:00
1:10
1:20
Time (h:mm)
R² = 0.892
R² = 0.896
fails to estimate fc
Observados
Horton
Kostiakov

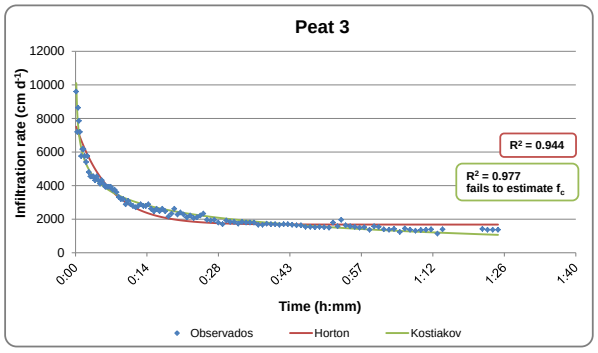
Peat 3
Infiltration rate (cm d-1)
12000
10000
8000
6000
4000
2000
0
0:00
0:14
0:28
0:43
0:57
1:12
1:26
1:40
Time (h:mm)
R² = 0.944
R² = 0.977
fails to estimate fc
Observados
Horton
Kostiakov

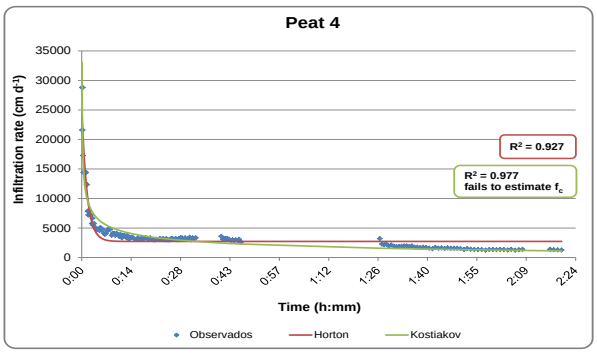
Peat 4
Infiltration rate (cm d-1)
35000
30000
25000
20000
15000
10000
5000
0
0:00
0:14
0:28
0:43
0:57
1:12
1:26
1:40
1:55
2:09
2:24
Time (h:mm)
R² = 0.927
R² = 0.977
fails to estimate fc
Observados
Horton
Kostiakov

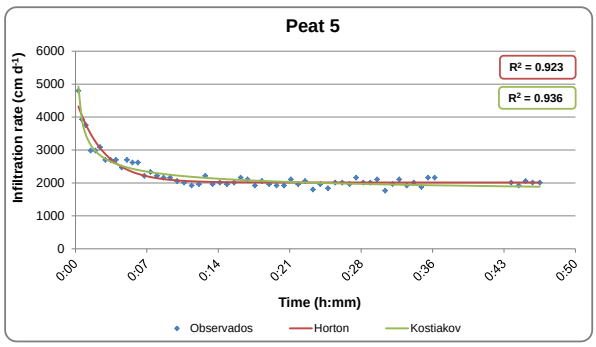
Peat 5
Infiltration rate (cm d-1)
6000
5000
4000
3000
2000
1000
0
0:00
0:07
0:14
0:21
0:28
0:36
0:43
0:50
Time (h:mm)
R² = 0.923
R² = 0.936
Observados
Horton
Kostiakov

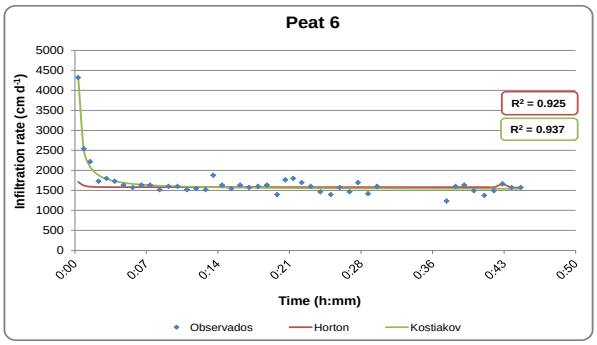
Peat 6
Infiltration rate (cm d-1)
5000
4500
4000
3500
3000
2500
2000
1500
1000
500
0
0:00
0:07
0:14
0:21
0:28
0:36
0:43
0:50
Time (h:mm)
R² = 0.925
R² = 0.937
Observados
Horton
Kostiakov

Clay

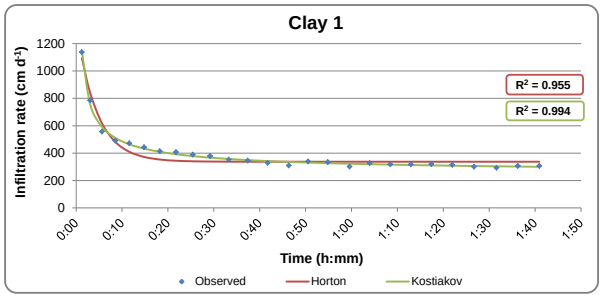
Clay 1
Infiltration rate (cm d-1)
1200
1000
800
600
400
200
0
0:00
0:10
0:20
0:30
0:40
0:50
1:00
1:10
1:20
1:30
1:40
1:50
Time (h:mm)
R² = 0.955
R² = 0.994
Observed
Horton
Kostiakov

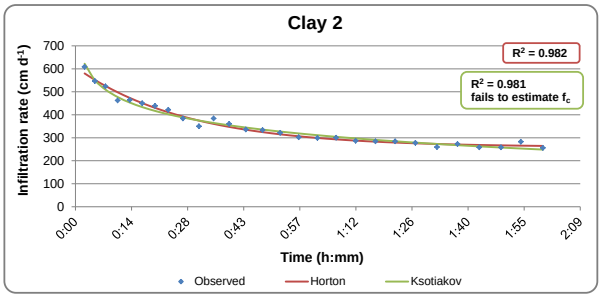
Clay 2
Infiltration rate (cm d-1)
700
600
500
400
300
200
100
0
0:00
0:14
0:28
0:43
0:57
1:12
1:26
1:40
1:55
2:09
Time (h:mm)
R² = 0.982
R² = 0.981
fails to estimate fc
Observed
Horton
Ksotiakov

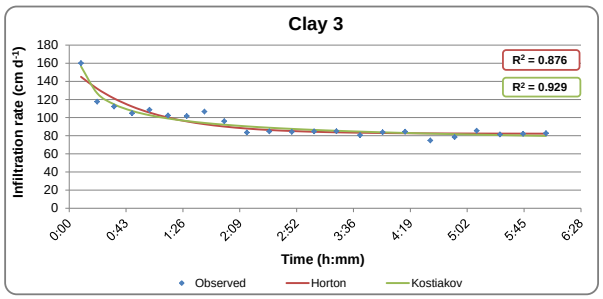
Clay 3
Infiltration rate (cm d-1)
180
160
140
120
100
80
60
40
20
0
0:00
0:43
1:26
2:09
2:52
3:36
4:19
5:02
5:45
6:28
Time (h:mm)
R² = 0.876
R² = 0.929
Observed
Horton
Kostiakov

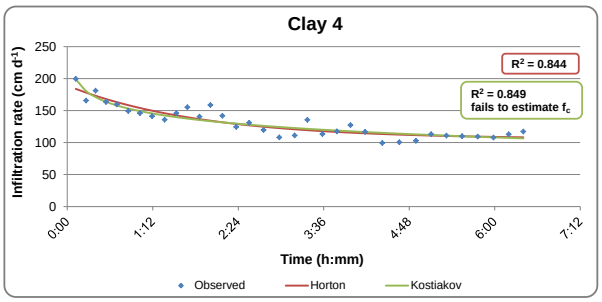
Clay 4
Infiltration rate (cm d-1)
250
200
150
100
50
0
0:00
1:12
2:24
3:36
4:48
6:00
7:12
Time (h:mm)
R² = 0.844
R² = 0.849
fails to estimate fc
Observed
Horton
Kostiakov

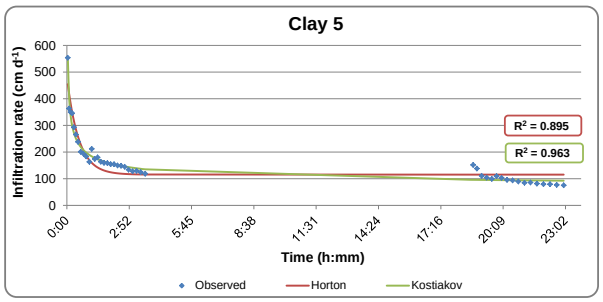
Clay 5
Infiltration rate (cm d-1)
600
500
400
300
200
100
0
0:00
2:52
5:45
8:38
11:31
14:24
17:16
20:09
23:02
Time (h:mm)
R² = 0.895
R² = 0.963
Observed
Horton
Kostiakov

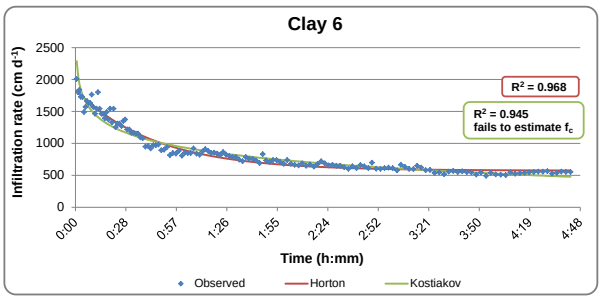
Clay 6
Infiltration rate (cm d-1)
2500
2000
1500
1000
500
0
0:00
0:28
0:57
1:26
1:55
2:24
2:52
3:21
3:50
4:19
4:48
Time (h:mm)
R² = 0.968
R² = 0.945
fails to estimate fc
Observed
Horton
Kostiakov

Peaty silt

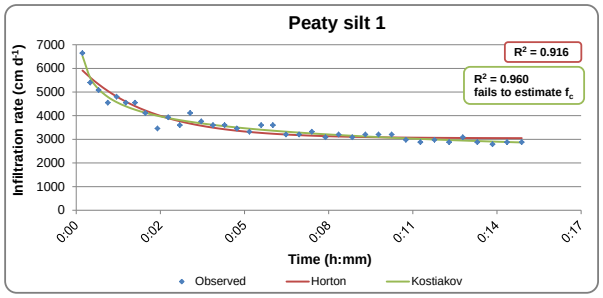
Peaty silt 1
Infiltration rate (cm d⁻¹)
7000
6000
5000
4000
3000
2000
1000
0
0:00
0:02
0:05
0:08
0:11
0:14
0:17
Time (h:mm)
R² = 0.916
R² = 0.960
fails to estimate f_c
Observed
Horton
Kostiakov

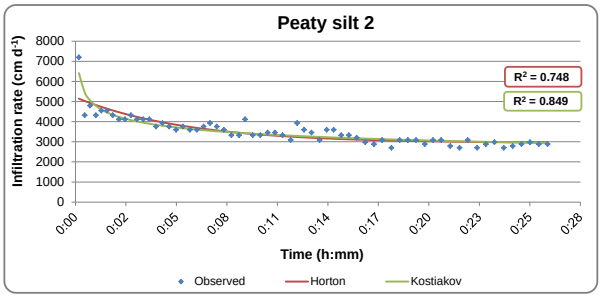
Peaty silt 2
Infiltration rate (cm d⁻¹)
8000
7000
6000
5000
4000
3000
2000
1000
0
0:00
0:02
0:05
0:08
0:11
0:14
0:17
0:20
0:23
0:25
0:28
Time (h:mm)
R² = 0.748
R² = 0.849
Observed
Horton
Kostiakov

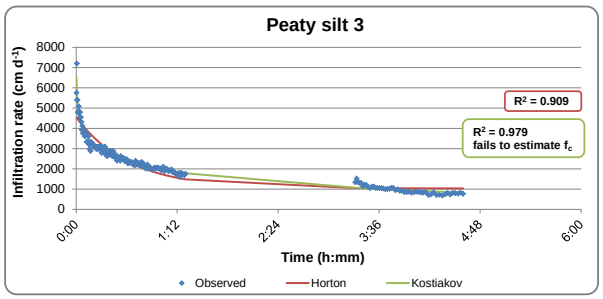
Peaty silt 3
Infiltration rate (cm d⁻¹)
8000
7000
6000
5000
4000
3000
2000
1000
0
0:00
1:12
2:24
3:36
4:48
6:00
Time (h:mm)
R² = 0.909
R² = 0.979
fails to estimate f_c
Observed
Horton
Kostiakov

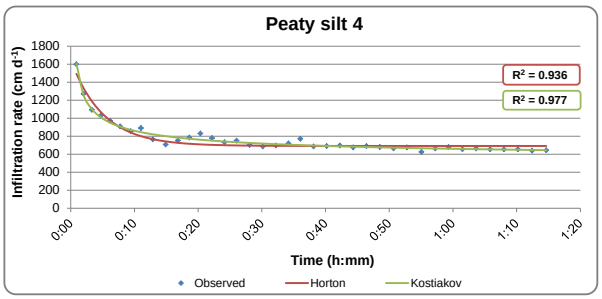
Peaty silt 4
Infiltration rate (cm d⁻¹)
1800
1600
1400
1200
1000
800
600
400
200
0
0:00
0:10
0:20
0:30
0:40
0:50
1:00
1:10
1:20
Time (h:mm)
R² = 0.936
R² = 0.977
Observed
Horton
Kostiakov

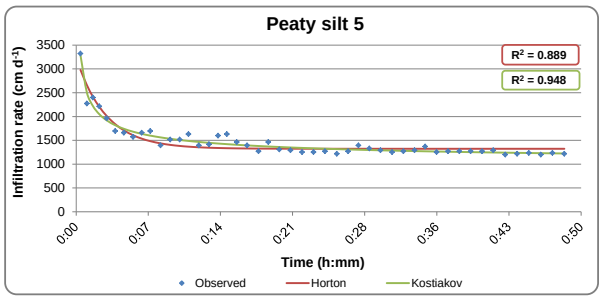
Peaty silt 5
Infiltration rate (cm d⁻¹)
3500
3000
2500
2000
1500
1000
500
0
0:00
0:07
0:14
0:21
0:28
0:36
0:43
0:50
Time (h:mm)
R² = 0.889
R² = 0.948
Observed
Horton
Kostiakov

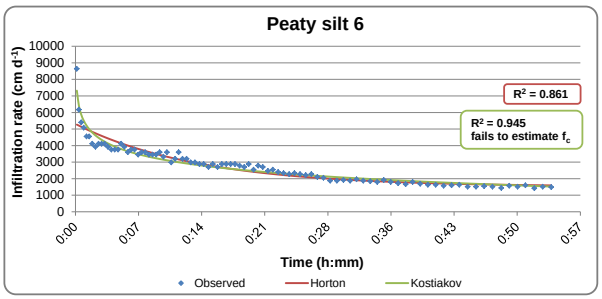
Peaty silt 6
Infiltration rate (cm d⁻¹)
10000
9000
8000
7000
6000
5000
4000
3000
2000
1000
0
0:00
0:07
0:14
0:21
0:28
0:36
0:43
0:50
0:57
Time (h:mm)
R² = 0.861
R² = 0.945
fails to estimate f_c
Observed
Horton
Kostiakov

Edaphized charophytes

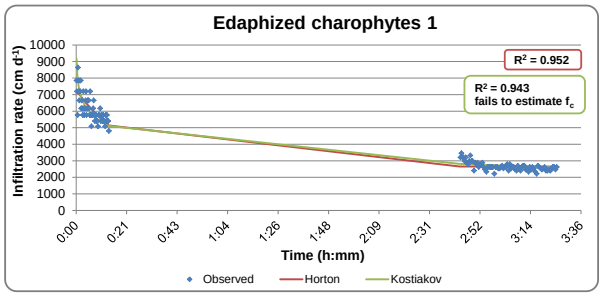

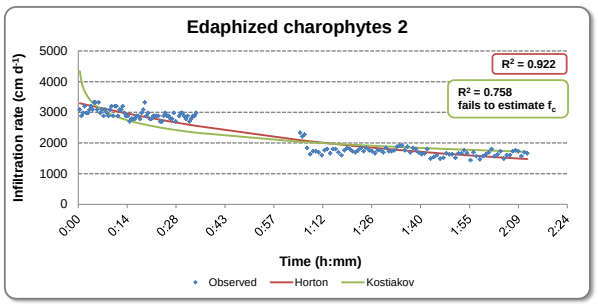

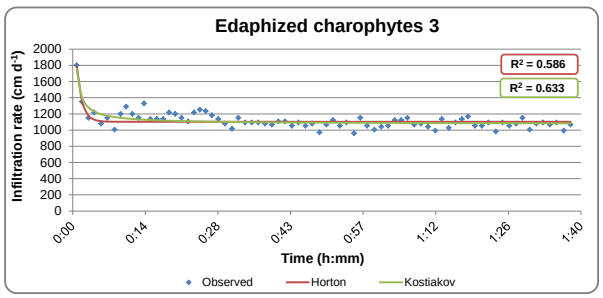

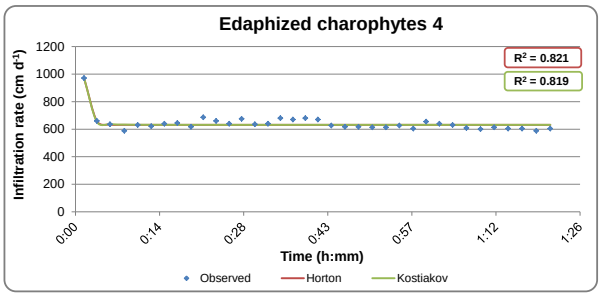

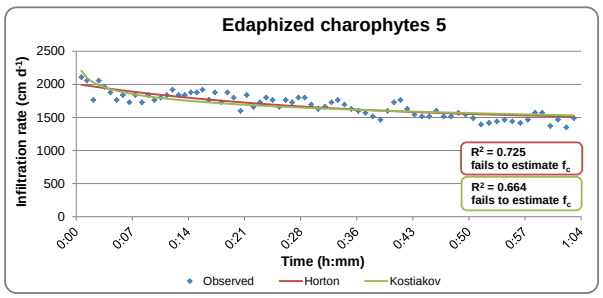

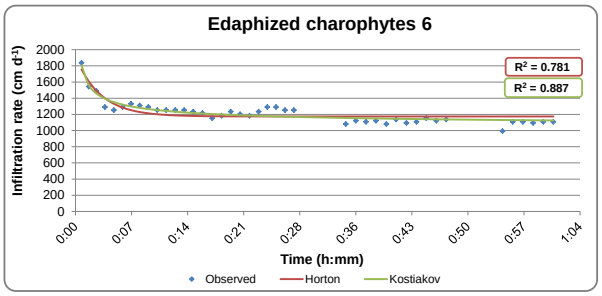

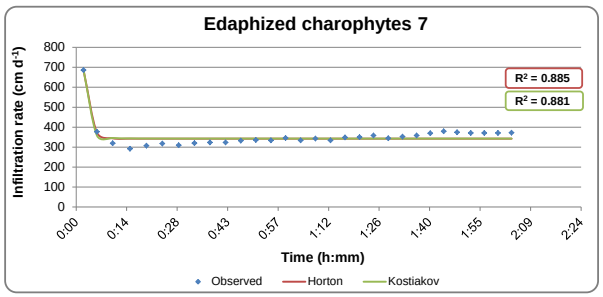

Charophytes-peat alternations

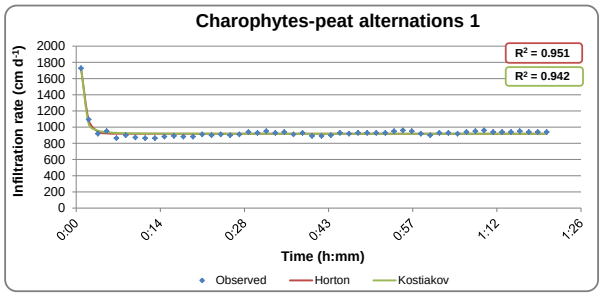

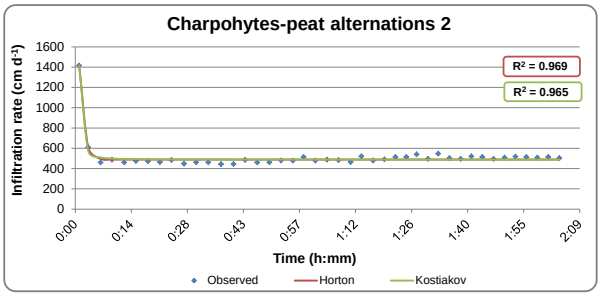

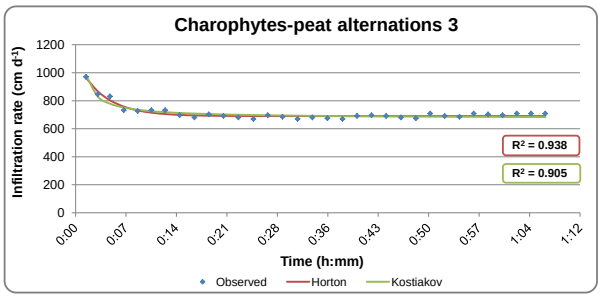

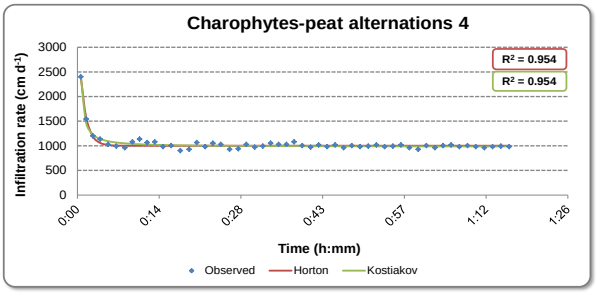

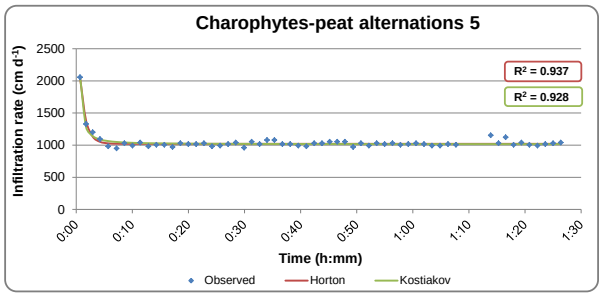

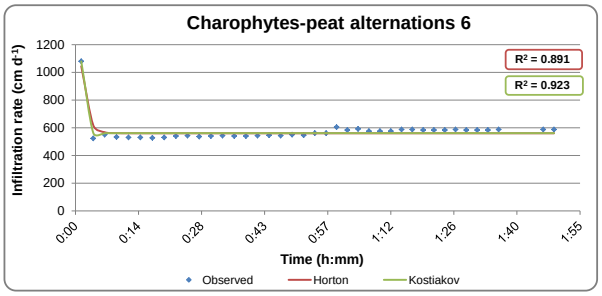

E.2.2. Linear fitting of accumulated infiltration curves for saturated hydraulic conductivity estimation as proposed by Wu et al. (1999)

Undisturbed charophytes

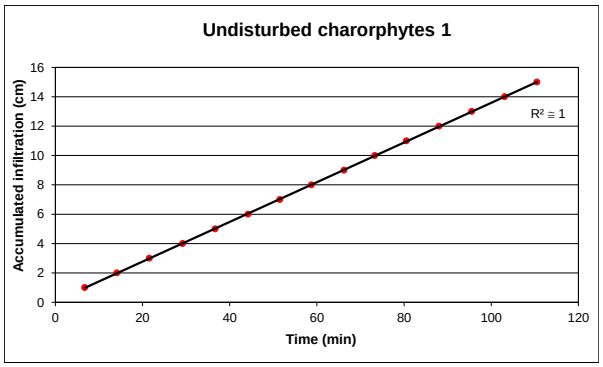

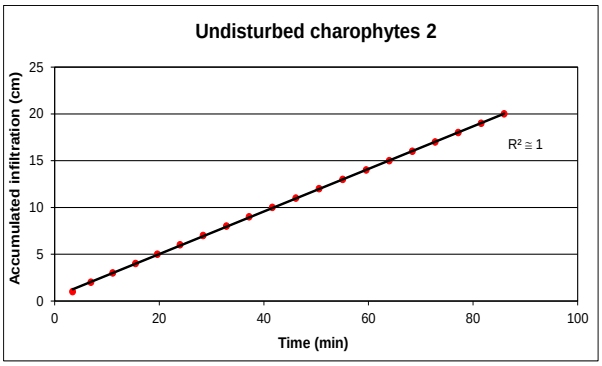

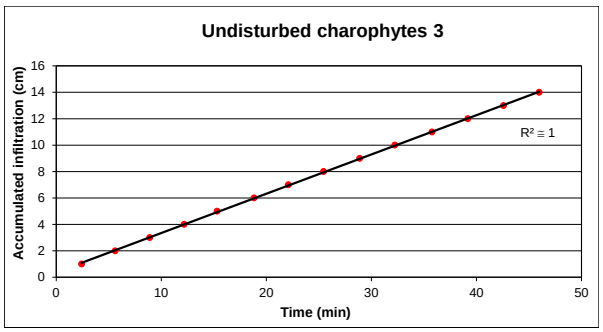

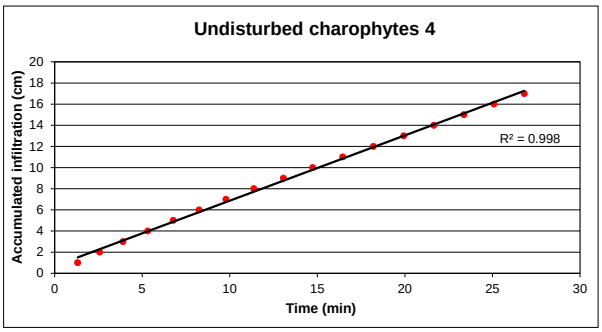

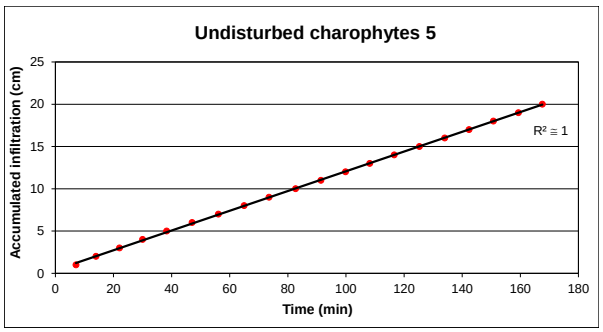

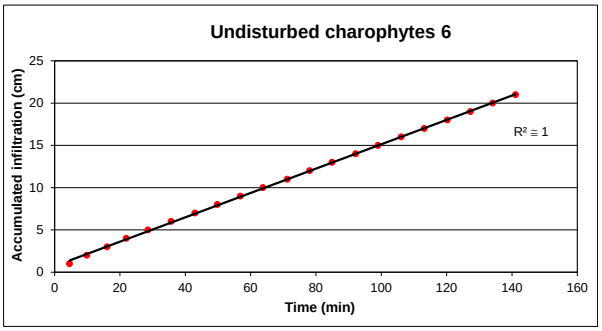

Silt

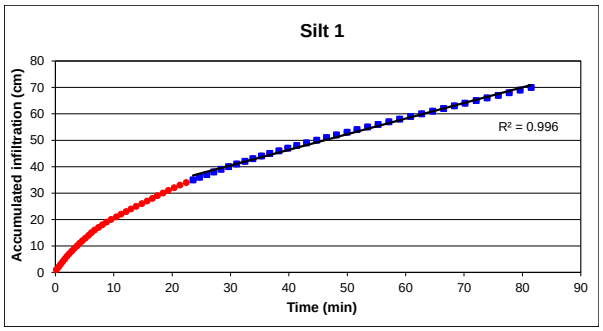
Silt 1
Accumulated infiltration (cm)
Time (min)
R² = 0.996

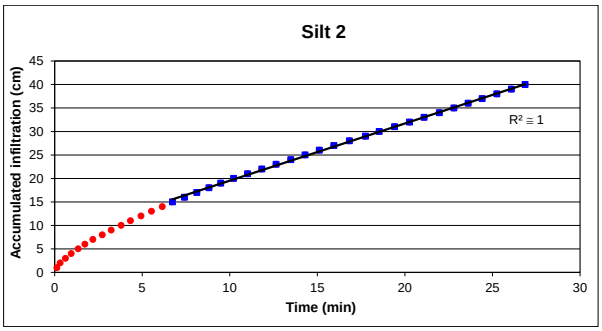
Silt 2
Accumulated infiltration (cm)
Time (min)
R² ≅ 1

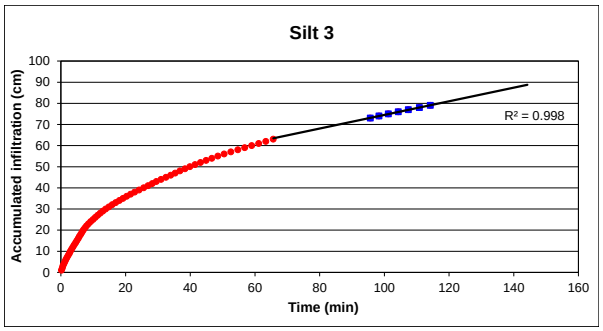
Silt 3
Accumulated infiltration (cm)
Time (min)
R² = 0.998

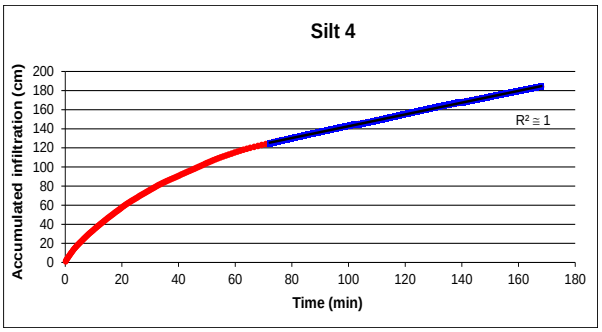
Silt 4
Accumulated infiltration (cm)
Time (min)
R² ≅ 1

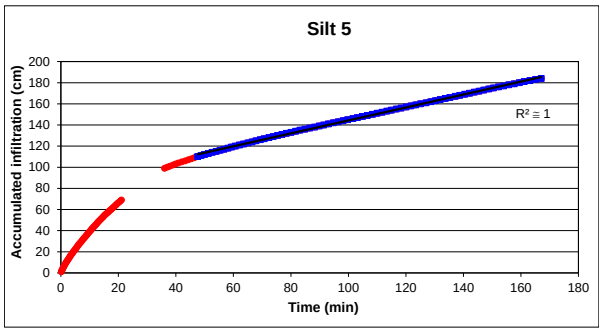
Silt 5
Accumulated infiltration (cm)
Time (min)
R² ≅ 1

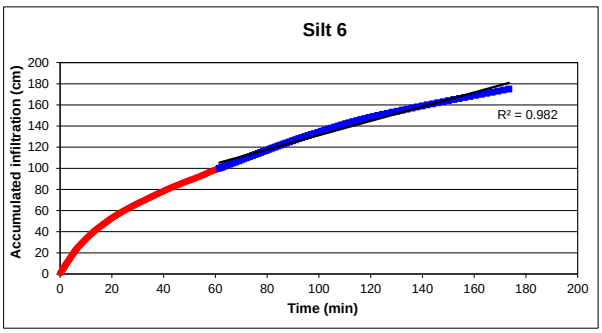
Silt 6
Accumulated infiltration (cm)
Time (min)
R² = 0.982

Peat

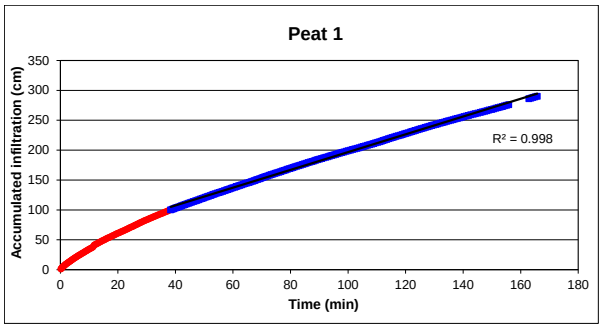
Peat 1
Accumulated infiltration (cm)
Time (min)
R² = 0.998

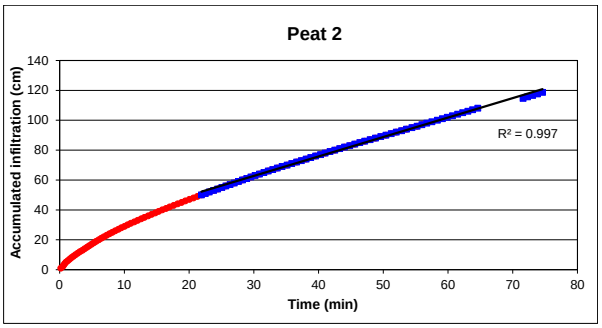
Peat 2
Accumulated infiltration (cm)
Time (min)
R² = 0.997

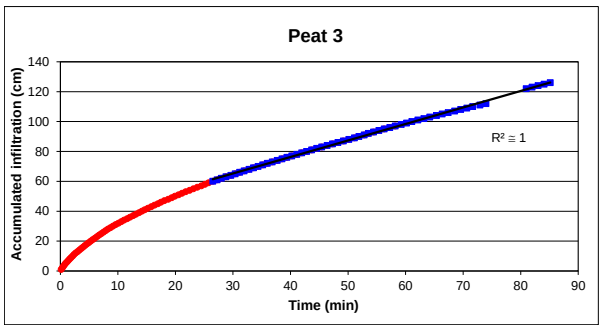
Peat 3
Accumulated infiltration (cm)
Time (min)
R² = 1

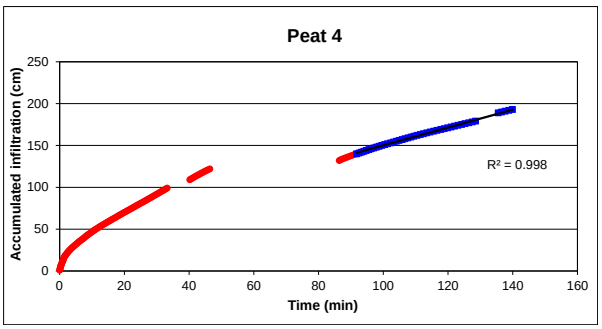
Peat 4
Accumulated infiltration (cm)
Time (min)
R² = 0.998

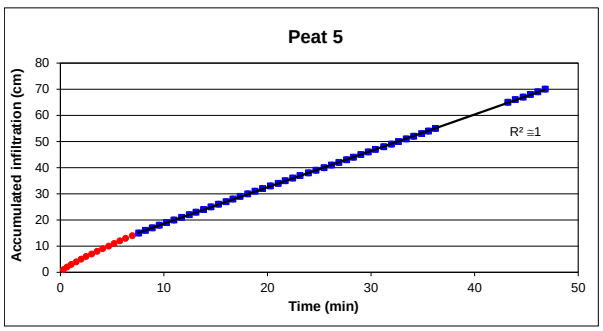
Peat 5
Accumulated infiltration (cm)
Time (min)
R² =1

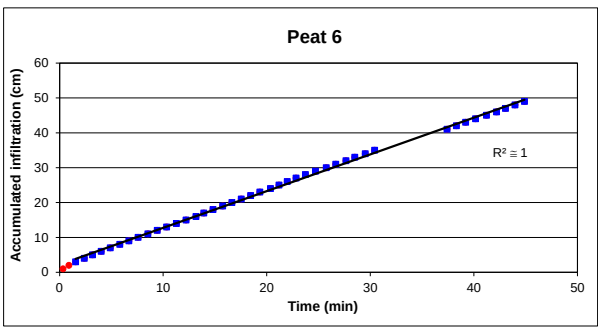
Peat 6
Accumulated infiltration (cm)
Time (min)
R² = 1

Clay

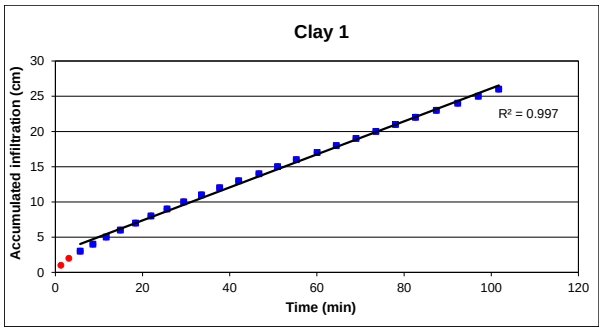
Clay 1
Accumulated infiltration (cm)
Time (min)
R² = 0.997

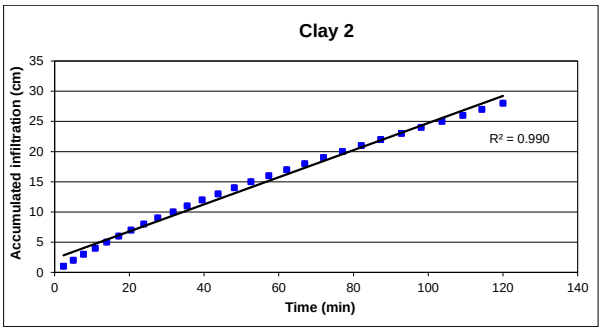
Clay 2
Accumulated infiltration (cm)
Time (min)
R² = 0.990

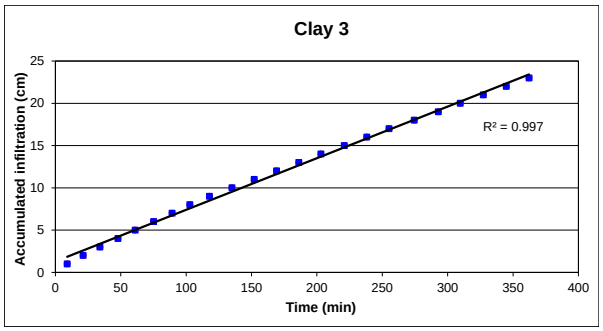
Clay 3
Accumulated infiltration (cm)
Time (min)
R² = 0.997

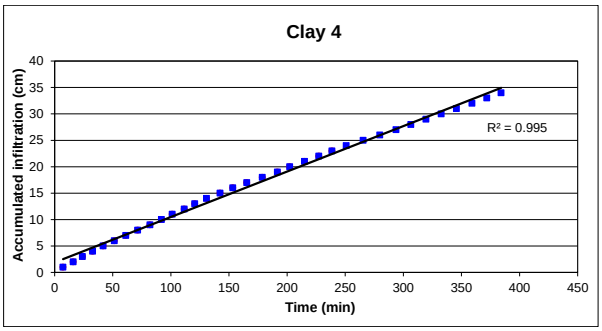
Clay 4
Accumulated infiltration (cm)
Time (min)
R² = 0.995

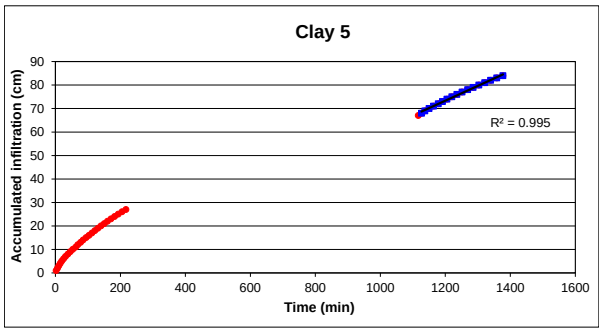
Clay 5
Accumulated infiltration (cm)
Time (min)
R² = 0.995

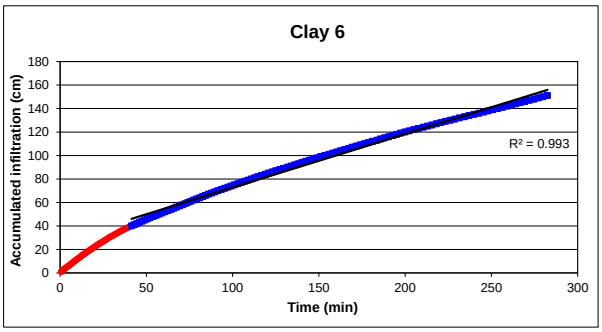
Clay 6
Accumulated infiltration (cm)
Time (min)
R² = 0.993

Peaty silt

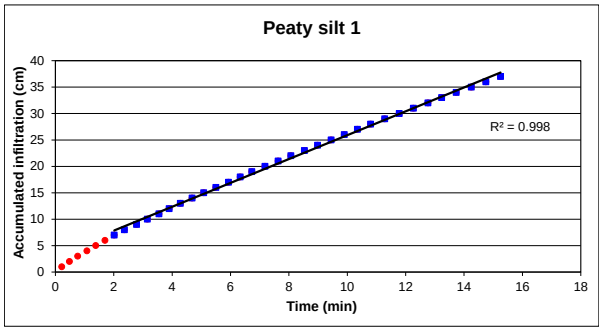
Peaty silt 1
Accumulated infiltration (cm)
Time (min)
R² = 0.998

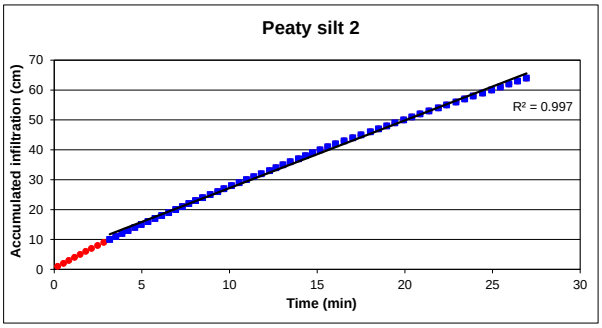
Peaty silt 2
Accumulated infiltration (cm)
Time (min)
R² = 0.997

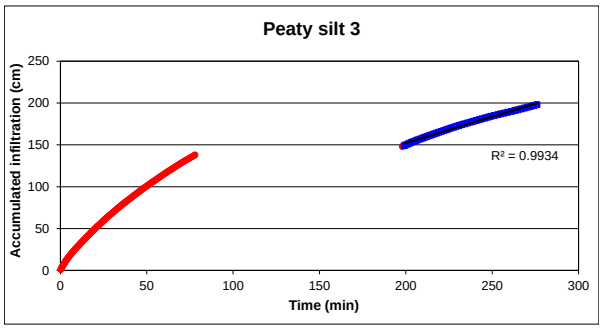
Peaty silt 3
Accumulated infiltration (cm)
Time (min)
R² = 0.9934

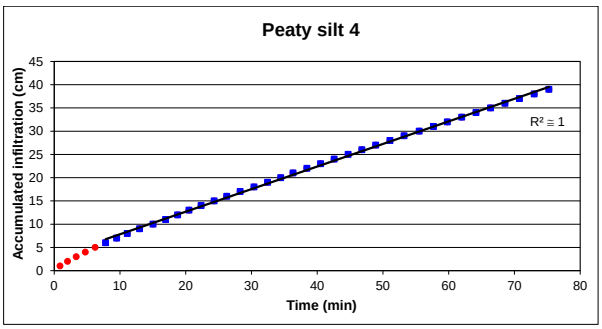
Peaty silt 4
Accumulated infiltration (cm)
Time (min)
R² = 1

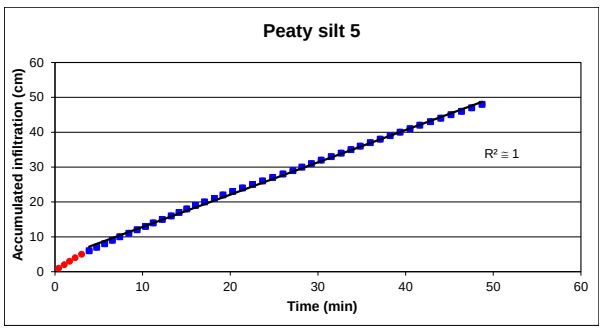
Peaty silt 5
Accumulated infiltration (cm)
Time (min)
R² = 1

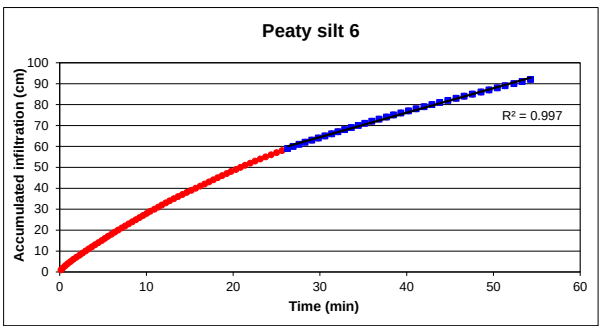
Peaty silt 6
Accumulated infiltration (cm)
Time (min)
R² = 0.997

Edaphized charophytes

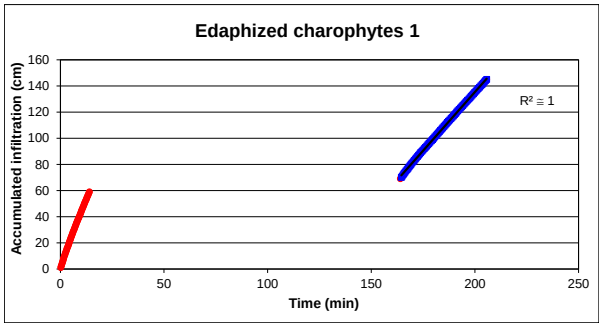

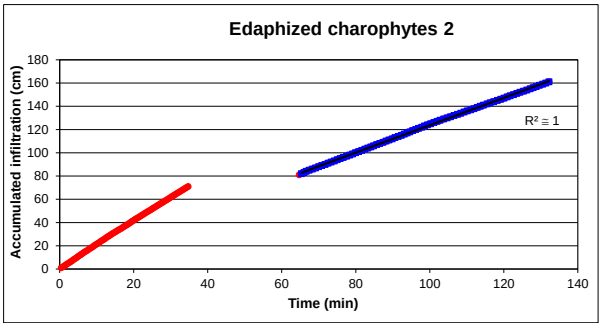

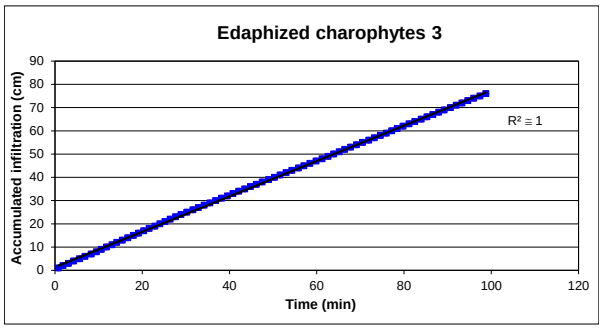

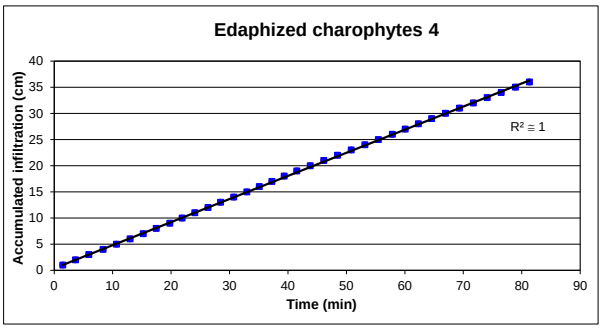

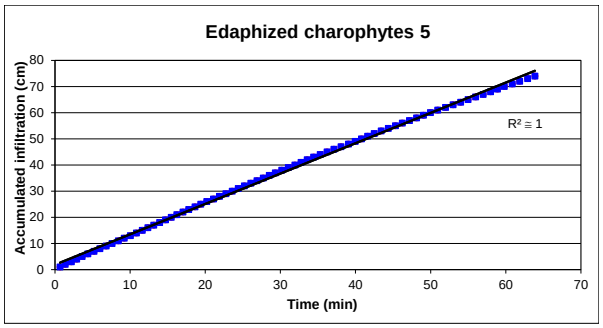

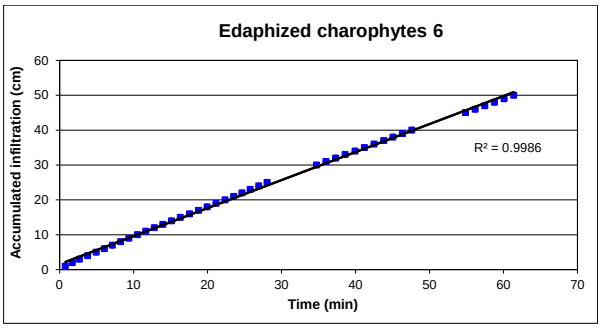

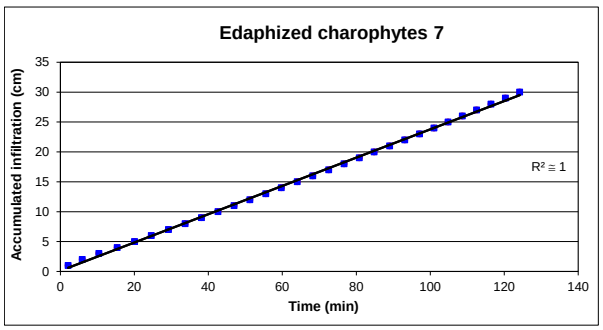

Charophytes-peat alternations

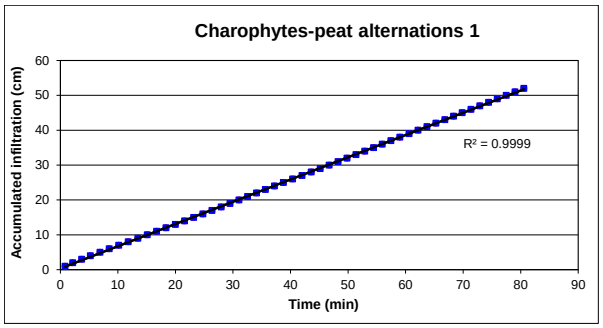

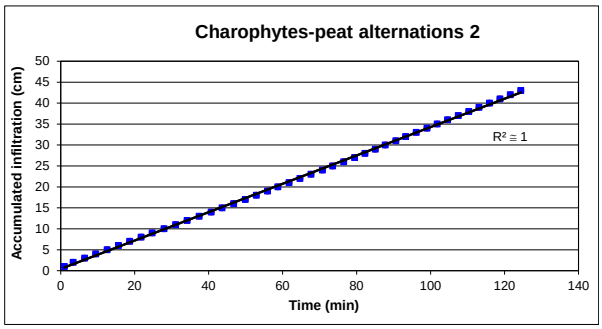

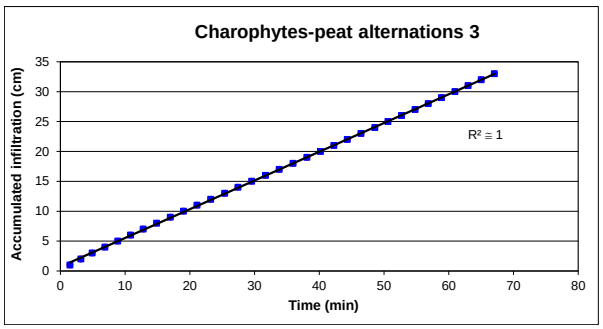

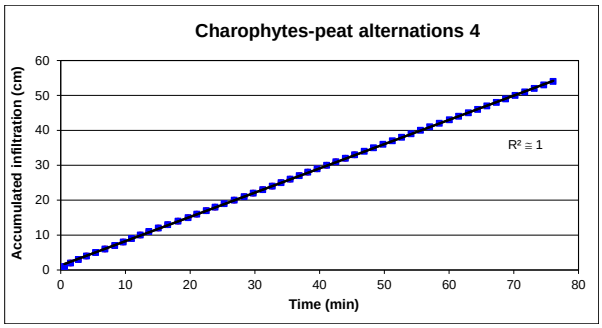

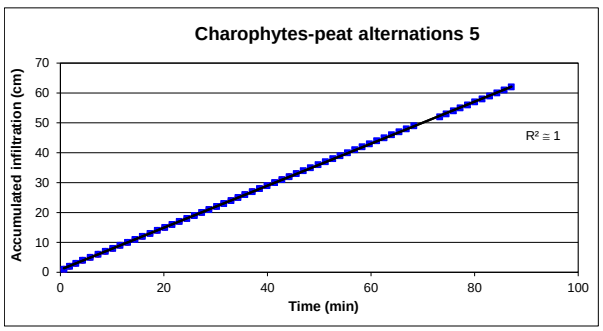

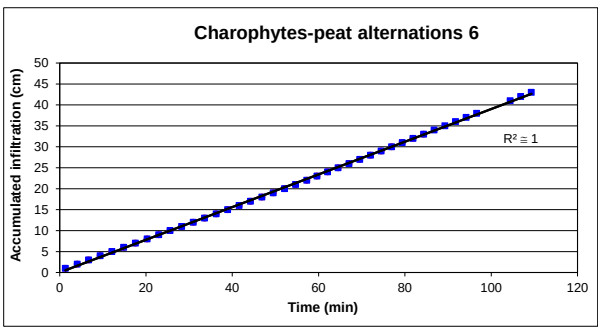

E.3.1. Water retention functions of charophytes and peat soils derived from Wind evaporation method

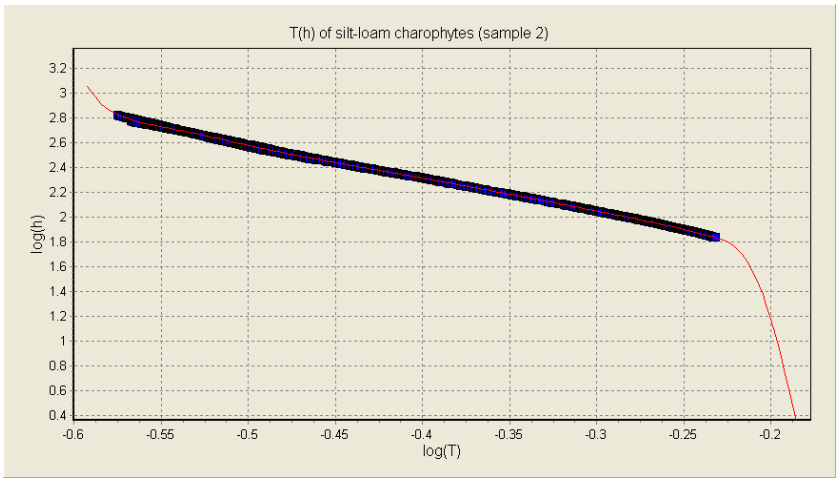

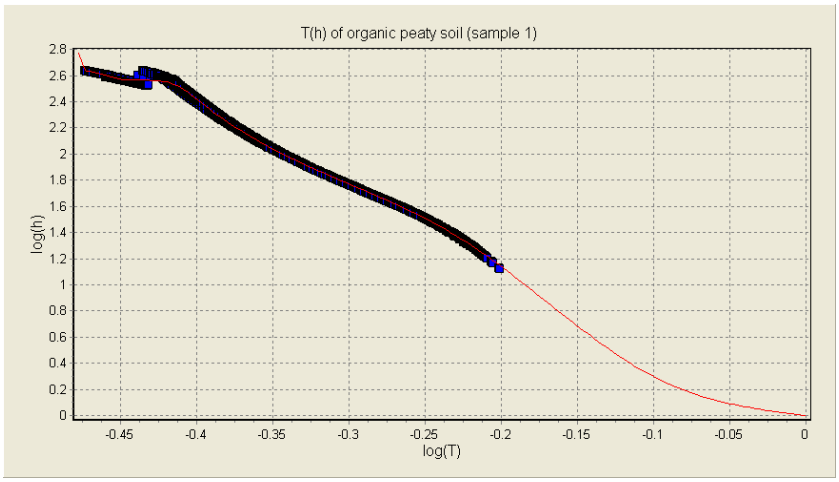

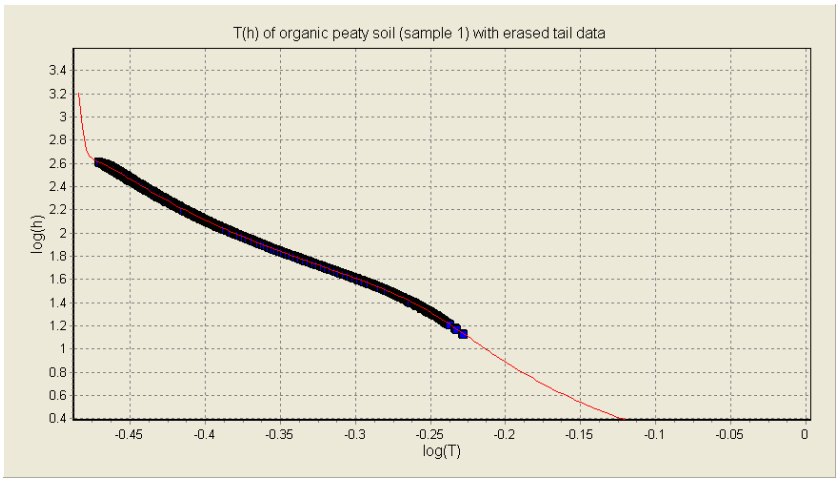

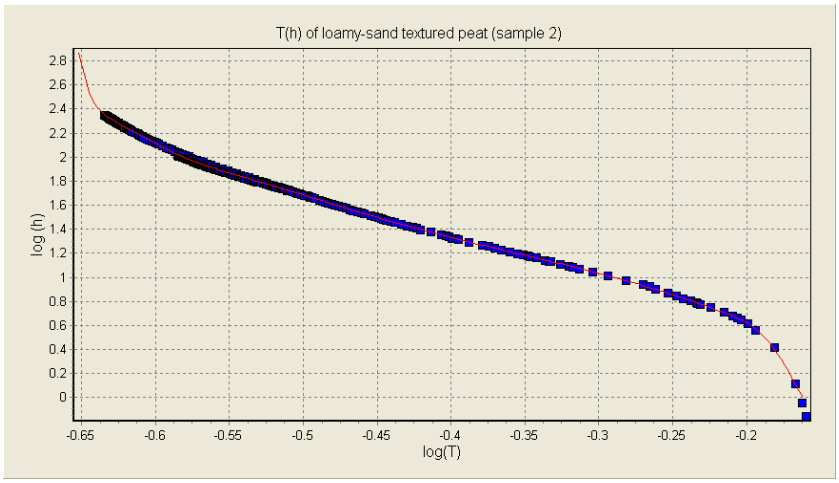
T(h) of loamy-sand textured peat (sample 2)
log (h)
log(T)

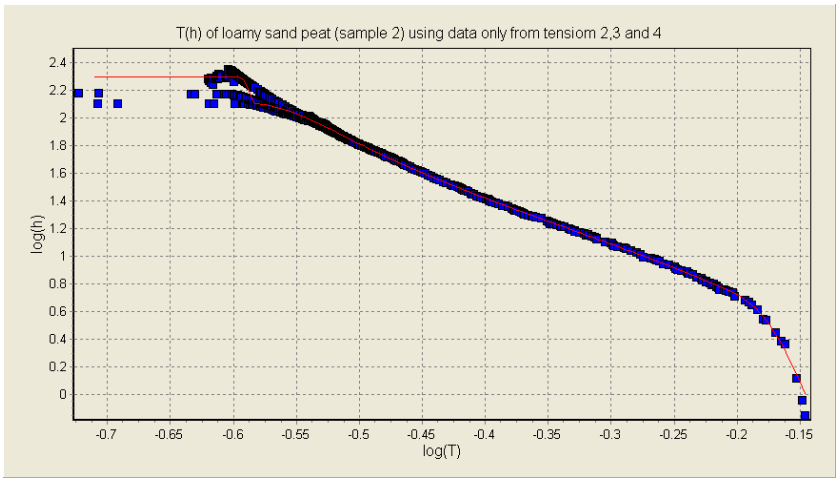
T(h) of loamy sand peat (sample 2) using data only from tensiom 2,3 and 4
log(h)
log(T)

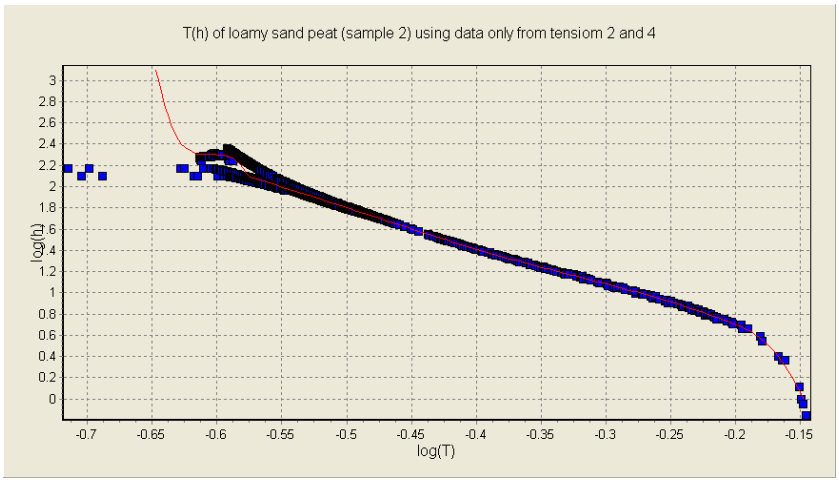
T(h) of loamy sand peat (sample 2) using data only from tensiom 2 and 4
log(h)
log(T)

E.3.2. Hydraulic conductivity functions of charophytes and peat soils derived from Wind evaporation method

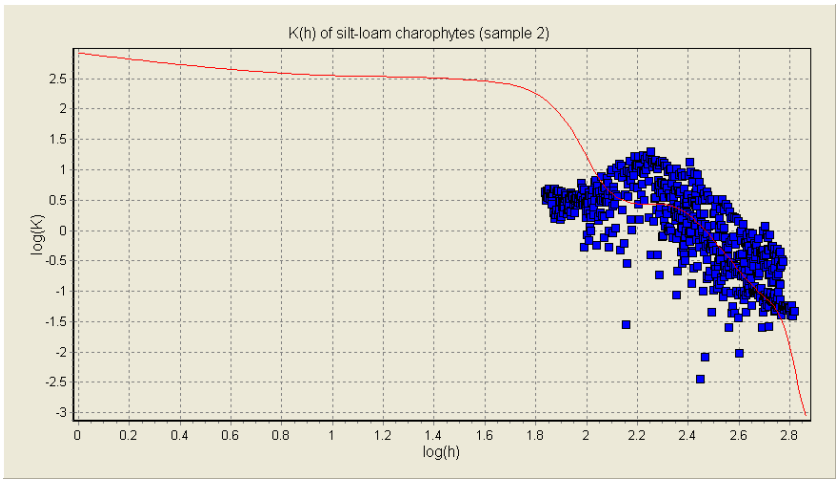

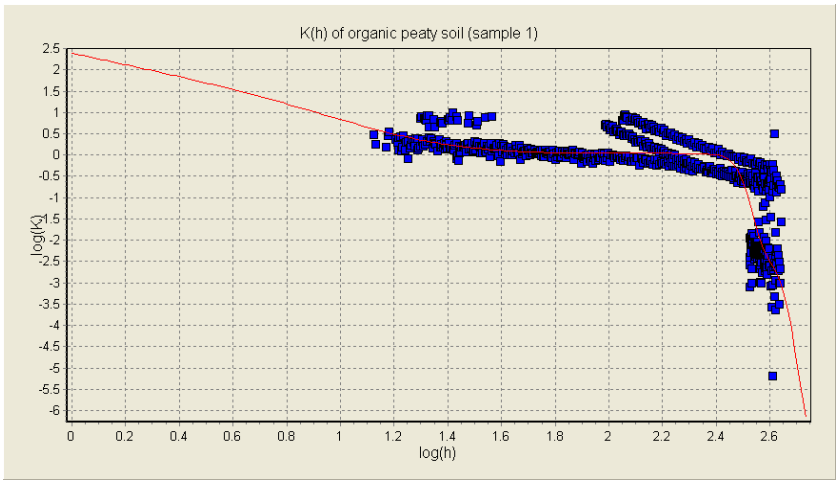

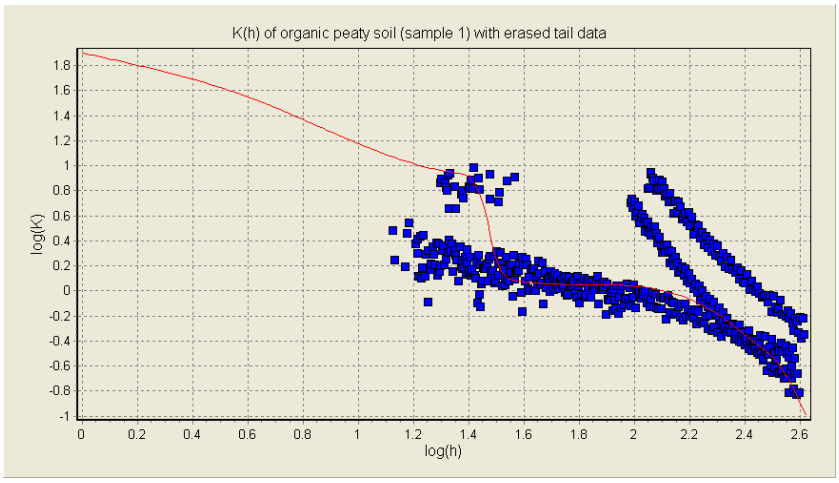

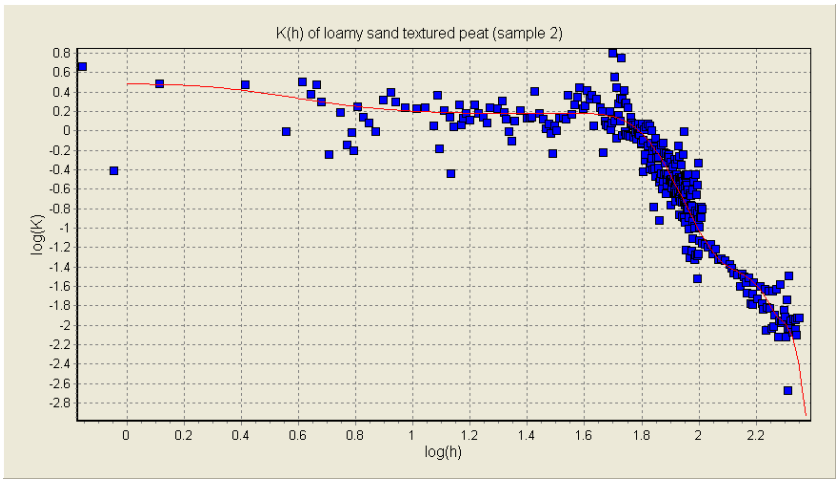
K(h) of loamy sand textured peat (sample 2)
log(K)
log(h)

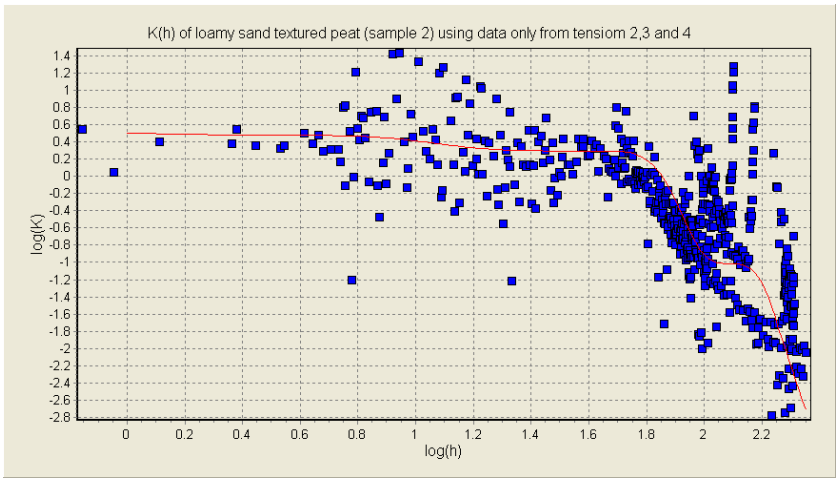
K(h) of loamy sand textured peat (sample 2) using data only from tensiom 2,3 and 4
log(K)
log(h)

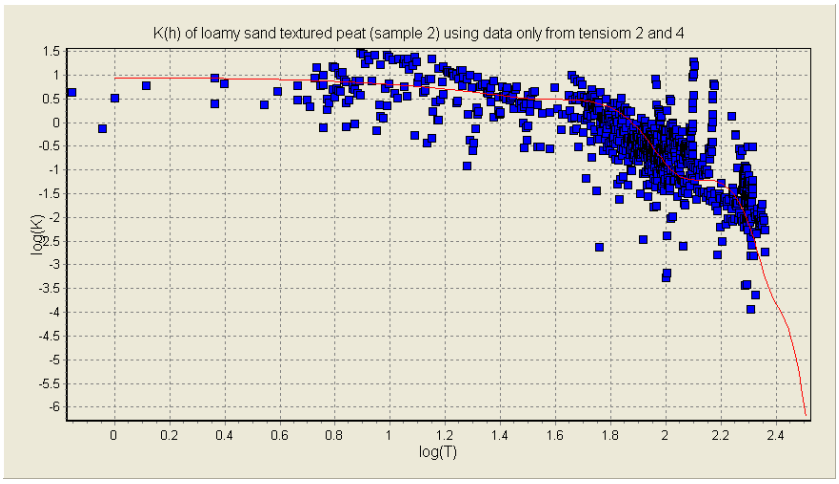
K(h) of loamy sand textured peat (sample 2) using data only from tensiom 2 and 4
log(K)
log(T)

APPENDIX F

Hydrochemistry

F. Hydrochemical data from groundwater and surface water monitoring points in Las Tablas de Daimiel National Park area in the period 2003-2010.

X (UTM)	Y (UTM)	Monitoring point	Date	µS cm^{-1}		mg l^{-1}	mg l^{-1}	mg l^{-1}	mg l^{-1}	mg l^{-1}	mg l^{-1}	mg l^{-1}	mg l^{-1}	mg l^{-1}	mg l^{-1}	mg l^{-1}	mg l^{-1}	mg l^{-1}	mg l^{-1}	mg l^{-1}	mg l^{-1}	mg l^{-1}
				EC	pH	SO4	Ca	HCO3	Cl	Mg	Na	K	DQO	TOC	NO3	NO2	NH4	PO4	SiO2	B	Br	N org
438683	4333348	G-01	17-may-06	16284	7.10	3900	780	322	2950	1050	1079	18	6.50	5.14	34	0.00		0.1472	18.60	0.327	5.2162	2.89
438683	4333348	G-01	21-mar-07	12614	7.02	4520	560	189	1880	1020	943	15	9.30	1.96	47	0.00	0.00	0.0000	19.70	0.344	0.6091	1.00
438683	4333348	G-01	13-sep-07	14893	7.52	5350	640	261	2640	1340	1215	18	7.80	7.44	26	0.00	0.33	0.1606	21.10	0.325	11.7267	2.12
438683	4333348	G-01	27-nov-07	15974	7.31	4620	590	241	2620	1200	1231	18	12.50	7.59	32	0.00	0.27	0.1338	19.60	0.412	48.0524	1.81
438683	4333348	G-01	27-dic-07	15704	7.23	4610	580	252	2680	1200	1299	19	10.90	8.19	27	0.00	0.00	0.1740	20.60	0.289	12.4752	3.07
438683	4333348	G-01	23-ene-08	15764	7.60	4560	560	238	2760	1240	1241	17	10.10	5.95	24	0.00	0.00	0.1222	16.20	0.321	13.1291	1.02
438683	4333348	G-01	23-abr-08	14943	7.34	4660	520	261	2440	1200	1143	17	7.80	4.25	33	0.00	0.00	0.0000	21.40	0.000	11.2367	1.43
438683	4333348	G-01	27-may-08	15383	7.92	5100	610	228	2100	1100	1147	16	7.80	5.59	34	0.00	0.00	0.0000	26.00	0.000	10.7631	2.30
438683	4333348	G-01	23-jun-08	14933	7.81	5000	600	238	2050	1060	1108	17	11.70	6.06	38	0.00	0.00	0.0000	28.00	0.000	10.2608	2.33
438683	4333348	G-01	5-may-09	12604	7.96	4580	560	191	1880	1070	882	14	7.00	4.29	47	0.00	0.00	0.0000	23.60	0.000	7.8610	1.29
438683	4333348	G-01	24-mar-10	16040	7.20	5340	860	243	2660	1290	1177	19	5.30	6.33	24	0.00	0.00	0.0000	21.60	0.000	11.1825	1.71
439548	4335023	G-02	17-jul-03	14004	7.10	3360	712	254	2920	897	1023	17	5.60		62	0.00	0.00	0.0000	32.10			
439548	4335023	G-02	28-jun-04	13794	7.30	3700	613	350	2200	932	904	27	10.30		43	0.76	0.00	0.0000	37.20			
439548	4335023	G-02	18-abr-06	13454	6.80	3840	742	238	3060	1120	876	16	5.90	5.56	76	0.00	0.49	0.0000	27.30	0.195	7.7332	1.50
439548	4335023	G-02	17-may-06	14994	6.99	3500	980	248	3240	1180	875	14	5.10	7.29	68	0.00	0.24	0.1338	29.20	0.196	9.2535	1.40
439548	4335023	G-02	20-jun-06	13334	6.98	2500	690	242	3250	1020	835	17	5.40	5.26	74	0.10	1.07	0.1338	29.80	0.206	5.4571	0.00
439548	4335023	G-02	24-jul-06	13193	6.85	3300	770	203	3200	1080	938	18	4.70	4.48	80	0.00	0.10	0.1338	30.40	0.000	8.6472	3.70
439548	4335023	G-02	29-ago-06	13413	7.62	3500	740	145	3160	1110	970	18	4.10	3.76	88	0.00	0.00	0.1204	26.50	0.000	7.2298	1.30
439548	4335023	G-02	18-sep-06	13444	6.75	3410	740	191	3050	1090	918	16	5.90	3.88	92	0.00	0.00	0.2141	31.40	0.192	8.7883	1.18
439548	4335023	G-02	17-nov-06	13563	7.09	3500	710	169	3020	1070	906	14	4.20	4.19	70	0.00	0.00	0.1740	32.50	0.156	8.6060	2.63
439548	4335023	G-02	14-dic-06	13393	7.09	3480	710	176	3000	1080	902	15	4.20	4.79	68	0.00	0.00	0.0000	29.00	0.155	9.2616	0.42
439548	4335023	G-02	19-ene-07	13123	7.05	3540	680	194	3060	1040	914	15	3.70	4.60	64	0.00	0.00	0.0000	33.50	0.000	10.6366	1.28
439548	4335023	G-02	21-feb-07	12233	6.85	3510	690	169	2820	1010	914	14	8.50	3.75	68	0.00	0.00	0.3212	32.30	0.244	7.1487	1.68
439548	4335023	G-02	21-mar-07	13884	6.96	3720	670	164	2960	1040	940	14	7.80	3.79	68	0.00	0.00	0.0000	32.80	0.000	6.0560	1.39
439548	4335023	G-02	18-abr-07	12534	7.31	3300	620	176	2880	1060	972	13	10.90	3.87	66	0.00	0.00	0.0937	31.10	0.000	5.3000	4.32
439548	4335023	G-02	29-may-07	13275	6.94	3450	700	172	3200	1140	979	17	9.30	3.64	64	0.00	0.18	0.0000	30.00	0.000	7.3040	3.14
439548	4335023	G-02	10-jul-07	15114	7.07	3780	740	226	3320	1140	960	16		3.38	72	0.00	0.08	0.1740	31.80	0.679	8.2251	2.64
439548	4335023	G-02	8-ago-07	13443	7.32	3740	710	206	3200	1160	1031	17	12.50	7.37	66	0.00	0.00	0.1740	32.20	0.000	8.0498	3.66
439548	4335023	G-02	13-sep-07	13923	7.33	3780	830	204	3140	1110	998	16	9.30	5.25	78	0.00	0.00	0.1606	32.80	0.000	7.7029	2.72
439548	4335023	G-02	9-oct-07	13523	7.25	3720	810	210	3100	1080	1002	18	10.90	4.92	74	0.00	0.00	0.0937	32.20	0.233	11.0966	1.95
439548	4335023	G-02	27-nov-07	13774	7.11	3620	800	195	3080	1100	989	15	10.10	4.70	47	0.00	0.00	0.1472	31.50	0.236	7.5291	3.62
439548	4335023	G-02	27-dic-07	13854	7.20	3600	720	188	3080	1060	1067	15	12.50	5.06	59	0.00	0.00	0.1472	34.20	0.000	10.0001	1.95
439548	4335023	G-02	23-ene-08	14154	7.87	3500	730	145	3550	1140	1010	13		3.58	70	0.00	0.00	0.0000	28.80	0.000	11.3456	2.19
439548	4335023	G-02	22-feb-08	13873	7.06	3360	660	137	3240	1060	928	13		3.57	68	0.00	0.00	0.1071	28.80	0.141	7.4872	2.86

X (UTM)	Y (UTM)	Monitoring point	Date	µS cm^{-1}		mg l^{-1}	mg l^{-1}	mg l^{-1}	mg l^{-1}	mg l^{-1}	mg l^{-1}	mg l^{-1}	mg l^{-1}	mg l^{-1}	mg l^{-1}	mg l^{-1}	mg l^{-1}	mg l^{-1}	mg l^{-1}	mg l^{-1}	mg l^{-1}	mg l^{-1}
				EC	pH	SO4	Ca	HCO3	Cl	Mg	Na	K	DQO	TOC	NO3	NO2	NH4	PO4	SiO2	B	Br	N org
439548	4335023	G-02	11-mar-08	14123	7.28	3600	760	145	3400	1200	979	15		4.64	60	0.00	0.00	0.0000	28.20	0.000	12.3045	2.24
439548	4335023	G-02	23-abr-08	14103	7.46	3550	720	185	3360	1220	972	14		5.76	60	0.00	0.00	0.1338	31.70	0.311	9.9507	2.29
439548	4335023	G-02	27-may-08	14113	7.92	3400	760	188	3200	1090	911	16	7.80	3.59	64	0.00	0.00	0.0000	34.20	0.000	9.7356	2.18
439548	4335023	G-02	23-jun-08	14193	7.83	3600	800	214	3260	1100	973	17	10.10	3.91	1	0.00	0.00	0.0000	42.20	0.000	9.7360	2.16
439548	4335023	G-02	21-jul-08	13973	7.70	3500	650	206	3100	1040	1013	16		3.88	64	0.00	0.00	0.0800	53.80	0.000	8.1840	1.62
439548	4335023	G-02	25-ago-08	13665	7.61	3600	620	147	2900	1060	994	15	8.50	29.75	64	0.00	0.00	0.0800	39.10	0.000	8.8369	1.28
439548	4335023	G-02	17-sep-08	13703	7.47	3400	600	183	3060	1070	1079	15		3.62	64	0.00	0.00	0.0800	40.30	0.000	7.9342	2.27
439548	4335023	G-02	5-may-09	14044	7.92	3420	630	159	2790	1080	917	14	9.30	3.40	63	0.00	0.00	0.0000	38.90	0.000	8.4420	3.03
442746	4335905	G-03	17-may-06	3024	6.32	592	250	221	570	114	268	15	1.50	3.32	33	0.00	0.29	1.8734	16.10	0.063	3.0171	3.31
442746	4335905	G-03	19-ene-07	9583	6.55	2200	590	476	1520	498	487	25	3.60	5.49	4	0.00	0.00	0.1472	51.40	0.000	1.5144	1.00
442746	4335905	G-03	28-may-07	9725	6.65	2300	560	480	1830	530	883	39	7.00	2.93	3	0.00	0.00	0.0000	54.60	0.337	3.4830	4.04
442746	4335905	G-03	26-nov-07	10924	6.76	2640	780	810	2080	570	1026	42	9.30	3.31	3	0.00	0.00	0.0803	56.20	0.346	4.2018	1.95
442746	4335905	G-03	27-may-08	10543	7.30	2800	640	354	1970	510	1012	41	7.00	1.83	4	0.00	0.00	0.0000	62.00	0.000	4.4360	2.58
442746	4335905	G-03	5-may-09	10514	7.54	2480	640	380	1890	500	981	40	6.20	1.85	4	0.00	0.00	0.0000	79.40	0.000	4.0010	2.14
442746	4335905	G-03	24-mar-10	5770	7.07	1990	690	221	970	268	364	26	2.70	3.18	70	0.00	0.00	0.0000	58.90	0.000	2.3487	2.14
439965	4332815	G-04	17-jul-03	6134	7.20	1960	490	310	576	314	343	12	5.30		0	0.00	0.17	0.0000	33.40			
439965	4332815	G-04	28-jun-04	4004	7.70	1200	352	360	360	169	154	6	11.40		5	0.00	0.00	0.0000	57.00			
439965	4332815	G-04	18-abr-06	8484	6.74	3180	680	360	1050	556	435	16	6.70	8.60	1	0.00	0.00	0.0000	36.90	0.176	3.3146	3.00
439965	4332815	G-04	16-may-06	8494	6.86	2540	722	342	1140	434	453	14	5.60	10.67	0	0.00	0.00	0.0937	37.00	0.199	3.2717	2.00
439965	4332815	G-04	20-jun-06	8724	6.74	3000	680	288	1140	590	413	16	6.80	10.40	4	0.00	0.00	0.1740	35.40	0.183	1.9457	0.00
439965	4332815	G-04	24-jul-06	8613	7.01	2960	610	310	1340	660	433	17	5.50	8.59	5	0.00	0.00	0.0000	35.80	0.000	2.8465	2.70
439965	4332815	G-04	29-ago-06	9453	7.33	3300	670	215	1430	700	508	19	5.70	8.50	1	0.00	0.00	0.0000	36.50	0.179	4.1274	1.10
439965	4332815	G-04	18-sep-06	9474	6.65	3200	720	366	1470	720	430	19	6.30	8.86	1	0.00	0.00	0.0000	37.00	0.174	3.5512	1.57
439965	4332815	G-04	17-nov-06	10673	6.85	3520	620	183	1660	780	526	20	7.00	9.82	1	0.00	0.00	0.0803	35.80	0.159	5.0919	1.73
439965	4332815	G-04	15-dic-06	10933	6.89	3720	670	216	1690	790	540	22	6.30	50.18	1	0.00	0.00	0.0803	32.80	0.150	5.0763	0.21
439965	4332815	G-04	18-ene-07	10983	6.84	3700	690	276	1710	810	773	22	6.50	10.15	0	0.00	0.00	0.1472	37.30	0.000	4.6713	0.64
439965	4332815	G-04	21-feb-07	11853	6.80	4150	650	416	2010	920	995	30	10.10	11.08	1	0.00	0.40	0.2542	37.40	0.244	3.1761	1.31
439965	4332815	G-04	20-mar-07	11654	6.68	4140	620	348	1740	880	778	22	11.70	10.90	1	0.00	0.10	0.1338	36.50	0.000	2.3978	1.44
439965	4332815	G-04	17-abr-07	10244	7.26	3650	630	390	1690	830	825	22	11.70	10.88	0	0.00	0.00	0.1204	35.00	0.000	2.2800	3.86
439965	4332815	G-04	30-may-07	11055	6.64	4050	740	376	1750	860	827	26	13.20	9.19	0	0.00	0.00	0.1204	35.10	0.214	4.1620	2.24
439965	4332815	G-04	27-jun-07	10355	7.49	3080	730	340	1740	760	547	22	11.70	6.46	0	0.00	0.00	0.1071	34.60	0.000	4.7941	2.38
439965	4332815	G-04	8-ago-07	8073	7.26	2900	590	320	1180	600	485	18	6.80	11.35	2	0.00	0.00	0.1070	35.50	0.000	2.6102	2.64
439965	4332815	G-04	13-sep-07	10683	7.30	3400	760	384	1630	690	752	21	11.70	10.43	2	0.00	0.00	0.1204	36.50	0.000	4.7121	2.87
439965	4332815	G-04	9-oct-07	9863	7.08	3300	696	374	1610	690	788	22	11.70	11.39	1	0.00	0.00	0.0000	35.50	0.000	4.4422	2.09

X (UTM)	Y (UTM)	Monitoring point	Date	µS cm^{-1}		mg l^{-1}	mg l^{-1}	mg l^{-1}	mg l^{-1}	mg l^{-1}	mg l^{-1}	mg l^{-1}	mg l^{-1}	mg l^{-1}	mg l^{-1}	mg l^{-1}	mg l^{-1}	mg l^{-1}	mg l^{-1}	mg l^{-1}	mg l^{-1}	mg l^{-1}
				EC	pH	SO4	Ca	HCO3	Cl	Mg	Na	K	DQO	TOC	NO3	NO2	NH4	PO4	SiO2	B	Br	N org
439965	4332815	G-04	21-nov-07	9454	6.97	3160	690	368	1550	650	736	20	12.50	13.10	2	0.00	0.00	0.1338	35.50	0.265	3.2019	4.15
439965	4332815	G-04	26-dic-07	10074	6.91	3180	670	360	1520	650	761	21	13.20	12.44	3	0.00	0.00	0.1204	36.70	0.000	3.9141	2.23
439965	4332815	G-04	21-ene-08	10664	7.38	3550	650	193	1780	760	800	22	13.20	10.69	1	0.00	0.00	0.1204	31.30	0.000	5.2988	0.73
439965	4332815	G-04	22-feb-08	10903	7.08	3560	620	190	1750	780	796	21	14.00	10.56	2	0.00	0.00	0.0000	32.20	0.176	4.1424	2.14
439965	4332815	G-04	11-mar-08	10503	7.18	3600	660	183	1750	710	780	21	12.50	11.26	1	0.00	0.00	0.0000	31.80	0.000	4.5578	2.99
439965	4332815	G-04	23-abr-08	11433	7.48	3500	620	224	1860	790	869	22	9.30	11.20	0	0.00	0.00	0.0000	32.60	0.000	4.8692	5.00
439965	4332815	G-04	28-may-08	11853	7.78	3600	650	238	1860	770	955	27	9.30	8.21	1	0.00	0.00	0.0000	38.00	0.000	5.1728	2.90
439965	4332815	G-04	23-jun-08	10973	7.66	3300	700	262	1810	710	807	21	12.50	10.80	1	0.00	0.90	0.0000	42.80	0.000	4.5338	2.74
439965	4332815	G-04	21-jul-08	10793	7.67	3300	630	279	1750	740	800	19	12.50	10.24	1	0.00	0.00	0.0000	41.50	0.000	3.3648	1.91
439965	4332815	G-04	25-ago-08	11135	7.59	3300	550	252	1730	760	855	21	10.10	6.04	1	0.00	0.00	0.0000	42.20	0.000	4.6382	2.47
439965	4332815	G-04	16-sep-08	11303	7.43	3700	600	292	1750	830	872	21	13.20	11.22	0	0.00	0.00	0.0000	44.30	0.000	4.2534	1.42
439965	4332815	G-04	5-may-09	13174	7.80	3980	690	307	2140	950	974	24	5.40	11.27	0	0.00	0.00	0.0000	41.70	0.000	5.1318	3.03
439965	4332815	G-04	24-mar-10	3690	7.45	1380	292	520	480	218	472	15	7.10	8.51	9	0.40	0.00	0.0000	63.00	0.000	1.1378	2.86
439758	4332389	G-05	17-may-06	12494	6.95	3660	760	396	2260	880	902	25	8.70	10.38	1	0.00	0.00	0.1204	28.50	0.201	5.7959	1.55
439758	4332389	G-05	18-ene-07	11923	7.13	3980	500	250	2020	970	964	23	6.80	3.21	1	0.00	0.00	0.0000	27.80	0.000	0.6987	1.00
439758	4332389	G-05	30-may-07	12995	7.21	3900	570	272	2060	930	896	23	12.50	8.81	1	0.00	0.00	0.0000	27.60	0.217	4.2850	4.64
439758	4332389	G-05	21-nov-07	13284	7.22	3760	650	408	2090	790	1137	26	14.80	14.23	0	0.00	0.00	0.1338	30.80	0.227	4.1256	4.15
439758	4332389	G-05	28-may-08	12363	7.97	3800	640	252	2180	850	981	23	11.70	9.18	0	0.00	0.00	0.0000	40.60	0.000	5.7916	3.92
439758	4332389	G-05	4-may-09	12704	7.91	4220	650	95	2040	960	991	22	7.00	10.60	3	0.00	0.00	0.0000	36.10	0.000	5.1620	2.16
439758	4332389	G-05	24-mar-10	3690	7.38	1422	380	241	260	212	142	6	7.50	8.09	6	0.00	0.00	0.0000	32.60	0.000	0.8731	1.71
439905	4332335	G-06	17-jul-03	10854	7.10	3280	610	360	1690	690	876	21	5.30		4	0.00	0.00	0.0000	24.20			
439905	4332335	G-06	28-jun-04	10774	7.50	3500	594	380	1820	695	889	23	6.70		0	0.00	0.00	0.0000	25.20			
439905	4332335	G-06	18-abr-06	11914	6.83	3900	666	476	2020	860	883	20	8.80	12.90	1	0.20	0.11	0.0000	32.70	0.173	7.2289	1.80
439905	4332335	G-06	17-may-06	10484	7.27	2840	698	372	1840	633	782	17	4.70	9.01	6	0.00	0.00	0.0937	21.60	0.173	5.5615	2.00
439905	4332335	G-06	20-jun-06	10124	6.97	2960	610	270	1680	690	715	19	6.10	7.42	13	0.00	0.00	0.1204	23.70	0.201	2.7876	0.00
439905	4332335	G-06	24-jul-06	9573	7.14	3180	590	352	1630	628	742	20	4.30	6.44	24	0.00	0.00	0.0000	22.20	0.000	4.3428	2.30
439905	4332335	G-06	29-ago-06	9573	7.69	3000	550	252	1600	710	551	19	3.90	5.62	18	0.00	0.00	0.0000	21.40	0.141	3.2029	0.64
439905	4332335	G-06	18-sep-06	9454	6.80	2950	590	366	1550	700	462	19	4.30	5.60	18	0.00	0.00	0.0000	23.80	0.164	3.5938	0.59
439905	4332335	G-06	17-nov-06	9683	7.03	3010	540	201	1510	660	512	18	4.00	6.52	21	0.00	0.00	0.0000	24.20	0.140	3.6197	1.94
439905	4332335	G-06	15-dic-06	9423	7.09	2990	400	203	1490	690	714	20	4.30	6.34	22	0.00	0.00	0.0000	21.70	0.143	3.9736	0.42
439905	4332335	G-06	18-ene-07	9463	7.15	3200	440	232	1540	760	754	19	4.10	6.59	20	0.00	0.00	0.0000	24.40	0.000	3.0762	0.86
439905	4332335	G-06	21-feb-07	9033	7.08	3120	370	297	1510	770	752	21	10.10	6.93	21	0.00	0.00	0.0000	23.50	0.239	2.3576	1.38
439905	4332335	G-06	20-mar-07	10354	7.03	3340	500	334	1620	730	738	19	9.30	6.64	11	0.00	0.00	0.0000	22.60	0.000	3.0451	0.72
439905	4332335	G-06	17-abr-07	9834	7.47	3320	510	348	1590	750	874	21	9.30	7.12	6	0.00	0.00	0.0000	21.70	0.000	3.6900	3.86

X (UTM)	Y (UTM)	Monitoring point	Date	µS cm^{-1}		mg l^{-1}	mg l^{-1}	mg l^{-1}	mg l^{-1}	mg l^{-1}	mg l^{-1}	mg l^{-1}	mg l^{-1}	mg l^{-1}	mg l^{-1}	mg l^{-1}	mg l^{-1}	mg l^{-1}	mg l^{-1}	mg l^{-1}	mg l^{-1}	mg l^{-1}
				EC	pH	SO4	Ca	HCO3	Cl	Mg	Na	K	DQO	TOC	NO3	NO2	NH4	PO4	SiO2	B	Br	N org
439905	4332335	G-06	30-may-07	10515	7.16	3300	560	320	1780	860	856	23	10.10	6.51	4	0.00	0.00	0.0000	21.70	0.000	4.0650	2.39
439905	4332335	G-06	27-jun-07	11065	7.71	3320	590	342	1850	800	828	21	9.30	6.61	5	0.00	0.00	0.0000	21.30	0.000	4.5673	2.23
439905	4332335	G-06	8-ago-07	10633	7.40	3660	530	346	1770	830	926	24	5.40	12.97	4	0.00	0.00	0.0937	23.10	0.000	4.4992	3.08
439905	4332335	G-06	13-sep-07	10883	7.36	3350	590	340	1960	800	909	22	12.50	9.01	5	0.00	0.00	0.1071	24.00	0.000	4.7660	2.57
439905	4332335	G-06	9-oct-07	10833	7.32	3300	550	350	1930	820	915	23	10.10	8.41	4	0.00	0.00	0.1071	21.60	0.000	3.6811	1.81
439905	4332335	G-06	21-nov-07	11234	7.16	3460	560	364	1890	810	977	23	12.50	11.36	6	0.00	0.00	0.1204	23.00	0.231	3.7095	3.55
439905	4332335	G-06	26-dic-07	11154	7.21	3410	620	362	1920	780	963	24	14.80	10.61	3	0.00	0.00	0.1071	22.00	0.000	5.0117	2.79
439905	4332335	G-06	21-ene-08	11174	7.62	3510	580	281	1940	800	948	23	13.20	7.32	3	0.00	0.00	0.0000	19.30	0.000	5.9675	3.06
439905	4332335	G-06	22-feb-08	10993	7.25	3340	580	256	1920	800	853	20	13.20	7.38	4	0.00	0.00	0.0000	20.80	0.128	4.8813	4.14
439905	4332335	G-06	11-mar-08	11273	7.57	3560	580	277	1940	790	906	22	7.00	8.06	4	0.00	0.00	0.0000	20.20	0.000	5.3560	2.54
439905	4332335	G-06	23-abr-08	11363	7.51	3500	570	252	1950	800	919	22	7.80	7.52	2	0.00	0.00	0.0000	23.10	0.000	6.0477	2.29
439905	4332335	G-06	28-may-08	12143	7.84	3700	610	246	2040	810	926	20	8.50	10.27	2	0.00	0.00	0.0000	28.30	0.000	5.8660	3.05
439905	4332335	G-06	23-jun-08	11143	7.74	3600	600	272	1900	800	884	21	11.70	10.06	2	0.00	0.00	0.0000	32.60	0.000	5.0227	2.60
439905	4332335	G-06	21-jul-08	10823	7.70	3300	540	248	1950	790	952	19	12.50	6.55	8	0.00	0.00	0.0000	31.00	0.000	5.5846	1.91
439905	4332335	G-06	25-ago-08	10025	7.69	3300	530	220	1670	750	839	18	8.50	3.50	15	0.00	0.00	0.0000	33.20	0.000	4.0595	1.56
439905	4332335	G-06	16-sep-08	10243	7.55	3200	510	266	1700	720	893	18	9.30	5.97	17	0.00	0.00	0.0000	32.60	0.000	4.3357	1.56
439905	4332335	G-06	4-may-09	10294	7.79	3200	560	263	1840	790	823	21	7.00	6.30	20	0.00	0.00	0.0000	33.20	0.000	4.1790	1.59
439905	4332335	G-06	24-mar-10	11500	7.10	3460	640	420	1880	850	834	20	9.20	8.42	2	0.00	0.00	0.0000	30.20	0.000	5.2642	3.00
440278	4331730	G-07	17-sep-08	2563	7.53	730	220	236	172	108	116	7	1.30	1.13	20	0.00	0.00	0.0000	26.50	0.000	0.6359	1.73
438757	4331250	G-08	18-ene-07	3333	7.24	1180	342	192	213	156	121	5	3.20	15.97	1	0.00	0.00	0.0000	21.10	0.000	3.9720	1.00
438757	4331250	G-08	30-may-07	3455	7.26	1140	322	190	220	164	115	4	3.20	3.34	7	0.00	0.00	0.0000	26.30	0.201	1.0280	1.94
438757	4331250	G-08	21-nov-07	3904	7.20	980	300	259	266	164	124	5	2.80	6.81	14	0.00	0.00	0.0000	27.70	0.230	1.1281	5.33
438757	4331250	G-08	28-may-08	3553	7.80	1160	260	156	246	180	125	4	2.10	3.15	18	0.00	0.00	0.0000	34.70	0.000	1.1414	4.06
438757	4331250	G-08	4-may-09	3924	7.64	1250	390	139	330	182	124	5	2.60	3.63	38	0.00	0.00	0.0000	35.00	0.000	1.2110	1.73
436366	4330245	G-09	16-may-06	1713	7.52	360	152	19	480	121	100	9	2.40	3.78	1	0.00	0.27	0.0000	0.60	0.000	2.6037	0.86
436366	4330245	G-09	17-ene-07	1692	7.15	342	124	33	366	92	104	8	2.50	20.16	0	0.00	0.70	0.0000	0.10	0.000	2.2826	2.80
436366	4330245	G-09	30-may-07	1768	7.10	336	122	32	414	110	101	8	2.50	2.12	0	0.00	0.30	0.0000	0.10	0.051	2.7070	2.24
436366	4330245	G-09	21-nov-07	2334	7.12	390	152	30	462	111	132	5	3.40	5.07	0	0.00	1.20	0.0000	0.10	0.000	2.7550	3.26
436366	4330245	G-09	28-may-08	2403	7.52	448	186	15	534	108	133	6	10.90	2.32	0	0.00	1.20	0.0000	0.10	0.000	3.0083	3.19
436366	4330245	G-09	4-may-09	3094	7.70	610	220	121	440	126	122	7	3.40	2.96	64	0.00	0.00	0.0000	0.30	0.000	2.6100	2.02
436366	4330245	G-09	24-mar-10	2530	5.22	628	252	13	512	113	111	4	3.50	2.86	1	0.00	2.00	0.0000	0.10	0.000	2.5898	1.57
434352	4329680	G-10	16-may-06	4494	6.82	1460	529	364	530	236	169	15	5.10	4.49	23	1.72	0.21	0.2542	30.00	0.159	2.8343	0.00
434352	4329680	G-10	24-jul-06	4083	6.87	1210	400	370	528	206	162	12	3.20	4.22	8	0.00	0.00	0.1204	33.00	0.148	2.2077	0.64
434352	4329680	G-10	29-ago-06	4123	7.42	1170	392	306	480	208	164	10	3.40	4.08	7	0.00	0.00	0.0803	31.50	0.000	2.6981	0.39

X (UTM)	Y (UTM)	Monitoring point	Date	µS cm^{-1}		mg l^{-1}	mg l^{-1}	mg l^{-1}	mg l^{-1}	mg l^{-1}	mg l^{-1}	mg l^{-1}	mg l^{-1}	mg l^{-1}	mg l^{-1}	mg l^{-1}	mg l^{-1}	mg l^{-1}	mg l^{-1}	mg l^{-1}	mg l^{-1}	mg l^{-1}
				EC	pH	SO4	Ca	HCO3	Cl	Mg	Na	K	DQO	TOC	NO3	NO2	NH4	PO4	SiO2	B	Br	N org
434352	4329680	G-10	18-sep-06	4144	6.54	1070	408	404	512	216	150	9	3.60	4.55	5	0.00	0.00	0.1472	33.10	0.000	2.3785	0.22
434352	4329680	G-10	16-nov-06	4193	6.86	1210	380	114	504	208	157	9	3.20	4.36	9	0.00	0.00	0.0000	35.10	0.132	2.1188	0.63
434352	4329680	G-10	12-dic-06	4193	6.82	1230	376	234	452	196	170	12	2.50	4.12	4	0.00	0.00	0.0000	34.20	0.135	3.1175	0.86
434352	4329680	G-10	17-ene-07	4033	6.84	1224	396	267	456	204	159	8	3.00	4.25	4	0.00	0.00	0.0000	36.30	0.000	1.8610	1.24
434352	4329680	G-10	20-feb-07	3943	6.54	1200	376	370	432	200	163	9	3.70	4.24	5	0.00	0.00	0.0000	33.80	0.283	1.6142	23.50
434352	4329680	G-10	21-mar-07	4114	6.57	1214	404	416	428	192	166	9	19.50	4.08	5	0.00	0.00	0.0000	35.30	0.109	1.4600	1.70
434352	4329680	G-10	17-abr-07	3864	7.39	1150	416	404	436	200	170	8	3.60	4.47	3	0.00	0.15	0.0669	33.70	0.000	1.0548	1.28
434352	4329680	G-10	30-may-07	4015	7.03	1120	376	339	432	196	161	9	3.70	3.29	3	0.00	0.00	0.0000	33.80	0.207	2.0690	2.39
434352	4329680	G-10	10-jul-07	4194	6.85	1170	430	426	482	200	154	9	6.70	6.12	3	0.00	0.12	0.2007	34.50	0.388	2.1628	2.49
434352	4329680	G-10	23-ago-07	4264	6.95	1220	444	416	462	206	178	10	3.20	5.38	9	0.00	0.00	0.2810	33.90	0.000	2.0176	5.74
434352	4329680	G-10	13-sep-07	4383	7.05	1250	470	492	472	184	189	12	3.10	4.73	5	0.00	0.00	0.2944	39.70	0.000	3.9910	4.84
434352	4329680	G-10	9-oct-07	4163	7.08	1180	472	498	470	180	222	13	3.20	4.16	6	0.00	0.00	0.2542	38.80	0.637	2.9818	16.03
434352	4329680	G-10	22-nov-07	4594	6.85	1192	460	494	464	188	208	12	6.10	6.99	4	0.00	0.00	0.2007	38.70	0.225	1.2869	2.37
434352	4329680	G-10	27-dic-07	4344	6.71	1180	456	484	460	172	243	13	4.00	5.50	6	0.00	0.00	0.1873	40.10	0.000	2.5863	2.51
434352	4329680	G-10	22-ene-08	4354	7.38	1030	376	383	480	190	186	13	3.70	4.49	6	0.00	0.00	0.0000	34.50	0.000	2.4096	0.87
434352	4329680	G-10	22-feb-08	4333	6.94	1020	346	341	480	192	178	13	3.60	4.41	10	0.00	0.00	0.0000	35.60	0.117	2.2951	7.00
434352	4329680	G-10	11-mar-08	4473	6.78	1020	362	362	500	184	195	14	3.20	5.72	8	0.00	0.00	0.0000	35.10	0.000	3.0308	3.59
434352	4329680	G-10	24-abr-08	4383	7.37	1090	370	340	510	190	197	13	3.70	9.51	9	0.00	0.00	0.0000	41.20	0.000	3.2626	1.43
434352	4329680	G-10	28-may-08	4203	7.55	1120	380	260	530	180	197	13	2.80	2.89	6	0.00	0.00	0.0000	40.20	0.000	2.4913	3.77
434352	4329680	G-10	23-jun-08	4273	7.37	1220	390	290	500	186	198	13	13.20	5.21	5	0.00	0.00	0.0000	51.20	0.000	2.4727	2.19
434352	4329680	G-10	21-jul-08	4723	7.49	1090	380	330	480	180	198	11	3.10	3.53	4	0.00	0.00	0.0000	51.60	0.000	3.0151	1.47
434352	4329680	G-10	25-ago-08	4475	7.54	1080	340	235	470	190	197	11	2.90	0.00	6	0.00	0.00	0.0000	51.00	0.000	3.5419	1.85
434352	4329680	G-10	16-sep-08	4363	7.41	1200	350	360	430	200	255	11	2.30	2.81	5	0.00	0.00	0.0000	51.00	0.000	2.4782	1.88
434352	4329680	G-10	4-may-09	4354	7.53	1230	440	244	530	200	186	15	2.80	3.22	8	0.00	0.00	0.0000	50.00	0.000	2.2852	1.88
434352	4329680	G-10	24-mar-10	4450	6.65	1360	510	532	524	240	195	12	3.50	3.24	3	0.00	0.00	0.0000	46.70	0.000	2.5746	2.29
434350	4329683	G-11	18-abr-06	6234	6.60	2280	708	380	500	320	184	14	13.40	17.40	1	0.18	4.00	0.0000	48.00	0.229	3.1975	1.70
434350	4329683	G-11	16-may-06	6474	6.73	1960	809	384	560	204	247	12	22.80	31.82	1	5.00	1.68	0.0803	47.70	0.239	2.7944	1.80
434350	4329683	G-11	20-jun-06	6624	6.63	2450	766	328	544	344	197	15	14.20	25.08	22	6.80	0.12	0.1071	48.10	0.239	2.1638	5.20
434350	4329683	G-11	24-jul-06	6743	6.79	2760	780	352	620	396	264	16	14.70	22.86	18	9.20	0.00	0.0669	50.20	0.000	3.0186	2.10
434350	4329683	G-11	29-ago-06	7043	7.20	2950	740	228	610	440	274	19	38.30	23.95	28	0.00	0.00	0.0000	45.10	0.201	2.9732	1.30
434350	4329683	G-11	18-sep-06	6854	6.50	2800	780	400	612	384	193	18	31.30	26.91	30	0.00	0.00	0.0000	46.50	0.231	4.5959	7.06
434350	4329683	G-11	16-nov-06	7013	6.78	2850	770	179	616	368	198	20	25.70	29.14	28	0.00	0.00	0.0000	39.00	0.219	5.4345	1.51
434350	4329683	G-11	12-dic-06	7023	6.80	2720	710	320	616	384	285	23	12.60	28.72	28	0.00	0.00	0.0000	36.80	0.205	3.4568	0.21
434350	4329683	G-11	17-ene-07	7013	6.62	2830	740	268	620	394	291	22	26.00	27.24	29	0.00	0.00	0.0000	40.10	0.254	3.6415	1.50

X (UTM)	Y (UTM)	Monitoring point	Date	µS cm^{-1}		mg l^{-1}	mg l^{-1}	mg l^{-1}	mg l^{-1}	mg l^{-1}	mg l^{-1}	mg l^{-1}	mg l^{-1}	mg l^{-1}	mg l^{-1}	mg l^{-1}	mg l^{-1}	mg l^{-1}	mg l^{-1}	mg l^{-1}	mg l^{-1}	mg l^{-1}
				EC	pH	SO4	Ca	HCO3	Cl	Mg	Na	K	DQO	TOC	NO3	NO2	NH4	PO4	SiO2	B	Br	N org
434350	4329683	G-11	21-feb-07	6673	6.45	2710	710	320	636	356	288	22	23.80	30.21	25	0.00	0.00	0.2141	37.30	0.325	2.4562	1.96
434350	4329683	G-11	21-mar-07	7304	6.49	2890	780	396	644	360	290	22	24.10	30.50	20	0.00	0.00	0.0937	39.10	0.226	2.4493	6.49
434350	4329683	G-11	17-abr-07	7164	6.92	2680	750	398	664	408	317	23	22.20	31.41	27	0.00	0.00	0.0937	34.80	0.208	2.2200	7.88
434350	4329683	G-11	30-may-07	7795	6.75	2900	840	382	760	450	298	21	22.80	20.31	21	0.00	0.00	0.1071	34.30	0.270	4.0050	6.13
434350	4329683	G-11	10-jul-07	7594	6.80	2980	850	592	790	444	285	23	26.30	28.19	6	16.00	0.20	0.0937	43.10	0.535	3.9552	9.38
434350	4329683	G-11	8-ago-07	7173	6.86	2870	870	444	740	424	317	23	21.90	40.40	29	0.00	0.00	0.0000	41.50	0.000	6.6732	10.11
434350	4329683	G-11	13-sep-07	7283	6.80	3000	860	420	820	432	324	22	23.10	35.78	26	0.00	0.00	0.0000	40.10	0.241	5.2395	9.82
434350	4329683	G-11	9-oct-07	7173	6.82	2760	840	412	800	404	326	23	25.00	35.88	27	0.00	0.00	0.0000	41.30	0.000	4.3231	10.45
434350	4329683	G-11	22-nov-07	7314	6.70	2800	840	486	780	400	334	23	25.70	36.81	31	0.00	0.00	0.0000	41.90	0.300	3.5888	10.36
434350	4329683	G-11	27-dic-07	6944	6.73	2620	780	460	700	380	328	23	25.00	35.63	36	0.00	0.00	0.0000	42.50	0.204	3.9487	15.75
434350	4329683	G-11	22-ene-08	7004	7.10	2580	720	387	800	430	307	23	20.00	29.80	28	0.00	0.00	0.0000	39.40	0.232	5.0264	7.89
434350	4329683	G-11	22-feb-08	6953	6.76	2400	630	329	748	392	283	20	19.70	29.29	33	0.00	0.00	0.0000	43.50	0.204	3.9678	12.57
434350	4329683	G-11	11-mar-08	7183	7.74	2500	690	370	790	410	322	23	20.90	31.70	37	0.00	0.00	0.0000	42.30	0.000	5.4891	7.93
434350	4329683	G-11	24-abr-08	7133	7.28	2470	680	372	790	400	316	22	20.30	30.92	29	0.00	0.00	0.0000	48.80	0.218	5.3134	15.14
434350	4329683	G-11	28-may-08	6993	7.96	3100	750	152	740	410	297	21	18.10	25.81	34	0.00	0.00	0.0000	46.80	0.000	7.8794	12.33
434350	4329683	G-11	23-jun-08	7313	7.65	3100	810	170	760	440	323	22	24.70	30.83	30	0.00	0.00	0.0000	56.20	0.000	4.4033	9.09
434350	4329683	G-11	19-jul-08	7363	7.55	2900	750	390	710	400	348	19	20.90	30.23	28	0.00	0.00	0.0000	53.80	0.000	4.0896	13.25
434350	4329683	G-11	25-ago-08	7445	7.30	2600	700	242	700	390	318	19	20.00	3.00	27	0.00	0.00	0.0000	55.00	0.000	3.8304	11.23
434350	4329683	G-11	16-sep-08	7333	7.20	2700	760	380	740	410	361	19	20.60	30.92	37	0.00	0.00	0.0000	59.30	0.000	4.2563	1.85
434350	4329683	G-11	4-may-09	7274	7.76	2740	710	283	460	380	276	20	14.40	26.41	41	0.00	0.00	0.0000	78.60	0.199	3.7200	10.53
434350	4329683	G-11	24-mar-10	2440	7.14	960	334	180	132	95	83	8	6.10	7.23	21	0.00	0.00	0.0000	13.90	0.000	0.4185	2.14
436757	4331990	G-12	17-may-06	2384	6.84	380	174	630	228	136	132	9	1.10	1.04	7	0.00	0.00	0.0000	26.20	0.065	0.4911	0.43
436757	4331990	G-12	29-ago-06	1730	7.64	326	122	406	205	115	106	12	1.00	0.74	6	0.00	0.00	0.0000	26.30	0.000	0.5928	0.39
436757	4331990	G-12	18-sep-06	1783	6.50	330	124	414	208	117	101	12	1.10	1.09	5	0.00	0.00	0.0000	27.50	0.000	0.3990	0.21
436757	4331990	G-12	14-dic-06	1738	6.91	292	98	386	204	114	99	11	0.80	1.51	4	0.00	0.00	0.0000	26.00	0.054	0.4252	0.88
436757	4331990	G-12	19-ene-07	1665	6.85	282	102	440	198	120	101	11	1.10	0.86	4	0.00	0.00	0.0000	28.60	0.000	0.3548	0.95
436757	4331990	G-12	20-feb-07	1720	6.47	226	112	606	185	116	96	12	1.20	0.84	3	0.00	0.00	0.0000	27.20	0.072	0.2408	2.74
436757	4331990	G-12	21-mar-07	1686	6.51	209	114	568	171	111	99	12	0.70	0.77	2	0.00	0.00	0.0000	28.20	0.000	0.2000	1.54
436757	4331990	G-12	18-abr-07	1526	7.24	190	118	620	178	112	107	12	0.70		3	0.00	0.10	0.1338	27.30	0.000		
436757	4331990	G-12	30-may-07	2625	7.04	420	98	420	286	160	146	9	1.10	1.29	7	0.00	0.00	0.0000	26.80	0.000	0.6450	1.50
436757	4331990	G-12	10-jul-07	1675	6.80	220	148	612	213	112	98	12	1.80	1.55	4	0.00	0.00	0.2141	27.80	0.090	0.5405	2.05
436757	4331990	G-12	23-ago-07	1750	6.96	260	152	608	204	116	110	12	0.70	1.78	5	0.00	0.00	0.2141	27.50	0.000	0.4499	1.51
436757	4331990	G-12	13-sep-07	1722	7.15	266	156	628	206	118	109	11	0.80	1.43	4	0.00	0.00	0.1740	28.10	0.000	0.5436	3.02
436757	4331990	G-12	9-oct-07	1715	7.05	270	158	628	210	119	114	12	0.50	1.56	4	0.00	0.00	0.2141	27.10	0.000	0.5633	3.34

X (UTM)	Y (UTM)	Monitoring point	Date	µS cm^{-1}		mg l^{-1}	mg l^{-1}	mg l^{-1}	mg l^{-1}	mg l^{-1}	mg l^{-1}	mg l^{-1}	mg l^{-1}	mg l^{-1}	mg l^{-1}	mg l^{-1}	mg l^{-1}	mg l^{-1}	mg l^{-1}	mg l^{-1}	mg l^{-1}	mg l^{-1}
				EC	pH	SO4	Ca	HCO3	Cl	Mg	Na	K	DQO	TOC	NO3	NO2	NH4	PO4	SiO2	B	Br	N org
436757	4331990	G-12	27-nov-07	1754	7.26	264	148	610	193	116	111	11	1.20	1.44	3	0.00	0.00	0.0000	27.50	0.072	0.5459	2.09
436757	4331990	G-12	27-dic-07	1726	6.92	270	145	590	194	114	112	11	0.90	1.44	4	0.00	0.00	0.0000	28.10	0.000	0.5251	3.07
436757	4331990	G-12	23-ene-08	1693	7.39	263	150	566	201	105	107	11	0.90	0.62	3	0.00	0.00	0.0000	24.20	0.000	0.8378	0.29
436757	4331990	G-12	22-feb-08	1673	7.05	245	138	522	198	102	94	10	0.70	0.61	4	0.00	0.00	0.0054	25.20	0.000	0.5033	4.00
436757	4331990	G-12	11-mar-08	1688	7.00	258	143	544	197	100	100	11	0.70	1.25	3	0.00	0.00	0.0000	24.60	0.000	0.6903	5.24
436757	4331990	G-12	23-abr-08	1340	7.38	260	126	452	196	102	100	11	1.00	1.31	2	0.00	0.00	0.0000	24.20	0.000	0.3661	1.86
436757	4331990	G-12	28-may-08	1497	7.85	221	66	388	182	104	99	11	0.90	0.00	2	0.00	0.00	0.0000	32.00	0.618	0.4704	1.15
436757	4331990	G-12	23-jun-08	1445	7.76	230	67	378	192	97	128	10	0.60	0.88	1	0.00	0.00	0.0000	35.10	0.000	0.4860	3.06
436757	4331990	G-12	21-jul-08	1463	7.65	220	61	376	188	105	112	10	0.70	0.00	3	0.00	0.00	0.0000	35.60	0.000	0.5699	1.91
436757	4331990	G-12	4-may-09	1484	7.94	244	94	440	178	110	96	11	0.70	0.00	4	0.00	0.00	0.0000	34.70	0.052	0.9499	1.57
436757	4331990	G-12	24-mar-10	5910	6.97	2520	630	279	540	378	305	10	2.60	4.96	2	0.00	0.00	0.0000	11.50	0.000	1.6649	2.00
440114	4337728	G-13	17-jul-03	4184	7.30	1240	429	193	352	170	133	9	1.60		36	0.00	0.00	0.0000	39.90			
440114	4337728	G-13	28-jun-04	5544	7.30	1860	631	200	560	213	173	13	2.80		16	0.31	0.00	0.0000	45.00			
440114	4337728	G-13	5-may-09	5444	7.93	1910	570	118	380	232	171	10	1.50	0.00	17	0.00	0.00	0.0000	59.40	0.000	2.0980	1.44
440114	4337728	G-13	24-mar-10	3770	7.22	1450	460	167	360	200	144	5	1.50	0.76	40	0.00	0.00	0.0000	42.60	0.000	1.3885	1.00
446625	4338600	G-14	17-may-06	6314	6.75	2440	651	270	306	348	146	14	2.20	2.76	110	1.20	0.00	0.3078	29.70	0.188	0.9953	0.88
446625	4338600	G-14	19-ene-07	4773	7.10	1930	492	256	284	240	169	13	2.20	8.84	80	0.00	0.00	0.6022	30.50	0.000	11.7008	1.00
446625	4338600	G-14	28-may-07	4895	7.10	2060	550	246	286	288	158	13	1.10	1.48	48	0.00	0.00	0.0000	29.30	0.229	1.0240	1.94
446625	4338600	G-14	22-nov-07	5214	7.31	1930	436	249	197	304	157	15	1.90	4.40	96	0.00	0.00	0.0000	29.40	0.283	0.9220	5.03
446625	4338600	G-14	27-may-08	4913	8.00	2120	420	196	182	310	171	13	1.40	1.65	98	0.00	0.00	0.0000	38.60	0.247	1.2643	1.87
446625	4338600	G-14	4-may-09	5024	7.88	2080	440	175	242	330	165	15	1.60	1.84	120	0.00	0.00	0.0000	36.40	0.000	1.2330	1.29
446625	4338600	G-14	24-mar-10	6510	7.34	2500	600	233	370	390	247	35	9.70	16.62	330	0.17	0.00	0.3800	24.80	0.000	3.2808	1.00
443746	4333939	G-15	17-may-06	1432	7.36	464	208	175	185	86	8	0	0.80	2.53	30	0.00	0.00	0.0000	30.10	0.000	0.6554	2.65
443746	4333939	G-15	19-ene-07	1430	7.50	504	168	140	181	94	69	5	1.10	2.74	29	0.00	0.00	0.0000	32.30	0.000	1.2428	1.00
443746	4333939	G-15	28-may-07	1521	7.45	508	170	142	190	88	69	4	0.70	1.37	33	0.00	0.00	0.0000	30.10	0.550	0.7210	4.64
443746	4333939	G-15	26-nov-07	1600	7.36	508	188	155	203	88	77	4	1.40	3.45	39	0.00	0.00	0.0000	29.20	0.059	0.6984	2.37
443746	4333939	G-15	27-may-08	1659	7.90	570	216	173	194	87	76	7	1.80	1.65	32	0.00	0.00	0.0000	38.20	0.000	0.8348	2.44
443746	4333939	G-15	5-may-09	1574	8.05	540	182	106	188	88	76	4	0.70	0.95	31	0.00	0.00	0.0000	37.90	0.000	1.9740	1.15
443746	4333939	G-15	24-mar-10	1632	7.36	560	206	168	180	85	82	4	0.90	1.16	31	0.00	0.00	0.0000	33.90	0.000	0.8579	2.29
444180	4329090	G-17	16-may-06	2314	7.06	608	242	286	322	150	79	7	1.10	2.82	30	0.00	0.00	0.0000	28.90	0.116	1.1262	1.80
444180	4329090	G-17	18-ene-07	1356	7.20	312	154	194	186	78	47	5	0.60	1.59	37	0.00	0.00	0.0000	21.50	0.058	0.6019	1.07
444180	4329090	G-17	28-may-07	1695	7.22	420	166	193	239	102	69	6	1.30	2.02	31	0.00	0.00	0.0000	24.80	0.094	0.9000	1.65
444180	4329090	G-17	26-nov-07	1796	7.45	432	188	238	272	112	76	6	1.10	1.61	32	0.00	0.00	0.0000	25.30	0.109	0.8227	1.81
444180	4329090	G-17	27-may-08	1244	7.91	306	132	122	162	59	45	4	0.90	0.00	36	0.00	0.00	0.0000	23.10	0.000	0.7123	1.45

X (UTM)	Y (UTM)	Monitoring point	Date	µS cm^{-1}		mg l^{-1}	mg l^{-1}	mg l^{-1}	mg l^{-1}	mg l^{-1}	mg l^{-1}	mg l^{-1}	mg l^{-1}	mg l^{-1}	mg l^{-1}	mg l^{-1}	mg l^{-1}	mg l^{-1}	mg l^{-1}	mg l^{-1}	mg l^{-1}	mg l^{-1}
				EC	pH	SO4	Ca	HCO3	Cl	Mg	Na	K	DQO	TOC	NO3	NO2	NH4	PO4	SiO2	B	Br	N org
451573	4329577	G-18	16-may-06	659	7.33	90	100	222	64	23	27	2	0.60	1.64	27	0.00	0.08	0.0000	11.10		0.1798	1.00
451573	4329577	G-18	18-ene-07	677	7.45	86	81	198	55	24	28	2	0.60	2.21	24	0.00	0.00	0.0000	12.30		0.1396	0.86
451573	4329577	G-18	28-may-07	677	7.43	85	79	199	57	26	28	2	0.70	1.11	23	0.00	0.00	0.0000	11.40	0.000	0.1570	1.35
451573	4329577	G-18	26-nov-07	703	7.74	87	80	193	62	26	29	2	0.90	0.70	24	0.00	0.00	0.0000	11.50	0.000	0.1302	2.23
451573	4329577	G-18	27-may-08	613	8.00	78	62	134	61	22	27	2	0.60	0.00	23	0.00	0.00	0.0000	15.00	0.000	0.1817	1.89
451573	4329577	G-18	24-mar-10	698	7.37	92	93	233	51	24	29	2	0.60	0.00	24	0.30	0.00	0.0000	16.20	0.000	0.2103	1.29
436734	4331700	S-1	17-jul-03	3824	7.70	1510	542	316	141	128	86	9	14.80		0	0.00	0.00	0.0000	13.30	0.334		
436826	4331904	S-1	28-jun-04	3904	7.60	1300	397	173	198	130	106	13	17.20	52.11	0	0.00	0.15	0.0000	43.50		5.1373	4.70
436838	4331893	S-1	18-abr-06	11464	6.99	4050	970	247	1320	690	497	59	29.70	99.85	0	0.11	0.43	0.0000	27.10	0.415	7.7753	2.80
436896	4331914	S-1	17-may-06	16994	7.42	8650	1790	218	1800	1390	905	71	53.20		1	0.07	0.07	0.2141	27.60	0.611		
436896	4331914	S-1	24-mar-10	1406	7.52	664	240	128	80	59	48	7	3.80	5.92	24	0.92	0.00	0.0000	0.50	0.056	0.2717	4.71
438365	4332840	S-2	17-jul-03	4864	7.90	1810	550	130	300	204	137	11	25.90		0	0.00	0.00	0.0000	45.50	0.372		
438587	4333223	S-2	28-jun-04	4084	7.60	1500	431	172	210	158	110	12	19.40	43.50	0	0.00	0.00	0.0000	55.00		12.9551	0.65
438456	4333024	S-2	17-nov-06	17103	7.33	4050	780	368	4220	1300	1220	51	30.40	14.76	10	0.00	0.66	1.2043	19.90	0.458	0.7493	7.98
438484	4333039	S-2	21-feb-07	4183	7.12	1520	400	218	416	228	193	20	12.80	16.11	4	2.00	0.00	1.4720	18.70	0.278	1.7700	2.47
438484	4333039	S-2	18-abr-07	4864	7.72	1530	428	194	600	242	290	22	13.10		0	0.42	0.42	0.1472	6.30	0.241		
438484	4333039	S-2	29-may-07	4475	7.70	1420	428	261	512	236	192	19	13.00	13.40	0	0.00	0.00	0.4014	16.30	0.355	1.8695	2.24
438484	4333039	S-2	10-jul-07	10324	7.12	2120	790	520	2920	730	701	41	29.70	32.54	0	6.90	0.00	0.1606	21.60	0.607	7.5773	5.57
438484	4333039	S-2	23-abr-08	6963	8.01	1700	530	229	1540	450	427	19	18.00	19.38	1	0.00	0.00	0.0000	17.30	0.244	6.0219	3.71
438449	4333059	S-2	27-may-08	8693	7.93	2600	760	320	1680	540	506	22	21.90	21.17	6	0.00	0.00	0.0000	24.80	0.594	5.8516	2.31
438449	4333059	S-2	24-mar-10	1362	7.75	664	236	111	74	58	46	8	3.60	6.77	18	0.25	0.00	0.2600	1.90	0.050	0.2731	8.86
439581	4334750	S-3	17-jul-03	4614	7.50	1870	641	274	155	168	95	11	28.50		2	0.00	0.14	0.0000	59.40	0.352		
439555	4334943	S-3	28-jun-04	4264	7.70	1580	467	180	210	150	107	15	17.20		1	0.00	0.00	0.0000	51.00			
439776	4334939	S-3	27-may-08	26385	7.01	8900	650	384	4000	2200	2218	136		353.60	30	0.00	0.00	0.0000	3.20	0.000	17.5330	36.30
439829	4332742	S-4	17-jul-03	3824	7.90	1540	518	156	100	119	50	7	12.80		0	0.00	0.11	0.0000	12.90	0.275		
439938	4332913	S-4	28-jun-04	4194	7.50	1400	430	223	192	137	102	13	18.40		0	0.00	0.00	0.0000	48.80			
439916	4332883	S-4	27-jun-07	5895	6.92	1810	400	297	540	280	351	71	15.30	37.20	0	0.00	0.19	0.0800	22.90	0.318	1.9135	7.29
439916	4332883	S-4	8-ago-07	3693	7.06	1740	488	219	208	166	152	19	16.60	36.17	0	0.00	2.70	0.6022	60.60	0.000	2.2895	7.18
439916	4332883	S-4	24-mar-10	1413	7.59	656	246	141	71	55	47	7	6.50	7.72	14	0.28	0.00	0.1100	3.10	0.054	0.2508	3.57
440103	4331359	S-5	18-sep-06	3134	7.44	1140	360	246	195	148	105	7	3.60	4.54	17	0.00	0.00	0.0000	17.70	0.000	1.0570	0.65
440115	4331360	S-5	17-nov-06	3063	7.90	1080	320	193	186	132	95	5	3.50	5.48	11	0.00	0.00	0.0000	11.70	0.125	0.7989	0.42
440103	4331359	S-5	12-dic-06	3293	7.55	1120	328	180	184	122	97	7	5.10	5.40	10	0.00	0.00	0.0000	9.10	0.090	0.7700	0.88
440112	4331363	S-5	18-ene-07	3043	7.45	1050	336	235	186	118	98	6	3.20	4.18	13	0.00	0.00	0.0000	17.80	0.000	0.6468	1.02
440103	4331359	S-5	21-feb-07	2923	7.45	1090	350	213	179	120	86	9	4.30	4.44	8	0.00	0.00	0.0000	7.90	0.134	0.7751	3.03

X (UTM)	Y (UTM)	Monitoring point	Date	µS cm^{-1}		mg l^{-1}	mg l^{-1}	mg l^{-1}	mg l^{-1}	mg l^{-1}	mg l^{-1}	mg l^{-1}	mg l^{-1}	mg l^{-1}	mg l^{-1}	mg l^{-1}	mg l^{-1}	mg l^{-1}	mg l^{-1}	mg l^{-1}	mg l^{-1}	mg l^{-1}	mg l^{-1}
				EC	pH	SO4	Ca	HCO3	Cl	Mg	Na	K	DQO	TOC	NO3	NO2	NH4	PO4	SiO2	B	Br	N org
440116	4331363	S-5	20-mar-07	3224	7.48	1240	392	225	195	134	106	7	3.40	5.34	9	0.26	0.00	0.0000	11.40	0.100	0.4800	8.19
440103	4331359	S-5	17-abr-07	3154	7.07	1130	382	203	190	121	98	6	4.30		7	0.00	0.00	0.0803	19.00	0.000		
440103	4331359	S-5	30-may-07	2945	7.50	1080	300	198	196	142	95	6	3.20	3.42	3	0.00	0.00	0.0000	21.40	0.206	0.7307	2.39
440103	4331359	S-5	27-jun-07	3165	7.55	1090	302	165	202	142	100	8	4.30	5.08	0	0.00	0.00	0.0000	18.50	0.000	0.7642	15.03
440103	4331359	S-5	8-ago-07	2973	7.46	1100	368	206	202	124	100	6	2.80	6.69	6	0.00	0.00	0.1606	18.80	0.000	0.8539	3.81
440103	4331359	S-5	13-sep-07	2973	7.51	1120	382	225	204	121	107	6	3.20	5.35	12	0.00	0.00	0.0937	17.50	0.000	0.7265	4.38
440103	4331359	S-5	9-oct-07	2963	6.96	1120	380	249	203	130	105	7	4.70	6.01	6	0.00	0.00	0.0000	16.80	0.201	1.1614	3.90
440103	4331359	S-5	22-nov-07	3374	7.21	934	300	246	199	117	101	6	3.90	16.80	11	0.00	0.00	0.1338	15.30	0.209	0.5275	4.59
440103	4331359	S-5	27-dic-07	2914	7.56	910	300	235	189	120	107	6	2.40	5.29	9	0.00	0.00	0.0000	15.40	0.000	0.9683	2.51
440103	4331359	S-5	22-ene-08	2924	7.78	950	300	220	195	119	111	7	2.70	3.80	6	0.00	0.00	0.0000	10.40	0.000	0.7089	3.35
440115	4331361	S-5	22-feb-08	2933	7.48	920	280	220	194	123	99	6	2.50	4.42	7	0.00	0.00	0.0000	7.60	0.095	0.7674	2.14
440103	4331359	S-5	11-mar-08	3513	7.64	960	310	230	210	122	115	6	2.20	4.90	4	0.00	0.00	0.0000	7.20	0.000	0.6191	3.74
440103	4331359	S-5	23-abr-08	2783	7.54	850	220	139	182	116	109	6	2.40	4.50	2	0.00	0.00	0.0000	9.20	0.000	0.9906	3.86
440103	4331359	S-5	28-may-08	2903	7.66	1070	304	132	189	124	109	7	3.40	4.51	2	0.00	0.00	0.0000	8.80	0.000	1.0566	1.73
440103	4331359	S-5	4-may-09	1819	7.77	626	220	188	158	104	53	6	1.70	1.54	26	0.00	0.00	0.0000	21.60	0.084	0.7400	1.71
440103	4331359	S-5	24-mar-10	1050	7.79	446	146	139	52	63	34	7	2.40	3.41	26	1.40	0.00	0.1200	0.30	0.130	0.2402	2.29
437907	4330819	S-6	17-jul-03	3854	7.80	1640	582	280	133	142	81	12	13.60		0	0.00	0.00	0.0000	12.60	0.404		
438009	4331009	S-6	28-jun-04	3874	7.70	1410	412	136	192	141	101	13	14.00	9.23	1	0.00	0.00	0.0000	34.10		1.1374	4.90
438099	4330937	S-6	18-abr-06	3444	6.94	1430	384	127	223	164	108	8	10.00	24.90	0	0.00	1.20	0.1338	0.20	0.170	1.6152	1.00
438112	4330925	S-6	16-may-06	4794	7.15	2060	604	79	306	214	141	9	13.70	10.22	1	0.00	0.24	0.1204	0.50	0.218	1.2514	3.00
438110	4330924	S-6	20-jun-06	3334	7.38	1300	394	132	244	162	107	8	8.10	8.28	4	2.00	0.00	0.1338	0.40	0.181	1.0644	1.60
438140	4330956	S-6	24-jul-06	3773	6.89	1650	450	116	282	186	119	10	7.60	17.71	9	0.00	0.00	0.3747	2.90	0.175	1.6180	3.40
438170	4330927	S-6	29-ago-06	5003	7.39	2020	570	66	370	232	153	15	14.40	6.40	0	0.00	0.00	0.0937	9.50	0.189	1.2293	1.18
438571	4331151	S-6	18-sep-06	3324	7.33	1210	368	177	276	176	110	8	8.30	5.27	10	0.00	0.00	0.3479	9.00	0.538	0.8049	1.30
438175	4330934	S-6	17-nov-06	2953	7.72	1030	328	130	236	136	90	5	5.00	5.48	3	0.00	0.00	0.0000	1.40	0.144	0.7382	0.21
438140	4330956	S-6	12-dic-06	3293	7.55	1250	376	163	213	150	102	8	5.10	6.02	9	0.00	0.00	0.0000	9.20	0.121	0.5288	1.54
438140	4330956	S-6	20-feb-07	2883	7.15	1120	348	126	187	122	83	7	6.00	18.43	5	0.00	0.00	0.0000	1.80	0.128	1.3579	0.86
438140	4330956	S-6	30-may-07	3505	7.42	1260	320	126	292	170	128	8	5.10	5.13	2	0.00	0.00	0.0000	4.40	0.273	1.1010	3.14
438140	4330956	S-6	24-mar-10	1410	7.73	668	240	142	77	60	47	7	4.20	5.13	26	0.49	0.00	0.0000	0.70	0.055	0.2569	5.57
437696	4331152	S-6-bis	17-nov-06	5953	7.39	2610	720	159	428	290	152	11	22.80		8	0.00	0.00	0.2409	15.80	0.453		
437696	4331152	S-6-bis	10-jul-07	10004	6.95	4200	1080	205	1180	650	329	32	30.00	48.16	0	0.00	7.80	3.7468	39.00	0.645	4.5460	11.72
434357	4329694	S-7	28-jun-04	3724	7.70	1390	412	195	179	140	95	14	15.60	45.58	0	0.00	0.00	0.0000	37.90		3.9930	12.20
434386	4329701	S-7	18-abr-06	7274	7.55	3120	730	444	750	480	309	17	29.40	78.48	1	0.20	4.00	0.1338	18.10	0.209	5.1993	3.20
434387	4329702	S-7	16-may-06	7664	7.55	2580	826	456	830	326	360	16	52.40	78.67	0	0.08	5.16	0.0937	21.20	0.248	3.2913	2.00
434407	4329752	S-7	20-jun-06	8344	7.51	3300	766	280	884	586	354	18	57.90	75.60	0	0.12	6.50	0.1071	16.70	0.265	6.9934	7.40
434381	4329712	S-7	24-jul-06	9903	6.93	4180	910	460	1280	790	415	25	30.40	104.20	3	3.20	5.50	0.1472	8.80	0.291	7.0058	1.50
434381	4329712	S-7	29-ago-06	11883	8.00	4890	1110	160	1530	930	490	34	75.20	124.80	0	0.08	0.29	0.2275	27.50	0.377	9.1014	13.92

X (UTM)	Y (UTM)	Monitoring point	Date	µS cm^{-1}		mg l^{-1}	mg l^{-1}	mg l^{-1}	mg l^{-1}	mg l^{-1}	mg l^{-1}	mg l^{-1}	mg l^{-1}	mg l^{-1}	mg l^{-1}	mg l^{-1}	mg l^{-1}	mg l^{-1}	mg l^{-1}	mg l^{-1}	mg l^{-1}	mg l^{-1}
				EC	pH	SO4	Ca	HCO3	Cl	Mg	Na	K	DQO	TOC	NO3	NO2	NH4	PO4	SiO2	B	Br	N org
434369	4329711	S-7	18-sep-06	13174	7.65	5600	1240	162	1630	1050	520	38	101.80	84.46	0	0.08	0.78	0.2275	29.10	0.000	5.7290	17.06
434381	4329712	S-7	16-nov-06	8273	7.38	3480	660	183	820	550	371	21	71.30	57.01	19	0.59	0.00	0.0937	30.10	0.243	5.3196	1.47
434381	4329712	S-7	12-dic-06	7753	7.33	3120	590	290	788	560	334	20	50.90	64.75	37	0.00	0.00	0.0000	23.40	0.152	6.3059	13.48
434376	4329723	S-7	17-ene-07	7643	7.07	3820	580	275	812	570	329	18	50.90	53.33	34	0.00	0.00	0.3613	12.00	0.000	3.5858	5.80
434381	4329712	S-7	20-feb-07	6363	6.92	2520	530	273	684	444	302	15	30.00	64.80	1	0.77	7.70	0.1204	16.30	0.255	4.1870	9.81
434381	4329720	S-7	21-mar-07	7824	6.86	3080	550	266	784	540	357	18	49.30	58.61	1	0.40	3.60	0.1338	5.00	0.208	3.2300	9.42
434381	4329712	S-7	17-abr-07	5154	7.77	2460	490	157	736	472	328	15	30.40	5.77	0	0.00	3.80	0.0000	6.20	0.000	1.2412	1.18
434381	4329712	S-7	30-may-07	7435	6.92	2700	540	162	850	550	312	13	29.10	35.03	6	0.00	0.00	0.0000	7.70	0.318	5.2680	10.32
434381	4329712	S-7	10-jul-07	11594	6.85	5100	1060	201	1710	940	514	28	65.00	84.50	0	0.18	2.20	0.2944	3.20	0.518	8.1681	3.22
434438	4329818	S-7	8-ago-07	16513	7.17	7600	1600	293	2080	1340	932	42	72.00	228.00	1	0.19	9.60	0.2409	28.30	0.422	17.1728	36.63
434381	4329712	S-7	13-sep-07	21965	6.72	8800	1460	239	3160	1900	1078	52		262.50	1	0.00	0.00	0.2542	43.50	0.678	19.4898	1.81
434381	4329712	S-7	9-oct-07	21604	6.64	8800	1350	205	2840	1780	1107	52		212.30	1	0.00	0.00	0.2409	37.70	0.000	24.0172	1.95
434428	4329819	S-7	22-nov-07	21666	6.75	8200	1370	195	3020	1800	1237	55		229.10	1	0.00	0.00	0.4951	38.30	0.651	13.2181	16.14
434428	4329819	S-7	27-dic-07	21407	6.84	8100	1250	181	3000	1800	1314	49		223.35	2	0.00	0.00	0.2542	40.50	0.558	18.6033	20.63
434428	4329819	S-7	22-ene-08	20427	6.68	8150	1320	181	3100	1860	955	43		16.68	42	0.00	0.00	0.0000	31.20	0.536	18.8239	16.62
434440	4329827	S-7	22-feb-08	17813	6.38	7200	1190	168	2720	1600	945	41	67.30	16.67	50	0.00	0.00	0.0000	32.20	0.479	18.7463	20.86
434421	4329816	S-7	11-mar-08	20993	6.88	8200	1300	186	3200	1880	1044	49		17.65	36	0.00	0.00	0.0000	31.20	0.473	25.5065	29.47
434404	4329803	S-7	24-abr-08	15433	7.20	5500	970	185	2290	1200	915	38	48.50	13.91	30	0.00	0.00	0.0000	28.30	0.454	23.0335	26.86
434392	4329795	S-7	28-may-08	23445	6.06	8400	1300	288	2900	1600	1529	55	72.80	166.60	44	0.00	0.00	0.0000	21.80	0.674	22.2017	15.87
434412	4329811	S-7	23-jun-08	33765	6.74	10400	1060	368	4500	2300	2259	97		414.40	30	0.00	0.00	0.0000	31.20	1.010	42.7382	37.03
434432	4329827	S-7	21-jul-08	145621	7.07	48000	840	1940	21500	14000	9889	320		0.00	0	0.00	0.00	0.0000	6.80		111.7184	160.44
434432	4329827	S-7	24-mar-10	1406	7.71	652	242	140	74	61	47	7	4.50	5.44	27	0.76	0.00	0.0000	0.30	0.059	0.2583	3.57
449385	4339230	S-IW	18-may-04	3574	7.90	1400	426	270	157	140	91	13	5.90		10	0.10	0.00	0.2007	7.10			
449387	4339238	S-IW	28-jun-04	4204	7.70	1570	467	183	186	156	100	10	4.70	4.80	14	0.00	0.00	0.0000	20.40		0.4216	3.29
449385	4339230	S-IW	31-may-07	2585	7.22	890	250	168	173	98	115	18	5.80		12	0.00	0.00	1.0036	20.20	0.261		
449385	4339230	S-IW	27-jun-07	5045	7.90	1920	410	261	446	252	288	35	7.00	7.84	0	0.00	0.00	0.9768	7.10	0.000	1.5079	10.42
449385	4339230	S-IW	8-ago-07	3543	7.89	1572	496	242	179	160	128	14	5.70	9.35	1	0.94	0.00	0.6691	39.90	0.000	0.5914	2.05
449385	4339230	S-IW	24-mar-10	1487	7.72	732	268	157	80	64	60	8	2.90	3.92	34	0.87	0.00	0.0000	3.50	0.060	0.2564	1.71

APPENDIX G

SWAP model calibrations and validations

G. Calibration and validation plots of SWAP vadose zone water flow models for typical soil profiles (Fig. 6.31) in Las Tablas de Daimiel National Park not shown in Figure 6.32.

Peaty silt (soil profile I)

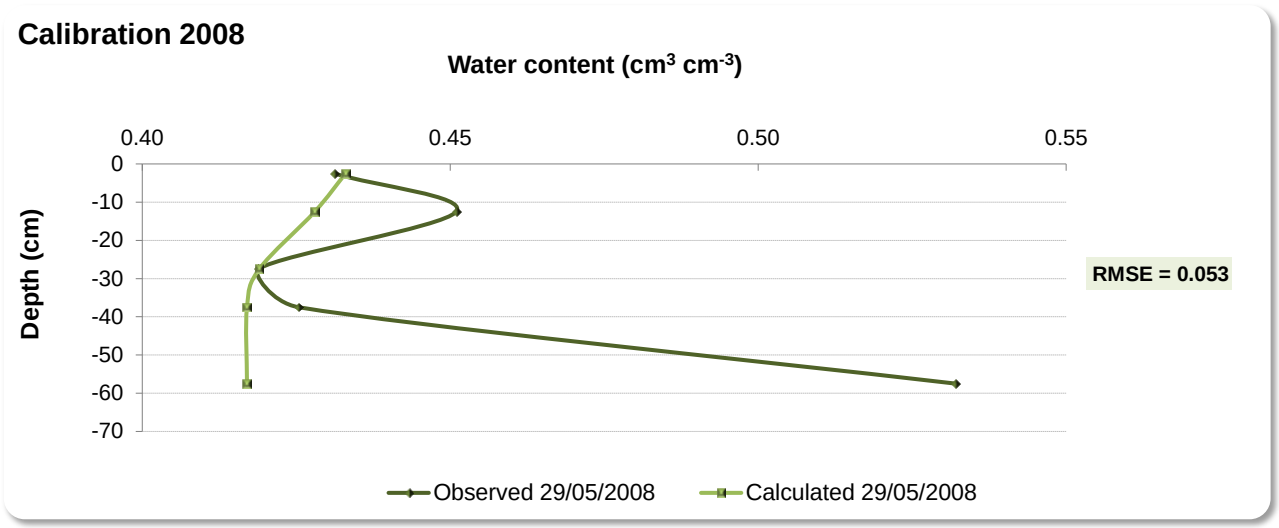

Peaty silt (soil profile III)

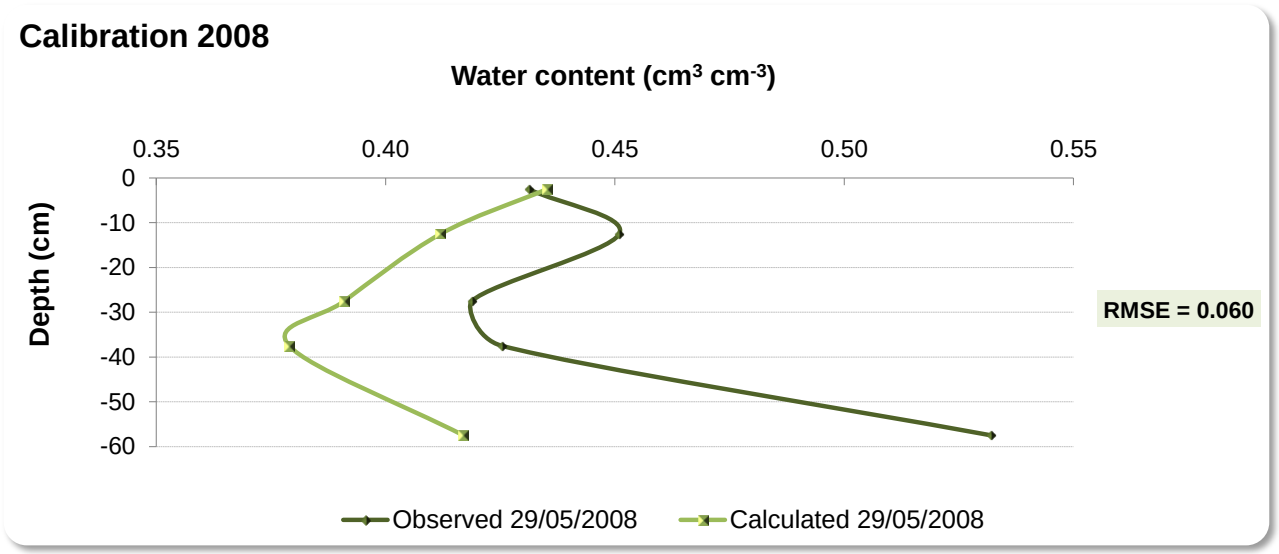

Saline charophytes overlying clay (soil profile V)

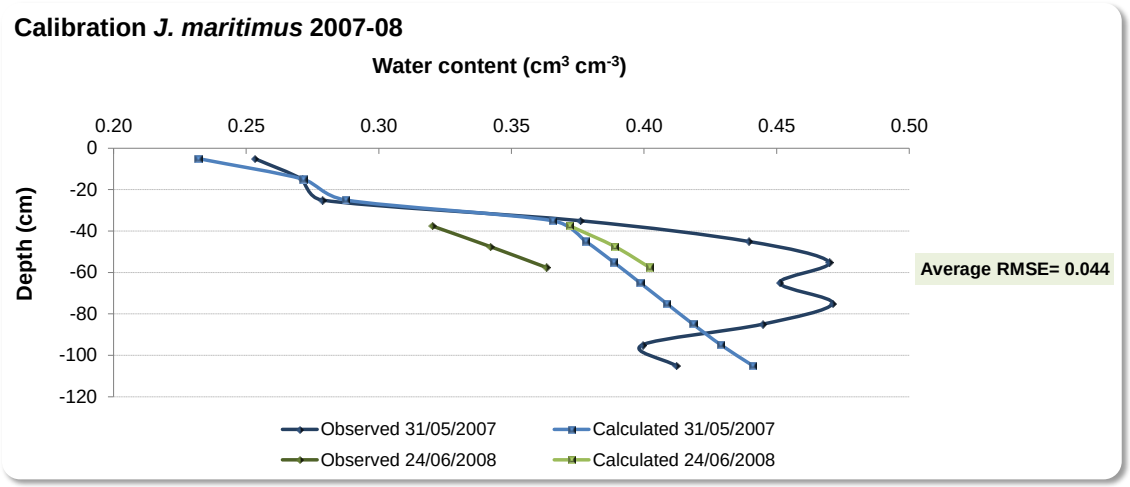

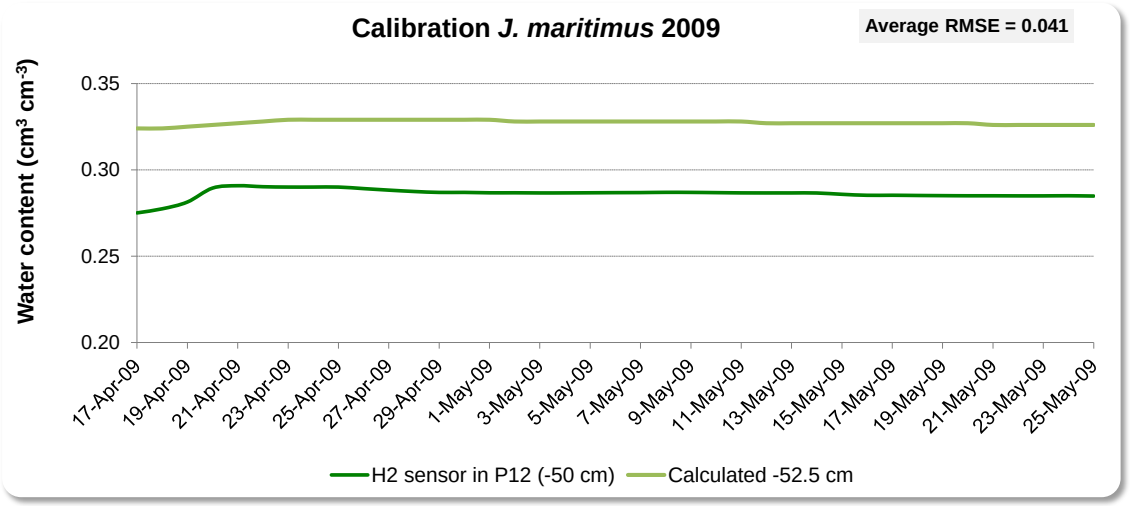

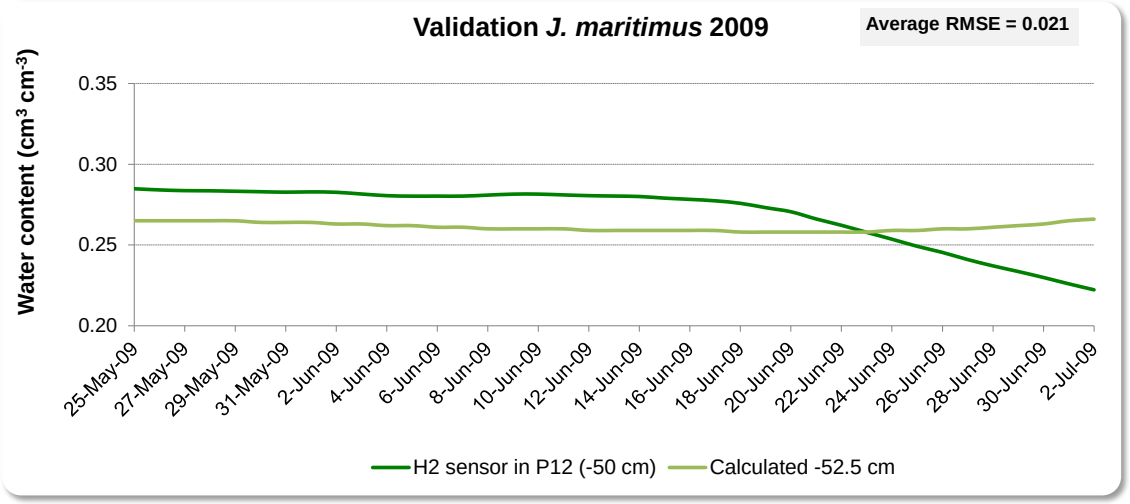

Charophytes-Peat alternations (soil profile VIII)